

Baligh El Hefni · Daniel Bouskela

# Modeling and Simulation of Thermal Power Plants with ThermoSysPro

A Theoretical Introduction and a  
Practical Guide



# Modeling and Simulation of Thermal Power Plants with ThermoSysPro

Baligh El Hefni · Daniel Bouskela

# Modeling and Simulation of Thermal Power Plants with ThermoSysPro

A Theoretical Introduction and a Practical  
Guide



Springer

Baligh El Hefni  
EDF R&D  
Chatou, France

Daniel Bouskela  
EDF R&D  
Chatou, France

ISBN 978-3-030-05104-4      ISBN 978-3-030-05105-1 (eBook)  
<https://doi.org/10.1007/978-3-030-05105-1>

Library of Congress Control Number: 2018962771

© Springer Nature Switzerland AG 2019

This work is subject to copyright. All rights are reserved by the Publisher, whether the whole or part of the material is concerned, specifically the rights of translation, reprinting, reuse of illustrations, recitation, broadcasting, reproduction on microfilms or in any other physical way, and transmission or information storage and retrieval, electronic adaptation, computer software, or by similar or dissimilar methodology now known or hereafter developed.

The use of general descriptive names, registered names, trademarks, service marks, etc. in this publication does not imply, even in the absence of a specific statement, that such names are exempt from the relevant protective laws and regulations and therefore free for general use.

The publisher, the authors and the editors are safe to assume that the advice and information in this book are believed to be true and accurate at the date of publication. Neither the publisher nor the authors or the editors give a warranty, express or implied, with respect to the material contained herein or for any errors or omissions that may have been made. The publisher remains neutral with regard to jurisdictional claims in published maps and institutional affiliations.

This Springer imprint is published by the registered company Springer Nature Switzerland AG  
The registered company address is: Gewerbestrasse 11, 6330 Cham, Switzerland

# Preface

Modelling and simulation is becoming an essential tool to assess the behavior of large complex energy systems against ever more stringent safety, availability, environmental, economic and societal constraints prompted by the ongoing energy transition. Indeed, the large number of requirements to be considered and the complex physical interactions between systems and their environment call for efficient means for quantitative and qualitative analysis of the systems physical and functional behavior.

System modelling, also called 0D/1D modelling, is the discipline at the cross-roads between detailed 3D physical modelling such as computational fluid dynamics and functional modelling such as control system design. It aims at representing the physical behavior of the whole system using first principle physical laws. These laws are averaged in space and are closed with empirical correlations in order to compute the quantities of interest to the engineer while avoiding unrealistic assumptions and minimizing computational time. Physical modelling is most often used for simulation which consists in predicting the system's behavior from given initial conditions over a given time period. Thanks to 0D/1D modelling, the time periods can extend over several time scales (from seconds to years), and simulation can usually be performed much faster than real time on ordinary laptops. This convenience is especially needed for simulation over long time periods. 0D/1D modelling is also used for assessing and monitoring the system current state in combination with other techniques such as data assimilation that aim at using the knowledge embedded in the models to improve data quality.

0D/1D modelling can cover the whole system engineering lifecycle, from preliminary design to commissioning, operation and maintenance. It can be used for diverse tasks such as the optimal sizing of a refueling cavity, the optimal plant startup that consists in minimizing startup delay while meeting operational constraints, the assessment of steam generator clogging while the plant is in operation, the monitoring and diagnostics of efficiency degradation due to thermal losses, operators training, etc.

This book is about the science and art of physical system modelling applied to thermal power plants with a library of component models called ThermoSysPro which is used at EDF (and also other organizations) for the engineering of power plants at the design and operation phases. The ambition is to show how to make power plant models that provide convincing simulation results. To that end, it contains EDF's long standing experience in power plant modelling and simulation. The equations used in the component models are presented in detail with their validity domains using mathematical notation in a tool-independent way. They are justified with respect to fundamental knowledge in thermodynamics and heat transfer using analytical derivations or proofs when necessary. For each component model, a small test-case with simulation results is given. Models of thermal power plants (fossil fuel fired and solar) are presented with results of numerical simulation and practical hints on how to build them with the library. In addition, comparison with real manufacturer data is provided in the case of a combined cycle power plant. Some insight is also given on the internal structure of the library for the interested reader.

The whole space of the book is dedicated to the physical and mathematical aspects of power plant modelling. Although they are important, the numerical aspects are not considered. This is made possible thanks to the Modelica technology that emerged at the turn of the twenty-first century and that is now fully operational in several commercial and open source tools. It allows to translate automatically models equations into efficient simulation code. Therefore, although this book relies on Modelica to produce numerical results, it is not an introduction to modeling and simulation with Modelica, so it does not present the language nor does it mention the associated techniques. Moreover, the lessons learned from this book can be used with any kind of tool, not only Modelica tools.

The book is intended to students and confirmed practitioners in power plant modelling and simulation. All models presented in the book can be found in the ThermoSysPro library which is released under open source license and freely available to the public.

Chatou, France  
October 2018

Daniel Bouskela  
Baligh El Hefni

# Acknowledgements

First thanks to the PRISME department of EDF Lab for their support to the accomplishment of this book.

Many thanks to Audrey Jardin for fruitful comments and to Benoît Bride for providing combustion component models.

Thanks to all ThermoSysPro enthusiastic users for their comments and feedback on the library.

Thanks to the Modelica community who developed the Modelica language that made ThermoSysPro possible.

Thanks to Peter Fritzson and the OpenModelica team for their support of ThermoSysPro in the OpenModelica open source platform.

Finally, thanks to the Eureka ITEA cluster program and dedicated team for providing the innovative framework that boosted the development of Modelica and ThermoSysPro.

# Contents

<b>1</b>	<b>Introduction to Modeling and Simulation . . . . .</b>	<b>1</b>
1.1	Systems, Complex Systems, and Cyber-Physical Systems . . . . .	1
1.2	What is System Modeling? . . . . .	2
1.3	What is Simulation? . . . . .	3
1.4	What is 0D/1D Modeling? . . . . .	4
1.5	What is a 0D/1D Thermal Hydraulic Component Models Library? . . . . .	7
1.6	What are 0D/1D Models Useful for? . . . . .	8
	References . . . . .	10
<b>2</b>	<b>Introduction to Thermodynamics and Heat Transfer . . . . .</b>	<b>11</b>
2.1	What Are Thermodynamics and Thermal Hydraulics? . . . . .	11
2.2	Thermodynamic Processes . . . . .	12
2.3	Properties of Substances . . . . .	12
2.3.1	Density and Specific Volume . . . . .	13
2.3.2	Pressure . . . . .	13
2.3.3	Temperature . . . . .	14
2.3.4	Energy . . . . .	14
2.3.5	Enthalpy . . . . .	16
2.3.6	Entropy . . . . .	17
2.4	State of a Physical System . . . . .	18
2.5	Selection of the State Variables . . . . .	19
2.6	Definition of a Thermodynamic System . . . . .	21
2.7	Types of Thermodynamic Systems . . . . .	21
2.7.1	Isolated System . . . . .	21
2.7.2	Closed System . . . . .	22
2.7.3	Open System . . . . .	22
2.8	Laws of Thermodynamics . . . . .	23
2.8.1	First Law . . . . .	23
2.8.2	Second Law . . . . .	29

2.9	Thermodynamic Cycles . . . . .	32
2.9.1	The Brayton Cycle . . . . .	32
2.9.2	The Rankine Cycle . . . . .	35
2.10	The Ideal Gas Law . . . . .	38
2.11	Polytropic Processes . . . . .	39
2.12	Heat Transfer Processes . . . . .	40
	References . . . . .	42
<b>3</b>	<b>Averaged Physical Quantities . . . . .</b>	<b>43</b>
3.1	Fluxes and Flows of Specific Extensive Quantities . . . . .	44
3.2	Average Density . . . . .	46
3.3	Average of Specific Extensive Quantities . . . . .	46
3.4	Average of Other Quantities . . . . .	48
3.5	Average of Phase-Related Quantities . . . . .	49
3.6	Notation . . . . .	49
<b>4</b>	<b>Governing Equations . . . . .</b>	<b>51</b>
4.1	Single-Phase Flow . . . . .	55
4.1.1	General Formulation of the Balance Equations . . . . .	55
4.1.2	Mass Balance Equation . . . . .	57
4.1.3	Momentum Balance Equation . . . . .	58
4.1.4	Energy Balance Equation . . . . .	60
4.2	Two-Phase Water/Steam Flow . . . . .	62
4.2.1	Definitions . . . . .	62
4.2.2	Mass Balance Equation . . . . .	65
4.2.3	Momentum Balance Equation . . . . .	67
4.2.4	Energy Balance Equation . . . . .	72
4.2.5	Computing the Phase Velocities for the Mixture Model . . . . .	75
4.2.6	Computing Condensation and Evaporation Mass Flow Rates in Drum Boilers . . . . .	77
4.3	Computing Quantities on the Control Volumes Boundaries . . . . .	78
4.3.1	Computation of the Mass Flow Rate . . . . .	78
4.3.2	Computation of the Specific Enthalpy . . . . .	80
4.3.3	Computation of the Thermal Flow Due to Diffusion . . . . .	83
4.3.4	Computation of the Pressure . . . . .	84
	References . . . . .	89
<b>5</b>	<b>Static Systems . . . . .</b>	<b>91</b>
5.1	General Form of the Static Balance Equations . . . . .	92
5.2	Computing the Physical States for Static Balance Equations . . . . .	93
5.2.1	Origin of the Singularities for the Computation of the Volumes Specific Enthalpies When Diffusion Is Neglected . . . . .	93

5.2.2	Computing the Volume Specific Enthalpies . . . . .	96
5.2.3	Computing the Volume Pressures and Mass Flow Rates . . . . .	97
Reference . . . . .		98
<b>6</b>	<b>Modeling and Simulation of Thermal Power Plants . . . . .</b>	<b>99</b>
6.1	Introduction . . . . .	99
6.2	Typical Usage of Power Plant Models . . . . .	101
6.3	The ThermoSysPro Library . . . . .	101
6.4	How to Develop a Power Plant Model . . . . .	102
6.4.1	Using the ThermoSysPro Library . . . . .	102
6.4.2	Conceptual Steps . . . . .	106
6.4.3	Recurrent Difficulty: Finding the Steady-State Initial Conditions . . . . .	107
6.4.4	Practical Steps . . . . .	111
6.4.5	Practical Hints . . . . .	113
6.5	Dynamic Model of a Real Combined Cycle Power Plant . . . . .	114
6.5.1	Description of a Combined Cycle Power Plant . . . . .	114
6.5.2	Description of the Phu My Combined Cycle Power Plant . . . . .	116
6.5.3	Description of the Model . . . . .	117
6.6	Dynamic Model of a Once-Through Supercritical Coal-Fired Power Plant . . . . .	134
6.6.1	Description of a Once-Through Supercritical Coal-Fired Power Plant . . . . .	134
6.6.2	Description of the Model . . . . .	136
6.7	Dynamic Model of a 1 MWe Concentrated Solar Power Plant (CSP) with a PTSC . . . . .	147
6.7.1	Description of the Concentrated Solar Power Plant . . . . .	147
6.7.2	Description of the Model . . . . .	148
References . . . . .		152
<b>7</b>	<b>Boiler (Steam Generator) Modeling . . . . .</b>	<b>153</b>
7.1	Detailed Modeling of the Boiler . . . . .	153
7.2	Simplified Modeling of the Boiler . . . . .	154
7.2.1	Modeling Principles . . . . .	154
7.2.2	Nomenclature . . . . .	155
7.2.3	Governing Equations . . . . .	157
7.2.4	Modelica Component Model: <i>FossilFuelBoiler</i> . . . . .	161
7.2.5	Test-Case . . . . .	161

<b>8</b>	<b>Combustion Chamber Modeling . . . . .</b>	165
8.1	Combustion Chamber for a Gas Turbine . . . . .	165
8.1.1	Modeling Principles . . . . .	166
8.1.2	Nomenclature . . . . .	167
8.1.3	Governing Equations . . . . .	169
8.1.4	Modelica Component Model: <i>GTCombustionChamber</i> . . . . .	171
8.1.5	Test-Case . . . . .	172
8.2	Combustion Chamber for Boiler Furnace . . . . .	174
8.2.1	Modeling Principles . . . . .	175
8.2.2	Nomenclature . . . . .	175
8.2.3	Governing Equations . . . . .	178
8.2.4	Modelica Component Model: <i>GenericCombustion1D</i> . . . . .	180
8.2.5	Component Model Validation . . . . .	180
	Reference . . . . .	185
<b>9</b>	<b>Heat Exchanger Modeling . . . . .</b>	187
9.1	Introduction . . . . .	187
9.2	Analysis Methods . . . . .	189
9.2.1	Nomenclature . . . . .	189
9.2.2	Assumptions . . . . .	193
9.2.3	Overall Heat Transfer Coefficient . . . . .	193
9.2.4	Convective Heat Transfer Coefficient . . . . .	194
9.2.5	The Log Mean Temperature Difference Method (LMTD) . . . . .	200
9.2.6	The Effectiveness and the Number of Transfer Units Method (NTU) . . . . .	204
9.2.7	The UA Method . . . . .	208
9.2.8	The Efficiency Method . . . . .	208
9.2.9	Taking into Account Phase Transitions . . . . .	208
9.2.10	Simple Heat Exchangers . . . . .	211
9.3	Dynamic Heat Exchangers . . . . .	211
9.4	Shell-and-Tube Heat Exchanger Modeling . . . . .	214
9.4.1	Introduction . . . . .	214
9.4.2	Tube Bundle Heat Exchanger . . . . .	215
9.4.3	Shell-Side Heat Exchanger Modeling . . . . .	222
9.4.4	Heat Exchanger Wall . . . . .	228
9.5	Shell Heat Exchangers . . . . .	231
9.5.1	Introduction . . . . .	231
9.5.2	Dynamic Modeling of a Water Heater . . . . .	232
9.5.3	Dynamic Modeling of a Simple Condenser . . . . .	240

9.5.4	Dynamic Modeling of a Condenser . . . . .	250
9.5.5	Static Modeling of a Water Heater . . . . .	254
9.6	Plate Heat Exchanger Modeling . . . . .	263
9.6.1	Dynamic Modeling of a Plate Heat Exchanger . . . . .	263
9.6.2	Static Modeling of a Plate Heat Exchanger . . . . .	270
9.7	Simple Heat Exchanger Modeling . . . . .	274
9.7.1	Static Condenser with Correlations Given by the 9th HEI Standard (1996) . . . . .	274
	References . . . . .	281
<b>10</b>	<b>Steam Turbine Modeling . . . . .</b>	<b>283</b>
10.1	Basic Description . . . . .	283
10.2	Stodola Turbine Modeling . . . . .	290
10.2.1	Nomenclature . . . . .	291
10.2.2	Assumptions . . . . .	292
10.2.3	Governing Equations . . . . .	292
10.2.4	Modelica Component Model: <i>StodolaTurbine</i> . . . . .	293
10.2.5	Test-Case . . . . .	294
	References . . . . .	295
<b>11</b>	<b>Gas Turbine Modeling . . . . .</b>	<b>297</b>
11.1	Basic Principles . . . . .	297
11.2	Reference Quantities . . . . .	300
11.3	Static Modeling of Compressor . . . . .	301
11.3.1	Nomenclature . . . . .	301
11.3.2	Governing Equations . . . . .	302
11.3.3	Modelica Component Model: <i>Compressor</i> . . . . .	303
11.3.4	Test-Case . . . . .	303
11.4	Static Modeling of the Combustion Turbine . . . . .	305
11.4.1	Nomenclature . . . . .	305
11.4.2	Assumptions . . . . .	306
11.4.3	Governing Equations . . . . .	306
11.4.4	Modelica Component Model: <i>CombustionTurbine</i> . . . . .	307
11.4.5	Test-Case . . . . .	307
<b>12</b>	<b>Centrifugal Pump Modeling . . . . .</b>	<b>311</b>
12.1	Basic Description . . . . .	311
12.2	Static Centrifugal Pump . . . . .	318
12.2.1	Nomenclature . . . . .	318
12.2.2	Governing Equations . . . . .	319
12.2.3	Modelica Component Model: <i>StaticCentrifugalPump</i> . . . . .	322
12.2.4	Test-Case . . . . .	322

12.3	Centrifugal Pump . . . . .	324
12.3.1	Nomenclature . . . . .	325
12.3.2	Governing Equations . . . . .	325
12.3.3	Modelica Component Model: <i>CentrifugalPump</i> . . . . .	326
12.3.4	Test-Case . . . . .	327
	References . . . . .	329
<b>13</b>	<b>Pressure Loss Modeling . . . . .</b>	<b>331</b>
13.1	Bernoulli's Equation . . . . .	331
13.2	Closure Laws: Coefficient of Friction . . . . .	332
13.2.1	Single-Phase Flow . . . . .	333
13.2.2	Homogeneous Two-Phase Flow Model . . . . .	336
13.3	General Assumptions for Pressure Loss Modeling . . . . .	337
13.4	Pipe and Singular Pressure Loss Modeling . . . . .	337
13.4.1	Nomenclature . . . . .	338
13.4.2	Governing Equations . . . . .	338
13.4.3	Modelica Component Models: <i>PipePressureLoss</i> and <i>SingularPressureLoss</i> . . . . .	339
13.4.4	Test-Case . . . . .	340
13.5	Lumped Straight Pipe Modeling . . . . .	341
13.5.1	Nomenclature . . . . .	341
13.5.2	Governing Equations . . . . .	342
13.5.3	Modelica Component Model: <i>LumpedStraightPipe</i> . . . . .	343
13.5.4	Test-Case . . . . .	343
13.6	Bend Modeling . . . . .	345
13.6.1	Nomenclature . . . . .	346
13.6.2	Assumptions . . . . .	347
13.6.3	Governing Equations . . . . .	347
13.6.4	Modelica Component Model: <i>Bend</i> . . . . .	348
13.6.5	Test-Case . . . . .	348
13.7	Diaphragm Modeling . . . . .	349
13.7.1	Nomenclature . . . . .	350
13.7.2	Assumptions . . . . .	350
13.7.3	Governing Equations . . . . .	350
13.7.4	Modelica Component Model: <i>Diaphragm</i> . . . . .	351
13.7.5	Test-Case . . . . .	352
13.8	Control Valve Modeling . . . . .	352
13.8.1	Nomenclature . . . . .	353
13.8.2	Assumptions . . . . .	354
13.8.3	Governing Equations . . . . .	354
13.8.4	Modelica Component Model: <i>ControlValve</i> . . . . .	355
13.8.5	Test-Case . . . . .	356

13.9	Three-Way Valve Modeling . . . . .	357
13.9.1	Modelica Component Model: <i>ThreeWayValve</i> . . . . .	358
13.9.2	Test-Case . . . . .	359
13.10	Switch Valve Modeling . . . . .	360
13.10.1	Nomenclature . . . . .	362
13.10.2	Assumptions . . . . .	362
13.10.3	Governing Equations . . . . .	362
13.10.4	Modelica Component Model: <i>SwitchValve</i> . . . . .	363
13.10.5	Test-Case . . . . .	363
13.11	Check Valve Modeling . . . . .	365
13.11.1	Nomenclature . . . . .	366
13.11.2	Governing Equations . . . . .	366
13.11.3	Modelica Component Model: <i>CheckValve</i> . . . . .	367
13.11.4	Test-Case . . . . .	368
13.12	Dynamic Check Valve Modeling . . . . .	369
13.12.1	Nomenclature . . . . .	369
13.12.2	Governing Equations . . . . .	370
13.12.3	Modelica Component Model: <i>DynamicCheckValve</i> . . . . .	372
13.12.4	Test-Case . . . . .	373
13.13	Dynamic Relief Valve Modeling . . . . .	374
13.13.1	Nomenclature . . . . .	375
13.13.2	Assumptions . . . . .	376
13.13.3	Governing Equations . . . . .	376
13.13.4	Modelica Component Model: <i>DynamicReliefValve</i> . . . . .	378
13.13.5	Test-Case . . . . .	378
	References . . . . .	381
14	<b>Volume Modeling . . . . .</b>	383
14.1	Simple Dynamic Volume Modeling . . . . .	383
14.1.1	Nomenclature . . . . .	384
14.1.2	Assumptions . . . . .	385
14.1.3	Governing Equations . . . . .	385
14.1.4	Modelica Component Model: <i>VolumeATh</i> . . . . .	386
14.1.5	Test-Case . . . . .	386
14.2	Dynamic Drum Modeling . . . . .	389
14.2.1	Nomenclature . . . . .	390
14.2.2	Assumptions . . . . .	393
14.2.3	Governing Equations . . . . .	394
14.2.4	Modelica Component Model: <i>DynamicDrum</i> . . . . .	397
14.2.5	Test-Case . . . . .	397

14.3	Pressurizer Modeling . . . . .	400
14.3.1	Nomenclature . . . . .	401
14.3.2	Assumptions . . . . .	403
14.3.3	Governing Equations . . . . .	404
14.3.4	Modelica Component Model: <i>Pressurizer</i> . . . . .	406
14.3.5	Test-Case . . . . .	408
14.4	Two-Phase Cavity Modeling . . . . .	410
14.4.1	Nomenclature . . . . .	412
14.4.2	Assumptions . . . . .	416
14.4.3	Governing Equations . . . . .	417
14.4.4	Modelica Component Model: <i>TwoPhaseCavity</i> . . . . .	421
14.4.5	Test-Case . . . . .	421
14.5	Tank Modeling . . . . .	422
14.5.1	Nomenclature . . . . .	422
14.5.2	Governing Equations . . . . .	424
14.5.3	Modelica Component Model: <i>Tank</i> . . . . .	426
14.5.4	Test-Case . . . . .	426
14.6	Static Drum Modeling . . . . .	428
14.6.1	Nomenclature . . . . .	429
14.6.2	Assumptions . . . . .	430
14.6.3	Governing Equations . . . . .	431
14.6.4	Modelica Component Model: <i>StaticDrum</i> . . . . .	431
14.6.5	Test-Case . . . . .	433
14.7	Static Mixer Modeling . . . . .	434
14.7.1	Nomenclature . . . . .	435
14.7.2	Assumptions . . . . .	435
14.7.3	Governing Equations . . . . .	435
14.7.4	Modelica Component Model: <i>Mixer3</i> . . . . .	436
14.7.5	Test-Case . . . . .	436
14.8	Static Splitter Modeling . . . . .	438
14.8.1	Nomenclature . . . . .	439
14.8.2	Assumptions . . . . .	439
14.8.3	Governing Equations . . . . .	439
14.8.4	Modelica Component Model: <i>Splitter3</i> . . . . .	440
14.8.5	Test-Case . . . . .	440
14.9	Steam Dryer Modeling . . . . .	442
14.9.1	Nomenclature . . . . .	443
14.9.2	Assumptions . . . . .	443
14.9.3	Governing Equations . . . . .	443
14.9.4	Modelica Component Model: <i>SteamDryer</i> . . . . .	444
14.9.5	Test-Case . . . . .	444
	References . . . . .	446

<b>15 Internal Combustion Engine Modeling . . . . .</b>	447
15.1 Nomenclature . . . . .	449
15.2 Governing Equations . . . . .	452
15.3 Modelica Component Model: <i>InternalCombustionEngine</i> . . . . .	457
15.4 Test-Case . . . . .	458
15.4.1 Test-Case Parameterization and Boundary Conditions . . . . .	458
15.4.2 Model Calibration . . . . .	459
15.4.3 Simulation Results . . . . .	459
<b>16 Solar Collector Modeling . . . . .</b>	461
16.1 Linear Parabolic Trough Collector (PTSC) . . . . .	462
16.1.1 Nomenclature . . . . .	462
16.1.2 Assumptions . . . . .	465
16.1.3 Governing Equations . . . . .	465
16.1.4 Modelica Component Model: <i>SolarCollector</i> . . . . .	467
16.1.5 Test-Case . . . . .	467
16.2 Linear Fresnel Reflector (LFR) . . . . .	467
16.2.1 Nomenclature . . . . .	469
16.2.2 Governing Equations . . . . .	470
16.2.3 Modelica Component Model: <i>FresnelField</i> . . . . .	471
16.2.4 Test-Case . . . . .	471
References . . . . .	474
<b>17 Implementation of the Fluid Equations into Component Models . . . . .</b>	477
17.1 The Staggered Grid Scheme . . . . .	477
17.1.1 Nomenclature . . . . .	477
17.1.2 Principle of the Staggered Grid Scheme . . . . .	478
17.1.3 Volume Components and Flow Components . . . . .	480
17.1.4 Connecting Volume Components to Flow Components . . . . .	481
17.1.5 Structure of the Connectors . . . . .	484
17.1.6 Case of Static Volume Components . . . . .	486
17.1.7 Flow Network Global Orientation . . . . .	491
17.2 Fundamental Choices for ThermoSysPro . . . . .	492
17.2.1 Current Situation with ThermoSysPro V3.x . . . . .	492
17.2.2 Future Directions for ThermoSysPro V4.x . . . . .	494
References . . . . .	494

# About the Authors

**Dr.-Ing. Baligh El Hefni** has 35 years of research, industry and teaching experience. He specialised in physical modelling of various types of power plants. In 2002, he joined EDF Research & Development division (R&D). He contributed to the development of power plants modeling activities, within the EDF and its subsidiaries, thanks to the use of ThermoSysPro library (developed by the authors). This has allowed him to collaborate with major industrial players, research and academics in the framework of many European projects (DLR, Dassault-Systèmes, Dassault-Aviation, Siemens, IFP, OpenModelica ...), in which EDF's contribution was recognized. The main objectives of these projects are: to improve the modeling languages, the tools, the methods (stat estimation), and to extend the modeling domains (multi-mode systems, property modeling). The experience in the power plant modeling has allowed him to develop solid competencies and a specific know-how that has allowed him to expand our activity towards the development of solar power plants, and collaborate with CENER (Spain), Chinese Academy of Sciences (China), CEA (France) and other partners. He is in charge of training courses of the modelling of power plants and energy systems, for EDF staff and partners. He was also in charge of the same training at Ecole Centrale de Paris "Engineering Training School".

**Daniel Bouskela** graduated from Ecole Centrale de Paris (France). He is currently Senior Researcher at EDF Research and Development Division where his main interests are in the domain of the modeling and simulation of energy systems.

Daniel Bouskela is strongly involved in European and French cooperative projects. He was in particular the leader of the European MODRIO project. He is the co-author of the open source ThermoSysPro Modelica library for the modeling and simulation of power plants.

# Chapter 1

## Introduction to Modeling and Simulation



**Abstract** Power plant modeling plays a key role in many purposes, like process design assessment, the assessment, and prediction of plant performance, operating procedure evaluation, control system design, and system prognosis and diagnosis. The present chapter introduces the discipline of 0D/1D modeling applied to thermal hydraulics and their main applications to real-life systems: how 0D/1D modeling relates to the 3D physical equations, what are the fundamental assumptions underlying 0D/1D physical models and the main limitations of the numerical solvers commonly used for such models, what is the rationale for a 0D/1D component models library and what kinds of real-life systems can be modeled and simulated for different purposes (plant sizing, control, operation and maintenance, prognosis, diagnosis and monitoring). Also, in this chapter, many questions are answered: what is a system, what is a model and modeling, what is simulation and why is modeling important?

### 1.1 Systems, Complex Systems, and Cyber-Physical Systems

A usual systems engineering definition of a system is that it is “a set of interrelated parts that work together to accomplish a common purpose or mission” (Cloutier et al. 2015).

Systems are decomposed into subsystems and objects at the lowest level. They are dynamically structured using abstract concepts such as modes, states, events, and trajectories. Modes refer to the logical or functional states of the system (e.g. started, stopped, closed, open, dysfunctional, under maintenance), whereas states refer to the physical states of the system (e.g. temperature, mass flow rate, angular velocity). Events cause switching between modes. Trajectories are the evolution in time of the states. Systems interact with their environment via inputs and outputs. The inputs represent the action of the environment on the system, whereas the outputs represent the influence of the system on the environment.

For instance, a cooling system whose mission is to cool machines can be decomposed into three subsystems: a pumping system composed of pumps that circulates water around the equipment to be cooled, a feed water system composed of a tank and switch valves that ensures sufficient water pressure at the pumping system inlet, and a group of heat exchangers that transfers heat to the environment. A given pump can be in various normal or dysfunctional modes: started, stopped, cavitating, broken, etc. The pump hydraulic state is most frequently described by the pump head (the variation of pressure through the pump) and the pump volumetric flow rate (the amount of liquid volume that goes through the pump casing per time unit). The mechanical state of the pump can be given by the angular velocity and the torque of the shaft. However, if the shaft is broken into two parts, then the mechanical state involves the angular velocities and the torques of each end of the broken shaft. Therefore, the state of a broken shaft has twice as many state variables as a normal one. This shows that mode switching can cause a complete structural change in the system description. The temperature of the environment is an input of the system (in such case it is assumed that the system does not change the temperature of the environment), and the heat released to the environment is an output of the system.

Although there is no widely accepted definition of a complex system, we will consider as complex systems the systems composed of numerous tightly interacting subsystems. Cyber-physical systems are complex systems having software and physical subsystems in tight interaction or deeply intertwined. Good examples of cyber-physical systems are power plants, cars, planes, power grids, etc. Cyber-physical systems exhibit *emerging* behaviors that are not necessarily foreseen at design time and that appear at operation time due to the multiple interactions (the whole is more than the sum of its parts). One of the main challenges of physical modeling and simulation is to be able to predict emerging behaviors. However, the objective of this book is not to show how to do that, but to provide the fundamental knowledge in terms of physical equations for the thermal hydraulic parts of the systems that are necessary for this goal in particular, and more generally for any other purpose requiring the understanding of the physical behavior of the system.

## 1.2 What is System Modeling?

Generally speaking, modeling is the process of representing a particular concept, physical phenomenon, or real-world object using abstract notations including but not limited to mathematical symbols. In this book, modeling is referred to as deriving from physical laws a valid set of mathematical equations that describe the system *physical behavior* in order to assess quantitatively how the system performs its duties according to some prescribed mission, e.g., to verify whether a power plant complies with operating rules during start-up or shutdown. Other ways of modeling complex systems such as state diagrams or other kinds of schemas, in particular for the purpose of expressing requirements, assumptions, or *logical*

*behavior*, are not considered here. However, such models are necessary for the design of control systems and can be considered as the environment of the physical system (i.e., they interact with the physical system via inputs and outputs). Also, stochastic models are not explicitly dealt with, but randomness can be introduced into physical models by replacing scalar variables with distributions in the physical equations and using Monte Carlo simulations to compute the response of the system to uncertainties.

Physical modeling is not limited to assessing the dynamic behavior of the system. It can also be used to compute isolated operating points. This is called *static modeling*, as opposed to *dynamic modeling* that aims at computing systems trajectories. Static modeling is mainly used for system sizing and optimization at design time, while dynamic modeling is often used for system control design and optimization at operation time. System diagnosis may use static or dynamic modeling depending on the phenomena to be explored.

### 1.3 What is Simulation?

Simulation is an experiment conducted on a model. As mathematical models are considered here, simulations are numerical experiments conducted with a computer-executable version of the model, which is usually obtained by compiling with a compiler the model expressed in a computer language into a machine executable code. The computer language used for modeling is called a modeling language. The challenge for the user is then to write the model's equations in the modeling language.

There are roughly two kinds of modeling languages: imperative languages and equational languages. Imperative languages such as Fortran, C, C++, Java, Python, etc. are used for imperative programming, which consists in writing explicitly the algorithms that compute the model's equations. This requires a significant effort from the user who must translate manually the equations that express mathematical relations into sequence of computing instructions that computes the numerical solution of the equations. It is more convenient to perform this tedious task automatically by using an equational language that lets the user express the model's equations directly in equational form, hence, with very little transformation of the original equations as written on paper. Modelica is an equational language. Modelica compilers translate equational models into imperative programs, which are in turn compiled with regular compilers (C, C++, Fortran, etc.) to produce executable code. Modelica has been used in this book to write and verify models equations.

Experiments with the same model differ according to the numerical values provided to the inputs of the model and to the initial values of the state variables, which are also called inputs in the sequel. Those values must be physically consistent in order to provide correct results. Consistency cannot be obtained using the model's equations because the unknowns are computed using the inputs as known

variables. In other words, the known variables are not constrained by the model's equations. So although, from a numerical point of view, any input can produce numerical results, any input cannot produce *valid* numerical results. Therefore, consistency of the inputs must be achieved by other means such as data assimilation, for instance, which is the science of producing the best estimate of the initial state of a system by combining information from observations of that system (e.g. via sensors) with an appropriate model of the system (i.e., the model at hand to be initialized), see Swinbank et al. (2003). This technique which uses continuous optimization algorithms is successfully used in meteorology and can be applied to any physical system provided it has only continuous inputs to be assimilated (this excludes the assimilation of logical inputs such as the on–off position of a switch). Another technique, which is used in this book, is to compute the inputs from the knowledge of the nominal operating point using inverse computation on square systems of equations (i.e., having as many unknowns as equations). The drawback of this technique is that one has to make a choice between redundant information in order to obtain a square system (e.g., if two valve positions influence a single state, one has to make a choice between the two valve positions). This technique is used in this book as it is more readily available with existing modeling and simulation tools than optimization techniques.

To summarize, a simulation run consists essentially in solving an initial value problem, i.e., a differential-algebraic equation with correct initial values for the state variables and correct values for the inputs. Inputs with fixed values all along a simulation run are often called parameters. This will be looked at in more detail in the sequel.

## 1.4 What is 0D/1D Modeling?

Physical equations are functions of space and time. 3D models involve the three space coordinates. However, when dealing with space and time, it is often desirable to reduce the number of space coordinates to speed-up the computation of trajectories as the full model's equations must be computed at each time step. Reducing the dimensionality of the problem by going from three space coordinates down to one or even zero space coordinates is called 0D/1D modeling as opposed to 3D modeling. This is obtained by exploiting the geometrical properties of the model such as the cylindrical symmetry of a pipe. In the sequel, this discussion is restricted to thermal hydraulic systems which are the scope of this book.

Thermal hydraulics is the application of fluid dynamics for heat and mass transfer in energy systems such as power plants. Phenomena studied include convection, conduction, radiation, phase change, single-phase (liquid or vapor), two-phase (liquid and vapor), and multi-phase flows (for example water/steam with air). The most common fluids used in power plants are water/steam and flue gases, but other fluids can be used as well such as molten salt.

The dynamic physical behavior of thermal hydraulic systems is described with partial derivative equations (PDEs) that express the three fundamental conservation laws of mass (1.1), momentum (1.2), and energy (1.3).

$$\frac{D}{Dt} \int_V \rho \cdot dV = 0 \quad (1.1)$$

$$\frac{D}{Dt} \int_V \rho \cdot \vec{v} \cdot dV = \vec{f} \quad (1.2)$$

$$\frac{D}{Dt} \int_V \rho \cdot u \cdot dV = \dot{Q} + \dot{W} \quad (1.3)$$

where  $D/Dt$  stands for the material derivative (that takes into account the fluid motion),  $V$  is the fluid volume,  $\rho$  is the fluid density,  $\vec{v}$  is the fluid velocity,  $\vec{f}$  are the external volume and surface forces acting upon the fluid (such as pressure and friction),  $u$  is the fluid internal energy,  $\dot{Q}$  and  $\dot{W}$  are, respectively, the amount of heat and work received by the fluid per unit time.

These equations are closed by closure laws (fluid correlations) that compute unknown quantities found in  $\vec{f}$  such as pressure loss or heat exchange coefficients as functions of the pressure  $P$  and the temperature  $T$  of the fluid. State equations are used to compute  $\rho$  and  $u$  with respect to  $P$  and  $T$ .

The 0D/1D modeling approach consists in averaging physical quantities over the cross-sectional area  $A$  perpendicular to the main flow direction  $x$ , then along the main flow direction  $x$ :

$$\int_V \bullet dV = \int_{\Delta x} \left[ \int_A \bullet dA \right] \cdot dx \quad (1.4)$$

where  $\Delta x$  is a length increment and  $V = A \cdot \Delta x$ .

In practice, this method consists in:

1. Dividing the system into control volumes  $V = A \cdot \Delta x$  along the main flow direction;
2. Averaging the physical quantities using (1.4) for all individual control volumes;
3. Connecting the control volumes along the main flow direction to account for the variation of the physical quantities along that direction in steps corresponding to the lengths  $\Delta x$  of the control volumes.

$\Delta x$  is adapted to the study at hand. It, therefore, can be small or large without limitation.  $\Delta x$  is equal to zero for components considered as a singularities such as valves. It is large for long pipes or large vessels when no information is needed regarding the distribution of physical quantities along the component length. One

must note that the choice of  $\Delta x$  does not induce any approximation in itself as computed quantities are considered as averaged quantities over  $V = A \cdot \Delta x$ , but the larger  $\Delta x$ , the lower the resolution of the computation in space.

0D/1D modeling gives the ability to choose the space resolution of realistic models described from first principle physics. It, therefore, allows to adjust the space resolution in order to compute large transients for complex systems for engineering studies that often require simulation speed orders of magnitude faster than real time. Therefore, the main benefit of this method is to allow the realistic modeling and simulation of complex systems over large transients.

As the only differential variable left in 0D/1D models is  $dt$ , 0D/1D models are sets of differential-algebraic equations (DAEs):

$$C \cdot \dot{x} = f(x, p, u) \quad (1.5)$$

where  $C$  is a coefficient matrix,  $x$  is the state vector of the system,  $\dot{x}$  is the time derivative of  $x$  (not to be confounded with the length increment  $\Delta x$  above),  $p$  are fixed parameters (such as fixed boundary conditions), and  $u$  are inputs of the system (such as variable boundary conditions). Note that  $x$  may contain time derivatives.

If  $C$  is invertible, then (1.5) can be transformed into an ordinary differential equation (ODE) and integrated with standard ODE numerical solvers:

$$\dot{x} = C^{-1} \cdot f(x, p, u) \quad (1.6)$$

If  $C$  is not invertible, then (1.5) is a true DAE that cannot be transformed into an ODE and its resolution is more problematic.

If  $C$  is not invertible because it contains rows equal to zero, then (1.5) can be written as the following DAE:

$$\begin{cases} \dot{x} = D^{-1} \cdot f(x, a, p, u) \\ 0 = g(x, a, p, u) \end{cases} \quad (1.7a, b)$$

where  $a$  are the algebraic variables, i.e., the variables from  $x$  in (1.5) with zero coefficients for  $\dot{x}$ , coefficient matrix  $D$  is coefficient matrix  $C$  without the rows and columns corresponding to the algebraic variables  $a$ , and  $x$  are the remaining differential variables, i.e., the variables from  $x$  in (1.5) with nonzero coefficients for  $\dot{x}$ .

Equation (1.7b) is a frequent case that appears when dynamics are neglected. It can be solved with numerical solvers that combine the resolution of ODEs with algebraic equations. If the size of  $x$  is equal to zero, then (1.7a, b) boils down to (1.7b) and the model is purely static. This case is frequently encountered in sizing problems. Off-the-shelf Modelica tools solve (1.7a, b) although they allow to express the problem as (1.5). If  $C$  is not invertible, then a division by zero occurs at simulation time.

If  $C$  contains predicates (i.e., Boolean conditions) that depend on elements of  $x$ , and if the predicates are such that  $C$  is not invertible at some instants  $t$ , then the system may be considered as a series of commuting DAEs such as (1.7a, b) with

varying structure (i.e., varying sizes for  $x$ ,  $a$ ,  $p$ , and  $u$ ) from one DAE to the other. Such systems are called multi-mode systems. There is currently no industrial tool able to solve such systems although a prototype was developed in the framework of the ITEA2 MODRIO project (2012–2016); (Elmqvist et al. 2014; Bouskela 2016), and the development of an industrial tool is ongoing in the framework of the FUI ModeliScale project (started in 2018).

## 1.5 What is a 0D/1D Thermal Hydraulic Component Models Library?

When using DAEs such as (1.5) to represent the fundamental equations of thermal hydraulics, integration of (1.1)–(1.3) must be performed over the various component volumes considered in the system model (pipes, valves, pumps, heat exchangers, turbines, etc.). The various ways of choosing the appropriate closure laws and of performing the integration over the various component volumes commonly found in the systems to be modeled result in the different 0D/1D component models that populate the library.

Therefore, a library component model is a DAE such as (1.5) that depends on inputs  $u$  and parameters  $p$ . The parameters are set according to the problem at hand. They usually represent quantities that are given as designers' assumptions or as measured quantities on the system or on its environment. The inputs are given as test scenarios or as outputs from neighboring components. The latter case is known as *connecting* the model component to its neighboring components. The way to perform such connections has a strong influence on the structure of the component models. The way to organize the component models in the library in order to be able to compose a full model by interconnecting them is referred to as the *structure of the library* in the sequel.

In order for library component models to be fully reusable, i.e., to be used in any model without modification, they should exhibit the following good properties:

1. Be acausal;
2. Be properly parameterized.

Being acausal means that when written as (1.7a, b), the DAE may be solved in any of the variables  $x$ ,  $\dot{x}$ ,  $a$ ,  $p$ , or  $u$ . This is needed because the outputs of one component model are the inputs of its connected ones, and therefore, the known or unknown status of the variables depends on the way the component models are

connected together to form the full model. The process of assigning this status to all variables in the model is known as *causality analysis*<sup>1</sup> and is performed automatically by Modelica tools.

Be properly parameterized means that a proper set of parameters should be defined in order to account for most possible usages of the component model, while keeping the size of the set as small as possible.

## 1.6 What are 0D/1D Models Useful for?

The purpose of 0D/1D models is not to discover or study new physical phenomena, but to understand the physical behavior of systems using the standard laws of physics complemented with physical correlations for various engineering purposes at design, commissioning, or operation time. To that end, it is only necessary to monitor a small number of significant variables called the *variables of interest*. This is why the space averaging operations to reduce the dimensionality of the problem from 3 to 1 or 0 are acceptable, provided that uncertainty margins are correctly computed to take into account requirements related to safety limits for instance. This allows fast computation of the system behavior all along its trajectory in time.

In the very early phases of system design, one is generally concerned with the logical behavior of the system in order to verify that the system will correctly perform its missions from a functional standpoint. The physical aspects are not very important at this stage. However, at the detailed design phase, when functions must be implemented into physical pieces of equipment, it becomes important to evaluate different implementation alternatives quantitatively in order to make sure that the system's requirements, in particular those involving real-time physical constraints such as safety, are satisfied while avoiding oversizing (as lack of precise quantitative assessment most often results in excessive operational margins), oversizing leading in turn to delays and over costs. This can be achieved using 0D/1D models, in particular static models for the sizing of nominal operating points, and dynamic models for the design, verification, and validation of control systems.

At commission time, 0D/1D models can be used to prepare the acceptance tests.

---

<sup>1</sup>The word *causality* in *causality analysis* should not be confounded with the word *causality* in *physical causality* which means that causes always precede their effects. However, there is a relationship between the two notions. The objective of causality analysis is to assign each unknown variable to a unique equation that computes this variable and vice versa. State derivatives are assigned in the most obvious way to equations such as (1.7a). Such assignments are conformant with physical causality as state derivatives (predictors) are thus computed from the state past values. However, algebraic variables are assigned to equations such as (1.7b) whose physical causalities are lost as algebraic equations are obtained by neglecting the dynamics of the system that force the physical causalities. The result of the analysis may, thus, not reflect the physical causality of the real system for the algebraic variables. This is why algebraic variables should not be used in a model when causalities are important, such as the feedback loop of a control system.

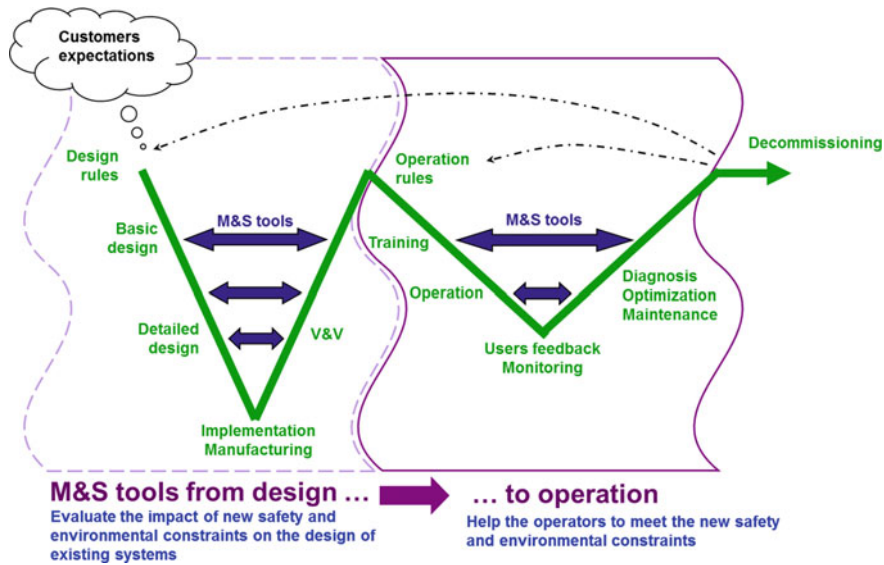


**Fig. 1.1** Using 0D/1D models from system design to system operation. (*Source* MODRIO project, with permission from the author: Audrey Jardin)

At operation time, 0D/1D models are useful to predict the short-term behavior of the system to make the right operation decision, for instance, to optimize plant start-ups while complying with equipment operational constraints. Operators can be trained for the conduct of difficult transients (i.e., transients that are rarely performed and are subject to tight safety constraints) using 0D/1D models. 0D/1D models can also be used in combination with plant onsite measurements to monitor and assess the plant performance degradations such as wear or clogging in order to provide key economic performance indicators for the plant and anticipate on maintenance actions in order to reduce plant shutdown for maintenance and comparatively increase plant availability.

Beyond individual power plants, there is a growing need to assess the collective behavior of energy networks when submitted to perturbations such as changes in regulatory, economic, or weather conditions, and how well the power system can adapt to dynamic and changing conditions, see, e.g., EPRI (2016). The growth in variable generation such as solar (photovoltaic and thermodynamic) and wind is a strong driver for the use of 0D/1D for large-scale energy systems. This new need prompted the launch of the ModeliScale project that aims at upscaling Modelica to very large multi-mode physical systems.

Figure 1.1 presents the different stages of the systems lifecycle, from design to operation, where 0D/1D models are useful.

## References

- Bouskela D (2016) Multi-mode physical modelling of a drum boiler, complex adaptive systems. *Proc Comput Sci* 95:516–523
- Cloutier R, Baldwin C, Bone MA (2015) Systems engineering simplified. CRC Press, Taylor & Francis
- Elmqvist H, Mattsson SE, Otter M (2014) Modelica extensions for multi-mode DAE systems. In: Proceedings of the 10th international Modelica conference
- EPRI (2016) Electric Power System Flexibility, challenges and opportunity. Available from <https://www.epri.com/#/pages/product/3002007374/?lang=en>
- MODRIO project (2012–1016), ITEA 2 11004 MODRIO. Available from <https://github.com/modelica/modrio> and <https://www.modelica.org/external-projects/modrio>
- Swinbank R, Shutyaev V, Lahoz WA (2003) Data assimilation for the earth system. In: Series IV: earth end environmental sciences, vol 26. Kluwer

# Chapter 2

## Introduction to Thermodynamics and Heat Transfer



**Abstract** Thermodynamics is the science that deals with the exchange of energy in the form of heat and work and with the different states (solid, liquid, gas, etc.) and properties (density, viscosity, thermal conductivity, etc.) of substances that are related to energy and temperature. Thermodynamics is formalized into three basic laws, the first law being the conservation of energy, and the second and third laws being related to the notion of entropy and is completed by the three main laws for heat transfer: radiation, convection, and conduction. In this chapter, we introduce first the properties of substances (density, pressure, and temperature), energy, enthalpy, and entropy, then the concept of state variables, the different types of thermodynamic systems, the first and second thermodynamic laws, the thermodynamics cycles (ideal and actual Brayton cycles, ideal and actual Rankine cycles), the ideal gas law, and the three heat transfer processes (radiation, convection, and conduction). It is shown why these different notions are essential in order to compute the complete thermal-hydraulic state of the system, which is the main challenge of 0D/1D modeling and simulation for that field.

### 2.1 What Are Thermodynamics and Thermal Hydraulics?

Thermodynamics can be defined in two ways: the science of heat and thermal machines or the science of large systems (i.e., composed of many particles) in equilibrium. In this book, the two aspects will be considered because power plants are thermal machines that produce mechanical energy using heat and mass transfer. As thermal machines, they are subjected to thermodynamic cycles (cf. Sect. 2.9), and as they use fluids to transfer energy from the reactor to the turbine, they are subjected to the laws of thermal hydraulics which is the combination of hydraulics with thermodynamics.

The two main concepts in thermodynamics are heat and temperature. These two quantities are defined and used in two ways that reflect the two aspects of thermodynamics: via the efficiency of thermal machines and via statistics (averages) over volumes containing large numbers of particles. These quantities are governed

by the first and second laws of thermodynamics. Heat and temperature are related via the concept of entropy, with the fundamental formula:

$$dS = \frac{\delta Q_{\text{rev}}}{T} \quad (2.1)$$

where  $dS$  is the variation of entropy of the system that receives  $\delta Q_{\text{rev}}$  amount of heat energy during a reversible process at temperature  $T$ .

The two additional concepts used for hydraulics are the conservation of mass and the conservation of momentum.

## 2.2 Thermodynamic Processes

A thermodynamic process is a change in the system state from an initial state in equilibrium to a final state in equilibrium. When the initial and final states are the same, the process is called a *cycle*.

A *reversible process* is a process in which the system is in equilibrium at each step. This corresponds to an ideal infinitely slow transformation of the system where each step of the process is a system state.

An *irreversible process* is a process that is not reversible. This corresponds to real processes where changes between the initial and final states occur out of equilibrium.

## 2.3 Properties of Substances

Properties of substances are quantities such as mass, temperature, volume, and pressure. Properties are used to define the current physical state of a substance.

Thermodynamic properties are divided into two general classes: intensive and extensive properties.

An intensive property is independent of the mass of the substance. Temperature, pressure, specific volume, and density are examples of intensive properties.

The value of an extensive property is directly proportional to the mass of the substance. The internal energy or the enthalpy is an example of extensive properties. Mass and volume are also extensive properties.

Thus, if a quantity of matter in a given state is divided into two equal parts in mass, each part will have the same value of the intensive property as the original and half the value of the extensive property.

Relationships between properties are expressed in the form equations which are called equations of state. The most famous state equation is the ideal gas law that relates the pressure, volume, and temperature of an ideal gas (cf. Sect. 2.10).

### 2.3.1 Density and Specific Volume

Density, also called mass density, is an intensive property defined as the mass of a substance per unit volume:

$$\rho = \frac{m}{V} \quad (2.2)$$

where  $m$  is the mass and  $V$  is the volume of the body.

The specific volume is the inverse of the density:

$$v = \frac{V}{m} = \frac{1}{\rho} \quad (2.3)$$

The SI unit for volume is  $\text{m}^3$  (cubic meters), for density is  $\text{kg m}^{-3}$  (kilograms per cubic meter), and for specific volume is  $\text{m}^3 \text{ kg}^{-1}$  (cubic meters per kilogram).

### 2.3.2 Pressure

Pressure is an intensive property. The pressure at a point of fluid continuum is defined as the normal compressive force per unit area at that point.

Atmospheric pressure serves as a suitable reference for pressure measurement. Pressure above the atmospheric pressure is called the gauge pressure. Pressure below the atmospheric pressure is called vacuum or subatmospheric pressure. The relationships between the pressures stated for different references are shown in Fig. 2.1.

The SI unit for pressure is Pa (pascal). Pressure is also commonly expressed in bars ( $1 \text{ bar} = 10^5 \text{ Pa}$ ).

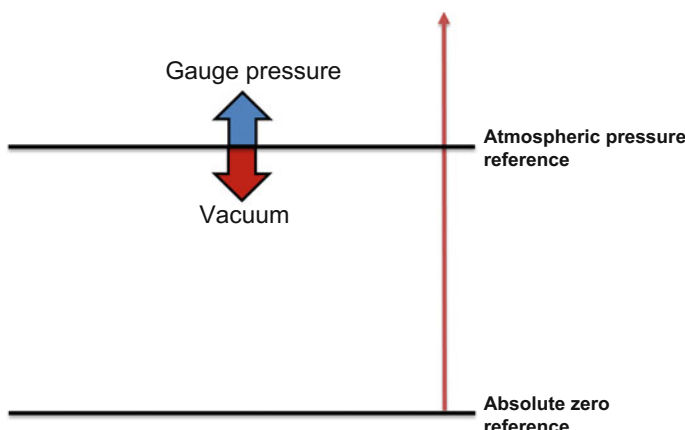


**Fig. 2.1** Pressure references

### 2.3.3 Temperature

Temperature is an intensive property. Equation (2.1) can be seen as a definition of the thermodynamic temperature; therefore, although temperature is a familiar property, it is a rather abstract concept as it involves entropy (cf. Sect. 2.3.6).

The SI unit for temperature is K (kelvins). Temperature is also commonly expressed in the °C (Celsius) or °F (Fahrenheit) scales, but (2.1) and equations derived from (2.1) are only valid for the thermodynamic (or absolute) temperature scale expressed in kelvins.

### 2.3.4 Energy

Energy is an extensive property that represents the ability to produce work. Work is produced by moving an object with a mechanical force. It is defined by the following equation:

$$W = \int_{\vec{r}_i}^{\vec{r}_f} \vec{f} \cdot d\vec{r} \quad (2.4)$$

where  $\vec{f}$  is the mechanical force applied to the object at position  $\vec{r}$ ,  $\vec{r}_i$  is the initial position of the object, and  $\vec{r}_f$  is the final position of the object.

Energy can be transferred to other systems, but cannot be neither created nor destroyed.

There are many different types of energy, for example, potential energy, kinetic energy, and internal energy.

Potential energy is a stored energy that contains the potential to do work when released. For instance, the potential energy due to gravitation is:

$$E_g = m \cdot g \cdot z \quad (2.5)$$

where  $g$  is the acceleration due to gravity and  $z$  is the elevation of the object.

Kinetic energy is the energy created by movement:

$$E_c = \frac{1}{2} m \cdot v^2 \quad (2.6)$$

where  $v$  is the velocity of the object.

Heat is the energy transferred between two bodies due to a temperature difference between the two bodies. When a body at temperature  $T_1$  receives at constant volume a quantity  $Q$  of heat, then its temperature rises to  $T_2$  according to the following equation:

$$Q = C_v \cdot (T_2 - T_1) \quad (2.7)$$

$C_v$  is the heat capacity at constant volume of the substance of the body, assumed to be quasi-constant between  $T_1$  and  $T_2$ .

Internal energy, often denoted  $U$ , is the energy contained within the system excluding potential energy and kinetic energy. Internal energy cannot be directly measured, but can be computed using thermodynamic functions such as (2.8) below.

For an isochoric process (i.e., at constant volume), the change in internal energy  $dU$  is defined as:

$$dU = C_v \cdot dT \quad (2.8)$$

where  $C_v$  is the heat capacity at constant volume and  $dT$  is the temperature difference during the thermodynamic process.

Therefore, by definition

$$C_v = \left( \frac{\partial U}{\partial T} \right)_V \quad (2.9)$$

The specific internal energy is defined as the internal energy per mass unit:

$$u = \frac{U}{m} = \frac{1}{\rho} \cdot \frac{U}{V} \quad (2.10)$$

The specific heat capacity at constant volume is defined as

$$c_v = \left( \frac{\partial u}{\partial T} \right)_V \quad (2.11)$$

and therefore for an isochoric process,

$$du = c_v \cdot dT \quad (2.12)$$

The SI unit for energy is J (joules). The SI unit for specific internal energy is  $\text{J kg}^{-1}$  (joules per kilogram). The SI unit for  $C_v$  is  $\text{J K}^{-1}$  (joules per kelvin). The SI unit for  $c_v$  is  $\text{J kg}^{-1} \text{ K}^{-1}$  (joules per kilogram per kelvin).

### 2.3.5 Enthalpy

Enthalpy is an extensive property that is defined as:

$$H = U + P \cdot V \quad (2.13)$$

where  $U$  is the internal energy,  $P$  is the pressure, and  $V$  is the volume of the substance.

Enthalpy has thus the dimensionality of energy. The purpose of enthalpy is to embed within the same quantity internal energy and mechanical energy due to pressure forces.

For an isobaric process (i.e., at constant pressure), the change in enthalpy  $dH$  is defined as:

$$dH = C_p \cdot dT \quad (2.14)$$

where  $C_p$  is the heat capacity at constant pressure and  $dT$  is the temperature difference during the thermodynamic process.

Therefore, by definition

$$C_p = \left( \frac{\partial H}{\partial T} \right)_P \quad (2.15)$$

The specific enthalpy is defined as the enthalpy per mass unit:

$$h = \frac{H}{m} = \frac{1}{\rho} \cdot \frac{H}{V} = u + \frac{P}{\rho} \quad (2.16)$$

The specific heat capacity at constant pressure is defined as

$$c_p = \left( \frac{\partial h}{\partial T} \right)_P \quad (2.17)$$

and therefore for an isobaric process,

$$dh = c_p \cdot dT \quad (2.18)$$

As shown by (2.18), only differences in specific enthalpies can be provided by measuring differences in temperatures on an isobaric process. Therefore, specific enthalpies are defined like any other energy quantity within an additive constant. Integrating (2.18) from  $T_{\text{ref}}$  to  $T$  under the assumption that  $c_p$  remains quasi-constant between  $T_{\text{ref}}$  and  $T$  yields:

$$h - h_{\text{ref}} = c_p \cdot (T - T_{\text{ref}}) \quad (2.19)$$

where  $h_{\text{ref}}$  is the reference value of the specific enthalpy at the reference temperature  $T_{\text{ref}}$ . The values for  $T_{\text{ref}}$  and  $h_{\text{ref}}$  can be chosen freely for each substance.

Usually, the triple point is used to define the reference point. In water/steam properties tables such as NBS/NRC,  $h_{\text{ref}} = 0$  at the triple point  $T_{\text{ref}} = 0.01 \text{ }^{\circ}\text{C}$  and  $P_{\text{ref}} = 611.2 \text{ Pa}$  (Haar et al. 1975; Wagner and Kruse 1998). For diatomic gases such as O<sub>2</sub>, N<sub>2</sub>, CO<sub>2</sub>, and SO<sub>2</sub> containing gaseous water,  $h_{\text{ref}} = L \cdot x$  where  $L = 2,501,569 \text{ J/kg}$  is the latent heat of vaporization at 0.01 °C of water and  $x$  is the mass fraction of gaseous water in the gases. Therefore, under the same conditions, the specific enthalpies of the diatomic gases are zero because  $h_{\text{ref}} = 0$  when  $x = 0$ .

For an isobaric and isochoric transformation,  $dV = dP = 0$  and from (2.13):

$$dH = dU \quad (2.20)$$

The SI unit for enthalpy is J (joules). The SI unit for specific enthalpy is J kg<sup>-1</sup> (joules per kilogram). The SI unit for  $C_p$  is J K<sup>-1</sup> (joules per kelvin). The SI unit for  $c_p$  is J kg<sup>-1</sup> K<sup>-1</sup> (joules per kilogram per kelvin).

### 2.3.6 Entropy

Entropy is an extensive property of the thermodynamic system defined by (2.1) that is related to the number of possible configurations  $\Omega$  of the thermodynamic system.

$$S = k_B \cdot \log \Omega \quad (2.21)$$

where  $k_B$  is the Boltzmann constant.

As entropy and temperature are defined using the same relation (2.1), entropy and temperature are two different quantities related to the same concept of thermal disorder, characterized by the number of possible system configurations  $\Omega$ . The striking difference between the two quantities is that one (temperature) is intensive and intuitive, whereas the other (entropy) is extensive and counter-intuitive.

The specific entropy is defined as the entropy per mass unit:

$$s = \frac{S}{m} = \frac{1}{\rho} \cdot \frac{S}{V} \quad (2.22)$$

The SI unit for entropy is J K<sup>-1</sup> (joules per kelvin). The SI unit for specific entropy is J K<sup>-1</sup> kg<sup>-1</sup> (joules per kelvin per kilogram).

## 2.4 State of a Physical System

The concept of physical state is central to physical modeling and simulation as the goal is to compute the system physical state given various inputs such as initial conditions that define the initial state, boundary conditions that define the influence of the environment of the system on the system, and other assumptions regarding the system properties that cannot be computed by the model such as geometrical factors, efficiencies, loss factors, and various correction coefficients. It is worth noting here that defining the initial state can be anticipated to be difficult as it must be given as an input to the model (via the initial conditions) *and* must be consistent with the model equations to be an eligible state. It will be shown in Chap. 6 how to compute the initial state as an inverse problem. It will be shown in Chap. 5 why approximations made on static systems can lead to difficulties in computing the system state and how to overcome them.

The state of a physical system (or the physical state of a system) is given by a complete set of mutually independent physical quantities that depend only on the current equilibrium of the system and not on the path followed by the system to reach equilibrium. Those physical quantities that characterize the state are thus the properties of the system, as introduced in the previous section (cf. Sect. 2.1). They are also called *state functions* as they depend only on the current state and not of the history of past states. The set of state functions is the *state representation* of the system. It is often called *state vector*, and its elements are often called *state variables* or simply *states* as a shorthand expression. Its size is the *degree of freedom* of the system as the quantities that it contains are independent of each other. These definitions are quite general and apply to any kind of physical system and to thermodynamic systems in particular.

As there are, in general, more state variables than degrees of freedom for a given system, there are possibly many different ways to choose the state representation of a system. The state functions that are not part of the state representation are often called property relations or property functions. Property functions are related to the state variables by explicit functions (hence their names).

For example, the mechanical state of a particle can be given by its position  $\vec{r}$  and its momentum  $\vec{p}$ . Therefore, its state representation is  $\{\vec{r}, \vec{p}\}$  and its number of degrees of freedom is 6 since  $\vec{r}$  and  $\vec{p}$  have each three space coordinates. The mechanical state of  $n$  particles is given by their respective positions  $\vec{r}_i$  and momentums  $\vec{p}_i$ . Therefore the state representation of the system of the  $n$  particles is  $\{\vec{r}_i, \vec{p}_i\}_{1 \leq i \leq n}$  which is very large when  $n$  is the order of magnitude of the Avogadro number ( $6.022 \times 10^{23}$ ).

The thermodynamic state of a system is defined only when the system is in thermodynamic equilibrium, i.e., when it has reached a spatially uniform temperature throughout the system for a sufficient length of time. In other words, the temperature  $T$  of a system is defined only when it is in thermodynamic equilibrium.

The thermodynamic state of a single-phase system can be defined choosing the pressure  $P$  and temperature  $T$  of the system as state variables. The state

representation of the system is  $\{P, T\}$ , and consequently, the system has two degrees of freedom since  $\{P, T\}$  has two elements.  $(P, T)$  is the state vector. The density  $\rho$  is a state function since it is an explicit function of  $P$  and  $T$ :  $\rho = f_\rho(P, T)$ . Alternatively, one could choose  $\{\rho, T\}$  as the state representation of the system, and the pressure would be related to the state as  $P = f_P(\rho, T)$ . In case of a two-phase system at saturation, the pressure  $P$  is a function of the temperature  $T$ . Therefore, the thermodynamic state can be described with only one variable, e.g.,  $T$ , and the number of degrees of freedom is 1.

Physical quantities that depend on the history of the system past states cannot be chosen as state variables. For instance, the internal energy is a state function, but heat and work are not state functions (cf. Sect. 2.8.1).

When a system is not in spatially thermodynamic equilibrium, it must be divided into subsystems small enough so that each of them can be considered in local thermodynamic equilibrium. For example, a boiler with a liquid and steam phases must be at least divided into two subsystems, one for each phase, if the two phases are not in thermal equilibrium, i.e., if the temperature of the liquid phase is different from the temperature of the steam phase, which is generally the case as the liquid receives feed water under the saturation line.

## 2.5 Selection of the State Variables

As explained above, there are several possible choices for the state vector. Looking at the mass, energy, and momentum balance equations (cf. 4.7, 4.11, and 4.28), the most obvious choices for the state variables are the density  $\rho$ , the internal energy  $u$ , and the mass flow rates  $\dot{m}$ .

On the other hand, the most natural choices for the thermodynamic state variables are  $P$  and  $T$ , because these are measurable quantities, to the contrary of other thermodynamic quantities such as the specific enthalpy which are not directly measurable. Consequently, state equations are known as functions of pressure and temperature, e.g.,

$$\rho = f_\rho(P, T) \quad (2.23)$$

$$h = f_h(P, T) \quad (2.24)$$

The problem with the choice of  $P$  and  $T$  is that  $P$  and  $T$  are not independent variables in the case of two-phase flow when two-phase flow is considered as a mixture of both phases (homogeneous or separated flow models; cf. Sect. 4.2.1):  $P = f_P(T)$  on the saturation line.

To alleviate this problem, the vapor mass fraction (or the quality; cf. Sect. 4.2.1)  $x$  could replace  $T$  as state variable when going from single-phase flow to two-phase flow. This would, however, lead to difficult dynamic change of state variables at simulation time when going through a phase transition. To avoid this, it is better to

choose as state variable a quantity that captures both temperature and mass fraction effects such as  $u$  or  $h$  instead of  $T$  or  $x$  for fluids that may undergo phase transitions. For water/steam flows, it is customary to choose  $P$  and  $h$  as state variables.

Consequently, the state Eq. (2.24) must be inverted to compute  $T$ :

$$T = f_T(P, h) \quad (2.25)$$

For flue gases, it is possible to keep  $P$  and  $T$  because such fluids do not undergo phase transitions.

Using the state equations, it is possible to express  $\rho$  and  $u$  as functions of  $P$  and  $h$  or as functions of  $P$  and  $T$ .

When using  $P$  and  $h$  as state variables, the left-hand side of the mass and energy balance equations (cf. 4.7 and 4.28) must be rewritten using the following transformations:

$$\rho = f_\rho(P, h) \quad (2.26)$$

$$h = u + \frac{P}{\rho} \quad (2.27)$$

$$\frac{d\rho}{dt} = \left( \frac{\partial \rho}{\partial P} \right)_h \cdot \frac{dP}{dt} + \left( \frac{\partial \rho}{\partial h} \right)_P \cdot \frac{dh}{dt} \quad (2.28)$$

$$\frac{d(\rho \cdot V)}{dt} = \rho \cdot \frac{dV}{dt} + V \cdot \left[ \left( \frac{\partial \rho}{\partial P} \right)_h \cdot \frac{dP}{dt} + \left( \frac{\partial \rho}{\partial h} \right)_P \cdot \frac{dh}{dt} \right] \quad (2.29)$$

$$\begin{aligned} \frac{d(\rho \cdot V \cdot u)}{dt} &= (\rho \cdot h - P) \cdot \frac{dV}{dt} \\ &\quad + V \cdot \left[ \left( h \cdot \left( \frac{\partial \rho}{\partial P} \right)_h - 1 \right) \cdot \frac{dP}{dt} + \left( h \cdot \left( \frac{\partial \rho}{\partial h} \right)_P + \rho \right) \cdot \frac{dh}{dt} \right] \end{aligned} \quad (2.30)$$

Using the right-hand side of the mass balance Eq. 4.7, (2.30) can also be written as:

$$\begin{aligned} \frac{d(\rho_a \cdot V_a \cdot u_a)}{dt} &= \frac{d(\rho_a \cdot V_a)}{dt} \cdot u_a + \rho_a \cdot V_a \cdot \frac{du_a}{dt} \\ &= V_a \cdot \left[ \left( \frac{P_a}{\rho_a} \cdot \left( \frac{\partial \rho_a}{\partial P} \right)_h - 1 \right) \cdot \frac{dP_a}{dt} + \left( \rho_a + \frac{P_a}{\rho_a} \cdot \left( \frac{\partial \rho_a}{\partial h} \right)_P \right) \cdot \frac{dh_a}{dt} \right] \\ &\quad + \left( h_a - \frac{P_a}{\rho_a} \right) \cdot \sum_{b \in V(a)} \dot{m}(b \rightarrow a) \end{aligned} \quad (2.31)$$

In (2.31), subscript  $a$  denotes average values over volume  $a$  that are introduced in Chap. 3.

## 2.6 Definition of a Thermodynamic System

For the purpose of this book, a thermodynamic system is defined as a system that is at least in local equilibrium so that it can be divided into finite volumes  $a_i$ , each volume having a well-defined temperature  $T_{a_i}$ .

The way to optimally divide a thermodynamic system into volumes is introduced in Chap. 3 and explained in further details in Chap. 17 (cf. the staggered grid scheme).

A thermodynamic system is delimited by a boundary that can be real or virtual and can exchange (or not) mass and energy with its surroundings. Therefore, the volumes  $a_i$  of a thermodynamic system are themselves thermodynamic systems.

## 2.7 Types of Thermodynamic Systems

There are classically three main types of thermodynamic systems: open systems, closed systems, and isolated systems, depending on whether the system under consideration exchanges mass and energy with its surroundings (cf. Fig. 2.2).

### 2.7.1 Isolated System

It is the simplest of all thermodynamic systems in which no transfer of mass or energy takes place across its boundary with the surroundings. Hot water kept in a thermos flask is an example of a closed system (as long as it is not open to pour the water out and the thermal leaks through its wall are neglected). Isolated systems are ideal systems of no practical use, so they will not be considered in the sequel.

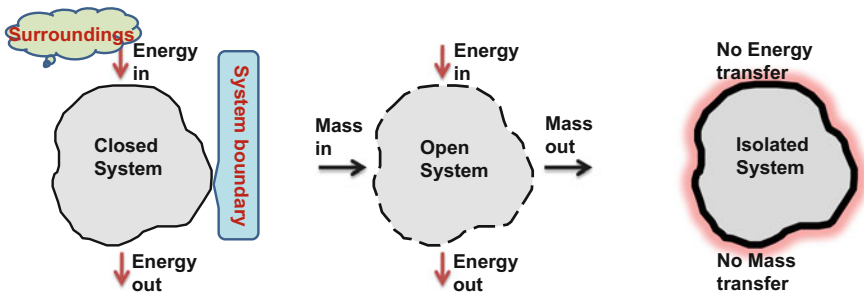


**Fig. 2.2** Types of thermodynamic systems

### 2.7.2 *Closed System*

A closed system is a system in which transfer of energy but no transfer of mass takes place across its boundary with the surroundings. Therefore, a closed system is a fixed mass system. A piston in which a gas is being compressed or expanded with no leaks is an example of a closed system. The mass of gas remains constant throughout the piston cycle, but the gas is heated or cooled depending on the position of the piston.

### 2.7.3 *Open System*

An open system is a system that exchanges mass and energy with its surroundings. An example of open system is boiling water in an open vessel, where transfer of heat as well as mass in the form of steam takes place between the vessel and its surroundings.

Due to the constant inflows and outflows of mass and energy, an open system is generally in local equilibrium only, so it must often be divided into smaller volumes  $a_i$  of mass  $m_{a_i}$ .

As open systems are divided into volumes  $a_i$ , it is more appropriate to use quantities per volume unit or, equivalently modulo the density  $\rho_{a_i}$ , quantities per mass unit for the extensive variables, e.g.,  $h_{a_i}$  (specific enthalpy) instead of  $H_{a_i}$  (enthalpy),  $u_{a_i}$  (specific internal energy) instead of  $U_{a_i}$  (internal energy),  $s_{a_i}$  (specific entropy) instead of  $S_{a_i}$  (entropy). Intensive variables  $T_{a_i}$  (temperature),  $P_{a_i}$  (pressure) are left unchanged.

The thermodynamic state of an open system is therefore the set of all thermodynamic states of volumes  $a_i$ , which can be represented as  $\{P_{a_i}, T_{a_i}\}$  if all volumes  $a_i$  are in a single-phase state.

In addition to the thermodynamic state variables, the system state depends also upon the ingoing or outgoing mass flow rates. Therefore, the thermal-hydraulic state of volume  $a_i$  is defined by its hydraulic state in addition to its thermodynamic state. The hydraulic state of volume  $a_i$  is the set  $\{\dot{m}_{b_j:a_i}\}$ , the  $\dot{m}_{b_j:a_i}$  being the ingoing or outgoing mass flow rates between volume  $a_i$  and its neighboring volumes  $b_j$ .

The full thermal-hydraulic state of volume  $a_i$  is then  $\{P_a, T_a, \dot{m}_{b_j:a_i}\}$ , and the full thermal-hydraulic state of the system is the set of all states of volumes  $a_i$  (the index  $i$  has been dropped for the sake of simplicity inside the state vector).

To summarize, the state of an open thermodynamic system is given by a vector (whose size may be very large), each vector element being composed of the variables that characterize the thermodynamic state of the control volumes and of the variables that define the ingoing or outgoing mass flow rates through the control volumes.

## 2.8 Laws of Thermodynamics

Two laws of thermodynamics describe the relationships between the properties of substances: The first law states the conservation of energy, and the second law states the limitations in converting heat into work. Those two laws are complemented by a third law that states that the entropy of a system approaches a constant value called the residual entropy of the system as the temperature approaches absolute zero (0 K). This implies that the temperature of absolute zero can never be reached. Only the two first laws are used in practice regarding heat transfer, so the third law will not be developed any further.

### 2.8.1 First Law

The first law of thermodynamics expresses the conservation of energy: Energy can never be created nor destroyed, but it can be converted from one form to another, for instance, from heat to mechanical work.

#### Closed systems

For a closed system, the first law is expressed as:

$$\Delta E = Q + W \quad (2.32)$$

where  $\Delta E$  is the variation of the total energy of the system when it receives  $Q$  heat energy and  $W$  work energy from its surroundings.  $Q$  (respectively  $W$ ) is counted positively when the system receives heat (respectively work) and negatively when the system produces heat (respectively work). To the contrary of  $E$  which is a state function,  $Q$  and  $W$  are not state functions because of the second law of thermodynamics, one consequence of which is that work and heat produced depend on a particular path the process: different paths with different efficiencies produce different ratios of work to heat so that work and heat produced depend on the past state history and not on the current state as required for state functions.

The differential formulation of the first law is:

$$dE = \delta Q + \delta W \quad (2.33)$$

As  $E$  is a state function,  $dE$  is a total differential of state functions, whereas  $\delta Q$  and  $\delta W$  just represent small increments that cannot be represented as differential of state functions, since  $Q$  and  $W$  are not state functions.

$E$  is the sum of all forms of energy that are captured inside the substance:

$$dE = dU + dE_C + dE_P + \sum_i \mu_i \cdot dN_i \quad (2.34)$$

where  $U$  is the internal energy,  $E_C$  is the kinetic energy, and  $E_P$  is the potential energy.  $\mu_i$  are the chemical potential of species  $i$  having  $dN_i$  moles if the system contains species of different types that may interact chemically.

If only internal energy is involved in the variation of  $E$ , then

$$dU = \delta Q + \delta W \quad (2.35)$$

For an expansion or a compression,  $\delta W = -P \cdot dV$ . Then using the definition of the enthalpy (2.13) with (2.35) yields:

$$dH = dU + P \cdot dV + V \cdot dP = \delta Q + V \cdot dP \quad (2.36)$$

For an adiabatic process (i.e., with no heat exchange to the outside),  $\delta Q = 0$ . Then from (2.36):

$$dH = V \cdot dP \quad (2.37)$$

For an isobaric process,  $dP = 0$ . Then from (2.36):

$$dH = \delta Q \quad (2.38)$$

Therefore, for an adiabatic and isobaric process:

$$dH = 0 \quad (2.39)$$

The first law for a closed system is illustrated below with the example of a piston cylinder with no leaks that contains gas (cf. Fig. 2.3). The system is the volume inside the piston. It is closed as the mass of gas is kept constant inside the piston. The piston is not adiabatic so the gas absorbs heat  $Q$  from the outside. When heated, the gas expands and pushes the piston upwards: The gas is doing work  $W = P \cdot \Delta V$  on the piston.

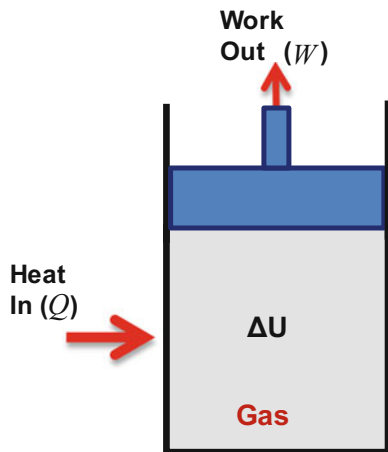
The change in internal energy of the gas inside the piston is:

$$\Delta U = Q - P \cdot \Delta V \quad (2.40)$$

where  $\Delta V$  is the variation of the volume of the piston which is positive during the expansion.

If the movement of the piston is sufficiently slow so that thermodynamic equilibrium is attained at each time instant (i.e., if the process is reversible), then taking the derivative of (2.40) w.r.t. time and dividing (2.40) by the mass of the gas inside the piston which is constant yields:

**Fig. 2.3** Closed thermodynamic system



$$\frac{du}{dt} = \dot{q} + \frac{P}{\rho^2} \cdot \frac{d\rho}{dt} \quad (2.41)$$

where  $\dot{q}$  is the heat received per time unit and per mass unit of the gas.

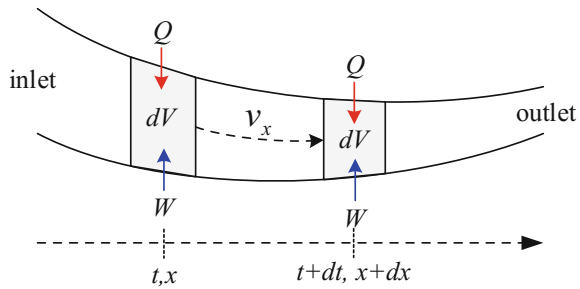
### Open systems

As open systems exchange mass with their surroundings, we will consider fluid systems only.

For open systems, (2.33) applies provided that the differential  $d\bullet$  is replaced by the total differential  $D\bullet$  that takes into account the fact that the fluid moves across the boundary of the system: The total differential acts as though the control volume  $dV$  moves with the fluid at the same velocity, hence as though the control volume is closed (as the mass flow rate through boundaries of the control volume moving at the fluid velocity is zero). In the sequel, to simplify the notations, it assumed that the fluid moves along the main direction  $x$  of 0D/1D modeling.

$$\frac{DE}{Dt} = \int_V (\partial_t(\rho \cdot e) + \partial_x(\rho \cdot e \cdot v_x)) \cdot dV = \dot{Q} + \dot{W} \quad (2.42)$$

where  $\partial_t$  denotes the differential w.r.t. time  $t$ ,  $\partial_x$  denotes the gradient w.r.t. position  $x$ , and  $v_x$  is the fluid velocity along  $x$  at time  $t$  and position  $x$  (cf. Fig. 2.4). The integral is taken over the volume  $V$  of the body.  $\rho$  is the fluid density, and  $e$  is the specific total energy (i.e., the total energy per mass unit) so that  $dE = \rho \cdot e \cdot dV$ .  $\dot{Q}$  and  $\dot{W}$  are respectively the heat and work received by the system per time unit. Note that the main difference between the expressions of the first law for the closed and open systems is that time appears explicitly in the expression for open systems due to the introduction of the fluid velocity. In (2.42), the differential is explicitly taken with respect to time and space which is not the case with (2.33). Therefore, (2.42)

**Fig. 2.4** Fluid stream

implies that the system is in local equilibrium over volume  $dV$  at each time step  $dt$  along its trajectory  $dx$ , so that the process along the fluid motion is reversible, which is not the case for (2.33).

Using the divergence theorem, (2.42) writes (cf. Sect. 4.1.1):

$$\partial_t E = - \int_{A_x} \rho \cdot e \cdot v_x \cdot dA_x + \dot{Q} + \dot{W} \quad (2.43)$$

where  $A_x$  is the area of the control volume boundary perpendicular to the flow direction.

For a fluid stream (cf. Fig. 2.4), as the fluid crosses the control volume boundary only at the inlet and the outlet, (2.43) yields:

$$\partial_t E = \underbrace{\dot{m}_{\text{in}} \cdot e_{\text{in}} - \dot{m}_{\text{out}} \cdot e_{\text{out}}}_{\text{advection term}} + \dot{Q} + \dot{W} \quad (2.44)$$

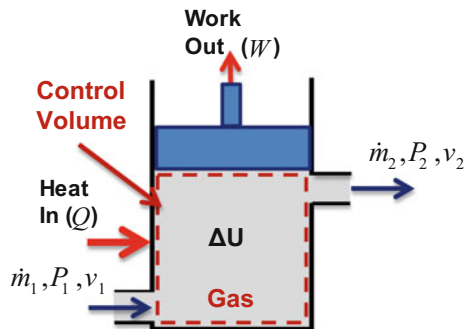
where  $\dot{m}_{\text{in}}$  and  $\dot{m}_{\text{out}}$  are averaged values of the mass flow rate respectively at the inlet and at the outlet that are defined in Chap. 3.

The expressions of the first law for closed systems (2.33) and for open systems (2.44) are very similar, with the following differences for open systems:

1. Open systems are assumed to undertake reversible processes along the fluid motion (which is not the case for closed systems).
2. The differential is explicitly taken with respect to time (which is not necessarily the case for closed systems).
3. There is an additional advection term on the right-hand side of the equation due to fluid transport.

Therefore, the expression of the first law for open systems is not anymore purely thermodynamic as for closed systems. Energy transfer aspects are introduced via the advection term that features the mass flow rate. Consequently, two additional equations are needed to compute the mass flow rate which are the conservation of momentum (to compute the fluid velocity) and the conservation of mass (to compute the fluid density), the mass flow rate being the product of those two

**Fig. 2.5** Open thermodynamic system



quantities. The combination of thermodynamics with hydraulics is often called thermal hydraulics (or thermofluids).

As the first law for open systems assumes that the process is reversible along the fluid motion, it cannot be used for irreversible processes, for instance, inside machines. For that purpose, the second law must be used instead with the concept of efficiencies.

The first law for an open system is illustrated below with the example of a piston cylinder with a gas admission and a gas exhaust (cf. Fig. 2.5). The control volume of the system is shown by the dotted line: It comprises the piston volume but not the admission and exhaust pipes. Therefore, it is an open system: Mass, heat, work, and momentum can flow across the control surface of the volume from the admission pipe to the exhaust pipe.

The change in total energy inside the piston includes the internal, potential, and kinetic energies transferred from and to the pipes and work done by pressure forces inside the pipes, at the inlet and the outlet of the piston.

Assuming that the piston moves sufficiently slowly so that at each instant equilibrium is attained, it is then possible to use (2.44) on the control volume shown in Fig. 2.5:

$$\frac{dE}{dt} = \dot{m}_{in} \cdot e_{in} - \dot{m}_{out} \cdot e_{out} + \dot{Q} - P \cdot \frac{dV}{dt} \quad (2.45)$$

with  $e_{in} = u_1 + \frac{P_1}{\rho_1} + \frac{v_1^2}{2} + g \cdot z_1$  and  $e_{out} = u_2 + \frac{P_2}{\rho_2} + \frac{v_2^2}{2} + g \cdot z_2$ .

Inside the piston, the total energy is assumed to be equal to the internal energy [the other forms of energy are neglected; cf. (2.34)].

Then,

$$\begin{aligned} \frac{d(\rho \cdot V \cdot u)}{dt} &= \dot{m}_1 \cdot \left( h_1 + \frac{v_1^2}{2} + g \cdot z_1 \right) - \dot{m}_2 \cdot \left( h_2 + \frac{v_2^2}{2} + g \cdot z_2 \right) \\ &\quad + \dot{Q} - P \cdot \frac{dV}{dt} \end{aligned} \quad (2.46)$$

with  $h_1 = u_1 + \frac{P_1}{\rho_1}$  and  $h_2 = u_2 + \frac{P_2}{\rho_2}$ .

Using the conservation of the mass inside the piston

$$\frac{d(\rho \cdot V)}{dt} = \dot{m}_1 - \dot{m}_2 \quad (2.47)$$

the left-hand term of (2.46) writes:

$$\frac{d(\rho \cdot V \cdot u)}{dt} = (\dot{m}_1 - \dot{m}_2) \cdot u + \rho \cdot V \cdot \frac{du}{dt} \quad (2.48)$$

Then

$$\begin{aligned} \rho \cdot V \cdot \frac{du}{dt} &= \dot{m}_1 \cdot \left( h_1 - u + \frac{v_1^2}{2} + g \cdot z_1 \right) - \dot{m}_2 \cdot \left( h_2 - u + \frac{v_2^2}{2} + g \cdot z_2 \right) \\ &\quad + \dot{Q} - P \cdot \frac{dV}{dt} \end{aligned} \quad (2.49)$$

This expression is significantly more complex than the one for the closed system; cf. (2.41).

*Remark* Under the assumption that  $\dot{m}_1 \approx \dot{m}_2$ ,  $\dot{m}_1 - \dot{m}_2 \approx 0$  so the term  $(\dot{m}_1 - \dot{m}_2) \cdot u$  can be neglected in (2.49), yielding a simpler equation where the internal energy of the fluid does not appear on the right-hand side.

$$\begin{aligned} \rho \cdot V \cdot \frac{du}{dt} &= \dot{m}_1 \cdot \left( h_1 + \frac{v_1^2}{2} + g \cdot z_1 \right) - \dot{m}_2 \cdot \left( h_2 + \frac{v_2^2}{2} + g \cdot z_2 \right) \\ &\quad + \dot{Q} - P \cdot \frac{dV}{dt} \end{aligned} \quad (2.50)$$

If the assumption of a reversible process cannot be made for the system, then the system can only be observed over a cycle. As over a cycle, considering the global process, the system operates under constant external (atmospheric) pressure and its volume remains constant (the volume of the piston is the same at the start of each cycle), the process is isobaric and isochoric. Then from (2.20):

$$\Delta H_{\text{cycle}} = \Delta U_{\text{cycle}} = Q - W \quad (2.51)$$

where  $W$  is the work produced by the system. As the system is open, over a cycle the system does not go back to its initial state, so the variation of enthalpy is not zero, but is given by:

$$\Delta H_{\text{cycle}} = (\dot{m}_2 \cdot h_2 - \dot{m}_1 \cdot h_1) \cdot \Delta t \quad (2.52)$$

where  $\Delta t$  is the cycle duration. Combining (2.51) with (2.52) yields:

$$0 = (\dot{m}_1 \cdot h_1 - \dot{m}_2 \cdot h_2) \cdot \Delta t + Q - W \quad (2.53)$$

Considering that  $\Delta t$  is close to zero, dividing (2.53) by  $\Delta t$  and taking the limit when  $\Delta t \rightarrow 0$  yield

$$0 = \dot{m}_1 \cdot h_1 - \dot{m}_2 \cdot h_2 + \dot{Q} - \dot{W} \quad (2.54)$$

This expression corresponds to the steady-state version of (2.50) (i.e.,  $du/dt = 0$ ) by considering that  $\dot{W}$  encapsulates the potential energy and kinetic energy provided to the fluid in addition to the work done on the piston. It is therefore as one would expect a less detailed energy balance of the system (irreversibility leads to loss of information).

### 2.8.2 Second Law

The second law of thermodynamics can be expressed in several ways, the simplest being that heat energy flows spontaneously from a hot body to a cold body. So if heat energy  $Q$  is spontaneously transferred from a body at temperature  $T_1$  to a body at temperature  $T_2$ , then  $T_1 > T_2$ .

Let us consider a body at temperature  $T$  undergoing a reversible process in contact with a source at temperature  $T_0$ .  $\delta Q_{\text{rev}}$  is the heat energy received by the body from the source at each infinitesimal step of the reversible process. As the process is reversible, there is sufficient time to reach equilibrium at each step, so the temperature  $T$  of the body is defined at each step. The temperature  $T_0$  of the source remains constant throughout the cycle (by definition of a source as an infinite reservoir).

By definition, the variation of entropy of the body is:

$$\Delta S = \int \frac{\delta Q_{\text{rev}}}{T} \quad (2.55)$$

$S$  is a state function as  $\Delta S$  does not depend on the particular path chosen for the integral (all reversible processes are equivalent if they have the same initial and final states). Therefore, for a cycle,  $\Delta S = 0$ .

Let us consider the complete system  $\Sigma = \text{body} + \text{source}$ .  $\Sigma$  is an isolated system as it contains everything.

The variation of the entropy of  $\Sigma$  is:

$$\Delta S_{\Sigma} = \Delta S + \Delta S_{\text{source}} = \int \frac{\delta Q_{\text{rev}}}{T} + \frac{-Q_{\text{rev}}}{T_0} = \int \left( \frac{1}{T} - \frac{1}{T_0} \right) \cdot \delta Q_{\text{rev}} \quad (2.56)$$

If  $T \leq T_0$ , heat flows from the source to the body. Then  $\frac{1}{T} - \frac{1}{T_0} \geq 0$  and  $\delta Q_{\text{rev}} \geq 0$ .

If  $T \geq T_0$ , heat flows from the body to the source. Then  $\frac{1}{T} - \frac{1}{T_0} \leq 0$  and  $\delta Q_{\text{rev}} \leq 0$ .

Therefore, in both cases,  $\Delta S_{\Sigma} \geq 0$ . The second law of thermodynamics generalizes this result by stating formally that the entropy of an isolated system increases.

Let us now consider an irreversible process for the body where  $Q$  is the heat energy received by the body from the source at temperature  $T_0$ . The variation of the entropy of the source is still

$$\Delta S_{\text{source}} = -\frac{Q}{T_0} \quad (2.57)$$

because the process is still reversible for the source since the temperature of the source does not change.

Then,

$$\Delta S_{\Sigma} = \Delta S + \Delta S_{\text{source}} = \Delta S - \frac{Q}{T_0} \quad (2.58)$$

As the entropy of an isolated system increases,  $\Delta S_{\Sigma} \geq 0$ . Then,

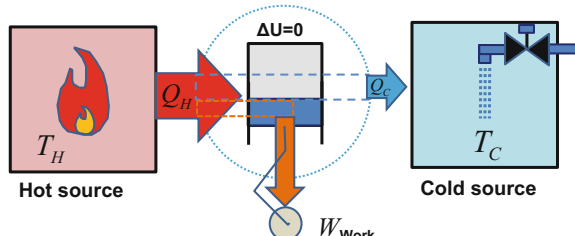
$$\Delta S \geq \frac{Q}{T_0} \quad (2.59)$$

As heat energy flows spontaneously from a hot body to a cold body, mechanical work must be provided to move heat energy from the cold body to the hot body. For instance, refrigeration or air-conditioning systems must be provided with mechanical work in order to respectively cool pieces of equipment or rooms.

Equation (2.59) shows that an engine cannot perform a cycle when connected to a single source providing heat energy to the engine, because then  $\Delta S > 0$  as  $Q > 0$  (in a cycle  $\Delta S = 0$ ). Consequently, an engine must be connected to at least two sources.

Let us consider an engine connected to a hot source and a cold source (cf. Fig. 2.6). The hot source is at temperature  $T_H$  and the cold source is at temperature  $T_C$  with  $T_C < T_H$ . The engine receives heat  $Q_H$  from the hot source, produces mechanical work  $W$ , and releases heat  $Q_C$  to the cold source (in a way, the engine operates like a watermill that receives energy in the form of heat instead of hydraulic power, the temperature gradient between the hot and cold sources replacing the pressure gradient between the upstream and downstream sides of the mill).

**Fig. 2.6** A thermal engine operating between a hot source and a cold source



The first law applied to the engine yields:

$$\Delta U_{\text{eng}} = Q_{\text{H}} - Q_{\text{C}} - W \quad (2.60)$$

The whole system  $\Sigma$  comprising the engine with the hot and the cold sources is isolated. Then the second law applied to  $\Sigma$  yields:

$$\Delta S_{\Sigma} = \Delta S_{\text{H}} + \Delta S_{\text{eng}} + \Delta S_{\text{C}} = \frac{-Q_{\text{H}}}{T_{\text{H}}} + \Delta S_{\text{eng}} + \frac{Q_{\text{C}}}{T_{\text{C}}} \geq 0 \quad (2.61)$$

Over a cycle,  $\Delta U_{\text{eng}} = 0$  and  $\Delta S_{\text{eng}} = 0$ .

Then from (2.60)

$$W = Q_{\text{H}} - Q_{\text{C}} \quad (2.62)$$

and from (2.61)

$$\frac{Q_{\text{C}}}{T_{\text{C}}} - \frac{Q_{\text{H}}}{T_{\text{H}}} \geq 0 \quad (2.63)$$

The efficiency of the engine is the amount of work produced for a given amount of heat energy delivered by the hot source:

$$\eta_{\text{eng}} = \frac{W}{Q_{\text{H}}} \quad (2.64)$$

From (2.62) and (2.63):

$$\eta_{\text{eng}} = 1 - \frac{Q_{\text{C}}}{Q_{\text{H}}} \leq 1 - \frac{T_{\text{C}}}{T_{\text{H}}} \quad (2.65)$$

The efficiency  $\eta_{\text{eng}}$  of the engine cannot be greater than  $\eta_{\text{rev}}$ :

$$\eta_{\text{eng}} \leq \eta_{\text{rev}} = 1 - \frac{T_{\text{C}}}{T_{\text{H}}} \quad (2.66)$$

$\eta_{\text{rev}}$  is the maximum efficiency of the engine for a reversible cycle.  $\eta_{\text{rev}}$  is always strictly less than 1 as  $T_{\text{C}}$  cannot reach 0 K according to the third law.  $\eta_{\text{rev}}$  does not depend on the engine, but on the temperatures of the hot and cold sources! This reflects the fact that reversible processes are independent of the structure of the system (i.e., the way it is conceived, built, and operated). That explains why real systems always undergo irreversible processes, and the challenge for the engineer is to maximize their efficiencies (taking of course into account all other additional constraints such as safety, dependability, costs, environmental regulations, human comfort).

To summarize, the second law combined with the first law is also about the quality of energy: It states a limitation on the amount of heat energy that can be converted into mechanical work. It also forbids the possibility of perpetual motion, where mechanical energy and thermal energy would be indefinitely transformed into one another without any losses.

Heat that cannot be converted into work must be released to the environment, which causes thermal pollution. In power plants, the condenser is dedicated to that task: Heat released from the condensation of steam coming from the low-pressure stage of the turbine is transferred to the environment via a cooling circuit. In combined heat and power (CHP) plants, heat energy is reused to heat buildings, turning waste into a valuable product and raising the plant economic efficiency, if not the thermodynamic efficiency. In a combined cycle power plant (CCPP), heat from exhaust flue gases at the outlet of the combustion turbine in a Brayton cycle is reused to produce steam at the inlet of the steam turbine in a Rankine cycle.

## 2.9 Thermodynamic Cycles

### 2.9.1 The Brayton Cycle

The Brayton cycle is a thermodynamic cycle that describes the process of a heat engine that operates at constant pressure. It is the ideal cycle for gas turbine engines in which the working fluid undergoes a closed loop. The Brayton cycle is always open because the exhaust flue gas cannot be completely reused at the inlet of the compressor (cf. Fig. 2.7).

A gas turbine is a type of internal combustion engine. It has an upstream compressor coupled to a downstream turbine and a combustion chamber in between. The atmospheric air flows through the compressor that compresses it to

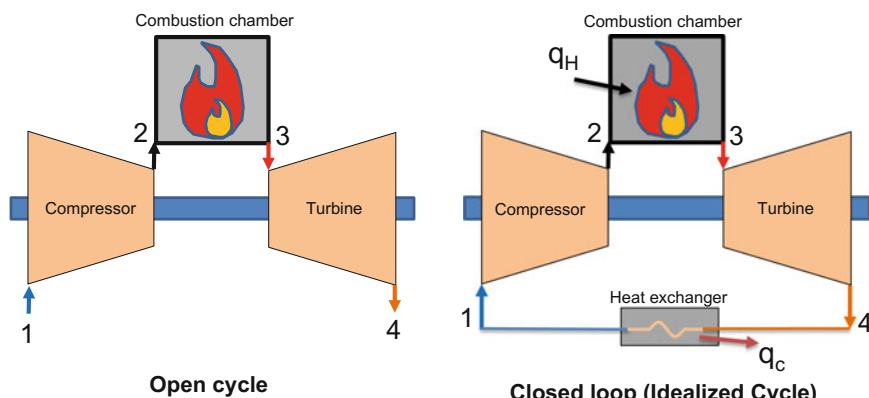


**Fig. 2.7** Schematic diagram of a gas turbine

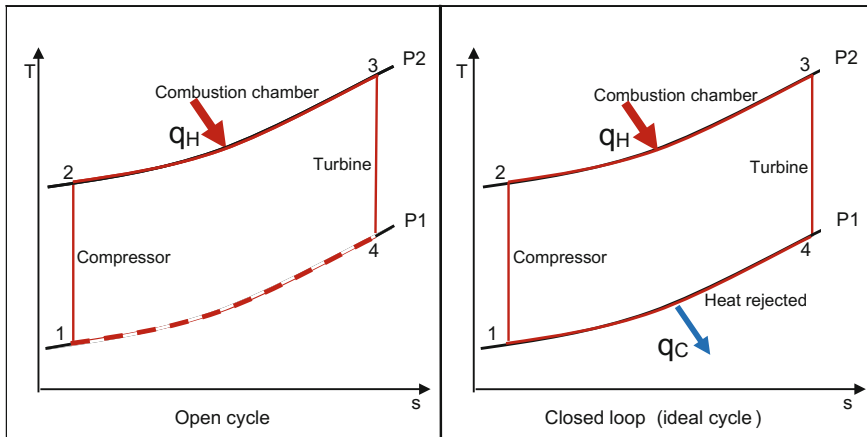


**Fig. 2.8** Ideal Brayton cycle in a  $T$ - $s$  diagram

higher pressure at the inlet of the combustion chamber. In the combustion chamber, heat is then added to the air flow by spraying fuel into the air and by igniting the fuel to generate a high-temperature flow. The high-temperature high-pressure gas enters the turbine, where it expands down to the exhaust pressure, producing work on the shaft, a fraction of which is provided to the compressor.

Figure 2.8 shows the diagram of the Brayton cycle on the temperature–entropy ( $T$ – $s$ ) diagram.

### Ideal Brayton cycle

The ideal Brayton cycle is a closed loop made of four reversible processes:

- Process 1–2: isentropic compression (inside the compressor); it is a vertical line.
- Process 2–3: constant pressure process, during which heat addition takes place (inside the combustion chamber);
- Process 3–4: isentropic expansion (inside the turbine); it is again a vertical line.
- Process 4–1: constant pressure heat rejection.

The first law per mass unit of gas can be written as follows where  $h_i$  denotes the specific enthalpy at point  $i$  in the cycle.

The work provided to the compressor is  $w_c = h_2 - h_1$ ;

The heat supplied by the combustion chamber is  $q_H = h_3 - h_2$ ;

The work provided by the turbine is  $w_t = h_3 - h_4$ ;

The heat rejected as thermal losses is  $q_C = h_4 - h_1$ .

The work cycle is given by the enclosed area (1–2–3–4) shown in Fig. 2.8.

The thermal efficiency of the ideal Brayton cycle (closed loop) is given by:

$$\begin{aligned}\eta_{\text{th}} &= \frac{\text{Heat added} - \text{Heat rejected}}{\text{Heat added}} = \frac{q_H - q_C}{q_H} \\ &= 1 - \frac{q_C}{q_H} = 1 - \frac{c_{p,C} \cdot (T_4 - T_1)}{c_{p,H} \cdot (T_3 - T_2)}\end{aligned}\quad (2.67)$$

where  $\eta_{\text{th}}$  is the thermal efficiency,  $c_{p,C}$  is the specific heat capacity of the cold fluid,  $c_{p,H}$  is the specific heat capacity of the hot fluid, and  $T_i$  is the fluid temperature in the cycle at point  $i$ .

### Actual Brayton cycle and component efficiencies

The actual Brayton cycle is based on real turbomachines that deviate from ideal isentropic ones (cf. Fig. 2.9). Therefore, it is quite important to analyze how much process losses are introduced on the overall performance of the gas turbine due to machine inefficiency. First, two isentropic definitions are introduced.

The compressor isentropic efficiency is defined as the ratio of isentropic compression work to the actual compression work:

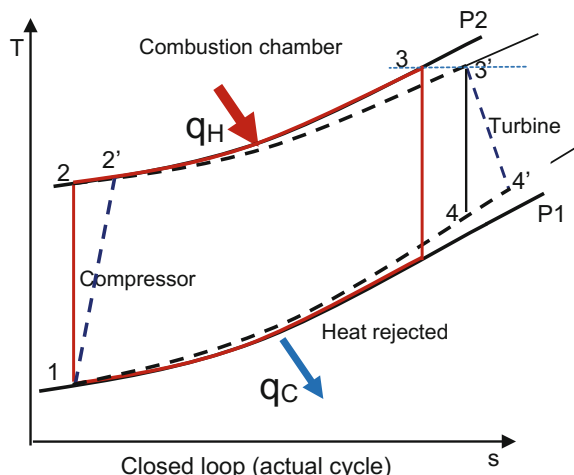
$$\eta_c = \frac{h_2 - h_1}{h_{2'} - h_1} \quad (2.68)$$

The turbine isentropic efficiency is defined as the ratio of the turbine actual work to the isentropic turbine work.

$$\eta_t = \frac{h_{3'} - h_{4'}}{h_{3'} - h_4} \quad (2.69)$$

Both compression processes and expansion processes in the turbine are shown in Fig. 2.9.

**Fig. 2.9** Actual Brayton cycle in a  $T-s$  diagram



## 2.9.2 The Rankine Cycle

The Rankine cycle is a thermodynamic cycle of a heat engine that converts heat into mechanical work. It is the most common of all power generation cycle, which usually uses water/steam as the working fluid (cf. Fig. 2.10). The heat source used in these power plants is usually nuclear fission or the combustion of fossil fuel such as coal, natural gas and oil, or solar radiation.

### Ideal Rankine cycle

In an ideal Rankine cycle, the pump and turbine are isentropic; i.e., the pump and turbine generate no entropy and hence, maximize the work output. Figure 2.11 shows the ideal Rankine cycle on a temperature–entropy ( $T$ – $s$ ) diagram, composed of four processes:

- Process 1–2: The saturated liquid is pumped from low to high pressure; the increase in pressure of the water going through the boiler feed pump takes place at the left of the saturated liquid line in the  $T$ – $s$  diagram.
- Process 2–3–4–5: The compressed liquid is driven to the boiler (steam generator), where it is heated at constant pressure by an external heat source to become a dry saturated steam or superheated steam.
- Process 5–6: The steam expands through a turbine, generating power; this decreases the temperature and pressure of the steam, and some condensation may occur.
- Process 6–1: The saturated steam (or wet steam) then enters the condenser where it is condensed at constant pressure to become a saturated liquid.

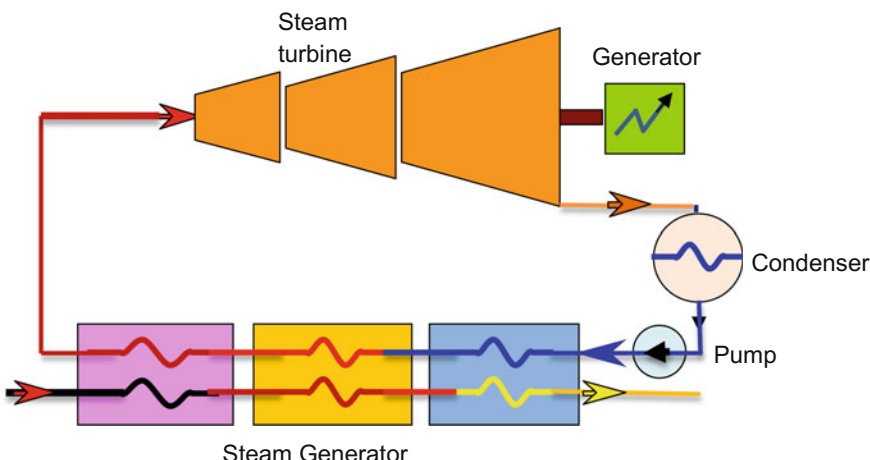
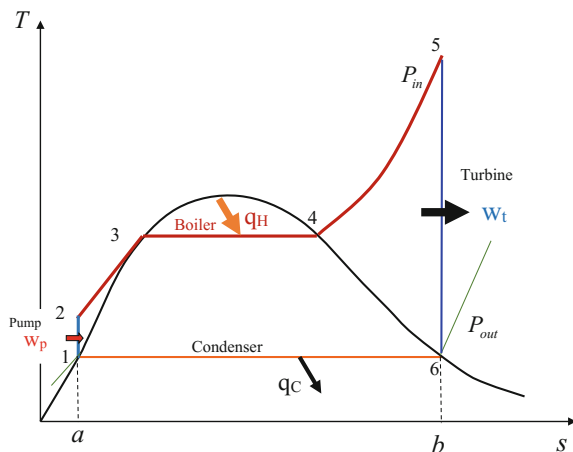


**Fig. 2.10** Schematic diagram of the Rankine steam power cycle

**Fig. 2.11** Ideal Rankine cycle in a  $T-s$  diagram



The efficiency of an ideal Rankine cycle is the ratio between output and input. It is given by:

$$\eta_{th} = \frac{\text{Area } 1 - 2 - 3 - 4 - 5 - 6 - 1}{\text{Area } a - 2 - 3 - 4 - 5 - b - a} \quad (2.70)$$

If the system is in steady state and the kinetic energy and potential energy differences between the inlet and outlet are negligible, the first law per mass unit of working fluid (water/steam) can be written as follows, where  $h_i$  denotes the specific enthalpy at point  $i$  in the cycle.

The work input to the feed pump is  $w_p = h_2 - h_1$ ;

The heat supplied by the boiler is  $q_H = h_5 - h_2$ ;

The work output by the turbine is  $w_t = h_5 - h_6$ ;

The heat rejected by the condenser is  $q_C = h_6 - h_1$ .

The thermal efficiency of the ideal Rankine cycle is given by:

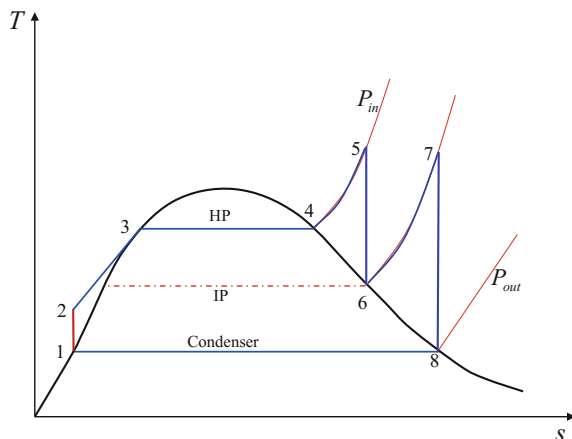
$$\eta_{th} = \frac{\text{Net work output}}{\text{Heat supplied by the boiler}} = \frac{w_t - w_p}{q_H} = 1 - \frac{q_C}{q_H} \quad (2.71)$$

### Rankine cycle efficiency improvement techniques

Some Rankine cycle efficiency improvement techniques are:

- Increase the superheating steam temperature  $T_5$  to higher temperatures in order to increase the work output and the efficiency of the cycle. It also decreases the moisture contents of the steam at the turbine exit.
- Increase the operating pressure of the boiler in order to increase the steam temperature and thus improve the cycle efficiency (i.e., increase area “1–2–3–4–

**Fig. 2.12** Ideal Rankine cycle with steam reheating in a  $T-s$  diagram



5–6–1’’). Note that for a fixed turbine inlet temperature, the cycle shifts to the left and the moisture content of the steam at the turbine exit increases.

- Lower the condenser pressure to help the turbine deliver more work as more steam expansion in the turbine is then possible (i.e., decrease area ‘‘a–1–6–b–a’’).
- Reheat the Rankine cycle. In a reheat system, a two-stage turbine (high-pressure turbine and low-pressure turbine) is employed to improve efficiency. Steam, after expansion inside the high-pressure turbine, is sent again to the boiler and heated until it reaches superheated conditions. It is then sent to expand in the low-pressure turbine (the second stage of the steam turbine) to attain condenser pressure (cf. Fig. 2.12). Reheating offers the ability to limit or eliminate moisture at the turbine exit. The presence of more than about 10% moisture in the turbine exhaust can cause erosion of the blades near the turbine exit and reduce energy conversion efficiency.
- Heat feed water heating. A water heater is a heat exchanger in which the latent heat of small amounts of steam is used to increase the temperature of the feed water (flowing to the steam generator). In a water heater, heat is transferred from the extracted steam (steam drawn from the turbine) to the feed water. So, the feed water can be mixed with the condensed extraction steam. In this case, it is assumed that the condensate and the feed water leaving the water heater are at the same pressure.

The thermal efficiency of the ideal Rankine cycle steam with reheating (cf. Fig. 2.12) is:

$$\eta_{th} = \frac{\text{Net work output}}{\text{Heat supplied by the boiler}} = \frac{(h_5 - h_6) + (h_7 - h_8) - (h_2 - h_1)}{(h_5 - h_2) + (h_7 - h_6)} \quad (2.72)$$

### Actual Rankine cycle and component efficiencies

The actual Rankine cycle is based on real thermal power plants that deviate from ideal isentropic ones (cf. Fig. 2.13). First, two isentropic definitions are introduced.

The pump isentropic efficiency is defined as the ratio of isentropic compression work to the actual compression work:

$$\eta_p = \frac{h_2 - h_1}{h_{2'} - h_1} \quad (2.73)$$

The turbine isentropic efficiency is defined as the ratio of the turbine actual work to the isentropic turbine work:

$$\eta_t_{-HP} = \frac{h_{5'} - h_6}{h_{5'} - h_6} \quad (2.74)$$

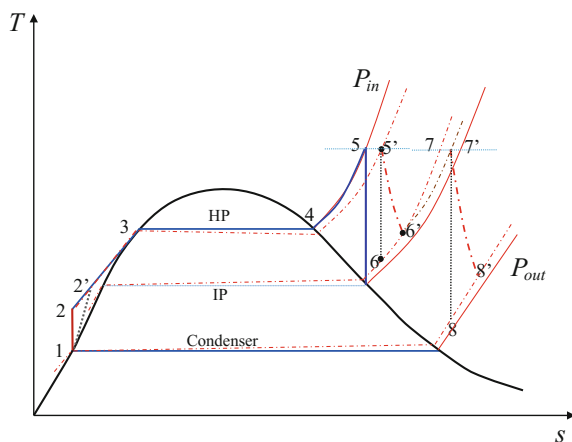
## 2.10 The Ideal Gas Law

The state of a gas is determined by its pressure, volume, and temperature. The equation that relates the pressure, temperature, and volume of a gas is called the gas state equation. In general, the state equation of a gas is complicated.

In a perfect or ideal gas, the change in density is directly proportional to the change in temperature at constant pressure or to the change in pressure at constant temperature. This is expressed as the ideal gas law which is given by:

$$P \cdot V = n \cdot R \cdot T \quad (2.75)$$

**Fig. 2.13** Real Rankine cycle with steam reheating in a  $T-s$  diagram



where  $P$  is the gas pressure,  $T$  is the gas temperature,  $V$  is the gas volume,  $n$  is the number of moles of the gas, and  $R$  is the ideal gas constant which is equal to the Avogadro constant multiplied by the Boltzmann constant:  $R = N_a \cdot k_B = 8.314 \text{ J K}^{-1} \text{ mol}^{-1}$ .

The number of moles is given by:

$$n = \frac{m}{M_g} \quad (2.76)$$

where  $m$  is the mass of the gas and  $M_g$  is the molar mass of the gas.

Another way of expressing the ideal gas law is to write it per mass unit of the gas:

$$\frac{P}{\rho} = R_g \cdot T \quad (2.77)$$

where  $\rho$  is the gas density and  $R_g$  is the specific gas constant:  $R_g = \frac{R}{M_g} = \frac{N_a \cdot k_B}{M_g}$ .

## 2.11 Polytropic Processes

A polytropic process follows the following state equation:

$$P \cdot V^n = C \quad (2.78)$$

where  $C$  is a constant,  $P$  is the gas pressure, and  $V$  is the gas volume.  $n$  is called the polytropic coefficient.

When  $n = 0$ , the process is isobaric.

When  $n = 1$ , the process is isothermal under the assumption of ideal gas law.

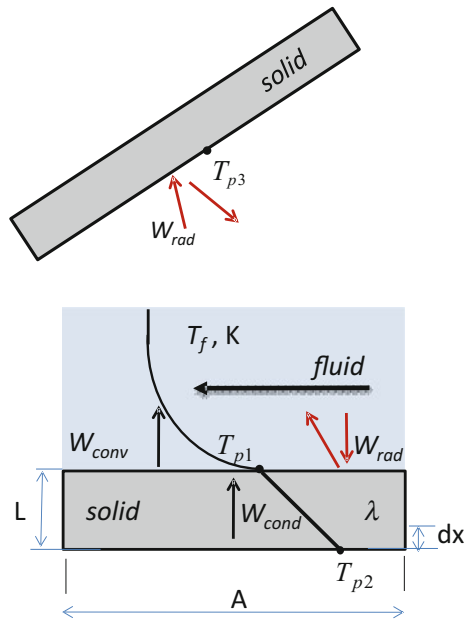
When  $1 < n < \gamma$ , with  $\gamma = c_p/c_v$ , work and heat flow in opposite directions, e.g., the process receives work and releases heat to the environment such as in a refrigerating cycle in the compression phase.

When  $n = \gamma$ , the process is isentropic under the assumption of ideal gas law.

When  $n > \gamma$ , work and heat flow in the same direction, e.g., the process provides work and releases heat to the environment such as an internal combustion engine cycle in the expansion phase.

When  $n \rightarrow +\infty$ , the process is isochoric.

**Fig. 2.14** Heat transfer by conduction, convection, and radiation



## 2.12 Heat Transfer Processes

There are three modes of heat transfer: conduction, radiation, and convection.

Consider two solid bodies at different temperatures (cf. Fig. 2.14). In case of vacuum between the two bodies, heat transfer occurs only by radiation between the two bodies. If a fluid flows between the two bodies, heat is also transferred by convection. If the fluid is initially at rest, then heat is transferred first via conduction between the two bodies then via natural convection when the fluid starts flowing due to fluid density differences induced by temperature gradient in the fluid.

In Fig. 2.14,  $T_{p1}$  and  $T_{p2}$  are the temperatures of the surfaces of the wall of the first body, and  $T_f$  is the temperature of the fluid. It is assumed that  $T_{p2} > T_{p1} > T_f$ .  $T_{p3}$  is the temperature of the surface of the second body.

### Conduction

Conduction involves physical contact between the bodies or the parts of bodies that exchange heat. *Fourier's law* gives the expression of the heat transfer by conduction per unit area in a plane solid wall between the two sides of the wall:

$$\dot{q} = -k \cdot \frac{dT}{dx} \quad (2.79)$$

where  $\dot{q}$  is the heat flux ( $\text{W/m}^2$ ),  $k$  ( $\text{W/m/K}$ ) is the thermal conductivity of the substance inside the wall, and  $\frac{dT}{dx}$  is the temperature gradient along the heat transfer direction (i.e., from wall to wall).

In steady-state conditions and for a linear distribution of the temperature in the solid (see Fig. 2.14), the thermal power transferred between the two sides of the wall is:

$$W_{\text{cond}} = k \cdot A \cdot \frac{(T_{p2} - T_{p1})}{L} \quad (2.80)$$

where  $A$  is the wall heat exchange surface and  $L$  is the thickness of the wall.

### **Radiation**

Radiation is thermal energy emitted by matter through space. It does not require contact or presence of any material between the emitting body and the receiving bodies.

The *Stefan–Boltzmann law* gives the upper limit of the radiation heat flux emitted by a blackbody (i.e., an ideal radiator) whose surface is at temperature  $T_s$ :

$$\dot{q}_{\max} = \sigma \cdot T_s^4 \quad (2.81)$$

where  $\dot{q}_{\max}$  is the maximum heat flux ( $\text{W/m}^2$ ) and  $\sigma$  is the Stefan–Boltzmann constant.

For a real surface, the heat flux emitted is less than the one from a blackbody at the same temperature:

$$\dot{q}_{\text{rad}} = \sigma \cdot \varepsilon \cdot T_s^4 \quad (2.82)$$

where  $\varepsilon$  is the emissivity of the surface ( $0 < \varepsilon < 1$ ).

In the frequent case where radiation occurs between a small surface at temperature  $T_{p1}$  surrounded by a much larger surface at temperature  $T_{p3}$ , the heat flux emitted by the small surface is:

$$\dot{q}_{\text{rad}} = \varepsilon \cdot \sigma \cdot (T_{p1}^4 - T_{p3}^4) \quad (2.83)$$

where  $\varepsilon$  is the emissivity of the small surface ( $0 < \varepsilon < 1$ ).

### **Convection**

Convection occurs when a fluid is in contact with two bodies at different temperatures (e.g., a hot zone and a cold zone in a fluid or in a solid). There is a movement of the fluid that carries heat from the hot zone toward the cold zone. When the movement of the fluid is due solely to differences in fluid temperature, the

convection is termed *natural convection*. The movement of the fluid can also be forced by the action of a pump or a fan; in such case, the convection is termed *forced convection*.

*Newton's law* gives the expression of the convection heat flux exchanged between the surface of a solid at the temperature  $T_{\text{p1}}$  and a fluid at the temperature  $T_f$  that flows on the surface of the solid:

$$\dot{q}_{\text{conv}} = h \cdot (T_{\text{p1}} - T_f) \quad (2.84)$$

where  $\dot{q}_{\text{conv}}$  is the heat flux ( $\text{W/m}^2$ ) transferred from the wall to the fluid and  $h$  is the convection heat transfer coefficient ( $\text{W/m}^2/\text{K}$ ).

The value of  $h$  is governed by operational parameters (wall or pipe geometry, mass flow rates, pressure, and temperature) as well as physical properties of the fluid (density, specific heat, viscosity, and thermal conductivity); cf. Sect. 9.2.4.

## References

- Haar L, Gallagher J, Kell G (1975) NBS/NRC steam tables: thermodynamic and transport properties and computer program for vapor and liquid states of water in SI units. Hemisphere Publishing Corporation, New York
- Wagner W, Kruse A (1998) The industrial standard IAPWS-IF97 for the thermodynamic properties and other properties of water and steam. Springer

# Chapter 3

## Averaged Physical Quantities



**Abstract** The present chapter introduces the mathematical definitions and notations for averaged physical quantities in control volumes, which are central to the 0D/1D modeling methodology. The intention is to show that the quantities used in 0D/1D modeling are exact quantities which represent average values in space and time for the sake of computational efficiency. This is done at the expense of resolution in space (but not in time). In Chap. 6 and the following sections, it will be shown that this limitation still gives acceptable simulation results.

### Nomenclature

$[G]$	Unit of quantity $G$
$A_{b:a}$	Cross-sectional area of boundary $b:a$ ( $\text{m}^2$ )
$A_{k,x}$	Cross-sectional area of phase $k$ at coordinate $x$ along the tube ( $\text{m}^2$ )
$A_x$	Flow cross-sectional area at coordinate $x$ ( $\text{m}^2$ )
$b:a$	Boundary between control volumes $b$ and $a$
$f_x$	Average of quantity $f$ over $A_x$ ( $[f]$ )
$f_{k,x}$	Phase average of phase $k$ -related quantity $f_k$ over $A_{k,x}$ ( $[f_k]$ )
$g$	Specific extensive quantity ( $[G]\cdot\text{kg}^{-1}$ )
$g_a$	Average value of specific extensive quantity $g$ inside volume $a$ ( $[G]\cdot\text{kg}^{-1}$ )
$g_{b:a}$	Average value of specific extensive quantity $g$ over $A_{b:a}$ ( $[G]\cdot\text{kg}^{-1}$ )
$g_x$	Average value of specific extensive quantity $g$ over $A_x$ for the left-hand side of the energy balance equation ( $[G]\cdot\text{kg}^{-1}$ )
$g_{x:}$	Average value of specific extensive quantity $g$ over $A_x$ for the right-hand side of the energy balance equation ( $[G]\cdot\text{kg}^{-1}$ )
$G_a$	Total value of specific extensive quantity $g$ inside $a$ ( $[G]$ )
$G_x$	Total value of specific extensive quantity $g$ in the tube from the origin up to coordinate $x$ ( $[G]$ )
$L$	Tube length (m)
$m_a$	Fluid mass inside volume $a$ (kg)
$m_x$	Total value of fluid mass in the tube from the origin up to coordinate $x$ along the tube (kg)

$\dot{m}(b \rightarrow a)$	Mass flow rate through boundary $b:a$ , counted positively when fluid flows from $b$ to $a$ ( $\text{kg s}^{-1}$ )
$\dot{m}(x)$	Mass flow rate through $A_x$ , counted positively when fluid flows along increasing $x$ ( $\text{kg s}^{-1}$ )
$\vec{n}(b \rightarrow a)$	Orientation of boundary $b:a$ , positively from $b$ to $a$
$v_x$	Average superficial velocity (or volumetric flux) over $A_x$ ( $\text{m s}^{-1}$ )
$V_a$	Volume of control volume $a$ ( $\text{m}^3$ )
$x$	Coordinate $x$ along the tube or the fluid vein (m)
$\rho_a$	Average fluid density in volume $a$ ( $\text{kg m}^{-3}$ )
$\rho_x$	Average fluid density over $A_x$ ( $\text{kg m}^{-3}$ )
$\varphi_g(b \rightarrow a)$	Flux of quantity $g$ through boundary $b:a$ , oriented positively from $b$ to $a$ ( $[g] \cdot \text{m}^{-2} \text{s}^{-1}$ )
$\Phi_g(b \rightarrow a)$	Flow of specific extensive quantity $g$ through boundary $b:a$ , oriented positively from $b$ to $a$ ( $[g] \cdot \text{s}^{-1}$ )
$\Phi_g(x)$	Flow of specific extensive quantity $g$ at coordinate $x$ along the tube, oriented positively with increasing $x$ ( $[g] \cdot \text{s}^{-1}$ )
$\langle f \rangle_x$	Average value of quantity $f$ over $A_x$ ( $[f]$ )
$\langle f_k \rangle_x$	Phase average of phase $k$ -related quantity $f_k$ over $A_{k,x}$ ( $[f_k]$ )

### 3.1 Fluxes and Flows of Specific Extensive Quantities

The definitions will be formulated for lumped models (see Fig. 3.1) and for distributed models (see Fig. 3.2).

Lumped systems are divided into finite volumes.  $g$  denotes a specific extensive quantity (e.g., specific enthalpy  $h$  or specific internal energy  $u$ ).  $\varphi_g(b \rightarrow a)$  denotes the flux of  $g$  through the boundary between volumes  $b$  and  $a$ , which is denoted  $b:a$ :

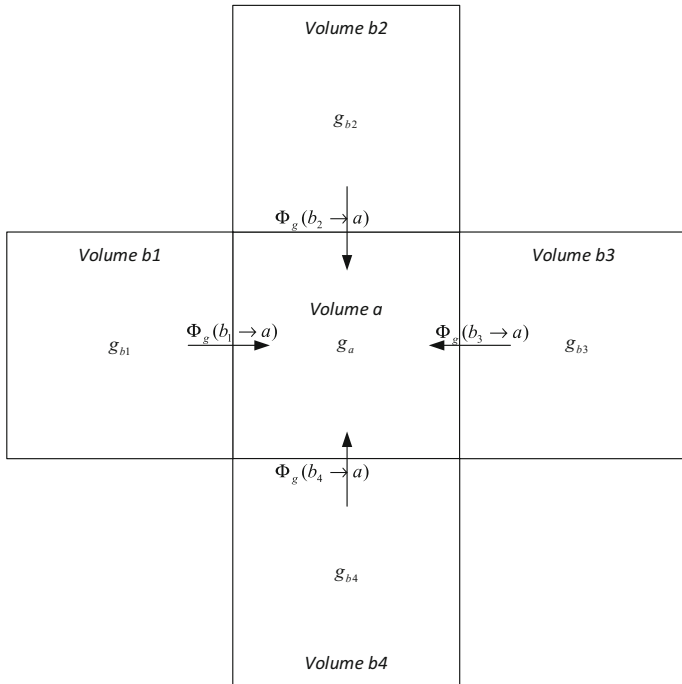
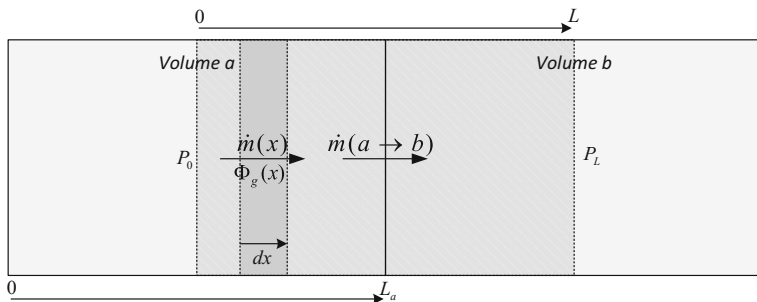
$$\varphi_g(b \rightarrow a) = \rho \cdot g \cdot \vec{v} \cdot \vec{n}(b \rightarrow a) \quad (3.1)$$

$\rho$  is the fluid density.  $\vec{v}$  is the fluid velocity through the boundary.  $\vec{n}(b \rightarrow a)$  denotes the orientation of the boundary, positively from  $b$  to  $a$ .

$\Phi_g(b \rightarrow a)$  denotes the flow of  $g$  through the boundary between volumes  $b$  and  $a$ :

$$\Phi_g(b \rightarrow a) = \int_{b:a} \varphi_g(b \rightarrow a) \cdot dA = \int_{b:a} \rho \cdot g \cdot \vec{v} \cdot \vec{n}(b \rightarrow a) \cdot dA \quad (3.2)$$

$\varphi_g(b \rightarrow a)$  and  $\Phi_g(b \rightarrow a)$  are scalars whose signs are positive when the flow crosses the boundary  $b:a$  from  $b$  to  $a$ .

**Fig. 3.1** Lumped model**Fig. 3.2** Distributed model

In particular, the mass flow rate from  $b$  to  $a$  through the boundary  $b:a$  is:

$$\dot{m}(b \rightarrow a) = \Phi_1(b \rightarrow a) = \int_{b:a} \rho \cdot \vec{v} \cdot \vec{n}(b \rightarrow a) \cdot dA \quad (3.3)$$

Distributed systems are divided into infinitely small volumes  $A_x \cdot dx$  spanning along the  $x$  space coordinate. As we are only interested in the  $x$  coordinate only, the vector notation is dropped for distributed systems.

$$\Phi_g(x) = \int_{A_x} \rho \cdot g \cdot v \cdot dA \quad (3.4)$$

$$\dot{m}(x) = \Phi_1(x) = \int_{A_x} \rho \cdot v \cdot dA \quad (3.5)$$

### 3.2 Average Density

In the lumped formulation, the average density over control volume  $a$  is:

$$\rho_a = \frac{1}{V_a} \cdot \int_a \rho \cdot dV = \frac{m_a}{V_a} \quad (3.6)$$

where  $m_a$  is the mass of the fluid inside  $a$  and  $V_a$  is the volume of  $a$ .

In the distributed formulation, the averaged density over the flow cross-sectional area  $A_x$  is:

$$\rho_x = \frac{1}{A_x} \cdot \int_{A_x} \rho \cdot dA = \frac{1}{A_x} \cdot \frac{\partial m_x}{\partial x} \quad (3.7)$$

### 3.3 Average of Specific Extensive Quantities

The average value  $g_a$  of the specific quantity  $g$  inside control volume  $a$  is defined as:

$$g_a = \frac{G_a}{m_a} \quad (3.8)$$

where  $m_a$  is the mass inside  $a$ , and  $G_a = \int_a \rho \cdot g \cdot dV$  is the total value of  $g$  inside  $a$ .

The average value  $g_{b:a}$  of  $g$  on the boundary  $b:a$  is defined such that:

$$\Phi_g(b \rightarrow a) = g_{b:a} \cdot \int_{b:a} \rho \cdot \vec{v} \cdot \vec{n}(b \rightarrow a) \cdot dA \quad (3.9)$$

Therefore using (3.3),

$$g_{b:a} = \frac{\Phi_g(b \rightarrow a)}{\dot{m}(b \rightarrow a)} \quad (3.10)$$

and

$$\Phi_g(b \rightarrow a) = g_{b:a} \cdot \dot{m}(b \rightarrow a) \quad (3.11)$$

Using the notation for distributed systems, the average value  $g_x$  of  $g$  over cross section  $A_x$  is defined such that:

$$G_x = \int_0^x \left[ \int_{A_x} \rho \cdot g \cdot dA \right] \cdot dx = \int_0^x \rho_x \cdot g_x \cdot A_x \cdot dx \quad (3.12)$$

Hence,

$$g_x = \frac{1}{\rho_x \cdot A_x} \cdot \frac{\partial G_x}{\partial x} = \frac{1}{\rho_x \cdot A_x} \cdot \int_{A_x} \rho \cdot g \cdot dA \quad (3.13)$$

The corresponding distributed definition of  $g_{b:a}$  is denoted  $g_x:$  as a shorthand for  $g_{x:x+dx}$  and is defined such that:

$$\Phi_g(x) = g_x: \cdot \int_{A_x} \rho \cdot v \cdot dA \quad (3.14)$$

Therefore using (3.5),

$$g_x: = \frac{\Phi_g(x)}{\dot{m}(x)} \quad (3.15)$$

and

$$\Phi_g(x) = g_x: \cdot \dot{m}(x) \quad (3.16)$$

So there are in fact two definitions of the average of  $g$  on cross section  $A_x$ ,  $g_x$  given by (3.13) and  $g_x:$  given by (3.15) which will be, respectively, related to the left- and right-hand sides of the balance equations in Chap. 4.

Using (3.13) and (3.7),

$$g_x = \frac{\int_{A_x} \rho \cdot g \cdot dA}{\int_{A_x} \rho \cdot dA}$$

Using (3.15), (3.4), and (3.5),

$$g_x = \frac{\int_{A_x} \rho \cdot g \cdot v \cdot dA}{\int_{A_x} \rho \cdot v \cdot dA}$$

Therefore, in general  $g_x \neq g_{x:}$  unless  $v$  has a constant profile  $v_x$  over  $A_x.$

The average superficial velocity (or volumetric flux)  $v_x$  over  $A_x$  is defined such that:

$$\dot{m}(x) = \rho_x \cdot v_x \cdot A_x \quad (3.17)$$

Therefore,

$$v_x = \frac{\dot{m}(x)}{\rho_x \cdot A_x} \quad (3.18)$$

Notice that

$$v_x = \frac{1}{\rho_x \cdot A_x} \cdot \int_{A_x} \rho \cdot v \cdot dA$$

$$v_{x:} = \frac{1}{\rho_x \cdot v_x \cdot A_x} \cdot \int_{A_x} \rho \cdot v^2 \cdot dA$$

In the sequel, it will be assumed that  $v_x = v_{x:}.$

### 3.4 Average of Other Quantities

For quantities other than the density or specific extensive quantities, the average values are taken over the flow cross-sectional area.

For lumped systems, the cross-sectional average of quantity  $f$  on the boundary  $b : a$  is:

$$f_{b:a} = \frac{1}{A_{b:a}} \cdot \int_{b:a} f \cdot dA \quad (3.19)$$

For distributed systems, the cross-sectional average is denoted:

$$f_x = \frac{1}{A_x} \cdot \int_{A_x} f \cdot dA \quad (3.20)$$

### 3.5 Average of Phase-Related Quantities

The average void fraction of phase  $k$  over cross-sectional area  $A_x$  is defined as:

$$\alpha_{k,x} = \frac{A_{k,x}}{A_x} \quad (3.21)$$

where  $A_{k,x}$  is the cross-sectional area of phase  $k$  and  $A_x$  is the total cross-sectional area.

The *phase* average of phase  $k$ -related quantity  $f_k$  over  $A_{k,x}$  is

$$f_{k,x} = \frac{1}{A_{k,x}} \int_{A_{k,x}} f_k \cdot dA \quad (3.22)$$

The average of the mixture quantity  $f$  over  $A_x$  is

$$f_x = \sum_k \alpha_{k,x} \cdot f_{k,x} \quad (3.23)$$

### 3.6 Notation

In the sequel, cross-sectional average values of quantity  $f$  are denoted  $f_x$ . They are denoted  $\langle f \rangle_x$  when necessary, e.g., in case of the average of a product.

In the same manner phase, cross-sectional average values of phase  $k$ -related quantity  $f_k$  are denoted  $f_{k,x}$ , or  $\langle f_k \rangle_{k,x}$  when necessary.

Volume average values of quantity  $g$  are denoted  $g_a$ , or  $\langle g \rangle_a$  when necessary.

# Chapter 4

## Governing Equations



**Abstract** The present chapter introduces the governing equations, whose structure is important to ensure the robustness of the library, and which are of two fundamental kinds: the dynamic mass, energy, and momentum conservation equations that compute the average physical state inside the control volumes, and the equations that compute the average physical state on the boundaries of the control volumes. Both kinds of equations, complemented with the closure equations for the computation of pressure losses or heat exchange coefficients, are necessary to compute the full thermal hydraulic state of the system. The main simplifications used for the efficient simulation of complex systems are presented and fully justified.

### Nomenclature

$[G]$	Unit of quantity $G$
$A_{b:a}$	Flow cross-sectional area of boundary $b:a$ ( $\text{m}^2$ )
$A_{g,x}$	Cross-sectional area of the gas phase at coordinate $x$ along the tube ( $\text{m}^2$ )
$A_{k,x}$	Cross-sectional area of phase $k$ at coordinate $x$ along the tube ( $\text{m}^2$ )
$A_{l,x}$	Cross-sectional area of the liquid phase at coordinate $x$ along the tube ( $\text{m}^2$ )
$A_x$	Flow cross-sectional area at coordinate $x$ ( $\text{m}^2$ )
$b:a$	Boundary between volumes $b$ and $a$ (-)
$c_p$	Specific heat at constant pressure ( $\text{J kg}^{-1} \text{K}^{-1}$ )
$c_v$	Specific heat at constant volume ( $\text{J kg}^{-1} \text{K}^{-1}$ )
$C_0$	Profile parameter for the drift-flux model (-)
$C_{0,x}$	Profile parameter (or flux concentration parameter, or distribution coefficient) (-)
$C_{\text{cond}}$	Time constant for the condensation rate ( $\text{s}^{-1}$ )
$C_{\text{evap}}$	Time constant for the evaporation rate ( $\text{s}^{-1}$ )
$dP_{f,x}$	Pressure loss along $dx$ at coordinate $x$ along the tube (Pa)
$D_{H,x}$	Tube hydraulic diameter at coordinate $x$ along the tube (m)
$D_x$	Tube diameter at coordinate $x$ along the tube (m)
$g$	Specific extensive quantity ( $[G]\cdot\text{kg}^{-1}$ )

$g$	Gravity constant ( $\text{m s}^{-2}$ )
$G_x$	Total value of specific extensive quantity $g$ in the tube from the origin up to coordinate $x$ ( $[G]$ )
$h_{b:a}$	Average specific enthalpy over $A_{b:a}$ ( $\text{J kg}^{-1}$ )
$h_{\text{bo},x}$	Heat transfer coefficient due to boiling at coordinate $x$ along the tube ( $\text{W m}^{-1} \text{K}^{-1}$ )
$h_{\text{g},a}^0$	Specific enthalpy of the liquid phase characteristic of the energy transfer due to mass transfer to the gas phase in volume $a$ ( $\text{J kg}^{-1}$ )
$h_{\text{l},a}^0$	Specific enthalpy of the liquid phase characteristic of the energy transfer due to mass transfer to the liquid phase in volume $a$ ( $\text{J kg}^{-1}$ )
$h_{\text{in}}$	Fluid specific enthalpy at the inlet ( $\text{J kg}^{-1}$ )
$h_{\text{out}}$	Fluid specific enthalpy at the outlet ( $\text{J kg}^{-1}$ )
$h_n$	Pump head (m)
$\bar{h}_n$	Dimensionless pump head (-)
$h_x$	Average specific enthalpy over $A_x$ ( $\text{J kg}^{-1}$ )
$h_{\text{g},x}$	Average specific enthalpy of the gas phase over $A_{\text{g},x}$ ( $\text{J kg}^{-1}$ )
$h_{\text{l},x}$	Average specific enthalpy of the liquid phase over $A_{\text{l},x}$ ( $\text{J kg}^{-1}$ )
$h_{\text{g},x}^0$	Specific enthalpy of the gas phase characteristic of the energy transfer due to mass transfer to the liquid phase at coordinate $x$ along the tube ( $\text{J kg}^{-1}$ )
$h_{\text{l},x}^0$	Specific enthalpy of the liquid phase characteristic of the energy transfer due to mass transfer to the gas phase at coordinate $x$ along the tube ( $\text{J kg}^{-1}$ )
$h_{w,x}$	Heat transfer coefficient at coordinate $x$ along the tube ( $\text{W m}^{-1} \text{K}^{-1}$ )
$j_x$	Average volumetric flux (or superficial velocity) over $A_x$ ( $\text{m s}^{-1}$ )
$j_{\text{g},x}$	Average superficial velocity of the gas phase over $A_{\text{g},x}$ ( $\text{m s}^{-1}$ )
$j_{\text{l},x}$	Average superficial velocity of the liquid phase over $A_{\text{l},x}$ ( $\text{m s}^{-1}$ )
$J$	Rotational inertia ( $\text{kg m}^2$ )
$J(b \rightarrow a)$	Total thermal diffusion through boundary $b:a$ , oriented positively from $b$ to $a$ (W)
$k$	Polytropic exponent (-)
$k$	Thermal conductivity ( $\text{W K}^{-1} \text{m}^{-2}$ )
$k_{b:a}$	Average thermal conductivity over $A_{b:a}$ ( $\text{W K}^{-1} \text{m}^{-2}$ )
$k_x$	Average thermal conductivity over $A_x$ ( $\text{W K}^{-1} \text{m}^{-2}$ )
$L$	Tube length (m)
$L_a$	Length of volume $a$ (m)
$L_x$	Average latent heat over $A_x$ ( $\text{J kg}^{-1}$ )
$\dot{m}_a(g \rightarrow l)$	Condensation mass flow rate from the gas phase to the liquid phase in volume $a$ ( $\text{kg s}^{-1}$ )
$\dot{m}_a(l \rightarrow g)$	Evaporation mass flow rate from the liquid phase to the gas phase in volume $a$ ( $\text{kg s}^{-1}$ )
$\dot{m}_{\text{cond}}$	Condensation mass flow rate ( $\text{kg s}^{-1}$ )
$\dot{m}_{\text{evap}}$	Evaporation mass flow rate ( $\text{kg s}^{-1}$ )

$\dot{m}_g(b \rightarrow a)$	Mass flow rate of the gas phase through boundary $b:a$ , oriented positively from $b$ to $a$ ( $\text{kg s}^{-1}$ )
$\dot{m}_l(b \rightarrow a)$	Mass flow rate of the liquid phase through boundary $b:a$ , oriented positively from $b$ to $a$ ( $\text{kg s}^{-1}$ )
$\dot{m}_g(x)$	Mass flow rate of the gas phase through $A_x$ ( $\text{kg s}^{-1}$ )
$\dot{m}_l(x)$	Mass flow rate of the liquid phase through $A_x$ ( $\text{kg s}^{-1}$ )
$M$	Molar mass of the mixture ( $\text{kg mol}^{-1}$ )
$M_g$	Molar mass of the gas phase ( $\text{kg mol}^{-1}$ )
$M_l$	Molar mass of the liquid phase ( $\text{kg mol}^{-1}$ )
$\vec{n}(b \rightarrow a)$	Orientation of boundary $b:a$ , positively from $b$ to $a$
$\vec{p}$	Fluid specific momentum ( $\text{m s}^{-1}$ )
$p_x$	Average fluid specific momentum over $A_x$ ( $\text{m s}^{-1}$ )
$P$	Fluid pressure (Pa)
$P_a$	Average pressure in volume $a$ (Pa)
$P_x$	Average pressure over $A_x$ (Pa)
$q$	Volumetric flow rate ( $\text{kg m}^{-3}$ )
$\bar{q}$	Dimensionless volumetric flow rate (-)
$r(x)$	Hyperbolic function (-)
$\mathfrak{R}$	Universal gas constant ( $\text{J mol}^{-1} \text{K}^{-1}$ )
$R_g$	Specific gas constant ( $\text{J kg}^{-1} \text{K}^{-1}$ )
$S$	Entropy ( $\text{J K}^{-1}$ )
$\text{sgn}(x)$	Sign function (-)
$T_{g,x}$	Temperature of the gas phase at coordinate $x$ along the tube (K)
$T_{l,x}$	Temperature of the liquid phase at coordinate $x$ along the tube (K)
$T_f$	Friction torque (N m)
$T_h$	Hydraulic torque (N m)
$\bar{T}_h$	Dimensionless hydraulic torque (-)
$T_m$	Motor torque (N m)
$u$	Fluid specific internal energy ( $\text{J kg}^{-1}$ )
$u_a$	Average specific internal energy inside volume $a$ ( $\text{J kg}^{-1}$ )
$u_x$	Average specific internal energy over $A_x$ ( $\text{J kg}^{-1}$ )
$\vec{v}$	Fluid velocity ( $\text{m s}^{-1}$ )
$v_x$	Average velocity over $A_x$ ( $\text{m s}^{-1}$ )
$v_{g,x}$	Average velocity of the gas phase over $A_{g,x}$ ( $\text{m s}^{-1}$ )
$v_{l,x}$	Average velocity of the liquid phase over $A_{l,x}$ ( $\text{m s}^{-1}$ )
$V_{gj,x}$	Drift velocity of the gas phase over $A_x$ ( $\text{m s}^{-1}$ )
$v_{gl,x}$	Average slip velocity between the gas phase and the liquid phase over $A_x$ ( $\text{m s}^{-1}$ )
$v_x(g \rightarrow l)$	Velocity of the gas phase entering the liquid phase at coordinate $x$ along the tube ( $\text{m s}^{-1}$ )
$v_x(l \rightarrow g)$	Velocity of the liquid phase entering the gas phase at coordinate $x$ along the tube ( $\text{m s}^{-1}$ )
$V(a)$	Set of volumes $b$ neighboring volume $a$
$V_a$	Volume of control volume $a$ ( $\text{m}^3$ )

$V_{g,a}$	Volume of the gas phase in volume $a$ ( $\text{m}^3$ )
$V_{l,a}$	Volume of the liquid phase in volume $a$ ( $\text{m}^3$ )
$\dot{W}_a$	Total heating power received by volume $a$ ( $\text{J s}^{-1}$ )
$\dot{W}_a(g \rightarrow l)$	Heat flow from the gas phase to the liquid phase in volume $a$ (W)
$\dot{W}_a(l \rightarrow g)$	Heat flow from the liquid phase to the gas phase in volume $a$ (W)
$\dot{W}_F(b \rightarrow a)$	Work produced by the forces acting on the boundary between $b$ and $a$ (W)
$\dot{W}_{g,a}$	Heat flow received from the wall into the gas phase in volume $a$ (W)
$\dot{W}_{l,a}$	Heat flow received from the wall into the liquid phase in volume $a$ (W)
$x_{g,a}$	Vapor mass fraction in the gas phase of volume $a$ (-)
$x_{l,a}$	Vapor mass fraction in the liquid phase of volume $a$ (-)
$x_{g,0}$	Set point for the vapor mass fraction in the gas phase (-)
$x_{l,0}$	Set point for the vapor mass fraction in the liquid phase (-)
$x_x$	Quality at coordinate $x$ along the tube (-)
$x_{v,x}$	Vapor mass fraction at coordinate $x$ along the tube (-)
$z_a$	Altitude of volume $a$ (m)
$z_x$	Tube altitude at coordinate $x$ (m)
$\alpha_a$	Average void fraction over volume $a$ (-)
$\alpha_x$	Average void fraction over cross-sectional area $A_x$ (-)
$\gamma$	Specific heat ratio (-)
$\gamma_x(g \rightarrow l)$	Mass transfer rate from the gas phase into the liquid phase at coordinate $x$ along the tube ( $\text{kg s}^{-1} \text{m}^{-3}$ )
$\gamma_x(l \rightarrow g)$	Mass transfer rate from the liquid phase into the gas phase at coordinate $x$ along the tube ( $\text{kg s}^{-1} \text{m}^{-3}$ )
$\Delta P_f(a \rightarrow b)$	Pressure loss due to friction between volumes $a$ and $b$ oriented positively from $a$ to $b$ (Pa)
$\epsilon_x$	Tube roughness at coordinate $x$ along the tube (m)
$\eta_h$	Hydraulic efficiency (-)
$\theta_x$	Tube angle with the horizontal line at coordinate $x$ (rad)
$\lambda_{a:b}$	Friction coefficient at boundary $a:b$ (-)
$\lambda_x$	Friction coefficient at coordinate $x$ along the tube (-)
$\mu_x$	Fluid viscosity at coordinate $x$ along the tube ( $\text{kg m}^{-1} \text{s}^{-1}$ )
$\mu_{g,x}$	Viscosity of the gas phase at coordinate $x$ along the tube ( $\text{kg m}^{-1} \text{s}^{-1}$ )
$\mu_{l,x}$	Viscosity of the liquid phase at coordinate $x$ along the tube ( $\text{kg m}^{-1} \text{s}^{-1}$ )
$\xi_{a:b}$	Pressure loss coefficient at boundary $a:b$ (-)
$\xi_x$	Pressure loss coefficient at coordinate $x$ along the tube (-)
$\pi_{l:g,x}$	Interfacial liquid-gas perimeter at coordinate $x$ along the tube (m)
$\pi_{w,x}$	Wetted perimeter of the wall at coordinate $x$ along the tube (m)
$\pi_{w:g,x}$	Wetted perimeter of the wall for the gas at coordinate $x$ along the tube (m)

$\pi_{w:l,x}$	Wetted perimeter of the wall for the liquid at coordinate $x$ along the tube (m)
$\rho$	Fluid density ( $\text{kg m}^{-3}$ )
$\rho_{b:a}$	Average fluid density over $A_{b:a}$ ( $\text{kg m}^{-3}$ )
$\rho_{g,a}$	Average density of the gas phase in volume $a$ ( $\text{kg m}^{-3}$ )
$\rho_{l,a}$	Average density of the liquid phase in volume $a$ ( $\text{kg m}^{-3}$ )
$\rho_{g,x}$	Average density of the gas phase over $A_x$ ( $\text{kg m}^{-3}$ )
$\rho_{l,x}$	Average density of the liquid phase over $A_x$ ( $\text{kg m}^{-3}$ )
$\tau_{l:g,x}$	Interfacial friction from the liquid phase acting on the gas phase at coordinate $x$ along the tube ( $\text{N m}^{-2}$ )
$\tau_{w:g,x}$	Friction from the wall acting on the gas phase at coordinate $x$ along the tube ( $\text{N m}^{-2}$ )
$\tau_{w:l,x}$	Friction from the wall acting on the liquid phase at coordinate $x$ along the tube ( $\text{N m}^{-2}$ )
$\tau_{w,x}$	Friction stress from the wall acting on the fluid at coordinate $x$ along the tube ( $\text{N m}^{-2}$ )
$\varphi_{w,x}$	Heat flux from the wall at coordinate $x$ along the tube ( $\text{W m}^{-2}$ )
$\varphi_{w:g,x}$	Heat flux received from the wall into the gas phase at coordinate $x$ along the tube ( $\text{W m}^{-2}$ )
$\varphi_{w:l,x}$	Heat flux received from the wall into the liquid phase at coordinate $x$ along the tube ( $\text{W m}^{-2}$ )
$\varphi_x(g \rightarrow l)$	Heat flux from the gas phase into the liquid phase at coordinate $x$ along the tube ( $\text{W m}^{-2}$ )
$\varphi_x(l \rightarrow g)$	Heat flux from the liquid phase into the gas phase at coordinate $x$ along the tube ( $\text{W m}^{-2}$ )
$\Phi_g(b \rightarrow a)$	Flow of specific extensive quantity $g$ through boundary $b:a$ , oriented positively from $b$ to $a$ ( $[g].\text{s}^{-1}$ )
$\Phi_g(x)$	Flow of specific extensive quantity $g$ at coordinate $x$ along the tube, oriented positively with increasing $x$ ( $[g].\text{s}^{-1}$ )
$\nabla T(b \rightarrow a)$	Average value of the temperature gradient over $A_{b:a}$ oriented positively from $b$ to $a$ ( $\text{K m}^{-1}$ )

## 4.1 Single-Phase Flow

### 4.1.1 General Formulation of the Balance Equations

The evolution of the physical state in time is given by the three balance equations: mass, energy, and momentum. In this section, the general formula for balance equations is given for  $g$  being a scalar specific extensive quantity.

Then in the following sections, the three balance equations will be derived by replacing  $g$  by the constant 1 for the mass balance equation, by the  $x$ -coordinate  $p_x$

of the specific momentum for the momentum balance equation, and by the specific internal energy  $u$  for the energy balance equation.

The general balance equation for the specific quantity  $g$  of a fluid with density  $\rho$  in control volume  $V_a$  is:

$$\frac{D}{Dt} \int_{V_a} \rho \cdot g \cdot dV = \Sigma \quad (4.1)$$

where  $\Sigma$  denotes terms depending on the balance equation [cf. (1.1)–(1.3)].

Developing the material derivative  $D/Dt$ :

$$\int_{V_a} \frac{\partial}{\partial t} (\rho \cdot g) \cdot dV = - \int_{V_a} \vec{\nabla} \cdot (\rho \cdot g \cdot \vec{v}) \cdot dV + \Sigma \quad (4.2)$$

with

$$\vec{\nabla} = \begin{pmatrix} \frac{\partial}{\partial x} \\ \frac{\partial}{\partial y} \\ \frac{\partial}{\partial z} \end{pmatrix} \quad (4.3)$$

Using the divergence theorem on the right-hand side of (4.2) and moving the time derivative outside the integral of the left-hand side of (4.2)<sup>1</sup>:

<sup>1</sup>In principle, the partial derivative with respect to time in (4.2) can be moved out of the integral only if the integration volume  $V_a$  is constant (i.e., does not vary in time). However, if the integration volume is not constant, one can consider a constant volume  $V'_a$  sufficiently large so as to contain  $V_a$  at all times and consider the fluid density  $\rho'$  that is equal to the fluid density  $\rho$  inside  $V_a$  and equal to zero outside of  $V_a$  and inside  $V'_a$ . Then

$$\int_{V_a} \rho \cdot g \cdot dV = \int_{V'_a} \rho' \cdot g \cdot dV$$

and

$$\int_{V_a} \frac{\partial}{\partial t} (\rho \cdot g) \cdot dV = \int_{V'_a} \frac{\partial}{\partial t} (\rho' \cdot g) \cdot dV$$

As  $V'_a$  is constant, the time derivative can be moved out of the integral

$$\int_{V_a} \frac{\partial}{\partial t} (\rho \cdot g) \cdot dV = \int_{V'_a} \frac{\partial}{\partial t} (\rho' \cdot g) \cdot dV = \frac{d}{dt} \int_{V'_a} \rho' \cdot g \cdot dV = \frac{d}{dt} \int_{V_a} \rho \cdot g \cdot dV$$

Control volumes varying in time are in particular to be found in tank models or two-phase cavity models (cf. Sects. 14.5.2 and 14.4.3).

$$\frac{d}{dt} \int_{V_a} \rho \cdot g \cdot dV = - \sum_{b \in V(a)} \int_{b:a} \rho \cdot g \cdot \vec{v} \cdot \vec{n}(a \rightarrow b) \cdot dA + \Sigma \quad (4.4)$$

where  $V(a)$  is the set of volumes  $b$  neighboring volume  $a$ .

Using (4.4) with (3.2), (3.6), and (3.8) yields the lumped formulation of the balance equation for  $g$ :

$$\frac{d(\rho_a \cdot V_a \cdot g_a)}{dt} = \sum_{b \in V(a)} \Phi_g(b \rightarrow a) + \Sigma \quad (4.5)$$

Using (4.4) with (3.4) and (3.13) on volume  $A_x \cdot \delta x$  where  $\delta x$  is a small length increment (cf. Fig. 3.2):

$$\delta x \cdot \frac{d(\rho_x \cdot A_x \cdot g_x)}{dt} = -(\Phi_g(x + \delta x) - \Phi_g(x)) + \delta \Sigma$$

Dividing by  $\delta x$  and taking the limit when  $\delta x$  tends to zero yields the distributed formulation of the balance equation for  $g$ :

$$\frac{\partial(\rho_x \cdot A_x \cdot g_x)}{\partial t} = -\frac{\partial \Phi_g(x)}{\partial x} + \frac{\partial \Sigma}{\partial x} \quad (4.6)$$

## 4.1.2 Mass Balance Equation

### 4.1.2.1 Lumped Formulation

Using (4.5) with  $g_a = 1$  and  $\Sigma = 0$  yields [cf. (3.3)]:

$$\frac{d(\rho_a \cdot V_a)}{dt} = \sum_{b \in V(a)} \dot{m}(b \rightarrow a) \quad (4.7)$$

### 4.1.2.2 Distributed Formulation

Using (4.6) with  $g_x = 1$  and  $\Sigma = 0$  yields:

$$\frac{\partial(\rho_x \cdot A_x)}{\partial t} = -\frac{\partial \Phi_1(x)}{\partial x} \quad (4.8)$$

Therefore, using (3.5):

$$\frac{\partial(\rho_x \cdot A_x)}{\partial t} = -\frac{\partial}{\partial x} \dot{m}(x) \quad (4.9)$$

or equivalently using (3.18):

$$\frac{\partial(\rho_x \cdot A_x)}{\partial t} = -\frac{\partial(\rho_x \cdot v_x \cdot A_x)}{\partial x} \quad (4.10)$$

### 4.1.3 Momentum Balance Equation

#### 4.1.3.1 Distributed Formulation

For the momentum balance equation, according to Newton's law,  $g$  is the component of interest of the average specific momentum  $\vec{p} = \vec{v}$ .

Hence,  $g_x = p_x = v_x$ ,  $v_x$  being the superficial velocity.

$\Sigma$  accounts for the pressure, gravity, and friction forces acting on the fluid. Then from (4.6), the momentum balance equation is:

$$\begin{aligned} \frac{\partial(\rho_x \cdot v_x \cdot A_x)}{\partial t} &= -\frac{\partial \Phi_v(x)}{\partial x} - \frac{\partial(A_x \cdot P_x)}{\partial x} + \frac{\partial A_x}{\partial x} \cdot P_x \\ &\quad - A_x \cdot \rho_x \cdot g \cdot \sin \theta_x - \text{sgn}(v_x) \cdot \pi_{w,x} \cdot \tau_{w,x} \end{aligned} \quad (4.11)$$

$P_x$  is the average pressure,  $\tau_{w,x}$  is the friction stress from the wall acting on the fluid,  $\theta_x$  is the tube angle with the horizontal line,  $\text{sgn}$  is the sign function, and  $\pi_{w,x}$  is the wetted perimeter of the wall. In (4.11),  $g$  is the gravity constant.  $\sin \theta_x = \partial z_x / \partial x$  where  $z_x$  is the elevation of the pipe at coordinate  $x$ .

The average pressure  $P_x$  is given by:

$$P_x = \frac{1}{A_x} \cdot \int_{A_x} P \cdot dA \quad (4.12)$$

On the right-hand side of (4.11), the second and third terms are, respectively, the forces acting on the fluid due to hydraulic and wall pressure, the fourth term is the gravity force, and the fifth term is the wall friction force.

Using (3.16) and (3.17) yields:

$$\Phi_v(x) = v_x \cdot \dot{m}(x) = \rho_x \cdot v_x^2 \cdot A_x \quad (4.13)$$

Then (4.11) can be rewritten as:

$$\frac{\partial(\rho_x \cdot v_x \cdot A_x)}{\partial t} = -\frac{\partial}{\partial x}(\rho_x \cdot v_x^2 \cdot A_x) - A_x \cdot \frac{\partial P_x}{\partial x} - A_x \cdot \rho_x \cdot g \cdot \sin \theta_x - \text{sgn}(v_x) \cdot \pi_{w,x} \cdot \tau_{w,x} \quad (4.14)$$

or equivalently using (3.18):

$$\frac{\partial}{\partial t} \dot{m}(x) = -\frac{\partial}{\partial x} \left( \frac{\dot{m}^2(x)}{\rho_x \cdot A_x} \right) - A_x \cdot \frac{\partial P_x}{\partial x} - A_x \cdot \rho_x \cdot g \cdot \sin \theta_x - \text{sgn}(\dot{m}(x)) \cdot \pi_{w,x} \cdot \tau_{w,x} \quad (4.15)$$

Using the mass balance Eq. (4.10) inside (4.14), the momentum balance equation can also be written as:

$$\frac{\partial v_x}{\partial t} = -\frac{\partial}{\partial x} \left( \frac{v_x^2}{2} \right) - \frac{1}{\rho_x} \cdot \frac{\partial P_x}{\partial x} - g \cdot \frac{\partial z_x}{\partial x} - \text{sgn}(v_x) \cdot \frac{\pi_{w,x}}{\rho_x \cdot A_x} \cdot \tau_{w,x} \quad (4.16)$$

If the fluid is incompressible (i.e., the density is constant w.r.t.  $x$ ) and if viscous effects are neglected (no pressure losses), then (4.16) yields the Bernoulli theorem:

$$P_x + \frac{\rho \cdot v_x^2}{2} + \rho \cdot g \cdot z_x = \text{cte} \quad (4.17)$$

$P_x + \frac{\rho \cdot v_x^2}{2}$  is defined as the total pressure,  $P_x$  being the static pressure.

#### 4.1.3.2 Lumped Formulation

Integrating (4.15) over the whole pipe length yields:

$$\begin{aligned} L \cdot \frac{d\langle \dot{m}(a \rightarrow b) \rangle}{dt} &= \frac{\dot{m}^2(0)}{\rho_0 \cdot A_0} - \frac{\dot{m}^2(L)}{\rho_L \cdot A_L} + A_0 \cdot P_0 - A_L \cdot P_L \\ &+ \int_0^L \frac{\partial A_x}{\partial x} \cdot P_x \cdot dx - g \cdot \int_0^L A_x \cdot \rho_x \cdot \sin \theta_x \cdot dx \\ &- \int_0^L \text{sgn}(\dot{m}(x)) \cdot \pi_{w,x} \cdot \tau_{w,x} \cdot dx \end{aligned} \quad (4.18)$$

where

$$\langle \dot{m}(a \rightarrow b) \rangle = \frac{1}{L} \cdot \int_0^L \dot{m}(x) \cdot dx \quad (4.19)$$

is the average mass flow rate over the whole volume going from  $A_0$  to  $A_L$ . The integration path extends from the center of volume  $a$  to the center of volume  $b$ .

Note that this equation is valid whatever the position of  $A_0$  within  $a$  and  $A_L$  within  $b$ , so that the volume used for computing  $\langle \dot{m}(a \rightarrow b) \rangle$  does not necessarily have to extend from the center of volume  $a$  to the center of volume  $b$ .

Note also that according to (3.6):

$$\rho_a = \frac{1}{V_a} \cdot \int_0^{L_a} \rho_x \cdot A_x \cdot dx \quad (4.20)$$

where  $L_a$  is the length of volume  $a$ . Here, the integration path extends from the left edge of volume  $a$  to the right edge of volume  $a$ .

So, comparing (4.20) with (3.7), in general  $\rho_a \neq \rho_0$  unless  $A_0$  is chosen such that  $\frac{1}{A_0} \cdot \int_{A_0} \rho \cdot dA = \frac{1}{V_a} \cdot \int_0^{L_a} \rho_x \cdot A_x \cdot dx$  (idem for  $\rho_L$  w.r.t. volume  $b$ ).

#### 4.1.4 Energy Balance Equation

##### 4.1.4.1 Lumped Formulation

For the energy balance equation, according to the first law of thermodynamics,  $g_a$  is the average specific internal energy  $u_a$  and  $\Sigma$  is the heat and work provided to the fluid (cf. Sect. 2.8.1).

Then from (4.5), the mass balance equation is:

$$\begin{aligned} \frac{d(\rho_a \cdot V_a \cdot u_a)}{dt} &= \sum_{b \in V(a)} \Phi_u(b \rightarrow a) + \sum_{b \in V(a)} J(b \rightarrow a) \\ &\quad + \sum_{b \in V(a)} \dot{W}_F(b \rightarrow a) + \dot{W}_a \end{aligned} \quad (4.21)$$

where  $J(b \rightarrow a)$  is the heat received by thermal diffusion from  $b$  to  $a$ ,  $\dot{W}_F(b \rightarrow a)$  is the work produced by the forces acting on the boundary between  $b$  and  $a$ , and  $\dot{W}_a$  is the total heat power received from the wall.

Diffusion is not neglected at this point because it becomes the predominant phenomenon for heat transfer when mass flow rates go to zero. It is given by:

$$J(b \rightarrow a) = - \int_{b:a} k \cdot \nabla \vec{T} \cdot \vec{n}(b \rightarrow a) \cdot dA = -\nabla T(b \rightarrow a) \cdot \int_{b:a} k \cdot dA \quad (4.22)$$

where  $\nabla T(b \rightarrow a)$  is the average value of the temperature gradient on the boundary, oriented positively from  $b$  to  $a$  (which means that  $\nabla T(b \rightarrow a) > 0$  when  $T_a > T_b$ ) and  $k$  is the fluid thermal conductivity.

Using the average thermal conductivity on the boundary:

$$k_{b:a} = \frac{1}{A_{b:a}} \cdot \int_{b:a} k \cdot dA \quad (4.23)$$

one gets:

$$J(b \rightarrow a) = -k_{b:a} \cdot \nabla T(b \rightarrow a) \cdot A_{b:a} \quad (4.24)$$

If only pressure forces are considered to compute  $\dot{W}_F$  (i.e., if work produced by friction and gravity forces is neglected); cf. (3.2):

$$\dot{W}_F(b \rightarrow a) = \Phi_{P/\rho}(b \rightarrow a) \quad (4.25)$$

Noticing that

$$\Phi_u(b \rightarrow a) + \Phi_{P/\rho}(b \rightarrow a) = \Phi_h(b \rightarrow a) \quad (4.26)$$

with the specific enthalpy  $h$  defined as

$$h = u + \frac{P}{\rho} \quad (4.27)$$

from (4.21) and (3.11), the energy balance equation can be written as:

$$\frac{d(\rho_a \cdot V_a \cdot u_a)}{dt} = \sum_{b \in V(a)} (h_{b:a} \cdot \dot{m}(b \rightarrow a) - k_{b:a} \cdot \nabla T(b \rightarrow a) \cdot A_{b:a}) + \dot{W}_a \quad (4.28)$$

$h_{b:a}$  being the average specific enthalpy on the boundary:

$$h_{b:a} = \left( u + \frac{P}{\rho} \right)_{b:a} \quad (4.29)$$

To account for the kinetic and the potential energies, one should replace  $u$  in (4.29) by

$$e = u + \frac{p^2}{2} + g \cdot z \quad (4.30)$$

where  $\vec{p}$  is the specific momentum.

#### 4.1.4.2 Distributed Formulation

The distributed formulation of the energy balance equation can be directly derived from the lumped formulation (4.28) following the same principle as the derivation of (4.6) from (4.5):

$$\frac{\partial}{\partial t} (\rho_x \cdot A_x \cdot u_x) = -\frac{\partial}{\partial x} \left( h_{x:} \cdot \dot{m}(x) - A_x \cdot k_x \cdot \frac{\partial T_x}{\partial x} \right) + \varphi_{w,x} \cdot \pi_{w,x} \quad (4.31)$$

where  $k_x$  is the average of  $k$  over cross-sectional  $A_x$ , and  $\varphi_{w,x}$  is the heat flux from the wall.

From (3.13), notice that:

$$u_x = \frac{1}{\rho_x \cdot A_x} \cdot \int_{A_x} \rho \cdot u \cdot dA \quad (4.32)$$

whereas from (3.15):

$$h_{x:} = \frac{\Phi_h(x)}{\dot{m}(x)} \quad (4.33)$$

Then, the distributed formulation of the energy balance equation can also be written as:

$$\frac{\partial}{\partial t} (\rho_x \cdot A_x \cdot u_x) = -\frac{\partial}{\partial x} \left( h_{x:} \cdot \rho_x \cdot v_x \cdot A_x - A_x \cdot k_x \cdot \frac{\partial T_x}{\partial x} \right) + \varphi_{w,x} \cdot \pi_{w,x} \quad (4.34)$$

Note that strictly speaking,  $h_{x:} \neq h_x$  with  $h_x$  given by (4.33) and  $h_x = \frac{1}{\rho_x \cdot A_x} \cdot \int_{A_x} \rho \cdot h \cdot dA$ ; cf. (3.13). However, the distinction between  $h_{x:}$  and  $h_x$  will not always be made in the sequel.

## 4.2 Two-Phase Water/Steam Flow

### 4.2.1 Definitions

Two-phase flow will be formulated here as a mixture model or as a two-fluid model.

For a vertical pipe with a rising average flow, the different flow configurations as a function of gas proportion (gas–liquid flow) are: (a) bubble flow, (b) slug of plug, (c) churn, (d), annular, and (e) wispy annular flow; cf. Fig. 4.1.

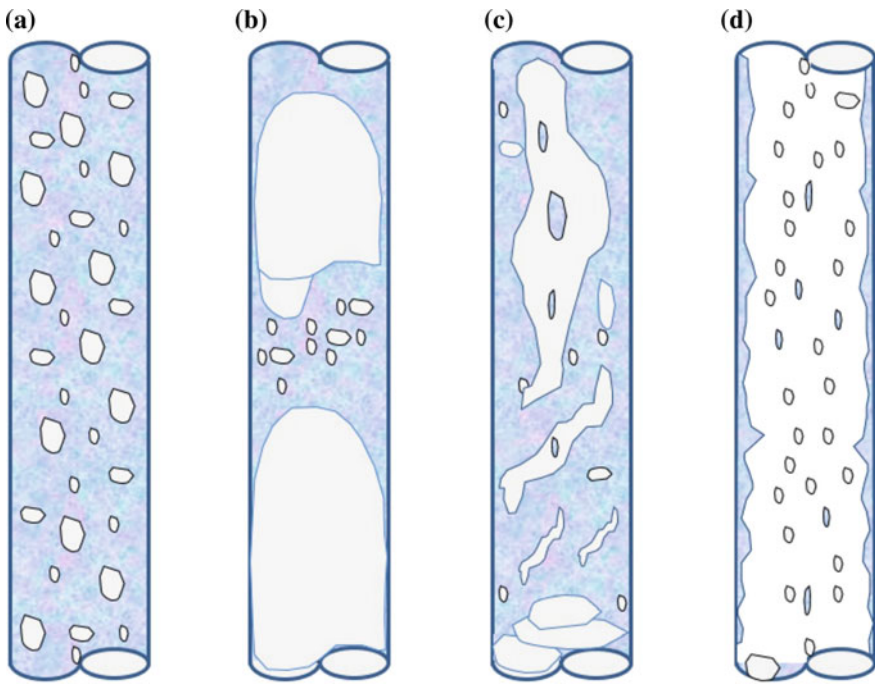


**Fig. 4.1** Flow configurations for a vertical tube: **a** dispersed bubble flow, **b** plug flow, **c** churn flow (stirred), and **d** annular flow

For the mixture model, the two phases are considered to be at equilibrium (momentum and energy), but may have different velocities. The fluid equations are formulated as one single-phase fluid with two-phase properties properly defined. This formulation is useful when the two phases are strongly mixed, thus removing degrees of freedom between them (e.g., one temperature state instead of two).

For the two-fluid model, the two phases are considered to be out of equilibrium. Therefore, the number of degrees of freedom cannot be reduced by using mixture models. The fluid equations are formulated as two single-phase fluids, exchanging mass, momentum, and energy through the interface separating the two phases. However, this formulation is only practical when the interface has a simple geometry such as in smooth-stratified flow (e.g., the plane steam/water interface in a boiler or in a condenser).

It is possible to use together mixture and two-fluid equations, depending on the respective evolution of the state variables between the two phases (i.e., whether they remain at equilibrium or not), ending up in a model with three (mixture mass, energy, and momentum), four (e.g., mixture mass and energy, two-fluid momentum), five (e.g., two-fluid mass and energy, mixture momentum), or six (two-fluid mass, energy, and momentum) equations.

When the two phases are saturated, one phase (e.g., steam) may contain a few amounts (e.g., droplets) of the other phase (e.g., water). The two-phase model can then be extended to a two-mixture model, the first mixture being predominantly steam (with droplets) and the other being predominantly water (with bubbles). This does not change the overall number of equations. In this case, the subscript l and g will, respectively, denote the predominantly liquid and gas phases (or dense and light phases).

The two-fluid model is useful, for instance, for describing the shrink–swell phenomenon in boilers, because the two phases cannot be considered at thermodynamic equilibrium.

The average void fraction over volume  $a$  is defined as:

$$\alpha_a = \frac{V_{g,a}}{V_a} \quad (4.35)$$

where  $V_{g,a}$  is the volume of the gas phase within volume  $a$ .

The average void fraction over the cross-sectional area  $A_x$  is defined as:

$$\alpha_x = \frac{A_{g,x}}{A_x} \quad (4.36)$$

where  $A_{g,x}$  is the cross-sectional area of the vapor phase.

The mass flow rates for each phase are:

$$\dot{m}_l(x) = \rho_{l,x} \cdot v_{l,x} \cdot A_{l,x} = (1 - \alpha_x) \cdot \rho_{l,x} \cdot v_{l,x} \cdot A_x = \rho_{l,x} \cdot j_{l,x} \cdot A_x \quad (4.37a)$$

$$\dot{m}_g(x) = \rho_{g,x} \cdot v_{g,x} \cdot A_{g,x} = \alpha_x \cdot \rho_{g,x} \cdot v_{g,x} \cdot A_x = \rho_{g,x} \cdot j_{g,x} \cdot A_x \quad (4.37b)$$

where  $v_{l,x}$  is the velocity of the liquid,  $v_{g,x}$  is the velocity of the gas,  $j_{l,x}$  is the superficial velocity of the liquid, and  $j_{g,x}$  is the superficial velocity of the gas.

$$j_{l,x} = (1 - \alpha_x) \cdot v_{l,x} \quad (4.38a)$$

$$j_{g,x} = \alpha_x \cdot v_{g,x} \quad (4.38b)$$

The total volumetric flux (or superficial velocity) is:

$$j_x = j_{l,x} + j_{g,x} \quad (4.39)$$

$v_{gl,x}$  is the slip velocity between the vapor and the liquid phase:

$$v_{gl,x} = v_{g,x} - v_{l,x} \quad (4.40)$$

The total mass flow rate is:

$$\begin{aligned}\dot{m}(x) &= \dot{m}_l(x) + \dot{m}_g(x) \\ &= (1 - \alpha_x) \cdot \rho_{l,x} \cdot v_{l,x} \cdot A_x + \alpha_x \cdot \rho_{g,x} \cdot v_{g,x} \cdot A_x\end{aligned}\quad (4.41)$$

The quality is defined as:

$$x_x = \frac{\dot{m}_g(x)}{\dot{m}(x)} \quad (4.42)$$

Using (4.37b) and (4.41):

$$x_x = \frac{\alpha_x \cdot \rho_{g,x} \cdot v_{g,x}}{(1 - \alpha_x) \cdot \rho_{l,x} \cdot v_{l,x} + \alpha_x \cdot \rho_{g,x} \cdot v_{g,x}} \quad (4.43)$$

The density of the mixture is:

$$\rho_x = (1 - \alpha_x) \cdot \rho_{l,x} + \alpha_x \cdot \rho_{g,x} \quad (4.44)$$

In order to have an expression for the mass flow rate of the mixture similar to the expression for the mass flow rate of the single-phase flow

$$\dot{m}(x) = \rho_x \cdot v_x \cdot A_x \quad (4.45)$$

using (4.41), the velocity of the mixture is defined as:

$$v_x = \frac{(1 - \alpha_x) \cdot \rho_{l,x} \cdot v_{l,x} + \alpha_x \cdot \rho_{g,x} \cdot v_{g,x}}{\rho_x} \quad (4.46)$$

The specific enthalpy  $h_x$  of the mixture is defined such that:

$$h_x \cdot \dot{m}(x) = h_{l,x} \cdot \dot{m}_l(x) + h_{g,x} \cdot \dot{m}_g(x) \quad (4.47)$$

where  $h_{l,x}$  and  $h_{g,x}$  are, respectively, the values of the specific enthalpy for the liquid and the gas.

Using (4.47) with (4.41) and (4.42) yields:

$$h_x = (1 - x_x) \cdot h_{l,x} + x_x \cdot h_{g,x} \quad (4.48)$$

## 4.2.2 Mass Balance Equation

### 4.2.2.1 Distributed Two-Fluid Formulation

Equation (4.10) is written for each fluid using the void fraction [cf. (4.36)], taking into account the mass transfer between the two fluids.

$$\frac{\partial((1 - \alpha_x) \cdot \rho_{l,x} \cdot A_x)}{\partial t} = -\frac{\partial}{\partial x} [(1 - \alpha_x) \cdot \rho_{l,x} \cdot v_{l,x} \cdot A_x] + \gamma_x(g \rightarrow l) \cdot A_x \quad (4.49a)$$

$$\frac{\partial(\alpha_x \cdot \rho_{g,x} \cdot A_x)}{\partial t} = -\frac{\partial}{\partial x} (\alpha_x \cdot \rho_{g,x} \cdot v_{g,x} \cdot A_x) + \gamma_x(l \rightarrow g) \cdot A_x \quad (4.49b)$$

where

$$\gamma_x(g \rightarrow l) = \frac{1}{A_x} \cdot \int_{A_x} \gamma(g \rightarrow l) \cdot dA \quad (4.50a)$$

$$\gamma_x(l \rightarrow g) = \frac{1}{A_x} \cdot \int_{A_x} \gamma(l \rightarrow g) \cdot dA \quad (4.50b)$$

$\gamma(g \rightarrow l)$  and  $\gamma(l \rightarrow g)$  being, respectively, the local mass transfer rate from the gas phase into the liquid phase, and local mass transfer rate from the liquid phase into the gas phase.

#### 4.2.2.2 Distributed Mixture Formulation

Supposing that the net mass transfer between the two phases is null, then:

$$\gamma_x(g \rightarrow l) + \gamma_x(l \rightarrow g) = 0 \quad (4.51)$$

With this assumption, adding (4.49a) and (4.49b) then using (4.41) and (4.44) yields:

$$\frac{\partial(\rho_x \cdot A_x)}{\partial t} = -\frac{\partial}{\partial x} (\rho_x \cdot v_x \cdot A_x) \quad (4.52)$$

The mass balance equation for the mixture is identical to the single-phase formulation (4.10).

#### 4.2.2.3 Lumped Two-Fluid Formulation

Equation (4.7) is written for each fluid, taking into account the mass transfer between the two fluids.

$$\frac{d(\rho_{l,a} \cdot V_{l,a})}{dt} = \sum_{b \in V(a)} \dot{m}_l(b \rightarrow a) + \dot{m}_a(g \rightarrow l) \quad (4.53a)$$

$$\frac{d(\rho_{g,a} \cdot V_{g,a})}{dt} = \sum_{b \in V(a)} \dot{m}_g(b \rightarrow a) + \dot{m}_a(l \rightarrow g) \quad (4.53b)$$

where  $\dot{m}_a(g \rightarrow l)$  and  $\dot{m}_a(l \rightarrow g)$  denote, respectively, the mass flow rate from the gas phase to the liquid phase, and the mass flow rate from the liquid phase to the gas phase within volume  $a$ .

$$\dot{m}_a(g \rightarrow l) = \frac{1}{V_a} \cdot \int_a \gamma(g \rightarrow l) \cdot dV \quad (4.54a)$$

$$\dot{m}_a(l \rightarrow g) = \frac{1}{V_a} \cdot \int_a \gamma(l \rightarrow g) \cdot dV \quad (4.54b)$$

#### 4.2.2.4 Lumped Mixture Formulation

Supposing that the net mass flow rate between the two phases is null, then:

$$\dot{m}_a(g \rightarrow l) + \dot{m}_a(l \rightarrow g) = 0 \quad (4.55)$$

With this assumption, adding Eqs. (4.53a) and (4.53b) yields:

$$\frac{d(\rho_a \cdot V_a)}{dt} = \sum_{b \in V(a)} \dot{m}(b \rightarrow a) \quad (4.56)$$

The mass balance equation for the mixture is identical to the single-phase formulation (4.7).

#### 4.2.3 Momentum Balance Equation

##### 4.2.3.1 Distributed Two-Fluid Formulation

Equation (4.14) is written for each fluid using the void fraction [cf. (4.36)], taking into account the momentum transfer between the two fluids.

$$\begin{aligned}
\frac{\partial((1 - \alpha_x) \cdot \rho_{l,x} \cdot v_{l,x} \cdot A_x)}{\partial t} = & -\frac{\partial}{\partial x} \left[ (1 - \alpha_x) \cdot \rho_{l,x} \cdot v_{l,x}^2 \cdot A_x \right] \\
& - (1 - \alpha_x) \cdot A_x \cdot \frac{\partial P_x}{\partial x} - (1 - \alpha_x) \cdot A_x \cdot \rho_{l,x} \cdot g \cdot \sin \theta_x \\
& - \operatorname{sgn}(v_{l,x}) \cdot \pi_{w:l,x} \cdot \tau_{w:l,x} + \operatorname{sgn}(v_{g,l,x}) \cdot \pi_{l:g,x} \cdot \tau_{l:g,x} \\
& + \gamma_x(g \rightarrow l) \cdot v_x(g \rightarrow l) \cdot A_x
\end{aligned} \tag{4.57a}$$

$$\begin{aligned}
\frac{\partial(\alpha_x \cdot \rho_{g,x} \cdot v_{g,x} \cdot A_x)}{\partial t} = & -\frac{\partial}{\partial x} (\alpha_x \cdot \rho_{g,x} \cdot v_{g,x}^2 \cdot A_x) \\
& - \alpha_x \cdot A_x \cdot \frac{\partial P_x}{\partial x} - \alpha_x \cdot A_x \cdot \rho_{g,x} \cdot g \cdot \sin \theta_x \\
& - \operatorname{sgn}(v_{g,x}) \cdot \pi_{w:g,x} \cdot \tau_{w:g,x} - \operatorname{sgn}(v_{g,l,x}) \cdot \pi_{l:g,x} \cdot \tau_{l:g,x} \\
& + \gamma_x(l \rightarrow g) \cdot v_x(l \rightarrow g) \cdot A_x
\end{aligned} \tag{4.57b}$$

$v_x(g \rightarrow l)$  is the velocity of the gas phase entering the liquid phase,  $\pi_{w:l,x}$  is the wetted perimeter of the wall for the liquid, and  $\tau_{w:l,x}$  is the friction from the wall acting on the liquid.  $\gamma_x(g \rightarrow l)$  is defined by (4.50a).

$v_x(l \rightarrow g)$  is the velocity of the liquid phase entering the gas phase,  $\pi_{w:g,x}$  is the wetted perimeter of the wall for the gas, and  $\tau_{w:g,x}$  is the friction from the wall acting on the gas.  $\gamma_x(l \rightarrow g)$  is defined by (4.50b).

$\pi_{l:g,x}$  is the interfacial perimeter, and  $\tau_{l:g,x}$  is the interfacial friction from the liquid acting on the gas.

#### 4.2.3.2 Distributed Mixture Formulation

Supposing that the net momentum transfer between the two phases is null (mechanical equilibrium at the interface), then:

$$\gamma_x(g \rightarrow l) \cdot v_x(g \rightarrow l) + \gamma_x(l \rightarrow g) \cdot v_x(l \rightarrow g) = 0 \tag{4.58}$$

With this assumption, adding (4.57a) and (4.57b) yields:

$$\begin{aligned}
\frac{\partial(\rho_x \cdot v_x \cdot A_x)}{\partial t} = & -\frac{\partial}{\partial x} \left( \rho_x \cdot v_x^2 \cdot A_x + \alpha_x \cdot (1 - \alpha_x) \cdot \frac{\rho_{l,x} \cdot \rho_{g,x}}{\rho_x} \cdot v_{gl,x}^2 \cdot A_x \right) \\
& - A_x \cdot \frac{\partial P_x}{\partial x} - A_x \cdot \rho_x \cdot g \cdot \sin \theta_x - \operatorname{sgn}(v_x) \cdot \pi_{w,x} \cdot \tau_{w,x}
\end{aligned} \tag{4.59}$$

The first term on the right-hand side of the equation is obtained by using the (not so obvious) identity:

$$(1 - \alpha_x) \cdot \rho_{l,x} \cdot v_{l,x}^2 + \alpha_x \cdot \rho_{g,x} \cdot v_{g,x}^2 \equiv \rho_x \cdot v_x^2 + \alpha_x \cdot (1 - \alpha_x) \cdot \frac{\rho_{l,x} \cdot \rho_{g,x}}{\rho_x} \cdot v_{gl,x}^2 \quad (4.60)$$

*Proof*

$$\begin{aligned} (1 - \alpha_x) \cdot \rho_{l,x} \cdot v_{l,x}^2 + \alpha_x \cdot \rho_{g,x} \cdot v_{g,x}^2 &= \frac{(1 - \alpha_x) \cdot \rho_{l,x} \cdot \rho_x \cdot v_{l,x}^2 + \alpha_x \cdot \rho_{g,x} \cdot \rho_x \cdot v_{g,x}^2}{\rho_x} \\ &= \frac{(1 - \alpha_x) \cdot \rho_{l,x} \cdot [(1 - \alpha_x) \cdot \rho_{l,x} + \alpha_x \cdot \rho_{g,x}] \cdot v_{l,x}^2}{\rho_x} \\ &\quad + \frac{\alpha_x \cdot \rho_{g,x} \cdot [(1 - \alpha_x) \cdot \rho_{l,x} + \alpha_x \cdot \rho_{g,x}] \cdot v_{g,x}^2}{\rho_x} \\ &= \frac{[(1 - \alpha_x)^2 \cdot \rho_{l,x}^2 + \alpha_x \cdot (1 - \alpha_x) \cdot \rho_{l,x} \cdot \rho_{g,x}] \cdot v_{l,x}^2}{\rho_x} \\ &\quad + \frac{[\alpha_x^2 \cdot \rho_{g,x}^2 + \alpha_x \cdot (1 - \alpha_x) \cdot \rho_{l,x} \cdot \rho_{g,x}] \cdot v_{g,x}^2}{\rho_x} \\ &= \frac{(1 - \alpha_x)^2 \cdot \rho_{l,x}^2 \cdot v_{l,x}^2 + \alpha_x^2 \cdot \rho_{g,x}^2 \cdot v_{g,x}^2}{\rho_x} \\ &\quad + \frac{\alpha_x \cdot (1 - \alpha_x) \cdot \rho_{l,x} \cdot \rho_{g,x} \cdot (v_{l,x}^2 + v_{g,x}^2)}{\rho_x} \\ &= \frac{(1 - \alpha_x)^2 \cdot \rho_{l,x}^2 \cdot v_{l,x}^2 + \alpha_x^2 \cdot \rho_{g,x}^2 \cdot v_{g,x}^2}{\rho_x} \\ &\quad + \frac{\alpha_x \cdot (1 - \alpha_x) \cdot \rho_{l,x} \cdot \rho_{g,x} \cdot [(v_{g,x} - v_{l,x})^2 + 2 \cdot v_{g,x} \cdot v_{l,x}]}{\rho_x} \\ &= \frac{[(1 - \alpha_x) \cdot \rho_{l,x} \cdot v_{l,x} + \alpha_x \cdot \rho_{g,x} \cdot v_{g,x} \cdot \rho_{g,x}]^2}{\rho_x} \\ &\quad + \frac{\alpha_x \cdot (1 - \alpha_x) \cdot \rho_{l,x} \cdot \rho_{g,x} \cdot (v_{g,x} - v_{l,x})^2}{\rho_x} \\ &= \frac{(\rho_x \cdot v_x)^2 + \alpha_x \cdot (1 - \alpha_x) \cdot \rho_{l,x} \cdot \rho_{g,x} \cdot v_{gl,x}^2}{\rho_x} \\ &= \rho_x \cdot v_x^2 + \alpha_x \cdot (1 - \alpha_x) \cdot \frac{\rho_{l,x} \cdot \rho_{g,x}}{\rho_x} \cdot v_{gl,x}^2 \end{aligned}$$

The proof uses (4.40), (4.44), and (4.46).

The momentum balance equation for the mixture is different from the single-phase formulation (4.14), the difference term being:

$$\delta_{\text{gl},x} = \alpha_x \cdot (1 - \alpha_x) \cdot \frac{\rho_{l,x} \cdot \rho_{g,x}}{\rho_x} \cdot v_{\text{gl},x}^2 \cdot A_x \quad (4.61)$$

on the right-hand side of (4.59).

However, if  $v_{l,x} = v_{g,x}$  (homogeneous flow model; cf. Sect. 4.2.5.1), then  $\delta_{\text{gl},x} = 0$  and the momentum balance equation for the mixture is identical to the single-phase formulation (4.14).

#### 4.2.3.3 Lumped Two-Fluid Formulation

Equation (4.18) is written for each fluid, taking into account the momentum transfer between the two fluids.

$$\begin{aligned} L \cdot \frac{d\langle \dot{m}_l(a \rightarrow b) \rangle}{dt} &= \frac{\dot{m}_l^2(0)}{\rho_{l,0} \cdot (1 - \alpha_0) \cdot A_0} - \frac{\dot{m}_l^2(L)}{\rho_{l,L} \cdot (1 - \alpha_L) \cdot A_L} \\ &\quad + (1 - \alpha_0) \cdot A_0 \cdot P_0 - (1 - \alpha_L) \cdot A_L \cdot P_L \\ &\quad + \int_0^L \frac{\partial((1 - \alpha_x) \cdot A_x)}{\partial x} \cdot P_x \cdot dx \\ &\quad - g \cdot \int_0^L (1 - \alpha_x) \cdot A_x \cdot \rho_{l,x} \cdot \sin \theta_x \cdot dx \\ &\quad - \int_0^L \operatorname{sgn}(\dot{m}(x)) \cdot \pi_{w:l,x} \cdot \tau_{w:l,x} \cdot dx \\ &\quad + \int_0^L \operatorname{sgn}(v_{\text{gl},x}) \cdot \pi_{l:g,x} \cdot \tau_{l:g,x} \cdot dx \\ &\quad + \int_0^L \gamma_x(g \rightarrow l) \cdot v_x(g \rightarrow l) \cdot A_x \cdot dx \end{aligned} \quad (4.62a)$$

$$\begin{aligned}
L \cdot \frac{d\langle \dot{m}_g(a \rightarrow b) \rangle}{dt} = & \frac{\dot{m}_g^2(0)}{\rho_{g,0} \cdot \alpha_0 \cdot A_0} - \frac{\dot{m}_g^2(L)}{\rho_{g,L} \cdot \alpha_L \cdot A_L} \\
& + \alpha_0 \cdot A_0 \cdot P_0 - \alpha_L \cdot A_L \cdot P_L \\
& + \int_0^L \frac{\partial(\alpha_x \cdot A_x)}{\partial x} \cdot P_x \cdot dx \\
& - g \cdot \int_0^L \alpha_x \cdot A_x \cdot \rho_{g,x} \cdot \sin \theta_x \cdot dx \\
& - \int_0^L \text{sgn}(\dot{m}(x)) \cdot \pi_{w:g,x} \cdot \tau_{w:g,x} \cdot dx \\
& - \int_0^L \text{sgn}(v_{gl,x}) \cdot \pi_{l:g,x} \cdot \tau_{l:g,x} \cdot dx \\
& + \int_0^L \gamma_x(l \rightarrow g) \cdot v_x(l \rightarrow g) \cdot A_x \cdot dx
\end{aligned} \tag{4.62b}$$

$v_x(g \rightarrow l)$  is the velocity of the gas phase entering the liquid phase,  $\pi_{w:l,x}$  is the wetted perimeter of the wall for the liquid, and  $\tau_{w:l,x}$  is the friction from the wall acting on the liquid.  $\gamma_x(g \rightarrow l)$  is defined by (4.50a).

$v_x(l \rightarrow g)$  is the velocity of the liquid phase entering the gas phase,  $\pi_{w:g,x}$  is the wetted perimeter of the wall for the gas, and  $\tau_{w:g,x}$  is the friction from the wall acting on the gas.  $\gamma_x(l \rightarrow g)$  is defined by (4.50b).

$\pi_{l:g,x}$  is the interfacial perimeter, and  $\tau_{l:g,x}$  is the interfacial friction from the liquid acting on the gas.

#### 4.2.3.4 Lumped Mixture Formulation

Supposing that the net momentum transfer between the two phases is null (mechanical equilibrium at the interface), then:

$$\gamma_x(g \rightarrow l) \cdot v_x(g \rightarrow l) + \gamma_x(l \rightarrow g) \cdot v_x(l \rightarrow g) = 0 \tag{4.63}$$

With this assumption, adding (4.62a) and (4.62b) in the same manner as for (4.59) yields:

$$\begin{aligned}
L \cdot \frac{d\langle \dot{m}(a \rightarrow b) \rangle}{dt} = & \frac{\dot{m}^2(0)}{\rho_0 \cdot A_0} - \frac{\dot{m}^2(L)}{\rho_L \cdot A_L} \\
& + \alpha_0 \cdot (1 - \alpha_0) \cdot \frac{\rho_{l,0} \cdot \rho_{g,0}}{\rho_0} \cdot v_{gl,0}^2 \cdot A_0 \\
& - \alpha_L \cdot (1 - \alpha_L) \cdot \frac{\rho_{l,L} \cdot \rho_{g,L}}{\rho_L} \cdot v_{gl,L}^2 \cdot A_L \\
& + (A_0 \cdot P_0) - (A_L \cdot P_L) + \int_0^L \frac{\partial A_x}{\partial x} \cdot P_x \cdot dx \\
& - g \cdot \int_0^L A_x \cdot \rho_x \cdot \sin \theta_x \cdot dx - \int_0^L \operatorname{sgn}(\dot{m}(x)) \cdot \pi_{w,x} \cdot \tau_{w,x} \cdot dx
\end{aligned} \tag{4.64}$$

If  $v_{l,x} = v_{g,x}$  (homogeneous flow model; cf. Sect. 4.2.5.1), then  $v_{gl,0}^2 = v_{gl,L}^2 = 0$  and the momentum balance equation is identical to the single-phase formulation (4.18).

#### 4.2.4 Energy Balance Equation

##### 4.2.4.1 Distributed Two-Fluid Formulation

Equation (4.34) is written for each fluid, taking into account the energy transfer between the two fluids.

$$\begin{aligned}
& \frac{\partial}{\partial t} [(1 - \alpha_x) \cdot \rho_{l,x} \cdot A_x \cdot u_{l,x}] \\
& = -\frac{\partial}{\partial x} \left( h_{l,x} \cdot \dot{m}_l(x) - (1 - \alpha_x) \cdot A_x \cdot k_{l,x} \cdot \frac{\partial T_{l,x}}{\partial x} \right) \\
& + \varphi_{w:l,x} \cdot \pi_{w:l,x} + h_{l,x}^0 \cdot \gamma_x(g \rightarrow l) \cdot A_x + \varphi_x(g \rightarrow l) \cdot \pi_{l:g,x}
\end{aligned} \tag{4.65a}$$

$$\begin{aligned}
& \frac{\partial}{\partial t} (\alpha_x \cdot \rho_{g,x} \cdot A_x \cdot u_{g,x}) \\
& = -\frac{\partial}{\partial x} \left( h_{g,x} \cdot \dot{m}_g(x) - \alpha_x \cdot A_x \cdot k_{g,x} \cdot \frac{\partial T_{g,x}}{\partial x} \right) \\
& + \varphi_{w:g,x} \cdot \pi_{w:g,x} + h_{g,x}^0 \cdot \gamma_x(l \rightarrow g) \cdot A_x + \varphi_x(l \rightarrow g) \cdot \pi_{l:g,x}
\end{aligned} \tag{4.65b}$$

with  $h_{l,x}^0$  and  $h_{g,x}^0$  being the specific enthalpies of the liquid and gas phases characteristic of the energy transfer due to the mass transfer between the two phases

(e.g., saturation enthalpies),  $\varphi_x(g \rightarrow l)$  and  $\varphi_x(l \rightarrow g)$  being, respectively, the heat flux from the gas phase to the liquid phase, and the heat flux from the liquid phase to the gas phase,  $\varphi_{w:l,x}$  and  $\varphi_{w:g,x}$  being, respectively, the heat flux received from the wall into the liquid and gas phases.

#### 4.2.4.2 Distributed Mixture Formulation

Supposing that the net energy transfer between the two phases is null (thermal equilibrium at the interface), then:

$$\begin{aligned} h_{l,x}^0 \cdot \gamma_x(g \rightarrow l) \cdot A_x + h_{g,x}^0 \cdot \gamma_x(l \rightarrow g) \cdot A_x \\ + \varphi_x(g \rightarrow l) \cdot \pi_{l:g,x} + \varphi_x(l \rightarrow g) \cdot \pi_{l:g,x} = 0 \end{aligned} \quad (4.66)$$

Supposing also that the two phases are at thermal equilibrium, then:

$$T_{l,x} = T_{g,x} = T_x \quad (4.67)$$

With these assumptions, adding (4.65a) and (4.65b) yields:

$$\frac{\partial}{\partial t} (\rho_x \cdot A_x \cdot u_x) = - \frac{\partial}{\partial x} \left( h_x \cdot \dot{m}(x) - A_x \cdot k_x \cdot \frac{\partial T_x}{\partial x} \right) + \varphi_{w,x} \cdot \pi_{w,x} \quad (4.68)$$

with  $h_x$  given by (4.48) and

$$u_x = \frac{(1 - \alpha_x) \cdot \rho_{l,x} \cdot u_{l,x} + \alpha_x \cdot \rho_{g,x} \cdot u_{g,x}}{\rho_x} \quad (4.69)$$

$$k_x = (1 - \alpha_x) \cdot k_{l,x} + \alpha_x \cdot k_{g,x} \quad (4.70)$$

$$\varphi_{w,x} \cdot \pi_{w,x} = \varphi_{w:l,x} \cdot \pi_{w:l,x} + \varphi_{w:g,x} \cdot \pi_{w:g,x} \quad (4.71)$$

With these definitions, the energy balance equation for the mixture is identical to the single-phase formulation (4.31).

#### 4.2.4.3 Lumped Two-Fluid Formulation

Equation (4.28) is written for each fluid, taking into account the energy transfer between the two fluids.

$$\begin{aligned} & \frac{d}{dt} [(1 - \alpha_a) \cdot \rho_{l,a} \cdot V_a \cdot u_{l,a}] \\ &= \sum_{b \in V(a)} (h_{l,b:a} \cdot \dot{m}_l(b \rightarrow a) - (1 - \alpha_{b:a}) \cdot A_{b:a} \cdot k_{l,b:a} \cdot \nabla T_l(b \rightarrow a)) \\ &+ \dot{W}_{l,a} + h_{l,a}^0 \cdot \dot{m}_a(g \rightarrow l) + \dot{W}_a(g \rightarrow l) \end{aligned} \quad (4.72a)$$

$$\begin{aligned} & \frac{d}{dt} (\alpha_a \cdot \rho_{g,a} \cdot V_a \cdot u_{g,a}) \\ &= \sum_{b \in V(a)} (h_{g,b:a} \cdot \dot{m}_g(b \rightarrow a) - \alpha_{b:a} \cdot A_{b:a} \cdot k_{g,b:a} \cdot \nabla T_g(b \rightarrow a)) \\ &+ \dot{W}_{g,a} + h_{g,a}^0 \cdot \dot{m}_a(l \rightarrow g) + \dot{W}_a(l \rightarrow g) \end{aligned} \quad (4.72b)$$

with  $h_{l,a}^0$  and  $h_{g,a}^0$  being the specific enthalpies of the liquid and gas phases characteristic of the energy transfer due to the mass transfer between the two phases (e.g., saturation enthalpies),  $\dot{W}_a(g \rightarrow l)$  and  $\dot{W}_a(l \rightarrow g)$  being, respectively, the heat flux from the gas phase to the liquid phase, and the heat flux from the liquid phase to the gas phase,  $\dot{W}_{l,a}$  and  $\dot{W}_{g,a}$  being, respectively, the heat flux received from the wall into the liquid and gas phases.

#### 4.2.4.4 Lumped Mixture Formulation

Supposing that the net energy transfer between the two phases is null (thermal equilibrium at the interface), then:

$$\begin{aligned} & h_{l,a}^0 \cdot \dot{m}_a(g \rightarrow l) + h_{g,a}^0 \cdot \dot{m}_a(l \rightarrow g) \\ &+ \dot{W}_a(g \rightarrow l) + \dot{W}_a(l \rightarrow g) = 0 \end{aligned} \quad (4.73)$$

Supposing also that the two phases are at thermal equilibrium, then:

$$\nabla T_l(b \rightarrow a) = \nabla T_g(b \rightarrow a) = \nabla T(b \rightarrow a) \quad (4.74)$$

With these assumptions, the energy balance equation is:

$$\frac{d(\rho_a \cdot V_a \cdot u_a)}{dt} = \sum_{b \in V(a)} (h_{b:a} \cdot \dot{m}(b \rightarrow a) - k_{b:a} \cdot \nabla T(b \rightarrow a) \cdot A_{b:a}) + \dot{W}_a \quad (4.75)$$

with the following definitions similar to the ones for the distributed formulation (cf. Sect. 4.2.4.2):

$$u_a = \frac{(1 - \alpha_a) \cdot \rho_{l,a} \cdot u_{l,a} + \alpha_a \cdot \rho_{g,a} \cdot u_{g,a}}{\rho_a} \quad (4.76)$$

$$h_{b:a} = (1 - x_{b:a}) \cdot h_{l,b:a} + x_{b:a} \cdot h_{g,b:a} \quad (4.77)$$

$$k_{b:a} = (1 - \alpha_{b:a}) \cdot k_{l,b:a} + \alpha_{b:a} \cdot k_{g,b:a} \quad (4.78)$$

$$\dot{W}_a = \dot{W}_{l,a} + \dot{W}_{g,a} \quad (4.79)$$

With these definitions, the energy balance equation for the mixture is identical to the single-phase formulation (4.28).

#### 4.2.5 Computing the Phase Velocities for the Mixture Model

##### 4.2.5.1 Homogeneous Flow Model

The homogeneous flow model is a mixture model with equal velocities for each phase:

$$v_{l,x} = v_{g,x} \quad (4.80)$$

Then

$$v_{l,x} = v_{g,x} = v_x \quad (4.81)$$

and from (4.43), (4.44), and (4.36)

$$x_x = \alpha_x \cdot \frac{\rho_{g,x}}{\rho_x} = \frac{A_{g,x} \cdot \rho_{g,x}}{A_x \cdot \rho_x} \quad (4.82)$$

$x_x$  is equivalent to the vapor mass fraction.

Using (4.43) and (4.80), the relation between the void fraction and the vapor mass fraction becomes:

$$\alpha_x = \frac{x_x}{x_x + (1 - x_x) \cdot \frac{\rho_{g,x}}{\rho_{l,x}}} \quad (4.83)$$

Using (4.83) with (4.82), the mixture density can then be written as:

$$\frac{1}{\rho_x} = \frac{(1 - x_x)}{\rho_{l,x}} + \frac{x_x}{\rho_{g,x}} \quad (4.84)$$

If there are no mass, momentum, or energy transfer between the two phases, then the mixture balance equations are identical to the single-phase balance equations when using the appropriate definitions for the mixture quantities.

So when using the appropriate definitions for the mixture quantities, the mixture behaves like a single-phase fluid.

#### 4.2.5.2 Drift-Flux Model

The objective of the drift-flux model is to compute the slip between the liquid and gas phases for mixture models in pipes when  $v_{l,x} \neq v_{g,x}$ .

The slip between the two phases is described as a combination of two mechanisms:

- The profiles of velocities and phases distribution vary across the cross-sectional area of the pipe. In particular, the gas concentration tends to be higher in the center of the pipe, where the velocity of the mixture is the fastest (cf. Fig. 4.1).
- The gas rises through the liquid due to buoyancy.

$C_{0,x}$  is the profile parameter (also called flux concentration parameter or distribution coefficient) that accounts for the first mechanism.  $C_{0,x}$  is defined as (Collier and Thom 1996):

$$C_{0,x} = \frac{\langle \alpha \cdot j \rangle_x}{\alpha_x \cdot j_x} \quad (4.85)$$

$V_{gj,x}$  is the drift velocity that accounts for the second mechanism.  $V_{gj,x}$  is defined as:

$$V_{gj,x} = \frac{\langle \alpha \cdot v_{gj} \rangle_x}{\alpha_x} \quad (4.86)$$

with  $v_{gj}$  defined as:

$$v_{gj} = v_g - j \quad (4.87)$$

Multiplying (4.87) by the void fraction  $\alpha$  and integrating over cross-sectional area  $A_x$ :

$$\langle \alpha \cdot v_{gj} \rangle_x = \langle \alpha \cdot v_g \rangle_x - \langle \alpha \cdot j \rangle_x \quad (4.88)$$

As according to Banerjee et al. (2010)

$$\langle \alpha \cdot v_g \rangle_x = \langle \alpha \rangle_x \cdot \langle v_g \rangle_{g,x} = \alpha_x \cdot v_{g,x} \quad (4.89)$$

(4.88) may be rewritten as:

$$\langle \alpha \cdot v_{gj} \rangle_x = \alpha_x \cdot v_{g,x} - \langle \alpha \cdot j_x \rangle_x \quad (4.90)$$

Using (4.85) and (4.86):

$$\alpha_x \cdot V_{gj,x} = \alpha_x \cdot v_{g,x} - C_{0,x} \cdot \alpha_x \cdot j_x \quad (4.91)$$

Dividing (4.91) by  $\alpha_x$  yields the average velocity of the gas phase over cross-sectional area  $A_x$ :

$$v_{g,x} = C_0 \cdot j_x + V_{gj,x} \quad (4.92)$$

Using (4.92) with (4.38), (4.39), and (4.40), the average slip velocity between the two phases is:

$$v_{gl,x} = \frac{(C_0 - 1) \cdot j_x + V_{gj,x}}{1 - \alpha_x} \quad (4.93)$$

$C_0 = 1$  and  $V_{gj,x} = 0$  yield the homogeneous flow model ( $v_{l,x} = v_{g,x}$ ).

$C_0$  and  $V_{gj,x}$  are computed using empirical correlations.

An example of correlations for the computation of  $C_0$  and  $V_{gj,x}$  established after the PATRICIA GV2 experiments on steam generators (De Crecy 1985) is:

$$C_0 = 1 - 0.0617 \cdot (1 - x_x^4) \quad (4.94)$$

$$V_{gj,x} = (1 - x_x^4) \cdot \left( 1.382 - 8.155 \cdot \sqrt{\frac{\rho_{g,x}}{\rho_{l,x}}} + 15.7 \cdot \frac{\rho_{g,x}}{\rho_{l,x}} \right) \quad (4.95)$$

Other correlations have been developed by EPRI, which take into account the pipe orientation and the phase flow respective directions (up or down, co-current or counter-current).

#### 4.2.6 Computing Condensation and Evaporation Mass Flow Rates in Drum Boilers

Drum boilers are considered as single volumes  $a$  in which each phase is considered as a separate two-phase mixture: The liquid phase contains bubbles and the vapor phase contains droplets, as explained in Sect. 4.2.1. The two phases are not in thermal equilibrium so there is an exchange of mass and energy between the two phases.

As the formation of droplets in the steam phase (condensation) and the formation of bubbles in the liquid phase (evaporation) are very complex phenomena, the following phenomenological equations are used to compute the condensation and evaporation mass flow rates:

$$\dot{m}_a(g \rightarrow l) = \dot{m}_{\text{cond}} = \begin{cases} 0 & \text{if } x_{g,a} > x_{g,0} \\ C_{\text{cond}} \cdot \rho_{g,a} \cdot V_{g,a} \cdot (x_{g,0} - x_{g,a}) & \text{if } x_{g,a} \leq x_{g,0} \end{cases} \quad (4.96a)$$

$$\dot{m}_a(l \rightarrow g) = \dot{m}_{\text{evap}} = \begin{cases} 0 & \text{if } x_{l,a} < x_{l,0} \\ C_{\text{evap}} \cdot \rho_{l,a} \cdot V_{l,a} \cdot (x_{l,a} - x_{l,0}) & \text{if } x_{l,a} \geq x_{l,0} \end{cases} \quad (4.96b)$$

In (4.96),  $x_{g,0}$  and  $x_{l,0}$  are the set points of a natural controller for the vapor mass fraction  $x_{g,a}$  in the vapor phase and the vapor mass fraction  $x_{l,a}$  in the liquid phase.  $C_{\text{cond}}$  and  $C_{\text{evap}}$  are time constants of the controller that must be adjusted manually to account for the condensation and evaporation rates (i.e., how fast evaporation and condensation take place).  $\rho_{g,a}$  and  $\rho_{l,a}$  are, respectively, the density of the gas and liquid phases, and  $V_{g,a}$  and  $V_{l,a}$  are, respectively, the volumes of the gas and liquid phases.

## 4.3 Computing Quantities on the Control Volumes Boundaries

### 4.3.1 Computation of the Mass Flow Rate

The objective is to compute the mass flow rates  $\dot{m}(a \rightarrow b)$  that cross the boundaries between volume  $a$  and its neighboring volumes  $b$  (cf. Fig. 4.2).

Let us go back to the lumped momentum Eq. (4.18). If the fluctuation of  $\dot{m}(x)$  around its average value  $\langle \dot{m} \rangle$  is sufficiently small, i.e., if  $L$  is small compared to the mass flow rate wavelength (e.g., no water hammer), then all  $\dot{m}(x)$  for  $x \in [0, L]$  including  $\dot{m}(a \rightarrow b)$  are approximately equal to the average mass flow rate  $\langle \dot{m}(a \rightarrow b) \rangle$ ; cf. (4.19).

Then, with the additional assumption that  $A_x$  is constant and equal to  $A$ :

$$\begin{aligned} L \cdot \frac{d}{dt} \dot{m}(a \rightarrow b) &= \frac{\dot{m}^2(a \rightarrow b)}{A} \cdot \left( \frac{1}{\rho_0} - \frac{1}{\rho_L} \right) + A \cdot (P_0 - P_L) \\ &\quad - A \cdot g \cdot \int_0^L \rho_x \cdot \frac{\partial z_x}{\partial x} \cdot dx - \text{sgn}(\dot{m}(a \rightarrow b)) \cdot \int_0^L \pi_{w,x} \cdot \tau_{w,x} \cdot dx \end{aligned} \quad (4.97)$$

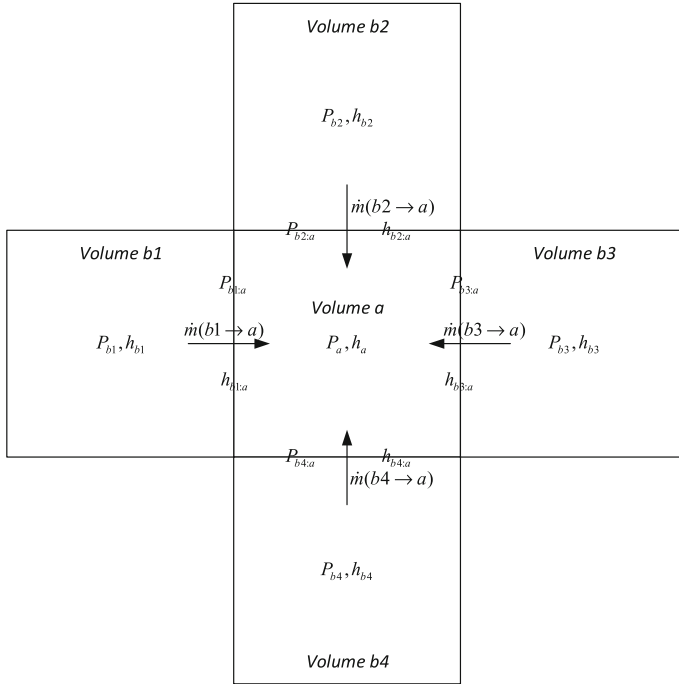


**Fig. 4.2** Volume *a* and its neighboring volumes *b* (Bouskela and El Hefni 2014)

Note that what this equation really computes is the average mass flow rate  $\langle \dot{m}(a \rightarrow b) \rangle$ .

With the additional assumptions

$$\left\{ \begin{array}{l} P_a = P_0 \\ P_b = P_L \\ \rho_a = \rho_0 \\ \rho_b = \rho_L \\ \rho_{b:a} \cdot (z_b - z_a) = \int_0^L \rho_x \cdot \frac{\partial z_x}{\partial x} \cdot dx \end{array} \right. \quad (4.98)$$

then

$$\begin{aligned} \frac{L}{A} \cdot \frac{d}{dt} \dot{m}(a \rightarrow b) &= \frac{\dot{m}^2(a \rightarrow b)}{A^2} \cdot \left( \frac{1}{\rho_a} - \frac{1}{\rho_b} \right) \\ &\quad + P_a - P_b - \rho_{b:a} \cdot g \cdot (z_b - z_a) - \Delta P_f(a \rightarrow b) \end{aligned} \quad (4.99)$$

where  $\Delta P_f(a \rightarrow b)$  is given by (13.14) for turbulent flow.

### 4.3.2 Computation of the Specific Enthalpy

The objective is to compute  $h_{b:a}$  from  $h_b$  and  $h_a$  (cf. Fig. 4.2). To that end, we consider the distributed system of Fig. 4.3 and assume that

$$\begin{cases} h_a = h_0 \\ h_b = h_L \\ h_{b:a} = h_{L/2} \end{cases} \quad (4.100)$$

We consider the distributed energy balance Eq. (4.31) and assume that  $L$  is sufficiently small so that  $\dot{m}(x)$ ,  $k_x$ , and  $A_x$  are approximately constant over the whole volume. Their values are, respectively, denoted  $\dot{m}$ ,  $k$ , and  $A$ . We also assume that the process is adiabatic so that  $\dot{W}_x = \varphi_{w,x} \cdot \pi_{w,x} = 0$ .

Notice then that:

$$\dot{m} = \dot{m}(a \rightarrow b) = -\dot{m}(b \rightarrow a) \quad (4.101)$$

We will also make the assumption that  $h_{x:} = h_x$  (cf. Sect. 4.1.4.2), and consider steady-state regimes.

Then

$$0 = \frac{d}{dx} \left( h_x \cdot \dot{m} - A \cdot k \cdot \frac{dT}{dx} \right) \quad (4.102)$$

In (4.102), partial derivatives have been replaced with ordinary derivatives as time is not considered.

We consider that

$$dh \approx c_p \cdot dT \quad (4.103)$$

which is only exact for isobaric transformations [cf. (2.18)].

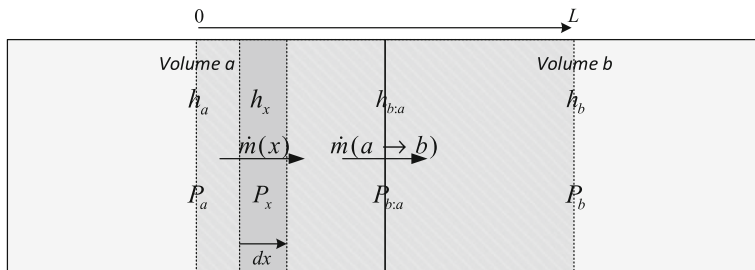


**Fig. 4.3** Distributed system between volume  $a$  and volume  $b$

Then, considering the assumptions above:

$$0 = \dot{m} \cdot \frac{dh_x}{dx} - \frac{1}{\alpha} \cdot \frac{d^2 h_x}{dx^2} \quad (4.104)$$

with

$$\alpha = \frac{c_p}{A \cdot k} \quad (4.105)$$

The solution of this ODE is, for  $\dot{m} \neq 0$ :

$$h_x = \frac{1}{1 - e^{P_e}} \cdot [h_L - h_0 \cdot e^{P_e} + (h_0 - h_L) \cdot e^{P_e \frac{x}{L}}] \quad (4.106)$$

with:

$$P_e = Re \cdot Pr = \alpha \cdot \dot{m} \cdot L \quad (4.107)$$

$P_e$  is the Peclet number,  $Re$  is the Reynolds number, and  $Pr$  is the Prandtl number.

For  $\dot{m} = 0$ :

$$h_{x,0} = \left(1 - \frac{x}{L}\right) \cdot h_0 + \frac{x}{L} \cdot h_L \quad (4.108)$$

The problem with this expression is that it does not provide a single formula for  $\dot{m} = 0$  and  $\dot{m} \neq 0$ , although the switch from one formula to the other is differentially continuous.

As the boundary between volumes  $a$  and  $b$  is located at  $x = L/2$ , one can easily check that:

$$h_{b:a} = h_{L/2} = \hat{s}(P_e) \cdot h_0 + \hat{s}(-P_e) \cdot h_L \quad (4.109)$$

with

$$\hat{s}(x) = \frac{1}{1 + e^{-\frac{x}{2}}} \quad (4.110)$$

$\hat{s}(x)$  is plotted in Fig. 4.4.

Using (4.100):

$$h_{b:a} = \hat{s}(P_e) \cdot h_a + \hat{s}(-P_e) \cdot h_b \quad (4.111)$$

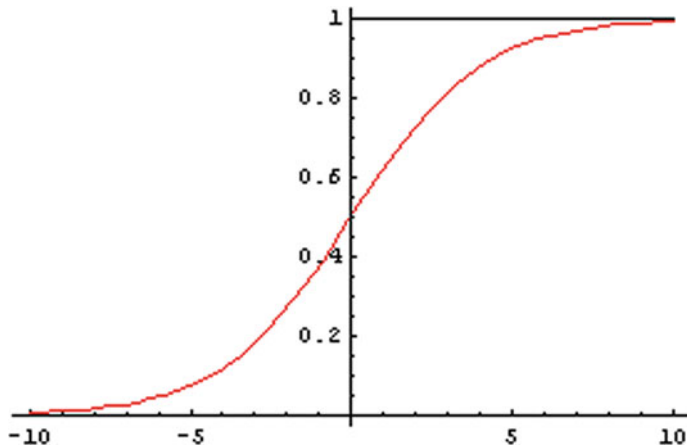


Fig. 4.4 Plot of  $\hat{s}(x)$

This expression is valid for any value of  $\dot{m}$  (including  $\dot{m} = 0$ ).

When the Peclet number is large, diffusion is outweighed by convection, and  $\hat{s}$  can be replaced for  $x \neq 0$  by the step function:

$$s(x) = \begin{cases} 1 & \text{if } x > 0 \\ 0 & \text{if } x < 0 \end{cases} \quad (4.112)$$

then

$$h_{b:a} = s(\dot{m}(b \rightarrow a)) \cdot h_b + s(\dot{m}(a \rightarrow b)) \cdot h_a \quad (4.113)$$

which simply means that:

$$h_{b:a} = \begin{cases} h_b & \text{if } \dot{m}(b \rightarrow a) > 0 \\ h_a & \text{if } \dot{m}(a \rightarrow b) > 0 \end{cases} \quad (4.114)$$

Equation (4.113) is well known as the upwind scheme (or the donor cell method).

Note that the upwind scheme neglects diffusion and for that reason does not provide a value for  $h_{b:a}$  when  $\dot{m} = 0$ .

Note also that this proof is valid for the systems that comply with the assumptions made at the beginning of this paragraph. A generalization of the upwind scheme for non-adiabatic processes is given in Chap. 17; cf. (17.3).

### 4.3.3 Computation of the Thermal Flow Due to Diffusion

From the definition of  $\nabla T(b \rightarrow a)$  given in Sect. 4.1.4.1:

$$\nabla T(b \rightarrow a) = \left( \frac{dT}{dx} \right)_{b:a} = \left( \frac{dT}{dx} \right)_{L/2} \quad (4.115)$$

In (4.115), partial derivatives have been replaced with ordinary derivatives as time is not considered.

Using (4.24) and (4.103) with the assumptions (4.100), one gets:

$$J(b \rightarrow a) = \frac{A \cdot k}{c_p} \cdot \left( \frac{dh_x}{dx} \right)_{L/2} \quad (4.116)$$

Taking the derivative of (4.106) at  $x = L/2$  for  $\dot{m} \neq 0$ :

$$J(b \rightarrow a) = \frac{A \cdot k}{c_p \cdot L} \cdot \frac{P_e}{e^{\frac{P_e}{2}} - e^{-\frac{P_e}{2}}} \cdot (h_b - h_a) \quad (4.117)$$

Taking the derivative of (4.108) at  $x = L/2$  for  $\dot{m} = 0$ :

$$J_0(b \rightarrow a) = \frac{A \cdot k}{c_p \cdot L} \cdot (h_b - h_a) \quad (4.118)$$

$J_0(b \rightarrow a)$  is the energy flux when  $\dot{m} = 0$ .

Introducing

$$\gamma_{b:a} = \left( \frac{A \cdot k}{c_p \cdot L} \right)_{b:a} \quad (4.119)$$

$$r(x) = \begin{cases} \frac{x}{e^{\frac{P_e}{2}} - e^{-\frac{P_e}{2}}} & \text{if } x \neq 0 \\ 1 & \text{if } x = 0 \end{cases} \quad (4.120)$$

then

$$P_e = -\frac{1}{\gamma_{b:a}} \cdot \dot{m}(b \rightarrow a) \quad (4.121)$$

$$J_0(b \rightarrow a) = \gamma_{b:a} \cdot (h_b - h_a) \quad (4.122)$$

$$J(b \rightarrow a) = r(P_e) \cdot J_0(b \rightarrow a) \quad (4.123)$$

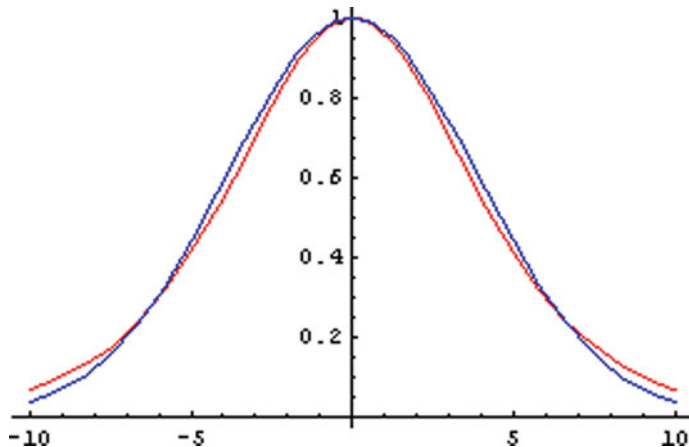


**Fig. 4.5** Approximation of  $r(x)$  (red curve) by  $\hat{r}(x)$  (blue curve)

To avoid the inconvenient switch between  $x \neq 0$  and  $x = 0$ , one can replace the function  $r$  by the Gaussian:

$$\hat{r}(x) = e^{-0.033x^2} \quad (4.124)$$

The plots of  $r(x)$  and  $\hat{r}(x)$  are given in Fig. 4.5.

#### 4.3.4 Computation of the Pressure

The objective is to compute  $P_{b:a}$  from  $P_b$  and  $P_a$ ; cf. Fig. 4.2. To that end, we consider the distributed system of Fig. 4.3 and assume that  $L$  is sufficiently small so that  $\dot{m}(x)$ ,  $\theta_x$ ,  $\lambda_x$ , and  $A_x$  are approximately constant over the whole volume. Their values are, respectively, denoted  $\dot{m}$ ,  $\theta$ ,  $\lambda$ , and  $A$ . Without loss of generality, we will also assume that  $\dot{m} \geq 0$  and that

$$\begin{cases} P_a = P_0 \\ P_{b:a} = P_{L/2} \\ P_b = P_L \end{cases} \quad (4.125)$$

We consider the momentum balance Eq. (4.15) and assume steady state.

Then

$$0 = \frac{\dot{m}^2}{A^2} \cdot \frac{d}{dx} \left( \frac{1}{\rho_x} \right) + \frac{dP_x}{dx} + \rho_x \cdot g \cdot \sin \theta + \frac{dP_{f,x}}{dx} \quad (4.126)$$

where  $dP_{f,x}$  is given by (13.5).

In (4.126), partial derivatives have been replaced with ordinary derivatives as time is not considered.

Then

$$-\frac{dP_x}{dx} = -\frac{\dot{m}^2}{A^2} \cdot \frac{1}{\rho_x^2} \cdot \frac{d\rho_x}{dx} + \rho_x \cdot g \cdot \sin \theta + k \cdot \frac{\dot{m}^2}{\rho_x} \quad (4.127)$$

with using (13.9),

$$k = \frac{1}{2} \cdot \frac{\lambda}{D_H \cdot A^2} \quad (4.128)$$

The variation of  $\rho_x$  with  $P_x$  and  $h_x$  is given by

$$\frac{d\rho_x}{dx} = \left( \frac{\partial \rho_x}{\partial P_x} \right)_h \cdot \frac{dP_x}{dx} + \left( \frac{\partial \rho_x}{\partial h_x} \right)_P \cdot \frac{dh_x}{dx} \quad (4.129)$$

Assuming high Peclet numbers, from (4.106)

$$\frac{dh_x}{dx} \approx \frac{h_L - h_0}{L} \cdot P_e \cdot e^{-P_e \cdot (1 - \frac{x}{L})} \approx 0 \quad (4.130)$$

As  $0 \leq x \leq L$  and  $P_e$  is large, when  $x$  is not close to  $L$ ,  $dh_x \approx 0$ . Then, from (4.129)

$$\frac{d\rho_x}{dx} = \left( \frac{\partial \rho_x}{\partial P_x} \right)_h \cdot \frac{dP_x}{dx} \quad (4.131)$$

If the fluid is incompressible, then

$$\left( \frac{\partial \rho_x}{\partial P_x} \right)_h = 0 \quad (4.132)$$

and therefore  $d\rho_x/dx = 0$  which means that  $\rho_x$  is constant over the whole pipe length:  $\rho_x = \rho_{b,a} \forall x \in [0, L]$ .

Integrating (4.127) over the pipe length from 0 to  $x$  yields

$$P_0 - P_x = \left( \rho_{b:a} \cdot g \cdot \sin \theta + k \cdot \frac{\dot{m}^2}{\rho_{b:a}} \right) \cdot x \quad (4.133)$$

Using (4.133) for  $x = L/2$  and  $x = L$  yields

$$P_0 - P_L = 2 \cdot (P_0 - P_{L/2}) \quad (4.134)$$

Therefore, from (4.134) and (4.125), if the fluid is incompressible

$$P_{b:a,\text{incomp}} = \frac{P_a + P_b}{2} \quad (4.135)$$

If the fluid is compressible, one can no longer assume that  $\rho_x$  is constant.

Assuming  $dh_x = c_p \cdot dT_x$  implies  $dT_x/dx = 0$  [cf. (4.130)], which means that  $T_x$  is constant over the whole pipe length:  $T_x = T_{b:a} \forall x \in [0, L]$ .

The case of an ideal gas is considered in the sequel. Then

$$\frac{P_x}{\rho_x} = R_g \cdot T_{b:a} \quad (4.136)$$

Differentiating (4.136) yields:

$$\frac{d\rho_x}{dx} = \frac{1}{R_g \cdot T_{b:a}} \cdot \frac{dP_x}{dx} \quad (4.137)$$

Inserting (4.136) and (4.137) into (4.127) yields:

$$\left( \frac{\chi}{P_x^2} - 1 \right) \cdot \frac{dP_x}{dx} = g \cdot \sin \theta \cdot \frac{P_x}{R_g \cdot T_{b:a}} + k \cdot \dot{m}^2 \cdot \frac{R_g \cdot T_{b:a}}{P_x} \quad (4.138)$$

with

$$\chi = \frac{\dot{m}^2 \cdot R_g \cdot T_{b:a}}{A^2} \quad (4.139)$$

For usual pipe geometries and fluid pressure,  $\chi/P_x^2 \ll 1$ . Then

$$-\frac{dP_x}{dx} = g \cdot \sin \theta \cdot \frac{P_x}{R_g \cdot T_{b:a}} + k \cdot \dot{m}^2 \cdot \frac{R_g \cdot T_{b:a}}{P_x} \quad (4.140)$$

For horizontal pipes ( $\theta = 0$ ):

$$-P_x \cdot \frac{dP_x}{dx} = k \cdot \dot{m}^2 \cdot R_g \cdot T_{b:a} \quad (4.141)$$

Integrating (4.141) over the pipe length from 0 to  $x$  yields

$$P_0^2 - P_x^2 = 2 \cdot k \cdot \dot{m}^2 \cdot R_g \cdot T_{b:a} \cdot x \quad (4.142)$$

Using (4.142) for  $x = L/2$  and  $x = L$  yields

$$P_0^2 - P_L^2 = 2 \cdot (P_0^2 - P_{L/2}^2) \quad (4.143)$$

Therefore, from (4.143) and (4.125), if the fluid is compressible and is an ideal gas:

$$P_{b:a,\text{comp,hor}}^2 = \frac{P_a^2 + P_b^2}{2} \quad (4.144)$$

If the fluid is compressible,  $P_{b:a}$  is not the mean value of  $P_b$  and  $P_a$  anymore, as stated by (4.135).

However, if  $L$  is sufficiently small so that

$$\frac{P_b}{P_a} = 1 - \varepsilon \quad (4.145)$$

where  $\varepsilon$  is a small number, then developing (4.144) to the first order in  $\varepsilon$ :

$$P_{b:a,\text{comp,hor}}^2 = \frac{P_a^2 + P_b^2}{2} = \frac{P_a^2}{2} \cdot \left[ 1 + \left( \frac{P_b}{P_a} \right)^2 \right] = \frac{P_a^2}{2} \cdot \left[ 1 + (1 - \varepsilon)^2 \right] \approx (1 - \varepsilon) \cdot P_a^2 \quad (4.146)$$

Then

$$P_{b:a,\text{comp,hor}} \approx \sqrt{1 - \varepsilon} \cdot P_a \approx \left( 1 - \frac{\varepsilon}{2} \right) \cdot P_a \quad (4.147)$$

Using (4.135):

$$P_{b:a,\text{incomp}} = \frac{P_a + P_b}{2} = \left( 1 - \frac{\varepsilon}{2} \right) \cdot P_a \quad (4.148)$$

Therefore, to the first order in  $\varepsilon$ :

$$P_{b:a,\text{comp,hor}} \approx P_{b:a,\text{incomp}} = \frac{P_a + P_b}{2} \quad (4.149)$$

For vertical pipes ( $\theta = \pi/2$ ), if the mass flow rate  $\dot{m}$  is close to zero, (4.140) becomes

$$-\frac{1}{P_x} \cdot \frac{dP_x}{dx} = g \cdot \frac{1}{R_g \cdot T_{b:a}} \quad (4.150)$$

Integrating (4.150) over the pipe length from 0 to  $x$  yields

$$P_x = P_0 \cdot e^{-\frac{g \cdot x}{R_g \cdot T_{b:a}}} \quad (4.151)$$

Using (4.151) and (4.125) for  $x = L/2$  and  $x = L$  yields

$$P_{b:a,comp,ver}^2 = P_a \cdot P_b \quad (4.152)$$

If  $L$  is sufficiently small so that (4.145) holds:

$$P_{b:a,comp,ver}^2 = P_a \cdot P_b = (1 - \varepsilon) \cdot P_a^2 \quad (4.153)$$

Then

$$P_{b:a,comp,ver} = \sqrt{P_a \cdot P_b} = \sqrt{1 - \varepsilon} \cdot P_a \approx \left(1 - \frac{\varepsilon}{2}\right) \cdot P_a \quad (4.154)$$

Hence, using (4.148)

$$P_{b:a,comp,ver} \approx P_{b:a,incomp} = \frac{P_a + P_b}{2} \quad (4.155)$$

As a conclusion,

$$P_{b:a} = \frac{P_a + P_b}{2} \quad (4.156)$$

holds provided that (1) the fluid is incompressible, or (2) if the fluid is compressible, that  $\varepsilon$  given by (4.145) can be considered as a small number, i.e., that  $\varepsilon^2 \ll 1$ , or in other words that an error magnitude of  $\varepsilon^2$  is acceptable for the computation of  $P_{b:a}$  (this corresponds to an error magnitude of 1% for a pressure loss magnitude of 10% between  $a$  and  $b$ ).

## References

- Banerjee S, Hetsroni G, Hewitt GF, Prasser H-M, Yadigaroglu G (2010) Modelling and computation of multiphase flows. 27th short courses, Zurich, Switzerland
- Bouskela D, El Hefni B (2014) A physical solution for solving the zero-flow singularity in static thermal-hydraulics mixing models. In: Proceedings of the 10th international Modelica conference, Lund, Sweden
- Collier JG, Thom JR (1996) Convective boiling and condensation. Oxford University Press
- De Crecy F (1985) Etude du comportement du secondaire des générateurs de vapeur. Résultat des expériences Patricia GV2. Technical report TT/SETRE/173, CEA

# Chapter 5

## Static Systems



**Abstract** This chapter deals with the important special case of static systems, which are systems described by static conservation equations, and which are extensively used, e.g., for the purpose of sizing. The differential term in the static conservation equations vanishes, which means that the state variables that describe the physical state of the system do not appear explicitly in the equations. In spite of this difficulty, it is shown how the physical state can still be efficiently computed.

### Nomenclature

$[G]$	Unit of quantity $G$
$A$	Flow cross-sectional area ( $\text{m}^2$ )
$A_{b:a}$	Flow cross-sectional area of boundary $b:a$ ( $\text{m}^2$ )
$b:a$	Boundary between volumes $b$ and $a$
$g$	Gravity constant ( $\text{m s}^{-2}$ )
$g_a$	Average value of specific extensive quantity $g$ inside volume $a$ ( $[G] \text{ kg}^{-1}$ )
$P_e$	Peclet number
$G_x$	Total value of specific extensive quantity $g$ in the tube from the origin up to coordinate $x$ ( $[G]$ )
$h$	Specific enthalpy ( $\text{J kg}^{-1}$ )
$h_a$	Average specific enthalpy inside volume $a$ ( $\text{J kg}^{-1}$ )
$h_{b:a}$	Average specific enthalpy over $A_{b:a}$ ( $\text{J kg}^{-1}$ )
$J(b \rightarrow a)$	Total thermal diffusion through boundary $b : a$ , positively from $b$ to $a$ ( $\text{W}$ )
$\dot{m}(b \rightarrow a)$	Mass flow rate through boundary $b:a$ , positively from $b$ to $a$ ( $\text{kg s}^{-1}$ )
$P$	Fluid pressure ( $\text{Pa}$ )
$P_a$	Average fluid pressure in volume $a$ ( $\text{Pa}$ )
$s(x)$	Step function
$\hat{s}(x)$	Hyperbolic function
$\text{sgn}(x)$	Sign function
$\hat{W}_a$	Total heating power received by volume $a$ ( $\text{J s}^{-1}$ )
$V_a$	Volume of volume $a$ ( $\text{m}^3$ )
$z_a$	Altitude of volume $a$ ( $\text{m}$ )

$z_x$	Pipe altitude at coordinate $x$ (m)
$\alpha$	Diffusion constant ( $\text{s kg}^{-1} \text{m}^{-1}$ )
$\gamma_{b:a}$	Diffusion mass flow rate through $A_{b:a}$ ( $\text{kg s}^{-1}$ )
$\Delta P$	Variation of pressure (Pa)
$\Delta P_f(a \rightarrow b)$	Pressure loss due to friction between volumes $a$ and $b$ oriented positively from $a$ to $b$ (Pa)
$\rho_a$	Average fluid density in volume $a$ ( $\text{kg m}^{-3}$ )
$\rho_{b:a}$	Average fluid density over $A_{b:a}$ ( $\text{kg m}^{-3}$ )

## 5.1 General Form of the Static Balance Equations

The static formulation is obtained from the dynamic formulation by setting in (4.5)

$$\frac{dG_a}{dt} = \frac{d(\rho_a \cdot V_a \cdot g_a)}{dt} = 0 \quad (5.1)$$

This yields for the mass, momentum, and energy balance Eqs. 4.7, 4.18, and 4.28:

$$0 = \sum_{b \in V(a)} \dot{m}(b \rightarrow a) \quad (5.2)$$

$$0 = \frac{\dot{m}^2(a \rightarrow b)}{A^2} \cdot \left( \frac{1}{\rho_a} - \frac{1}{\rho_b} \right) + P_a - P_b - \rho_{b:a} \cdot g \cdot (z_b - z_a) - \Delta P_f(a \rightarrow b) \quad (5.3)$$

$$0 = \sum_{b \in V(a)} (h_{b:a} \cdot \dot{m}(b \rightarrow a) + J(b \rightarrow a)) + \dot{W}_a \quad (5.4)$$

See (4.99) for the derivation of (5.3).

In the case of completely static systems, i.e., when only operating points are considered, all balance equations are static (in fact, all time derivatives are set to zero).

In other cases, some balance equations may be static and another dynamic. For instance, incompressible systems usually have static mass and momentum balance equations, but may have dynamic energy balance equation to account for thermal inertia.

An important class of systems having static balance equations are singularities, i.e., systems that have a quasi-null volume such as singular pressure losses (valves, bends, etc.):  $V_a \approx 0$ . The volume being considered as zero, the differential term in the balance equations vanishes, so the balance equations are static. So systems with

static balance equations are not necessarily static, in the sense that the time dependence of their behavior is not taken into account. It just means that the corresponding inertia is neglected.

When the variation of  $G_a$  is very fast,  $\frac{dG_a}{dt} \rightarrow +\infty$ , which can be considered as a step function acting as an instantaneous transition between the two values  $G_a^-$  before the event and  $G_a^+$  after the event. The balance equation is then often replaced by two static balance equations involving  $G_a^-$  before the event and  $G_a^+$  after the event. This approximation is motivated for practical reasons: (1) It is easier to model fast transients as ideal switches, and (2) ideal switches are faster to simulate because it is less CPU consuming to detect zero-crossings than to integrate stiff differential equations. This approximation is obviously not valid when the dynamics of fast transients are to be taken into account such as water hammer; see, e.g., Wylie and Streeter (1993). This leads to two conditional algebraic equations with discontinuity across the event.

Example of a check valve: The variation of fluid momentum is assumed to be very fast when opening or closing a check valve. Hence, the valve switches instantaneously between two states:

- Valve open: The pressure difference between the valve inlet and outlet is zero.
- Valve closed: The mass flow rate through the valve is zero.

The momentum balance equation is then statically written as:

$$\begin{cases} \Delta P = 0 & \text{if the valve is open} \\ \dot{m} = 0 & \text{if the valve is closed} \end{cases}$$

## 5.2 Computing the Physical States for Static Balance Equations

The static formulations (5.2)–(5.4) of the balance equations are quite simple. However, the main problem that arises when using them is that the corresponding state variables disappear as differential variables. It is therefore not obvious to compute the physical state of the system.

### 5.2.1 *Origin of the Singularities for the Computation of the Volumes Specific Enthalpies When Diffusion Is Neglected*

For static systems, when diffusion is neglected, the static energy balance Eq. (5.4) becomes:

$$0 = \sum_{b \in V(a)} h_{b:a} \cdot \dot{m}(b \rightarrow a) + \dot{W}_a \quad (5.5)$$

For the sake of simplicity, in the following of this paragraph,  $\dot{m}_b$  is used as a shorthand notation for  $\dot{m}(b \rightarrow a)$  and  $\dot{W}_a$  is assumed to be equal to zero without loss of generality.

Then, the static mass and energy balance Eqs. (5.2) and (5.5) write:

$$0 = \sum_b \dot{m}_b \quad (5.6)$$

$$0 = \sum_b h_{b:a} \cdot \dot{m}_b \quad (5.7)$$

The value of the enthalpy  $h_{b:a}$  is given by the upwind scheme (4.113) and rewritten below using the shorthand notation for  $\dot{m}(b \rightarrow a)$ :

$$h_{b:a} = s(\dot{m}_b) \cdot h_b + s(-\dot{m}_b) \cdot h_a \quad (5.8)$$

In the sequel, the following relations are used:

$$|x| = \operatorname{sgn}(x) \cdot x \quad (5.9)$$

$$\operatorname{sgn}(x) = s(x) - s(-x) \quad (5.10)$$

$$s(x) = 1 - s(-x) \quad (5.11)$$

$$s(x) \cdot s(-x) = 0 \quad (5.12)$$

$$s^2(x) = s(x) \quad (5.13)$$

where  $\operatorname{sgn}$  is the sign function.

Then from (5.6)–(5.8) and (5.11),

$$\begin{aligned} \sum_b h_{b:a} \cdot \dot{m}_b &= \sum_b s(\dot{m}_b) \cdot \dot{m}_b \cdot h_b + h_a \cdot \sum_b s(-\dot{m}_b) \cdot \dot{m}_b \\ &= \sum_b s(\dot{m}_b) \cdot \dot{m}_b \cdot h_b + h_a \cdot \left( \sum_b \dot{m}_b - \sum_b s(\dot{m}_b) \cdot \dot{m}_b \right) \quad (5.14) \\ &= \sum_b s(\dot{m}_b) \cdot \dot{m}_b \cdot h_b - h_a \cdot \sum_b s(\dot{m}_b) \cdot \dot{m}_b = 0 \end{aligned}$$

Therefore,

$$h_a = \frac{\sum_b s(\dot{m}_b) \cdot \dot{m}_b \cdot h_b}{\sum_b s(\dot{m}_b) \cdot \dot{m}_b} \quad (5.15)$$

when

$$\sum_b s(\dot{m}_b) \cdot \dot{m}_b \neq 0 \quad (5.16)$$

To find out when condition (5.16) is satisfied, using (5.6) and (5.9)–(5.11):

$$\begin{aligned} \sum_b |\dot{m}_b| &= \sum_b \text{sgn}(\dot{m}_b) \cdot \dot{m}_b = \sum_b (s(\dot{m}_b) - s(-\dot{m}_b)) \cdot \dot{m}_b \\ &= \sum_b s(\dot{m}_b) \cdot \dot{m}_b - \sum_b s(-\dot{m}_b) \cdot \dot{m}_b \\ &= \sum_b s(\dot{m}_b) \cdot \dot{m}_b - \sum_b (1 - s(\dot{m}_b)) \cdot \dot{m}_b \\ &= 2 * \sum_b s(\dot{m}_b) \cdot \dot{m}_b - \sum_b m_b = 2 * \sum_b s(\dot{m}_b) \cdot \dot{m}_b \end{aligned} \quad (5.17)$$

Hence,

$$h_a = 2 \cdot \frac{\sum_b s(\dot{m}_b) \cdot \dot{m}_b \cdot h_b}{\sum_b |\dot{m}_b|} \quad (5.18)$$

when

$$\sum_b |\dot{m}_b| \neq 0 \quad (5.19)$$

So when all mass flow rates are equal to zero, the mixing enthalpy  $h_a$  is indeterminate ( $h_a = 0/0$ ).

Although the indetermination occurs only at an isolated point (all mass flow rates equal to zero), it is not obvious to extend  $h_a$  in order to remove the singularity at zero (contrary to other functions with isolated singularities such as  $\sin(x)/x$ ).

In particular, it is not sufficient to replace  $s$  by  $\hat{s}$  defined in (4.110) (or in other words get rid of the upwind scheme by introducing diffusion in the flow reversing formula given by (5.8)) because the derivation (5.14) is still valid for  $\hat{s}$  and then

$$h_a = \frac{\sum_b \hat{s}(\hat{\dot{m}}_b) \cdot \dot{m}_b \cdot h_b}{\sum_b \hat{s}(\hat{\dot{m}}_b) \cdot \dot{m}_b}$$

with

$$\hat{\dot{m}}_b = \frac{\dot{m}_b}{\gamma_{b:a}}$$

The singularity still remains since  $\sum_b \hat{s}(\hat{\dot{m}}_b) \cdot \dot{m}_b = 0$  when all mass flow rates are equal to zero.

### 5.2.2 Computing the Volume Specific Enthalpies

The zero-flow singularity is removed by reintroducing diffusion in the energy balance equation:

$$0 = \sum_{b \in V(a)} (h_{b:a} \cdot \dot{m}(b \rightarrow a) + J(b \rightarrow a)) + \dot{W}_a \quad (5.20)$$

which is the same as (5.4).

When all mass flow rates  $\dot{m}(b \rightarrow a) = 0$ :

$$0 = \sum_{b \in V(a)} J_0(b \rightarrow a) + \dot{W}_a \quad (5.21)$$

Using (4.122),

$$h_a = \frac{\sum_{b \in V(a)} \gamma_{b:a} \cdot h_b + \dot{W}_a}{\sum_{b \in V(a)} \gamma_{b:a}} \quad (5.22)$$

Equation (5.22) gives the value for the mixing specific enthalpy  $h_a$  although  $h_a$  does not appear explicitly in the static energy balance Eq. (5.20).

Using (4.121)–(4.123), the static energy balance Eq. (5.20) can be written as

$$0 = \sum_{b \in V(a)} (h_{b:a} \cdot \dot{m}(b \rightarrow a) + (h_b - h_a) \cdot \dot{m}_e(b \rightarrow a)) + \dot{W}_a \quad (5.23)$$

with

$$\dot{m}_e(b \rightarrow a) = r \left( -\frac{1}{\gamma_{b:a}} \cdot \dot{m}(b \rightarrow a) \right) \cdot \gamma_{b:a} \quad (5.24)$$

The terms  $\dot{m}_e(b \rightarrow a)$  are in general small but are always strictly positive, so they never go to zero even when all mass flow rates go to zero. As they have the

same physical unit as a mass flow rate (kg/s), they act as small positive mass flow rates that remove naturally in a  $C^\infty$  way the singularity of the mixing enthalpy at zero flows.

### 5.2.3 Computing the Volume Pressures and Mass Flow Rates

The static momentum balance Eq. (5.3) may be reformulated as:

$$A^2 \cdot \Delta P = f(\dot{m}) \quad (5.25)$$

where  $\Delta P = P_a - P_b$  and  $\dot{m} = \dot{m}(b \rightarrow a)$ .

This equation shows that pressure differences are computed rather than absolute pressure values provided that  $A > 0$ . Therefore, pressure states remain undetermined, unless at least one pressure reference is given in the network, and there exists an open path (i.e., not closed by, e.g., a valve to avoid  $A = 0$ ) from any control volume in the network to a pressure reference. In such case, (5.25) can be used iteratively from one volume to another along that path to link the control volume of interest to the pressure reference. Pressure references are provided with pressure source boundary conditions: A pressure source can deliver unlimited mass flow rate at a constant pressure value (it behaves like an infinite reservoir). Therefore, a pressure source is a volume  $a$  whose static mass and energy balance Eqs. (5.2) and (5.4) are, respectively, replaced by (5.26) and (5.27):

$$P_a = P_{\text{ref}} \quad (5.26)$$

$$h_a = h_{\text{ref}} \quad (5.27)$$

where  $P_{\text{ref}}$  and  $h_{\text{ref}}$  are, respectively, the pressure and specific enthalpy reference of the fluid.

In Fig. 5.1, circles represent volumes with static mass and energy balance equations such as (5.2) and (5.4). Straight lines represent pipes with static momentum balance equations like (5.3) such that the pipes hydraulic diameters never go to zero.

The left diagram has as many unknowns (six pressures, seven mass flow rates) as equations (six mass balance equations, seven momentum balance equations). However, it cannot compute absolute pressure values, as only pressure differences are computed. Therefore, the system is singular: It has an infinite number of solutions.

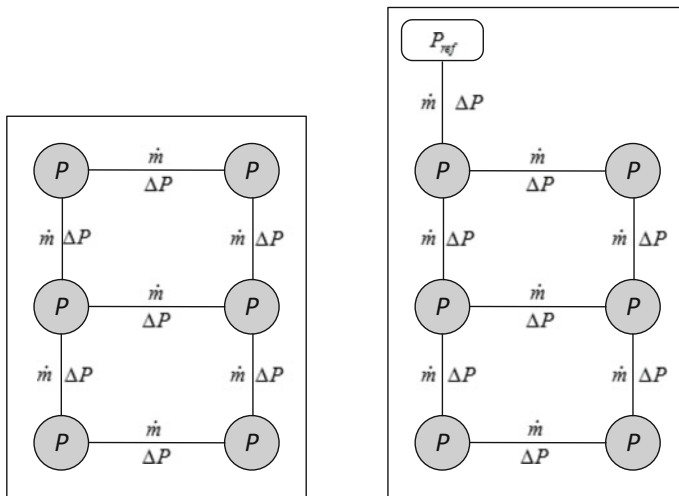


**Fig. 5.1** Incorrect (left) and correct (right) static flow networks

The right diagram is correct as a pressure reference  $P_{ref}$  is provided.

It is also possible to provide mass flow rate references instead of pressure references. The system is then defined as an inverse problem.

## Reference

Wylie EB, Streeter VL (1993) Fluid transients in systems. Prentice Hall

# Chapter 6

## Modeling and Simulation of Thermal Power Plants



**Abstract** Three power plant models are presented, which are used as reference cases: a dynamic model of a combined cycle power plant (CCGT), a model of a once-through supercritical coal-fired power plant, and a model of a concentrated solar power plant (CSP). The component models of the ThermoSysPro library are used to build the Brayton and Rankine cycles of the plants. The basic operating principles of fossil fuel-fired power plants are recalled, and steps and advice to develop efficient simulation models are given: choice of the component models, parameterization data, model calibration, and model validation versus simulation results of typical transients such as load variation, full trip, and plant start-up.

### 6.1 Introduction

Power plants constitute the main part of installed capacity in global power generation. A power plant can be defined as a single machine or as a set of pieces of equipment that generate electrical energy.

A power plant can be of several types depending mainly on the type of fuel used as primary energy source and on the thermodynamic cycles used to produce work for the generator. Accordingly, the major classifications for power generation are: nuclear power plant, fossil fuel power plant, gas turbine power plant, combined cycle power plant (gas turbine + steam cycle), diesel power plant, solar thermal power plant, geothermal power plant, and hydroelectric power plant.

Nuclear power plants, fossil fuel power plants, gas turbine power plants, combined cycle power plants, diesel power plants, solar thermal power plants, and geothermal power plants are designated under the generic term of *thermal power plants* because they convert heat into electrical energy. Accordingly, the heat source used in thermal power plants is nuclear fission, combustion of biomass or fossil fuel such as coal, natural gas and oil, solar radiation, or geothermal energy.

Steam power plants are based on the Rankine cycle where steam is used as the working fluid in the steam turbine. Powered by the steam, the turbine rotates at high speed and its rotational energy is transferred to the generator to produce electricity.

Gas turbine power plants are based on the Brayton cycle. Combined cycle power plants use both the gas turbine cycle (i.e., the Brayton cycle) and the steam turbine cycle (i.e., the Rankine cycle). Rankine and Brayton cycles are introduced in Sect. 2.9.

Power plant modeling and simulation play a key role for component and system design verification and optimization. They are in particular widely used for system sizing, control system verification, safety assessment, and the preparation of the acceptance tests for system commissioning. They are also increasingly used to assist the operator in the proper conduct of difficult transients, monitor the plant performance, and diagnose the causes of malfunctions or degradation to improve plant operation and prepare maintenance actions.

Modeling and simulation of power plants are the difficult art of predicting plants' behavior using the mathematical equations that express the physical laws of the involved phenomena and their interactions. Difficulties stem from the complexity of the process that requires to use a large number of equations from different fields of physics. The usual solution to this problem is to provide libraries of pre-defined model equations for commonly used components, such as pumps, valves, pipes, and also more sophisticated ones such as steam generators, heat exchangers, steam turbines, gas turbines, combustion chambers, so that the user can build the model of a power plant by assembling components. The component models should also come in different levels of complexity so that the detail of the model can be adjusted to the problem at hand. For instance, technical economic studies require rather coarse static models that are fit for cost optimization (i.e., they should be adapted to optimization algorithms that require continuous and low CPU-consuming models). Control system design requires dynamic models that represent well the system inertias without going too much into physics. System diagnosis requires detailed physical insight into the phenomena to be analyzed (e.g., heat exchanger clogging) when it is needed to identify the causes of malfunctions or when little history data are available (otherwise, machine learning can be sufficient).

The component models that populate the component model libraries can be seen as incomplete models of small- to medium-size components or subsystems. They are incomplete in the sense that they cannot be used alone: They must be connected to one another to produce a complete numerical model, i.e., a model that can be numerically solved. Each component model has input and/or output ports to exchange variable values (e.g., mass flow rates, pressures, temperatures) and parameters that are placeholders for component properties that are assumed to be fixed during a simulation run (e.g., boundary conditions, some substance properties, component geometry).

In this chapter, three full power plant models are presented, which are used as reference cases: the model of a combined cycle power plant (CCGT), the model of a once-through supercritical coal-fired power plant, and the model of a concentrated solar power plant (CSP).

The basic operating principles of the plants are recalled, and the way to develop the models is described in detail: modeling steps and advice, components choice, model parameterization data and calibration, simulation results (load variation, large transients, full trip, etc.), and model validation. The simulation results for the CCGT are compared to real plant data provided by the plant manufacturer.

## 6.2 Typical Usage of Power Plant Models

Power plant models are useful to:

- Find the best design of the power plant that meets required economic criteria;
- Validate and compare control strategies and control system design;
- Optimize power plant design and operation using static and dynamic optimization algorithms;
- Prepare acceptance tests for power plant commissioning;
- Assess and monitor power plant performances (e-monitoring);
- Simulate plant transients, including large operational transients such as load variation, system start-up or shutdown, and system islanding (sudden separation of the plant from the power grid);
- Evaluate power plant parameters that are not accessible with measuring devices;
- Study the impact of equipment replacement on the operation of the plant.

This list is not limitative.

## 6.3 The ThermoSysPro Library

The library used for the modeling of the reference cases is ThermoSysPro (TSP).

ThermoSysPro is a Modelica library (i.e., that contains component models expressed in the Modelica language) for the modeling and simulation of power plants and energy systems at large. Most of the library is released under open-source license. A thorough introduction to the Modelica modeling language and related techniques can be found in Fritzson (2011). The library can be downloaded with OpenModelica from <https://openmodelica.org/openmodelicaworld/tools> (it is listed as one of the system libraries).

Although ThermoSysPro is a Modelica library, the description of the physical equations is given in Chaps. 7–16 using mathematical notations independent of any programming language and tools.

## 6.4 How to Develop a Power Plant Model

### 6.4.1 Using the ThermoSysPro Library

The ThermoSysPro library is structured in packages that contain component models organized by physical domains. For instance, the *Combustion* package contains all components relative to combustion. Each package is further organized by sub-packages that contain component models according to their role in the modeling process. For instance, the *Combustion* package contains 4 sub-packages:

- *Combustion.BoundaryConditions* that contains boundary conditions such as a fuel source;
- *Combustion.CombustionChambers* that contains the different components for the modeling of combustion chambers. These components are described in Chaps. 7 and 8;
- *Combustion.Connectors* that contains the description of the connectors for combustion component models;
- *Combustion.Sensors* that contains the sensors that are useful when connecting the physical model to the model of a control system.

Other packages contain more sub-packages, but they all follow the above principle.

To develop a full model, it is necessary to connect component models together in order to obtain a complete set of equations, i.e., a system that has as many unknowns as equations. Such a system is said to be square. This is done by dragging and dropping component models from the library into the sheet that contains the full model to be developed, and by connecting the different component models together. The connections are made by connecting so-called *connectors*.

A connector is a group of variables of a given component that are meant to be exposed to other components. They constitute the interface of the component with the other components. The structure of a given connector depends on the physical domain, so there are roughly as many different types of connectors as there are physical domains in the library. The following discussion will bear on fluid connectors, as they are the main connectors used in ThermoSysPro, but the same arguments apply to all types of connectors.

Fluid components have fluid connectors that enable to connect fluid components together. They can also have connectors of other types if one wants to connect them to components of other types such as mechanical components or control blocks.

The precise meaning of the connectors depends on the structure of the library. In ThermoSysPro, the role of the connectors is to share variables between different component models, but other Modelica libraries may have a different usage of the connectors such as automatically generating simple balance equations. Therefore, connecting two ThermoSysPro connectors implies that the corresponding variables in each connector are equal. The rationale for the connector system in ThermoSysPro is detailed in Chap. 17.

To understand the practical role of the connectors, let us consider a simple fluid system consisting of two steam cavities connected via a pipe and a control valve (cf. Fig. 6.1). The two steam cavities are labeled Volumes 1 and 2 in Fig. 6.1. They are initially, respectively, at pressure  $P_1$  and  $P_2$  with  $P_1 > P_2$ . After initial time, steam will flow from Volume 1 to Volume 2 until  $P_1 = P_2$ .

The fluid connectors are represented by blue- and red-filled squares on the sides of the components. They are oriented in such a way that mass flow rates are positive when they enter a component via a blue square and exit a component via a red square. Therefore, the mass flow rate inside the pipe is positive when the fluid flows in the direction of the arrow in Fig. 6.1. Otherwise, it is negative. This constitutes a practical way to detect backflows. Given the initial conditions of the system, one expects that the mass flow rate will always be positive during simulation runs.

Other connectors are represented by other symbols. In Fig. 6.1, the control system signal output (from the control block) and the actuator signal input (to the valve itself) are represented by triangles in different shades of blue that point in the direction of the signal.

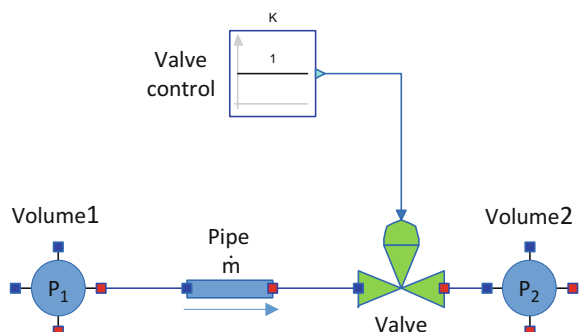
Back to the fluid connectors, the components are connected by drawing lines between exactly two fluid connectors in order to constitute a complete system of equations. The volumes compute the specific enthalpies and the pressures of the fluid inside the steam cavities. The pipe and the valve compute the mass flow rate or the pressure drop across each of those components (one or the other, but not both), depending on the computational causality of the system (which is established automatically by the Modelica compiler; cf. Sect. 1.5).

For the sake of clarity, in this example we only consider the hydraulic equations of the system (so the thermal equations are omitted).

$$V_1 \cdot \frac{\partial \rho_1}{\partial t} = \dot{m}_1 \quad (6.1)$$

$$V_2 \cdot \frac{\partial \rho_2}{\partial t} = \dot{m}_2 \quad (6.2)$$

**Fig. 6.1** Two steam cavities connected via a pipe and a control valve



$$P_{\text{pipe,in}} - P_{\text{pipe,out}} = k_{\text{pipe}} \cdot \frac{\dot{m}_{\text{pipe}} \cdot |\dot{m}_{\text{pipe}}|}{\rho_{\text{pipe}}} \quad (6.3)$$

$$(P_{\text{valve,in}} - P_{\text{valve,out}}) \cdot C_v^2 = K \cdot \frac{\dot{m}_{\text{valve}} \cdot |\dot{m}_{\text{valve}}|}{\rho_{\text{valve}} \cdot \rho_{\text{water,60 }^{\circ}\text{F}}} \quad (6.4)$$

Equations (6.1) and (6.2) represent, respectively, Volumes 1 and 2. They are contained in the *Volume* component which is instantiated twice in the model. Equation (6.3) represents the pipe, and (6.4) represents the valve, each of those components being instantiated only once in the model.

The characteristics (model parameters or model data) of the components are given as inputs:  $V_1$  and  $V_2$  which are the volumes of Volumes 1 and 2,  $k_{\text{pipe}}$  which is a pressure loss factor that depends on the geometry of the pipe, and  $C_v$  which is a pressure loss factor called flow coefficient that depends on the geometry and position of the valve set by the control system.

Therefore, the unknowns of the system are:  $\rho_1$  and  $\rho_2$  which are the densities of the fluid inside Volumes 1 and 2,  $\dot{m}_1$  and  $\dot{m}_2$  which are the mass flow rates, respectively, leaving Volume 1 and entering Volume 2,  $P_{\text{pipe,in}}$  and  $P_{\text{pipe,out}}$  which are, respectively, the pressures at the inlet and the outlet of the pipe,  $P_{\text{valve,in}}$  and  $P_{\text{valve,out}}$  which are, respectively, the pressures at the inlet and the outlet of the valve,  $\dot{m}_{\text{pipe}}$  and  $\dot{m}_{\text{valve}}$  which are, respectively, the mass flow rates inside the pipe and the valve.

At this point, we have four equations for ten unknowns. Six equations are missing; thus, the system is not square.

However, as stated above, the role of the ThermoSysPro fluid connectors is to share variables between two and only two connected connectors. As the outlet of Volume 1 is connected to the inlet of the pipe, the pressure and mass flow rate at the outlet of Volume 1 are identical to the pressure and mass flow rate at the inlet of the pipe. The same argument applies to all other connected connectors in Fig. 6.1.

Therefore, the three fluid connections generate the following identities:

$$\begin{cases} P_1 \equiv P_{\text{pipe,in}} \\ \dot{m}_1 \equiv \dot{m}_{\text{pipe}} \end{cases} \quad (C1)$$

$$\begin{cases} P_{\text{pipe,out}} \equiv P_{\text{valve,in}} \\ \dot{m}_{\text{pipe}} \equiv \dot{m}_{\text{valve}} \end{cases} \quad (C2)$$

$$\begin{cases} P_{\text{valve,out}} \equiv P_2 \\ \dot{m}_{\text{valve}} \equiv \dot{m}_2 \end{cases} \quad (C3)$$

The connectors generate the six missing equations, so we now have ten equations for ten unknowns: The system is square. For the sake of numerical efficiency,

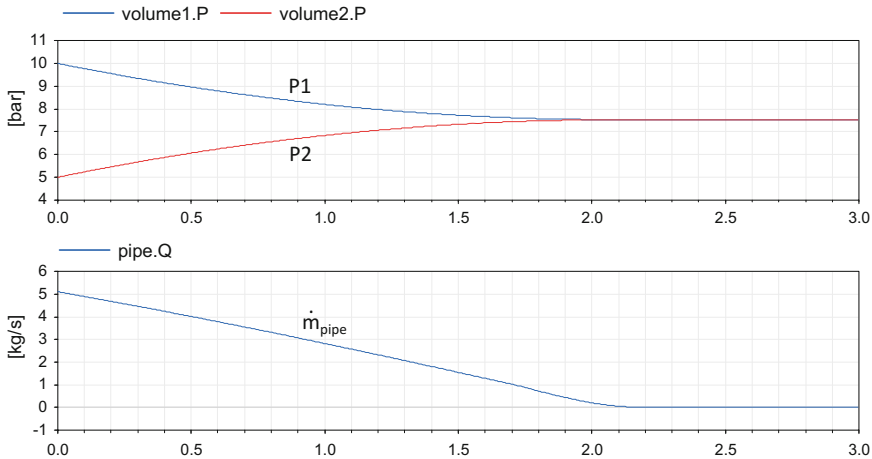


**Fig. 6.2** Simulation results of the two steam cavity problems of Fig. 6.1

the connection equations should be used to substitute the redundant variables in (6.1)–(6.4) rather than being merely added to (6.1)–(6.4).

However, to be solved the system must also be non-singular and the initial conditions fully and consistently defined (cf. Sect. 6.4.3). The system can be singular when static equations are involved (cf. Chap. 5). Here, the system is non-singular because the pressures are well defined throughout the system as the volumes use compressible mass balance equations. The initial conditions are well defined because the initial values for  $\rho_1$  and  $\rho_2$  can be computed from the given initial values for  $P_1$  and  $P_2$  using the fluid state equations.

The connection equations (C1)–(C3) yield the structure of the fluid connector for the hydraulic system. Each connector contains two variables, the first being a pressure and the second a mass flow rate. However, caution must be taken to understand which pressure and which mass flow rate are represented in a connector of a given component, taking into account the fact that the system is broken down into components according to the staggered grid scheme. Moreover, in order to handle the thermal aspects of the system, two specific enthalpies are added to the actual ThermoSysPro fluid connector. This is explained in detail in Chap. 17.

The result of the simulation is shown in Fig. 6.2, the two volumes having a capacity of  $10 \text{ m}^3$  each and the steam being close to saturation.

### 6.4.2 Conceptual Steps

The development of a numerical model is an iterative process that follows the following conceptual steps:

1. Formulation of the problem.
2. Definition of the architecture of the model (i.e., its decomposition into subsystems and components) as a trade-off between realism and simplicity.
3. Definition of the boundary conditions. Boundary conditions define the influence of the environment of the system on the system. For a power plant, boundary conditions are typically the temperature, pressure, and mass flow rate of the cold source, or the temperature and pressure of the atmosphere. If only a subsystem of the plant is considered, then boundary conditions include physical conditions (i.e., pressure, temperature, mass flow rate, thermal or mechanical power, etc.) of the surrounding plant physical subsystems, and possibly positions of the actuators governed by the control system if the control system is partially or not included in the model.
4. Definition of the model inputs. For a thermal power plant, the inputs are design quantities such as steam generator geometry and machine characteristics, operational quantities such as valve positions, and other physical quantities such as heat transfer coefficients, friction pressure loss coefficients. Inputs whose values are constant during a simulation run are called parameters.
5. Definition of the model outputs. The outputs are the quantities of interest that characterize the state of the system (pressures, temperatures, mass flow rates), the performance of the system (power produced, economic efficiency, etc.), or other kinds of information. The outputs are related to the system state via functions often called system observers (when the output is a state, then the corresponding observer is the identity function).
6. Data collection to feed in the model inputs. Data can be collected from various sources such as expert knowledge, design results, on-site measurements. Data contribute to the definition of inputs, as inputs must reflect the type of collected data and must be related to the system state via model functions which are inverse system observers because, contrary to observers, they relate the outside of the model to the inside of the model.
7. Development of the model: The model is built by connecting the component models together as explained in Sect. 6.4.1 and by feeding in the model inputs.
8. Definition of the initial state and calibration of the model. For a power plant, the initial state is most often a nominal steady state such as the plant operating steadily at full or partial load. It is usually defined by setting outputs to values corresponding to the nominal state, e.g., drum pressure, temperature and water level, electric generator power. The calibration of the model consists in finding the values of the variables with no prescribed values (i.e., the unknown variables) from the variables with prescribed values (i.e., the known variables) by solving the model equations. Therefore, inputs and outputs can be both known and unknown variables (only for the computation of the initial state). Computing

unknown inputs from known outputs is called solving an *inverse problem*. The Modelica compiler determines the model computational causalities to generate automatically the inverse model for the computation of the initial state (although it is sometimes convenient to build manually a separate inverse model when the computational causalities derived by the compiler are not satisfactory).

9. Simulation of the model. Simulation consists in finding numerically the model's initial state and then solving the model's differential-algebraic equations (DAEs) at each time step, from the initial time corresponding to the initial state until the final time signaled by some criteria. The simulation may be constrained by some scenario given as time series on the inputs. Standard variable of fixed step solvers such as DASSL, LSODAR, Euler can be used to solve the DAEs.
10. Verification and validation of the model, i.e., checking whether results comply with engineering expertise. This is the most critical and difficult step, as there is no way to formally prove that a model is correct. Therefore, models are usually constantly modified according to needs defined by case study scenarios and the precision required for the results.
11. Verification and validation of the system design, i.e., checking whether results comply with system requirements. This is usually done by inspecting plots of the variables and comparing them to required values as given by the system specifications.

Those steps are quite general and are not tool dependent.

### 6.4.3 Recurrent Difficulty: Finding the Steady-State Initial Conditions

When solving differential-algebraic equations (DAEs), cf. (1.7), a recurrent difficult problem is to find consistent initial conditions, i.e., conditions that satisfy (1.7) at initial time ( $t = 0$ ) and make physical sense.

For the following discussion, (1.7) is reproduced below in a simplified form for the sake of clarity. In the following, uppercase letters denote vectors, whereas lowercase letters denote vector elements.

$$\begin{cases} \dot{X} = f(X, P) \\ Y = X \end{cases} \quad (6.5)$$

where  $X$  is the state vector,  $\dot{X}$  is the derivative of the state vector,  $P$  are the parameters (i.e., fixed inputs during a simulation run), and  $Y$  are the outputs (i.e., the variables of interest). In (6.5), outputs are a mere replication of the state variables.

Equation (6.5) is an initial value problem: The differential equation is solved provided that an initial state denoted  $X_0$  is given by the user. Any state  $X_0$  is mathematically valid provided that it complies with the definition domain of function  $f$ . Therefore, in general, there are infinitely many mathematically valid initial states

$X_0$ , whereas only a few of them are physically valid. The physically valid states are those that can be (indirectly) measured at the outputs, which implies that they correspond to steady states (i.e.,  $\dot{X}_0 = 0$ ) or at least to slowly varying states (i.e.,  $\dot{X}_0$  close to zero) as state derivatives are difficult, if not impossible, to measure.

Therefore, the initial state is defined by

$$\begin{cases} 0 = f(X_0, P) \\ Y_0 = X_0 \end{cases} \quad (6.6)$$

where  $Y_0$  is the outputs at initial time, which usually correspond to nominal values for a particular steady-state regime, e.g., 100% or 50% load.

The problem of finding the initial state is hence posed as an inverse problem: The nominal values of all or some elements of the output  $Y_0$  are given, and the objective is to compute the corresponding nominal values of all or some elements of the system state  $X_0$  and of the parameters  $P$  whose values are unknown. When dealing with square systems, the limitation is that the total number of unknown values that can be computed cannot exceed the number of equations. Therefore, if the causality of one input (i.e., one element of  $X_0$  or  $P$ ) is switched to unknown, then the causality of exactly one output (i.e., one element of  $Y_0$ ) must be switched to known and the corresponding value for the output provided by the user.

Let us illustrate this procedure on the following simple example, chosen not to describe a real system, but to show the practical implementation difficulties of the method on equations reflecting those commonly found in power plant models.

$$\begin{cases} \dot{x}_1 = -0.3 \cdot (x_2 + 1) \cdot (x_2 - x_4 - 1) \\ \dot{x}_2 = -0.3 \cdot (x_1 - 0.1 \cdot p) \cdot (x_1 - 10) \\ \dot{x}_3 = -x_2 \cdot |x_2| + (x_3 - x_4)^2 \\ \dot{x}_4 = x_4 \\ y = x_1 \end{cases} \quad (6.7)$$

In (6.7),  $X_\phi = [x_1 \ x_2 \ x_3]^\top$  is the physical state, whereas  $X_c = [x_4]$  is the control state. Therefore, the physical steady state of the system is defined as  $\dot{X}_\phi = [\dot{x}_1 \ \dot{x}_2 \ \dot{x}_3]^\top = [0 \ 0 \ 0]^\top$ . It is assumed that all physical states are positive.  $Y = [y]$  is the output,  $P = [p]$  is the parameter,  $X = [x_1 \ x_2 \ x_3 \ x_4]^\top$  is the full state, and  $\dot{X} = [\dot{x}_1 \ \dot{x}_2 \ \dot{x}_3 \ \dot{x}_4]^\top$  is the derivative of the full state.

The idea is to initialize the physical part of the system at steady state. An initial impulse is given to the system by the control system so that the system leaves the physical steady state immediately after initial time. Hence, the derivative of  $x_4$  is not zero at initial time (it is set to 1).

Therefore, it is assumed that at initial time,  $\dot{X} = [0 \ 0 \ 0 \ 1]^\top$ . The parameter  $p$  is unknown.

To compute the initial state  $X_0$ , all derivatives but  $\dot{x}_4$  in (6.7) are set to zero and a value is assigned to one output such that it corresponds to a nominal value for the system. As  $y$  is the sole output, the nominal value is assigned to  $y$ , which is 0.2.

Therefore, the algebraic system to be solved to find the initial state and the parameter value is:

$$\begin{cases} 0 = (x_2 + 1) \cdot (x_2 - x_4 - 1) \\ 0 = (x_1 - 0.1 \cdot p) \cdot (x_1 - 10) \\ 0 = -x_2 \cdot |x_2| + (x_3 - x_4)^2 \\ 1 = x_4 \\ y = x_1 \\ y = 0.2 \end{cases} \quad (6.8)$$

This is a square system with six unknowns and six equations. It is, however, unclear at first glance whether it has a solution, and if a solution exists, whether it is unique.

The first algebraic equation of (6.8) has two roots:  $x_2 = 2$  and  $x_2 = -1$ . The third equation has no solution with  $x_2 = -1$ . Therefore, only  $x_2 = 2$  must be considered. For  $x_2 = 2$ ,  $x_3 = 1 \pm 2$ . As physical states are assumed to be positive, the only possible solution is  $x_3 = 3$ .  $x_1 = y = 0.2$ . The second algebraic equation in (6.8) yields  $p = 2$ .

To sum up, (6.8) has two solutions,  $X_0 = [0.2 \ 2 \ -1 \ 1]^T$  and  $X_0 = [0.2 \ 2 \ 3 \ 1]^T$ , but only the second solution is physically valid, and the solution for the parameter is  $p = 2$ .

Let us now try to solve (6.8) with a numerical solver. Dymola is used for this experiment. The Modelica code is given in Fig. 6.3. The whole set of equations in the “initial equation” and “equation” sections is used to compute the initial state, i.e.,  $X_0$  and  $\dot{X}_0$ , whereas only the set of equations in the “equation” section is used to

**Fig. 6.3** Modelica model of system (6.7) with initial conditions specified by (6.8)

```
model Example
  parameter Real p(fixed=false);
  output Real y(start=0.2, fixed=true);

  Real x_1;
  Real x_2;
  Real x_3;
  Real x_4;

  initial equation
    0 = der(x_1);
    0 = der(x_2);
    0 = der(x_3);
    1 = der(x_4);

  equation
    der(x_1) = -0.3*(x_2 + 1)*(x_2 - x_4 - 1);
    der(x_2) = -0.3*(x_1 - 0.1*p)*(x_1 - 10);
    der(x_3) = -x_2*abs(x_2) + (x_3 - x_4)^2;
    der(x_4) = x_4;

    y = x_1;

end Example;
```

compute subsequent states  $X_{t>0}$  and  $\dot{X}_{t>0}$  after initial time. Therefore, the Modelica model is strictly equivalent to (6.8) at initial time and (6.7) after initial time.

The computing causalities of  $p$  and  $y$  are inverted by setting the modifier *fixed* to false for variable  $p$  and the modifier *fixed* to true for variable  $y$ . The target value for  $y$  is indicated by setting the modifier *start* to 0.2 for  $y$ .

When simulating the model, the solver chooses the solution  $x_2 = -1$  and therefore complains that the system has no solution for  $x_3$ . The solver chooses  $x_2 = -1$  because it starts iterating from  $x_2 = 0$  when no *guess value* is provided. Otherwise, it starts iterating from the guess value. A guess value is an approximate value of the solution guessed by the user. To force the solver choose the other root  $x_2 = 2$ , one has to provide a guess value for  $x_2$  that is closer to  $x_2 = 2$  than to  $x_2 = -1$ .  $x_2 = 4$  is chosen. Figure 6.4 shows that the guess value for  $x_2$  is indicated by setting the modifier *start* to 4 for  $x_2$ .

The solver finds then the unphysical solution  $x_3 = -1$ ; cf. Fig. 6.6a. To force the solver find the physical solution  $x_3 = 3$ , a proper guess value must be provided for  $x_3$ . The guess value chosen is 2; cf. Fig. 6.5.

The solver then finds the right physical solution; cf. Figure 6.6.

For models of complex systems, the algebraic system of equations to be solved is much more complex and requires expertise from the user to set the proper computing causalities and guess values, but the principle of the method stays the same.

**Fig. 6.4** Modelica model of system (6.7) with initial conditions (6.8) with a guess value for  $x_2$

```
model Example
  parameter Real p(fixed=false);
  output Real y(start=0.2, fixed=true);

  Real x_1;
  Real x_2;
  Real x_3;
  Real x_4;

  initial equation
    0 = der(x_1);
    0 = der(x_2);
    0 = der(x_3);
    1 = der(x_4);

  equation
    der(x_1) = -0.3*(x_2 + 1)*(x_2 - x_4 - 1);
    der(x_2) = -0.3*(x_1 - 0.1*p)*(x_1 - 10);
    der(x_3) = -x_2*abs(x_2) + (x_3 - x_4)^2;
    der(x_4) = x_4;

    y = x_1;

end Example;
```

**Fig. 6.5** Modelica model of system (6.7) with initial conditions (6.8) with guess values for  $x_2$  and  $x_3$

```

model Example
  parameter Real p(fixed=false);
  output Real y(start=0.2, fixed=true);

  Real x_1;
  Real x_2(start=4);
  Real x_3(start=2);
  Real x_4;

initial equation
  0 = der(x_1);
  0 = der(x_2);
  0 = der(x_3);
  1 = der(x_4);

equation
  der(x_1) = -0.3*(x_2 + 1)*(x_2 - x_4 - 1);
  der(x_2) = -0.3*(x_1 - 0.1*p)*(x_1 - 10);
  der(x_3) = -x_2*abs(x_2) + (x_3 - x_4)^2;
  der(x_4) = x_4;

  y = x_1;

end Example;

```

#### 6.4.4 Practical Steps

The practical steps for power plant model development are driven by the conceptual steps and the difficulty in finding the initial state because complex algebraic equations are involved in such models. Model development requires dealing with many unknown variables that must be computed by model inversion. To overcome this difficulty, the idea is to build and validate the model gradually by increasing slowly its size. This consists in practice in iterating on steps 2–10 of Sect. 6.4.2 while introducing progressively new component models into the model.

Here are the most common practical steps for model development:

1. Create a new model and give it a meaningful name.
2. Insert the first component into the model by drag-and-drop from the library. It is important to start the model with a component that defines a pressure reference for the system such as the condenser, a drum, or a steam generator.
3. Give meaningful names to the inserted component in order to provide better readability for the end user (e.g., Drum\_HP for the high-pressure drum, Condenser for the condenser, Valve\_MP for a medium-pressure valve, Turbine\_LP for the low-pressure turbine, Pump\_FW for a feed water pump).
4. Insert as many boundary conditions as unconnected ports of the model, and connect them so that the overall causality of the model is correct (cf. e.g., TestDynamicDrum in Sect. 14.2.5). The causality defines which variables are given as inputs (the known variables) and which variables are computed as

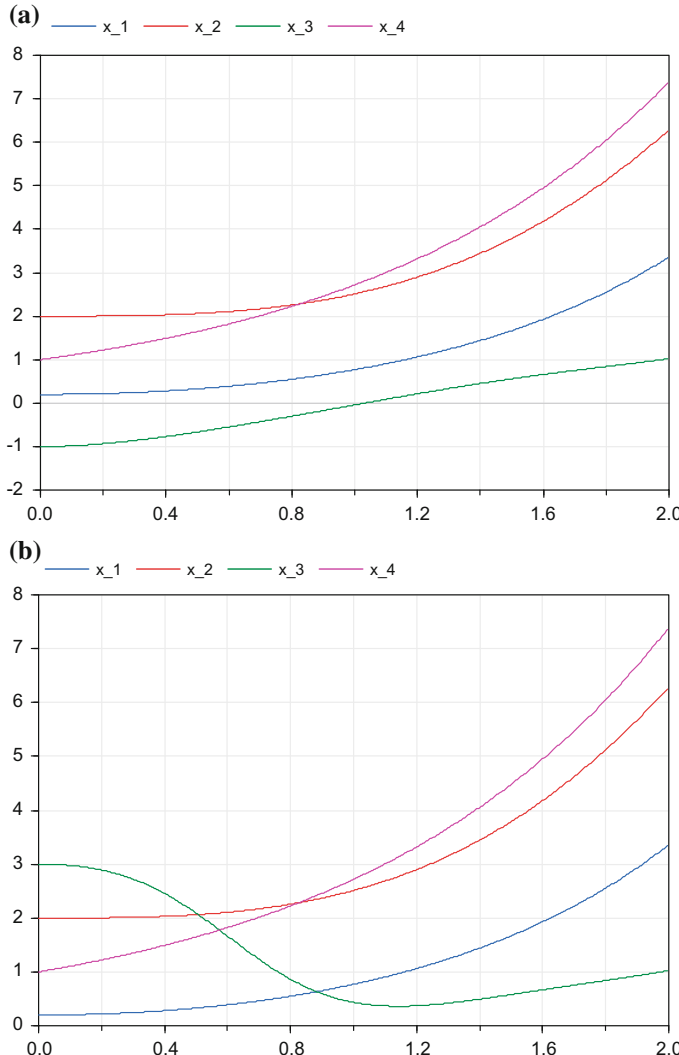


**Fig. 6.6** **a** Plot of the unphysical solution of (6.7) starting from steady-state conditions (6.8) with  $y = 0.2$ . **b** Plot of the physical solution of (6.7) starting from steady-state conditions (6.8) with  $y = 0.2$

outputs (the unknown variables) by the model equations. The causality is correct when the model can be computed, i.e., when the system is square for a Modelica model.

5. Replace the default values of the parameters in the boundary conditions by the collected data. The default values are those given in the library.

6. Define the calibration of the model by setting the values of variables of interest, which are normally outputs of the model, to values corresponding to a known operating point, such that the causality of the model is correct. For instance, one can set the fluid pressure in the condenser to a known operating value in order to compute the value of the mass flow rate of the cold source. Other examples of parameters to be calibrated are friction pressure loss coefficients, Stodola's ellipse coefficients, tube diameters, heat exchange surfaces.
7. Translate (compile) the model to produce the executable simulation code.
8. Provide an initialization script that sets the guess values for the guess variables of the model. A guess variable is a variable that must be provided a guess value to compute the initial state (cf. Sect. 6.4.3). The very first initialization script must be created from the engineer's expertise and knowledge of the plant operating points. This is usually the most difficult task.
9. Run the model, first for calibration, and in subsequent steps to calculate transients.
10. Verify the model by checking the results of the simulation. If the results are correct, save the model with a new version number.
11. Use the results of the model to create a new initialization script that is more accurate than the preceding one.
12. Insert another component and iterate from step 3.

The above steps are quite general, but they require some special functionalities that are not available in all tools, namely the ability to compute the initial state by inverse calculation and the ability to identify the guess variables automatically selected by the tool. Many Modelica tools provide these facilities.

#### 6.4.5 Practical Hints

Practical hints are given below:

- The topology of the model should be close to the technical diagrams (P&ID for instance) in order to provide a better readability for the end user. However, in general, the model cannot be graphically identical to technical diagrams because components that are usually not present in technical diagrams such as mergers, splitters, or pipes must be explicitly added to the model. This is due to the fact that technical diagrams such as P&ID represent the architecture of the system in a rather functional way where the piping represents flow directions, whereas the model represents the architecture of the system in a physical way where the piping represents physical fluid flow.
- For model calibration of a non-existing power plant, it is necessary to know the order of magnitude of the parameter values of the system design.
- For model calibration of an existing power plant, it is necessary to set as many variables to known measurement values as possible (temperatures, pressures, mass flow rates, levels in drum, etc.) taken from on-site sensors for a given load

(e.g., 75, 100%). This method ensures that all needed performance parameters, size characteristics, and input data can be computed by model inversion (friction pressure loss coefficients, pipes' diameters, maximum mass flow rate coefficients of the valves, heat exchange surfaces, heat exchange efficiencies, Stodola's ellipse coefficients, turbine efficiencies, pumps characteristics, etc.).

- After model calibration, it is recommended to check carefully all parameters computed by model inversion.
- A convergence problem can be indicative of a bad choice for the physical quantities imposed on the model for the calibration of the unknown parameters. It may also be due to an error in the initialization script file (guess variables not found in the script or guess values poorly estimated in the script). It is then necessary to check the consistency of the initialization script with respect to the guess variables generated by the compiler, and check the consistency of the guess values with respect to design or operation data.
- When physical quantities vary in space, it is necessary to set correctly the discretization parameters of the component models (such as the number of segments).
- Pay close attention to the units of the physical quantities used in the model (e.g., bars vs. Pa, °C vs. K).

## 6.5 Dynamic Model of a Real Combined Cycle Power Plant

### 6.5.1 Description of a Combined Cycle Power Plant

Combined cycle power plants use both the gas turbine Brayton cycle (cf. Sect. 2.9.1) and the steam turbine Rankine cycle (cf. Sect. 2.9.2). A basic configuration for a combined cycle power plant consists of one or more gas turbines used in conjunction with a dedicated heat recovery steam generator (HRSG) connected through the turbine exhaust path (cf. Fig. 6.7). The steam produced in the HRSG (at one or more pressure levels) is fed to a steam turbine driving an electric generator. This greatly increases the overall efficiency of the power plant.

The gas turbine has an upstream compressor coupled to a downstream turbine, and a combustion chamber in between. It is normally fueled with natural gas, although low-sulfur fuel oil can also be used. The atmospheric air flows through the compressor to be brought to higher pressure. In the combustion chamber, energy is added by spraying fuel into the air, and the combustion of the mixture generates high-temperature flue gases. Then, the hot flue gases flow through the turbine, where they expand to the exhaust pressure, producing work on the shaft. A significant part of the shaft work is used to drive the compressor and other devices such as an electric generator that may be coupled to the shaft. The rest is used by the alternator to generate electricity.

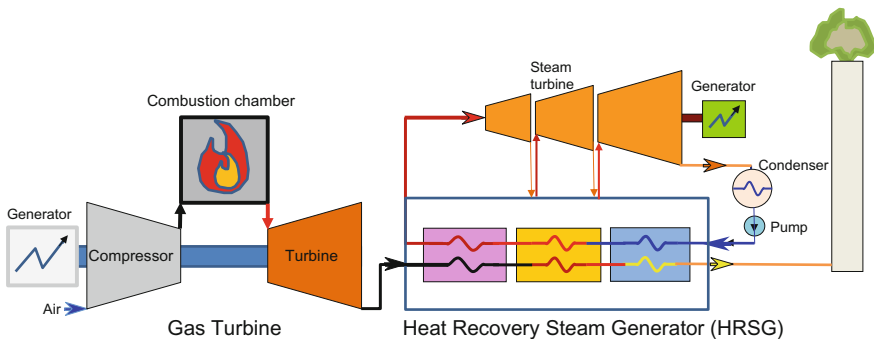


**Fig. 6.7** Schematic diagram of a combined cycle power plant

The hot effluent (exhaust flue gases) of the gas turbine is used in the steam cycle of the plant where it provides heat to generate steam in the steam generator. The generated steam expands in the steam turbine and produces additional electrical energy. The steam cycle includes: the steam turbine, a boiler (with several tubular heat exchangers that transfer the exhaust gas heat to the water), three evaporating loops (at low, intermediate, and high pressure), several pumps, valves and pipes, and a condenser.

### **The low-pressure (LP) loop**

At the exit of the condenser, water is pumped and heated in the LP economizer and then is sent to the LP drum. The water leaving the LP drum goes to the LP evaporator, the IP loop, and the HP loop. The produced steam is transmitted to the LP super-heater, then to a mixer (to mix the steam at the exit of the LP super-heater with the steam at exit of the IP turbine), and then to the LP turbine.

### **The intermediate pressure (IP) loop**

At the exit of the LP drum, water is pumped and heated in the IP economizer and then is sent to the IP drum. The water leaving the IP drum goes to the IP evaporator, and the produced steam is transmitted to the first IP super-heater, then to a mixer (to mix the steam at the exit of the IP super-heater with the steam at exit of the HP turbine), then to the second IP super-heater, then to the third IP super-heater, and then to the IP turbine.

### **The high-pressure (HP) loop**

At the exit of the LP drum, water is pumped and heated in the first, the second, the third, and the fourth HP economizers and then is sent to the HP drum. The water leaving the HP drum goes to the HP evaporator. The produced steam is transmitted to the first HP super-heater, then to the second HP super-heater, then to the third HP super-heater, and then to the HP turbine.

## **The condenser**

At the exit of the LP turbine, the steam is condensed in the condenser, and then the water is pumped and sent to the LP economizer.

### ***6.5.2 Description of the Phu My Combined Cycle Power Plant***

The Phu My combined cycle power plant is located in the Phu My power generation complex in the town of Phu My, Vietnam. The power plant consists of a 2–2–1 (2 gas turbines, 2 HRSG, and 1 steam turbine) combined cycle generating 729 MWe net power, 468 MWe in simple cycle mode with manual bypass system. The main fuel is natural gas. Diesel oil fuel is used as a backup fuel for an annual limited continuous period of 5 days. The net efficiency of the combined cycle with gas is 56.3%. The plant is composed of two gas turbines (GT), two heat recovery steam generators (HRSG) with three levels of pressure and reheat, one steam turbine, one river water cooling condenser.

The plant characteristics are (under ambient conditions of 32 °C, 1 atm., and 80% air humidity):

- Gas turbine (GT)
  - Compressor compression rate: 14,
  - Nominal power: 226.2 MWe.
- Steam generator (HRSG)
  - Thermal power: **361 MWth**,
  - HRSG with three levels of pressure,
  - High-pressure circuit at nominal power: 126.8 bar, 568 °C,  $2 \times 273$  t/h,
  - Intermediate pressure circuit at nominal power:  $2 \times 28.7$  t/h with reheat: 25.25 bar, 568 °C,  $2 \times 302.5$  t/h,
  - Low-pressure circuit at nominal power: 4.8 bar, 259 °C,  $2 \times 34.4$  t/h.
- Steam turbine
  - Nominal power: **277 MWe**,
  - High pressure at nominal power: 125 bar, 566 °C, 546 t/h; relative power: 22%,
  - Intermediate pressure at nominal power: 25 bar, 567 °C, 605 t/h; relative power: 30%,
  - Low pressure at nominal power: 5 bar, 260.5 °C, 673.7 t/h; relative power: 48%,
  - Exhaust steam: 61 mbar abs, 696.3 t/h.

- Condenser

- Steam flow rate: 696.3 t/h (**193.417 kg/s**),
- Thermal power: **428 MW<sub>th</sub>**,
- Inlet water temperature: 27 °C; outlet water temperature: 33 °C,
- 2 × 100% vacuum pumps; vacuum pressure: 61 mbar.

### 6.5.3 Description of the Model

This chapter presents the dynamic model of a combined cycle power plant called *CombinedCyclePowerPlant* developed by EDF with Modelica.

The full 1D dynamic model is built by connecting the component models in a technological way, so that its topology reflects the functional schema of a real combined cycle power plant. The model contains two main parts: the water/steam cycle and the flue gases subsystem. Only one train is modeled, so identical behavior is assumed for each HRSG and for each gas turbine.

The structure of the combined cycle power plant model is shown in Fig. 6.8: (1) gas turbine; (2), (4), and (6) HP super-heaters; (3), (5), and (9) IP super-heaters; (11) LP super-heater; (7) HP evaporator; (12) IP evaporator; (16) BP evaporator; (8), (10), (13), and (15) HP economizers; (14) IP economizer; (17) LP economizer; (18) HP drum; (19) IP drum; (20) LP drum; (22) HP pump; (21) IP pump; (23) LP pump; (24) HP steam governor valve; (25) IP steam governor valve; (26) HP steam turbine; (27) IP steam turbine; (28) LP steam turbine; (29) volume; (30) condenser; (31) HP drum-level control; (32) IP drum-level control; (33) LP drum-level control; (34) HP evaporating loop; (35) IP evaporating loop; (36) LP evaporating loop; and (37) electric generator. Table 6.1 lists the ThermoSysPro (TSP) components used in the model.

The physical equations of each component model are given in Chaps. 7–16.

The model contains 673 component models totaling 10,802 variables, 257 differentiated variables, 2752 equations, and 1855 non-trivial equations (obtained after elimination of simple equations).

Two models are used: one to simulate the power generator step reduction load (cf. Fig. 6.8a) and the other to simulate the full GT trip (cf. Fig. 6.8b). In the model used to simulate the GT trip, the gas turbine is replaced by a boundary condition.

The two models are available in the *ThermoSysPro.Examples* package.

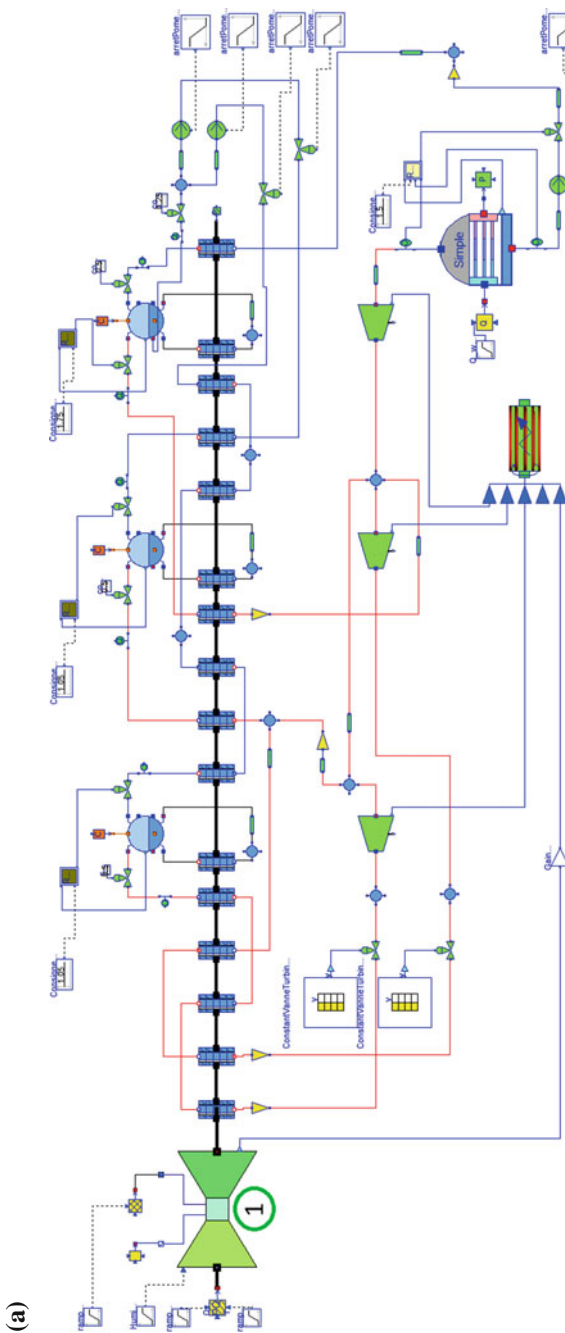


**Fig. 6.8** **a** Model of the power generator step reduction load (1 gas turbine + 1 HRSG + steam turbine + condenser). **b** Model used for the full GT trip. **c**. Models of the drum (left) and condenser (right) water-level controls

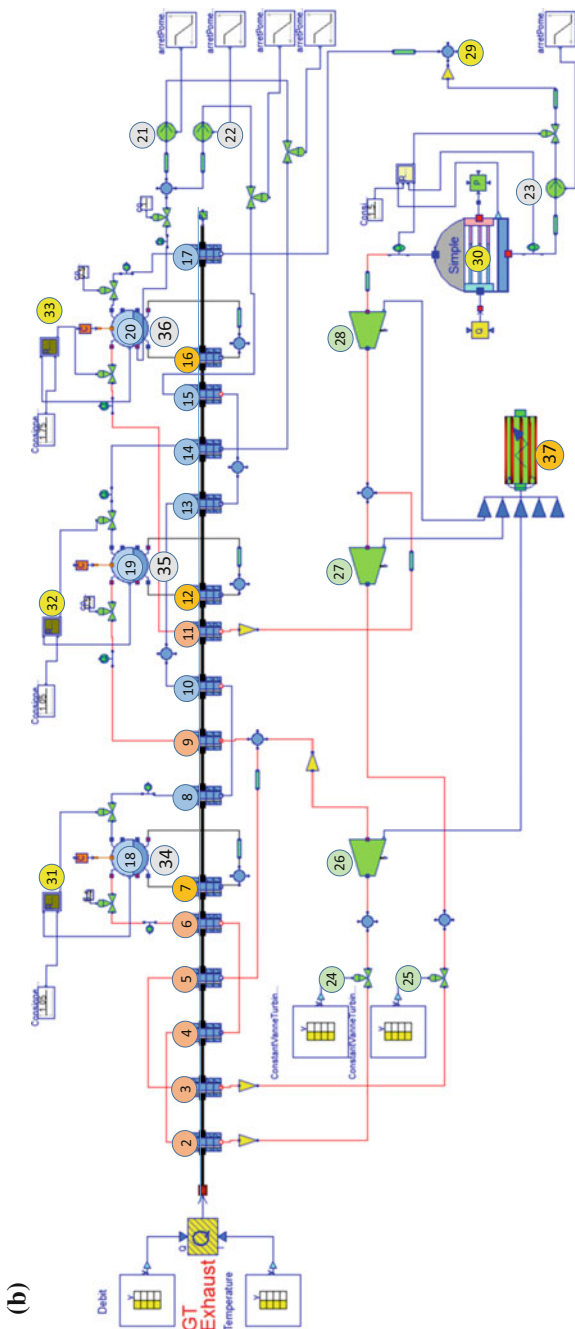


Fig. 6.8 (continued)

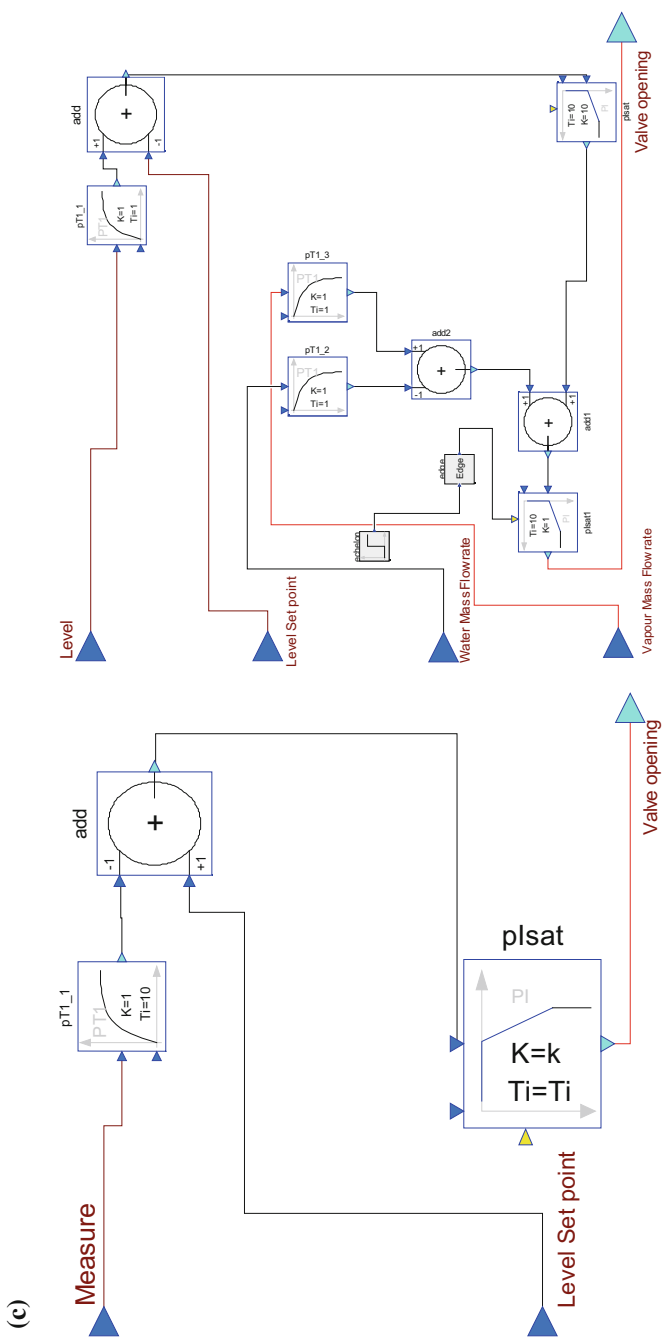


Fig. 6.8 (continued)

### 6.5.3.1 Model Topology of the HRSG (Water/Steam Cycle “1 Train”)

The model consists of 16 heat exchangers (3 evaporators, 6 economizers, and 7 super-heaters), 3 evaporating loops (low, intermediate, and high pressure), 3 drums, 3 steam turbine stages (HP, IP, and LP), 3 pumps, 12 valves, several pressure drops, several mixers, several collectors, 1 condenser, 1 generator, several sensors, sources, sinks, and the control system limited to the drum-level control.

An important feature of this model is that the thermodynamic cycle is completely closed through the condenser. This is something quite difficult to achieve, due to the difficulty of solving numerically large algebraic loops.

The list of components used for the development of the HRSG model is given in Table 6.1.

The dynamic 1D heat exchanger model *DynamicExchangerWaterSteamFlueGases* consists of three sub-models: (1) the water/steam flow model which is a two-phase flow model, (2) the wall model, and (3) the flue gases flow model (see Fig. 6.9).

**Table 6.1** ThermoSysPro components used in the HRSG model

Components	Model name in TSP	Package name in TSP
Condenser	<i>SimpleDynamicCondenser</i>	<i>WaterSteam.HeatExchangers</i>
Drums	<i>DynamicDrum</i>	<i>WaterSteam.Volumes</i>
Generator	<i>Generator</i>	<i>WaterSteam.Machines</i>
Heat exchangers	<i>DynamicExchangerWaterSteamFlueGases</i> <b>contains</b> <i>DynamicTwoPhaseFlowPipe</i> <i>StaticWallFlueGasesExchanger</i> <i>HeatExchangerWall</i>	<i>MultiFluids.HeatExchangers</i> <b>contains</b> <i>WaterSteam.HeatExchangers</i> <i>FlueGases.HeatExchangers</i> <i>Thermal.HeatTransfer</i>
Pipes	<i>PipePressureLoss</i>	<i>WaterSteam.PressureLosses</i>
Pumps	<i>StaticCentrifugalPump</i>	<i>WaterSteam.Machines</i>
Mass flow sensor	<i>SensorQ</i>	<i>WaterSteam.Sensors</i>
Steam turbines	<i>StodolaTurbine</i>	<i>WaterSteam.Machines</i>
Valves	<i>ControlValve</i>	<i>WaterSteam.PressureLosses</i>
Mixers	<i>VolumeB</i> , <i>VolumeC</i>	<i>WaterSteam.Volumes</i>
Splitters	<i>VolumeA</i> , <i>VolumeD</i>	<i>WaterSteam.Volumes</i>
Level controls	<i>Drum_LevelControl</i> <i>Condenser_LevelControl</i>	<i>Examples.PowerPlants.</i> <i>Control</i>

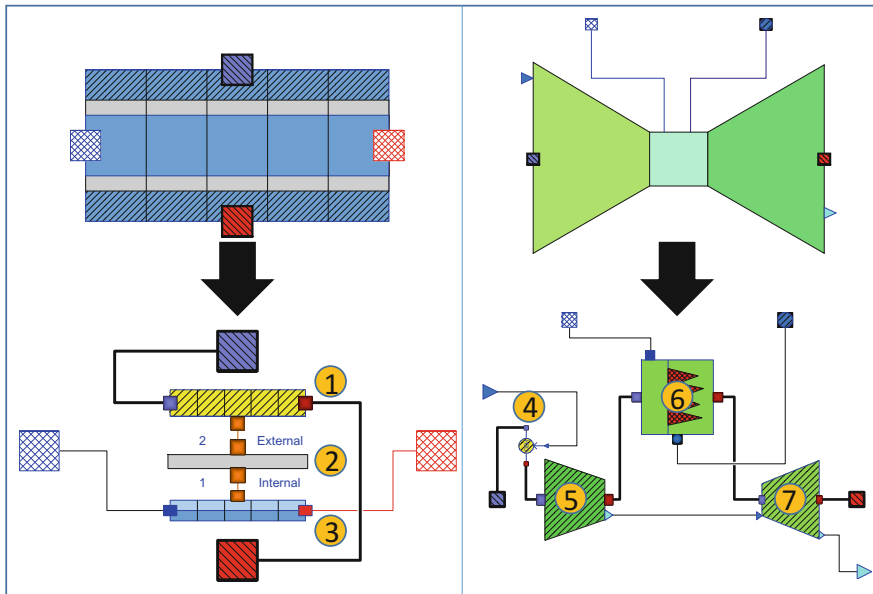


**Fig. 6.9** Heat exchanger: flue gases/water steam model and gas turbine model

### 6.5.3.2 Model Topology of the Control System (Limited to the Drum- and Condenser-Level Controls)

The real drum-level control is quite complex, so it is replaced in the model by simple PI controllers (cf. Fig. 6.8c).

Each drum is controlled by a separate controller which consists in a PI controller that takes as input the water level inside the drum.

The condenser is controlled with a PI controller that takes as inputs the condenser water level, the incoming steam mass flow rate, and the outgoing water mass flow rate.

### 6.5.3.3 Model Topology of the Gas Turbine (GT)

The model consists of four sub-models: (4) air humidity model, (5) compressor, (6) combustion chamber, and (7) gas turbine (cf. Fig. 6.9).

The list of component models used for the development of the GT model is given in Table 6.2.

**Table 6.2** ThermoSysPro components used in the gas turbine (GT) model

Components	Model name in TSP	Package name in TSP
Compressor	<i>Compressor</i>	<i>FlueGases.Machines</i>
Combustion chamber	<i>GTCCombustionChamber</i>	<i>Combustion. CombustionChambers</i>
Gas turbine	<i>CombustionTurbine</i>	<i>FlueGases.Machines</i>
Air humidity	<i>AirHumidity</i>	<i>FlueGases.BoundaryConditions</i>

### 6.5.3.4 Model Parameterization and Boundary Conditions

All geometrical data are provided to the model (tube and exchanger lengths, diameters, volumes, corrective terms for the heat exchange coefficients, corrective terms for the pressure losses, etc.). The characteristics of the main components of the model are:

#### Heat exchangers (*EconomiseurBP*):

- Number of pipes = 3444
- Internal diameter of the pipes = 0.0328 m
- External diameter of the pipes = 0.038 m
- Length of the pipes = 20.726 m
- Inlet altitude of the pipes = 0
- Outlet altitude of the pipes = 10.767 m
- Longitudinal length step = 0.092 m
- Transverse length step = 0.0869 m
- Pipes' thermal conductivity = 47 W/m/K
- Cross-sectional area = 5 m<sup>2</sup>
- Increase factor of the heat exchange surface = 11.67376
- Corrective term for the friction pressure loss = 0.5.

#### Heat exchangers (*EvaporateurHP*):

- Number of pipes = 1476
- Internal diameter of the pipes = 0.0328 m
- External diameter of the pipes = 0.038 m
- Length of the pipes = 20.7 m
- Inlet altitude of the pipes = 0
- Outlet altitude of the pipes = 10.83 m
- Longitudinal length step = 0.092 m
- Transverse length step = 0.0869 m
- Pipes' thermal conductivity = 47 W/m/K
- Cross-sectional area = 5 m<sup>2</sup>
- Increase factor of the heat exchange surface = 11.86442
- Corrective term for the friction pressure loss = 1.

**Heat exchangers (SurchauffeurHP1):**

- Number of pipes = 246
- Internal diameter of the pipes = 0.0328 m
- External diameter of the pipes = 0.038 m
- Length of the pipes = 20.4 m
- Inlet altitude of the pipes = 0
- Outlet altitude of the pipes = 10.83 m
- Longitudinal length step = 0.111 m
- Transverse length step = 0.0869 m
- Pipes' thermal conductivity = 37.61 W/m/K
- Cross-sectional area = 1 m<sup>2</sup>
- Increase factor of the heat exchange surface = 10.25056
- Corrective term for the friction pressure loss = 2.

**HP drum:**

- Cavity length = 16.27 m
- Cavity radius = 1.05 m
- Liquid level in the cavity = 1.05 m
- Steam mass flow rate at the outlet = 76.58 kg/s.

**HP turbine:**

- Minimum isentropic efficiency = 0.75
- Steam specific enthalpy at the outlet =  $3106 \times 10^3$  J/kg
- Steam pressure at the inlet =  $125.2 \times 10^5$  Pa.

**LP pump:**

- $a_1$  (pump) =  $-6000 \text{ s}^2/\text{m}^5$
- $a_2$  (pump) = 0
- $a_3$  (pump) = 400 m
- $b_1$  (pump) =  $-3.7751 \text{ s}^2/\text{m}^6$
- $b_2$  (pump) =  $3.61 \text{ s}/\text{m}^3$
- $b_3$  (pump) =  $-0.0075464$
- Nominal rotational speed = 1400 rev/min.

**Feed water valve (LP drum):**

- Water pressure at the outlet =  $5.2 \times 10^5$  Pa
- Maximum mass flow coefficient of the valve = 250 U.S.

**Condenser:**

- Cavity volume = 1000 m<sup>3</sup>
- Cavity cross-sectional area = 100 m<sup>2</sup>
- Fraction of initial water volume in the drum = 0.15
- Fluid initial pressure = 6100 Pa
- Pipes' diameter = 0.018 m

- Pipes' wall thickness = 0.002 m
- Pipes' length = 10 m
- Number of pipes = 28,700.

### **Gas turbine:**

- Compressor: isentropic efficiency = 0.76
- Nominal compression rate ratio = 1
- Compressor:  $X^4$  coefficient of the efficiency = 0
- Compressor:  $X^3$  coefficient of the efficiency = 0
- Compressor:  $X^2$  coefficient of the efficiency = -0.634857
- Compressor:  $X^1$  coefficient of the efficiency = 1.46222
- Compressor:  $X^0$  coefficient of the efficiency = 0.1725914
- Turbine: nominal expansion rate = 0.079094
- Turbine: fluid temperature at the outlet = 620.61 K
- Turbine: corrected mass flow (reduced mass flow rate) = 0.01731
- Air pressure at the inlet of the combustion chamber =  $14.042 \times 10^5$  Pa
- Air temperature at the inlet = 302.56 K
- Air pressure at the inlet =  $1.003 \times 10^5$  Pa
- Air mass flow rate at the inlet = 593.42 kg/s
- CO<sub>2</sub> mass fraction in the air at the inlet = 0
- H<sub>2</sub>O mass fraction in the air at the inlet = 0
- O<sub>2</sub> mass fraction in the air at the inlet = 0.20994
- SO<sub>2</sub> mass fraction in the air at the inlet = 0
- Water mass flow rate at the inlet = 0
- Fuel temperature at the inlet = 458.16 K
- Fuel mass flow rate at the inlet = 13.521 kg/s
- Lower heating value of the fuel =  $46989 \times 10^3$  J/kg
- Fuel humidity = 0
- C mass fraction in the fuel = 0.74
- H mass fraction in the fuel = 0.25
- Fuel specific heat capacity = 2255 J/kg/K
- Fuel density = 0.838 kg/m<sup>3</sup>.

#### **6.5.3.5 Model Calibration**

Table 6.3 shows, for each component in the model, the unknown variables computed by model inversion and, for each unknown variable, the corresponding known variable.

**Table 6.3** Variables computed by model inversion

Component name	Unknown variables	Corresponding known variables
<i>CombustionChamber</i>	<b>C_Kcham:</b> Pressure loss coefficient	<b>Pea:</b> Air pressure at the inlet
<i>CombustionTurbine</i>	<b>1—T_Qred:</b> Reduced mass flow rate <b>2—T_is_eff_n:</b> Nominal isentropic efficiency	<b>1—tau:</b> Expansion rate <b>2—Ts:</b> Flue gases temperature at the outlet
<i>Compressor</i>	<b>1—C_tau_n:</b> Nominal compression rate <b>2—C_is_eff_n:</b> Nominal isentropic efficiency	<b>1—is_eff:</b> Isentropic efficiency <b>2—Xtau:</b> Normal/nominal compression rate ratio
<i>HP_DownComer</i>	<b>K_HP_DownComer:</b> Friction pressure loss coefficient	<b>Q:</b> Mass flow rate
<i>HP_Economizer_1</i>	<b>Fouling_EHP1:</b> Corrective term for the heat exchange coefficient	<b>K:</b> Total heat exchange coefficient
<i>HP_Economizer_2</i>	<b>Fouling_EHP2:</b> Corrective term for the heat exchange coefficient	<b>K:</b> Total heat exchange coefficient
<i>HP_Economizer_3</i>	<b>Fouling_EHP3:</b> Corrective term for the heat exchange coefficient	<b>K:</b> Total heat exchange coefficient
<i>HP_Economizer_4</i>	<b>Fouling_EHP4:</b> Corrective term for the heat exchange coefficient	<b>K:</b> Total heat exchange coefficient
<i>HP_Evaporator</i>	<b>Fouling_EvHP:</b> Corrective term for the heat exchange coefficient	<b>HP_Drum.Cv.Q:</b> Steam mass flow rate
<i>HP_FeedValve</i>	<b>CvmaxValveAHP:</b> Maximum Cv of the HP drum feed water valve	<b>HP_Drum.zl:</b> Liquid level in drum
<i>HP_PressureLoss_2</i>	<b>K_Dp_HP_2:</b> Friction pressure loss coefficient	<b>C1.P:</b> Pressure at the inlet
<i>HP_SteamValve</i>	<b>CvmaxValveVHP:</b> Maximum Cv of the IP drum steam valve	<b>HP_SteamValve.C1.P:</b> Pressure at the inlet
<i>HP_SuperHeater_1</i> <i>HP_SuperHeater_2</i> <i>HP_SuperHeater_3</i>	<b>Fouling_SHP:</b> Corrective term for the heat exchange coefficient (the same parameter for all three components)	<b>HP3_SuperHeater.</b> <b>Cws2.h:</b> Fluid specific enthalpy at the outlet
<i>HP_Turbine</i>	<b>1—CstHP:</b> Stodola's HP ellipse coefficient <b>2—EtaIsNomHP:</b> Nominal isentropic efficiency	<b>1—Pe:</b> Pressure at the inlet <b>2—C2.h:</b> Fluid specific enthalpy at the outlet
<i>HP_Turbine_Valve</i>	<b>Cvmax_THP:</b> Maximum CV, HP	<b>C1.P:</b> Pressure at the inlet
<i>HP_IP_PressureLoss</i>	<b>K_Dp_HP_IP:</b> Friction pressure loss coefficient	<b>Q:</b> Mass flow rate
<i>IP_DownComer</i>	<b>K_IP_DownComer:</b> Friction pressure loss coefficient	<b>Q:</b> Mass flow rate
<i>IP_Economizer</i>	<b>Fouling_EMP:</b> Corrective term for the heat exchange coefficient	<b>K:</b> Total heat exchange coefficient
<i>IP_Evaporator</i>	<b>Fouling_EvMP:</b> Corrective term for the heat exchange coefficient	<b>IP_Drum.Cv.Q:</b> Steam mass flow rate

(continued)

**Table 6.3** (continued)

Component name	Unknown variables	Corresponding known variables
<i>IP_SteamValve</i>	<b>CvmaxValveVMP:</b> Maximum Cv of the IP drum steam valve	<b>IP_SteamValve.C1.P:</b> Pressure at the inlet
<i>IP_SuperHeater_1</i> <i>IP_SuperHeater_2</i> <i>IP_SuperHeater_3</i>	<b>Fouling_SMP:</b> Corrective term for the heat exchange coefficient (the same parameter for all three components)	<b>IP3_SuperHeaterCws2.</b> <b>h:</b> Fluid specific enthalpy at the outlet
<i>IP_Turbine</i>	<b>CstMP:</b> Stodola's IP ellipse coefficient	<b>Pe:</b> Pressure at the inlet
<i>LP_Economizer</i>	<b>Fouling_EBP:</b> Corrective term for the heat exchange coefficient	<b>K:</b> Total heat exchange coefficient
<i>IP_FeedValve</i>	<b>CvmaxValveAMP:</b> Maximum Cv of the IP drum feed water valve	<b>IP_Drum.zl:</b> Liquid level in drum
<i>LP_Evaporator</i>	<b>Fouling_EvBP:</b> Corrective term for the heat exchange coefficient	<b>LP_Drum.Cv.Q:</b> Steam mass flow rate
<i>LP_Pump</i>	<b>LP_Pump_a1:</b> $x^2$ Coefficient of the pump characteristics (hn)	<b>LP_FeedValve.C2.P:</b> Pressure at the outlet
<i>LP_SteamValve</i>	<b>CvmaxValveABP:</b> Maximum Cv of the LP drum feed water valve	<b>LP_Drum.zl:</b> Liquid level in drum
<i>LP_SuperHeater</i>	<b>Fouling_SBP:</b> Corrective term for the heat exchange coefficient	<b>K:</b> Total heat exchange coefficient
<i>LP_Turbine</i>	<b>1—CstBP:</b> Stodola's LP ellipse coefficient <b>2—EtaIsNomBP:</b> Nominal isentropic efficiency	<b>1—Pe:</b> Pressure at the inlet <b>2—C2.h:</b> Fluid specific enthalpy at the outlet
<i>IP_Turbine_Valve</i>	<b>Cvmax_TMP:</b> Maximum CV; MP	<b>C1.P:</b> Pressure at the inlet

#### 6.5.3.6 Scenarios' Description

For simulation runs, two scenarios are selected.

The first scenario is a power generator step reduction from 100 to 40.5% load (cf. Fig. 6.10):

- Initial state (combined cycle): 100% load,
- Final state (combined cycle): 40.5% load (800 s slope).

The second scenario is a full GT trip (sudden stopping of the gas turbine):

- Initial state (GT exhaust): flue gases temperature = 620.6 °C and flue gases mass flow rate = 606.94 kg/s,
- Final state (GT exhaust): flue gases temperature = 150 °C and flue gases mass flow rate = 50 kg/s (600 s slope).

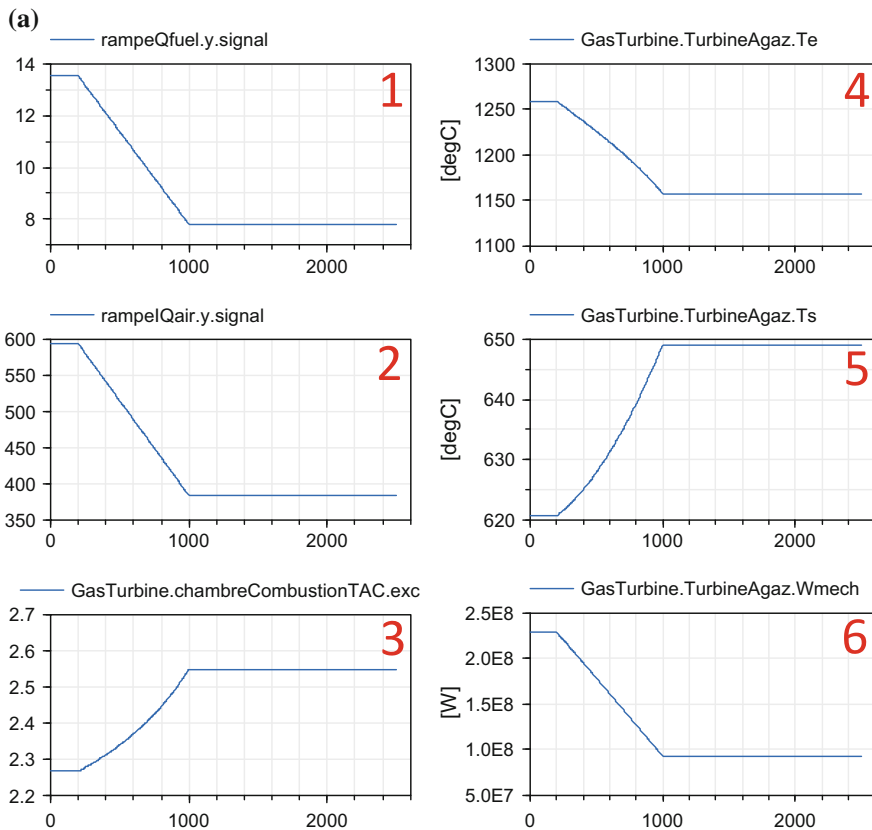


**Fig. 6.10** **a** Simulation results for the power generator step reduction scenario ( $-59.5\%$ ): (1) natural gas mass flow rate, (2) air mass flow rate, (3) excess air mass flow rate, (4) temperature at the inlet of the combustion turbine, (5) gas turbine exhaust temperature, and (6) mechanical power of the combustion turbine. **b** Simulation results for the power generator step reduction scenario ( $-59.5\%$ ): (7) mechanical power produced by the HP, IP, and LP steam turbines, (8) generator power, and (9) HRSG temperature at the outlet, and (10–12) steam mass flow rates produced in the HP, IP, and LP drums. **c** Simulation results for the power generator step reduction scenario ( $-59.5\%$ ): (13–15) HP, IP, and LP drum pressures, and (16–18) HP, IP, and LP drum water levels

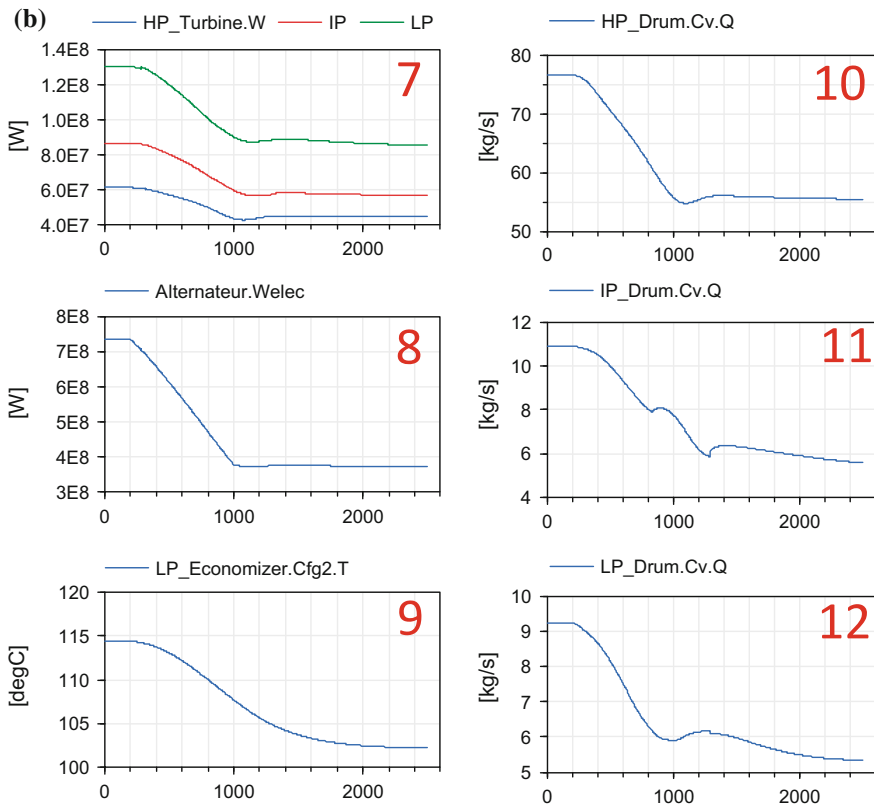
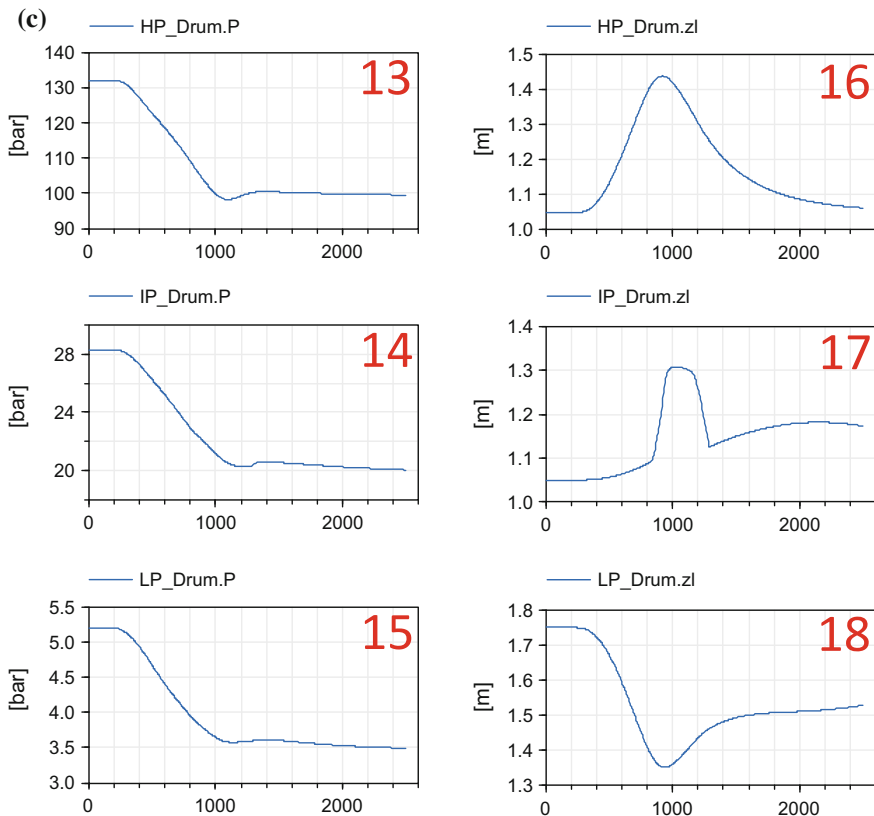


Fig. 6.10 (continued)



**Fig. 6.10** (continued)

#### 6.5.3.7 Simulation Results

The dynamic model is capable of simulating the dynamic behavior of the entire combined cycle power plant.

Utilized software: Dymola 2017 and OpenModelica 1.9.6, with the DASSL solver set at tolerance  $10^{-4}$ .

The model computes precisely:

- The excess air in the gas turbine;
- The distribution of water and steam mass flow rates;
- The pressure, temperature, and specific enthalpy distribution across the network;
- The drum levels and condenser level;
- The performance parameters for all pieces of equipment;
- The global efficiencies of the water/steam cycle and gas turbine;
- The thermal power of the heat exchangers;
- The electrical power generated by the generator.

The following phenomena are simulated:

- Flow reversal;
- Local boiling or condensation;
- Swell and shrink effect in drums.

Figure 6.10 shows the results for 2500 s of simulation of the “power generator step reduction from 100 to 40.5% load” scenario. Curves 1 and 2 display, respectively, the variation of the natural gas and air mass flow rates at the inlets. The results show that the excess air (curve 3) and the exhaust temperature of the combustion turbine (curve 5) increase when the power produced decreases.

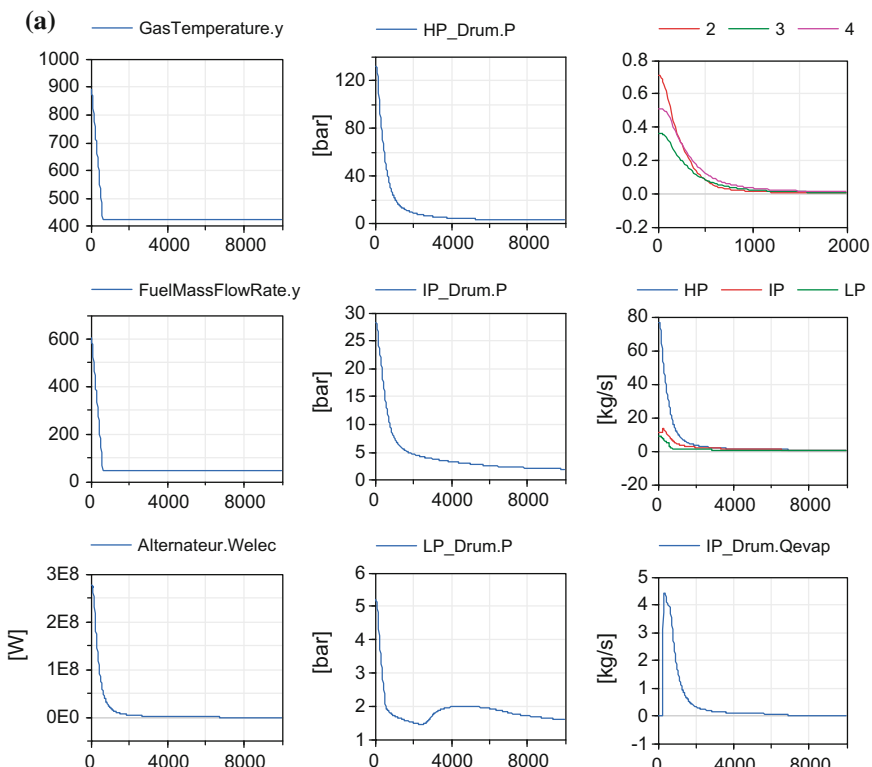


**Fig. 6.11** **a** Simulation results for the GT trip scenario (top to bottom and then left to right): (1) flue gases temperature at the inlet of the HRSG, (2) flue gases mass flow rate at the inlet of the HRSG, (3) generator power, (4–6) HP, IP, and LP drum pressures, (7) vapor mass fraction in the HP evaporator at different pipe positions, (8) steam mass flow rate produced in the HP, IP, and LP drums, and (9) evaporation mass flow rate from the liquid phase in the IP drum. **b** Simulation results for the GT trip scenario (top to bottom and then left to right): (1) condenser mass flow rate at the inlet and the outlet, (2) HRSG temperature at the outlet, (3) mechanical power produced in the HP, IP, and LP steam turbines, (4–6) steam mass flow rate produced in the HP, IP, and LP drums, and (7–9) water level in the HP, IP, and LP drums

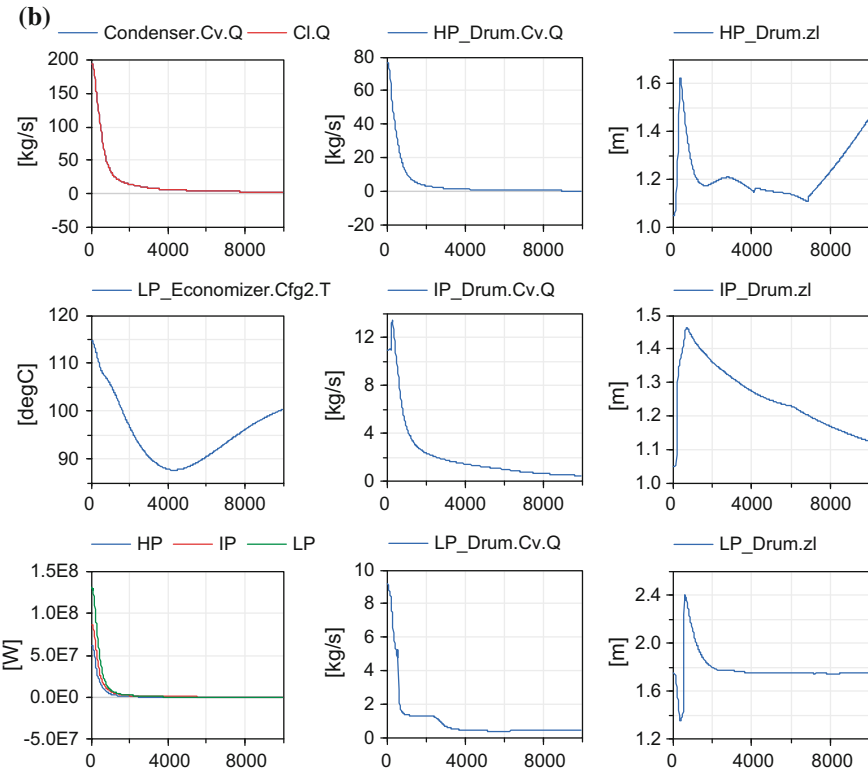


**Fig. 6.11** (continued)

The power variation of the gas turbine, steam turbine, and generator is shown in curves 6, 7, and 8.

Curves 16 and 17 show the effect of swelling in drums: The water level inside the drum increases when the pressure inside the drum decreases (curves 13 and 14); cf. also Sect. 14.2.5.3.

Figure 6.11 shows the results for 10,000 s ( $\approx 2.8$  h) of simulation of the full GT trip scenario. The results are fairly consistent with the engineer's expertise.

In particular, it is possible to simulate a GT trip until the full stopping of the plant.

However, the recirculation flows in the evaporators do not go to zero as expected. This problem originates from the topology of the evaporating loops: The down-comer sucks water from the bottom of the drum, whereas the riser propels the water/steam mixture toward the top of the drum inside the steam phase. Consequently, the pressure at the input of the down-comer (which is at the drum pressure + water head inside the drum from water level down to the bottom of the drum) stays higher than the pressure at the output of the riser (which is at the drum pressure). The difference in pressure between the input of the down-comer and the output of the riser (the water head inside the drum) does not go to zero because

the water level inside the riser does not go down to reach the water level inside the drum when the energy provided to the riser to evaporate water decreases. The modeling and simulation of such phenomenon are impossible (or at least very difficult) with current state-of-the-art tools because they require multi-mode modeling and simulation to account for the progressive disappearance of water and the appearance of steam in the segment of the riser that is above drum level as water recedes from top to bottom in the riser to let steam in the drum enter the riser (cf. also Sect. 1.4).

**Table 6.4** (a) Comparison between simulation results and GE gas design results for 100% load.  
 (b) Comparison between simulation results and GE gas design results for 40.5% load

(a)		Simulation	GE	Unit
100% load				
Mechanical power developed by the combustion turbine	228.8	226.2	MW	
Mechanical power developed by the steam turbine	278.33	277.20	MW	
Flue gases temperature at the inlet of the HRSG	620.60	620.60	°C	
Flue gases temperature at the outlet of the HRSG	114.7	90.0	°C	
HP_Drum: Fluid average pressure	132.1	132.1	bar	
IP_Drum: Fluid average pressure	28.3	28.3	bar	
LP_Drum: Fluid average pressure	5.2	5.2	bar	
HP_Drum: Steam mass flow rate at the outlet	76.58	76.58	kg/s	
IP_Drum: Steam mass flow rate at the outlet	10.9	10.9	kg/s	
LP_Drum: Steam mass flow rate at the outlet	9.23	9.23	kg/s	
HP_Steam Turbine: Fluid pressure at the inlet	125.20	125.20	bar	
IP_Steam Turbine: Fluid pressure at the inlet	25.13	25.13	bar	
LP_Steam Turbine: Fluid pressure at the inlet	4.77	4.77	bar	
Condenser: Steam mass flow rate at the inlet	193.43	193.43	kg/s	
(b)				
40.5% load		Simulation	GE	Unit
Mechanical power developed by the combustion turbine	92.56	91.50	MW	
Mechanical power developed by the steam turbine	187.03	186.50	MW	
Flue gases temperature at the inlet of the HRSG	648.99	648.90	°C	
Flue gases temperature at the outlet of the HRSG	102.5	90.0	°C	
HP_Drum: Fluid average pressure	99.48	92.0	bar	
IP_Drum: Fluid average pressure	20.05	19.9	bar	
LP_Drum: Fluid average pressure	3.493	3.3	bar	
HP_Drum: Steam mass flow rate at the outlet	55.42	52.64	kg/s	
IP_Drum: Steam mass flow rate at the outlet	5.60	9.16	kg/s	
LP_Drum: Steam mass flow rate at the outlet	5.337	3.47	kg/s	
HP_Steam Turbine: Fluid pressure at the inlet	92.16	89.33	bar	

(continued)

**Table 6.4** (continued)

(b)				
40.5% load		Simulation	GE	Unit
IP_Steam Turbine: Fluid pressure at the inlet	17.84	17.77	bar	
LP_Steam Turbine: Fluid pressure at the inlet	3.39	3.22	bar	
Condenser: Steam mass flow rate at the inlet	132.72	130.54	kg/s	

### 6.5.3.8 Model Validation

General electric (GE) is the supplier of the combustion turbine and the steam turbine. NEM is the supplier of the HRSG.

Table 6.4a, b shows the results of the comparison between simulation results and plant design data provided by GE and NEM (Fouquet 2004) for 100 and 40.5% loads. The figures obtained by simulation are close to those published by the suppliers, with two exceptions:

1. Exhaust temperature at the outlet of the HRSG. The simulated power is very close to the value provided by the suppliers. The difference between simulation and the suppliers lies in the value of the exhaust temperature: In general, a realistic operating value for the exhaust temperature of a standard CCPP is around 120 °C, whereas 90 °C is more an ideal goal that optimizes the efficiency of the HRSG. The simulation result is closer to the real operating value.
2. Operating conditions inside the drum. Some results at 40.5% load are different due to the lack of information regarding the water-level control and the real pump characteristics as a function of the load. Although those differences are quite significant, they do not put into question any of the results because the important information regarding the operation of the plant is the generated power and the operating conditions inside the gas and steam turbines.

This demonstrates the physical validity and numerical robustness of the model.

## 6.6 Dynamic Model of a Once-Through Supercritical Coal-Fired Power Plant

### 6.6.1 Description of a Once-Through Supercritical Coal-Fired Power Plant

Once-through supercritical pulverized coal power plant enables to generate more power than the subcritical ones. The efficiency of a coal-fired power plant is indeed around 48% for a supercritical one, while it is usually around less than 40% for a subcritical one.

The once-through steam generators are characterized by the absence of drum between the evaporator and the super-heater: The flow in the water-walls is

continuously transformed in sequence from liquid at the inlet to saturated steam and then superheated steam at the outlet without separation between liquid and steam.

For water/steam, the critical point is reached at a pressure of 220.064 bars, a temperature of 647.096 K, and a density of 0.322 g/cm<sup>3</sup>. Beyond this point, the fluid is supercritical.

The plant is based on the Rankine cycle where water is used as the working fluid. It incorporates many processes and systems, including fuel handling, furnace, boiler (steam generation), several-stage steam turbine, feed water system (heaters), condenser, flue gas cleanup, and an electric generator.

The diagram of the plant is shown in Fig. 6.12. The water flows sequentially through the feed water heaters, the economizers, and inside the water-walls of the boiler which acts as an evaporator and a super-heater. Then, the steam goes through three super-heaters (low, intermediate, and high temperature). At the outlet of the last super-heater, the steam goes to the high-pressure (HP) steam turbine, where it is expanded, and then returns to the boiler. The steam then passes through two heaters (low and high temperature) and goes through the intermediate pressure (IP) steam turbine, where it is expanded. At the exit of the low-pressure (LP) steam turbine, the steam is condensed in the condenser, and then the water is pumped and sent into the feed water heaters.

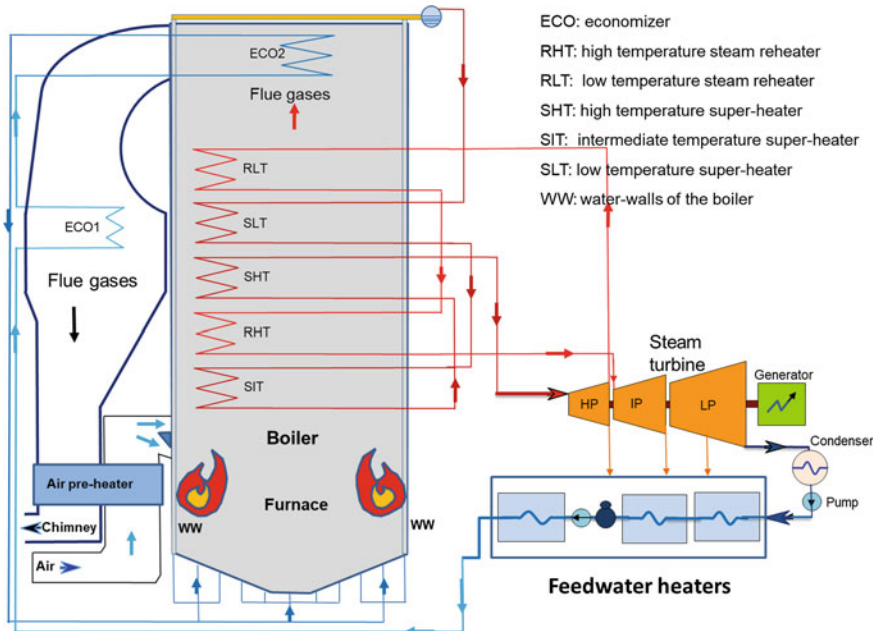


**Fig. 6.12** Diagram of a once-through (without drum) supercritical coal-fired power plant

Along the way from storage to furnace, solid fuels are ground so that it is easier to mix them with air (about 30% of excess air). Both fuel (in pulverized form) and air are blown into the burner of the furnace where combustion takes place.

In the water-tube boiler, the hot products of combustion circulate outside the membrane water-walls and water flows inside the tubes. After passing over the boiler and super-heater tubes, the flue gases flow through the dust collector, the economizers, the air preheater and are finally exhausted to the atmosphere through the chimney.

Air taken from the atmosphere is first passed through the air preheater, where it is heated by the flue gases.

### **6.6.2 Description of the Model**

This chapter presents the dynamic model of a pulverized supercritical coal-fired power plant called *SupercriticalCoalPowerPlant* developed by EDF with Modelica.

This model is an improved version of a module that was used for a study, developed in the framework of the Energy Technologies Institute project (ETI project: CCS System Modeling Tool Kit).

#### **6.6.2.1 Technical Specifications**

The power plant specifications and data used in this study are based on the parameters developed by the European Benchmarking Task Force (EBTF) under the EU-funded CESAR project (CESAR FP7 Project 2011).

The nominal design conditions of the power plant are given in Table 6.5 (CESAR Project 2011; Rioual 2014), while the properties of the coal used in this study, corresponding to a Douglas premium coal, are given in Table 6.6 in two forms: proximate analysis and ultimate analysis. The ultimate analysis determines quantitatively all coal component elements, whereas the proximate analysis determines only the percentage of moisture, ash, volatile matter, and fixed carbon with a simpler apparatus.

#### **6.6.2.2 Model Topology**

The objectives of the model are: Check the performances and design (the sizing of the components) given by the CESAR project, and validate by simulation the load change transient. Also, this model can be used to simulate the plant dynamic behavior in a large operating scenario.

The full 1D dynamic model was built by connecting the component models in a technological way, so that its topology reflects the functional schema of a real

**Table 6.5** Nominal design conditions

Parameters	Value
Gross power output	819 MWe
Auxiliary power consumption	65 MWe
Net power output	754 MWe
Net efficiency	45%
Design coal	South African Douglas premium
Steam condition	Supercritical
Main steam (at the steam turbine inlet)	600 °C, 270 bar
Cold reheat (at the reheater inlet)	366 °C, 64 bar
Hot reheat (at the reheater outlet)	620 °C, 60 bar
Final feed water (at the boiler inlet)	308 °C, 320 bar
Condenser pressure/temperature	48 mbar/32 °C
Boiler feed water pumps	2 × 50% + 1 × 30% start-up
Condensate pumps	2 × 50%
Feed water heaters	5 × LP heaters + 3 × HP heaters
Flue gas temperature	128 °C
HP isentropic efficiency	92%
IP isentropic efficiency	94%
LP isentropic efficiency	88%

**Table 6.6** Douglas premium coal composition

Proximate analysis (%)		Ultimate analysis (%)	
Moisture	8.0	Carbon	66.52
Ash	14.2	Nitrogen	1.56
Volatiles	22.9	Hydrogen	3.78
Fixed carbon	54.9	Total sulfur	0.52
High heating value (HHV) (MJ/kg)	26.23	Chlorine	0.01
Low heating value (LHV) (MJ/kg)	25.17	Oxygen	5.41

pulverized coal power plant. The model contains two main circuits: the water/steam circuit and the air–flue gases circuit. The water/steam cycle is closed through the condenser.

The structure of the model is shown in Fig. 6.13: (1) air preheater and air heater; (2) furnace; (3) and (4) water-tube boiler (evaporator and super-heater); (5) and (6) HP super-heaters; (7) and (8) IP super-heaters; (9) economizer; (10), (11), (12), and (13) HP feed water heaters; (14), (15), (16), (17), and (18) IP and LP feed water heaters; (19) and (20) HP steam turbine; (21), (22), and (23) IP steam turbine; (24), (25), (26), and (27) LP steam turbine; (28) tank; (29) condenser; (30) and (31) pumps; (32) electric generator; and (33), (34), (35), and (36) control system. Table 6.7 lists the ThermoSysPro components used in the model.

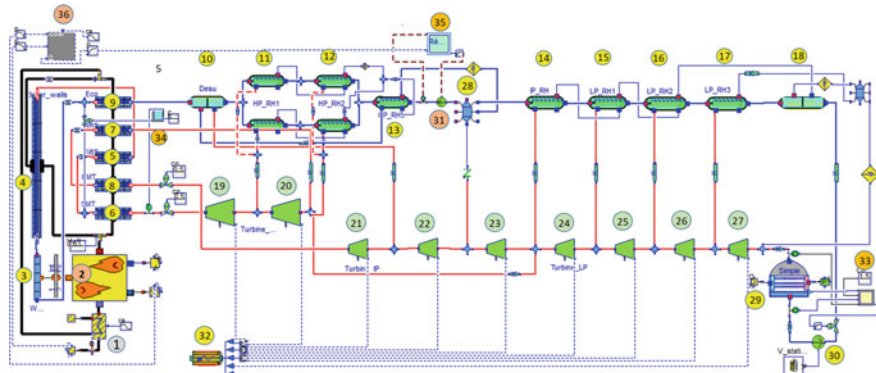


**Fig. 6.13** Supercritical pulverized coal power plant model

**Table 6.7** ThermoSysPro components used in the model

Components	Model name in TSP	Package name in TSP
Check valves	<i>CheckValve</i>	<i>WaterSteam.PressureLosses</i>
Combustion chamber	<i>GenericCombustion1D</i>	<i>Combustion.CombustionChambers</i>
Condenser	<i>SimpleDynamicCondenser</i>	<i>WaterSteam.HeatExchangers</i>
Generator	<i>Generator</i>	<i>WaterSteam.Machines</i>
Heat exchangers (4) to (9)	<i>DynamicExchanger</i> <i>WaterSteam.FlueGases</i> <b>contains</b> <i>DynamicTwoPhaseFlowPipe</i> <i>StaticWallFlueGasesExchanger</i> <i>HeatExchangerWall</i>	<i>MultiFluids.HeatExchangers</i> <b>contains</b> <i>WaterSteam.HeatExchangers</i> <i>FlueGases.HeatExchangers</i> <i>Thermal.HeatTransfer</i>
Heat exchanger (3)	<i>DynamicOnePhaseFlowPipe</i>	<i>WaterSteam.HeatExchangers</i>
Heat exchangers (10) to (17)	<i>NTUWaterHeater</i>	<i>WaterSteam.HeatExchangers</i>
Heat exchanger (18)	<i>StaticWaterWaterExchangerDTorWorEff</i>	<i>WaterSteam.HeatExchangers</i>
Heat source	<i>HeatSource</i>	<i>Thermal.BoundaryConditions</i>
Pipes	<i>InvSingularPressureLoss</i>	<i>WaterSteam.PressureLosses</i>
Pipes	<i>PipePressureLoss</i>	<i>WaterSteam.PressureLosses</i>
Pipes	<i>SingularPressureLoss</i>	<i>WaterSteam.PressureLosses</i>
Pumps	<i>StaticCentrifugalPump</i>	<i>WaterSteam.Machines</i>
Sensor	<i>SensorT</i>	<i>WaterSteam.Sensors</i>

(continued)

**Table 6.7** (continued)

Components	Model name in TSP	Package name in TSP
Steam turbines	<i>StodolaTurbine</i>	<i>WaterSteam.Machines</i>
Valves	<i>ControlValve</i>	<i>WaterSteam.PressureLosses</i>
Check valve	<i>CheckValve</i>	<i>WaterSteam.PressureLosses</i>
Mixers	<i>Mixer2</i>	<i>FlueGases.Junctions</i>
Mixer/splitters	<i>VolumeB, VolumeA, VolumeD, VolumeI, VolumeD, VolumeATH</i>	<i>WaterSteam.Volumes</i>
Wall	<i>HeatExchangerWall</i>	<i>Thermal.HeatTransfer</i>
Control system	<i>Condenser_LevelControl, MassFlowControl, TemperatureControl MassFlowRateAirCoalWater</i>	<i>Examples.PowerPlants. Control</i>

The model contains 614 component models, generating 9301 variables, 157 differentiated variables, 2811 equations, and 1751 non-trivial equations.

The physical equations of each component model are given in Chaps. 7–16.

### 6.6.2.3 Dynamic Pulverized Coal-Fired Boiler

The most complex subsystem of the plant is the boiler associated with the furnace where the combustion of the fuel takes place and steam is generated. It is split into a pair of interacting circuits: the water/steam circuit and the flue gases circuit. The flue gases leave the combustion chamber to be separated into two unequal flows: A small one (about 5%) is sent to the water-walls, while the rest goes through the heat exchangers.

The components of the detailed dynamic model are (cf. Fig. 6.14):

- One-dimensional combustion chamber (2);
- One-dimensional water-walls (WW) (3) and (4);
- One-dimensional steam super-heaters (SLT, SIT\_SHT) (5) and (6);
- One-dimensional steam heaters (RLT, RIT\_RHT) (7) and (8);
- One-dimensional economizers (ECO) (9);
- Air preheater (1);
- Air heater (1);
- Valves;
- Volumes;
- Mass flow rate control system (air, coal, and water) (36);
- Temperature control system (at the inlet of HP steam turbine).

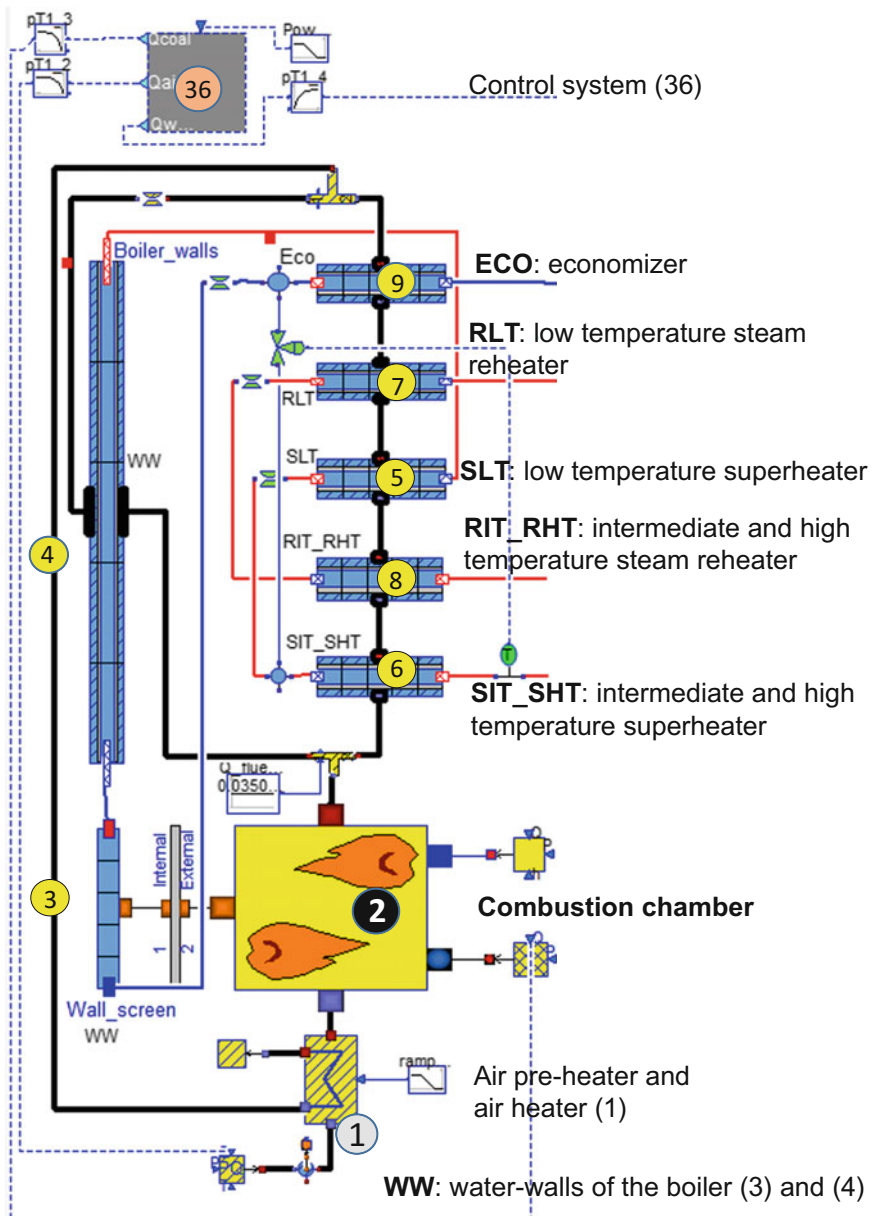


Fig. 6.14 Dynamic pulverized coal-fired boiler model

It is necessary to have the detailed geometry of the furnace, the water-walls, and the heat exchangers, to develop a detailed model of the boiler. The boiler components have been designed in order to match the set of conditions given by the ETI project (cf. Table 6.5). The boiler characteristics are given accordingly in Table 6.8.

**Table 6.8** Boiler parameters

Components	Combustion chamber	Boiler walls	SIT_SHT (6)	RIT_RHT (8)	SLT (5)	RLT (7)	ECO (9)	Air heater
Total exchange surface ( $\text{m}^2$ )	4449.9	3897	4225	14,346	6584	18,167	10,563	7475
Convective heat transfer coefficient ( $\text{W/m}^2/\text{K}$ )	15	14.8						
Total heat transfer coefficient ( $\text{W/m}^2/\text{K}$ )			109.6	87.4	104.2	142.4	75.4	350

#### 6.6.2.4 Steam Turbines and Feed Water Heaters

The coal-fired power plant is composed of three levels of pressure (high, intermediate, and low pressure); cf. Fig. 6.15. The characteristic parameters of the turbines are given in Table 6.9.

Reheating is carried out by transit of water through different feed water heaters; cf. Fig. 6.15.

The LP feed water system is located between the condenser (29) and the tank (28). The HP feed water system is located between the tank and the economizer (9). The parameter characteristics of the feed water heaters are given in Table 6.10.

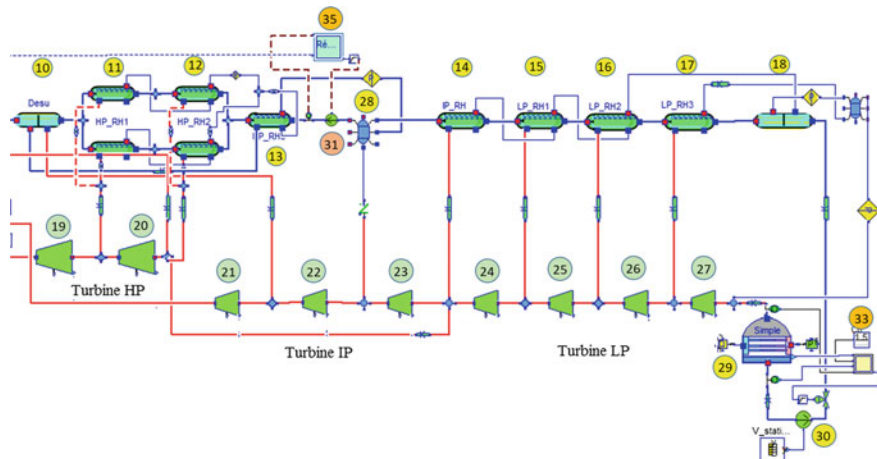


**Fig. 6.15** Steam turbines and feed water heater model

**Table 6.9** Steam turbine parameters

Turbine	HP1 (19)	HP2 (20)	IP1 (21)	IP2 (22)	IP3 (23)	LP1 (24)	LP2 (25)	LP3 (26)	LP4 (27)
Isentropic efficiency (%)	0.94	0.92	0.94	0.94	0.94	0.91	0.91	0.91	0.91

**Table 6.10** Feed water heater parameters (SCond: heat exchange surface for the condensation zone, KCond: heat transfer coefficient for the condensation zone, Sdrain: drain surface, Kdrain: heat transfer coefficient for the cooling drain)

Component feed water	HP1 (11)	HP2 (12)	HP3 (13)	IP (14)	LP1 (15)	LP2 (16)	LP3 (17)
SCond ( $\text{m}^2$ )	3385	3335	750	795	1408	1477	3255
KCond ( $\text{W/m}^2/\text{K}$ )	1588	1588	1588	1730.5	1530.5	1530.5	1535.2
Sdrain ( $\text{m}^2$ )	2098	1698	1098	239	504	482.5	200
Kdrain ( $\text{W/m}^2/\text{K}$ )	1279	1200	1200	2795	155.7	109.55	100

### 6.6.2.5 Model Topology of the Control Systems

Several control systems are implemented in the model, in order to represent some aspects of a real power plant (cf. Fig. 6.16):

- **T\_LevelControl\_OuvNew** controls the steam temperature inside the boiler. Indeed, the variation of temperature at the boiler outlet can be affected by the fouling coefficients, excess air, feed water temperature, changes in fuel, ash deposits, etc.

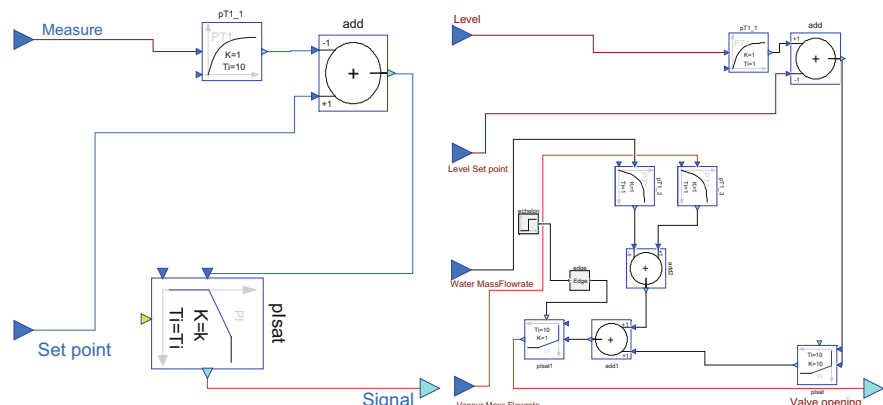


**Fig. 6.16** Model used for the boiler steam temperature and feed water mass flow rate control (left), and model used for the condenser water-level control (right)

- **Condenser\_LevelControl** controls the condenser level.
- **Pump\_MassFlowControl** controls the feed water mass flow rate.
- **MassFlowRateAirCoalWater** calculates the mass flow rate of the air, coal, and feed water as a function of the power produced.

### 6.6.2.6 Model Calibration

Table 6.11 shows, for each component in the model, the unknown variables computed by model inversion and, for each unknown variable, the corresponding known variable.

**Table 6.11** Variables computed by model inversion

Components	Unknown variables	Corresponding known variables
<i>CheckValve</i>	<b>K_Cvalve:</b> Friction pressure loss	<b>Q:</b> Mass flow rate
<i>controlValveHP</i>	<b>CvmaxValveHP:</b> HP steam valve maximum Cv	<b>C1,P:</b> Pressure at the inlet
<i>controlValveIP</i>	<b>CvmaxValveIP:</b> IP steam valve maximum CV	<b>C1,P:</b> Pressure at the inlet
<i>lumpedStraightPipe_HP</i>	<b>K_HP:</b> Friction pressure loss	<b>Q:</b> Mass flow rate
<i>lumpedStraightPipe_HPI</i>	<b>K_HPI:</b> Friction pressure loss	<b>Q:</b> Mass flow rate
<i>lumpedStraightPipe_HPIP</i>	<b>K_HPIP:</b> Friction pressure loss	<b>Q:</b> Mass flow rate
<i>lumpedStraightPipe_IP1</i>	<b>K_IP1:</b> Friction pressure loss	<b>Q:</b> Mass flow rate
<i>lumpedStraightPipe_IP3</i>	<b>K_IP3:</b> Friction pressure loss	<b>Q:</b> Mass flow rate
<i>lumpedStraightPipe_LP1</i>	<b>K_LP1:</b> Friction pressure loss	<b>Q:</b> Mass flow rate
<i>lumpedStraightPipe_LP2</i>	<b>K_LP2:</b> Friction pressure loss	<b>Q:</b> Mass flow rate
<i>lumpedStraightPipe_LP3</i>	<b>K_LP3:</b> Friction pressure loss	<b>Q:</b> Mass flow rate
<i>TurbineHP</i>	<b>CstHP:</b> Stodola's HP ellipse coefficient	<b>Pe:</b> Pressure at the inlet
<i>TurbineHPI</i>	<b>CstHP1:</b> Stodola's HP ellipse coefficient	<b>Pe:</b> Pressure at the inlet
<i>TurbineIP1</i>	<b>CstIP1:</b> Stodola's IP1 ellipse coefficient	<b>Pe:</b> Pressure at the inlet
<i>TurbineIP2</i>	<b>CstIP2:</b> Stodola's IP2 ellipse coefficient	<b>Pe:</b> Pressure at the inlet

(continued)

**Table 6.11** (continued)

Components	Unknown variables	Corresponding known variables
<i>TurbineIP3</i>	<b>CstIP3:</b> Stodola's IP3 ellipse coefficient	<b>P<sub>e</sub>:</b> Pressure at the inlet
<i>TurbineLP1</i>	<b>CstLP1:</b> Stodola's LP1 ellipse coefficient	<b>P<sub>e</sub>:</b> Pressure at the inlet
<i>TurbineLP2</i>	<b>CstLP2:</b> Stodola's LP2 ellipse coefficient	<b>P<sub>e</sub>:</b> Pressure at the inlet
<i>TurbineLP3</i>	<b>CstLP3:</b> Stodola's LP3 ellipse coefficient	<b>P<sub>e</sub>:</b> Pressure at the inlet
<i>Turbine_nozzle</i>	<b>CstNoz:</b> Stodola's nozzle ellipse coefficient	<b>P<sub>e</sub>:</b> Pressure at the inlet
<i>singularPressureLoss_SBT</i>	<b>K_SBT:</b> Friction pressure loss	<b>C1.P:</b> Pressure at the inlet
<i>singularPressureLoss_RBT</i>	<b>K_RBT:</b> Friction pressure loss	<b>C1.P:</b> Pressure at the inlet
<i>singularPressureLoss_Eco</i>	<b>K_ECO:</b> Friction pressure loss	<b>C1.P:</b> Pressure at the inlet
<i>staticCentrifugalPump</i>	<b>a1_PompeEx:</b> $x^2$ coefficient of the pump characteristics (hn)	<b>C2.P:</b> Pressure at the outlet
<i>staticCentrifugalPump1</i>	<b>a1_PompeAlim:</b> $x^2$ coefficient of the pump characteristics (hn)	<b>C2.Q:</b> Mass flow rate

### 6.6.2.7 Scenarios' Description

For simulation runs, two scenarios are selected:

- A steady-state scenario at full load;
- A dynamic scenario representing a load variation from 100 to 50%.

### 6.6.2.8 Simulation Results

The dynamic model simulates the dynamic behavior of the entire once-through supercritical coal-fired power plant.

Figure 6.17 shows the results for 1200 s of simulation for the scenario “power generator step reduction from 100 to 50% load.”

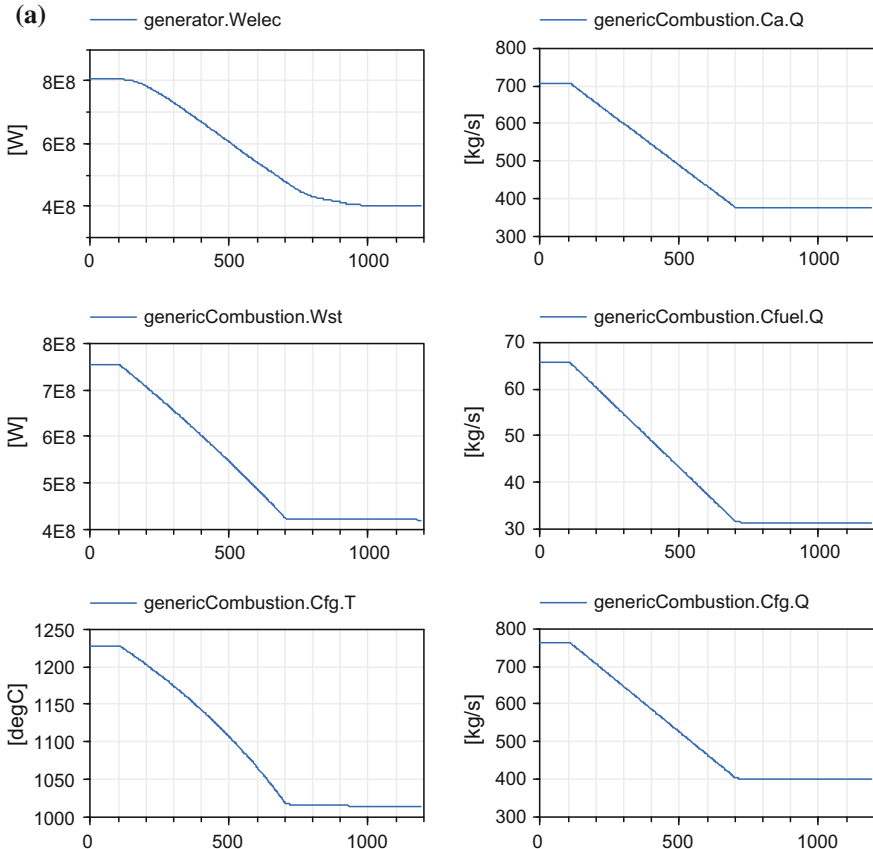


**Fig. 6.17** **a** Simulation results for the power generator step reduction scenario ( $-50\%$ ) (top to bottom and then left to right): (1) electrical power provided by the generator, (2) power transferred to water/steam in the combustion chamber, (3) flue gases temperature at the outlet of the combustion chamber, (4–6) air mass flow rate, coal mass flow rate, and flue gases mass flow rate. **b** Simulation results for the power generator step reduction simulation scenario ( $-50\%$ ) (top to bottom and then left to right): (1) water mass flow rate, (2) flue gases temperature at the outlet of the heat exchangers (SIT\_SHT, RIT\_RHT, SLT, RLT, and Eco), (3) air temperature at the inlet of the combustion chamber (outlet air heater) and flue gases exhaust temperature, (4) mechanical power produced by the HP steam turbine, (5) mechanical power produced by the IP steam turbine, and (6) mechanical power produced by the LP steam turbine. **c** Simulation results for the power generator step reduction simulation ( $-50\%$ ) (top to bottom and then left to right): (1) steam mass flow rate in the HP steam turbine, (2) steam pressure at the inlet of the HP steam turbine, (3) steam temperature at the inlet of the HP steam turbine, (4) steam mass flow rate in the IP steam turbine, (5) steam pressure at the inlet of the IP steam turbine, and (6) steam temperature at the inlet of the IP steam turbine

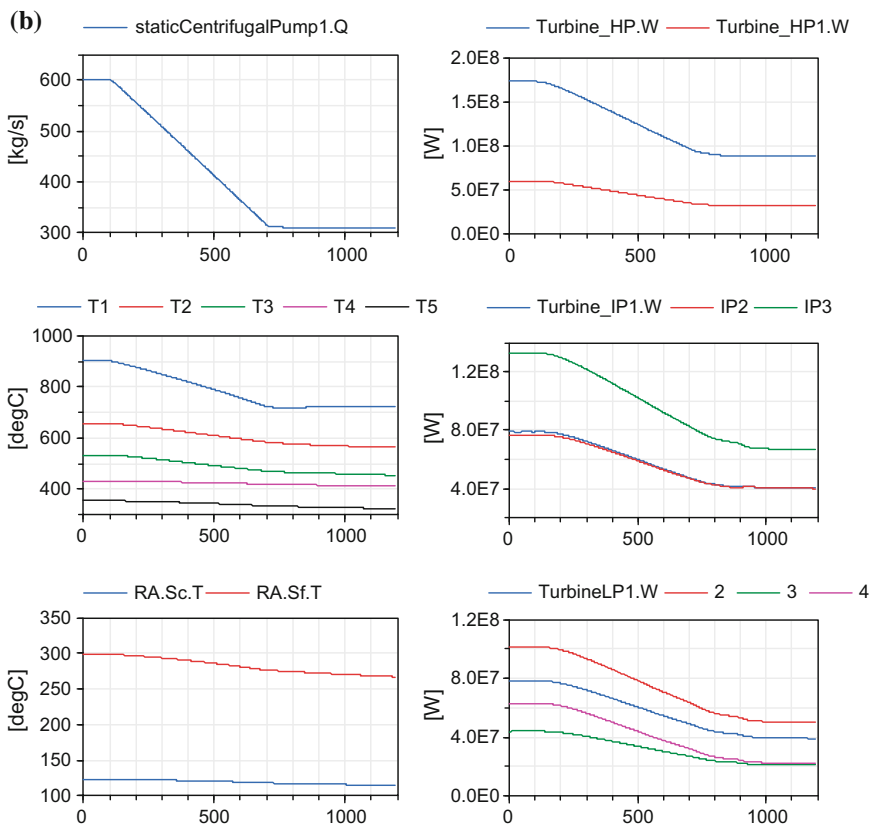


**Fig. 6.17** (continued)

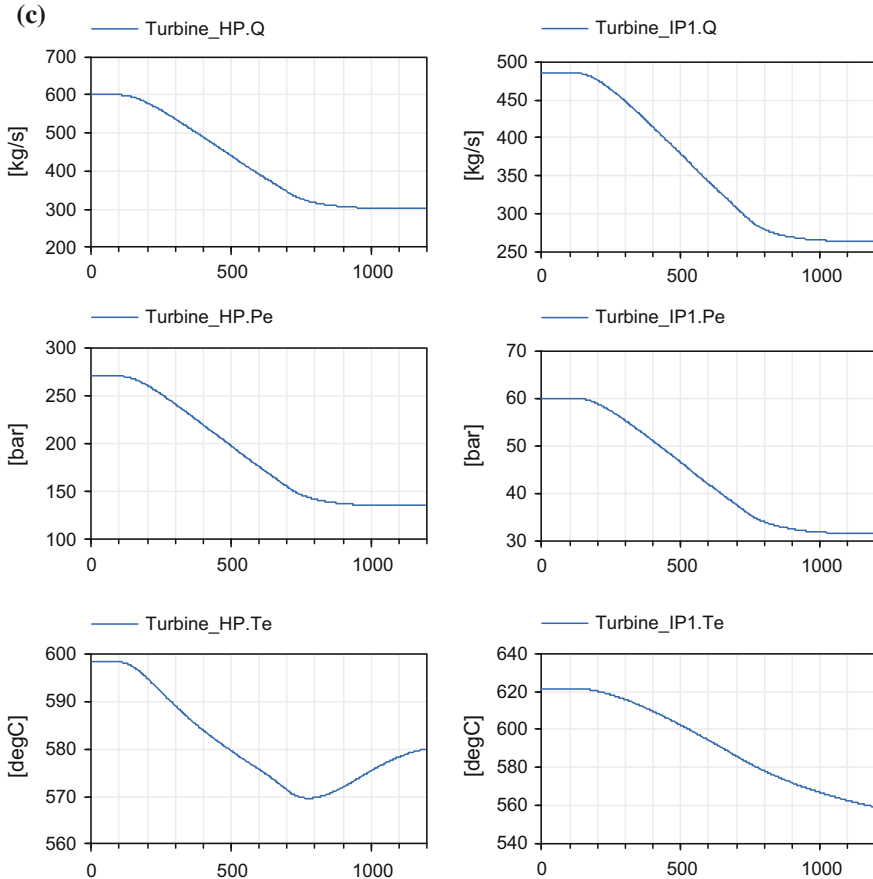


**Fig. 6.17** (continued)

## 6.7 Dynamic Model of a 1 MWe Concentrated Solar Power Plant (CSP) with a PTSC

### 6.7.1 Description of the Concentrated Solar Power Plant

Solar thermal power plants are key technology for electricity generation from renewable energy resources. Solar energy systems are considered as promising power generating sources due to their availability and topological advantages in local power generation. Among all concentrating solar power technologies available for power generation today, the linear parabolic trough collector (PTSC) is raising increasing interest.

The diagram of a concentrated solar power plant with a PTSC is shown in Fig. 6.18. The PTSC receiver (cf. Sect. 16.1) contains a parabolic reflective surface

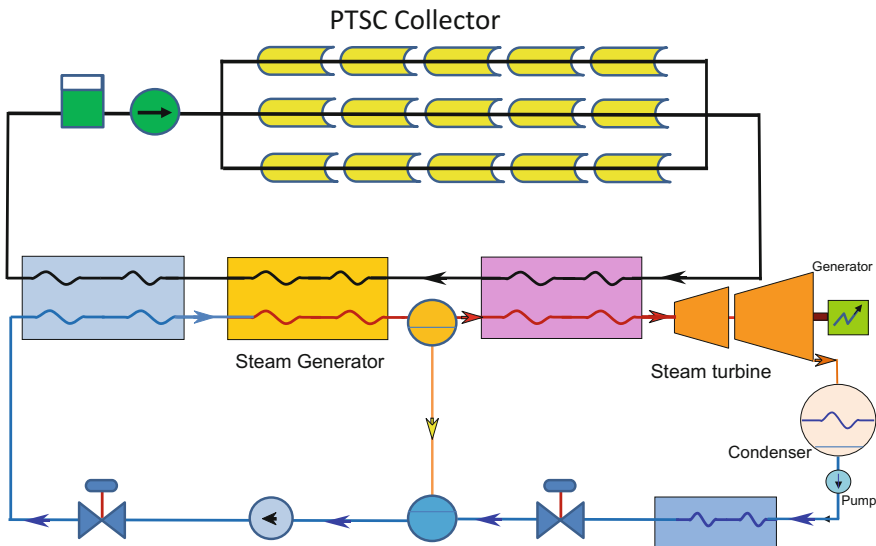


**Fig. 6.18** Diagram of a simple concentrated solar power plant with a PTSC

and a receiver tube. The PTSC receiver tube is located at the focus line of the parabolic reflective surface which allows transferring the absorbed solar energy to a synthetic heat transfer fluid pumped through the absorber tube. The absorber tubes heat up the synthetic oil to nearly 400 °C, and several heat exchangers transfer the heat from the synthetic oil to the water/steam in a Rankine cycle. In the water/steam cycle, water passes through the feed water heater, the feed water tank, the economizer and then flows inside the evaporator and the steam dryer. Then, the steam passes through the super-heater and water goes to the feed water tank. At the outlet of the super-heater, the steam goes to the high-pressure (HP) steam turbine, where it is expanded, and then goes through the intermediate–low-pressure (IP-LP) steam turbine, where it is expanded. At the exit of the low-pressure steam turbine, the steam is condensed in the condenser, and then the water is pumped and sent into the feed water heater.

### 6.7.2 Description of the Model

This chapter presents the dynamic model of a simple concentrated solar power plant with a PTSC called *ConcentratedSolarPowerPlant\_PTSC* developed by EDF with Modelica.

The model contains two main parts: the water/steam cycle and the oil cycle. Only one train of the PTSC is modeled.

The objective of this model is to validate the physics and the numerical robustness of the model for a very challenging scenario: the daily fluctuation of solar irradiation.

The interested reader in a complete model of a power plant with a tower receiver, molten salt storage, and steam generator can refer to El Hefni and Soler (2014).

### 6.7.2.1 Technical Specifications

The power plant specifications and data used in this study do not correspond to an existing installation.

The power plant components have been designed in order to match the set of conditions given below:

- Output power = 1 MWe
- Steam pressure at the inlet of the steam turbine =  $80 \times 10^5$  Pa
- Steam temperature at the inlet of the steam turbine = 681 K
- Steam mass flow rate at the inlet of the steam turbine = 1.133 kg/s
- Condenser pressure = 5000 Pa
- Oil temperature at the outlet of the receiver tube = 683 K
- Oil mass flow rate at the outlet of the oil pump = 7.4 kg/s
- HP steam turbine isentropic efficiency = 92%
- IP and LP steam turbine isentropic efficiency = 94%
- Focal length = 1.78518 m
- Rim angle = 70°
- Width of the collector or pipe length = 450 m
- Pipe diameter (absorber) = 0.07 m
- Internal glass diameter = 0.115 m
- Glass transmissivity = 0.95
- Glass absorptivity = 0.0302
- Tube absorptivity = 0.96
- Glass emissivity = 0.86
- Tube emissivity = 0.14
- Mirror reflectivity = 0.93
- Interception factor = 0.83
- Gas thermal conductivity between the tube and the glass = 0.0289141 W/m/K
- Convective heat transfer coefficient between the ambient and the glass = 3.06 W/m<sup>2</sup>/K.

The heat exchanger characteristics are given in Table 6.12.

### 6.7.2.2 Model Topology

The full 1D dynamic model was built by connecting the component models in a technological way.

**Table 6.12** Heat exchanger parameters

Components	Reflector	Receiver tube	Super-heater	Evaporator	Economizer	Feed water heater
Total surface (m <sup>2</sup> )	6750	254.46	30.16	188.5	7.56	10.31
Pipe length (m)	–	450 * 3	80 * 3	500 * 3	20 * 3	–
Pipe diameter (m)	–	0.07	0.04	0.04	0.04	–

The model contains two main circuits: the water/steam circuit and the oil circuit. Figure 6.19 and Table 6.13 show the structure of the model and the ThermoSysPro components used in the model: (1) linear parabolic trough collector (PTSC); (2) solar receiver pipe; (3) super-heater; (4) steam dryer; (5) evaporator; (6) economizer; (7) feed water tank; (8) feed water heater; (9) condenser; (10) HP steam turbine; (11) IP and LP steam turbine; (12) valves; (13), (14), and (15) pumps; and (16) electric generator.

Only one train of the PTSC is modeled. The model contains 279 component models generating 4503 variables, 364 differentiated variables, 787 equations, and 522 non-trivial equations.

The physical equations of each component model are given in Chaps. 7–16.

The list of component used for the development of the model is given in Table 6.13.

### 6.7.2.3 Model Calibration

Table 6.14 shows, for each component in the model, the unknown variables computed by model inversion and, for each unknown variable, the corresponding known variable.

### 6.7.2.4 Simulation Scenario and Results

The dynamic model is capable of simulating the dynamic behavior of the entire CSP plant.

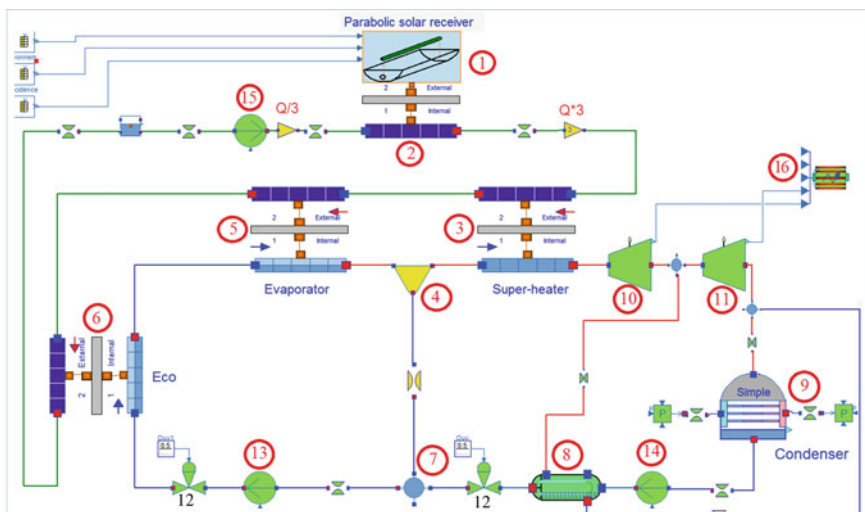


**Fig. 6.19** Model of the concentrated solar power plant

**Table 6.13** ThermoSysPro components used in the model

Components	Model name in TSP	Package name in TSP
Condenser	<i>SimpleDynamicCondenser</i>	<i>WaterSteam.HeatExchangers</i>
Gains	<i>MassFlowMultiplier</i>	<i>WaterSteam.Junctions</i>
Generator	<i>Generator</i>	<i>WaterSteam.Machines</i>
Heat exchangers (3), (5) and (6)	<b>described with</b> <i>DynamicTwoPhaseFlowPipe</i> <i>DynamicOnePhaseFlowPipe_Oil</i> <i>HeatExchangerWall</i>	<i>WaterSteam.HeatExchangers</i> <i>Solar.HeatExchangers</i> <i>Thermal.HeatTransfer</i>
Heat exchanger (2)	<i>DynamicOnePhaseFlowPipe_Oil</i>	<i>Solar.HeatExchangers</i>
Heat exchanger (8)	<i>NTUWaterHeating</i>	<i>WaterSteam.HeatExchangers</i>
Pipe	<i>InvSingularPressureLoss</i>	<i>WaterSteam.PressureLosses</i>
Pipes	<i>SingularPressureLoss</i>	<i>WaterSteam.PressureLosses</i> <i>Solar.PressureLosses</i>
Pumps	<i>StaticCentrifugalPump</i>	<i>WaterSteam.Machines</i> <i>Solar.Machines</i>
PTSC	<i>SolarCollector</i>	<i>Solar.SolarField</i>
Splitter/mixers	<i>VolumeA, VolumeC</i>	<i>WaterSteam.Volumes</i>
Steam dryer	<i>SteamDryer</i>	<i>WaterSteam.Junctions</i>
Steam turbines	<i>StodolaTurbine</i>	<i>WaterSteam.Machines</i>
Tank	<i>Tank</i>	<i>Solar.Volumes</i>
Valves	<i>ControlValve</i>	<i>WaterSteam.PressureLosses</i>
Wall	<i>HeatExchangerWall</i>	<i>Thermal.HeatTransfer</i>

**Table 6.14** Variables computed by model inversion and fixed variables

Components	Unknown variables	Corresponding known variables
<i>TurbineHP</i>	<b>Cst:</b> Stodola's HP ellipse coefficient	<b>Pe:</b> Pressure at the inlet
<i>TurbineIP-LP</i>	<b>Cst:</b> Stodola's MP-IP ellipse coefficient	<b>Pe:</b> Pressure at the inlet
<i>NTUWaterHeating</i>	<b>SCondDes:</b> Exchange surface for condensation and deheating	<b>Se.h:</b> Water specific enthalpy at the outlet of the feed water heater
<i>staticCentrifugalPump</i>	<b>a1_PompeAlim:</b> $x^2$ coefficient of the pump characteristics (hn)	<b>C2.Q:</b> Mass flow rate or <b>C2.P:</b> Pressure at the outlet

In order to challenge the dynamic simulation capabilities of the model, a high-amplitude transient is simulated corresponding to the scenario of the daily fluctuation of solar irradiation (DNI at Almeria in Spain, on March 1, 2012, from 08:00 to 19:00). This transient is used to check and validate the physics and the numerical robustness of the model.

The direct normal irradiance (DNI) is the solar radiation received per unit area by a surface that is held perpendicular (or normal) to the rays emitted from the sun along its trajectory in the sky.

The results of the simulation are given in Fig. 6.20 for three trains (loops). Curve 1 shows the daily variation of the DNI for alternating sunny and cloudy

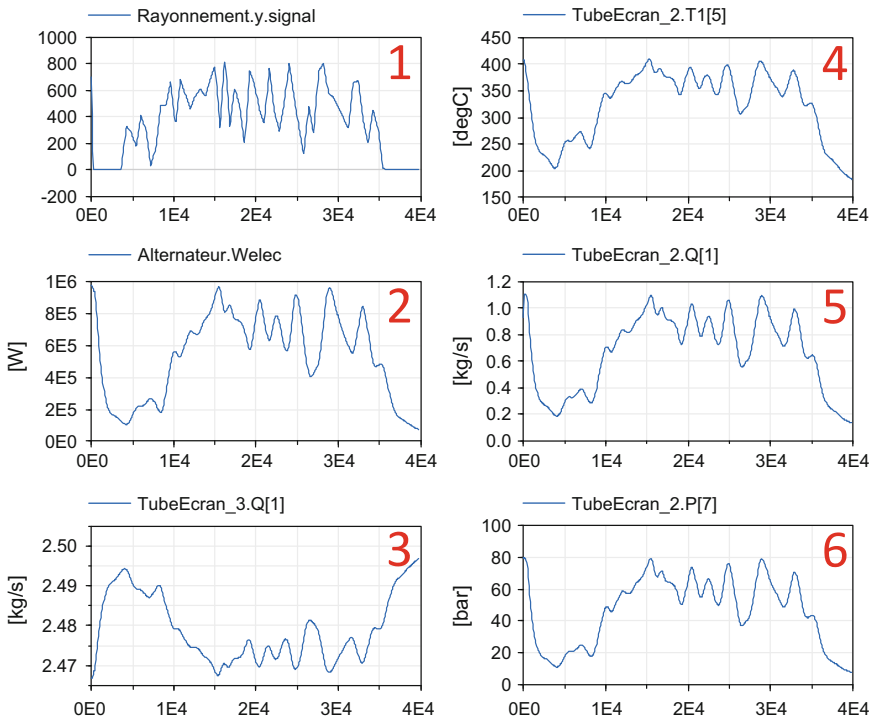


**Fig. 6.20** Simulation results for the concentrated solar power plant: (1) solar irradiation “DNI”, (2) net power produced, (3) oil mass flow rate for one train, (4) steam temperature at the inlet of the HP steam turbine, (5) steam mass flow rate at the inlet of the HP steam turbine, and (6) pressure at the inlet of the HP steam turbine

conditions. Curve 2 shows that when the DNI is zero (at simulation instants close to the start and toward the end of the transient), there is still some power produced due to the thermal inertia of the system.

## References

- CESAR FP7 project (2011) European best practice guidelines for assessment of CO<sub>2</sub> capture technologies. Deliverable D1.4.3
- El Hefni B, Soler R (2014) Dynamic multi-configuration model of a 145 MWe concentrated solar power plant with the ThermoSysPro Library. In: International conference on concentrating solar power and chemical energy systems, SolarPACES 2014
- Fouquet L (2004) Phu My 2.2: overall plant operation description. EDF Pôle Industrie, CNET: Y. PM.X.000.PPPP.OO.X.0872
- Fritzson P (2011) Introduction to modeling and simulation of technical and physical systems with modelica. Wiley-IEEE Press
- Rioual C (2014) Dynamic modelling of a supercritical coal-fired power. EDF Energy R&D UK Centre, ETI CCS Project Report, Milestone 20–WP5 Deliverables 5.3.5.a

# Chapter 7

## Boiler (Steam Generator) Modeling



**Abstract** Thermal power plants consist of a large number of facilities. One major component is the boiler together with the furnace where combustion of the fuel takes place and steam is generated. Boilers produce hot water or steam using thermal energy released by the combustion. Steam at the desired temperature and pressure is used to produce mechanical energy via a steam turbine. Hot water is used in district heating networks. This chapter describes the different models of water-tube boilers (detailed boilers, simplified boilers) and gives a detailed description of the physical equations for each of them: modeling assumptions and fundamental equations. A test-case is provided for each component model that includes the structure of the model, parameterization data, and results of simulation. It is a valuable aid to understand the chemical (combustion) phenomena that govern the operation of power plants and energy processes. It is a main support to develop models for industrial power plants. The full description of the physical equations is independent of the programming languages and tools.

### 7.1 Detailed Modeling of the Boiler

The boiler is the most complex subsystem of a power plant. It is split into a pair of interacting circuits: the water/steam circuit and the flue gases circuit. There are different components present in flue gases and water/steam circuits: boiler furnace with membrane water-walls, heat exchangers (economizers, evaporators, and super-heaters), drums, headers, volumes, mixers, splitters, and valves.

In water-tube boilers, the fuel is burnt inside a furnace. The hot products of combustion circulate outside the membrane water-walls and water flows inside the water-wall tubes. The modular modeling method is adopted to develop the detailed models of boilers. So, a detailed example of a water-tube boiler is presented in sect. 6.6 (cf. Fig 6.12). The feed water passes through the economizer and then flows inside the water-walls of the boiler which acts as an evaporator. Then, the steam goes through two super-heaters (low temperature and high temperature). At the outlet of the second super-heater, the steam goes to the HP steam turbine, where

it is expanded, and then returns to the boiler. The steam then passes through two heaters (low temperature and high temperature) and goes through the IP steam turbine, where it is expanded.

It is necessary to have the detailed geometry of the furnace, the water-walls, and the heat exchangers, to develop a detailed model of the boiler.

## 7.2 Simplified Modeling of the Boiler

In the absence of the detailed geometry of the boiler (furnace, water-walls, heat exchangers), the simplified boiler model can be used. The model consists of one combustion chamber with two circuits: the water/steam circuit and the flue gases circuit (Fig. 7.1). In the combustion chamber, energy is added by spraying fuel into the air, and the combustion of the mixture generates a high-temperature flow. During the combustion, oxygen is combined with different elements of fuel, like carbon, hydrogen, sulfur, and produces the respective oxides. This combination is exothermic; i.e., it is accompanied by a release of heat. Thus, the boiler produces hot water or steam using the thermal energy released by the combustion of fuel.

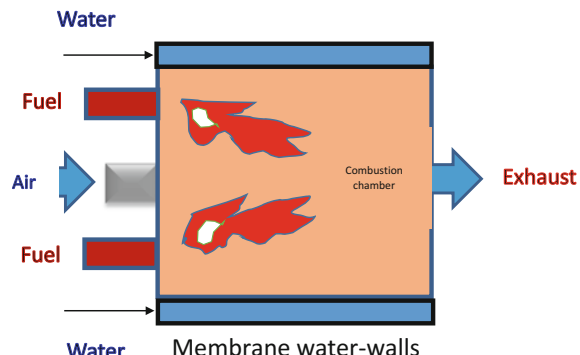
The boiler model is called *FossilFuelBoiler*. This component models the combustion inside the boiler furnace with heat transfer between the furnace and the cooling fluid flowing through the tubes. Thus, the exhaust gas composition, the combustion air ratio, the fluid specific enthalpy at the outlets, the power transferred to the water/steam, and the fluid pressure losses are computed as a function of the fluid characteristics, fuel composition, and air composition.

The fuels used in this component are coal, oil, gas, biomass, and solid waste.

### 7.2.1 Modeling Principles

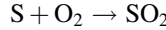
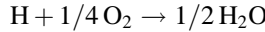
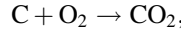
The objective of the model is to compute the flue gases mass flow rate and temperature, the mass fractions of the combustion products and the excess air at the

**Fig. 7.1** Schematic diagram of a boiler



outlet of the boiler from the mass flow rates and mass fractions of the species at the inlet of the boiler. In addition, the water/steam specific enthalpy and pressure are calculated at the outlet.

The species at the outlet are governed by the following exothermic chemical reactions:



The formation of nitrogen oxide ( $\text{NO}_2$ ) is neglected.

For a boiler, excess air is necessary to avoid having unburnt fuel in the exhaust fumes. It also allows to increase the convective exchange between the fumes and the tubes.

Excess air is defined by:

$$E_{X,a} = 100 \cdot \left( \frac{\text{dry air mass at the inlet}}{\text{stoichiometric dry air mass}} - 1 \right)$$

It is assumed that there is no accumulation of matter and energy inside the boiler. Therefore, only the static 0D model of the boiler is presented.

### 7.2.2 Nomenclature

Symbols	Definition	Unit	Mathematical definition
$c_{p,f}$	Fuel specific heat capacity	J/kg/K	
$E_X$	Dry air stoichiometry necessary for the combustion of one kilogram of fuel (theoretical dry air requirement)	–	Oxygen mass in air required to burn 1 kg of fuel divided by the oxygen mass in dry air at the inlet
$E_{X,a}$	Excess air	%	$100 \cdot \left( \frac{\dot{m}_a \cdot (1 - X_{\text{H}_2\text{O},a})}{\dot{m}_f \cdot E_X} - 1 \right)$
$h_{a,i}$	Air specific enthalpy at the inlet	J/kg	
$\tilde{h}_{a,r}$	Air reference specific enthalpy (cf. sect. 2.3.5)	J/kg	$2501569 \cdot X_{\text{H}_2\text{O},a}$
$h_f$	Fuel specific enthalpy at the inlet	J/kg	$c_{p,f} \cdot (T_f - 273.16)$
$\tilde{h}_{f,r}$	Fuel reference specific enthalpy (cf. sect. 2.3.5)	J/kg	0
$h_g$	Flue gases specific enthalpy after combustion	J/kg	

(continued)

(continued)

Symbols	Definition	Unit	Mathematical definition
$h_{g,o}$	Flue gases specific enthalpy at the outlet	J/kg	
$\tilde{h}_{g,r}$	Flue gases reference specific enthalpy (cf. sect. 2.3.5)	J/kg	$2501569 \cdot X_{h2o,g}$
$h_{ws,i}$	Water/steam specific enthalpy at the inlet	J/kg	
$h_{ws,o}$	Water/steam specific enthalpy at the outlet	J/kg	
LHV	Fuel lower heating value	J/kg	
$\dot{m}_a$	Air mass flow rate	kg/s	
$\dot{m}_f$	Fuel mass flow rate	kg/s	
$\dot{m}_g$	Flue gases mass flow rate	kg/s	
$\dot{m}_{ws}$	Water/steam mass flow rate	kg/s	
$M_C$	Carbon atomic mass	kg/kmol	12.01115
$M_H$	Hydrogen atomic mass	kg/kmol	1.00797
$M_O$	Oxygen atomic mass	kg/kmol	15.9994
$M_S$	Sulfur atomic mass	kg/kmol	32.064
$M_{co2}$	$CO_2$ molar mass	kg/kmol	$M_C + 2 \cdot M_O$
$M_{h2o}$	$H_2O$ molar mass	kg/kmol	$M_O + 2 \cdot M_H$
$M_{so2}$	$SO_2$ molar mass	kg/kmol	$M_S + 2 \cdot M_O$
$P_{g,i}$	Flue gases pressure at the inlet	Pa	
$P_{g,o}$	Flue gases pressure at the outlet	Pa	
$P_{ws,i}$	Water/steam pressure at the inlet	Pa	
$P_{ws,o}$	Water/steam pressure at the outlet	Pa	
$T_{a,i}$	Air temperature at the inlet	K	
$T_f$	Fuel temperature at the inlet	K	
$T_{f,o}$	Flue gases temperature at the outlet	K	
$T_g$	Flue gases temperature after combustion	K	
$W_l$	Thermal losses (such as but not limited to thermal losses through the wall)	W	
$X_{C,f}$	C mass fraction in the fuel	-	
$X_{H,f}$	H mass fraction in the fuel	-	
$X_{O,f}$	O mass fraction in the fuel	-	
$X_{S,f}$	S mass fraction in the fuel	-	
$X_{co2,a}$	$CO_2$ mass fraction in the air at the inlet	-	

(continued)

(continued)

Symbols	Definition	Unit	Mathematical definition
$X_{\text{co2,g}}$	CO <sub>2</sub> mass fraction in the flue gases	–	
$X_{\text{h2o,a}}$	H <sub>2</sub> O mass fraction in the air at the inlet	–	
$X_{\text{h2o,g}}$	H <sub>2</sub> O mass fraction in the flue gases	–	
$X_{\text{o2,a}}$	O <sub>2</sub> mass fraction in the air at the inlet	–	
$X_{\text{o2,g}}$	O <sub>2</sub> mass fraction in the flue gases	–	
$X_{\text{so2,a}}$	SO <sub>2</sub> mass fraction in the air at the inlet	–	
$X_{\text{so2,g}}$	SO <sub>2</sub> mass fraction in the flue gases	–	
$\eta$	Boiler efficiency ( $0 < \eta \leq 1$ )	–	Net thermal power at the outlet divided by the total thermal power at the inlet
$\eta_c$	Combustion efficiency ( $0 < \eta_c \leq 1$ )	–	$\frac{\text{Burnt fuel mass}}{\text{Input fuel mass}}$
$A_g$	Flue gases pressure loss coefficient	$\text{m}^{-4}$	
$A_{ws}$	Water/steam pressure loss coefficient	$\text{m}^{-4}$	
$\rho_g$	Flue gases density	$\text{kg/m}^3$	
$\rho_{ws}$	Water/steam density	$\text{kg/m}^3$	

### 7.2.3 Governing Equations

The *FossilFuelBoiler* model is based on the energy and momentum balance equations.

Equation 1

Title	Mass balance equation for the flue gases
Validity domain	$\forall \dot{m}_g, \forall \dot{m}_a$ and $\forall \dot{m}_f$
Mathematical formulation	$\dot{m}_g = \dot{m}_a + \dot{m}_f$
Comments	Flue gases result from the combustion of fuel with air If $\eta_c < 1$ , then there is unburnt fuel in the exhaust flue gases

Equation 2	
Title	Energy balance equation for the flue gases
Validity domain	$\dot{m}_g > 0, \forall \dot{m}_a \text{ and } \forall \dot{m}_f$
Mathematical formulation	$\dot{m}_g \cdot h_g = \dot{m}_a \cdot h_{a,i} + \dot{m}_f \cdot (h_f + \eta_c \cdot \text{LHV}) - W_l$
Comments	<p>This equation computes the flue gases specific enthalpy <math>h_g</math>. <math>\eta_c</math> and LHV are model inputs.</p> <p>The specific enthalpies <math>h_f</math> and <math>h_{a,i}</math> are computed using properties tables from the known temperatures <math>T_f</math> and <math>T_{a,i}</math> of the fuel and the air at the inlet. As the properties tables use different references, <math>h_f</math> and <math>h_{a,i}</math> must be explicitly replaced in Eq. (2) by <math>\tilde{h}_f</math> and <math>\tilde{h}_{a,i}</math> using (2.19). Then,</p> $h_f \rightarrow \tilde{h}_f = h_f - \tilde{h}_{f,r}$ $h_{a,i} \rightarrow \tilde{h}_{a,i} = h_{a,i} - \tilde{h}_{a,r}$ <p>where the sign <math>\rightarrow</math> means “is replaced by.”</p> <p>The same applies to <math>h_g</math> in order to compute the temperature <math>T_g</math> of the flue gases:</p> $h_g \rightarrow \tilde{h}_g = h_g - \tilde{h}_{g,r}$ <p>Cf. also comments of Eq. (4) in Chap. 15</p>

Equation 3	
Title	Power exchanged in the boiler between the flue gases and the water/steam circuits
Validity domain	$\forall \dot{m}_g, \forall \dot{m}_a, \forall \dot{m}_f \text{ and } \dot{m}_{ws} \neq 0$
Mathematical formulation	$\dot{m}_a \cdot h_{a,i} + \dot{m}_f \cdot (h_f + \eta_c \cdot \text{LHV}) - W_l - \dot{m}_g \cdot h_{g,o}$ $= \dot{m}_{ws} \cdot (h_{ws,o} - h_{ws,i})$
Comments	<p>This equation computes the water/steam specific enthalpy <math>h_{ws,o}</math>.</p> <p>Cf. comments of Eq. (2) regarding the use of reference specific enthalpies</p>

Equation 4	
Title	Boiler efficiency
Validity domain	$\dot{m}_a > 0 \text{ and } \dot{m}_f > 0$
Mathematical formulation	$\eta = 100 \cdot \frac{\dot{m}_{ws} \cdot (h_{ws,o} - h_{ws,i})}{\dot{m}_a \cdot h_{a,i} + \dot{m}_f \cdot (h_f + \text{LHV})}$
Comments	<p>Cf. comments of Eq. (2) regarding the use of reference specific enthalpies</p> <p>There are other ways to define the efficiency, such as taking into account the LHV only:</p> $\eta = 100 \cdot \frac{\dot{m}_{ws} \cdot (h_{ws,o} - h_{ws,i})}{\dot{m}_f \cdot \text{LHV}}$

---

Equation 5

---

Title	Momentum balance equation for the flue gases (pressure losses)
Validity domain	$\forall \dot{m}_f$
Mathematical formulation	$P_{f,o} = P_{f,i} - A_f \cdot \frac{\dot{m}_f \cdot  \dot{m}_f }{\rho_f}$
Comments	Cf. (13.18)

---

Equation 6

---

Title	Momentum balance equation for the water/steam (pressure losses)
Validity domain	$\forall \dot{m}_{ws}$
Mathematical formulation	$P_{w,o} = P_{w,i} - A_{ws} \cdot \frac{\dot{m}_{ws} \cdot  \dot{m}_{ws} }{\rho_{ws}}$
Comments	Cf. (13.18)

---

Equation 7

---

Title	Dry air stoichiometry for the combustion of one kilogram of fuel
Validity domain	$X_{h2o,a} < 1$ and $X_{o2,a} > 0$
Mathematical formulation	$E_X = M_O \cdot \frac{\frac{2 \cdot X_{C,f}}{M_C} + \frac{X_{H,f}}{2 \cdot M_H} + \frac{2 \cdot X_{S,f}}{M_S} - \frac{X_{O,f}}{M_O}}{X_{o2,a} \cdot \frac{1 - X_{h2o,a}}{1 - X_{h2o,a}}}$
Comments	<p>The chemical reactions considered for the combustion are:</p> $C + O_2 \rightarrow CO_2 \quad (1)$ $H + 1/4 O_2 \rightarrow 1/2 H_2O \quad (2)$ $S + O_2 \rightarrow SO_2 \quad (3)$ <p>The first chemical reaction requires two moles of oxygen and one mole of carbon to produce one mole of <math>CO_2</math>. Hence,</p> $\dot{N}_O^{(1)} = 2 \cdot \dot{N}_C$ <p>where <math>\dot{N}_O^{(1)}</math> and <math>\dot{N}_C</math> are respectively the molar flux of oxygen and carbon (i.e., number of moles per second) for the first reaction</p> <p>The mass of oxygen consumed by the first reaction for one kilogram of fuel is then,</p> $\dot{m}_O^{(1)} = M_O \cdot \dot{N}_O^{(1)} = M_O \cdot 2 \cdot \dot{N}_C$ $= M_O \cdot 2 \cdot \frac{X_{C,f}}{M_C} \cdot \dot{m}_f = M_O \cdot \frac{2 \cdot X_{C,f}}{M_C}$ <p>since <math>\dot{m}_f = 1 \text{ kg/s}</math></p> <p>Similarly, the mass of oxygen consumed by the second reaction and the mass of oxygen consumed by the third reaction for one kilogram of fuel are:</p> $\dot{m}_O^{(2)} = M_O \cdot \frac{X_{H,f}}{2 \cdot M_H}$ $\dot{m}_O^{(3)} = M_O \cdot \frac{2 \cdot X_{S,f}}{M_S}$ <p>The total mass of oxygen consumed is:</p> $\dot{m}_O = \dot{m}_O^{(1)} + \dot{m}_O^{(2)} + \dot{m}_O^{(3)}$ <p>As oxygen is present in the air and in the fuel:</p> $\dot{m}_O = \dot{m}_{O,a} + \dot{m}_{O,f}$

---

(continued)

(continued)

**Equation 7**

Title	Dry air stoichiometry for the combustion of one kilogram of fuel
	<p>From the definition of <math>E_X</math>, it follows that</p> $E_X = \frac{\dot{m}_{O,a}}{\frac{X_{O2,a}}{1 - X_{h2o,a}}}$ <p>Hence</p> $E_X = M_O \cdot \frac{\frac{2 \cdot X_{C,f}}{M_C} + \frac{X_{H,f}}{2 \cdot M_H} + \frac{2 \cdot X_{S,f}}{M_S} - \frac{X_{O,f}}{M_O}}{\frac{X_{O2,a}}{1 - X_{h2o,a}}} \text{ noticing that}$ $X_{O,f} = \frac{\dot{m}_{O,f}}{\dot{m}_f} = \dot{m}_{O,f}$ <p>since <math>\dot{m}_f = 1 \text{ kg/s}</math></p>

**Equation 8**

Title	$\text{CO}_2$ mass fraction in the flue gases
Validity domain	$\dot{m}_g \neq 0$
Mathematical formulation	$X_{\text{co2,g}} = \frac{\dot{m}_a \cdot X_{\text{co2,a}} + \dot{m}_f \cdot X_{f,C} \cdot \frac{M_{\text{co2}}}{M_C}}{\dot{m}_g}$
Comments	<p>The computation is similar to Eq. (7) using the chemical reaction <math>\text{C} + \text{O}_2 \rightarrow \text{CO}_2</math> that yields</p> $X_{\text{co2,g}} = \frac{\dot{m}_a \cdot X_{\text{co2,a}} + \frac{\dot{m}_f \cdot X_{C,f} \cdot M_{\text{co2}}}{M_C}}{\dot{m}_g}$

**Equation 9**

Title	$\text{H}_2\text{O}$ mass fraction in the flue gases
Validity domain	$\dot{m}_g \neq 0$
Mathematical formulation	$X_{\text{h2o,g}} = \frac{\dot{m}_a \cdot X_{\text{h2o,a}} + \dot{m}_f \cdot X_{H,f} \cdot \frac{M_{\text{h2o}}}{2 \cdot M_H}}{\dot{m}_g}$
Comments	<p>The computation is similar to Eq. (7) using the chemical reaction <math>\text{H} + 1/4 \text{O}_2 \rightarrow 1/2 \text{H}_2\text{O}</math> that yields</p> $X_{\text{h2o,g}} = \frac{\dot{m}_a \cdot X_{\text{h2o,a}} + \frac{\dot{m}_f \cdot X_{H,f} \cdot M_{\text{h2o}}}{2 \cdot M_H}}{\dot{m}_g}$

**Equation 10**

Title	$\text{O}_2$ mass fraction in the flue gases
Validity domain	$\dot{m}_g \neq 0$
Mathematical formulation	$X_{\text{o2,g}} = \frac{\dot{m}_a}{\dot{m}_g} \cdot X_{\text{o2,a}}$ $- M_O \cdot \frac{\dot{m}_f}{\dot{m}_g} \cdot \left( \frac{2 \cdot X_{C,f}}{M_C} + \frac{X_{H,f}}{2 \cdot M_H} + \frac{2 \cdot X_{S,f}}{M_S} \right) + \frac{\dot{m}_f}{\dot{m}_g} \cdot X_{O,f}$

(continued)

(continued)

Equation 10	
Title	O <sub>2</sub> mass fraction in the flue gases
Comments	The computation is similar to Eq. (7) (using the three chemical reactions) that yields $X_{\text{O}_2,\text{g}} = \frac{\dot{m}_{\text{a}} \cdot X_{\text{O}_2,\text{a}}}{\dot{m}_{\text{g}}} - \frac{\dot{m}_{\text{f}} \cdot M_{\text{O}} \cdot \left( \frac{2 \cdot X_{\text{C,f}}}{M_{\text{C}}} + \frac{X_{\text{H,f}}}{2 \cdot M_{\text{H}}} + \frac{2 \cdot X_{\text{S,f}}}{M_{\text{S}}} \right)}{\dot{m}_{\text{g}}} + \frac{\dot{m}_{\text{f}} \cdot X_{\text{O,f}}}{\dot{m}_{\text{g}}}$
Equation 11	
Title	SO <sub>2</sub> mass fraction in the flue gases
Validity domain	$\dot{m}_{\text{g}} \neq 0$
Mathematical formulation	$X_{\text{SO}_2,\text{g}} = \frac{\dot{m}_{\text{a}} \cdot X_{\text{SO}_2,\text{a}} + \dot{m}_{\text{f}} \cdot X_{\text{S,f}} \cdot \frac{M_{\text{SO}_2}}{M_{\text{S}}}}{\dot{m}_{\text{g}}}$
Comments	The computation is similar to Eq. (7) using the chemical reaction S + O <sub>2</sub> → SO <sub>2</sub> that yields $X_{\text{SO}_2,\text{g}} = \frac{\dot{m}_{\text{a}} \cdot X_{\text{SO}_2,\text{a}} + \frac{\dot{m}_{\text{t}} \cdot X_{\text{S,f}} \cdot M_{\text{SO}_2}}{M_{\text{S}}}}{\dot{m}_{\text{g}}}$

This set of equations must be completed by state equations for all substances in order to have a complete system of equations that can be solved. The state equations are to be given for  $h_{\text{a,i}}$ ,  $h_{\text{g,o}}$ ,  $T_{\text{g}}$ ,  $\rho_{\text{g}}$ , and  $\rho_{\text{ws}}$ .

### 7.2.4 Modelica Component Model: FossilFuelBoiler

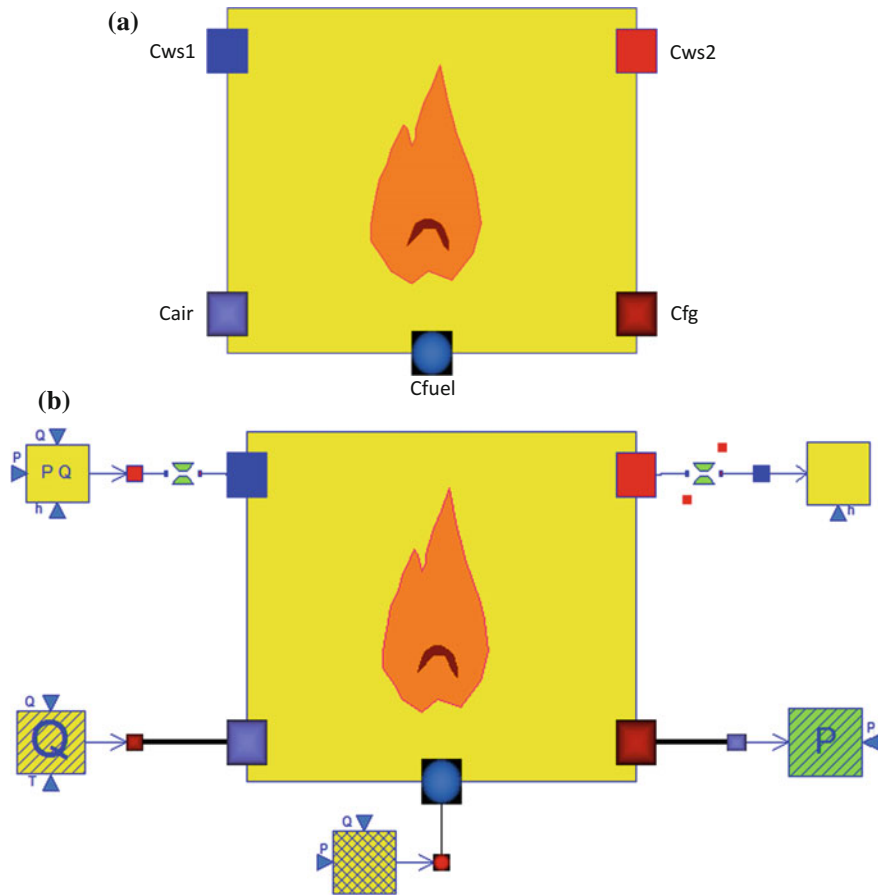
The governing equations are implemented in the *FossilFuelBoiler* located in the *MultiFluids.Boilers* sub-library.

Figure 7.2a represents the graphical icon of the component with its five connectors.

### 7.2.5 Test-Case

The model *TestFossilFuelBoiler* used to validate the *FossilFuelBoiler* component model is represented in Fig. 7.2b. It uses the following component models:

- One *FossilFuelBoiler* component model;
- One *SourceQ* component model (flue gases);
- One *SinkP* component model (flue gases);
- One *SourcePQ* component model (water/steam);



**Fig. 7.2** **a** Icon of the *FossilFuelBoiler* component model and **b** test-case for the *FossilFuelBoiler* component model

- One *Sink* component model (water/steam);
- One *FuelSourcePQ* model (fuel);
- Two *SingularPressureLoss* component models.

In the test-case scenario, the *TestFossilFuelBoiler* component receives: (1) the air mass flow rate, temperature, and composition at the inlet, (2) the flue gases pressure at the outlet, (3) the fuel pressure, mass flow rate, temperature, and composition at the inlet, and (4) the water pressure, the mass flow rate, and specific enthalpy at the inlet. The component computes: (1) the flue gases mass flow rate, pressure, and composition at the outlet, and (2) the water specific enthalpy and pressure at the outlet.

### 7.2.5.1 Test-Case Parameterization and Boundary Conditions

The model data are:

- Flue gases temperature at the outlet of the boiler = 386.16 K
- Flue gases pressure loss coefficient =  $0.05 \text{ m}^{-4}$
- Water/steam pressure loss coefficient =  $10^6 \text{ m}^{-4}$
- Thermal losses = 0
- Air pressure at the outlet of the boiler =  $1.0 \times 10^5 \text{ Pa}$
- Air temperature at the inlet = 298.16 K
- Air mass flow rate at the inlet = 27 kg/s
- $\text{CO}_2$  mass fraction in the air at the inlet = 0
- $\text{H}_2\text{O}$  mass fraction in the air at the inlet = 0
- $\text{O}_2$  mass fraction in the air at the inlet = 0.233
- $\text{SO}_2$  mass fraction in the air at the inlet = 0
- Water mass flow rate at the inlet of the boiler = 24 kg/s
- Water pressure at the inlet of the boiler =  $140 \times 10^5 \text{ Pa}$
- Water specific enthalpy at the inlet of the boiler =  $600 \times 10^3 \text{ J/kg}$
- Fuel temperature at the inlet = 338.16 K
- Fuel mass flow rate at the inlet = 1.45 kg/s
- Lower heating value of the fuel =  $48 \times 10^6 \text{ J/kg}$
- Fuel humidity = 0
- C mass fraction in the fuel = 0.75323
- H mass fraction in the fuel = 0.24403
- Fuel specific heat capacity = 1282 J/kg/K
- Fuel density = 0.72 kg/m<sup>3</sup>.

### 7.2.5.2 Model Calibration

The calibration procedure consists in setting (fixing) the value of the water/steam pressure at the outlet to a known measurement value and computing by model inversion the value of the pressure loss coefficient in the tubes.

Other possible calibration procedures:

1. Set the water/steam specific enthalpy at the outlet to a known measurement value, and compute the value of the fuel mass flow rate by model inversion.
2. Set the water/steam specific enthalpy at the outlet to a known measurement value, and compute the value of the water/steam mass flow rate by model inversion.

### 7.2.5.3 Simulation Results

The simulation of the test scenario is successful and produces the numerical results below:

- Water pressure at the outlet = 9,971,240 Pa
- Water/steam specific enthalpy at the outlet = 3,405,420 J/kg
- Boiler efficiency = 94.95%
- Combustion air ratio = 10%
- CO<sub>2</sub> mass fraction in the flue gases = 0.14066
- H<sub>2</sub>O mass fraction in the flue gases = 0.12064
- O<sub>2</sub> mass fraction in the flue gases = 0.02014.

# Chapter 8

## Combustion Chamber Modeling



**Abstract** Combustion is a chemical reaction that occurs between a fuel and an oxidizing agent that produces energy, usually in the form of heat and light. During combustion, oxygen is combined with different elements of the fuel, like carbon, hydrogen, sulfur, etc. and produces the respective oxides. Some excess air is always supplied to the burner, to ensure complete combustion. Insufficiency in combustion air may result in lower combustion efficiency, fouling of the heat transfer surface, atmospheric pollution (unburned fuel, soot, smoke, and carbon monoxide), and flame instability. This chapter describes the different models of combustion chambers and gives a detailed description of the physical equations for each of them: modeling assumptions, fundamental equations, and correlations with their validity domains. A test-case is given for each component model that includes the structure of the model, the parameterization data, and results of simulation. It is a valuable aid to understand the combustion phenomena that govern the operation of power plants. It is a main support to develop models for industrial power plants. The full description of the physical equations is independent of the programming languages and tools.

### 8.1 Combustion Chamber for a Gas Turbine

A gas turbine is a type of internal combustion engine. It has an upstream compressor coupled to a downstream turbine, and a combustion chamber in between; cf. Fig. 8.1. The compressor is used to increase the pressure of the atmospheric air that flows through it, in some cases up to 30 times higher than the atmospheric pressure. In the combustion chamber, energy is then added by spraying fuel into the air (oxidizer), and the combustion of the mixture generates a high-temperature flow. The hot flue gases enter the turbine, where they expand to the exhaust pressure, producing work on the shaft. An important part of the generated mechanical power is used by the compressor and the rest is converted into electricity in the generator. The exhaust gases are released into the atmosphere. Therefore, this cycle is classified as an open Brayton cycle (cf. Sect. 2.9.1).

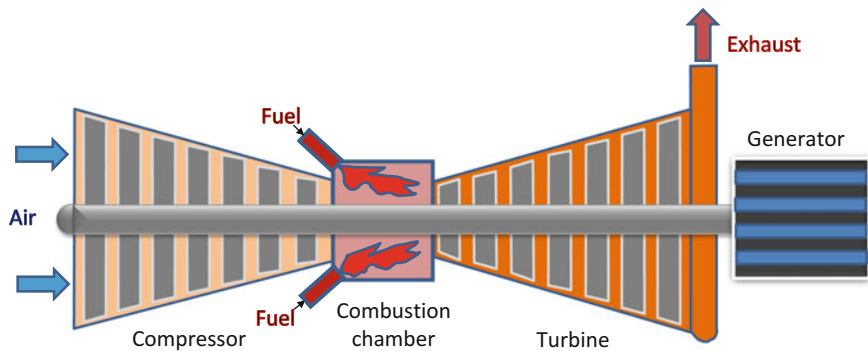
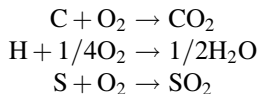


**Fig. 8.1** Schematic diagram of a gas turbine

### 8.1.1 *Modeling Principles*

The objective of the model is to compute the flue gas temperature, and the mass fractions of the species and of the excess air at the outlet from the mass flow rates and mass fractions of the species at the inlet.

The species at the outlet are governed by the following chemical reactions:



The formation of nitrogen oxide ( $\text{NO}_2$ ) is neglected.

For a gas turbine, excess air is needed to increase the mass of hot gas in the turbine and thus the power provided by the turbine.

The excess air factor is defined by:

$$E_{X,a} = \left( \frac{\text{dry air mass at the inlet}}{\text{stoichiometric dry air mass}} \right)$$

It is assumed that there is no accumulation of mass and energy inside the combustion chamber. Therefore, only the static 0D model of the combustion chamber is presented.

### 8.1.2 Nomenclature

Symbols	Definition	Unit	Mathematical definition
$A$	Average cross-sectional area of the combustion chamber	$\text{m}^2$	
$c_{\text{p,f}}$	Fuel specific heat capacity	$\text{J/kg/K}$	
$E_X$	Dry air stoichiometry necessary for the combustion of one kilogram of fuel (theoretical dry air requirement)	—	Oxygen mass required to burn 1 kg of fuel Oxygen mass in dry air at the inlet
$E_{X,a}$	Excess air factor	—	$\frac{\dot{m}_a \cdot (1 - X_{\text{H}_2\text{O},a})}{\dot{m}_f \cdot E_X}$
$h_{\text{a,i}}$	Air specific enthalpy at the inlet	$\text{J/kg}$	
$\tilde{h}_{\text{a,r}}$	Air reference specific enthalpy	$\text{J/kg}$	$2,501,569 \cdot X_{\text{H}_2\text{O},a}$
$h_{\text{at,i}}$	Air specific enthalpy at the inlet of the atomization compressor	$\text{J/kg}$	
$h_{\text{at,o}}$	Air specific enthalpy after isentropic expansion at the outlet of the atomization compressor	$\text{J/kg}$	
$h_f$	Fuel specific enthalpy at the inlet	$\text{J/kg}$	$c_{\text{p,f}} \cdot (T_f - 273.16)$
$\tilde{h}_{\text{f,r}}$	Fuel reference specific enthalpy	$\text{J/kg}$	0
$h_g$	Flue gases specific enthalpy after combustion	$\text{J/kg}$	
$h_{\text{g,o}}$	Flue gases specific enthalpy at the outlet	$\text{J/kg}$	
$\tilde{h}_{\text{g,r}}$	Flue gases reference specific enthalpy	$\text{J/kg}$	$2,501,569 \cdot X_{\text{H}_2\text{O},g}$
$h_{\text{ws,i}}$	Water/steam specific enthalpy at the inlet	$\text{J/kg}$	
$\tilde{h}_{\text{ws,r}}$	Water/steam reference specific enthalpy	$\text{J/kg}$	$2,501,569$
LHV	Fuel lower heating value	$\text{J/kg}$	
$\dot{m}_a$	Air mass flow rate	$\text{kg/s}$	
$\dot{m}_f$	Fuel mass flow rate	$\text{kg/s}$	
$\dot{m}_g$	Flue gases mass flow rate	$\text{kg/s}$	
$\dot{m}_m$	Average mass flow rate in the combustion chamber	$\text{kg/s}$	$\dot{m}_a + (\dot{m}_f + \dot{m}_{\text{ws}})/2$
$\dot{m}_{\text{ws}}$	Water/steam mass flow rate	$\text{kg/s}$	
$M_C$	Carbon atomic mass	$\text{kg/kmol}$	12.01115
$M_H$	Hydrogen atomic mass	$\text{kg/kmol}$	1.00797
$M_O$	Oxygen atomic mass	$\text{kg/kmol}$	15.9994
$M_S$	Sulfur atomic mass	$\text{kg/kmol}$	32.064
$M_{\text{CO}_2}$	$\text{CO}_2$ molar mass	$\text{kg/kmol}$	$M_C + 2 \cdot M_O$
$M_{\text{H}_2\text{O}}$	$\text{H}_2\text{O}$ molar mass	$\text{kg/kmol}$	$M_O + 2 \cdot M_H$
$M_{\text{SO}_2}$	$\text{SO}_2$ molar mass	$\text{kg/kmol}$	$M_S + 2 \cdot M_O$

(continued)

(continued)

Symbols	Definition	Unit	Mathematical definition
$P_{\text{at},i}$	Pressure at the inlet of the atomization compressor	Pa	With air atomization: $P_i \cdot (1 - \Lambda_{\text{at}})$ Without air atomization: $P_i$
$P_{\text{at},o}$	Pressure at the outlet of the atomization compressor	Pa	With air atomization: $P_i \cdot (1 + X P_{\text{at}})$ Without air atomization: $P_i$
$P_i$	Fluid pressure at the inlet	Pa	
$P_o$	Fluid pressure at the outlet	Pa	
$S_{\text{at},i}$	Entropy at the inlet of the atomization compressor	J/kg/K	
$T_{\text{a},i}$	Air temperature at the inlet	K	
$T_{\text{at}}$	Temperature at the inlet of the atomization compressor	K	
$T_{\text{g},o}$	Flue gases temperature at the outlet	K	
$T_f$	Fuel temperature at the inlet	K	
$v$	Flue gases velocity in the combustion chamber	m/s	$\dot{m}_m / (A \cdot \rho_m)$
$W_{\text{at}}$	Power of the atomization compressor	W	
$W_{\text{at},o}$	Thermal power extracted by the atomization refrigerant	W	
$W_f$	LHV power available in the fuel	W	$\dot{m}_f \cdot \text{LHV}$
$W_l$	Thermal power loss	W	
$X_{\text{C,f}}$	C mass fraction in the fuel	—	
$X_{\text{H,f}}$	H mass fraction in the fuel	—	
$X_{\text{O,f}}$	O mass fraction in the fuel	—	
$X_{\text{S,f}}$	S mass fraction in the fuel	—	
$X_{\text{CO}_2,a}$	$\text{CO}_2$ mass fraction in the air at the inlet	—	
$X_{\text{CO}_2,g}$	$\text{CO}_2$ mass fraction in the flue gases	—	
$X_{\text{H}_2\text{O},a}$	$\text{H}_2\text{O}$ mass fraction in the air at the inlet	—	
$X_{\text{H}_2\text{O},g}$	$\text{H}_2\text{O}$ mass fraction in the flue gases	—	
$X_{\text{O}_2,a}$	$\text{O}_2$ mass fraction in the air at the inlet	—	
$X_{\text{O}_2,g}$	$\text{O}_2$ mass fraction in the flue gases	—	
$X_{\text{SO}_2,a}$	$\text{SO}_2$ mass fraction in the air at the inlet	—	
$X_{\text{SO}_2,g}$	$\text{SO}_2$ mass fraction in the flue gases	—	
$XM_{\text{at}}$	Atomization air mass flow rate coefficient	—	
$XP_{\text{at}}$	Atomization overpressure coefficient	—	
$\Delta P$	Pressure loss in the combustion chamber	Pa	$P_i - P_o$

(continued)

(continued)

Symbols	Definition	Unit	Mathematical definition
$\eta_{at}$	Atomization compressor isentropic efficiency	–	
$\eta_c$	Combustion efficiency	–	
$\Lambda$	Pressure loss coefficient in the combustion chamber	$m^{-4}$	
$\Lambda_{at}$	Atomization pressure loss coefficient	$m^{-4}$	
$\rho_i$	Air density at the inlet	$kg/m^3$	
$\rho_o$	Flue gases density at the outlet	$kg/m^3$	
$\rho_m$	Fluid average density	$kg/m^3$	$\frac{\rho_i + \rho_o}{2}$

### 8.1.3 Governing Equations

The *GTCombustionChamber* model is based on the mass and energy balance equations.

#### Equation 1

Title	Mass balance equation
Validity domain	$\forall \dot{m}_g, \forall \dot{m}_a, \forall \dot{m}_f$ and $\forall \dot{m}_{ws}$
Mathematical formulation	$\dot{m}_g = \dot{m}_a + \dot{m}_f + \dot{m}_{ws}$
Comments	Flue gases result from the combustion of fuel with air. The incoming water is completely vaporized and mixed with the flue gases in the combustion chamber

#### Equation 2

Title	Energy balance equation
Validity domain	$\dot{m}_g \neq 0, \forall \dot{m}_a, \forall \dot{m}_f$ and $\forall \dot{m}_{ws}$
Mathematical formulation	$\dot{m}_g \cdot h_{g,o} + W_{at,o} + W_l - \dot{m}_f \cdot (h_f + \eta_c \cdot LHV) - \dot{m}_a \cdot h_{a,i} - \dot{m}_{ws} \cdot h_{ws,i} - W_{at} = 0$
Comments	This equation calculates the specific enthalpy $h_{g,o}$ ; cf. comments of Eq. (2) in Chap. 7

#### Equation 3

Title	Energy balance equation (without air atomization)
Validity domain	$\dot{m}_g \neq 0, \forall \dot{m}_a, \forall \dot{m}_f$ and $\forall \dot{m}_{ws}$
Mathematical formulation	$\dot{m}_g \cdot h_{g,o} + W_l - \dot{m}_f \cdot (h_f + \eta_c \cdot LHV) - \dot{m}_a \cdot h_{a,i} - \dot{m}_{ws} \cdot h_{ws,i} = 0$

(continued)

(continued)

Equation 3	
Title	Energy balance equation (without air atomization)
Comments	This equation calculates the specific enthalpy $h_{g,o}$ ; cf. comments of Eq. (2) in Chap. 7
Equation 3	
Title	Power of the atomization compressor
Validity domain	$\eta_{isc} > 0$ and $\forall \dot{m}_a \geq 0$
Mathematical formulation	With air atomization $W_{at} = \dot{m}_a \cdot XM_{at} \cdot \eta_{isc} \cdot (h_{at,o} - h_{at,i})$ Without air atomization $W_{at} = 0$
Equation 4	
Title	Thermal power extracted by the atomization refrigerant
Validity domain	$\forall \dot{m}_a \geq 0$
Mathematical formulation	With air atomization $W_{at,o} = \dot{m}_a \cdot XM_{at} \cdot (h_{a,i} - h_{at,i})$ Without air atomization $W_{at,o} = 0$
Equation 5	
Title	Momentum balance equation for the fluid (pressure losses)
Validity domain	$\forall \dot{m}$
Mathematical formulation	$P_o = P_i - \Lambda \cdot \frac{\rho_m \cdot v  \cdot v }{2}$
Equation 6	
Title	Dry air stoichiometry for the combustion of one kilogram of fuel
Validity domain	$X_{h_2o,f} < 1$ and $X_{O_2,a} > 0$
Mathematical formulation	$E_X = M_O \cdot \frac{\frac{2 \cdot X_{C,f}}{M_C} + \frac{X_{H,f}}{2 \cdot M_H} + \frac{2 \cdot X_{S,f}}{M_S} - \frac{X_{O,f}}{M_O}}{X_{O_2,a}} \quad 1 - X_{h_2o,a}$
Comments	The derivation of this equation is identical to Eq. (7) in Chap. 7
Equation 7	
Title	CO <sub>2</sub> mass fraction in the flue gases
Validity domain	$\dot{m}_g \neq 0$
Mathematical formulation	$X_{co_2,g} = \frac{\dot{m}_a}{\dot{m}_g} \cdot X_{co_2,a} + \frac{\dot{m}_f}{\dot{m}_g} \cdot X_{f,C} \cdot \frac{M_{co_2}}{M_C}$
Comments	The derivation of this equation is similar to Eq. (8) in Chap. 7

---

Equation 8

---

Title	H <sub>2</sub> O mass fraction in the flue gases
Validity domain	$\dot{m}_g \neq 0$
Mathematical formulation	$X_{\text{H}_2\text{O},g} = \frac{\dot{m}_a}{\dot{m}_g} \cdot X_{\text{H}_2\text{O},a} + \frac{\dot{m}_f}{\dot{m}_g} \cdot X_{\text{H,f}} \cdot \frac{M_{\text{H}_2\text{O}}}{2 \cdot M_{\text{H}}}$
Comments	The derivation of this equation is similar to Eq. (9) in Chap. 7

---

Equation 9

---

Title	O <sub>2</sub> mass fraction in the flue gases
Validity domain	$\dot{m}_g \neq 0$
Mathematical formulation	$X_{\text{O}_2,g} = \frac{\dot{m}_a}{\dot{m}_g} \cdot X_{\text{O}_2,a} - M_{\text{O}} \cdot \frac{\dot{m}_f}{\dot{m}_g} \cdot \left( \frac{2 \cdot X_{\text{C,f}}}{M_{\text{C}}} + \frac{X_{\text{H,f}}}{2 \cdot M_{\text{H}}} + \frac{2 \cdot X_{\text{S,f}}}{M_{\text{S}}} \right) + \frac{\dot{m}_f}{\dot{m}_g} \cdot X_{\text{O,f}}$
Comments	The derivation of this equation is similar to Eq. (10) in Chap. 7

---

Equation 10

---

Title	SO <sub>2</sub> mass fraction in the flue gases
Validity domain	$\dot{m}_g \neq 0$
Mathematical formulation	$X_{\text{SO}_2,g} = \frac{\dot{m}_a}{\dot{m}_g} \cdot X_{\text{SO}_2,a} + \frac{\dot{m}_f}{\dot{m}_g} \cdot X_{\text{S,f}} \cdot \frac{M_{\text{SO}_2}}{M_{\text{S}}}$
Comments	The derivation of this equation is similar to Eq. (11) in Chap. 7

---

This set of equations must be completed by the state equations for all substances in order to have a complete system of equations that can be solved. The state equations are given by the thermal properties of the fluids (air and flue gases:  $h_{a,i}$ ,  $h_{at,i}$ ,  $h_{at,o}$ ,  $S_{at,i}$ ,  $T_{g,o}$ ,  $\rho_i$  and  $\rho_o$ ).

### 8.1.4 Modelica Component Model: GTCombustionChamber

The governing equations are implemented in the *GTCombustionChamber* located in the *Combustion. CombustionChambers* sub-library.

Figure 8.2a represents the graphical icon of the component with its four connectors.

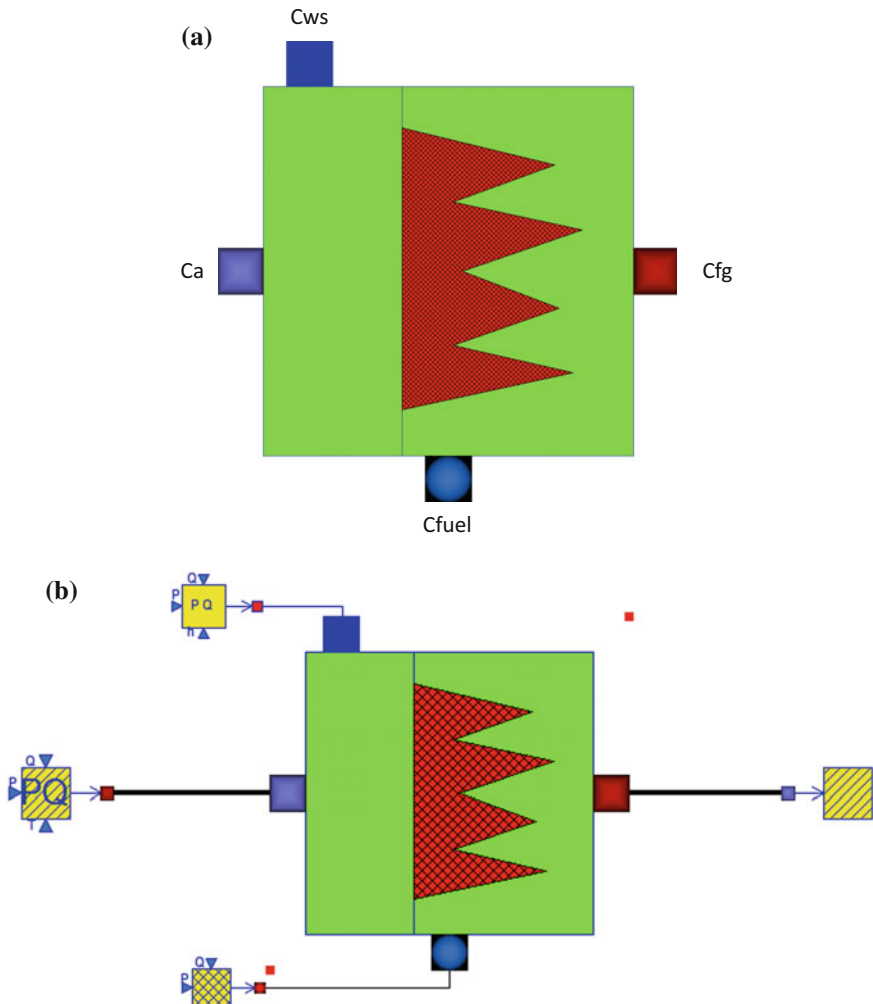


**Fig. 8.2** **a** Icon of the *GTCombustionChamber* component model. **b** Test-case for the *GTCombustionChamber* component model

### 8.1.5 Test-Case

The model *TestGTCombustionChamber* used to validate the *GTCombustionChamber* component model is represented in Fig. 8.2b. It uses the following component models:

- One *GTCombustionChamber* component model;
- One *SourcePQ* component model (for flue gases);
- One *Sink* component model (for flue gases);

- One *SourcePQ* component model (for water/steam);
- One *FuelSourcePQ* component model (for fuel).

In the test-case scenario, the *GTCombustionChamber* component receives:  
(1) the air pressure, mass flow rate, temperature, and composition at the inlet,  
(2) the fuel pressure, mass flow rate, temperature, and composition at the inlet, and  
(3) the water pressure, mass flow rate, and specific enthalpy at the inlet. The component model computes: the flue gases temperature, pressure, and composition at the outlet.

### 8.1.5.1 Test-Case Parameterization and Boundary Conditions

The model data are:

- Flue gases temperature at the outlet of the boiler = 386.16 K
- Flue gases pressure at the outlet of the boiler =  $14.1 \times 10^5$  Pa
- Thermal power losses =  $10^6$  W
- Air pressure at the inlet of the combustion chamber =  $15 \times 10^5$  Pa
- Air temperature at the inlet = 680 K
- Air mass flow rate at the inlet = 415 kg/s
- CO<sub>2</sub> mass fraction in the air at the inlet = 0
- H<sub>2</sub>O mass fraction in the air at the inlet = 0.01
- O<sub>2</sub> mass fraction in the air at the inlet = 0.23
- SO<sub>2</sub> mass fraction in the air at the inlet = 0
- Fuel temperature at the inlet = 410 K
- Fuel mass flow rate at the inlet = 9.3 kg/s
- Lower heating value of the fuel =  $47.5 \times 10^6$  J/kg
- Fuel humidity = 0
- C mass fraction in the fuel = 0.755
- H mass fraction in the fuel = 0.245
- Fuel specific heat capacity = 2255 J/kg/K
- Fuel density = 0.838 kg/m<sup>3</sup>.

### 8.1.5.2 Model Calibration

The calibration step consists in setting the value of the flue gases pressure at the outlet to a known measurement value and computing by model inversion the value of the pressure loss coefficient in the combustion chamber.

Other possible calibrations:

- Set the flue gases temperature at the outlet to a known measurement value and compute the value of the fuel mass flow rate by model inversion.

- Set the combustion air ratio to a known measurement value and compute the value of the air mass flow rate by model inversion.

### 8.1.5.3 Simulation Results

The simulation of the test scenario produces the numerical results below:

- Flue gases temperature at the outlet = 1500.7 K
- Combustion air ratio = 2.5945
- $\text{CO}_2$  mass fraction in the flue gases = 0.0606
- $\text{H}_2\text{O}$  mass fraction in the flue gases = 0.0578
- $\text{O}_2$  mass fraction in the flue gases = 0.1383
- Pressure loss coefficient in the combustion chamber =  $4.593 \text{ m}^{-4}$ .

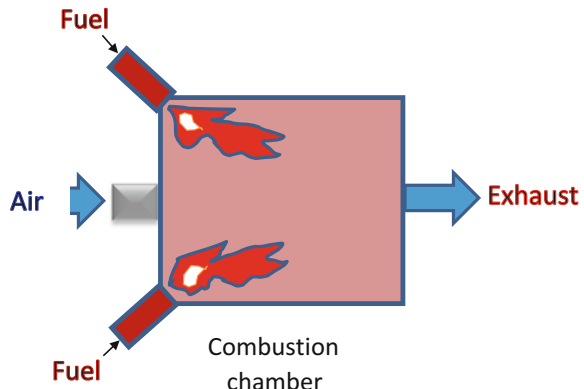
## 8.2 Combustion Chamber for Boiler Furnace

Combustion takes place in the furnace, which is one of the major components in thermal power plants. In the combustion chamber, energy is added by spraying fuel into the air. Combustion of the resulting mixture generates high-temperature flue gases (cf. Fig. 8.3) which circulate outside the membrane of the furnace that wraps the water-walls that contain the tubes where water flows and vaporizes.

The furnace model is called *GenericCombustion1D*. This component models the combustion inside the furnace with heat transfer between the furnace and the cooling fluid flowing through the tubes.

The fuels to be used in this component are: coal, oil, gas, biomass, and solid waste.

**Fig. 8.3** Schematic diagram of a generic combustion chamber

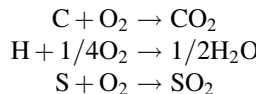


In this paragraph, the static 1D discretized model of a generic combustion chamber is presented.

### 8.2.1 Modeling Principles

The objective of the model is to compute the flue gas temperature, and the mass fractions of the species and of the excess air at the outlet from the mass flow rates and mass fractions of the species at the inlet.

The species at the outlet are governed by the following chemical reactions:



The formation of nitrogen oxide ( $\text{NO}_2$ ) is neglected.

For a boiler furnace, excess air is necessary to avoid having unburnt fuel in the exhaust fumes. It also allows to increase the convective exchange between the fumes and the tubes.

The excess air factor is defined by:

$$E_{X,a} = \left( \frac{\text{dry air mass at the inlet}}{\text{stoichiometric dry air mass}} \right)$$

As the residence time of the species in the combustion chamber is very short, it is assumed that there is no accumulation of mass and energy inside the chamber. Therefore, only the static 0D model of the boiler furnace is presented.

In addition, the radiative and convective heat exchange between the flue gases and the water-wall is represented in one dimension along the tubes of the water-wall.

### 8.2.2 Nomenclature

Symbols	Definition	Unit	Mathematical definition
$A$	Average cross-sectional area of the combustion chamber	$\text{m}^2$	
$c_{p,cd}$	Ashes specific heat capacity	$\text{J/kg/K}$	
$c_{p,f}$	Fuel specific heat capacity	$\text{J/kg/K}$	
$E_X$	Dry air stoichiometry necessary for the combustion of one kilogram of fuel (theoretical dry air requirement)	–	

(continued)

(continued)

Symbols	Definition	Unit	Mathematical definition
$E_{X,a}$	Excess air factor	–	$\frac{\dot{m}_a \cdot (1 - X_{h_2o,a})}{\dot{m}_f \cdot E_X}$
$h_{a,i}$	Air specific enthalpy at the inlet	J/kg	
$\tilde{h}_{a,r}$	Air reference specific enthalpy	J/kg	$2,501,569 \cdot X_{h_2o,a}$
$h_{bf}$	Low furnace ashes specific enthalpy at the outlet	J/kg	$c_{p,cd} \cdot (T_{bf} - 273.16)$
$h_c$	Convective/conductive (+fouling) heat exchange coefficient	W/m <sup>2</sup> /K	
$h_{c,r}$	Ashes reference specific enthalpy	J/kg	0
$h_{cv}$	Volatile ashes specific enthalpy at the outlet	J/kg	$c_{p,cd} \cdot (T_{g,o} - 273.16)$
$h_f$	Fuel specific enthalpy at the inlet	J/kg	$c_{p,f} \cdot (T_f - 273.16)$
$\tilde{h}_{f,r}$	Fuel reference specific enthalpy	J/kg	0
$h_{g,o}$	Flue gases specific enthalpy at the outlet	J/kg	
$\tilde{h}_{g,r}$	Flue gases reference specific enthalpy	J/kg	$2,501,569 \cdot X_{h_2o,g}$
$h_{ws,i}$	Water/steam specific enthalpy at the inlet	J/kg	
$\tilde{h}_{ws,r}$	Water/steam reference specific enthalpy	J/kg	2,501,569
$HHV_c$	Unburnt carbon higher heating value	J/kg	$32.8 \times 10^6$
$I_{CV}$	Unburnt particles ratio in the volatile ashes $0 \leq I_{CV} < 1$	–	
$I_{BF}$	Unburnt particle ratio in the low furnace ashes $0 \leq I_{BF} < 1$	–	
$LHV_d$	Fuel lower heating value of the dry matter	J/kg	
$LHV$	Fuel lower heating value (effective value or crude)	J/kg	$LHV_d \cdot (1 - X_{f,W}) - 25.1 \times 10^5 \cdot X_{f,W}$
$\dot{m}_a$	Air mass flow rate	kg/s	
$\dot{m}_{bf}$	Low furnace ashes mass flow rate	kg/s	$\dot{m}_f \cdot X_{CD,f} \cdot X_{bf} \cdot (1 - I_{BF})$
$\dot{m}_{cv}$	Volatile ashes mass flow rate	kg/s	$\frac{\dot{m}_f \cdot X_{CD,f} \cdot (1 - X_{bf})}{(1 - I_{BF})}$
$\dot{m}_f$	Fuel mass flow rate	kg/s	
$\dot{m}_g$	Flue gases mass flow rate	kg/s	
$\dot{m}_{ws}$	Water/steam mass flow rate	kg/s	
$\dot{m}_m$	Average mass flow rate in the combustion chamber	kg/s	$\dot{m}_a + (\dot{m}_f + \dot{m}_{ws})/2$
$M_C$	Carbon atomic mass	kg/kmol	12.01115

(continued)

(continued)

Symbols	Definition	Unit	Mathematical definition
$M_H$	Hydrogen atomic mass	kg/kmol	1.00797
$M_O$	Oxygen atomic mass	kg/kmol	15.9994
$M_S$	Sulfur atomic mass	kg/kmol	32.064
$M_{CO_2}$	$CO_2$ molar mass	kg/kmol	$M_C + 2 \cdot M_O$
$M_{H_2O}$	$H_2O$ molar mass	kg/kmol	$M_O + 2 \cdot M_H$
$M_{SO_2}$	$SO_2$ molar mass	kg/kmol	$M_S + 2 \cdot M_O$
$n$	Number of segments in the combustion chamber	—	
$P_i$	Fluid pressure at the inlet	Pa	
$P_o$	Fluid pressure at the outlet	Pa	
$R_{S,i}$	Corrective coefficient for the real heat exchange area for cell $i$	—	
$S_i$	Heat exchange area for cell $i$ (the projected area)	$m^2$	
$T_{a,i}$	Air temperature at the inlet	K	
$T_f$	Fuel temperature at the inlet	K	
$T_{g,o}$	Flue gases temperature at the outlet	K	
$T_{bf}$	Ashes temperature at the outlet of the low furnace	K	
$T_{w,i}$	Furnace wall temperature for each cell $i$	K	
$v$	Flue gases velocity in the combustion chamber	m/s	$\dot{m}_m / (A \cdot \rho_m)$
$W_l$	Thermal power loss	W	$\dot{m}_f \cdot LHV \cdot x_{W,l}$
$W_{s,i}$	Thermal power exchanged between the flue gases and the furnace wall for each cell $i$	W	
$W_s$	Total thermal power exchanged between the flue gases and the furnace wall	W	$\sum W_{s,i}$
$X_{bf}$	Ashes ratio in the low furnace $0 < X_{bf} < 1$	—	
$X_{C,f}$	C mass fraction in the fuel	—	
$X_{H,f}$	H mass fraction in the fuel	—	
$X_{O,f}$	O mass fraction in the fuel	—	
$X_{S,f}$	S mass fraction in the fuel	—	
$X_{w,f}$	$H_2O$ mass fraction in the fuel	—	
$X_{CD,f}$	Ashes mass fraction in the fuel	—	
$X_{CO_2,a}$	$CO_2$ mass fraction in the air at the inlet	—	
$X_{H_2O,a}$	$H_2O$ mass fraction in the air at the inlet	—	

(continued)

(continued)

Symbols	Definition	Unit	Mathematical definition
$X_{O_2,a}$	O <sub>2</sub> mass fraction in the air at the inlet	–	
$X_{SO_2,a}$	SO <sub>2</sub> mass fraction in the air at the inlet	–	
$X_{CO_2,g}$	CO <sub>2</sub> mass fraction in the flue gases	–	
$X_{H_2O,g}$	H <sub>2</sub> O mass fraction in the flue gases	–	
$X_{O_2,g}$	O <sub>2</sub> mass fraction in the flue gases	–	
$X_{SO_2,g}$	SO <sub>2</sub> mass fraction in the flue gases	–	
$x_{W,i}$	Thermal loss fraction in the body of the combustion chamber $0 < x_{W,i} < 1$	–	
$\Delta P$	Pressure loss in the combustion chamber	Pa	$P_i - P_o$
$\varepsilon$	Wall emissivity	–	
$\Lambda$	Pressure loss coefficient in the combustion chamber	m <sup>-4</sup>	
$\rho_i$	Air density at the inlet	kg/m <sup>3</sup>	
$\rho_o$	Flue gases density at the outlet	kg/m <sup>3</sup>	
$\rho_m$	Fluid average density	kg/m <sup>3</sup>	$\frac{\rho_i + \rho_o}{2}$
$\sigma$	Stefan–Boltzmann constant	W/m <sup>2</sup> /K <sup>4</sup>	$5.67 \times 10^{-8}$

### 8.2.3 Governing Equations

The *GenericCombustion1D* model is based on the mass, energy, and momentum balance equations.

Equation 1	
Title	Mass balance equation
Validity domain	$\forall \dot{m}_g, \forall \dot{m}_a, \forall \dot{m}_f$ and $\forall \dot{m}_{ws}$
Mathematical formulation	$\dot{m}_g = \dot{m}_a + \dot{m}_{ws} + \dot{m}_f \cdot (1 - X_{CD,f}) - \dot{m}_{cv} \cdot I_{cv} - \dot{m}_{bf} \cdot I_{BF}$

Equation 2	
Title	Energy balance equation
Validity domain	$\dot{m}_a > 0, \dot{m}_f > 0$ and $\dot{m}_{ws} \geq 0$
Mathematical formulation	$\begin{aligned} (\dot{m}_a + \dot{m}_{ws} + \dot{m}_f \cdot (1 - X_{CD,f})) \cdot h_{g,o} + W_l \\ + \dot{m}_{cv} \cdot h_{cv} + \dot{m}_{bf} \cdot h_{bf} \\ + (\dot{m}_{cv} \cdot I_{cv} + \dot{m}_{bf} \cdot I_{BF}) \cdot HHV_c + W_s \\ = \dot{m}_f \cdot (h_f + LHV) + \dot{m}_a \cdot h_{a,i} + \dot{m}_{ws} \cdot h_{ws,i} \end{aligned}$
Comments	This equation computes the specific enthalpy $h_{g,o}$ ; cf. comments of Eq. (2) in Chap. 7

Equation 3	
Title	Energy balance equation (thermal power exchanged between the flue gases and the furnace wall)
Validity domain	$\forall T_{g,o}$ and $\forall T_{w,i}$
Mathematical formulation	$W_s = \sum_{i=1}^n \sigma \cdot \varepsilon \cdot S_i \cdot R_{S,i} \cdot (T_{g,o}^4 - T_{w,i}^4)$ $+ \sum_{i=1}^n h_c \cdot S_i \cdot R_{S,i} \cdot (T_{g,o} - T_{w,i})$
Comments	Cf. (2.83)
Equation 4	
Title	Momentum balance equation for the fluid (pressure losses)
Validity domain	$\forall v$
Mathematical formulation	$P_o = P_i - \Lambda \cdot \frac{\rho_m \cdot v^2}{2}$
Equation 5	
Title	Dry air stoichiometry for the combustion of one kilogram of fuel
Validity domain	$X_{h_2o,f} < 1$ and $X_{O_2,a} > 0$
Mathematical formulation	$E_X = M_O \cdot \frac{\left[ \frac{2 \cdot X_{C,f}}{M_C} + \frac{X_{H,f}}{2 \cdot M_H} + \frac{2 \cdot X_{S,f}}{M_S} - \frac{X_{O,f}}{M_O} \right] - 2 \cdot \left( \frac{\dot{m}_{cv} \cdot I_{CV} + \dot{m}_{bf} \cdot I_{BF}}{M_C} \right)}{\frac{X_{O_2,a}}{1 - X_{h_2o,a}}}$
Comments	The derivation of this equation is similar to Eq. (7) in Chap. 7
Equation 6	
Title	$CO_2$ mass fraction in the flue gases
Validity domain	$\dot{m}_g \neq 0$
Mathematical formulation	$X_{co_2,g} = \frac{\dot{m}_a}{\dot{m}_g} \cdot X_{co_2,a} + \frac{\dot{m}_f}{\dot{m}_g} \cdot X_{C,f} \cdot \frac{M_{co_2}}{M_C}$ $- \frac{1}{\dot{m}_f} \cdot \frac{M_{co_2}}{M_C} \cdot (\dot{m}_{cv} \cdot I_{CV} + \dot{m}_{bf} \cdot I_{BF})$
Comments	The derivation of this equation is similar to Eq. (8) in Chap. 7
Equation 7	
Title	$H_2O$ mass fraction in the flue gases
Validity domain	$\dot{m}_g \neq 0$
Mathematical formulation	$X_{h_2o,g} = \frac{\dot{m}_a}{\dot{m}_g} \cdot X_{h_2o,a} + \frac{\dot{m}_f}{\dot{m}_g} \cdot X_{H,f} \cdot \frac{M_{h_2o}}{2 \cdot M_H}$ $+ \frac{\dot{m}_{ws}}{\dot{m}_g} + \frac{\dot{m}_f \cdot X_{w,f}}{\dot{m}_g}$
Comments	The derivation of this equation is similar to Eq. (9) in Chap. 7

Equation 8	
Title	O <sub>2</sub> mass fraction in the flue gases
Validity domain	$\dot{m}_g \neq 0$
Mathematical formulation	$X_{O_2,f} = \frac{\dot{m}_a}{\dot{m}_g} \cdot X_{O_2,a}$ $- M_O \cdot \frac{\dot{m}_f}{\dot{m}_g} \cdot \left( \frac{2 \cdot X_{C,f}}{M_C} + \frac{X_{H,f}}{2 \cdot M_H} + \frac{2 \cdot X_{S,f}}{M_S} \right)$ $+ \frac{\dot{m}_f}{\dot{m}_g} \cdot X_{O,f}$
Comments	The derivation of this equation is similar to Eq. (10) in Chap. 7

Equation 9	
Title	SO <sub>2</sub> mass fraction in the flue gases
Validity domain	$\dot{m}_g \neq 0$
Mathematical formulation	$X_{SO_2,g} = \frac{\dot{m}_a}{\dot{m}_g} \cdot X_{SO_2,a} + \frac{\dot{m}_f}{\dot{m}_g} \cdot X_{S,f} \cdot \frac{M_{SO_2}}{M_S}$
Comments	The derivation of this equation is similar to Eq. (11) in Chap. 7

This set of equations must be completed by the state equations for all substances in order to have a complete system of equations that can be solved. The state equations are given by the thermal properties of the fluids (air and flue gases:  $h_{a,i}$ ,  $T_{g,o}$ ,  $\rho_i$  and  $\rho_o$ ).

### 8.2.4 Modelica Component Model: GenericCombustion1D

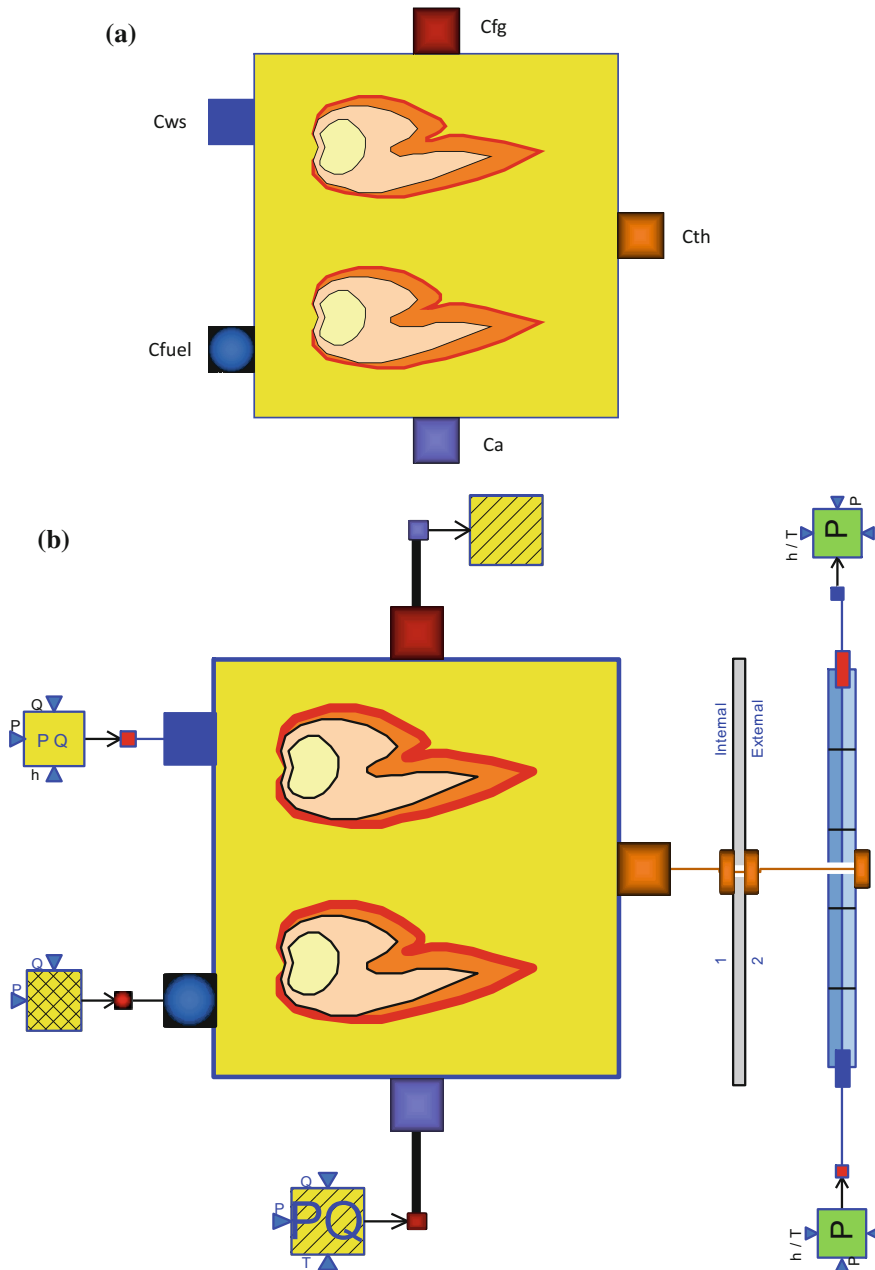
The governing equations are implemented in the *GenericCombustion1D* located in the *Combustion.CombustionChambers* sub-library.

Figure 8.4a represents the graphical icon of the component with its five connectors.

### 8.2.5 Component Model Validation

The model *TestGenericCombustion1D* used to validate the *GenericCombustion1D* component model is represented in Fig. 8.4b. It uses the following component models:

- One *GenericCombustion1D* component model;
- One *SourcePQ* component model (for flue gases);
- One *Sink* model (for flue gases);
- One *SourcePQ* component model (for water/steam);
- One *FuelSourcePQ* component model (for fuel);



**Fig. 8.4** **a** Icon of the *GenericCombustion1D* component model. **b** Test-case for the *GenericCombustion1D* component model

- One *DynamicTwoPhaseFlowPipe* component model;
- One *HeatExchangerWall* component model.

In the test-case scenario, the *GenericCombustion1D* component receives: (1) the air pressure, mass flow rate, temperature, and composition at the inlet, (2) the fuel pressure, mass flow rate, temperature, and composition at the inlet, (3) the water pressure, mass flow rate and specific enthalpy at the inlet, (4) the water pressure and specific enthalpy at the inlet of the water tube, and (5) the water pressure at the outlet of the water tube. The component computes: (1) the flue gases temperature, pressure, and composition at the outlet, and (2) the steam pressure and specific enthalpy at the outlet of the water tube.

### 8.2.5.1 Test-Case Parameterization and Boundary Conditions

The model data are:

- Average cross-sectional area of the combustion chamber =  $275 \text{ m}^2$
- Heat exchange area for each node = {639.92, 198.58, 466.48, 466.48, 466.48, 358.56, 358.56}  $\text{m}^2$
- Thermal loss fraction in the body of the combustion chamber = 0
- Unburnt particles ratio in the volatile ashes = 0.05
- Unburnt particle ratio in the low furnace ashes = 0.0
- Ashes specific heat capacity = 500 J/kg/K
- Ashes temperature at the outlet of the low furnace = 500 K
- Convection and conduction heat exchange coefficient = 8.8 W/m<sup>2</sup>/K
- Combustion chamber walls emissivity = 0.7
- Air pressure at the inlet =  $1.91 \times 10^5 \text{ Pa}$
- Air temperature at the inlet = 524.89 K
- Air mass flow rate at the inlet = 606.29 kg/s
- CO<sub>2</sub> mass fraction in the air at the inlet = 0
- H<sub>2</sub>O mass fraction in the air at the inlet = 0.01
- O<sub>2</sub> mass fraction in the air at the inlet = 0.23
- SO<sub>2</sub> mass fraction in the air at the inlet = 0
- Fuel temperature at the inlet = 358.15 K
- Fuel mass flow rate at the inlet = 57.2 kg/s
- Lower heating value of the fuel =  $29,245 \times 10^3 \text{ J/kg}$
- Fuel humidity = 0.08
- C mass fraction in the fuel = 0.719
- H mass fraction in the fuel = 0.0414
- N mass fraction in the fuel = 0.0208
- O mass fraction in the fuel = 0.086
- S mass fraction in the fuel = 0.0044
- Volatile matter mass fraction = 0.286
- Fuel specific heat capacity = 1200 J/kg/K

- Fuel density =  $1100 \text{ kg/m}^3$
- Water specific enthalpy at the water-tube boiler inlet =  $1292 \times 10^3 \text{ J/kg}$
- Water mass flow rate at the outlet of the water-tube boiler =  $486.69 \text{ kg/s}$
- Water pressure at the inlet of the water-tube boiler =  $201.12 \times 10^5 \text{ Pa}$
- Number of pipes of the water-tube boiler = 403
- Internal diameter of the pipes =  $0.0327 \text{ m}$
- External diameter of the pipes =  $0.038 \text{ m}$
- Length of the pipes =  $58 \text{ m}$
- Inlet altitude of the pipes =  $0 \text{ m}$
- Outlet altitude of the pipes =  $58 \text{ m}$
- Pipes conductivity =  $40 \text{ W/m/K}$
- Corrective term for the friction pressure loss = 3.5.

### 8.2.5.2 Model Calibration

The calibration step consists in setting the value of the flue gases pressure at the outlet to a known measurement value and computing by model inversion the value of the pressure loss coefficient in the combustion chamber.

Other possible calibrations:

1. Set the flue gases temperature at the outlet to a known measurement value and compute by model inversion the value of the fuel mass flow rate.
2. Set the combustion air ratio to a known measurement value and compute by model inversion the value of the air mass flow rate.
3. Set the water/steam mass flow rate at the outlet of the water tube to a known measurement value and compute by model inversion the value of the steam pressure at the outlet of the water tube.

### 8.2.5.3 Simulation Results

The simulation of the test scenario produces the numerical results below:

- Water pressure at the outlet =  $192.66 \times 10^5 \text{ Pa}$
- Specific enthalpy at the outlet of the water tube =  $2,816,480 \text{ J/kg}$
- Flue gases temperature at the outlet =  $1462.02 \text{ K}$
- Flue gases mass flow rate at the outlet =  $658.3 \text{ kg/s}$
- Combustion air ratio = 2.3
- $\text{CO}_2$  mass fraction in the flue gases = 0.227
- $\text{H}_2\text{O}$  mass fraction in the flue gases = 0.0483
- $\text{O}_2$  mass fraction in the flue gases = 0.025.

### 8.2.5.4 Model Validation

A detailed 3D model of the furnace of the Q600 boiler (pulverized coal units) was developed with the CFD Code\_Saturne tool by EDF (Dal-Secco 2005). In this model, the behavior of the water-walls is represented by a constant wall temperature at  $T = 400$  °C. In order to compare this model with the Modelica model, the water-walls in Fig. 8.4b are replaced by a *HeatSource* component model at temperature  $T = 400$  °C.

Table 8.1 shows the comparison between the 0D/1D simulation results obtained with Dymola and those obtained with the 3D CFD Code\_Saturne tool (displayed in Fig. 8.5).

**Table 8.1** Comparison between 0D/1D simulation results and 3D CFD simulation results

	0D/1D	3D CFD	Discrepancy (%)
Flue gases average temperature in the furnace (°C)	1189.6	1182.4	0.61

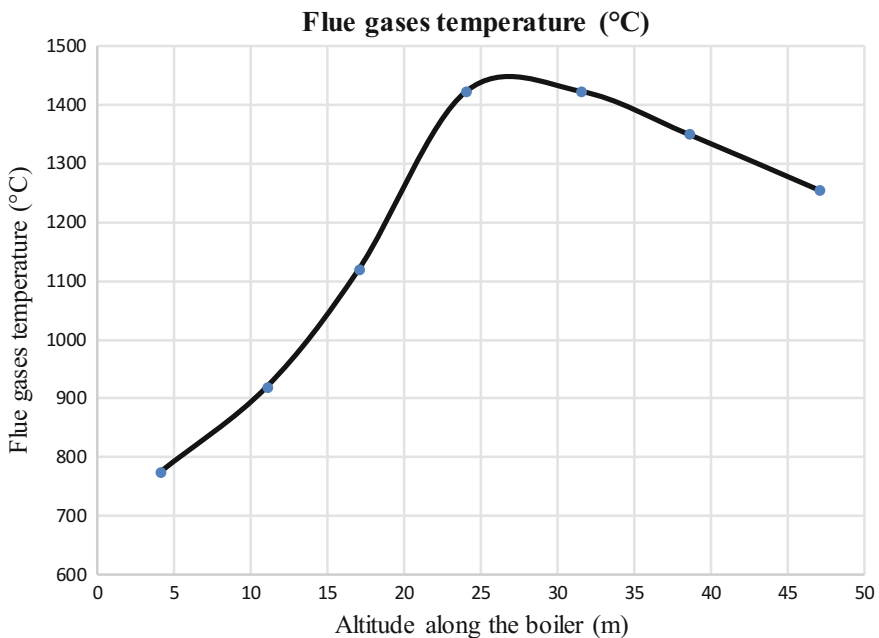


**Fig. 8.5** Simulation result obtained with the 3D CFD Saturne code for the Q600 power plant

## Reference

Dal-Secco S (2005) Synthèse des calculs paramétriques 3D réalisés avec Code\_Saturne sur une chaudière de type Q600. Analyse de l'influence de différents critères. EDF R&D technical report HI-81/04/014/A

# Chapter 9

## Heat Exchanger Modeling



**Abstract** A heat exchanger, as its name suggests, is a component that transfers heat between two fluids separated by a solid wall. The process of exchanging heat between different fluids is one of the most important and frequently encountered processes found in engineering practice, for example, boilers, condensers, water heaters, flue gases heaters. In some components, heat exchange is associated with a phase change of one of the fluids such as condensation or evaporation. This chapter presents the different heat exchanger design methods (LMTD, NTU, UA, and efficiency method) and the different correlations utilized to compute the convective heat transfer coefficient for single- and two-phase flow (evaporation and condensation). Then, models are presented for various types of heat exchangers: shell and tube, dynamic two-phase flow pipe, dynamic single-phase flow shell, water- or gas-wall, dynamic and static water heating, dynamic and static condensers, dynamic and static plate heat exchangers, and flue gases heat exchangers. A detailed description of the physical equations is given for each component model: modeling assumptions, fundamental equations, and correlations with their validity domains. A test-case is provided for each component model that includes the structure of the model, the parameterization data, the simulation results, the model validation, and in some cases the experimental validation. It is a valuable aid to understand the physical phenomena that govern the operation of power plants and energy processes. It is a main and full support to develop models for industrial power plants. The full description of the physical equations is independent of the programming languages and tools.

### 9.1 Introduction

There are different types of heat exchangers that can be divided into two general classes, depending on the relative flow orientation of the two fluids exchanging heat. If the two fluid flows cross one another in space, not necessarily at right angles, the exchanger is termed a cross-flow heat exchanger as shown in Fig. 9.1a.

This configuration is generally used in applications where a gas is forced over a tube bundle through which a liquid is pumped.

Heat exchangers in which the two fluid flows move in parallel directions in space are termed unidirectional heat exchangers. In the parallel-flow arrangement as shown in Fig. 9.1b, the hot and cold fluids enter the exchanger at the same end, flow in the same direction, and exit at the same end. In the counter-flow

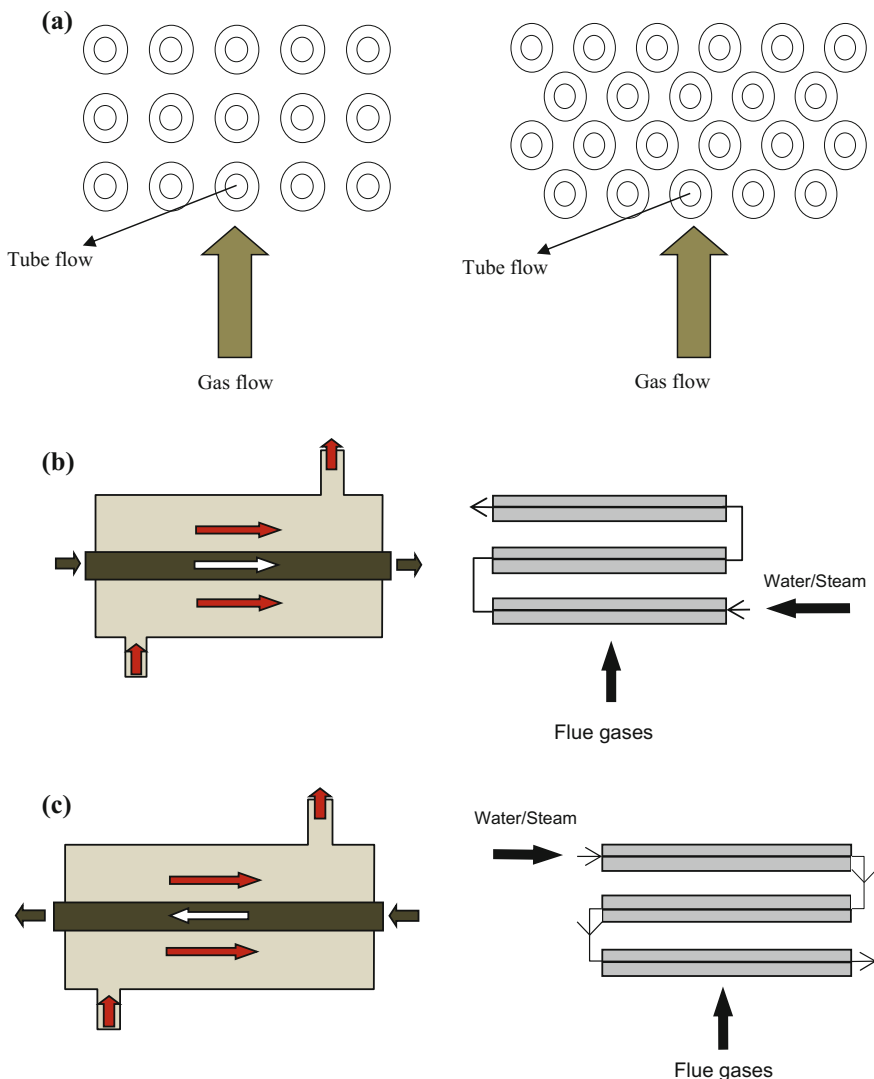


**Fig. 9.1** **a** Cross-flow heat exchanger, **b** parallel-flow heat exchanger, and **c** counter-flow heat exchanger

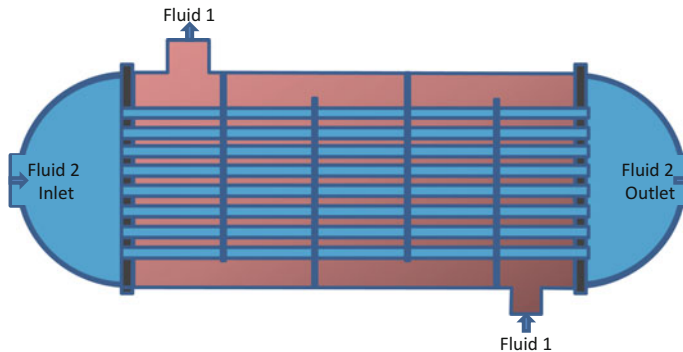


**Fig. 9.2** Shell-and-tube heat exchanger with one shell pass and one tube pass

arrangement, see Fig. 9.1c, the fluids enter at opposite ends, flow in opposite directions, and exit at opposite ends.

Flow conditions become more complicated for shell-and-tube heat exchangers, which are commonly used for liquid-to-liquid heat transfer and consist of a bundle of circular tubes mounted in a cylindrical shell. The simplest configuration, which involves a single shell pass and one tube pass, is shown in Fig. 9.2. Cross-baffles are generally installed in the exchanger in order to generate turbulence in the shell-side fluid and to promote a cross-flow component in the fluid velocity relative to the tubes. These effects contribute to a higher heat transfer coefficient on the outer tube surface.

## 9.2 Analysis Methods

### 9.2.1 Nomenclature

$A$	Internal or external heat exchange surface	$\text{m}^2$
$A$	Pipe internal cross-sectional area	$\text{m}^2$
$A_i$	Internal heat exchange surface of the pipes	$\text{m}^2$
$A_o$	External heat exchange surface of the pipes	$\text{m}^2$
$Bo$	Boiling number	—
$c_p$	Fluid specific heat capacity	$\text{J/kg/K}$
$c_{p,c}$	Cold fluid specific heat capacity	$\text{J/kg/K}$
$c_{p,h}$	Hot fluid specific heat capacity	$\text{J/kg/K}$
$c_{p,l}$	Specific heat capacity of the liquid phase	$\text{J/kg/K}$
$c_{p,v}$	Specific heat capacity of the vapor phase	$\text{J/kg/K}$
$c_{p,w}$	Specific heat capacity of the wall	$\text{J/kg/K}$

(continued)

(continued)

$c_{p,w,i}$	Specific heat capacity of the wall in cell $i$	J/kg/K
$C_R$	Heat capacity ratio	—
$D_e$	External diameter of one pipe	m
$D_i$	Internal diameter of one pipe	m
$E$	Dimensionless corrective term	—
$g$	Acceleration due to gravity	m/s <sup>2</sup>
$G$	Surface mass flow rate	kg/m <sup>2</sup> /s
$h_{c,i}$	Cold fluid specific enthalpy at the inlet	J/kg
$h_{c,o}$	Cold fluid specific enthalpy at the outlet	J/kg
$h_{h,i}$	Hot fluid specific enthalpy at the inlet	J/kg
$h_{h,o}$	Hot fluid specific enthalpy at the outlet	J/kg
$h_{fg}$	Latent energy of phase transition	J/kg
$h_{i:i+1}$	Fluid specific enthalpy at the boundary between cells $i$ and $i + 1$	J/kg
$k_f$	Fluid thermal conductivity	W/m/K
$K_{\text{cond}}$	Convective heat exchange coefficient due to condensation	W/m <sup>2</sup> /K
$K_{f,i}$	Convective heat exchange coefficient between fluid and the wall in cell $i$	W/m <sup>2</sup> /K
$K_i$	Internal convective heat exchange coefficient	W/m <sup>2</sup> /K
$K_o$	External convective heat exchange coefficient	W/m <sup>2</sup> /K
$K$	Heat transfer coefficient for single-phase flow only	W/m <sup>2</sup> /K
$K_{bo}$	Heat exchange coefficient for vaporization	W/m <sup>2</sup> /K
$K_{ev}$	Heat exchange coefficient for the vapor fraction	W/m <sup>2</sup> /K
$K_{ev(85^+)}$	Heat exchange coefficient for the vapor fraction $x > 85\%$	W/m <sup>2</sup> /K
$L$	Tube length	m
$M$	Water molar mass	kg/kmol
$\dot{m}$	Fluid mass flow rate	kg/s
$\dot{m}_c$	Cold fluid mass flow rate	kg/s
$\dot{m}_h$	Hot fluid mass flow rate	kg/s
$\dot{m}_{i:i+1}$	Mass flow rate crossing the boundary between cells $i$ and $i + 1$ , oriented positively from $i$ to $i + 1$	kg/s
$N$	Number of tubes	—
$Nu$	Nusselt number	—
$P_c$	Critical point pressure	Pa
$P_i$	Fluid pressure in cell $i$	Pa

(continued)

(continued)

$P_{i:i+1}$	Pressure at the boundary between cells $i$ and $i + 1$	Pa
$P_{\text{red}}$	Reduced pressure	—
$P_{\text{sat}}$	Pressure on the saturation line	Pa
$Pr$	Prandtl number	—
$Pr_l$	Prandtl number of the liquid phase	—
$Pr_v$	Prandtl number of the vapor phase	—
$Re$	Reynolds number	—
$Re_l$	Reynolds number of the liquid phase	—
$Re_v$	Reynolds number of the vapor phase	—
$r_i$	Internal radius of the pipes	m
$r_o$	External radius of the pipes	m
$S$	Dimensionless corrective term	—
$T$	Fluid temperature	K
$T_c$	Cold fluid temperature	K
$T_{c,i}$	Cold fluid temperature at the inlet	K
$T_{c,o}$	Cold fluid temperature at the outlet	K
$T_h$	Hot fluid temperature	K
$T_{h,i}$	Hot fluid temperature at the inlet	K
$T_{h,o}$	Hot fluid temperature at the outlet	K
$T_i$	Fluid temperature in cell $i$	K
$T_{\text{sat}}$	Saturation temperature of the fluid	K
$T_w$	Wall temperature	K
$T_{w,i}$	Wall temperature in cell $i$	K
$T_{w1}$	Internal wall temperature of the pipe	K
$T_{w2}$	External wall temperature of the pipe	K
$U$	Internal overall heat exchange coefficient for two fluids separated by a plane wall	W/m <sup>2</sup> /K
$U_i$	Internal overall heat exchange coefficient for two fluids separated by a cylindrical wall	W/m <sup>2</sup> /K
$U_o$	External overall heat exchange coefficient for two fluids separated by a cylindrical wall	W/m <sup>2</sup> /K
$u_i$	Specific internal energy in cell $i$	J/kg
$V_i$	Fluid volume of cell $i$	m <sup>3</sup>
$V_{w,i}$	Wall volume of cell $i$	m <sup>3</sup>
$W$	Heat exchange power	W
$W_r$	Real heat exchange power	W
$W_{\max}$	Maximum power exchangeable	W
$x$	Vapor mass fraction	—
$X_{lt}$	Lockhart–Martinelli number	—
$z_i$	Altitude of cell $i$	m

(continued)

(continued)

$\Delta A_i$	Internal or external heat exchange surface for cell $i$	$\text{m}^2$
$(\Delta P)_{ii+1}^a$	Advection pressure loss crossing the boundary between cells $i$ and $i + 1$	Pa
$(\Delta P)_{ii+1}^g$	Gravity pressure loss crossing the boundary between cells $i$ and $i + 1$	Pa
$(\Delta P)_{ii+1}^f$	Friction pressure loss crossing the boundary between the cells $i$ and $i + 1$	Pa
$\Delta S_i$	Heat exchange area for cell $i$	$\text{m}^2$
$\Delta T_m$	Mean value of the temperature difference	K
$\Delta W_i$	Thermal power received by fluid 1 or 2 from the wall for cell $i$	W
$\Delta W_{1,i}$	Thermal power received by fluid 1 from the wall for cell $i$	W
$\Delta W_{2,i}$	Thermal power received by fluid 2 from the wall for cell $i$	W
$\Delta x_{i:i+1}$	Tube segment length between the centers of cells $i$ and $i + 1$	m
$\varepsilon$	Exchanger effectiveness	—
$\lambda$	Metal thermal conductivity	W/m/K
$\lambda_c$	Cold fluid thermal conductivity	W/m/K
$\lambda_f$	Fluid thermal conductivity	W/m/K
$\lambda_l$	Thermal conductivity of the liquid phase	W/m/K
$\lambda_v$	Thermal conductivity of the vapor phase	W/m/K
$\mu$	Fluid dynamic viscosity	kg/m/s
$\mu_c$	Cold fluid dynamic viscosity	kg/m/s
$\mu_l$	Dynamic viscosity of the liquid phase	kg/m/s
$\mu_v$	Dynamic viscosity of the vapor phase	kg/m/s
$\rho_l$	Density of the liquid phase	kg/m <sup>3</sup>
$\rho_i$	Fluid density in cell $i$	kg/m <sup>3</sup>
$\rho_{i:i+1}$	Fluid density at the boundary between cells $i$ and $i + 1$	kg/m <sup>3</sup>
$\rho_v$	Density of the vapor phase	kg/m <sup>3</sup>
$\rho_w$	Metal wall density	kg/m <sup>3</sup>
$\rho_{w,i}$	Metal wall density in cell $i$	kg/m <sup>3</sup>
$\varphi_w$	Heat flux through the wall	W/m <sup>2</sup>
$\Phi$	Corrective factor of Lockhart–Martinelli	—

### 9.2.2 Assumptions

The following assumptions are used when describing the different analysis methods in the sequel:

- Steady-state conditions;
- No zero flow;
- Adiabatic conditions (no heat is exchanged with the environment);
- Constant specific heat (i.e., temperature and pressure independent);
- Constant mass flow rates for both fluids across the heat exchanger tubes;
- Constant overall heat transfer coefficient  $U$  across the heat exchanger;
- Negligible axial conduction along the tubes.

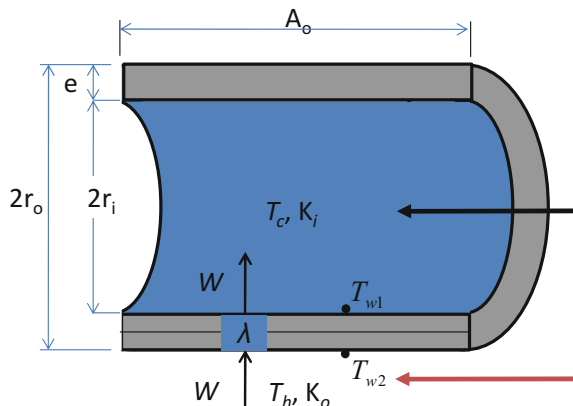
When describing the methods, it is assumed that neither the hot nor the cold fluids undergo phase transitions. However, it will be shown in a subsequent paragraph how the methods can be adapted to take into account phase transitions.

### 9.2.3 Overall Heat Transfer Coefficient

In all heat exchangers, the two fluids are separated by a solid wall; cf. Fig. 9.3. Heat transfer takes place by conduction through the wall, and by convection between each fluid and the wall. Radiation must be accounted for if there are significant temperature gradients between the fluid and the wall. In many practical cases, it is possible to neglect this phenomenon as temperature gradients are small enough.

The overall heat transfer coefficient is one of the most important parameters for the design and the analysis of heat exchanger performance. It is defined as the total heat exchanger thermal resistance.

**Fig. 9.3** Parallel-flow heat exchanger



Overall heat transfer coefficient for a plane wall:

$$U = \frac{1}{\frac{1}{K_i} + \frac{L}{\lambda} + \frac{1}{K_o}} \quad (9.1)$$

Overall heat transfer coefficient for the inner wall of a cylinder:

$$U_i = \frac{1}{\frac{1}{K_i} + \frac{r_i}{\lambda} \cdot \ln\left(\frac{r_o}{r_i}\right) + \left(\frac{r_i}{r_o}\right) \cdot \frac{1}{K_o}} \quad (9.2)$$

Overall heat transfer coefficient for the outer wall of a cylinder:

$$U_o = \frac{1}{\frac{1}{K_o} + \frac{r_o}{\lambda} \cdot \ln\left(\frac{r_o}{r_i}\right) + \left(\frac{r_o}{r_i}\right) \cdot \frac{1}{K_i}} \quad (9.3)$$

The coefficients (9.2) and (9.3) are related by the following constraint:

$$U_i \cdot A_i = U_o \cdot A_o \quad (9.4)$$

It should be noted that these equations are only valid for clean surfaces. The effect of fouling can be taken into account by introducing an additional thermal resistance term in  $U_i$  or  $U_o$ .

#### 9.2.4 Convective Heat Transfer Coefficient

Heat energy transferred between a solid surface (wall) and a moving fluid at different temperatures is known as convection. The movement of the fluid can be natural or forced. Movement due solely to differences in fluid temperature is called natural convection. When it is obtained by the action of a pump or a fan, it is called forced convection.

The convective heat transfer coefficient  $K_i$  is used in thermodynamics to calculate the heat transfer typically occurring by convection. It is defined according to Newton's law of cooling as:

$$W = K_i \cdot A \cdot (T_{w1} - T) \quad (9.5)$$

Convective heat transfer coefficient correlations are typically expressed in terms of dimensionless numbers. The dimensionless numbers used for forced convection are the Nusselt number  $Nu$ , the Reynolds number  $Re$ , and the Prandtl number  $Pr$ .

The convective heat transfer coefficient is related to the Nusselt number by:

$$Nu = \frac{K_i \cdot D_i}{\lambda} \quad (9.6)$$

The Nusselt number is usually formulated in terms of two dimensionless numbers as:

$$Nu = C \cdot Re^n \cdot Pr^m \quad (9.7)$$

with

$$Re = \frac{4 \cdot \dot{m}}{\pi \cdot D_i \cdot \mu} \quad (9.8)$$

$$Pr = \frac{c_p \cdot \mu}{\lambda} \quad (9.9)$$

The constants  $C$ ,  $n$ , and  $m$  are in general functions of the flow conditions and geometry. Therefore, the value of  $K_i$  is governed by operating parameters (geometrical shape of the pipes or wall, mass flow rate, pressure, and temperature) as well as physical properties of the fluid (density, specific heat, viscosity, and thermal conductivity).

Many correlations were developed by various authors to estimate the convective heat transfer coefficient in various cases: single-phase flow, two-phase flow, internal flow, external flow. They are presented in the sequel.

#### 9.2.4.1 General Correlations for Saturated Two-Phase Flow Boiling Heat Transfer Inside Horizontal and Vertical Tubes

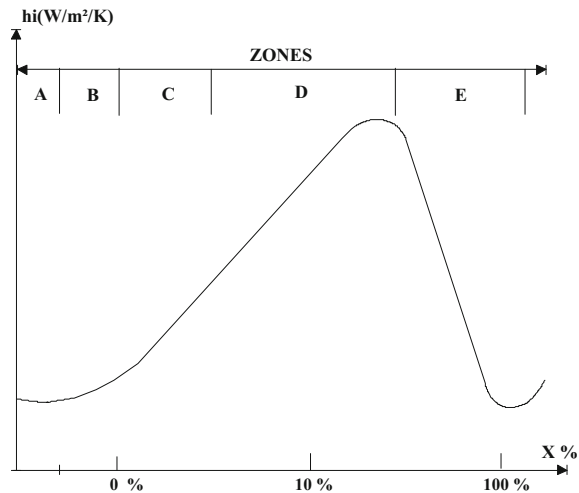
A large number of correlations have been proposed for flow boiling. In general, it is difficult to find the correlations adapted to the problem at hand.

For saturated boiling, several authors have proposed the following method to estimate the convective heat transfer coefficient (Gungor and Winterton 1986; CEA-GRETh 1997; Chen 1966).

Several distinct boiling mechanisms are considered; cf. Fig. 9.4:

- A. Natural convection: single-phase liquid flow, no boiling.
- B. Nucleate boiling: Vapor bubbles appear on the wall surface and are released into the liquid. The temperature of the core of the fluid is still under the saturation temperature.
- C. Transition to fully developed nucleate boiling: Small bubbles merge into large bubbles.
- D. Fully developed nucleate boiling.
- E. Drying of the wall: The wall is gradually insulated by steam. That may eventually lead to the melting of the wall if the wall melting point is reached.

**Fig. 9.4** Evolution of the heat transfer coefficient with the vapor mass fraction



### Dittus–Boelter Correlation

For single-phase flow in smooth straight pipes (regime **A**), one can use for  $K_i$  in (9.5) the Dittus–Boelter correlation, valid for  $10^4 < Re_l < 1.5 \times 10^5$ ,  $0.7 < Pr_l < 120$  and  $L/D_i > 60$ :

$$K_1 = 0.023 \cdot (\lambda_i/D_i) \cdot Re_l^{0.8} \cdot Pr_l^{0.4} \quad (9.10)$$

### Gungor–Chen Correlations

For regimes **B** to **D**, one can use for  $K_i$  in (9.5) the Gungor–Chen correlations (Gungor and Winterton 1986; CEA-GRETh 1997; Chen 1966) for evaporation.

The basic form of the correlation is:

$$K_{ev} = E \cdot K_1 + S \cdot K_{bo} \quad (9.11)$$

The heat transfer coefficient due to boiling is:

$$K_{bo} = 55 \cdot P_{red}^{0.12} (-\log_{10} P_{red})^{-0.55} M^{-0.5} \cdot \varphi_w^{0.67} \quad (9.12)$$

$\varphi_w$  is the heat flux through the wall:  $\varphi_w = W/A_w$ .

$E$  and  $S$  are dimensionless corrective terms:

$$E = 1 + 24000 \cdot \text{Bo}^{1.16} + 1.37 \cdot \left( \frac{1}{X_{tt}} \right)^{0.86} \quad (9.13)$$

$$S = \frac{1}{1 + 1.15 \times 10^{-6} \cdot E^2 \cdot Re_1^{1.17}} \quad (9.14)$$

and the other quantities are given by

$$\text{Bo} = \frac{\varphi_w}{h_{fg} \cdot G} \quad (9.15)$$

$$X_{tt} = \left( \frac{1-x}{x} \right)^{0.9} \cdot \left( \frac{\rho_v}{\rho_l} \right)^{0.5} \cdot \left( \frac{\mu_l}{\mu_v} \right)^{0.1} \quad (9.16)$$

$$P_{\text{red}} = \frac{P_{\text{sat}}}{P_c} \quad (9.17)$$

$$Re_l = \frac{G \cdot D_i \cdot (1-x)}{\mu_l} \quad (9.18a)$$

$$Re_v = \frac{G \cdot D_i \cdot x}{\mu_v} \quad (9.18b)$$

$$Pr_l = \frac{\mu_l \cdot c_{p,l}}{\lambda_l} \quad (9.19a)$$

$$Pr_v = \frac{\mu_v \cdot c_{p,v}}{\lambda_v} \quad (9.19b)$$

with  $G$  being the surface mass flow rate defined by  $G = \dot{m}/A$ ,  $\dot{m}$  being the mass flow rate through the pipe, and  $A$  being the pipe cross-sectional area.

### CEA-GRETh Correlation

For regime E ( $x > 0.85$ ), one can use for  $K_i$  in (9.5) the following correlation (CEA-GRETh 1997), whose basic form is:

$$K_{ev(85^+)} = K_{ev(85)} \cdot (1-x)/0.15 + K_{ev} \cdot (x-0.85)/0.15 \quad (9.20)$$

$K_{ev(85)}$  is the heat transfer coefficient due to boiling, calculated by the Gungor-Chen correlations at  $x = 0.85$ .

$K_{ev}$  is given by:

$$K_{ev} = 0.023 \cdot (\lambda_v/D_i) \cdot Re_v^{0.8} \cdot Pr_v^{0.4} \quad (9.21)$$

### Jens and Lottes Correlation

The heat transfer coefficient  $K_i$  in (9.5) for regimes **B** to **E** can be expressed as (Jens and Lottes 1951):

$$K_{ev} = 57.59 \cdot e^{(10^{-5} \cdot P_i / 15.5)} \cdot (T_w - T_{sat})^3 \quad (9.22)$$

valid for  $7 \times 10^5 < P_i < 172 \times 10^5$  Pa,  $388 < T_i < 613$  K,  $11 < G < 10,500$  kg/m<sup>2</sup>/s, and  $0 < \varphi < 12.5 \times 10^6$  W/m<sup>2</sup>.  $\varphi$  is the heat flux at the wall. The upper limit on  $\varphi$  comes from the fact that this correlation is not valid for the boiling crisis.

### Thom Correlation

The heat transfer coefficient for  $K_i$  in (9.5) for regimes **A** and **B** can be expressed as (Thom et al. 1965):

$$K_{ev} = 1970 \cdot e^{(10^{-5} \cdot P_i / 43.5)} \cdot (T_w - T_{sat}) \quad (9.23)$$

valid for  $51.7 \times 10^5 < P_i < 138 \times 10^5$  Pa,  $275.16 < T_{sat} - T_i < 353.16$  K,  $1040 < G < 3800$  kg/m<sup>2</sup>/s, and  $0 < \varphi < 12.5 \times 10^6$  W/m<sup>2</sup>.  $\varphi$  is the heat flux at the wall. The upper limit on  $\varphi$  comes from the fact that this correlation is not valid for the boiling crisis.

#### 9.2.4.2 General Correlations for Heat Transfer During Condensation

Condensation is the physical transformation by which vapor is converted into liquid. Condensation occurs when the vapor temperature drops below the saturation temperature. Because of the large internal energy difference between liquid and vapor, a significant amount of heat is released during condensation.

Condensation may occur in two possible ways depending on the condition of the surface: (1) film condensation that occurs when the condensate completely wets the surface in the form of a continuous liquid film, and (2) dropwise condensation that occurs under the action of gravity where the condensate flows continuously from the surface. The two phenomena do not occur simultaneously, but one after the other.

## Film Condensation on the Outer Surface of Horizontal Tubes and Tube Banks

The heat transfer coefficient due to condensation can be computed using the Nusselt theory (Nusselt 1916). For a vertical tier of  $N$  horizontal tubes, the average convection coefficient (Nusselt correlation) can be expressed as a factor (Incropera et al. 2006):

$$K_{\text{cond}} = 0.729 \cdot \left[ \frac{k_l^3 \cdot g \cdot \rho_l \cdot (\rho_l - \rho_v) \cdot h_{fg}}{\mu_l \cdot (T_{\text{sat}} - T_w) \cdot N \cdot D_e} \right]^{0.25} \quad (9.24)$$

### Film Condensation Inside Horizontal Tubes

The heat transfer coefficient can be expressed as (Chato 1962):

$$K_{\text{cond}} = 0.555 \cdot \left[ \frac{k_l^3 \cdot g \cdot \rho_l \cdot (\rho_l - \rho_v) \cdot h'_{fg}}{\mu_l \cdot (T_{\text{sat}} - T_w) \cdot D_i} \right]^{0.25} \quad (9.25)$$

$$h'_{fg} = h_{fg} + \frac{3}{8} \cdot c_{pl} \cdot (T_{\text{sat}} - T_w) \quad (9.26)$$

### Film Condensation Inside Horizontal, Vertical, and Inclined Tubes

The heat transfer coefficient can be expressed as (Shah 1979):

$$K_{\text{cond}} = 0.023 \cdot (\lambda_l/D) \cdot Re_l^{0.8} \cdot Pr_l^{0.4} \cdot \left[ (1-x)^{0.8} + \frac{3.8 \cdot x^{0.76} (1-x)^{0.04}}{P_{\text{red}}^{0.38}} \right] \quad (9.27)$$

valid for  $350 < Re_l < 63 \times 10^3$ ,  $0.002 < P_{\text{red}} < 0.44$ ,  $1 < Pr_l < 13$ ,  $7 \times 10^{-3} < D < 40 \times 10^{-3}$  m,  $294 < T_{\text{sat}} < 583$  K,  $3 < v_v < 300$  m/s,  $11 < G < 211$  kg/s/m<sup>2</sup>, and  $158 < \varphi < 1893 \times 10^3$  W/m<sup>2</sup>.  $v_v$  is the vapor velocity.  $D$  is the tube diameter.

#### 9.2.4.3 General Correlations for Heat Transfer Outside Tubes

For external flow involving fluid motion in a direction normal to the axis of a cylinder, the heat transfer coefficient can be expressed as (Hilpert 1933), for  $Pr \geq 0.7$ :

$$K_o = C \cdot (\lambda_f/D_e) \cdot Re^m \cdot Pr^{1/3} \quad (9.28)$$

The values of  $C$  and  $m$  depend on the Reynolds number as follows:

$$\begin{aligned} 0.4 < Re < 4 &\Rightarrow C = 0.989 \quad \text{and} \quad m = 0.330 \\ 4 < Re < 40 &\Rightarrow C = 0.911 \quad \text{and} \quad m = 0.385 \\ 40 < Re < 4000 &\Rightarrow C = 0.683 \quad \text{and} \quad m = 0.466 \\ 4000 < Re < 40,000 &\Rightarrow C = 0.193 \quad \text{and} \quad m = 0.618 \\ 40,000 < Re < 400,000 &\Rightarrow C = 0.027 \quad \text{and} \quad m = 0.805 \end{aligned}$$

### 9.2.5 The Log Mean Temperature Difference Method (LMTD)

#### 9.2.5.1 Principle of the Method

To design or to predict the performance of a heat exchanger, it is essential to have expressions that relate the total heat transfer rate to quantities such as the inlet and outlet fluid temperatures, the overall heat transfer coefficient, and the total surface area for heat transfer.

The LMTD method computes the exchanged thermal power between the hot and cold fluids using the following formula:

$$W = U \cdot A \cdot \Delta T_m \quad (9.29)$$

where  $\Delta T_m$  is the mean value of the temperature difference as defined by LMTD; cf. (9.41).

#### 9.2.5.2 Parallel-Flow Heat Exchangers

In a parallel-flow heat exchanger, the hot and cold fluids enter at the same end. The temperature distributions for the hot and cold fluids are shown in Fig. 9.5.

The thermal power released by the hot fluid across surface area  $dA$  is:

$$dW_h = -\dot{m}_h \cdot c_{p,h} \cdot dT_h \quad (9.30)$$

The thermal power received by the cold fluid across surface area  $dA$  is:

$$dW_c = \dot{m}_c \cdot c_{p,c} \cdot dT_c \quad (9.31)$$

The thermal power exchanged through the wall across surface area  $dA$  is given by:

$$dW = U \cdot dA \cdot (T_h - T_c) \quad (9.32)$$

As losses to the environment are assumed to be negligible:

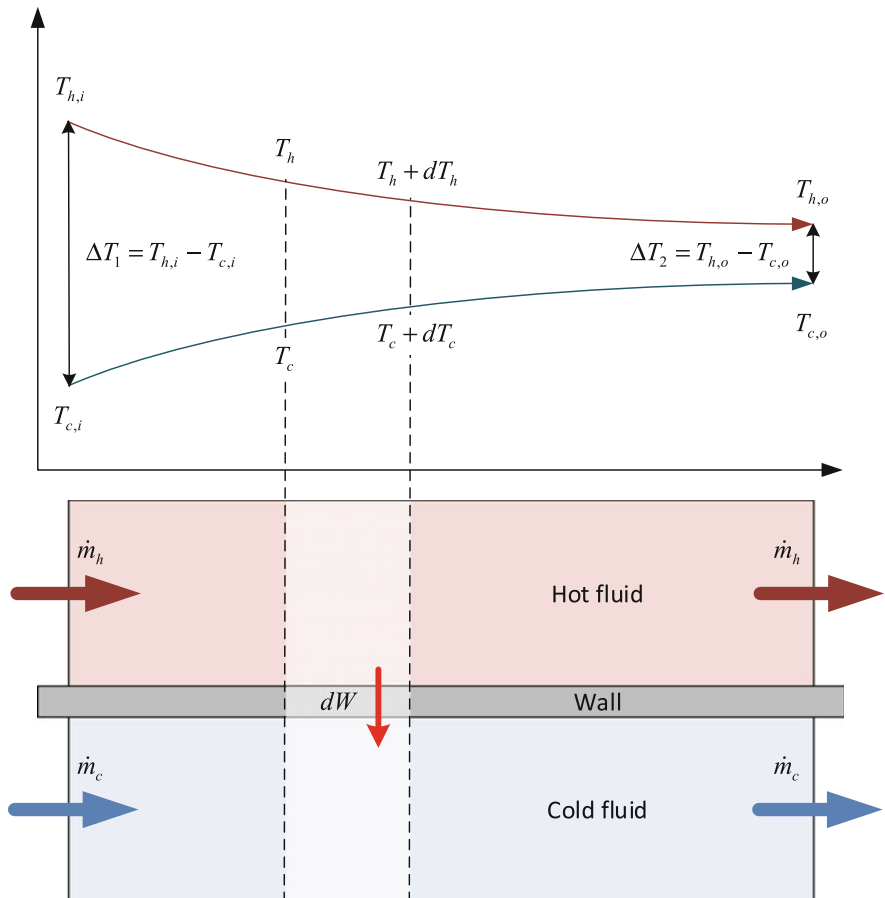


**Fig. 9.5** Temperature distribution for a parallel-flow heat exchanger

$$dW_h = dW_c = dW \quad (9.33)$$

Assuming constant mass flow rates and heat capacities between the inlet and the outlet, from (9.30) to (9.32) it follows that the total thermal power exchanged between the hot and cold fluids is:

$$W = \int_i^o dW = \dot{m}_h \cdot c_{p,h} \cdot (T_{h,i} - T_{h,o}) = \dot{m}_c \cdot c_{p,c} \cdot (T_{c,o} - T_{c,i}) \quad (9.34)$$

The relative magnitudes of the heat capacity rates of the hot and cold fluids determine the maximum amount of heat that can be transferred by a given heat exchanger.

From (9.30) to (9.33), it follows that:

$$dT_h - dT_c = d(T_h - T_c) = -dW \cdot \left( \frac{1}{\dot{m}_h \cdot c_{p,h}} + \frac{1}{\dot{m}_c \cdot c_{p,c}} \right) \quad (9.35)$$

In (9.35), substituting  $dW$  by (9.32) and integrating (9.35) over the whole exchanger length yields (as the mass flow rates and the specific heat capacities are assumed to be constant over the exchanger length; cf. Sect. 9.2.2):

$$\int_i^o \frac{d(T_h - T_c)}{T_h - T_c} = -U \cdot \left( \frac{1}{\dot{m}_h \cdot c_{p,h}} + \frac{1}{\dot{m}_c \cdot c_{p,c}} \right) \cdot \int_i^o dA \quad (9.36)$$

Equation (9.36) is valid if  $T_h > T_c$ ,  $\dot{m}_h \neq 0$  and  $\dot{m}_c \neq 0$ .

Hence,

$$\ln \left| \frac{(T_h - T_c)_o}{(T_h - T_c)_i} \right| = -U \cdot A \cdot \left( \frac{1}{\dot{m}_h \cdot c_{p,h}} + \frac{1}{\dot{m}_c \cdot c_{p,c}} \right) \quad (9.37)$$

This equation shows that the LMTD method is not valid when either the cold or the hot fluid mass flow rate is zero, or if the temperature of the cold fluid is equal to the temperature of the hot fluid.

Using (9.34) in (9.37) yields:

$$\ln \left| \frac{T_{h,o} - T_{c,o}}{T_{h,i} - T_{c,i}} \right| = -\frac{U \cdot A}{W} \cdot [(T_{h,i} - T_{c,i}) - (T_{h,o} - T_{c,o})] \quad (9.38)$$

Denoting  $\Delta T_1 = T_{h,i} - T_{c,i}$  and  $\Delta T_2 = T_{h,o} - T_{c,o}$ , (9.38) writes:

$$W = U \cdot A \cdot \frac{\Delta T_2 - \Delta T_1}{\ln \left| \frac{\Delta T_2}{\Delta T_1} \right|} \quad (9.39)$$

$\Delta T_2$  is always positive because  $T_{c,o}$  is always smaller than  $T_{h,o}$  (temperature crossing is impossible in a heat exchanger due to the second principle of thermodynamics). Also, unless the two fluids are at the same temperature,  $\Delta T_1$  is always larger than zero. Thus, the term  $|\Delta T_2/\Delta T_1|$  can be replaced by  $\Delta T_2/\Delta T_1$  in (9.39).

Comparing (9.39) with (9.29) yields:

$$\Delta T_m = \frac{\Delta T_2 - \Delta T_1}{\ln \left( \frac{\Delta T_2}{\Delta T_1} \right)} = \frac{\Delta T_1 - \Delta T_2}{\ln \left( \frac{\Delta T_1}{\Delta T_2} \right)} \quad (9.40)$$

Equation (9.40) is known as the log mean temperature difference method and is valid provided the two fluids are not at the same temperature and that the mass flow rate of each fluid is not zero.

### 9.2.5.3 Counter-Flow Heat Exchangers

In this paragraph, it is assumed that neither the hot fluid nor the cold fluid undergoes a phase transition.

In the counter-flow heat exchanger shown in Fig. 9.6, the fluids enter at opposite ends, flow in opposite directions, and exit at opposite ends. Note that the outlet temperature of the cold fluid may exceed the outlet temperature of the hot fluid.

The heat exchanged across surface area  $dA$  can also be expressed using Eqs. (9.30)–(9.32).

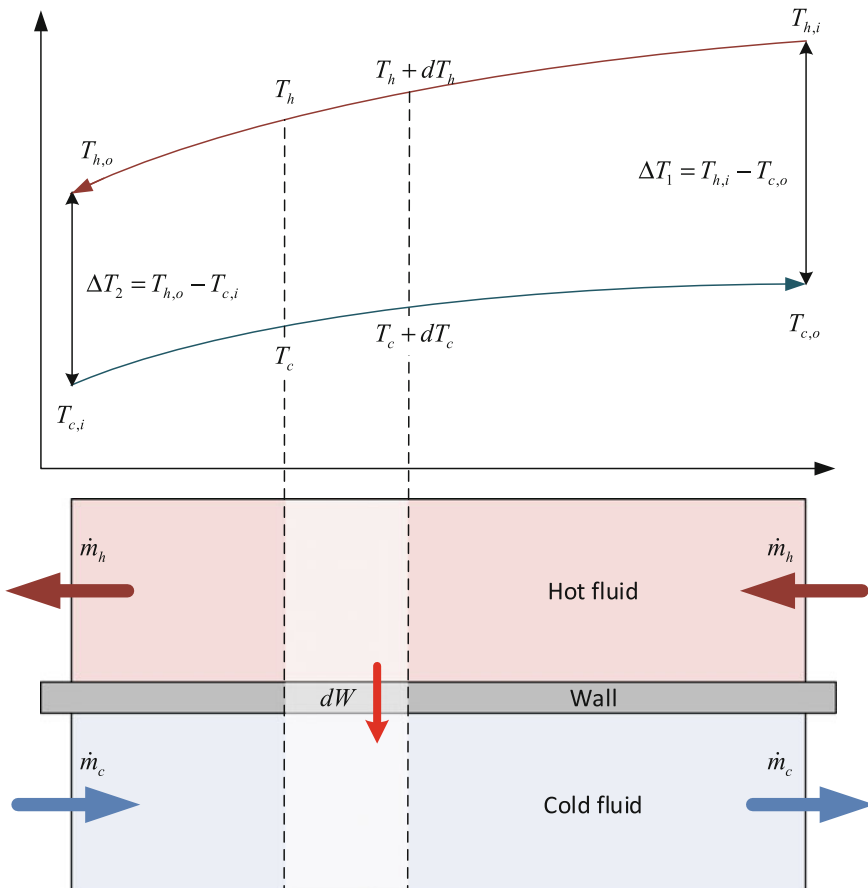


**Fig. 9.6** Temperature distribution for a counter-flow heat exchanger

Using a derivation similar to the case of a parallel-flow heat exchanger (i.e., by swapping  $T_{c,i}$  with  $T_{c,o}$  in Sect. 9.2.5.2), the formula that gives the mean temperature difference for a counter-flow heat exchanger is:

$$\Delta T_m = \frac{\Delta T_1 - \Delta T_2}{\ln\left(\frac{\Delta T_1}{\Delta T_2}\right)} \quad (9.41)$$

with  $\Delta T_1 = T_{h,i} - T_{c,o}$  and  $\Delta T_2 = T_{h,o} - T_{c,i}$ .

Therefore, the LMTD formula for counter-flow heat exchangers is the same as for parallel-flow heat exchangers, provided that the correct definitions of  $\Delta T_1$  and  $\Delta T_2$  are used for each type of heat exchanger. The method is valid provided the two fluids are not at the same temperature and that the mass flow rate of each fluid is not zero.

#### 9.2.5.4 Cross-flow Heat Exchangers

For cross-flow heat exchangers, the LMTD method can be used with a corrective factor (Incropera et al. 2006):

$$\Delta T_{lm} = F \cdot \Delta T_m \text{ for counter-flow} \quad (9.42)$$

$F$  is the correction factor, and  $\Delta T_m$  is computed under counter-flow conditions.

#### 9.2.6 *The Effectiveness and the Number of Transfer Units Method (NTU)*

##### 9.2.6.1 Definitions

LMTD requires an iterative procedure to compute the outlet temperatures for each fluid and the power exchanged between the two fluids. However, this method needs as inputs the fluid temperature at the inlets, the overall heat exchange coefficient, and the heat exchange surface, which therefore should be known.

The concept of the number of transfer units was first suggested by Nusselt and developed extensively by Kays and London (1964). The product  $U \cdot A$  is transformed to a dimensionless quantity by being divided with  $\dot{m} \cdot c_p$  yielding a number which represents the heat transfer capacity of the exchanger. The number of transfer units (NTU) is defined as the ratio of  $U \cdot A$  to the smallest of the two quantities  $\dot{m}_h \cdot c_{p,h}$  and  $\dot{m}_c \cdot c_{p,c}$ :

$$\text{NTU} = \frac{U \cdot A}{(\dot{m} \cdot c_p)_{\min}} \quad (9.43)$$

with  $(\dot{m} \cdot c_p)_{\min} = \min(\dot{m}_h \cdot c_{p,h}, \dot{m}_c \cdot c_{p,c})$ .

The effectiveness  $\varepsilon$  of a heat exchanger is the ratio of the actual heat transferred to the maximum heat that could be transferred in a counter-flow heat exchanger of infinite length:

$$\varepsilon = \frac{W}{W_{\max}} \quad (9.44)$$

The capacity ratio  $C_R$  is defined as:

$$C_R = \frac{(\dot{m} \cdot c_p)_{\min}}{(\dot{m} \cdot c_p)_{\max}} \quad (9.45)$$

with  $(\dot{m} \cdot c_p)_{\max} = \max(\dot{m}_h \cdot c_{p,h}, \dot{m}_c \cdot c_{p,c})$ .

The maximum heat transfer  $W_{\max}$  between the hot and cold fluids corresponds to the two possible limiting situations when the cold fluid is heated to the temperature of the hot fluid (i.e., when  $T_{c,o} = T_{h,i}$ ) or when the hot fluid is cooled to the temperature of the cold fluid (i.e., when  $T_{h,o} = T_{c,i}$ ); cf. Fig. 9.6.

When  $T_{c,o} = T_{h,i}$ , it follows from (9.34) that  $W_{\max} = \dot{m}_h \cdot c_{p,h} \cdot (T_{h,i} - T_{h,o}) = \dot{m}_c \cdot c_{p,c} \cdot (T_{h,i} - T_{c,i})$ . As  $T_{h,o} > T_{c,i}$ , then  $T_{h,i} - T_{h,o} < T_{h,i} - T_{c,i}$  and consequently  $\dot{m}_c \cdot c_{p,c} < \dot{m}_h \cdot c_{p,h}$ .

When  $T_{h,o} = T_{c,i}$ , a similar derivation leads to  $W_{\max} = \dot{m}_h \cdot c_{p,h} \cdot (T_{h,i} - T_{c,i})$  with  $\dot{m}_h \cdot c_{p,h} < \dot{m}_c \cdot c_{p,c}$ .

Hence, in both cases:

$$W_{\max} = (\dot{m} \cdot c_p)_{\min} \cdot (T_{h,i} - T_{c,i}) \quad (9.46)$$

From (9.44) and (9.46), it follows that:

$$W = \varepsilon \cdot (\dot{m} \cdot c_p)_{\min} \cdot (T_{h,i} - T_{c,i}) \quad (9.47)$$

### 9.2.6.2 Parallel-Flow Heat Exchangers

We consider the case where  $W_{\max}$  corresponds to  $\dot{m}_h \cdot c_{p,h} < \dot{m}_c \cdot c_{p,c}$ .

Then, using (9.43):

$$\text{NTU} = \frac{U \cdot A}{\dot{m}_h \cdot c_{p,h}} \quad (9.48)$$

From (9.45) and (9.34):

$$C_R = \frac{\dot{m}_h \cdot c_{p,h}}{\dot{m}_c \cdot c_{p,c}} = \frac{T_{c,o} - T_{c,i}}{T_{h,i} - T_{h,o}} \quad (9.49)$$

From (9.34) and (9.47):

$$\varepsilon = \frac{T_{h,i} - T_{h,o}}{T_{h,i} - T_{c,i}} \quad (9.50)$$

From (9.37) and (9.49), it follows that:

$$\ln \left| \frac{(T_h - T_c)_o}{(T_h - T_c)_i} \right| = - \frac{U \cdot A}{\dot{m}_h \cdot c_{p,h}} \cdot (1 + C_R) \quad (9.51)$$

From (9.48) and (9.51), it follows that:

$$\frac{T_{h,o} - T_{c,o}}{T_{h,i} - T_{c,i}} = e^{-NTU \cdot (1 + C_R)} \quad (9.52)$$

Rearranging the left-hand side of (9.52) and using (9.49) and (9.50), it follows that

$$\begin{aligned} \frac{T_{h,o} - T_{c,o}}{T_{h,i} - T_{c,i}} &= \frac{(T_{h,o} - T_{h,i}) + (T_{h,i} - T_{c,i}) + (T_{c,i} - T_{c,o})}{T_{h,i} - T_{c,i}} \\ &= \frac{(T_{h,i} - T_{c,i}) - (1 + C_R) \cdot (T_{h,i} - T_{h,o})}{T_{h,i} - T_{c,i}} = 1 - \varepsilon \cdot (1 + C_R) \end{aligned} \quad (9.53)$$

Substituting (9.53) into (9.52) yields for the parallel-flow heat exchanger:

$$\varepsilon = \frac{1 - e^{-NTU \cdot (1 + C_R)}}{1 + C_R} \quad (9.54)$$

The heat exchanger efficiency is always positive and lower than unity ( $0 \leq \varepsilon \leq 1$ ).

If  $\varepsilon = 1$ , then  $T_{h,o} - T_{c,i} = 0$ , which implies that the exchange surface  $A$  is infinite.

Equations (9.48) and (9.54) show that the NTU method is not valid for zero or negative flows (NTU negative).

In practice, the NTU method is used by providing as inputs values for  $A$  and  $U$  in addition to the flow characteristics for the two fluids. Then, NTU and  $\varepsilon$  are computed using (9.48) and (9.54). Finally, the power exchanged between the two fluids is computed using (9.47). The benefit as compared to the LMTD method is that if the value of  $\varepsilon$  can be estimated, then all quantities of interest can be computed without solving implicit algebraic equations.

### 9.2.6.3 Counter-Flow Heat Exchangers

A similar derivation for a counter-flow heat exchanger gives the following expression for the heat exchanger efficiency (Incropera et al. 2006):

$$\varepsilon = \frac{1 - e^{-\text{NTU} \cdot (1 - C_R)}}{1 - C_R \cdot e^{-\text{NTU} \cdot (1 - C_R)}} \quad (9.55)$$

### 9.2.6.4 Shell-and-Tube Heat Exchangers

The heat exchanger effectiveness relations for a shell-and-tube heat exchanger can be expressed as in Incopera et al. (2006); Kays and London (1964).

For a shell-and-tube heat exchanger with one shell pass and any multiple of two-tube passes:

$$\varepsilon_1 = 2 \cdot \left[ 1 + C_R + (1 + C_R^2)^{0.5} \cdot \frac{1 + e^{-\text{NTU} \cdot (1 + C_R^2)^{0.5}}}{1 - e^{-\text{NTU} \cdot (1 + C_R^2)^{0.5}}} \right]^{-1} \quad (9.56)$$

For a shell-and-tube heat exchanger with two shell passes and any multiple of four-tube passes:

$$\varepsilon_2 = \left[ \left( \frac{1 - \varepsilon_1 \cdot C_R}{1 - \varepsilon_1} \right)^2 - 1 \right] \left[ \left( \frac{1 - \varepsilon_1 \cdot C_R}{1 - \varepsilon_1} \right)^2 - C_R \right]^{-1} \quad (9.57)$$

For a cross-flow heat exchanger with single pass and with one fluid mixed and the other unmixed:

- a. For  $(\dot{m} \cdot c_p)_{\max}$  associated with the mixed fluid:

$$\varepsilon = \frac{1 - e^{-C_R \cdot (1 - e^{-\text{NTU}})}}{C_R} \quad (9.58)$$

- b. For  $(\dot{m} \cdot c_p)_{\max}$  associated with the unmixed fluid:

$$\varepsilon = 1 - e^{-\frac{1 - e^{-C_R \cdot \text{NTU}}}{C_R}} \quad (9.59)$$

### 9.2.7 The UA Method

The UA method relies on the LMTD method.

For parallel-flow heat exchangers, from (9.37) it follows that:

$$\ln\left(\frac{\Delta T_2}{\Delta T_1}\right) = -U \cdot A \cdot \left( \frac{1}{\dot{m}_h \cdot c_{p,h}} + \frac{1}{\dot{m}_c \cdot c_{p,c}} \right) \quad (9.60)$$

$$\frac{\Delta T_2}{\Delta T_1} = e^{-U \cdot A \cdot \left( \frac{1}{\dot{m}_h \cdot c_{p,h}} + \frac{1}{\dot{m}_c \cdot c_{p,c}} \right)} \quad (9.61)$$

with  $\Delta T_1 = T_{h,i} - T_{c,i}$  and  $\Delta T_2 = T_{h,o} - T_{c,o}$ .

For counter-current heat exchangers:

$$\ln\left(\frac{\Delta T_2}{\Delta T_1}\right) = -U \cdot A \cdot \left( \frac{1}{\dot{m}_h \cdot c_{p,h}} + \frac{1}{\dot{m}_c \cdot c_{p,c}} \right) \quad (9.62)$$

$$\frac{\Delta T_2}{\Delta T_1} = e^{-U \cdot A \cdot \left( \frac{1}{\dot{m}_h \cdot c_{p,h}} + \frac{1}{\dot{m}_c \cdot c_{p,c}} \right)} \quad (9.63)$$

with  $\Delta T_1 = T_{h,i} - T_{c,o}$  and  $\Delta T_2 = T_{h,o} - T_{c,i}$

Equation (9.61) and (9.63) show that the UA method is not valid for zero flows.

For the UA method, an estimated value of the product  $U \cdot A$  is given as input. The benefit is to avoid dealing explicitly with the exact exchange and the overall heat transfer coefficients.

### 9.2.8 The Efficiency Method

The efficiency method relies on the NTU method, but to the contrary of the NTU method, the efficiency  $\varepsilon$  is assumed to be known.

The exchanged power writes, cf. (9.47):

$$W = \varepsilon \cdot (\dot{m} \cdot c_p)_{\min} \cdot (T_{h,i} - T_{c,i}) \quad (9.64)$$

This method is a simplification of the NTU method as  $\varepsilon$  is directly provided as input.

### 9.2.9 Taking into Account Phase Transitions

The heat exchanger is divided into different zones (cf. Fig. 9.7):

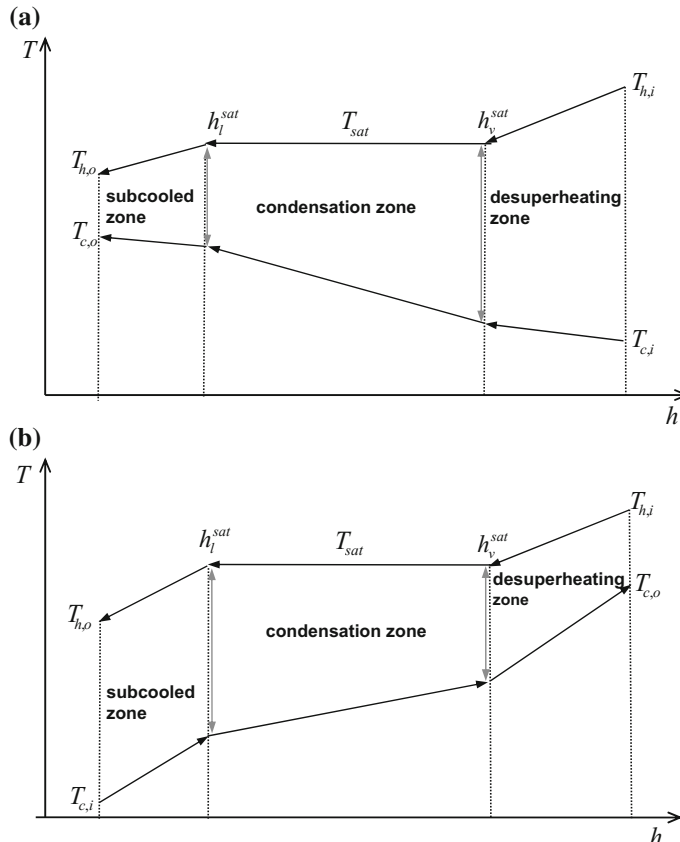


**Fig. 9.7** **a** Parallel-flow heat exchanger with three zones and **b** counter-current heat exchanger with three zones

- The zones where no phase transition takes place;
- The zones where phase transitions take place.

The different zones correspond to different fluid states:

- Subcooled zone: The fluid temperature is below the liquid saturation temperature.
- Supercooling (when the fluid temperature rises) or desuperheating (when the fluid temperature decreases) zones: The fluid temperature is above the steam saturation temperature.
- Two-phase zone: The fluid temperature is equal to the fluid saturation temperature.

Each zone has its own exchange surface and overall heat transfer coefficient.

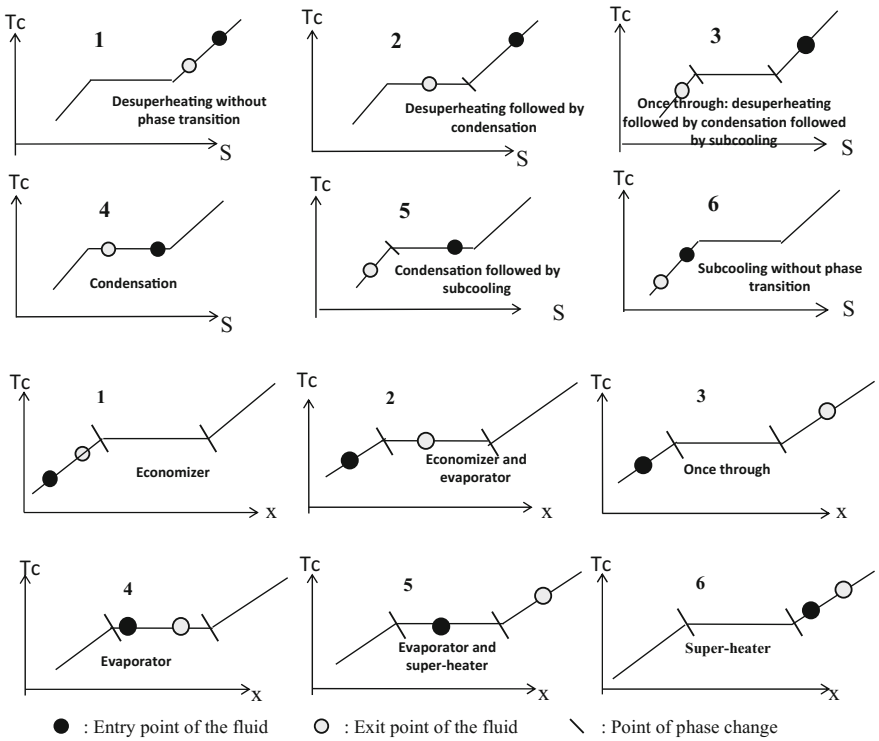


**Fig. 9.8** Phase transitions in heat exchangers

The fluid transformations in the different zones are illustrated in Fig. 9.8 on Mollier diagrams (the saturation line is not represented in these diagrams).

In case of two-phase flow, it is better to use the following equations to compute the heat exchanged power.

- If two-phase flow occurs on the hot side:

$$T_{h,i} = T_{h,o} = T_{\text{sat}} \quad (9.65)$$

$$W = \dot{m}_h \cdot (h_{h,i} - h_{h,o}) \quad (9.66)$$

- If two-phase flow occurs on the cold side:

$$T_{c,i} = T_{c,o} = T_{\text{sat}} \quad (9.67)$$

$$W = \dot{m}_c \cdot (h_{c,o} - h_{c,i}) \quad (9.68)$$

- All methods fail if two-phase flow occurs on both sides, because as the two sides are then at the same temperature, (9.41) goes to infinity for LMTD or  $c_p$  is undefined for NTU.

In addition, the LMTD or the NTU methods can be used for sizing the heat exchanger; i.e., compute the exchange surface, the mass flow rates, or the global heat transfer coefficient.

When using the NTU or the efficiency method, the value of the heat transfer capacity should be taken equal to the single-phase fluid heat transfer capacity value.

### 9.2.10 Simple Heat Exchangers

The objective of the methods presented so far is to compute the exchanged power  $W$  and the temperatures at the outlets for each fluid. In case  $W$  or one of the outlet temperatures is known, then it is sufficient to use (9.34).

## 9.3 Dynamic Heat Exchangers

The methods presented in Sect. 9.2 are subject to the assumptions of Sect. 9.2.2. To deal with situations that do not comply with these assumptions, the heat exchanger can be represented modeled as two discretized 1D fluid flows separated by a solid wall; cf. Fig. 9.9.

The following mass, energy, and momentum balance equations are written for each fluid with the assumption of cylindrical wall geometry. The cross-sectional area of each pipe is assumed to be constant and equal to  $A$ .

From (4.7) applied to cell  $i$  and its neighboring cells  $i - 1$  and  $i + 1$ , the mass balance equation writes:

$$V_i \cdot \frac{d\rho_i}{dt} = \dot{m}_{i-1:i} - \dot{m}_{i:i+1} \quad (9.69)$$

where  $\dot{m}_{i:i+1}$  is the mass flow rate crossing the boundary between cells  $i$  and  $i + 1$ , and  $V_i$  and  $\rho_i$  are respectively the volume of cell  $i$  and the fluid density in cell  $i$ .

From (4.28) applied to cell  $i$  and its neighboring cells  $i - 1$  and  $i + 1$ , and neglecting diffusion, the energy balance equation writes:

$$V_i \cdot \frac{d(\rho_i \cdot u_i)}{dt} = \dot{m}_{i-1:i} \cdot h_{i-1:i} - \dot{m}_{i:i+1} \cdot h_{i:i+1} + \Delta W_i \quad (9.70)$$

where  $h_{i:i+1}$  is the specific enthalpy of the fluid crossing the boundary between cells  $i$  and  $i + 1$ , and  $u_i$  is the fluid specific internal energy in cell  $i$ .  $\Delta W_i$  is the heat received (counted positively) or released (counted negatively) by cell  $i$  through the wall.

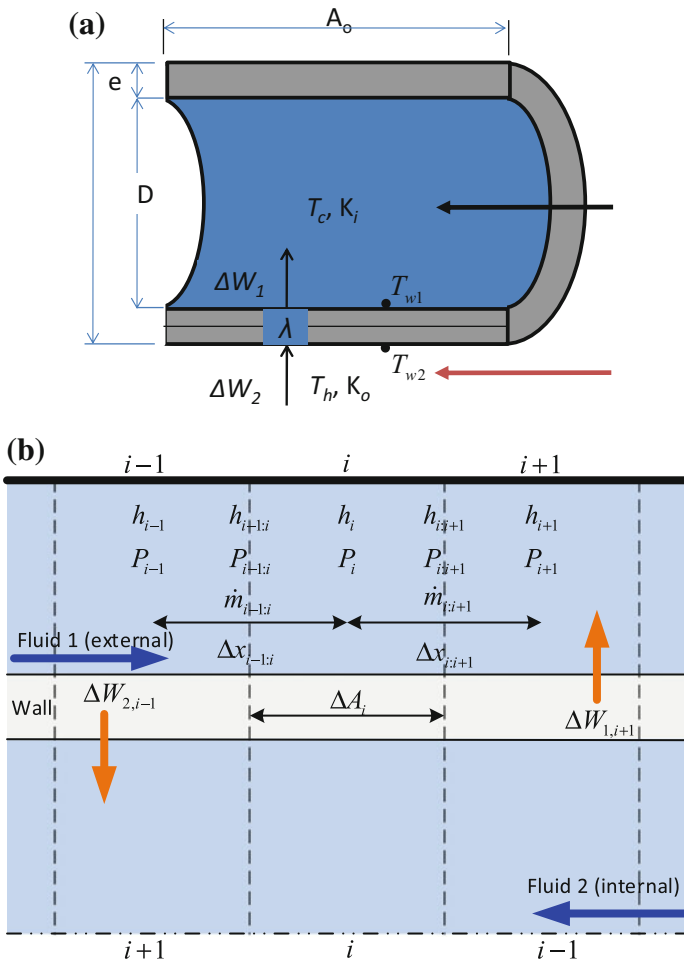


**Fig. 9.9** **a** Heat exchanger wall and **b** discretized heat exchanger (half cross section)

From (4.18) applied to neighboring cells  $i$  and  $i + 1$ , the momentum balance equation writes:

$$\frac{1}{A} \frac{d\dot{m}_{i:i+1}}{dt} \cdot \Delta x_{i:i+1} = P_i - P_{i+1} - (\Delta P)_{i:i+1}^a - (\Delta P)_{i:i+1}^f - (\Delta P)_{i:i+1}^g \quad (9.71)$$

where  $P_i$  is the fluid pressure in cell  $i$ , and  $\Delta x_{i:i+1}$  is the pipe length between the centers of cells  $i$  and  $i + 1$ .

$(\Delta P)_{i:i+1}^a$  is the advection pressure loss between cells  $i$  and  $i + 1$ :

$$(\Delta P)_{i:i+1}^a = \frac{\dot{m}_{i:i+1} \cdot |\dot{m}_{i:i+1}|}{A^2} \cdot \left( \frac{1}{\rho_{i+1}} - \frac{1}{\rho_i} \right) \quad (9.72)$$

$(\Delta P)_{i:i+1}^f$  is the friction pressure loss between cells  $i$  and  $i + 1$ :

$$(\Delta P)_{i:i+1}^f = \text{sgn}(\dot{m}_{i:i+1}) \cdot \frac{\pi_{w,i:i+1} \cdot \tau_{w,i:i+1}}{A} \quad (9.73)$$

$\pi_{w,i:i+1}$  and  $\tau_{w,i:i+1}$  are respectively the pipe wetted perimeter and friction between the centers of cells  $i$  and  $i + 1$  (cf. also Sect. 13.2.1).

$(\Delta P)_{i:i+1}^g$  is the friction pressure loss between the centers of cells  $i$  and  $i + 1$ :

$$(\Delta P)_{i:i+1}^g = \rho_{i:i+1} \cdot g \cdot (z_{i+1} - z_i) \quad (9.74)$$

where  $z_i$  is the altitude of cell  $i$  and  $g$  is the acceleration due to gravity.

The fluid density  $\rho_{i:i+1}$  at the boundary between cells  $i$  and  $i + 1$  is given by:

$$\rho_{i:i+1} = f_\rho(P_{i:i+1}, h_{i:i+1}) \quad (9.75)$$

$f_\rho$  is the state function that computes the density as a function of the pressure and the specific enthalpy.

The fluid pressure  $P_{i:i+1}$  at the boundary between cells  $i$  and  $i + 1$  is given by [cf. (4.156)]:

$$P_{i:i+1} = \frac{P_i + P_{i+1}}{2} \quad (9.76)$$

$h_{i:i+1}$  is given by the upwind scheme; cf. (4.113):

$$h_{i:i+1} = s(\dot{m}_{i:i+1}) \cdot h_i + (1 - s(\dot{m}_{i:i+1})) \cdot h_{i+1} \quad (9.77)$$

Heat exchange occurs by convection between the fluid and the wall. The heat received by each fluid from the wall is:

$$\Delta W_i = K_i \cdot \Delta A_i \cdot (T_{w,i} - T_i) \quad (9.78)$$

where  $\Delta A_i$  is the heat surface exchange between the fluid and the wall,  $K_i$  is the convective heat transfer coefficient,  $T_i$  is the fluid temperature, and  $T_{w,i}$  is the wall temperature for cell  $i$ .

The energy accumulation in the wall between fluids 1 and 2 is given by:

$$\rho_{w,i} \cdot V_{w,i} \cdot c_{p,w,i} \cdot \frac{dT_{w,i}}{dt} = -\Delta W_{1,i} - \Delta W_{2,i} \quad (9.79)$$

where  $\Delta W_{1,i}$  and  $\Delta W_{2,i}$  denote respectively the heat received by fluid 1 and fluid 2 from the wall, given by (9.78), and  $\rho_{w,i}$ ,  $c_{p,w,i}$  and  $V_{w,i}$  are respectively the wall density, specific heat capacity, and volume for cell  $i$ .

Equations (9.69) to (9.79) describe the heat exchange between the two fluids for a small segment of the exchanger and are valid for all flow conditions, including zero, reverse, or unsteady flow. It suffices to consider  $N$  such segments to represent a full heat exchanger of length  $L = \sum_1^N \Delta x_{i:i+1}$ . This method is therefore suitable for dynamic behavioral studies involving varying flow conditions. It is however more computationally demanding than the other methods presented in this chapter.

Notice that the mass and energy balance equations are centered on the cell volumes, whereas that the momentum balance equations are centered on the cell boundaries. As for  $N$  segments, there are  $N$  cell volumes and  $N + 1$  cell boundaries, there are  $N$  mass and energy balance equations for  $N + 1$  momentum balance equations, the latter being shifted by half a cell with respect to the former. This is the so-called staggered grid scheme, which is explained in further detail in Chap. 17. In the sequel, cell volumes are called thermal cells (because they carry the energy balance equations), and cell boundaries are called hydraulic cells (because they carry the momentum balance equations).

The drawback of this method as compared to the other ones introduced in this chapter is that it requires to discretize the flow and the wall into  $N$  sufficiently short segments so that the assumption of thermodynamic equilibrium is valid for each cell  $i$  and that there is no pressure wave between the centers of two neighboring cells. It is consequently inconvenient to use for system sizing as it makes inverse calculations impossible on global parameters such as heat exchanger efficiency. It also cannot be used in practice for fast transients such as water hammer as it would require to discretize the tube in a large number of small segments. For such transients, the method of characteristics can be used; cf. (Wylie and Streeter 1993).

## 9.4 Shell-and-Tube Heat Exchanger Modeling

### 9.4.1 Introduction

A shell-and-tube heat exchanger consists of a several tubes mounted inside a cylindrical shell. Two fluids exchange heat: One fluid flows over the outside of the tubes, while the second fluid flows through the tubes. The fluids can be single- or two-phase flow and can flow in a parallel or a cross-/counter-flow arrangement.

There are several shell-and-tube heat exchanger models in ThermoSysPro. Each model is decomposed into three sub-models: (1) the tube bundle, (2) the wall, and (3) the shell or the volume. Those three components are presented in this paragraph.

### 9.4.2 Tube Bundle Heat Exchanger

The tube bundle model is called *DynamicTwoPhaseFlowPipe*. This component represents a single- or two-phase fluid flowing inside the bundle (i.e., fluid 1 of Fig. 9.10a) with the heat transfer through the boundary between the fluid and the wall. Conduction inside the wall is not represented in this model. The fluid can also be subcritical or supercritical.

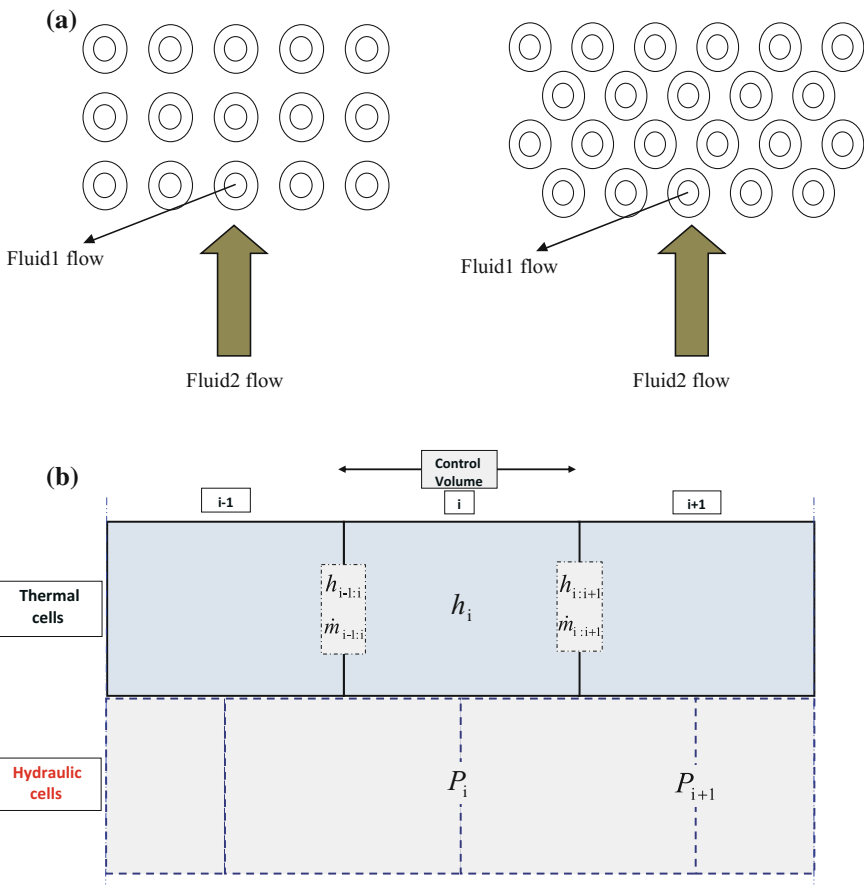


**Fig. 9.10** a Different types of tube bundle and b three sections of a 1D heat exchanger with shifted thermal and hydraulic cells

There is also a simpler version of the model called *DynamicOnePhaseFlowPipe* for single-phase flow only that differs from the two-phase flow version by the correlations utilized in the model.

#### 9.4.2.1 Nomenclature

Symbols	Definition	Unit	Mathematical definition
$A$	Internal cross section of the pipe bundle	$\text{m}^2$	$N_t \cdot \pi \cdot D^2 / 4$
$D$	Internal diameter of one pipe	$\text{m}$	
$D_t$	Sum of the internal diameter of the pipes in the bundle	$\text{m}$	$N_t \cdot D$
$h_{c,i}$	Convective heat exchange coefficient in thermal cell $i$	$\text{W}/\text{m}^2/\text{K}$	See Sect. 9.2.4
$h_i$	Fluid specific enthalpy in thermal cell $i$	$\text{J/kg}$	
$h_{i:i+1}$	Fluid specific enthalpy of the mass flow $\dot{m}_{i:i+1}$ at the boundary between thermal cells $i$ and $i + 1$ (or fluid specific enthalpy in hydraulic cell $i:i + 1$ located between thermal cells $i$ and $i + 1$ )	$\text{J/kg}$	
$L$	Pipe length	$\text{m}$	
$\dot{m}_{i:i+1}$	Mass flow rate crossing the boundary between cells $i$ and $i + 1$ (or mass flow rate in hydraulic cell $i:i + 1$ ) oriented positively from $i$ to $i + 1$	$\text{kg/s}$	
$N$	Number of hydraulic cells equal to the number of thermal cells plus one	–	
$N_t$	Number of pipes in parallel	–	
$P_i$	Fluid pressure in thermal cell $i$	$\text{Pa}$	
$T_i$	Fluid temperature in thermal cell $i$	$\text{K}$	
$T_{w,i}$	Wall temperature in thermal cell $i$	$\text{K}$	
$T_m$	Melting temperature of the metal tubes	$\text{K}$	
$u_i$	Specific internal energy in thermal cell $i$	$\text{J/kg}$	
$V_i$	Volume of thermal cell $i$	$\text{m}^3$	$A \cdot \Delta x_1$
$z_i$	Inlet altitude of hydraulic cell $i:i + 1$	$\text{m}$	
$z_{i+1}$	Outlet altitude of hydraulic cell $i:i + 1$	$\text{m}$	
$\alpha$	Corrective term for the heat exchange coefficient $h_{c,i}$ for each thermal cell	–	
$\Delta A_i$	Internal heat exchange area for thermal cell $i$	$\text{m}^2$	$\pi \cdot D \cdot \Delta x_1$
$\Delta W_i$	Thermal power exchanged in the water side for thermal cell $i$	$\text{W}$	
$\Delta x_1$	Length of a thermal cell	$\text{m}$	$L/(N - 1)$
$\Delta x_2$	Average length of a hydraulic cell	$\text{m}$	$L/N$
$(\Delta P)_{i:i+1}^a$	Advection pressure loss in hydraulic cell $i:i + 1$ when the fluid flows from $i$ to $i + 1$	$\text{Pa}$	

(continued)

(continued)

Symbols	Definition	Unit	Mathematical definition
$(\Delta P)_{ii+1}^f$	Friction pressure loss in hydraulic cell $i:i + 1$ when the fluid flows from $i$ to $i + 1$	Pa	
$(\Delta P)_{ii+1}^g$	Gravity pressure loss in hydraulic cell $i:i + 1$ when the fluid flows from $i$ to $i + 1$	Pa	
$\zeta$	Corrective term for the friction pressure loss for each cell	-	
$\Lambda_{ii+1}$	Friction pressure loss coefficient in cell $i:i + 1$	-	See Sect. 13.2
$\rho_i$	Fluid density in thermal cell $i$	kg/m <sup>3</sup>	
$\rho_{ii+1}$	Fluid density in hydraulic cell $i:i + 1$	kg/m <sup>3</sup>	
$\Phi_{lo}^2$	Lockhart and Martinelli corrective coefficient		See Sect. 13.2

#### 9.4.2.2 Assumptions

The tube bundle is modeled according to the following assumptions:

- Homogeneous fluid in each mesh cell (same velocity for the liquid and steam phases).
- 1D modeling (using the finite-volume method with the staggered grid scheme).
- Mass accumulation is considered in each mesh cell.
- The inertia of the fluid is taken into account.
- The phenomenon of longitudinal heat conduction in the metal wall and in the fluid is neglected.
- The thermophysical properties are calculated on the basis of the average pressure and enthalpy in each mesh cell.

#### 9.4.2.3 Governing Equations

The 1D formulation for dynamic heat exchangers is used (cf. Sect. 9.3).

The tube bundle is modeled as one tube equivalent to the  $N_t$  tubes of the bundle.

In the following equations, the balance equations of Sect. 9.3 are written using the fluid pressure  $P_i$ , the fluid specific enthalpy  $h_i$ , and the wall temperature  $T_{w,i}$  as state variables.

Notice that according to the staggered grid scheme, there are two different meshes: the thermal mesh that contains the mass and energy balance equations and the hydraulic mesh that contains the momentum balance equations. In principle, the cells of the two meshes are of equal length  $\Delta x_1 = L/(N - 1)$ , with  $N - 1$  thermal cells and  $N$  hydraulic cells, which implies that the two hydraulic cells at both ends of the pipe are of length  $\Delta x_1/2$ ; cf. Fig. 9.10b. However, for the sake of simplicity,

all hydraulic cells are assumed to be of the same length equal to the average length  $\Delta x_2 = L/N$ , thus slightly different from  $\Delta x_1$  when  $N$  is not too small.

In the following, equations labeled *n-a*, *n-b*, etc., denote possible alternatives. Therefore, either equation *n-a* or *n-b* should be used for a given simulation, but not both.

#### Equation 1a

Title	Dynamic mass balance equation
Validity domain	$\forall \dot{m}_{i:i+1}$
Mathematical formulation	$A \cdot \left[ \left( \frac{\partial \rho_i}{\partial P_i} \right)_h \cdot \frac{dP_i}{dt} + \left( \frac{\partial \rho_i}{\partial h_i} \right)_P \cdot \frac{dh_i}{dt} \right] \cdot \Delta x_1 = \dot{m}_{i-1:i} - \dot{m}_{i:i+1}$
Comments	This equation uses (9.69) and the expansion of the derivative of the density using $P$ and $h$ as state variables: $\frac{d\rho_i}{dt} = \left( \frac{\partial \rho_i}{\partial P_i} \right)_h \cdot \frac{dP_i}{dt} + \left( \frac{\partial \rho_i}{\partial h_i} \right)_P \cdot \frac{dh_i}{dt}$

#### Equation 1b

Title	Static mass balance equation
Validity domain	$\forall \dot{m}_{i:i+1}$ and the fluid is incompressible
Mathematical formulation	$0 = \dot{m}_{i-1:i} - \dot{m}_{i:i+1}$
Comment	This equation uses (9.69) and $\frac{d\rho_i}{dt} = 0$ as the fluid is incompressible

#### Equation 2a

Title	Energy balance equation
Validity domain	$\forall \dot{m}_{i:i+1}$
Mathematical formulation	$A \cdot \left[ \left( h_i \cdot \frac{\partial \rho_i}{\partial P_i} - 1 \right) \cdot \frac{dP_i}{dt} + \left( h_i \cdot \frac{\partial \rho_i}{\partial h_i} + \rho_i \right) \cdot \frac{dh_i}{dt} \right] \cdot \Delta x_1 = \dot{m}_{i-1:i} \cdot h_{i-1:i} - \dot{m}_{i:i+1} \cdot h_{i:i+1} + \Delta W_i$
Comments	The derivation of the mathematical formulation above is given below, using the relation between the specific internal energy and the specific enthalpy: $u_i = h_i - \frac{P_i}{\rho_i}$ The derivative term of (9.70) is expanded using $P$ and $h$ as state variables: $\begin{aligned} V_i \cdot \frac{d(\rho_i \cdot u_i)}{dt} &= V_i \cdot \left( \rho_i \cdot \frac{du_i}{dt} + u_i \cdot \frac{d\rho_i}{dt} \right) \\ &= V_i \cdot \left[ \left( \rho_i \cdot \frac{dh_i}{dt} - \frac{dP_i}{dt} + \frac{P_i}{\rho_i} \cdot \frac{d\rho_i}{dt} \right) + u_i \cdot \frac{d\rho_i}{dt} \right] \\ &= V_i \cdot \left[ \left( u_i + \frac{P_i}{\rho_i} \right) \cdot \left\{ \left( \frac{\partial \rho}{\partial P} \right)_h \cdot \frac{dP_i}{dt} + \left( \frac{\partial \rho}{\partial h} \right)_P \cdot \frac{dh_i}{dt} \right\} \right. \\ &\quad \left. + \rho_i \cdot \frac{dh_i}{dt} - \frac{dP_i}{dt} \right] \\ &= V_i \cdot \left[ \left( h_i \cdot \left( \frac{\partial \rho}{\partial P} \right)_h - 1 \right) \cdot \frac{dP_i}{dt} + \left( h_i \cdot \left( \frac{\partial \rho}{\partial h} \right)_P + \rho_i \right) \cdot \frac{dh_i}{dt} \right] \end{aligned}$

(continued)

(continued)

**Equation 2a**

The value of  $h_{ii+1}$  is given by the upwind scheme; cf. (4.114):

$$h_{ii+1} = \begin{cases} h_i & \text{if } \dot{m}_{ii+1} > 0 \\ h_{i+1} & \text{if } \dot{m}_{ii+1} < 0 \end{cases}$$

$h_{ii+1}$  is undefined for  $\dot{m}_{ii+1} = 0$ , but Eq. 2a is still valid for  $\dot{m}_{ii+1} = 0$  as it is not static

**Equation 2b**

Title	Incompressible flow energy balance equation
Validity domain	$\forall \dot{m}_{ii+1}$ and the fluid is incompressible
Mathematical formulation	$A \cdot \left( \rho_i \cdot \frac{dh_i}{dt} - \frac{dP_i}{dt} \right) \cdot \Delta x_1 = \dot{m}_{i-1:i} \cdot h_{i-1:i} - \dot{m}_{ii+1} \cdot h_{ii+1} + \Delta W_i$
Comments	This equation can be derived from Eq. 2a with $\frac{\partial \rho_i}{\partial P_i} = \frac{\partial \rho_i}{\partial h_i} = 0$ as the fluid is incompressible.

**Equation 2c**

Title	Simple incompressible flow energy balance equation
Validity domain	$\forall \dot{m}_{ii+1}$ and the fluid is incompressible
Mathematical formulation	$A \cdot \rho_i \cdot \frac{dh_i}{dt} \cdot \Delta x_1 = \dot{m}_{i-1:i} \cdot h_{i-1:i} - \dot{m}_{ii+1} \cdot h_{ii+1} + \Delta W_i$
Comments	This equation neglects the pressure derivative in Eq. 2b

**Equation 3a**

Title	Dynamic momentum balance equation
Validity domain	$\forall \dot{m}_{ii+1}$
Mathematical formulation	$\frac{1}{A} \cdot \frac{d\dot{m}_{ii+1}}{dt} \cdot \Delta x_2 = P_i - P_{i+1} - (\Delta P)_{ii+1}^a - (\Delta P)_{ii+1}^f - (\Delta P)_{ii+1}^g$ $(\Delta P)_{ii+1}^a = \frac{\dot{m}_{ii+1} \cdot  \dot{m}_{ii+1} }{A^2} \cdot \left( \frac{1}{\rho_{i+1}} - \frac{1}{\rho_i} \right)$ $(\Delta P)_{ii+1}^f = \zeta \cdot \frac{\Phi_{lo}^2 \cdot A_{ii+1} \cdot \Delta x_2 \cdot \dot{m}_{ii+1} \cdot  \dot{m}_{ii+1} }{2 \cdot D \cdot A^2 \cdot \rho_{ii+1}}$ $(\Delta P)_{ii+1}^g = \rho_{ii+1} \cdot g \cdot (z_{i+1} - z_i)$
Comments	By default, the flow is considered to be turbulent ( $Re > 2300$ ). This equation uses (9.71), (13.17), and (13.24). The friction coefficient $\Lambda_{ii+1}$ is computed using the Zigrang correlation; cf. (13.13). The two-phase aspects are captured by the Lockhart and Martinelli corrective coefficient $\Phi_{lo}^2$ ; cf. Sect. 13.2.2

Equation 3b	
Title	Static momentum balance equation
Validity domain	$\forall \dot{m}_{ii+1}$ and the fluid inertia can be neglected
Mathematical formulation	$P_i - P_{i+1} = (\Delta P)_{ii+1}^a + (\Delta P)_{ii+1}^f + (\Delta P)_{ii+1}^g$ $(\Delta P)_{ii+1}^a = \frac{\dot{m}_{ii+1} \cdot  \dot{m}_{ii+1} }{A^2} \cdot \left( \frac{1}{\rho_{i+1}} - \frac{1}{\rho_i} \right)$ $(\Delta P)_{ii+1}^f = \zeta \cdot \frac{\Phi_{lo}^2 \cdot \Lambda_{ii+1} \cdot \Delta x_2 \cdot \dot{m}_{ii+1} \cdot  \dot{m}_{ii+1} }{2 \cdot D \cdot A^2 \cdot \rho_{ii+1}}$ $(\Delta P)_{ii+1}^g = \rho_{ii+1} \cdot g \cdot (z_{i+1} - z_i)$
Comments	<p>This equation uses (9.71), (13.17), and (13.24). The friction coefficient <math>\Lambda_{ii+1}</math> is computed using the Zigrang correlation; cf. (13.13). The two-phase aspects are captured by the Lockhart and Martinelli corrective coefficient <math>\Phi_{lo}^2</math>; cf. Sect. 13.2.2.</p> <p>As the fluid inertia is neglected, it is assumed that</p> $\frac{1}{A} \cdot \frac{d\dot{m}_{ii+1}}{dt} \cdot \Delta x_2 \approx 0$ <p>e.g., that <math>\Delta x_2/A</math> or <math>d\dot{m}_{ii+1}/dt</math> are small</p>
Equation 4	
Title	Convective heat exchanged between the fluid and the wall
Validity domain	$\forall T_{w,i}$ and $\forall T_i$
Mathematical formulation	$\Delta W_i = \alpha \cdot h_{c,i} \cdot \Delta A_i \cdot (T_{w,i} - T_i)$
Comments	<p>This equation uses (9.78). The convection heat transfer coefficient <math>h_{c,i}</math> between the fluid and the wall is computed using the Dittus–Boelter correlation for one-phase flow and the Gungor–Chen correlation for two-phase flow; cf. Sect. 9.2.4.1</p>

#### 9.4.2.4 Modelica Component Model: *DynamicTwoPhaseFlowPipe*

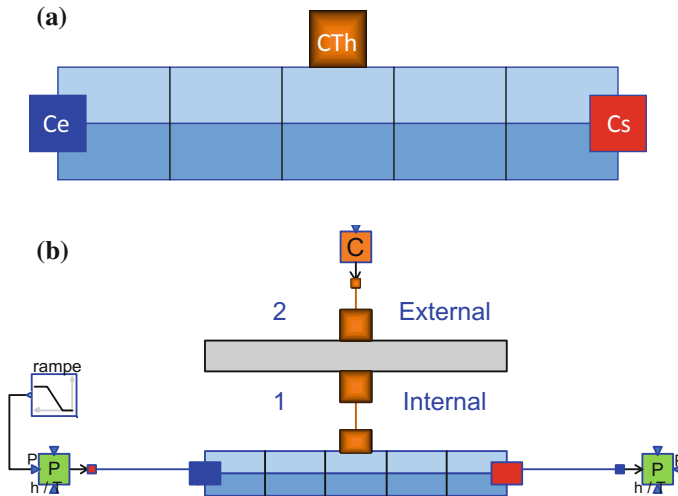
The governing equations are implemented in the *DynamicTwoPhaseFlowPipe* component model located in the *WaterSteam.HeatExchangers* sub-library for the case of single- and two-phase flow. They are also implemented in the *DynamicOnePhaseFlowPipe* component model located in the same sub-library for the simpler case of single-phase flow only.

Figure 9.11a represents the graphical icon of the component with its two connectors.

#### 9.4.2.5 Test-Case

The model *TestDynamicTwoPhaseFlowPipe* used to validate the *DynamicTwoPhaseFlowPipe* component model is represented in Fig. 9.11b. This model uses the following component models:

- One *DynamicTwoPhaseFlowPipe* component model;
- One *HeatExchangerWall* component model;



**Fig. 9.11** **a** Icon of the *DynamicTwoPhaseFlowPipe* component model and **b** test-case for the *DynamicTwoPhaseFlowPipe* component model

- One *HeatSource* component model;
- One *SourceP* component model;
- One *SinkP* component model;
- One *Ramp* block.

In the test-case scenario, the *DynamicTwoPhaseFlowPipe* component receives: (1) the fluid pressure, mass flow rate, and specific enthalpy at the fluid inlet, (2) the thermal power exchanged at the thermal connector, and (3) the fluid pressure at the fluid outlet. The component computes the distribution of the fluid specific enthalpy, mass flow rate, pressure and temperature and wall temperature. The corrective term for the friction pressure loss is obtained by inverse calculation.

#### Test-Case Parameterization and Boundary Conditions

The model data are:

- Water specific enthalpy at the inlet =  $800 \times 10^3$  J/kg/K
- Water mass flow rate at the outlet = 1 kg/s
- Water pressure at the inlet (for time  $\leq 300$  s) =  $20 \times 10^5$  Pa
- Water pressure at the inlet (for time  $\geq 600$  s) =  $19.8 \times 10^5$  Pa
- Water pressure at the outlet =  $19.9 \times 10^5$  Pa
- Number of pipes = 1
- Internal diameter of the pipes = 0.03 m
- External diameter of the pipes = 0.035 m
- Length of the pipes = 10 m

- Inlet altitude of the pipes = 0
- Outlet altitude of the pipes = 0
- Pipes' conductivity = 10 W/m/K
- Inlet power =  $2 \times 10^5$  W.

## Model Calibration

The calibration procedure consists in setting (fixing) a state variable at some point along the tube to a known measurement value and computing by model inversion the value of a parameter or a boundary condition.

The point along the tube is in general the inlet or the outlet of the tube.

The parameter can be the corrective term for the friction pressure loss. The boundary condition can be the fluid mass flow rate.

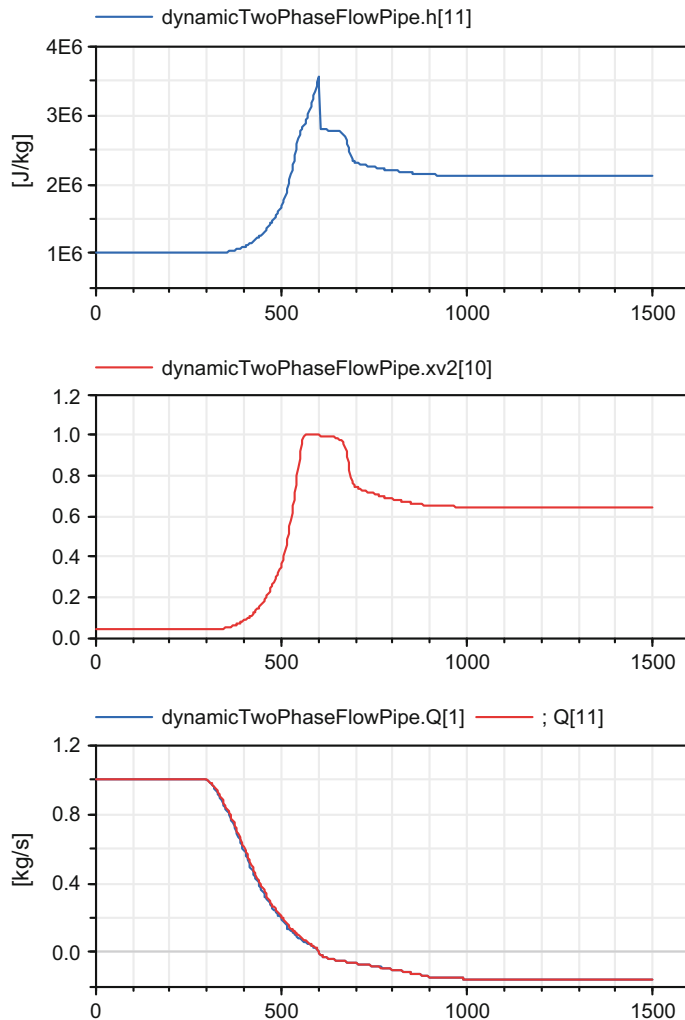
## Simulation Results

Figure 9.12 shows the results of the simulation for a scenario of pressure variation at the inlet of the pipe from  $20 \times 10^5$  to  $19.8 \times 10^5$  Pa.

### 9.4.3 Shell-Side Heat Exchanger Modeling

The shell model is called *DynamicOnePhaseFlowShell*. It represents the shell volume and the fluid part flowing outside one or several pipes (the tube bundle) with heat transfer through the pipes walls; cf. Fig. 9.13. Therefore, the model represents only the fluid circulating outside the bundle of parallel tubes (i.e., fluid 2 of Fig. 9.13) and the thermal exchange between the fluid and the outside walls of the tubes. The fluid is always liquid water. The physical equations of this model are the same as for the tube bundle heat exchanger (cf. Sect. 9.4.2) model, with different correlations for the friction pressure loss and the heat exchange coefficient between the fluid and the pipe walls.

The convection heat transfer coefficient  $h_c$  between the fluid and the tube bundle walls is computed using the Kern correlation (Sacadura 1978; Fraas and Ozisik 1965; Kern 1950).



**Fig. 9.12** Simulation results for *DynamicTwoPhaseFlowPipe*: evolution of the fluid specific enthalpy at the outlet (top), evolution of the vapor mass fraction at the outlet (middle), evolution of the mass flow rates at the inlet and at the outlet (bottom)

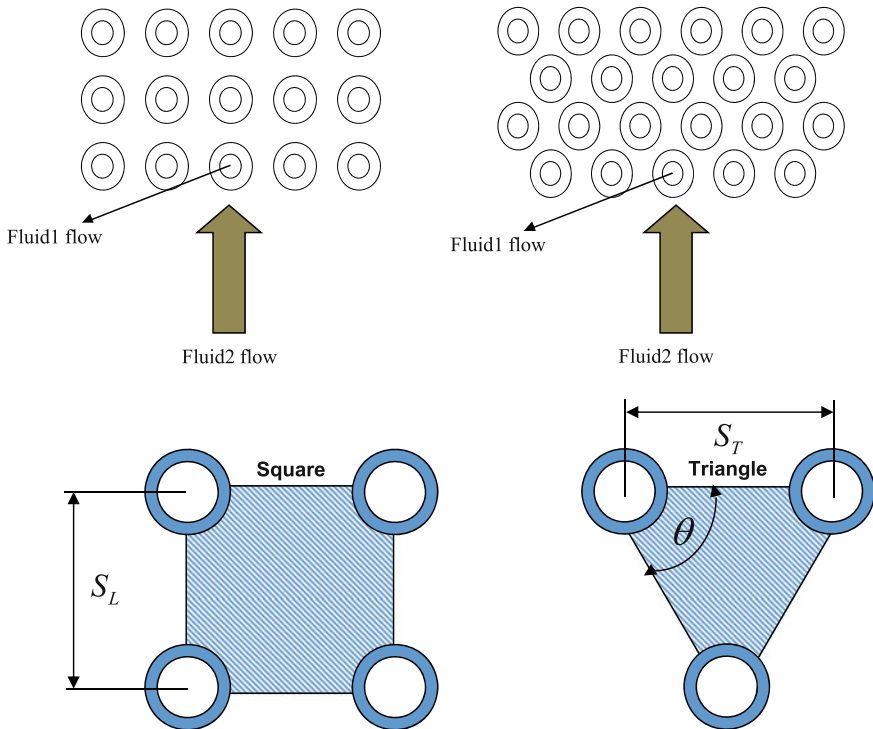


**Fig. 9.13** Geometry of the tube bundle

#### 9.4.3.1 Nomenclature

The following table complements the nomenclature for the tube bundle heat exchanger (cf. Sect. 9.4.2.1).

Symbols	Definition	Unit	Mathematical definition
$A$	Cross-sectional area of the fluid flow that is perpendicular to the pipes	$\text{m}^2$	$\pi \cdot D_s^2 / 4 - N_t \cdot \pi \cdot D_e^2 / 4$
$A_s$	Maximum cross-sectional area of the fluid that is parallel to the pipes	$\text{m}^2$	$D_s \cdot L_c \cdot \left( \frac{S_L - D_e}{S_L} \right)$
$c_{p,l,i}$	Specific heat capacity of the liquid phase for cell $i$	$\text{J/K/kg}$	
$D_e$	External diameter of one pipe	$\text{m}$	
$D_s$	Shell internal diameter	$\text{m}$	
$L_c$	Distance between two plates in the shell (support plate spacing in the cooling zone)	$\text{m}$	

(continued)

(continued)

Symbols	Definition	Unit	Mathematical definition
$Pr_{l,i}$	Prandtl number of the liquid phase for thermal cell $i$		$\frac{c_{p,l,i} \cdot \mu_{l,i}}{\lambda_{l,i}}$
$q_{S,i:i+1}$	Surface mass flow rate for hydraulic cell $i:i+1$	$\text{kg/s/m}^2$	$\frac{\dot{m}_{i:i+1}}{A_s}$
$Re_{l,i:i+1}$	Reynolds number of the liquid phase for hydraulic cell $i:i+1$	—	
$Re_{l,i}$	Reynolds number of the liquid phase for thermal cell $i$	—	
$S_L$	Longitudinal step; cf. Fig. 9.13	m	
$S_T$	Transverse step; cf. Fig. 9.13	m	
$\theta$	Average bend angle (pipe triangular step)	Degree	
$\lambda_{l,i}$	Liquid thermal conductivity for thermal cell $i$	$\text{W/m/K}$	
$\mu_{l,i:i+1}$	Liquid dynamic viscosity for hydraulic cell $i:i+1$	$\text{Pa s}$	
$\mu_{IT,i:i+1}$	Liquid dynamic viscosity at the wall temperature for hydraulic cell $i:i+1$	$\text{Pa s}$	
$\mu_{l,i}$	Liquid dynamic viscosity for thermal cell $i$	$\text{Pa s}$	

#### 9.4.3.2 Governing Equations

All equations are similar to the tube bundle heat exchanger (cf. Sect. 9.4.2), except the momentum balance equations that differ by the friction correlation. Therefore, only Eq. 3a is detailed below. The modification for Eq. 3b is similar.

Equation 3a	
Title	Dynamic momentum balance equation
Validity domain	$\forall \dot{m}_{i:i+1}$ and $400 < Re_{l,i:i+1} < 10^6$
Mathematical formulation	$\frac{1}{A_s} \cdot \frac{d\dot{m}_{i:i+1}}{dt} \cdot \Delta x_2 = P_i - P_{i+1} - (\Delta P)_{i:i+1}^a - (\Delta P)_{i:i+1}^f - (\Delta P)_{i:i+1}^g$ $(\Delta P)_{i:i+1}^a = \frac{\dot{m}_{i:i+1} \cdot  \dot{m}_{i:i+1} }{A_s^2} \cdot \left( \frac{1}{\rho_{i+1}} - \frac{1}{\rho_i} \right)$ $(\Delta P)_{i:i+1}^f = \frac{\Lambda_{i:i+1} \cdot \dot{m}_i \cdot  \dot{m}_i  \cdot (D_s/S_T) \cdot (L/L_c + 1)}{2 \cdot A_s^2 \cdot \rho_{i:i+1} \cdot N}$ $(\Delta P)_{i:i+1}^g = \rho_{i:i+1} \cdot g \cdot (z_{i+1} - z_i)$
Comments	<p>This equation uses (9.71). The friction coefficient <math>\Lambda_i</math> is computed using the following correlation (Kakaç et al. 2012):</p> $\Lambda_{i:i+1} = e^{0.576 - 0.19 \cdot \ln Re_{l,i:i+1}}$ <p>The Reynolds number for the liquid phase is given by:</p> $Re_{l,i:i+1} = \frac{q_{S,i:i+1} \cdot D_e}{\mu_{l,i:i+1}}$

Equation 4

Title	Convective heat exchanged between the fluid and the wall
Validity domain	$\forall T_{w,i}$ and $\forall T_i$
Mathematical formulation	$\Delta W_i = h_{c,i} \cdot \Delta A_i \cdot (T_{w,i} - T_i)$
Comments	<p>This equation uses (9.78). The convection heat transfer coefficient <math>h_{c,i}</math> between the fluid and the wall is computed using the following correlation (Sacadura 1978; Kern 1950):</p> $h_{c,i} = \begin{cases} \frac{\dot{q}_i}{D_e} \cdot 0.5 \cdot Re_{l,i}^{0.507} \cdot Pr_{l,i}^{0.33} & \text{for } Re_{l,i} < 2000 \\ \frac{\dot{q}_i}{D_e} \cdot 0.36 \cdot Re_{l,i}^{0.55} \cdot Pr_{l,i}^{0.33} \cdot \left( \frac{\mu_{l,i}}{\mu_{IT,i}} \right)^{0.14} & \text{for } 2000 < Re_{l,i} < 10^6 \end{cases}$ <p>For the sake of simplicity, <math>Re_{l,i} = Re_{l,i:i+1}</math></p>

#### 9.4.3.3 Modelica Component Model: *DynamicTwoPhaseFlowShell*

The governing equations are implemented in the *DynamicTwoPhaseFlowShell* component model located in the *WaterSteam.HeatExchangers* sub-library.

Figure 9.14a represents the graphical icon of the component with its three connectors.

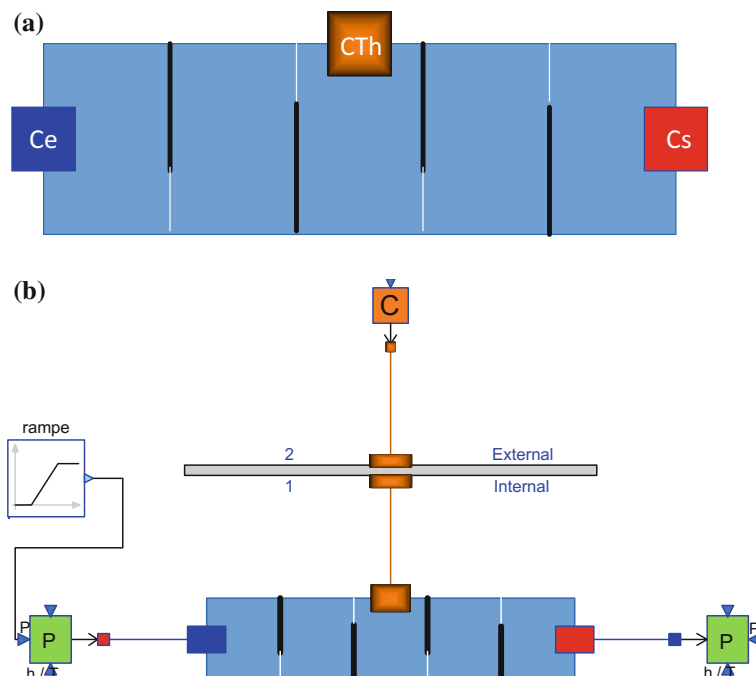


**Fig. 9.14** a Icon of the *DynamicOnePhaseFlowShell* component model and b test-case for the *DynamicOnePhaseFlowShell* component model

#### 9.4.3.4 Test-Case

The model *TestDynamicOnePhaseFlowShell* used to validate the *DynamicOnePhaseFlowShell* component model is represented in Fig. 9.14b. This model uses the following component models:

- One *DynamicOnePhaseFlowShell* component model;
- One *HeatExchangerWall* component model;
- One *HeatSource* component model;
- One *SourceP* component model;
- One *SinkP* component model;
- One *Ramp* block.

In the test-case scenario, the *DynamicOnePhaseFlowShell* component receives: (1) the fluid pressure, mass flow rate, and specific enthalpy at the fluid inlet, and (2) the thermal power exchanged at the thermal connector. The component computes the distribution of the fluid specific enthalpy, mass flow rate, pressure and temperature and wall temperature. The fluid pressure at the fluid outlet is obtained by inverse calculation.

#### Test-Case Parameterization and Boundary Conditions

The model data are:

- Water specific enthalpy at the inlet =  $600 \times 10^3$  J/kg/K
- Water pressure at the inlet (time  $\leq 300$  s) =  $20 \times 10^5$  Pa
- Water pressure at the inlet (time  $\geq 600$  s) =  $19.8 \times 10^5$  Pa
- Fluid mass flow rate at the inlet = 500 kg/s
- Number of pipes = 520
- Shell internal diameter = 1 m
- External diameter of the pipes = 0.019 m
- Length of the pipes = 12 m
- Inlet altitude of the pipes = 0
- Outlet altitude of the pipes = 0
- Pipes' conductivity = 10 W/m/K
- Outlet power =  $2 \times 10^7$  W.

#### Model Calibration

The calibration step consists in setting the value of the fluid mass flow rate at the inlet to known measurement value and computing by model inversion the values of the fluid pressure at the outlet.

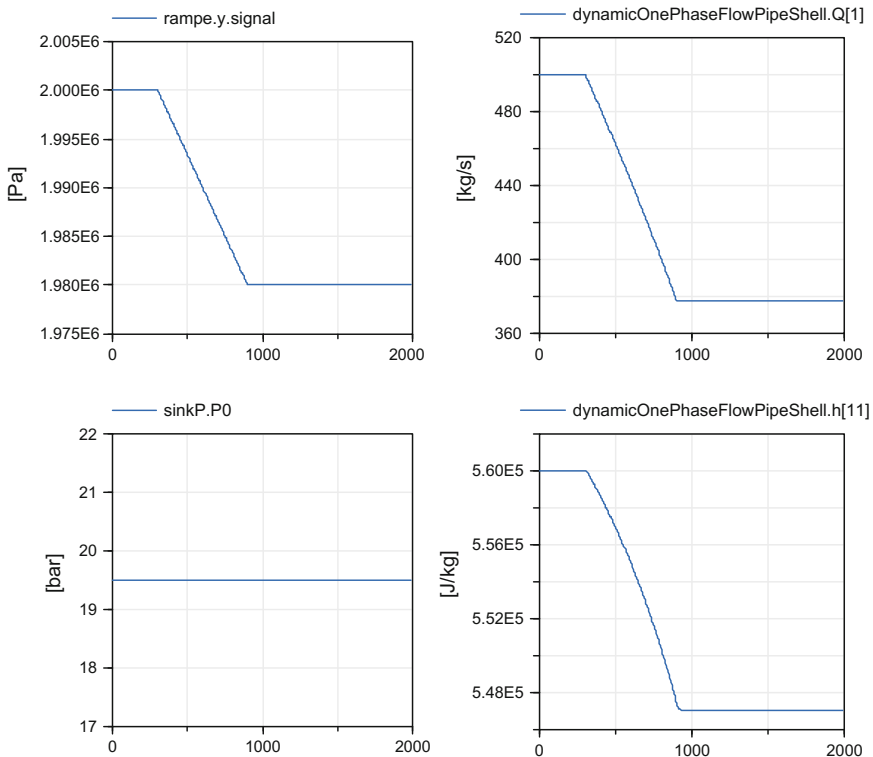


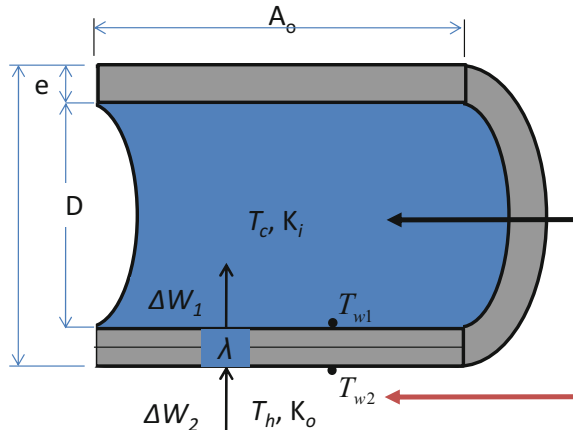
**Fig. 9.15** Simulation results for *DynamicOnePhaseFlowShell*: evolution of the water pressure at the inlet (top left), water pressure at the outlet (bottom left), evolution of the mass flow rate at the inlet (top right), and evolution of the water specific enthalpy at the outlet (bottom right)

## Simulation Results

Figure 9.15 shows the results of the simulation.

### 9.4.4 Heat Exchanger Wall

The wall transmits heat between the two fluids that are separated by the wall. The wall model is called *HeatExchangerWall*. This component represents the conductive heat flow through the wall of the tube bundle. The pipe wall is assumed to be cylindrical; cf. Fig. 9.16.

**Fig. 9.16** Wall geometry

#### 9.4.4.1 Nomenclature

Symbols	Definition	Unit	Mathematical definition
$c_{p,w}$	Specific heat capacity of the wall	J/kg/K	
$D$	Internal diameter of the pipes	m	
$e$	Wall thickness	m	
$L$	Pipe length	m	
$N_S$	Number of sections inside the wall	—	
$N_t$	Number of pipes in parallel	—	
$T_m$	Melting temperature of the tubes metal	K	
$T_{w,i}$	Average wall temperature in section $i$	K	
$T_{w1,i}$	Wall temperature in section $i$ of side 1 (internal wall side)	K	
$T_{w2,i}$	Wall temperature in section $i$ of side 2 (external wall side)	K	
$\Delta M_w$	Mass of a wall section	kg	
$\Delta W_{1,i}$	Thermal power transferred by conduction from the center of the wall to the wall internal surface, for each section $i$ Equivalently, thermal power received by the fluid from the wall internal surface for each section $i$	W	
$\Delta W_{2,i}$	Thermal power transferred by conduction from the wall external surface to the center of the wall, for each section $i$ Equivalently, thermal power received by the wall external surface from the fluid for each section $i$	W	

(continued)

(continued)

Symbols	Definition	Unit	Mathematical definition
$\Delta x$	Wall section length	m	$L/N_s$
$\lambda_w$	Wall thermal conductivity	W/m/K	
$\rho_w$	Wall density	kg/m <sup>3</sup>	

#### 9.4.4.2 Assumptions

The wall is modeled according to the following assumptions:

- 1D modeling.
- The energy accumulation is considered in each mesh cell.
- The phenomenon of longitudinal heat conduction in the wall is neglected.
- The thermal conductivity of the wall is constant in space and time.
- The heat flow through the wall is supposed to be positive when it is going from side 2 (external surface) to side 1 (internal surface) of the wall.

#### 9.4.4.3 Governing Equations

The *HeatExchangerWall* model is based on the dynamic energy balance equation on the wall, the heat capacity terms being lumped in the middle of the wall thickness. The heat flux in the wall is computed using the formulation of Fourier's equation expressed in cylindrical coordinates.

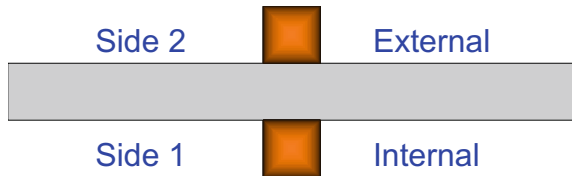
Equation 1

Title	Dynamic energy balance equation for the wall
Validity domain	$\forall T_{w,i}$
Mathematical formulation	$\Delta M_w \cdot c_{p,w} \cdot \frac{dT_{w,i}}{dt} = \Delta W_{2,i} - \Delta W_{1,i}$
Comments	This equation uses (9.79). Notice that the sign convention in (9.79) is different for fluid 2. $\Delta M_w$ is given by: $\Delta M_w = N_t \cdot \rho_w \cdot \pi \cdot \frac{(D + 2 \cdot e)^2 - D^2}{4} \cdot \Delta x$

Equation 2

Title	Fourier's equation in cylindrical coordinates (conduction through the internal side of the wall)
Validity domain	$\forall T_{w,i}$ and $\forall T_{w1,i}$
Mathematical formulation	$\Delta W_{1,i} = N_t \cdot \lambda_w \cdot \frac{2 \cdot \pi \cdot \Delta x}{\ln((e + D)/D)} \cdot (T_{w,i} - T_{w1,i})$
Comments	See Incropera et al. (2006) for a derivation of this equation

**Fig. 9.17** Icon of the *HeatExchangerWall* model




---

### Equation 3

Title	Fourier's equation in cylindrical coordinates (conduction through the external side of the wall)
Validity domain	$\forall T_{w,i}$ and $\forall T_{w2,i}$
Mathematical formulation	$\Delta W_{2,i} = N_t \cdot \lambda_w \cdot \frac{2 \cdot \pi \cdot \Delta x}{\ln((2 \cdot e + D)/(e + D))} \cdot (T_{w2,i} - T_{w,i})$
Comments	See Incropera et al. (2006) for a derivation of this equation

#### 9.4.4.4 Modelica Component Model: *HeatExchangerWall*

The governing equations are implemented in the *HeatExchangerWall* component model located in the *Thermal.HeatTransfer* sub-library.

Figure 9.17 represents the graphical icon of the component with its two connectors.

#### 9.4.4.5 Test-Case

The validation of the model component is done using the model featuring in Sect. 9.4.2.5.

## 9.5 Shell Heat Exchangers

### 9.5.1 Introduction

All heat exchangers described in this paragraph are water/steam heat exchangers with different closure laws, different computational causalities, depending on their function in the plant and whether dynamic or static behavior is considered. They use the modeling principles described in Sect. 9.3.

In the case of the water heater, the condenser, and the evaporator, the shell heat exchange is associated with a phase change in one of the fluids.

### 9.5.2 Dynamic Modeling of a Water Heater

The water heater model is called *DynamicWaterHeater*. It is a **two-phase** shell-and-tube heat exchanger; cf. Fig. 9.18. The feed water flows inside the tube bundle, while the steam and condensate flow outside those tubes (and inside the cavity). In the water heater, there are two distinct areas: (1) the *desuperheating* and *condensation* zone, located in the upper part of the component, and (2) the *sub-cooled* zone, located in the lower part of the component. In some water heaters, the condensate of the water heater located upstream from the current water heater is reinjected into the current water heater. During reinjection, part of the condensate may vaporize due to the pressure drop (this phenomenon is known as flash). The level of the condensate in the cavity is adjusted with a valve located at the outlet of the water heater.

The water heater is considered as a vertical or horizontal cylindrical cavity (as schematized in Fig. 9.18), containing a U-bent tube bundle with the feed water inlet and outlet located on the same side. The cavity is subdivided into the following zones:

- The *desuperheating* and *condensation* zone, where the superheated steam, flowing into the heater, exchanges heat with the liquid flowing through the tube bundle, until it becomes saturated steam and enters the condensation zone, where the saturated steam condenses as a consequence of the thermal exchange with the tube bundle, turning into liquid water that enters the subcooled zone. This zone is modeled by “Pipes 2” and “Pipes 3” in Fig. 9.19.
- The *subcooled* zone, where the liquid inside the cavity continues to exchange heat with the liquid flowing through the tube bundle. This zone is modeled by “Pipes 1” in Fig. 9.19.

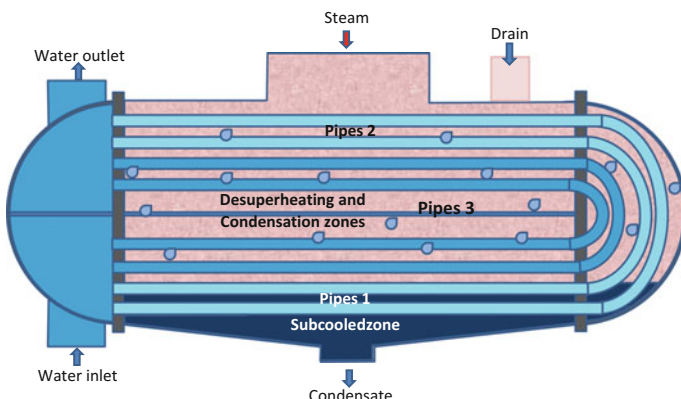


**Fig. 9.18** Schematic diagram of a water heater

Four configurations of the model are possible (see Fig. 9.19):

1. Horizontal water heater, with desuperheating, condensation, and subcooled zones;
2. Horizontal water heater, with desuperheating and condensation zones;
3. Vertical water heater, with desuperheating, condensation, and subcooled zones;
4. Separate vertical water heater with desuperheating, condensation and subcooled zones.

The model is divided into ten sub-models of different types which are connected together to make the full model (cf. Fig. 9.20a):

- Three *DynamicOnePhaseFlowPipe* component models;
- Three *HeatExchangerWall* component models;
- One *TwoPhaseCavity* component model;
- Three *Volume* component models.

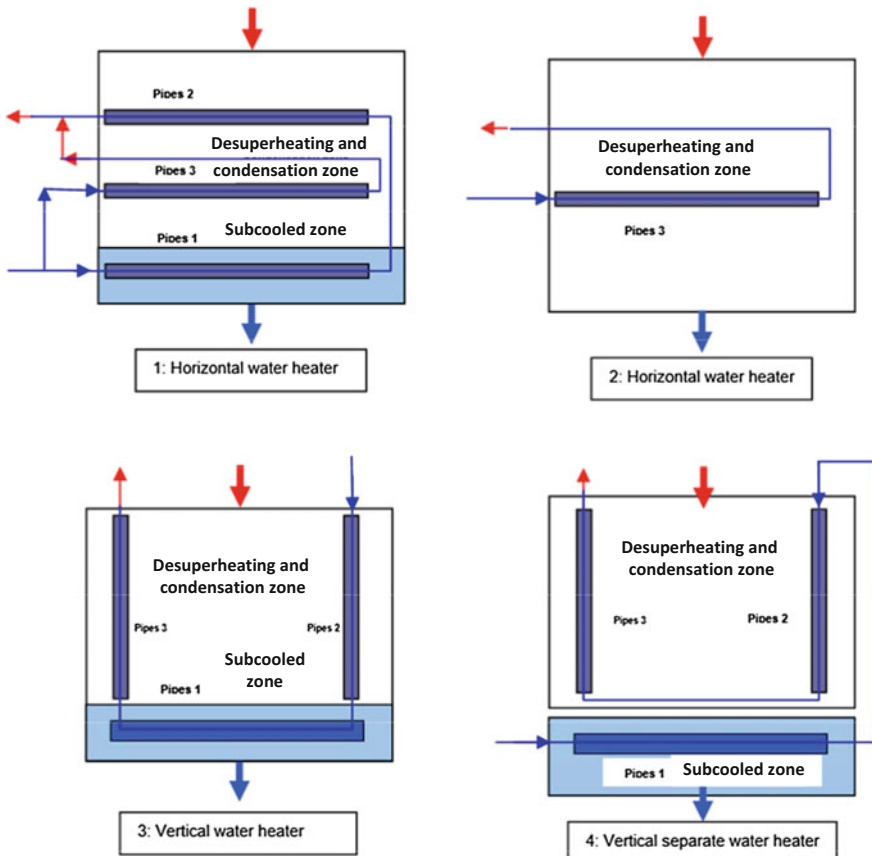


**Fig. 9.19** Water heater model configurations

By reassembling the sub-models, any water heating configuration of Fig. 9.19 can be modeled.

### 9.5.2.1 Modelica Component Model: *DynamicWaterHeater*

The *DynamicWaterHeater* component model is located in the *WaterSteam. HeatExchangers* sub-library.

Figure 9.20b represents the graphical icon of the component with its fluid, thermal, and sensor connectors.

### 9.5.2.2 Component Model Validation

To simulate the complex dynamic physical behavior in normal and accidental conditions of the water heater model, a test model has been developed by assembling the proper components from the ThermoSysPro library. The test model includes the level control system.

The model *TestDynamicWaterHeater* used to validate the *DynamicWaterHeater* component model is represented in Fig. 9.20c. It uses the following component models:

- One *DynamicWaterHeater* component model;
- Three *SingularPressureLoss* component models;
- One *LumpedStraightPipe* component model;
- One *IdealCheckValve* component model;
- One *ControlValve* component model;
- Two *SourceP* component models;
- One *SinkP* component model;
- One *Sink* component model;
- One *Constant* block;
- Five *TimeTable* blocks;
- One *RefQ* component model;
- One *Regulation* block (level of the condensate in the cavity).

In the test-case scenario, the *DynamicWaterHeater* component receives: (1) the steam pressure and specific enthalpy at the steam inlet, (2) the pressure of the condensate in the boundary conditions (*SinkP*), (3) the cooling fluid pressure and temperature at the cooling fluid inlet, and (4) the cooling fluid mass flow rate at the cooling fluid outlet. The component computes: (1) for the cavity, the mass flow rate of the steam, the specific enthalpy and pressure of the condensate at the condensate outlet, the volume of each phase, the specific enthalpy of each phase, the wall temperature, the liquid level in the cavity (by inverse calculation), and (2) for the cooling fluid the distribution of the fluid pressure, specific enthalpy, mass flow rate, temperature, and the distribution of the wall temperature.

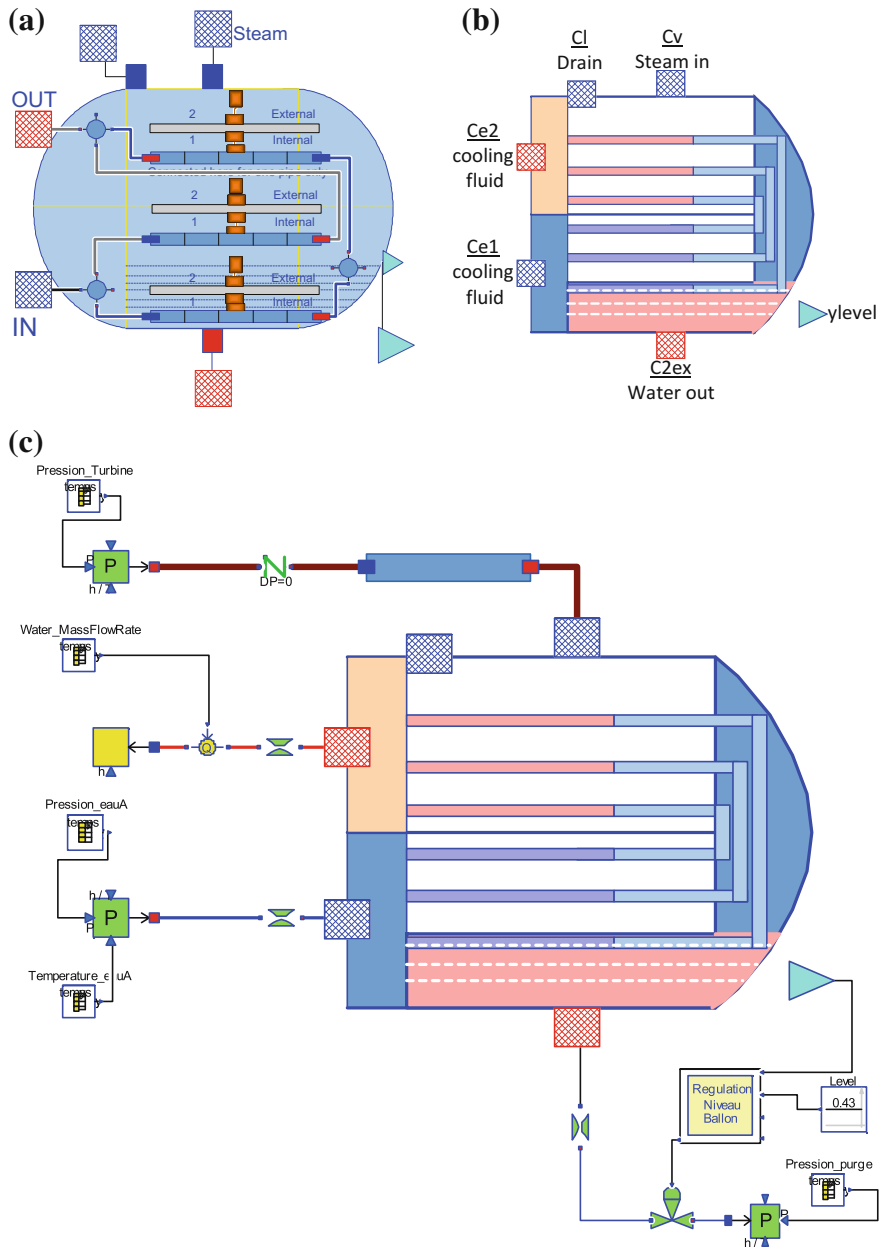


**Fig. 9.20** **a** Model of the *DynamicWaterHeater* component model, **b** icon of the *DynamicWaterHeater* component model, and **c** test-case for the *DynamicWaterHeater* component model

### Test-Case Parameterization and Boundary Conditions

In order to challenge the dynamic simulation capabilities of the model, a high-amplitude transient, called islanding that occurs when the plant is suddenly disconnected from the electrical grid, is simulated. This transient is used to check and validate the physics taken into account in the model and the numerical robustness of the model as it runs the water heater model into very different operating regimes. This allows to test the validity and applicability range of the model equations, and the numerical robustness of the Modelica model.

The boundary conditions of the model (scenario profiles) are presented in Fig. 9.21 and Table 9.1.

All geometrical data were provided to the model (tubes and exchangers lengths, diameters, volumes, corrective terms for the heat exchange coefficients, corrective terms for the pressure loss, etc.). The water heater characteristics are given below:

- Fraction of initial liquid volume in the cavity = 0.066
- Initial pressure in the cavity =  $22 \times 10^5$  Pa
- Radius of the cavity cross-sectional area = 1.130514 m
- Length of the drowned pipes in liquid (Pipes 1) = 13.2 m
- Length of Pipes 2 (in steam) = 13.2 m
- Length of Pipes 3 (in steam) = 26.4 m
- Support plate spacing in cooling zone (chicanes) = 2.56 m
- Internal diameter of the cooling pipes = 0.016 m
- Thickness of the cooling pipes = 0.001 m
- Longitudinal step = 0.027 m
- Transverse step = 0.02338 m
- Number of segments for one tube pass = 10
- Numbers of drowned pipes for Pipes 1 (drowned pipes) = 351
- Numbers of drowned pipes for Pipes 2 (in steam) = 351
- Numbers of drowned pipes for Pipes 3 (in steam) = 1319
- Numbers of pipes in a vertical row (tube bank) = 15
- Specific heat capacity of the metal of the cooling pipes = 506 J/kg/K
- Density of the metal of the cooling pipes = 7780 kg/m<sup>3</sup>
- Wall thermal conductivity of the cooling pipes = 35 W/m/K
- Corrective term for the friction pressure loss = 1.1136
- Corrective term for the heat exchange coefficient: steam side = 1
- Fluid pressure in the cavity =  $22.16584 \times 10^5$  Pa
- Cavity volume = 53 m<sup>3</sup>
- Wall mass = 50,000 kg
- Liquid level in cavity = 0.43 m
- Inlet altitude of the pipes = 0
- Outlet altitude of the pipes = 0.5 m
- Length of the pipe (*LumpedStraightPipe*) = 48.72 m
- Internal diameter of the pipe (*LumpedStraightPipe*) = 0.387 m
- Pressure loss coefficient of *singularPressureLossWaterOut* =  $30 \text{ m}^{-4}$

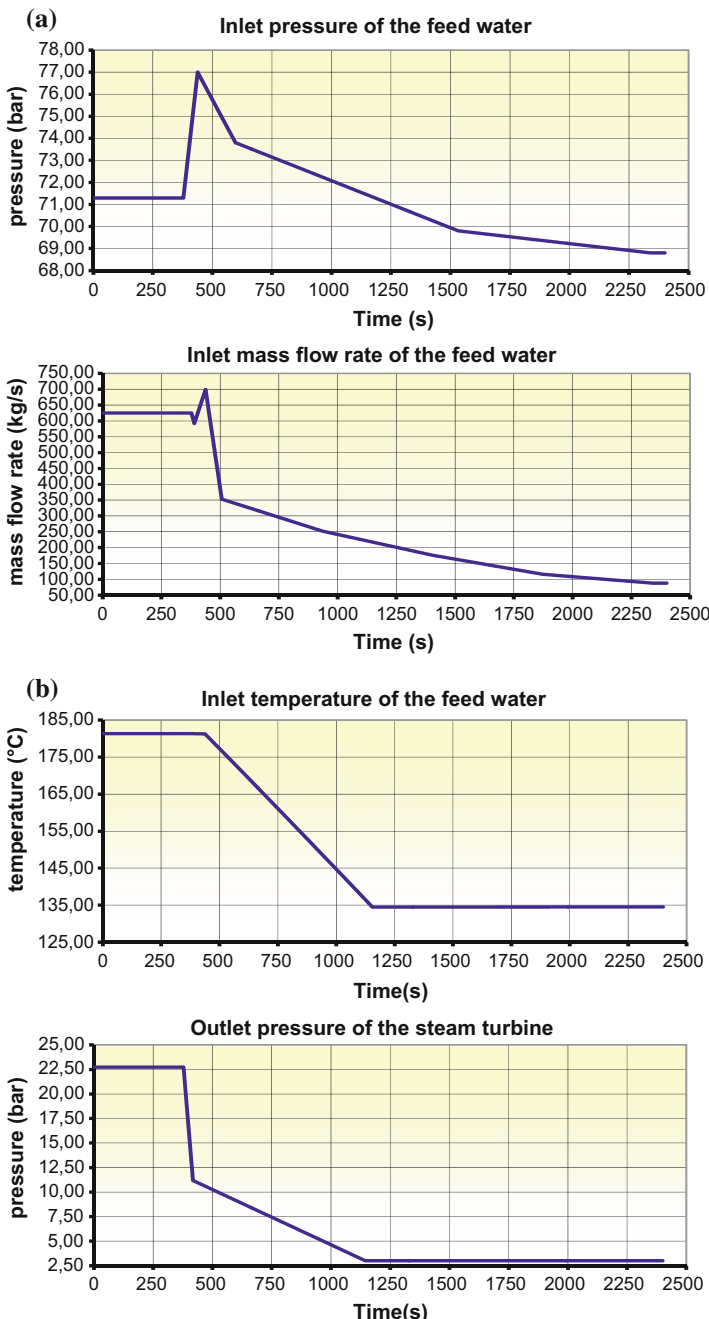


**Fig. 9.21** **a** Inlet pressure and mass flow rate of the feed water and **b** inlet temperature of the feed water and outlet pressure of the turbine

**Table 9.1** Drain pressure at the outlet

Time (s)	Pressure (Pa)
0	$10 \times 10^5$
378	$10 \times 10^5$
418	$7 \times 10^5$
1145	$2.9 \times 10^5$
2000	$2.9 \times 10^5$

- Pressure loss coefficient of *singularPressureLossWaterIn* =  $35 \text{ m}^{-4}$
- Pressure loss coefficient of *singularPressureLossPurge* =  $0.001 \text{ m}^{-4}$
- Inlet specific enthalpy of the steam *SourceP* =  $2650.6 \times 10^3 \text{ J/kg}$
- For Pipe 3: *inertia* = false.

### Model Calibration

The calibration procedure consists in setting:

- The liquid level in the cavity to a known measurement value ( $=0.43 \text{ m}$ ) to compute the value of Cvmax of the extraction valve by model inversion;
- The cavity pressure (outlet pressure of the steam pipe) (*PressureLoss\_Steam*) to a known measurement value ( $=22.16584 \times 10^5 \text{ Pa}$ ) to compute the value of the friction pressure loss coefficient of the steam pipe (*PressureLoss\_Steam*) by model inversion.

### Simulation Results and Experimental Validation of the Islanding Scenario

The model is able to compute precisely:

- The mass flow rate of the steam at the inlet;
- The mass flow rate of the condensate (drain);
- The thermal power of the water heater;
- The pressure, temperature, and specific enthalpy distributions inside the tubes;
- The cavity level and the cavity pressure.

The results of the simulation runs are given in Fig. 9.22. Figure 9.22a, b shows that the simulation results are very close to the measured values on site. The outflow drain (condensate) in Fig. 9.21d depends on the way the level is controlled inside the heater.

So, the physical validity of the component model is demonstrated in steady-state and islanding conditions. As islanding is the most demanding transient in normal operation, it can be considered that the component is valid for any transient under normal operating conditions of the power plant.

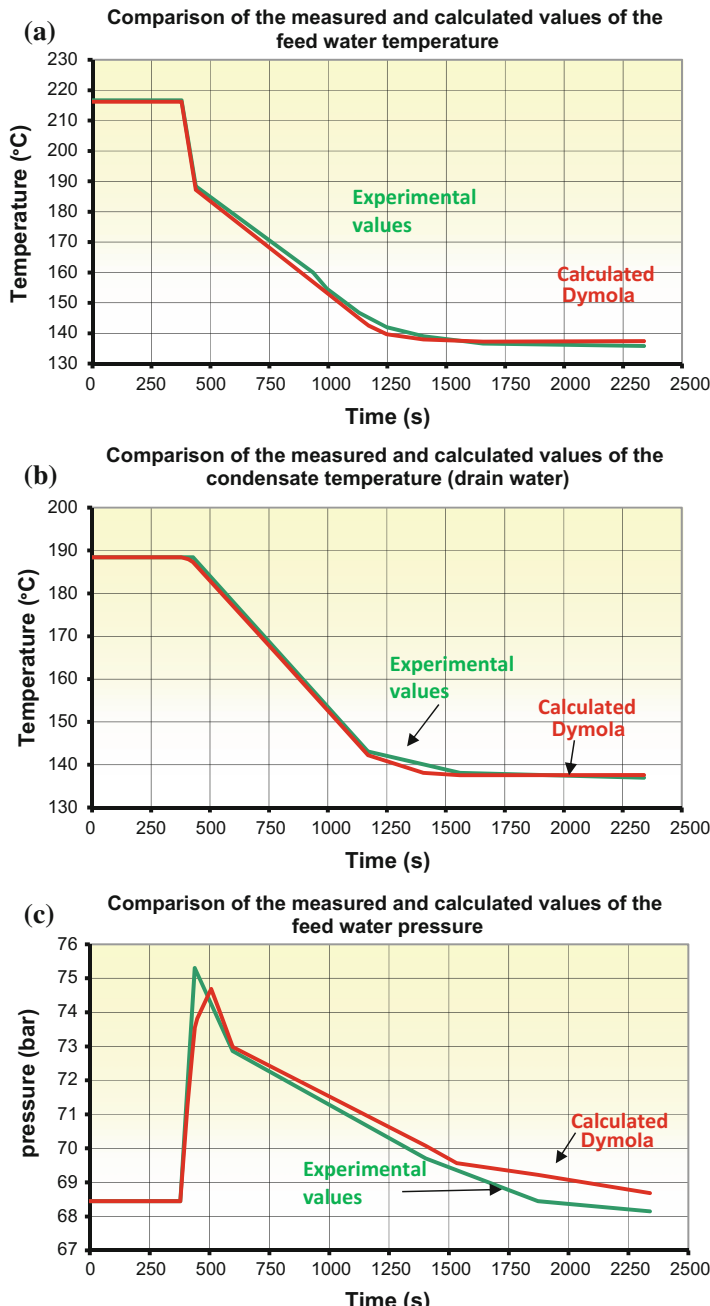


**Fig. 9.22** **a** Simulation results for *DynamicWaterHeater*: evolution of the feed water temperature at the outlet, **b** simulation results for *DynamicWaterHeater*: evolution of the condensate temperature at the outlet (water drain), **c** simulation results for *DynamicWaterHeater*: evolution of the feed water pressure at the outlet, and **d** simulation results for *DynamicWaterHeater*: evolution of the condensate mass flow rate at the outlet (water drain)

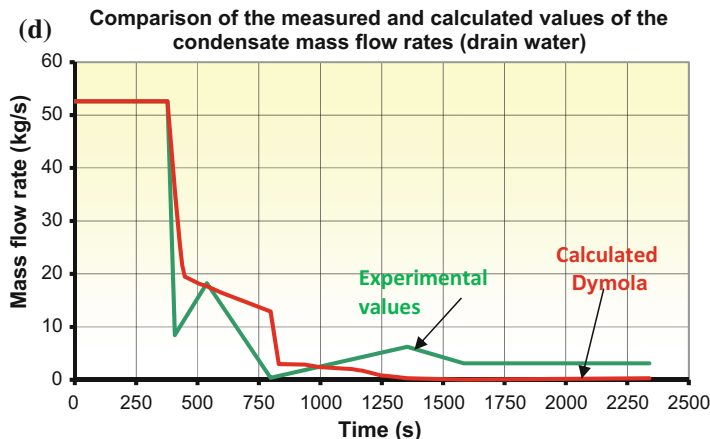


Fig. 9.22 (continued)

### Simulation Results for Flow Reversal and Zero-Flow Conditions

The boundary conditions for the flow reversal scenario are:

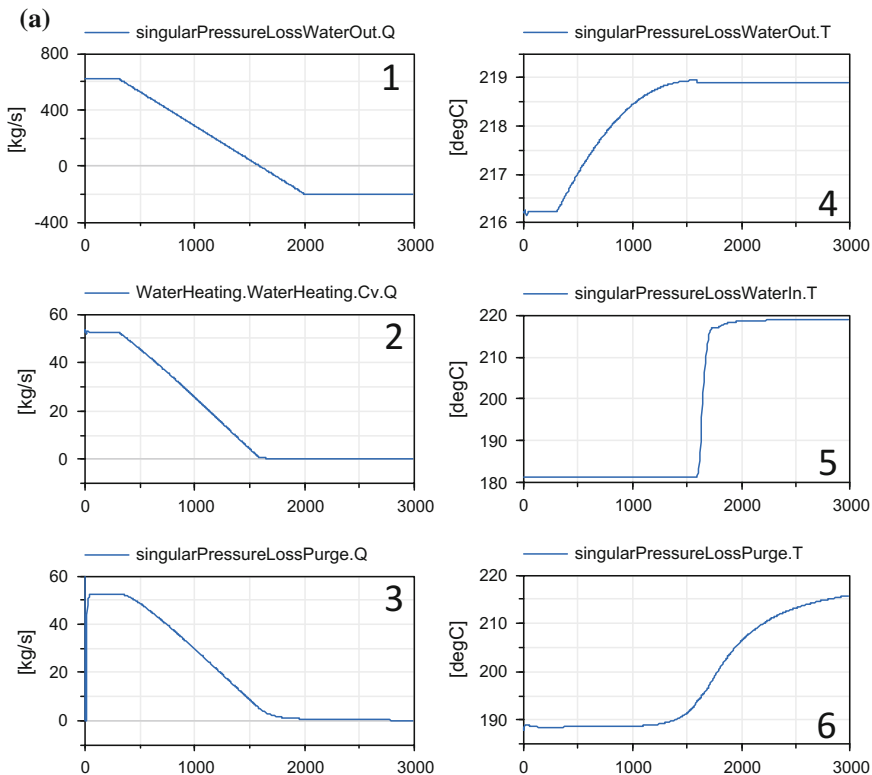
- Mass flow rate of the feed water at the inlet ( $t > 2000$  s):  $-200 \text{ kg/s}$
- Specific enthalpy of the feed water at the outlet for  $Q < 0$ :  $940 \times 10^3 \text{ J/kg}$ .

Figure 9.23 shows the results for the scenarios of flow reversal and zero flow in the water heater. The possibility of flow reversal and zero flow in the tube bundle of the component has been verified. But there are no data available for comparison with the simulation results.

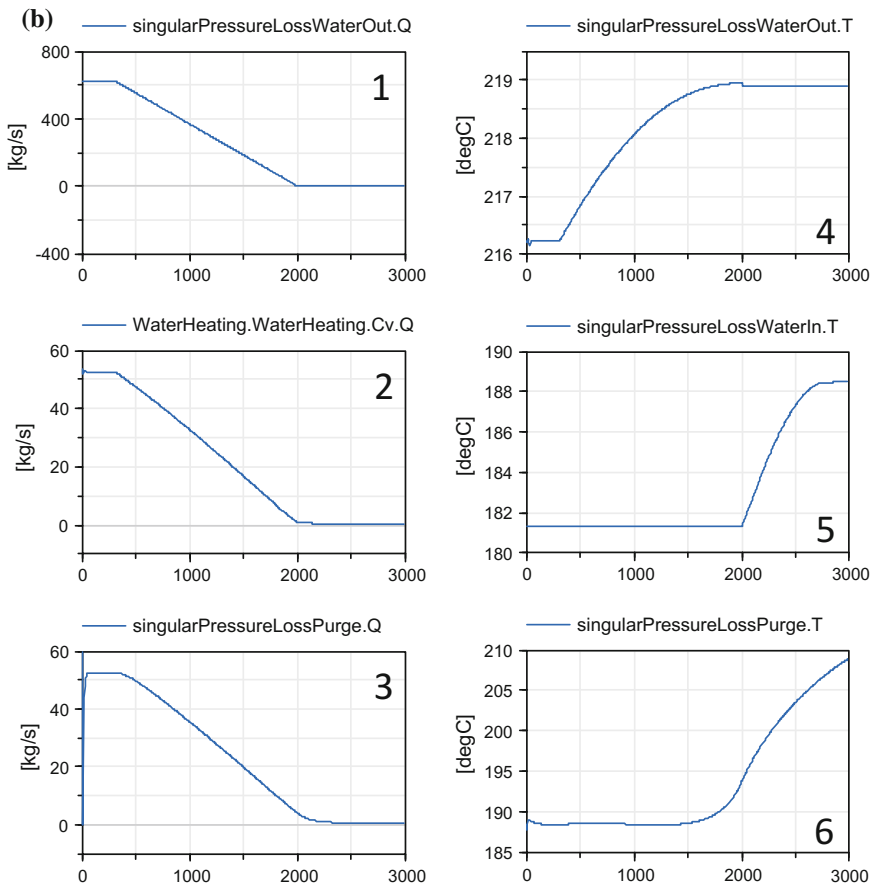
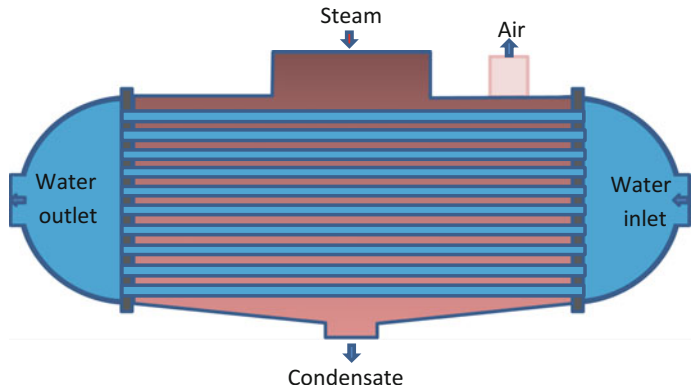
### 9.5.3 Dynamic Modeling of a Simple Condenser

The condenser is a large shell-and-tube heat exchanger composed of a bundle of circular tubes mounted in a cavity. The steam in the cavity flows outside the tube bundles, and the cooling water flows inside the tubes. The condenser is positioned at the outlet of the steam turbine in order to receive a large flow rate of low-pressure steam. Steam in the cavity undergoes a phase change from steam to water as a consequence of the thermal exchange with the tube bundle. External cooling water is pumped through the tube bundles of the condenser to evacuate the condensation heat of the steam. The condensate at the outlet is pumped and sent into the feed water heaters.

The condenser model is called *SimpleDynamicCondenser*. It is a two-phase shell-and-tube heat exchanger (cf. Fig. 9.24). The cooling water flows inside the tube bundles, while the steam and condensate flow outside those tubes and inside the cavity.



**Fig. 9.23** **a** Simulation results for *DynamicWaterHeater*: flow reversal scenario and **b** simulation results for *DynamicWaterHeater*: zero-flow scenario. (1) Mass flow rate of the feed water at the inlet, (2) mass flow rate of the steam at the inlet (corresponding to the steam turbine outlet), (3) mass flow rate of the water at the drain outlet, (4) temperature of the feed water at the outlet of the pipes, (5) temperature of the feed water at the inlet of the pipes, and (6) temperature of the water at the drain outlet

**Fig. 9.23** (continued)**Fig. 9.24** Schematic diagram of a condenser

### 9.5.3.1 Nomenclature

Symbols	Definition	Unit	Mathematical definition
$A_{vl}$	Heat exchange surface between steam and liquid in the cavity	$\text{m}^2$	
$A_t$	Internal cross section of the pipes of the tube bundle (cooling fluid)	$\text{m}^2$	$N_t \cdot \pi \cdot D^2 / 4$
$C_{\text{cond}}$	Condensation rate inside the cavity	$\text{s}^{-1}$	
$C_{\text{evap}}$	Evaporation rate inside the cavity	$\text{s}^{-1}$	
$D$	Internal diameter of one pipe of the tube bundle	m	
$g$	Acceleration due to gravity	$\text{m/s}^2$	
$h_{c,i}$	Cooling fluid specific enthalpy at the inlet of the tube bundle	$\text{J/kg}$	
$h_{c,o}$	Cooling fluid specific enthalpy at the outlet of the tube bundle	$\text{J/kg}$	
$h_l$	Liquid specific enthalpy in the cavity	$\text{J/kg}$	
$h_{l,o}$	Liquid specific enthalpy at the cavity outlet (drain)	$\text{J/kg}$	
$h_l^{\text{sat}}$	Liquid saturation enthalpy in the cavity	$\text{J/kg}$	
$h_v$	Steam specific enthalpy in the cavity	$\text{J/kg}$	
$h_{v,i}$	Steam specific enthalpy at the cavity inlet	$\text{J/kg}$	
$h_v^{\text{sat}}$	Steam saturation enthalpy in the cavity	$\text{J/kg}$	
$K_{vl}$	Convective heat exchange coefficient between the liquid and the steam in the cavity	$\text{W/m}^2/\text{K}$	
$L$	Tube bundle length (cooling fluid)	m	
$\dot{m}_c$	Cooling fluid (water) mass flow rate inside the tube bundle	$\text{kg/s}$	
$\dot{m}_{\text{cond}}$	Condensation mass flow rate inside the cavity	$\text{kg/s}$	
$\dot{m}_{\text{evap}}$	Evaporation mass flow rate inside the cavity	$\text{kg/s}$	
$\dot{m}_{l,o}$	Mass flow rate of outgoing condensate	$\text{kg/s}$	
$\dot{m}_{v,i}$	Mass flow rate of incoming vapor	$\text{kg/s}$	
$N_t$	Number of parallel pipes of the tube bundle (cooling fluid)	—	
$P$	Fluid pressure in the cavity	Pa	
$P_b$	Fluid pressure at the bottom of the cavity	Pa	$P + \rho_l \cdot g \cdot z_l$
$P_{c,i}$	Pressure of the cooling fluid at the inlet of the tube bundle	Pa	
$P_{c,o}$	Pressure of the cooling fluid at the outlet of the tube bundle	Pa	
$T_l$	Liquid temperature in the cavity	K	
$T_v$	Steam temperature in the cavity	K	
$V$	Volume of the cavity	$\text{m}^3$	$V_l + V_v$
$V_l$	Volume of the liquid in the cavity	$\text{m}^3$	$A_{vl} \cdot z_l$
$V_v$	Volume of the steam in the cavity	$\text{m}^3$	

(continued)

(continued)

Symbols	Definition	Unit	Mathematical definition
$W_{\text{out}}$	Power exchanged between the steam in the cavity and the cooling fluid in the tube bundle	W	
$W_{\text{vl}}$	Power exchanged between the vapor and the liquid phases in the cavity	W	
$x_l$	Vapor mass fraction in the liquid phase inside the cavity	–	
$x_v$	Vapor mass fraction in the vapor phase inside the cavity	–	
$X_{l_0}$	Vapor mass fraction in the liquid phase from which the bubbles in the liquid phase start to leave the liquid phase	–	
$X_{v_0}$	Vapor mass fraction in the gas phase from which the droplets in the vapor phase start to leave the vapor phase	–	
$z_l$	Liquid level in the cavity	m	$V_l/A_{\text{vl}}$
$z_1$	Inlet altitude of the pipes of the tube bundle (cooling fluid)	m	
$z_2$	Outlet altitude of the pipes of the tube bundle (cooling fluid)	m	
$\Delta P_f$	Friction pressure loss for the cooling fluid between the inlet and outlet of the tube bundle	Pa	
$\Delta P_g$	Pressure loss due to gravity for the cooling fluid between the inlet and outlet of the tube bundle	Pa	
$\Lambda$	Friction pressure loss coefficient for the cooling fluid	–	
$\rho_c$	Cooling fluid density	kg/m <sup>3</sup>	
$\rho_l$	Liquid density in the cavity	kg/m <sup>3</sup>	
$\rho_v$	Steam density in the cavity	kg/m <sup>3</sup>	

### 9.5.3.2 Assumptions

The condenser is modeled as a cavity containing a tube bundle with the following assumptions:

- The efficiency of the condenser is equal to 1 (100% of the mass flow rate of input steam is condensed).
- The energy accumulation in solids (pipes) is neglected.
- Heat exchange between the liquid and steam phases is taken into account.
- Pressure losses in the cavity are not taken into account.

- The liquid and steam phases are not necessarily in thermal equilibrium.
- The liquid and steam phases are assumed to be always in pressure equilibrium.
- The pressure at the bottom of the cavity is calculated as a function of the liquid level.

### 9.5.3.3 Governing Equations

The model represents the dynamics of the thermal hydraulic phenomena of the hot fluid inside the cavity and the power evacuated by the cooling liquid inside the pipes. The thermal power transferred to the cold fluid is calculated with a condensation efficiency equal to 1. The cavity is considered as a vertical or horizontal cylinder.

Regarding the cavity, the balance mass and energy equations of Sect. 4.2 are written for each phase (water and steam) using as state variables:

- $P$ : the mean pressure in the cavity;
- $h_l$ : the specific enthalpy of the liquid phase;
- $h_v$ : the specific enthalpy of the steam phase;
- $V_l$ : the volume of the liquid phase;
- $V_v$ : the volume of the steam phase.

The pipe bundle is represented as a simple pressure loss and a convective heat exchange with the cavity.

Equation 1

Title	Dynamic mass balance equation for the liquid phase
Validity domain	$\forall \dot{m}$ and $0 < V_l < V$
Mathematical formulation	$\rho_l \cdot \frac{dV_l}{dt} + V_l \cdot \left[ \left( \frac{\partial \rho_l}{\partial P} \right)_h \cdot \frac{dP}{dt} + \left( \frac{\partial \rho_l}{\partial h_l} \right)_P \cdot \frac{dh_l}{dt} \right] = \dot{m}_{\text{cond}} - \dot{m}_{\text{evap}} - \dot{m}_{l,o}$
Comments	<p>This equation establishes the mass balance between the outgoing liquid, the condensation, and the evaporation flows. The evaporation flow term is added for the sake of completeness as it should always be zero during normal operation of the condenser</p> <p>From (4.7):</p> $\begin{aligned} \frac{d(\rho_l \cdot V_l)}{dt} &= \rho_l \cdot \frac{dV_l}{dt} + V_l \cdot \left[ \left( \frac{\partial \rho_l}{\partial P} \right)_h \cdot \frac{dP}{dt} + \left( \frac{\partial \rho_l}{\partial h_l} \right)_P \cdot \frac{dh_l}{dt} \right] \\ &= \sum_i \dot{m}_i - \sum_o \dot{m}_o \end{aligned}$ <p>where <math>\dot{m}_i</math> and <math>\dot{m}_o</math> denote respectively the input and output mass flow rates into and from the liquid phase.</p> <p>It is assumed that the liquid and the steam are at the same pressure <math>P</math>. The condensation and evaporation mass flow rates are given by (4.96):</p> $\dot{m}_{\text{cond}} = \max(C_{\text{cond}} \cdot \rho_v \cdot V_v \cdot (X_{vo} - x_v), 0)$ $\dot{m}_{\text{evap}} = \max(C_{\text{evap}} \cdot \rho_l \cdot V_l \cdot (x_l - X_{lo}), 0)$

**Equation 2**

Title	Dynamic mass balance equation for the steam phase
Validity domain	$\forall \dot{m}$ and $0 < V_v < V$
Mathematical formulation	$\rho_v \cdot \frac{dV_v}{dt} + V_v \cdot \left[ \left( \frac{\partial \rho_v}{\partial P} \right)_h \cdot \frac{dP}{dt} + \left( \frac{\partial \rho_v}{\partial h_v} \right)_P \cdot \frac{dh_v}{dt} \right] = \dot{m}_{v,i} + \dot{m}_{evap} - \dot{m}_{cond}$
Comments	<p>This equation establishes the mass balance between the incoming steam, the condensation, and the evaporation flows. The evaporation flow term is added for the sake of completeness as it should always be zero during normal operation of the condenser.</p> <p>See also Eq. 1</p>

**Equation 3**

Title	Dynamic energy balance equation for the liquid phase
Validity domain	$\forall \dot{m}$ and $0 < V_l < V$
Mathematical formulation	$V_l \cdot \left[ \left( \frac{P}{\rho_l} \cdot \left( \frac{\partial \rho_l}{\partial P} \right)_h - 1 \right) \cdot \frac{dP}{dt} + \left( \frac{P}{\rho_l} \cdot \left( \frac{\partial \rho_l}{\partial h_l} \right)_P + \rho_l \right) \cdot \frac{dh_l}{dt} \right] = \dot{m}_{cond} \cdot \left[ h_l^{\text{sat}} - \left( h_l - \frac{P}{\rho_l} \right) \right] - \dot{m}_{evap} \cdot \left[ h_v^{\text{sat}} - \left( h_l - \frac{P}{\rho_l} \right) \right] - \dot{m}_{l,o} \cdot \left[ h_{l,o} - \left( h_l - \frac{P}{\rho_l} \right) \right] + W_{vl}$
Comments	<p>This equation establishes the energy balance between the outgoing liquid, the condensation, and the evaporation flows. The evaporation flow term is added for the sake of completeness as it should always be zero during normal operation of the condenser.</p> <p>From (4.28) and neglecting diffusion:</p> $\frac{d(\rho_l \cdot V_l \cdot u_l)}{dt} = \sum_i \dot{m}_i \cdot h_i - \sum_o \dot{m}_o \cdot h_o + W_{vl}$ <p>where <math>h_i</math> and <math>h_o</math> are respectively the specific enthalpies of the incoming and outgoing mass flows <math>\dot{m}_i</math> and <math>\dot{m}_o</math>.</p> <p>Developing the left-hand side yields:</p> $\frac{d(\rho_l \cdot V_l \cdot u_l)}{dt} = \rho_l \cdot V_l \cdot \frac{du_l}{dt} + u_l \cdot \frac{d(\rho_l \cdot V_l)}{dt}$ <p>Each term of this equation is calculated separately in the following.</p> <p>The mass balance equation is:</p> $\frac{d(\rho_l \cdot V_l)}{dt} = \sum_i \dot{m}_i - \sum_o \dot{m}_o$ <p>As the specific internal energy <math>u_l</math> is</p> $u_l = h_l - \frac{P}{\rho_l}$ <p>then</p> $u_l \cdot \frac{d(\rho_l \cdot V_l)}{dt} = \left( h_l - \frac{P}{\rho_l} \right) \cdot \left( \sum_i \dot{m}_i - \sum_o \dot{m}_o \right)$ <p>and</p> $\rho_l \cdot V_l \cdot \frac{du_l}{dt} = V_l \cdot \left[ \rho_l \cdot \frac{dh_l}{dt} - \left( \frac{dP}{dt} + \frac{P}{\rho_l} \cdot \frac{d\rho_l}{dt} \right) \right]$ <p>Expanding <math>d\rho_l/dt</math> as a function of the state variables <math>P_l</math> and <math>h_l</math> yields:</p>

(continued)

(continued)

**Equation 3**

$\rho_l \cdot V_l \cdot \frac{du_l}{dt}$ $= V_l \cdot \left[ \left( \frac{P}{\rho_l} \cdot \left( \frac{\partial \rho_l}{\partial h_l} \right)_p + \rho_l \right) \cdot \frac{dh_l}{dt} + \left( \frac{P}{\rho_l} \cdot \left( \frac{\partial \rho_l}{\partial P} \right)_h - 1 \right) \cdot \frac{dP}{dt} \right]$ <p>Finally, expanding the full energy balance equation with the results above yields:</p>	$V_l \cdot \left[ \left( \frac{P}{\rho_l} \cdot \left( \frac{\partial \rho_l}{\partial h_l} \right)_p + \rho_l \right) \cdot \frac{dh_l}{dt} + \left( \frac{P}{\rho_l} \cdot \left( \frac{\partial \rho_l}{\partial P} \right)_h - 1 \right) \cdot \frac{dP}{dt} \right]$ $= \sum_i \dot{m}_i \cdot \left[ h_i - \left( h_l - \frac{P}{\rho_l} \right) \right] - \sum_o \dot{m}_o \cdot \left[ h_o - \left( h_l - \frac{P}{\rho_l} \right) \right] + W_{vl}$
--	--

**Equation 4**

Title	Dynamic energy balance equation for the steam phase
Validity domain	$\forall \dot{m}$ and $0 < V_v < V$
Mathematical formulation	$V_v \cdot \left[ \left( \frac{P}{\rho_v} \cdot \left( \frac{\partial \rho_v}{\partial P} \right)_h - 1 \right) \cdot \frac{dP}{dt} + \left( \frac{P}{\rho_v} \cdot \left( \frac{\partial \rho_v}{\partial h_v} \right)_p + \rho_v \right) \cdot \frac{dh_v}{dt} \right]$ $= \dot{m}_v \cdot \left[ h_{v,i} - \left( h_v - \frac{P}{\rho_v} \right) \right] + \dot{m}_{evap} \cdot \left[ h_v^{sat} - \left( h_v - \frac{P}{\rho_v} \right) \right]$ $= -\dot{m}_{cond} \cdot \left[ h_l^{sat} - \left( h_v - \frac{P}{\rho_v} \right) \right] - W_{vl} + W_{out}$
Comments	This equation establishes the energy balance between the incoming steam, the condensation, and the evaporation flows. The evaporation flow term is added for the sake of completeness as it should always be zero during normal operation of the condenser. The derivation of this equation is similar to Eq. 3

**Equation 5**

Title	Power exchanged by convection between the two phases inside the cavity
Validity domain	$\forall T_l$ and $\forall T_v$
Mathematical formulation	$W_{vl} = K_{vl} \cdot A_{vl} \cdot (T_v - T_l)$
Comments	See (9.5)

**Equation 6**

Title	Power exchanged between the cavity and the pipe bundle
Validity domain	$\forall \dot{m}_c$ and $\forall \dot{m}_v$
Mathematical formulation	$W_{out} = \dot{m}_{v,i} \cdot (h_{v,i} - h_l) = \dot{m}_c \cdot (h_{c,i} - h_{c,o})$
Comments	All the steam power is transferred to the cooling fluid

Equation 7	
Title	Momentum balance equation for the cold fluid
Validity domain	$\forall \dot{m}_c$
Mathematical formulation	$P_{c,i} - P_{c,o} = \Delta P_f + \Delta P_g$ $\Delta P_f = \frac{\Lambda \cdot \dot{m}_c \cdot  \dot{m}_c }{2 \cdot A_t^2 \cdot \rho_c}$ $\Delta P_g = \rho_c \cdot g \cdot (z_2 - z_1)$
Comments	<p>The purpose of this equation is to compute the mass flow rate of the cooling fluid that is used to compute the power evacuated from the condenser (cf. Eq. 6)</p> <p>The friction coefficient <math>\Lambda</math>, cf. (13.17), can be calculated using the various correlations presented in Sect. 13.2</p>

In order to have a full system of equations that can be solved, this set of equations must be completed by the state equations for the following water and steam properties:  $h_l^{\text{sat}}$ ,  $h_v^{\text{sat}}$ ,  $\rho_c$ ,  $\rho_l$ ,  $\rho_v$ ,  $x_l$  and  $x_v$ .

### 9.5.3.4 Modelica Component Model: *SimpleDynamicCondenser*

The governing equations are implemented in the *SimpleDynamicCondenser* component model located in the *WaterSteam.HeatExchangers* sub-library.

Figure 9.25a represents the graphical icon of the component with its five connectors.

### 9.5.3.5 Test-Case

The model *TestSimpleDynamicCondenser* used to validate the *SimpleDynamicCondenser* component model is represented in Fig. 9.25b. This model uses the following component models:

- One *SimpleDynamicCondenser* component model;
- Four *SingularPressureLoss* component models;
- Two *SourceQ* component models;
- Two *SinkP* component models.

#### Test-Case Parameterization and Boundary Conditions

The model data are:

- Cavity volume = 1000 m<sup>3</sup>
- Cavity cross-sectional area = 100 m<sup>2</sup>
- Fraction of initial liquid volume in the cavity = 0.15
- Inlet altitude of the pipes = 0
- Outlet altitude of the pipes = 0.5 m

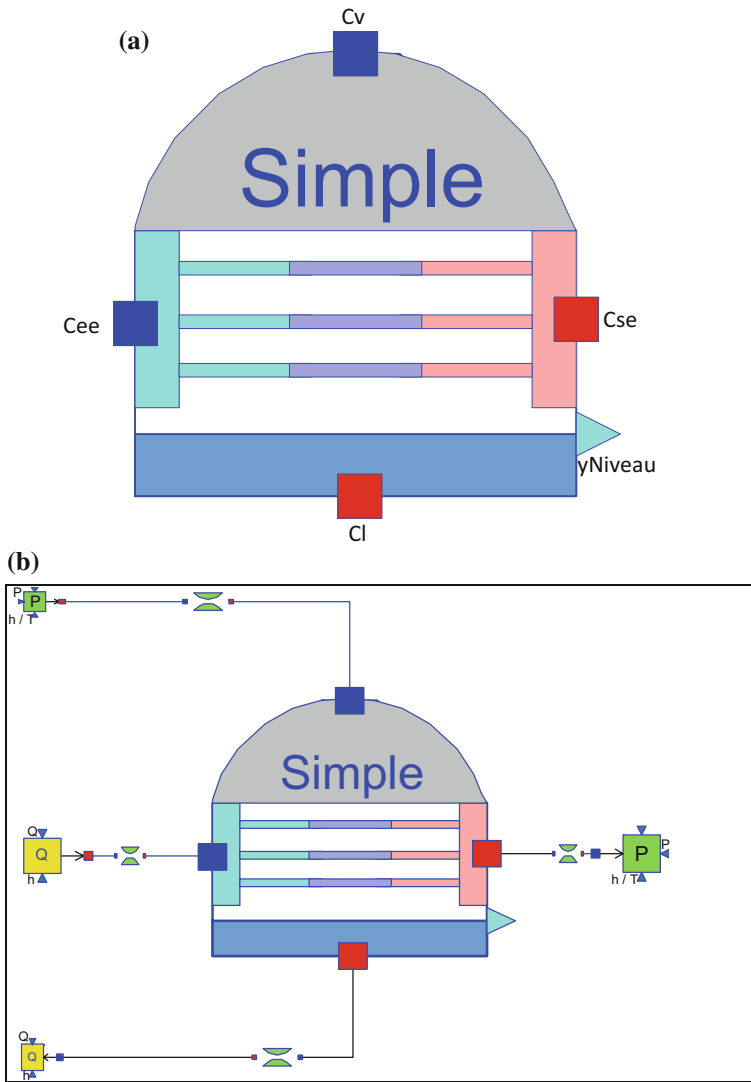


**Fig. 9.25** **a** Icon of the *SimpleDynamicCondenser* component model and **b** test-case for the *SimpleDynamicCondenser* component model

- Internal diameter of the pipes = 0.018 m
- Thickness of the pipes = 0.001 m
- Length of the pipes = 10 m
- Inlet altitude of the pipes = 0
- Outlet altitude of the pipes = 0
- Number of pipes in parallel = 28,700

- Mass flow rate of the hot fluid at the outlet (condensate) = 192 kg/s
- Mass flow rate of the hot fluid at the inlet (steam) = 192 kg/s
- Specific enthalpy of the hot fluid at the inlet (steam) = 2,401,000 J/kg
- Mass flow rate of the cold fluid at the inlet (cooling water) = 29804.5 kg/s
- Specific enthalpy of the cold fluid at the inlet (cooling water) =  $113 \times 10^3$  J/kg
- Pressure of the cold fluid at the outlet (cooling water) =  $10^5$  Pa
- Pressure loss coefficient of each *SingularPressureLoss* = 0.0001 m<sup>-4</sup>.

### Model Calibration

The calibration procedure consists in setting the specific enthalpy of the cold fluid at the outlet to a known measurement value and computing by model inversion the value of mass flow rate of the cold fluid at the inlet.

Another possible calibration consists in setting (fixing) the pressure of the cold fluid at the inlet to a known measurement value and computing by model inversion the value of the mass flow rate of the cold fluid at the inlet.

### Simulation Results

The simulation of the test scenario produces the numerical results below:

- Cavity pressure = 10,000 Pa
- Specific enthalpy of liquid in the cavity = 191,812 J/kg
- Specific enthalpy of the cold fluid at the outlet = 127,232 J/kg
- Pressure of the cold fluid at the inlet = 146,535 Pa.

#### **9.5.4 Dynamic Modeling of a Condenser**

A condenser is a two-phase heat exchanger; cf. Fig. 9.24. The cooling water flows inside the tube bundle, while the steam and condensate flow outside those tubes and inside the cavity.

The condenser model is called *DynamicCondenser*. It represents the dynamics of the thermohydraulic phenomena of the hot fluid inside the cavity and of the cooling fluid which flows through the tube bundle. In particular, the model features the thermal exchanges between the fluid in the cavity and the cooling fluid flowing through the tube bundle.

The condenser is considered as a vertical or horizontal cylindrical cavity, containing a tube bundle with the cooling water inlet and outlet located on opposite sides.

In the condenser, there are two zones: the desuperheating zone and the condensation zone.

The model is divided into three sub-models of different types which are connected together to make the full model (cf. Fig. 9.26a):

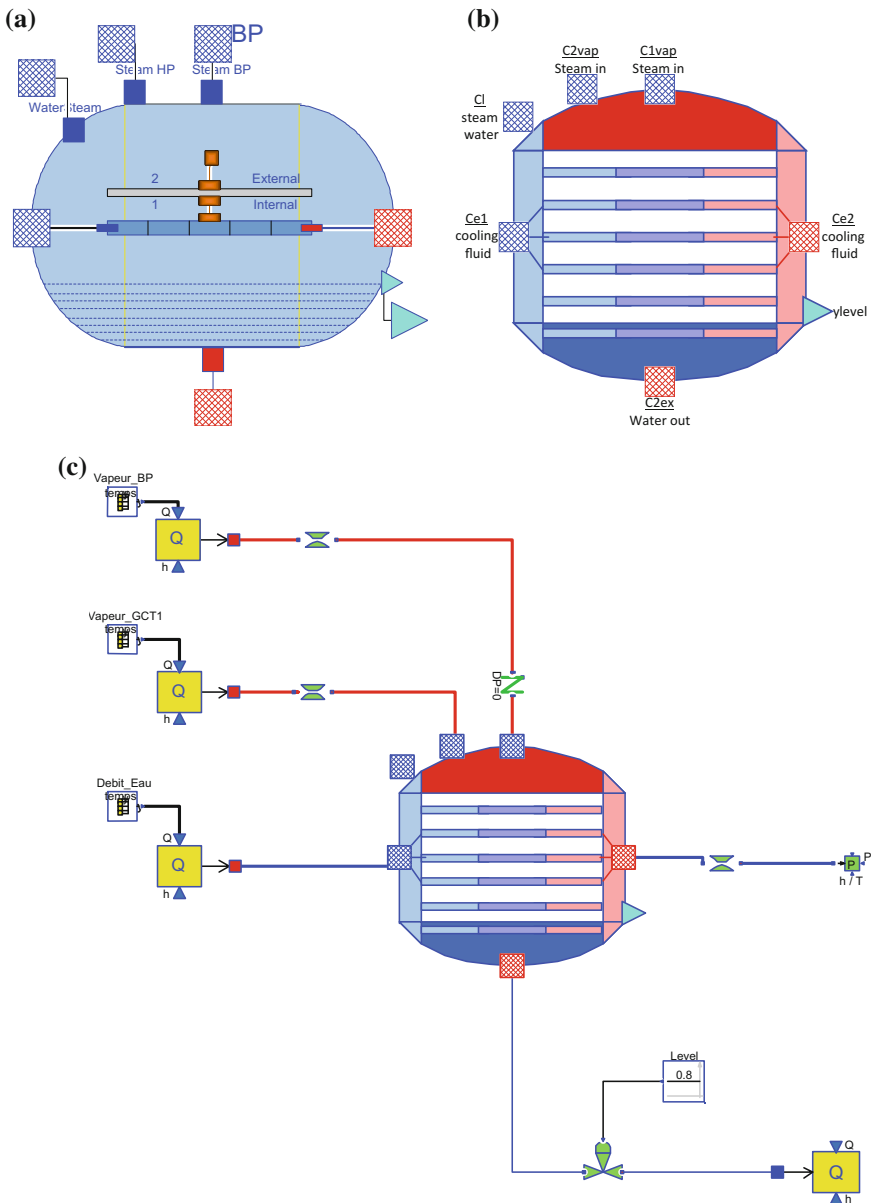


**Fig. 9.26** **a** Model of the *DynamicCondenser* component model, **b** icon of the *DynamicCondenser* component model, and **c** test-case for the *DynamicCondenser* component model

- One *DynamicOnePhaseFlowPipe* component model;
- One *HeatExchangerWall* component model;
- One *TwoPhaseCavityOnePipe* component model.

By reassembling the sub-models, any other configuration of the condenser can be modeled.

#### 9.5.4.1 Modelica Component Model: *DynamicCondenser*

The governing equations are implemented in the *DynamicCondenser* located in the *WaterSteam.HeatExchangers* sub-library.

Figure 9.26b represents the graphical icon of the component with its seven connectors.

#### 9.5.4.2 Test-Case

To simulate the complex dynamic physical behavior in normal conditions of the condenser model, a test model has been developed by assembling the necessary components from the ThermoSysPro library.

The model *TestDynamicCondenser* used to validate the *DynamicCondenser* component model is represented in Fig. 9.26c. This model uses the following component models:

- One *DynamicCondenser* component model;
- Three *SingularPressureLoss* component models;
- One *IdealCheckValve* component model;
- One *ControlValve* component model;
- Three *SourceQ* component models;
- One *SinkP* component model;
- One *SinkQ* component model;
- One *Constant* block;
- Three *TimeTable* blocks.

In the test-case scenario, the *DynamicCondenser* component receives: (1) the steam pressure and specific enthalpy at the steam inlet, (2) the condensate mass flow rate at the condensate outlet, (3) the cooling fluid mass flow rate and specific enthalpy at the cooling fluid inlet, and (4) the cooling fluid pressure at the cooling fluid outlet. The component computes: (1) for the cavity, the pressure, the specific enthalpy and the volume of each phase in the cavity, the pressure at the condensate outlet, the wall temperature, and the corrective term for the heat exchange coefficient (using inverse calculation), and (2) for the cooling fluid, the pressure at the inlet, the distribution of the fluid pressure, temperature, specific enthalpy, mass flow rate, and the distribution of the wall temperature.

### Test-Case Parameterization and Boundary Conditions

In order to challenge the dynamic simulation capabilities of the model, islanding with a turbine trip is used as the test scenario (cf. Sect. 9.5.2.2).

The boundary conditions of the model (scenario profiles) are presented in Table 9.2.

All geometrical data were provided to the model (tubes' and exchangers' lengths, diameters, volumes, corrective terms for the heat exchange coefficients, corrective terms for the pressure losses, etc.). The model data are:

**Table 9.2** (a) Mass flow rate of the LP steam at the inlet, (b) mass flow rate of the cooling water at the inlet, and (c) mass flow rate of the HP steam at the inlet

Time (s)	Mass flow rate (kg/s)
<i>(a) Mass flow rate of the LP steam at the inlet</i>	
0	310
22	310
24	150
25	80
28	15
31	$10^{-6}$
1000	$10^{-6}$
<i>(b) Mass flow rate of the cooling water at the inlet</i>	
0	19,000
8	19,000
9	1500
9.6	$10^{-6}$
100	$10^{-6}$
<i>(c) Mass flow rate of the HP steam at the inlet</i>	
0	$10^{-4}$
22	$10^{-4}$
24	2.02
25	100
26	150
28	300
29.7	590
30.2	600
30.5	590
31	570
35	250
40	100
45	15
47	$10^{-6}$
1000	$10^{-6}$

- Fraction of initial liquid volume in the cavity = 0.056
- Radius of the cavity = 8.15 m
- Cavity length = 12 m
- Pipes' length = 12 m
- Internal diameter of the cooling pipes = 0.016 m
- Thickness of the cooling pipes = 0.0005 m
- Number of pipes in the cavity = 52,176
- Numbers of pipes in a vertical row (tube bank) = 223
- Specific heat capacity of the metal of the cooling pipes = 506 J/kg/K
- Density of the metal of the cooling pipes = 7780 kg/m<sup>3</sup>
- Wall thermal conductivity of the cooling pipes = 20 W/m/K
- Wall mass = 50,000 kg
- Maximum flow coefficient of the valve = 15,000 U.S.
- Cavity pressure = 3199.2 Pa
- Condensate mass flow rate “Puit\_condenseur1” = 310 kg/s
- Specific enthalpy of the BP steam “Source\_vapeur” = 2,400,000 J/kg
- Specific enthalpy of the HP steam “Source\_Vsup1” = 2,759,000 J/kg
- Specific enthalpy of the cooling water “Source\_Eau” =  $50 \times 10^3$  J/kg
- Pressure of the cooling water “Puit\_Eau” =  $10^5$  Pa
- Pressure loss coefficient of each *SingularPressureLoss* model =  $10^{-4}$  m<sup>-4</sup>.

### Model Calibration

The calibration procedure consists in setting the cavity pressure to a known measurement value (=3199.2 Pa) and computing by model inversion the value of the corrective term of the heat exchange coefficient in the cavity (COP = 0.706066).

### Simulation Results

Figure 9.27 shows the results of the simulation for a scenario of islanding with a steam turbine trip. For this scenario, the most important quantity to be examined is the pressure in the condenser. The results (curve 4) show that the maximum pressure in the condenser is less than 0.15 bar.

#### 9.5.5 Static Modeling of a Water Heater

The static water heating component model is called *NTUWaterHeater*. The water heater is a two-phase shell-and-tube heat exchanger; cf. Fig. 9.28. A heat exchanger, as its name suggests, is designed to transmit heat from a hot fluid (brown flow) to a cold fluid (blue flow). The feed water flows inside the tube bundle, while the steam

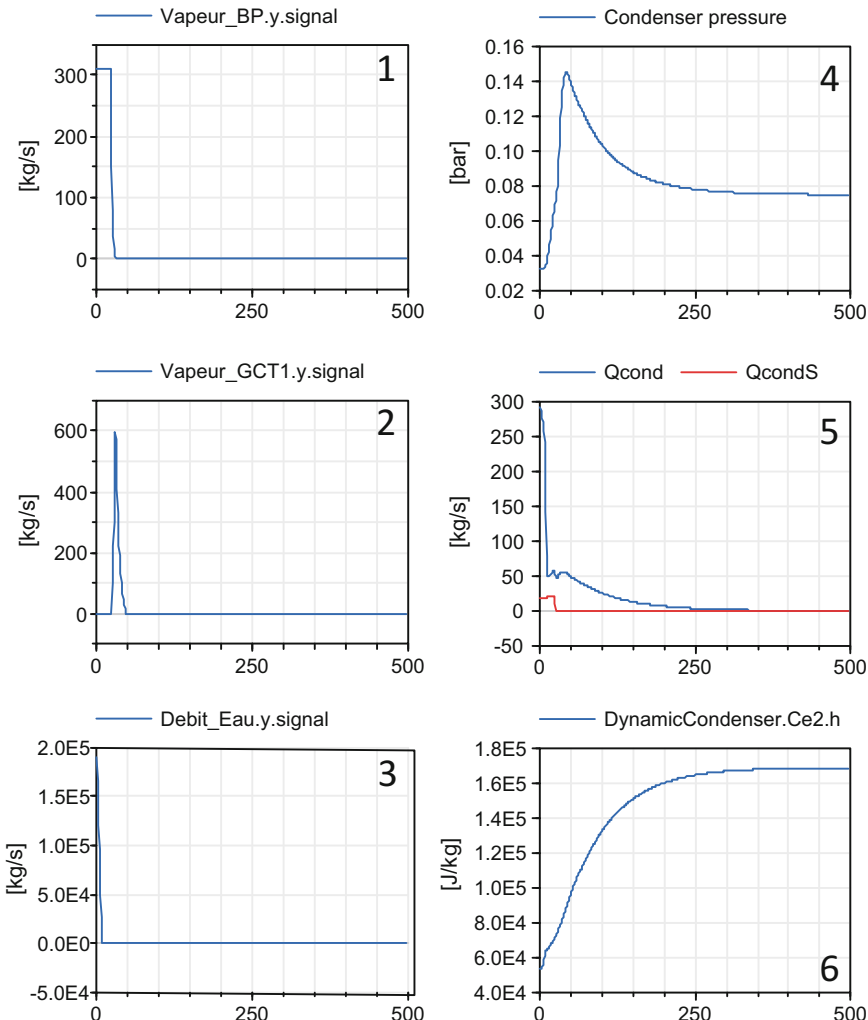


**Fig. 9.27** Simulation results for *DynamicCondenser*: (1) mass flow rate of the LP steam, (2) mass flow rate of the HP steam, (3) mass flow rate of the cooling water, (4) pressure in the cavity, (5) mass flow rates of the condensates, and (6) specific enthalpy of the cooling water at the outlet

and the condensate flow outside those tubes (and inside the cavity). In the static water heater, there are three distinct areas: (1) the desuperheating zone, (2) the condensation zone, both located in the upper part of the component, and (3) the subcooled zone, located in the lower part of the component. In some water heaters, the condensate of the water heater located upstream from the current water heater is reinjected into the current water heater. During reinjection, part of the condensate may vaporize due to the pressure drop (this phenomenon is known as flash).

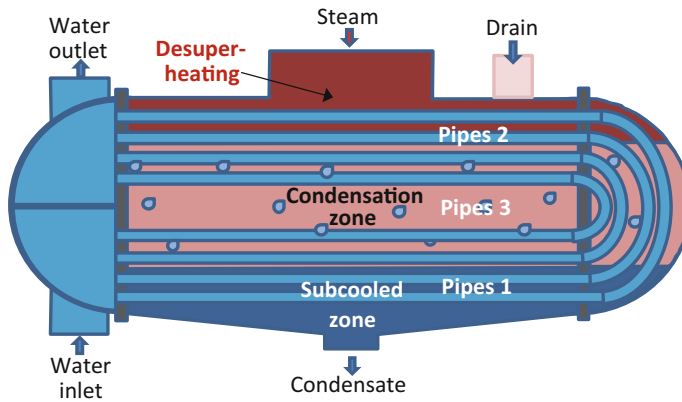


**Fig. 9.28** Schematic diagram of a water heating heat exchanger

### 9.5.5.1 Nomenclature

Symbols	Definition	Unit
$c_{p,c,cond}$	Cold fluid specific heat capacity of the condensation zone	J/kg/K
$c_{p,c,des}$	Cold fluid specific heat capacity of the desuperheating zone	J/kg/K
$c_{p,h,des}$	Hot fluid specific heat capacity of the desuperheating zone	J/kg/K
$c_{p,d,o}$	Specific heat capacity of the outlet drain	J/kg/K
$c_{p,c,d}$	Cold fluid specific heat capacity of the subcooled zone	J/kg/K
$h_{c,i}$	Cold fluid (water) specific enthalpy at the inlet	J/kg
$h_{c,o}$	Cold fluid (water) specific enthalpy at the outlet	J/kg
$h_{c,cond}$	Cold fluid (after drain cooling) specific enthalpy at the inlet of the condensation zone	J/kg
$h_{c,des}$	Cold fluid specific enthalpy at the inlet of the desuperheating zone	J/kg
$h_{d,i}$	Fluid specific enthalpy of the drain inlet	J/kg
$h_{h,i}$	Hot fluid (steam) specific enthalpy at the inlet	J/kg
$h_{h,o}$	Hot fluid (drain) specific enthalpy at the outlet	J/kg
$h_{h,sub}$	Hot fluid specific enthalpy at the inlet of the subcooled zone	J/kg
$h_l^{\text{sat}}$	Hot fluid saturation enthalpy of the liquid	J/kg
$h_v^{\text{sat}}$	Hot fluid saturation enthalpy of the steam	J/kg
$\dot{m}_c$	Cold fluid mass flow rate	kg/s
$\dot{m}_h$	Hot fluid mass flow rate	kg/s
$\dot{m}_{d,i}$	Mass flow rate of the input drain	kg/s
$\dot{m}_{d,o}$	Mass flow rate of the output drain	kg/s
$P_{c,i}$	Cold fluid pressure at the inlet	Pa
$P_{c,o}$	Cold fluid pressure at the outlet	Pa
$S_{\text{cond}}$	Exchange surface of the condensation zone	m <sup>2</sup>

(continued)

(continued)

Symbols	Definition	Unit
$S_{des}$	Exchange surface of the desuperheating zone	$\text{m}^2$
$S_{liq}$	Exchange surface of the subcooled zone	$\text{m}^2$
$T_{h,i}$	Hot fluid (steam) temperature at the inlet	K
$T_{h,\text{sub}}$	Hot fluid temperature at the inlet of the subcooled zone	K
$T_{\text{sat}}$	Saturation temperature of the hot fluid	K
$T_{c,i}$	Cold fluid (water) temperature at the inlet	K
$T_{c,o}$	Cold fluid temperature at the outlet	K
$T_{c,\text{cond}}$	Cold fluid temperature at the inlet of the condensation zone	K
$T_{c,\text{des}}$	Cold fluid temperature at the inlet of the desuperheating zone	K
$W_{\text{cond}}$	Thermal power exchanged in the condensation zone	W
$W_{\text{des}}$	Thermal power exchanged in the desuperheating zone	W
$W_{\text{sub}}$	Thermal power exchanged in the subcooled zone	W
$W_{\text{vapo}}$	Thermal power exchanged for the partial vaporization of the input drain (flash)	W
$x_d$	Vapor mass fraction in the subcooled zone	—
$\varepsilon_{\text{cond}}$	NTU effectiveness of the condensation zone; cf. Sect. 9.2.6	—
$\varepsilon_d$	NTU effectiveness of the subcooled zone	—
$\varepsilon_{\text{des}}$	NTU effectiveness of the desuperheating zone	—
$\Lambda$	Friction pressure loss coefficient for the cold fluid	$\text{m}^{-4}$
$\rho_c$	Cold fluid density	$\text{kg/m}^3$

### 9.5.5.2 Assumptions

The water heating heat exchanger is modeled according to the following assumptions:

- 0D modeling (with three zones).
- The phenomenon of longitudinal heat conduction in the wall and in the fluid is neglected.
- Counter-flow heat exchanger.
- The thermophysical properties are calculated on the basis of the average pressure and specific enthalpy in each mesh cell.

### 9.5.5.3 Governing Equations

The model is based on the static energy balance equation using the number of transfer units (NTU) method and the momentum balance equation.

The *NTUWaterHeater* component model represents the thermal exchanges between the fluid in the cavity and the cooling fluid flowing through the tube bundle. This model is subdivided into the following zones (as represented in Fig. 9.29):

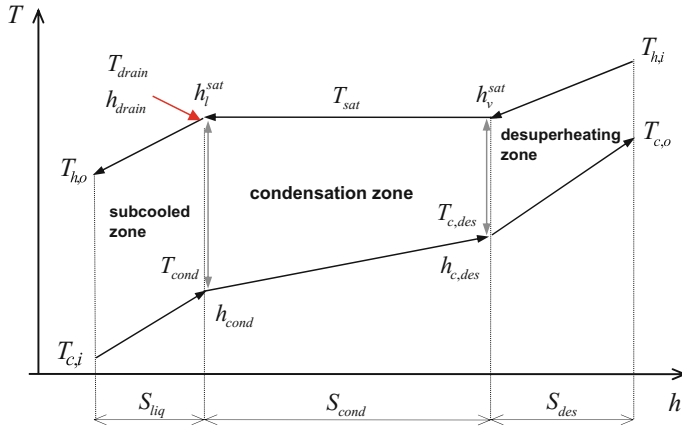


**Fig. 9.29** Division of the heat exchanger into three operating zones

- The *desuperheating zone*, where the superheated steam, flowing into the heater, exchanges heat with the liquid flowing through the tube bundle, until it becomes saturated steam and enters the condensation zone;
- The *condensation zone*, where the saturated steam condenses as a consequence of the thermal exchange with the tube bundle, turning into liquid water that enters the subcooled zone;
- The *subcooled zone*, where the liquid inside the cavity continues to exchange heat with the liquid flowing through the tube bundle.

The model is formulated in order to correctly handle possible flow reversal conditions.

#### Equation 1

Title	Thermal power exchanged in the desuperheating zone defined by $h_{h,i} > h_v^{sat}$
Validity domain	$\dot{m}_h > 0$ and $\dot{m}_c > 0$
Mathematical formulation	$W_{des} = \dot{m}_h \cdot (h_{h,i} - h_v^{sat})$ $= \dot{m}_c \cdot (h_{c,o} - h_{c,des})$ $= \min(\dot{m}_h \cdot c_{p,h,des}, \dot{m}_c \cdot c_{p,c,des}) \cdot \varepsilon_{des} \cdot (T_{h,i} - T_{c,des})$
Comments	<p>These equations are used only if <math>h_{h,i} &gt; h_v^{sat}</math> (i.e., presence of a desuperheating zone); cf. Sect. 9.2.6.</p> <p>If not (i.e., for <math>h_{h,i} \leq h_v^{sat}</math>), then <math>W_{des} = 0</math>.</p> <p>The objective of these equations is to compute the desuperheating power <math>W_{des}</math> and the specific enthalpy <math>h_{c,o}</math> of the cold fluid at the outlet. In addition, the desuperheating heat exchange surface <math>S_{des}</math> can be obtained from the effectiveness <math>\varepsilon_{des}</math>; cf. Sect. 9.2.6</p>

**Equation 2a**

Title	Thermal power exchanged in the condensation zone if $h_{h,i} > h_v^{\text{sat}}$
Validity domain	$\dot{m}_h > 0$ and $\dot{m}_c > 0$
Mathematical formulation	$\begin{aligned} W_{\text{cond}} &= \dot{m}_h \cdot (h_v^{\text{sat}} - h_l^{\text{sat}}) + W_{\text{vapo}} \\ &= \dot{m}_c \cdot (h_{c,\text{des}} - h_{c,\text{cond}}) \\ &= \dot{m}_c \cdot c_{p,c,\text{cond}} \cdot \epsilon_{\text{cond}} \cdot (T_{\text{sat}} - T_{c,\text{cond}}) \end{aligned}$
Comments	<p>These equations are used only if <math>h_{h,i} &gt; h_v^{\text{sat}}</math> (i.e., presence of a desuperheating zone); cf. Sect. 9.2.6.</p> <p>The objective of these equations is to compute the specific enthalpy <math>h_{c,\text{des}}</math> of the cold fluid at the outlet of this zone and the mass flow rate <math>\dot{m}_h</math> of the hot fluid (steam) at the input</p>

**Equation 2b**

Title	Thermal power exchanged in the condensation zone if $h_{h,i} \leq h_v^{\text{sat}}$
Validity domain	$\dot{m}_h > 0$ and $\dot{m}_c > 0$
Mathematical formulation	$\begin{aligned} W_{\text{cond}} &= \dot{m}_h \cdot (h_{h,i} - h_l^{\text{sat}}) + W_{\text{vapo}} \\ &= \dot{m}_c \cdot (h_{c,\text{des}} - h_{c,\text{cond}}) \\ &= \dot{m}_c \cdot c_{p,c,\text{cond}} \cdot \epsilon_{\text{cond}} \cdot (T_{\text{sat}} - T_{c,\text{cond}}) \end{aligned}$
Comments	<p>These equations are used only if <math>h_{h,i} \leq h_v^{\text{sat}}</math> (i.e., absence of the desuperheating zone); cf. Sect. 9.2.6.</p> <p>The objective of these equations is to compute the specific enthalpy <math>h_{c,\text{cond}}</math> of the cold fluid at the outlet of this zone and the mass flow rate <math>\dot{m}_h</math> of the hot fluid (steam) at the input</p>

**Equation 3**

Title	Thermal power exchanged in the drain by partial vaporization (flash)
Validity domain	$\dot{m}_{d,i} \geq 0$
Mathematical formulation	$W_{\text{vapo}} = \dot{m}_{d,i} \cdot x_d \cdot (h_v^{\text{sat}} - h_l^{\text{sat}})$
Comments	<p>This equation can also be written as</p> $W_{\text{vapo}} = \dot{m}_{d,i} \cdot (h_{d,i} - h_l^{\text{sat}})$ <p>since</p> $\dot{m}_{d,i} \cdot h_{d,i} = \dot{m}_{d,i} \cdot x_d \cdot h_v^{\text{sat}} + \dot{m}_{d,i} \cdot (1 - x_d) \cdot h_l^{\text{sat}}$

**Equation 4**

Title	Energy balance equation at the inlet of the subcooled zone (mixing of the hot fluid with the drain fluid) if $x_d = 0$
Validity domain	$\dot{m}_{d,o} \neq 0$
Mathematical formulation	$\dot{m}_{d,o} \cdot h_{h,\text{sub}} = \dot{m}_h \cdot h_l^{\text{sat}} + \dot{m}_{d,i} \cdot h_{d,i}$
Comments	<p>The objective of this equation is to compute the specific enthalpy <math>h_{h,\text{sub}}</math> at the inlet of the subcooled zone for the hot fluid.</p> <p>If <math>x_d &gt; 0</math>, then <math>h_{h,\text{sub}} = h_l^{\text{sat}}</math></p>

---

Equation 5

---

Title	Energy balance equation for subcooled zone (drain cooling) if $S_{\text{liq}} > 0$
Validity domain	$\dot{m}_c > 0$ and $\dot{m}_{d,o} > 0$
Mathematical formulation	$\begin{aligned} W_{\text{sub}} &= \dot{m}_{d,o} \cdot (h_{h,\text{sub}} - h_{h,o}) \\ &= \dot{m}_c \cdot (h_{c,\text{cond}} - h_{c,i}) \\ &= \min(\dot{m}_{d,o} \cdot c_{p,d,o}, \dot{m}_c \cdot c_{p,c,d}) \cdot \varepsilon_d \cdot (T_{h,\text{sub}} - T_{c,i}) \end{aligned}$
Comments	If $S_{\text{liq}} = 0$ , then $W_{\text{sub}} = 0$ and $h_{h,o} = h_{h,\text{sub}}$

---

Equation 6

---

Title	Mass balance equation for the hot fluid (mixing of the hot fluid with the drain fluid)
Validity domain	$\dot{m}_h > 0$ and $\dot{m}_{d,i} \geq 0$
Mathematical formulation	$\dot{m}_{d,o} = \dot{m}_h + \dot{m}_{d,i}$

---

Equation 7

---

Title	Momentum balance equation for the cold fluid (pressure loss equation in the water pipes)
Validity domain	$\forall \dot{m}_c$
Mathematical formulation	$P_{c,i} - P_{c,o} = \Lambda \cdot \frac{\dot{m}_c \cdot  \dot{m}_c }{\rho_c}$
Comments	Only pressure losses due friction are taken into account

---

In order to have a full system of equations that can be solved, this set of equations must be completed by the state equations for the following water and steam properties:  $h_l^{\text{sat}}$ ,  $h_v^{\text{sat}}$ ,  $\rho_c$ ,  $c_p$  and  $T_{\text{sat}}$ .

### 9.5.5.4 Modelica Component Model: *NTUWaterHeater*

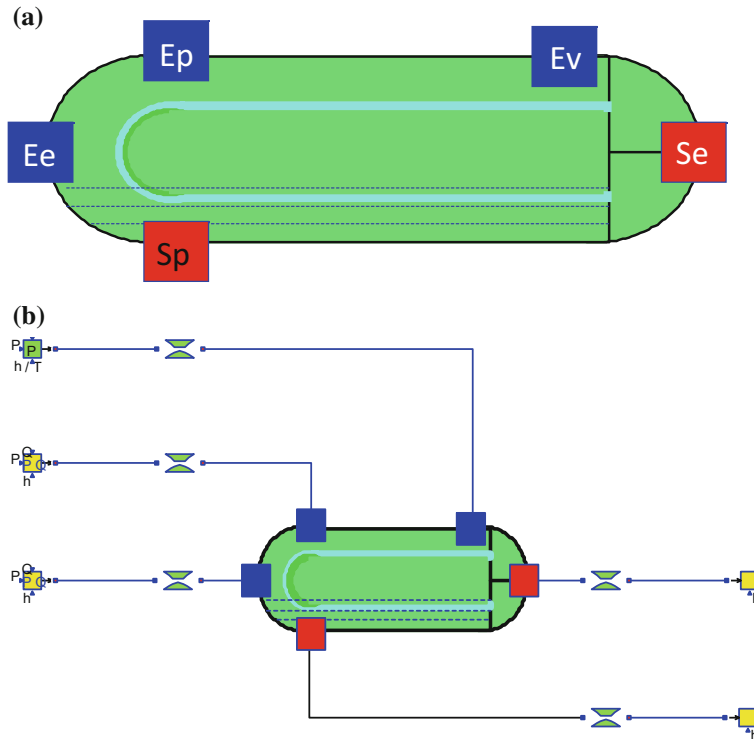
The governing equations are implemented in the *NTUWaterHeater* component model located in the *WaterSteam.HeatExchangers* sub-library.

Figure 9.30a represents the graphical icon of the component with its five connectors.

### 9.5.5.5 Test-Case

The model *TestNTUWaterHeater* used to validate the *NTUWaterHeater* component model is represented in Fig. 9.30b. This model uses the following component models:

- One *NTUWaterHeater* component model;
- Five *SingularPressureLoss* component models;



**Fig. 9.30** **a** Icon of the *NTUWaterHeater* component model and **b** test-case for the *NTUWaterHeater* component model

- One *SourceP* model component model;
- Two *SourcePQ* component models;
- Two *SinkP* component models.

In the test-case scenario, the *NTUWaterHeater* component receives: (1) the steam pressure and specific enthalpy at the steam inlet, (2) the drain pressure, mass flow rate, and specific enthalpy at the drain inlet, and (3) the cold fluid pressure, mass flow rate, and specific enthalpy at the inlet. The component computes: (1) the steam mass flow rate at the steam inlet, (2) the drain pressure, mass flow rate, and specific enthalpy at the drain outlet, and (3) the cold fluid pressure and specific enthalpy at the outlet.

## Test-Case Parameterization and Boundary Conditions

The model data are:

- Exchange surface for the condensation and deheating =  $5752 \text{ m}^2$
- Drain surface ( $>0$ : with drain cooling) =  $1458 \text{ m}^2$
- Water pressure at the inlet =  $82.7 \times 10^5 \text{ Pa}$
- Water specific enthalpy at the inlet =  $780,830 \text{ J/kg}$
- Water mass flow rate at the inlet =  $1788.9 \text{ kg/s}$
- Drain pressure at the inlet =  $27.79 \times 10^5 \text{ Pa}$
- Drain specific enthalpy at the inlet =  $889,890 \text{ J/kg}$
- Drain mass flow rate at the inlet =  $118.02 \text{ kg/s}$
- Water pressure at the outlet =  $80.19 \times 10^5 \text{ Pa}$
- Water specific enthalpy at the outlet =  $872,080 \text{ J/kg}$
- Water specific enthalpy at the outlet of drain =  $780,130 \text{ J/kg}$
- Steam pressure at the inlet =  $17.49 \times 10^5 \text{ Pa}$
- Steam specific enthalpy at the inlet =  $2,432,500 \text{ J/kg}$
- Pressure loss coefficient of each *SingularPressureLoss* model =  $10^{-4} \text{ m}^{-4}$ .

## Model Calibration

The calibration phase consists in setting the pressure at the outlet of the cold fluid, the specific enthalpy of the cold fluid at the outlet (water), the specific enthalpy of the hot fluid at the outlet (drain) to known measurement values and computing by model inversion the values of the friction pressure loss of the cold fluid, the heat exchange coefficient for the subcooled zone, and the heat exchange coefficient for the condensation zone.

## Simulation Results

The simulation of the test scenario produces the numerical results below:

- Hot fluid (steam) mass flow rate =  $112.603 \text{ kg/s}$
- Friction pressure loss coefficient for the cold fluid =  $68.979$
- Heat exchange coefficient for the condensation zone =  $3500.27 \text{ W/m}^2/\text{K}$
- Heat exchange coefficient for the subcooled zone =  $1327.7 \text{ W/m}^2/\text{K}$
- Thermal power exchanged =  $199.02 \times 10^6 \text{ W}$
- Cold fluid temperature at the outlet =  $476.97 \text{ K}$
- Hot fluid temperature at the outlet =  $456.92 \text{ K}$ .

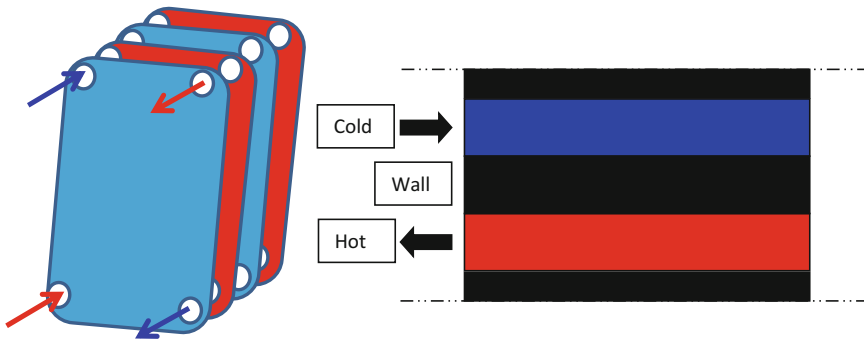


**Fig. 9.31** Schematic diagram of a plate heat exchanger

## 9.6 Plate Heat Exchanger Modeling

The plate heat exchanger is composed of a large number of plates arranged in a thousand sheets that are separated from each other by a small space where fluids flow. The plates are not flat: They exhibit a wavy surface in a specific pattern in order to create a turbulent flow that generates a better heat transfer. This type of exchanger is widely used in the food industry because it can easily be taken apart for cleanup; cf. Fig. 9.31.

### 9.6.1 Dynamic Modeling of a Plate Heat Exchanger

The plate heat exchanger model is called *DynamicPlateHeatExchanger*. This model represents a single-phase counter-flow thermal exchange between the hot fluid and the cold fluid. The two fluids are separated by a wall through which heat transfer takes place by conduction. Between the fluids and the wall, heat transfer takes place by convection.

#### 9.6.1.1 Nomenclature

Symbols	Definition	Unit	Mathematical definition
$c_{p,c,i}$	Cold fluid specific heat in thermal cell $i$	J/kg/K	
$c_{p,h,i}$	Hot fluid specific heat in thermal cell $i$	J/kg/K	
$D_h$	Hydraulic diameter	m	
$e_m$	Wall thickness	m	
$h_{c,i}$	Cold fluid specific enthalpy in thermal cell $i$	J/kg	

(continued)

(continued)

Symbols	Definition	Unit	Mathematical definition
$h_{c,i:i+1}$	Cold fluid specific enthalpy in hydraulic cell $i:i + 1$	J/kg	
$h_{h,i}$	Hot fluid specific enthalpy in thermal cell $i$	J/kg	
$h_{h,i:i+1}$	Hot fluid specific enthalpy in hydraulic cell $i:i + 1$	J/kg	
$K_{c,i}$	Convective heat exchange coefficient for the cold fluid in thermal cell $i$	W/m <sup>2</sup> /K	
$K_{h,i}$	Convective heat exchange coefficient for the hot fluid in thermal cell $i$	W/m <sup>2</sup> /K	
$\dot{m}_{c,i:i+1}$	Cold fluid mass flow rate in hydraulic cell $i:i + 1$	kg/s	
$\dot{m}_{h,i:i+1}$	Hot fluid mass flow rate in hydraulic cell $i:i + 1$	kg/s	
$N$	Number of hydraulic cells	—	
$N_c$	Number of channels of each fluid	—	$(N_p - 1)/2$
$N_p$	Number of plates	—	
$P_{c,i}$	Cold fluid pressure at the outlet of thermal cell $i$	Pa	
$P_{h,i}$	Hot fluid pressure at the outlet of thermal cell $i$	Pa	
$Pr_{c,i}$	Prandtl number of the cold fluid in thermal cell $i$	—	$\frac{\mu_{c,i} \cdot c_{p,c,i}}{\lambda_{c,i}}$
$Pr_{h,i}$	Prandtl number of the hot fluid in thermal cell $i$	—	$\frac{\mu_{h,i} \cdot c_{p,h,i}}{\lambda_{h,i}}$
$Re_{c,i:i+1}$	Reynolds number of the cold fluid in hydraulic cell $i:i + 1$	—	$\frac{4 \cdot \dot{m}_{c,i:i+1}}{\pi \cdot D_h \cdot \mu_{c,i} \cdot N_c}$
$Re_{h,i:i+1}$	Reynolds number of the hot fluid in hydraulic cell $i:i + 1$	—	$\frac{4 \cdot \dot{m}_{h,i:i+1}}{\pi \cdot D_h \cdot \mu_{h,i} \cdot N_c}$
$S_p$	Plate area	m <sup>2</sup>	
$T_{c,i}$	Temperature of the cold fluid in thermal cell $i$	K	
$T_{h,i}$	Temperature of the hot fluid in thermal cell $i$	K	
$T_{w,c,i}$	Wall temperature of for cold fluid in thermal cell $i$	K	
$T_{w,h,i}$	Wall temperature for the hot fluid in thermal cell $i$	K	
$U_i$	Global heat transfer coefficient for thermal cell $i$	W/m <sup>2</sup> /K	
$V_c$	Cold fluid volume	m <sup>3</sup>	
$V_h$	Hot fluid volume	m <sup>3</sup>	
$\Delta A_i$	Heat exchange surface for thermal cell $i$	m <sup>2</sup>	$\frac{S_p \cdot (N_p - 2)}{N - 1}$
$\Delta W_i$	Thermal power released by the hot fluid to the cold fluid for thermal cell $i$	W	

(continued)

(continued)

Symbols	Definition	Unit	Mathematical definition
$\lambda_{c,i}$	Cold fluid thermal conductivity in thermal cell $i$	W/m/K	
$\lambda_{h,i}$	Hot fluid thermal conductivity in thermal cell $i$	W/m/K	
$\lambda_m$	Metal thermal conductivity	W/m/K	
$\Lambda_c$	Friction pressure loss coefficient of the entire length of the exchanger for the cold fluid	$m^{-4}$	
$\Lambda_h$	Friction pressure loss coefficient of the entire length of the exchanger for the hot fluid	$m^{-4}$	
$\mu_{c,i}$	Cold fluid dynamic viscosity in thermal cell $i$	Pa s	
$\mu_{c,i:i+1}$	Cold fluid dynamic viscosity in hydraulic cell $i:i + 1$	Pa s	
$\mu_{h,i}$	Hot fluid dynamic viscosity in thermal cell $i$	Pa s	
$\mu_{h,i:i+1}$	Hot fluid dynamic viscosity in hydraulic cell $i:i + 1$	Pa s	
$\rho_{c,i}$	Cold fluid density in thermal cell $i$	kg/m <sup>3</sup>	
$\rho_{h,i}$	Hot fluid density in thermal cell $i$	kg/m <sup>3</sup>	

### 9.6.1.2 Assumptions

The heat exchanger is modeled according to the following assumptions:

- Single-phase flow in each mesh cell.
- 1D modeling (using the finite-volume method).
- Counter-flow heat exchanger.
- The energy accumulation in the wall is neglected.
- The phenomenon of longitudinal heat conduction in the wall and in the fluid is neglected.
- The thermophysical properties are calculated on the basis of the average pressure and specific enthalpy in each mesh cell.

### 9.6.1.3 Governing Equations

The *DynamicPlateHeatExchanger* component model is based on the dynamic energy and momentum balance equations, which are originally given as 1D partial

differential equations. The model is formulated in order to correctly handle possible flow reversal conditions.

---

#### Equation 1

Title	Steady-state mass balance equation (hot fluid)
Validity domain	$\forall \dot{m}_{h,i:i+1}$
Mathematical formulation	$\dot{m}_{h,i-1:i} - \dot{m}_{h,i:i+1} = 0$
Comments	Cf. (5.2)

---

#### Equation 2

Title	Steady-state mass balance equation (cold fluid)
Validity domain	$\forall \dot{m}_{c,i:i+1}$
Mathematical formulation	$\dot{m}_{c,i-1:i} - \dot{m}_{c,i:i+1} = 0$
Comments	Cf. (5.2)

---

#### Equation 3

Title	Dynamic energy balance equation (hot fluid)
Validity domain	$\forall \dot{m}_{h,i:i+1}$
Mathematical formulation	$\frac{V_h}{N-1} \cdot \rho_{h,i} \cdot \frac{dh_{h,i}}{dt} = \dot{m}_{h,i-1:i} \cdot h_{h,i-1:i} - \dot{m}_{h,i:i+1} \cdot h_{h,i:i+1} - \Delta W_i$
Comments	The fluid is assumed to be incompressible. The derivation of this equation is similar to Eq. 2c in Sect. 9.4.2

---

#### Equation 4

Title	Dynamic energy balance equation (cold fluid)
Validity domain	$\forall \dot{m}_{c,i:i+1}$
Mathematical formulation	$\frac{V_c}{N-1} \cdot \rho_{c,i} \cdot \frac{dh_{c,i}}{dt} = \dot{m}_{c,i-1:i} \cdot h_{c,i-1:i} - \dot{m}_{c,i:i+1} \cdot h_{c,i:i+1} + \Delta W_i$
Comments	The fluid is assumed to be incompressible. The derivation of this equation is similar to Eq. 2c in Sect. 9.4.2

---

#### Equation 5

Title	Heat exchanged between the hot and cold fluids
Validity domain	$\forall T_{h,i}$ and $\forall T_{c,i}$
Mathematical formulation	$\Delta W_i = U_i \cdot \Delta A_i \cdot (T_{h,i} - T_{c,i})$
Comments	<p>See (9.5).  The global heat transfer coefficient <math>U_i</math> between the two fluids is given by:</p> $\frac{1}{U_i} = \frac{1}{K_{h,i}} + \frac{1}{\lambda_m} + \frac{1}{K_{c,i}} \quad (1)$ $\frac{1}{e_m}$ <p>Equation (1) above is obtained by considering the power transferred by convection from the hot fluid to the wall, then by conduction through the wall [cf. (2.80)], and finally by convection from the wall to the cold fluid, yielding</p>

(continued)

(continued)

**Equation 5**

$$\begin{aligned}\Delta W_i &= K_{h,i} \cdot \Delta A_i \cdot (T_{h,i} - T_{w,h,i}) \\ &= \frac{\lambda_m}{e_m} \cdot \Delta A_i \cdot (T_{w,h,i} - T_{w,c,i}) \quad (2) \\ &= K_{c,i} \cdot \Delta A_i \cdot (T_{w,c,i} - T_{c,i})\end{aligned}$$

and by combining (2) above with (3) below

$$T_{h,i} - T_{c,i} = (T_{h,i} - T_{w,h,i}) + (T_{w,h,i} - T_{w,c,i}) + (T_{w,c,i} - T_{c,i}) \quad (3)$$

$K_{h,i}$  and  $K_{c,i}$  can be directly provided by the user, or computed with the Dittus–Boelter correlation, cf. (9.10):

$$K_{h,i} = 0.023 \cdot \lambda_{h,i} \cdot Re_{h,i}^{0.8} \cdot Pr_{h,i}^{0.4} / D_h$$

$$K_{c,i} = 0.023 \cdot \lambda_{c,i} \cdot Re_{c,i}^{0.8} \cdot Pr_{c,i}^{0.4} / D_c$$

It is assumed that  $Re_{h,i} = Re_{h,i+1}$  and  $Re_{c,i} = Re_{c,i+1}$

**Equation 6**

Title	Momentum balance equation (hot fluid)
Validity domain	$\forall \dot{m}_{h,ii+1}$
Mathematical formulation	$P_{h,i+1} = P_{h,i} - \frac{\Lambda_h}{N} \cdot \frac{\dot{m}_{h,ii+1} \cdot  \dot{m}_{h,ii+1} }{N_c^2 \cdot \rho_{h,i}}$
Comments	<p>Only pressure losses due to friction are taken into account; cf. (13.17). The friction coefficient <math>\Lambda_h</math> can be directly provided by the user or computed using a correlation.</p> <p>The following correlation is used for some specific plate heat exchangers with hydraulic diameter <math>D_h = 0.0356951</math>:</p> $\Lambda_h = 14423.2 \cdot c_1 \cdot \bar{m}_{h,ii+1}^{-0.097} \cdot \left( 1472.47 + 1.54 \cdot (N_c - 1)/2 + 104.97 \cdot \bar{m}_{h,ii+1}^{-0.25} \right)$ <p>with</p> $\bar{m}_{h,ii+1} = \frac{\dot{m}_{h,ii+1}}{N_c \cdot \mu_{h,ii+1}}$ <p><math>c_1</math> is a correction coefficient: <math>c_1 = 1.12647</math></p>

**Equation 7**

Title	Momentum balance equation (cold fluid)
Validity domain	$\forall \dot{m}_{c,ii+1}$
Mathematical formulation	$P_{c,i+1} = P_{c,i} - \frac{\Lambda_c}{N} \cdot \frac{\dot{m}_{c,ii+1} \cdot  \dot{m}_{c,ii+1} }{N_c^2 \cdot \rho_{c,i}}$
Comments	<p>Only pressure losses due to friction are taken into account; cf. (13.17). The friction coefficient <math>\Lambda_c</math> can be directly provided by the user or computed using a correlation.</p> <p>The following correlation is used for some specific plate heat exchangers with hydraulic diameter <math>D_h = 0.0356951</math>:</p> $\Lambda_c = 14423.2 \cdot c_1 \cdot \bar{m}_{c,ii+1}^{-0.097} \cdot \left( 1472.47 + 1.54 \cdot (N_c - 1)/2 + 104.97 \cdot \bar{m}_{c,ii+1}^{-0.25} \right)$ <p>with</p> $\bar{m}_{c,ii+1} = \frac{\dot{m}_{c,ii+1}}{N_c \cdot \mu_{c,ii+1}}$ <p><math>c_1</math> is a correction coefficient: <math>c_1 = 1.12647</math></p>

In order to have a full system of equations that can be solved, this set of equations must be completed by the state equations for the following water and steam properties:  $c_{p,c}$ ,  $c_{p,h}$ ,  $\rho_c$ ,  $\rho_h$ ,  $\mu_c$ ,  $\mu_h$ ,  $\lambda_c$  and  $\lambda_h$ .

#### 9.6.1.4 Modelica Component Model: *DynamicPlateHeatExchanger*

The governing equations are implemented in the *DynamicPlateHeatExchanger* located in the *WaterSteam.HeatExchangers* sub-library.

Figure 9.32a represents the graphical icon of the component with its four connectors.

#### 9.6.1.5 Test-Case

The model *TestDynamicPlateHeatExchanger* used to validate the *DynamicPlateHeatExchanger* component model is represented in Fig. 9.32b. This model uses the following component models:

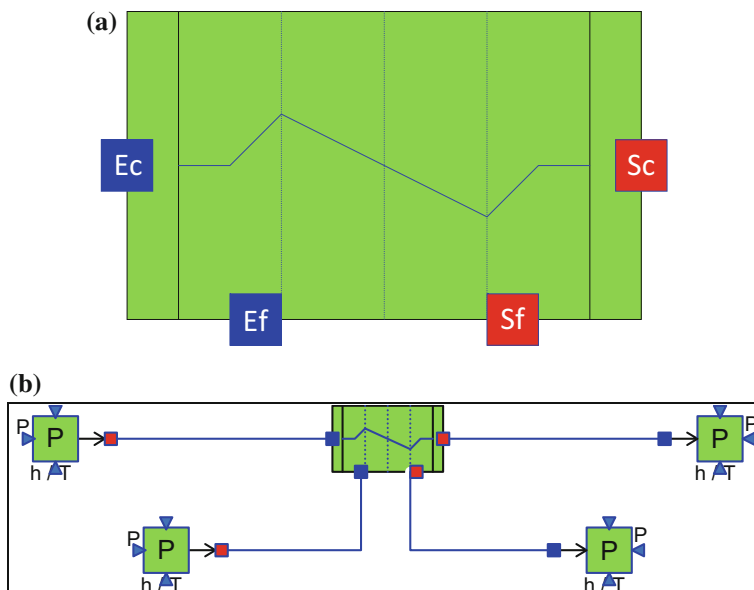


**Fig. 9.32** **a** Icon of the *DynamicPlateHeatExchanger* component model and **b** test-case for the *DynamicPlateHeatExchanger* component model

- One *DynamicPlateHeatExchanger* component model;
- Two *SourceP* component models;
- Two *SinkP* component models.

In the test-case scenario, the *DynamicPlateHeatExchanger* component receives: (1) the hot fluid pressure and temperature at the hot fluid inlet, (2) the hot fluid pressure at the hot fluid outlet (3) the cold fluid pressure and temperature at the cold fluid inlet, and (4) the cold fluid pressure at the cold fluid outlet. The component computes for the two fluids: the distribution of the fluid pressure, temperature, specific enthalpy, mass flow rate, and the distribution of thermal power exchanged.

### Test-Case Parameterization and Boundary Conditions

The model data are:

- Metal thermal conductivity = 15.0 W/m/K
- Heat transfer coefficient for the hot side = 6000 W/m<sup>2</sup>/K
- Heat transfer coefficient for the cold side = 3000 W/m<sup>2</sup>/K
- Pressure loss coefficient for the hot side = 100 m<sup>-4</sup>
- Pressure loss coefficient for the cold side = 100 m<sup>-4</sup>
- Hot-side volume = 1 m<sup>3</sup>
- Cold-side volume = 1 m<sup>3</sup>
- Wall thickness =  $6 \times 10^{-4}$  m
- Plate area = 2 m<sup>2</sup>
- Number of plates = 499
- Correction coefficient = 1.12647
- Number of segments = 5
- Hot water temperature at the inlet = 340 K
- Hot water pressure at the inlet =  $3 \times 10^5$  Pa
- Hot water pressure at the outlet =  $10^5$  Pa
- Cold water temperature at the inlet = 290 K
- Cold water pressure at the inlet =  $3 \times 10^5$  Pa
- Cold water pressure at the outlet =  $10^5$  Pa.

### Model Calibration

The calibration procedure consists in setting the fluid mass flow rate of the hot fluid at the inlet to a known measurement value and computing by model inversion the value of the outlet pressure of the hot fluid.

Other possible calibration procedure: setting the fluid specific enthalpy of the hot fluid at the outlet to a known measurement value and computing by model inversion the value of the plate area.

## Simulation Results

The simulation of the test scenario produces the numerical results below:

- Hot fluid mass flow rate = 1036.03 kg/s
- Hot fluid specific enthalpy at the outlet = 161,481 J/kg
- Cold fluid mass flow rate = 1084.24 kg/s
- Cold fluid specific enthalpy at the outlet = 184,313 J/kg.

### 9.6.2 Static Modeling of a Plate Heat Exchanger

The plate heat exchanger model is called *StaticPlateHeatExchanger*. This model is the steady-state version of the dynamic plate heat exchanger model (cf. Sect. 9.6.1).

#### 9.6.2.1 Nomenclature

Symbols	Definition	Unit	Mathematical definition
$A$	Heat exchange surface	$\text{m}^2$	$(N_p - 2) \cdot S_p$
$\dot{m}_h$	Hot fluid mass flow rate	$\text{kg/s}$	
$\dot{m}_c$	Cold fluid mass flow rate	$\text{kg/s}$	
$N_c$	Number of channels of each fluid	–	$(N_p - 1)/2$
$N_p$	Number of plates	–	
$P_{c,i}$	Cold fluid pressure at the inlet	$\text{Pa}$	
$P_{c,o}$	Cold fluid pressure at the outlet	$\text{Pa}$	
$P_{h,i}$	Hot fluid pressure at the inlet	$\text{Pa}$	
$P_{h,o}$	Hot fluid pressure at the outlet	$\text{Pa}$	
$T_{c,i}$	Cold fluid temperature at the inlet	$\text{K}$	
$T_{c,o}$	Cold fluid temperature at the outlet	$\text{K}$	
$T_{h,i}$	Hot fluid temperature at the inlet	$\text{K}$	
$T_{h,o}$	Hot fluid temperature at the outlet	$\text{K}$	
$U$	Global heat transfer coefficient (internal overall heat exchange coefficient)	$\text{W/m}^2/\text{K}$	
$W$	Thermal power exchanged between the two fluids	$\text{W}$	
$\Delta T_1$	Temperature difference 1; cf. (9.39) and (9.41)	$\text{K}$	For counter flow $T_{h,i} - T_{c,o}$ For parallel flow $T_{h,i} - T_{c,i}$

(continued)

(continued)

Symbols	Definition	Unit	Mathematical definition
$\Delta T_2$	Temperature difference 2; cf. (9.39) and (9.41)	K	For counter flow $T_{h,o} - T_{c,i}$ For parallel flow $T_{h,o} - T_{c,o}$
$\Lambda_c$	Friction pressure loss coefficient of the entire length of the exchanger for the cold fluid	$m^{-4}$	
$\Lambda_h$	Friction pressure loss coefficient of the entire length of the exchanger for the hot fluid	$m^{-4}$	
$\rho_c$	Cold fluid density	$kg/m^3$	
$\rho_h$	Hot fluid density	$kg/m^3$	

### 9.6.2.2 Assumptions

The heat exchanger is modeled according to the following assumptions:

- Single-phase flow in each mesh cell.
- The energy accumulation in the wall is neglected.
- The phenomenon of longitudinal heat conduction in the wall and in the fluid is neglected.
- The specific heats and mass flow rates of both fluids are constant.
- The thermophysical properties are calculated on the basis of the average pressure and specific enthalpy in each mesh cell.

### 9.6.2.3 Governing Equations

The *StaticPlateHeatExchanger* model is utilized using the LMTD method (cf. Sect. 9.2.5) for the energy balance equation and is similar to the *DynamicPlateHeatExchanger* model (cf. Sect. 9.6.1) regarding the mass and momentum balance equations, with  $N = 1$  (there is only one segment, and the model is not discretized).

---

#### Equation 1

---

Title	Energy balance equation (hot fluid)
Validity domain	$\forall \dot{m}_h$
Mathematical formulation	$W = \dot{m}_h \cdot c_{p,h} \cdot (T_{h,i} - T_{h,o})$

---

#### Equation 2

---

Title	Energy balance equation (cold fluid)
Validity domain	$\forall \dot{m}_c$
Mathematical formulation	$W = \dot{m}_c \cdot c_{p,c} \cdot (T_{c,o} - T_{c,i})$

## Equation 3

Title	Heat exchanged between the fluid and the wall
Validity domain	$\dot{m}_h \neq 0, \dot{m}_c \neq 0, \Delta T_1 \neq 0$ and $\Delta T_2 \neq 0$
Mathematical formulation	$W = U \cdot A \cdot \frac{\Delta T_2 - \Delta T_1}{\ln \left( \frac{\Delta T_2}{\Delta T_1} \right)}$
Comments	Cf. (9.40) for parallel flow and (9.41) for counter-flow heat exchangers

## Equation 4

Title	Momentum balance equation (hot fluid)
Validity domain	$\forall \dot{m}_h$
Mathematical formulation	$P_{h,o} = P_{h,i} - \Lambda_h \cdot \frac{\dot{m}_h \cdot  \dot{m}_h }{N_c^2 \cdot \rho_h}$
Comments	See Eq. 6 of Sect. 9.6.1.3

## Equation 5

Title	Momentum balance equation (cold fluid)
Validity domain	$\forall \dot{m}_c$
Mathematical formulation	$P_{c,o} = P_{c,i} - \Lambda_c \cdot \frac{\dot{m}_c \cdot  \dot{m}_c }{N_c^2 \cdot \rho_c}$
Comments	See Eq. 7 of Sect. 9.6.1.3

**9.6.2.4 Modelica Component Model: *StaticPlateHeatExchanger***

The governing equations are implemented in the *StaticPlateHeatExchanger* located in the *WaterSteam.HeatExchangers* sub-library.

Figure 9.33a represents the graphical icon of the component with its four connectors.

**9.6.2.5 Test-Case**

The model *TestStaticPlateHeatExchanger* used to validate the *StaticPlateHeatExchanger* component model is represented in Fig. 9.33b. This model uses the following component models:

- One *StaticPlateHeatExchanger* component model;
- Two *SourceP* component models;
- Two *SinkP* component models.

In the test-case scenario, the *StaticPlateHeatExchanger* component receives: (1) the hot fluid pressure and temperature at the hot fluid inlet, (2) the hot fluid pressure at the hot fluid outlet, (3) the cold fluid pressure and temperature at the cold fluid inlet, and (4) the cold fluid pressure at the cold fluid outlet. The

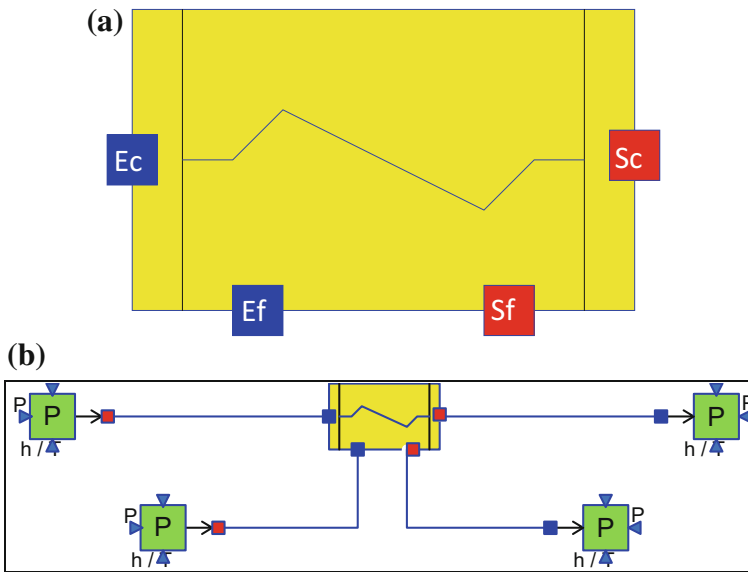


**Fig. 9.33** **a** Icon of the *StaticPlateHeatExchanger* component model and **b** test-case for the *StaticPlateHeatExchanger* component model

component computes for the two fluids: the mass flow rate and temperature at the outlet, and the thermal power exchanged.

#### Test-Case Parameterization and Boundary Conditions

The model data are:

- Metal thermal conductivity = 15 W/m/K
- Heat transfer coefficient for the hot side = 6000 W/m<sup>2</sup>/K
- Heat transfer coefficient for the cold side = 3000 W/m<sup>2</sup>/K
- Pressure loss coefficient for the hot side = 100 m<sup>-4</sup>
- Pressure loss coefficient for the cold side = 100 m<sup>-4</sup>
- Wall thickness =  $6 \times 10^{-4}$  m
- Plate area = 2 m<sup>2</sup>
- Number of plates = 499
- Correction coefficient = 1.12647
- Hot water temperature at the inlet = 340 K
- Hot water pressure at the inlet =  $3 \times 10^5$  Pa
- Hot water pressure at the outlet =  $10^5$  Pa
- Cold water temperature at the inlet = 290 K
- Cold water pressure at the inlet =  $3 \times 10^5$  Pa
- Cold water pressure at the outlet =  $10^5$  Pa.

## Model Calibration

The calibration procedure consists in setting the fluid mass flow rate of the hot fluid at the inlet to a known measurement value and computing by model inversion the value of the outlet pressure of the hot fluid.

Other possible calibration: setting the fluid specific enthalpy of the hot fluid at the outlet to a known measurement value and computing by model inversion the value of the plate area.

## Simulation Results

The simulation of the test scenario produces the numerical results below:

- Hot fluid mass flow rate = 1036.78 kg/s
- Hot fluid specific enthalpy at the outlet = 160,997 J/kg
- Cold fluid mass flow rate = 1085.45 kg/s
- Cold fluid specific enthalpy at the outlet = 184,364 J/kg.

## 9.7 Simple Heat Exchanger Modeling

### 9.7.1 Static Condenser with Correlations Given by the 9th HEI Standard (1996)

The condenser considered here is a large shell-and-tube-type heat exchanger as shown in Fig. 9.24. It is composed of a bundle of circular tubes mounted in a cavity. The steam in the cavity flows outside the tube bundles and the cooling water flows inside the tubes. The condenser is positioned at the outlet of the steam turbine in order to receive a large flow rate of low-pressure steam. The steam in the cavity undergoes a phase change from steam to water as a consequence of the thermal exchange with the tube bundle. External cooling water is pumped through the tube bundles of the condenser to evacuate the steam condensation heat. The condensate at the outlet is pumped and sent into feed water heaters.

The condenser model is called *StaticCondenser*.

### 9.7.1.1 Nomenclature

Symbols	Definition	Unit	Mathematical definition
$A$	Heat exchange surface	$\text{m}^2$	
$C$	Fouling coefficient	—	
$C_{\text{ref}}$	Reference fouling coefficient	—	
$h_{c,i}$	Cold fluid specific enthalpy at the inlet	J/kg	
$h_{c,o}$	Cold fluid specific enthalpy at the outlet	J/kg	
$h_{d,i}$	Specific enthalpy at the inlet (from drain)	J/kg	
$h^{\text{h}}$	Hot fluids mixing specific enthalpy	J/kg	
$h_{l,o}$	Liquid specific enthalpy at the outlet of the condenser (drain)	J/kg	$h_l^{\text{sat}} + \frac{(P_b - P)}{\rho_l}$
$h_l^{\text{sat}}$	Hot fluid saturation enthalpy of the liquid	J/kg	
$h_{t,i}$	Specific enthalpy of the steam coming from the turbine	J/kg	
$h_{v,i}$	Specific enthalpy of the steam coming from the boiler outlet or from the turbine inlet valve	J/kg	
$h_{\text{cond}}$	Heat exchange coefficient: correlation given by the manufacturers	$\text{W}/\text{m}^2/\text{K}$	
$K_{\text{cond}}$	Reference heat exchange coefficient	$\text{W}/\text{m}^2/\text{K}$	
$\dot{m}_c$	Cold fluid (water) mass flow rate	kg/s	
$\dot{m}_{c,\text{ref}}$	Cold fluid (water) reference mass flow rate	kg/s	
$\dot{m}_{d,i}$	Water mass flow rate at the inlet (drain)	kg/s	
$\dot{m}_{d,o}$	Water mass flow rate at the outlet of the condenser	kg/s	
$\dot{m}_{t,i}$	Mass flow rate of the steam coming from the turbine	kg/s	
$\dot{m}_{v,i}$	Mass flow rate of the steam coming from the boiler outlet or from the turbine inlet valve	kg/s	
$P$	Steam pressure inside the condenser (cavity pressure)	Pa	
$P_b$	Fluid pressure at the bottom of the cavity (drain outlet)	Pa	$P + \rho_l \cdot g \cdot z_l$
$P_{c,i}$	Cold fluid pressure at the inlet	Pa	
$P_{c,o}$	Cold fluid pressure at the outlet	Pa	
$T_{c,i}$	Cold fluid (water) temperature at the inlet	K	
$T_{c,o}$	Cold fluid (water) temperature at the outlet	K	
$T_{c,\text{ref}}$	Cold fluid (water) reference temperature	K	
$T^{\text{sat}}$	Saturation temperature	K	
$W$	Heat power released to the cold fluid (thermal power exchanged)	W	

(continued)

(continued)

Symbols	Definition	Unit	Mathematical definition
$z_l$	Water level in the condenser	m	
$\Delta P_c$	Cold fluid pressure loss between the inlet and the outlet	Pa	$P_{c,i} - P_{c,o}$
$\Lambda_c$	Cold fluid friction pressure loss coefficient	$m^{-4}$	
$\rho_c$	Cold fluid density	$kg/m^3$	
$\rho_l$	Water density at the extraction point (i.e., at the liquid outlet of the condenser)	$kg/m^3$	

### 9.7.1.2 Assumptions

The condenser is modeled according to the following assumptions:

- The efficiency of the condenser is equal to 1 (100% of mass flow rate of the input steam is condensed).
- The energy accumulation in the wall is neglected.

### 9.7.1.3 Governing Equations

The *StaticCondenser* model is based on the static energy balance equation using the LMTD method, cf. Sect. 9.2.5, and the static and momentum balance equations.

Equation 1	
Title	Power received by the cold fluid
Validity domain	$\forall \dot{m}_c$
Mathematical formulation	$W = \dot{m}_c \cdot (h_{c,o} - h_{c,i})$

Equation 2	
Title	Mass balance equation of the hot fluids
Validity domain	$\forall \dot{m}_{t,i}, \forall \dot{m}_{v,i}$ and $\forall \dot{m}_{d,i}$
Mathematical formulation	$\dot{m}_{d,o} = \dot{m}_{t,i} + \dot{m}_{v,i} + \dot{m}_{d,i}$
Comments	<p>There are three sources of hot fluid:</p> <ol style="list-style-type: none"> <li>1. Steam coming from the turbine,</li> <li>2. Steam coming from the boiler outlet or from the turbine inlet valve,</li> <li>3. Water or steam coming from the drain, e.g., outlets of water heaters.</li> </ol>

**Equation 3**

Title	Specific mixing enthalpy of the hot fluids
Validity domain	$\dot{m}_{d,o} \neq 0, \forall \dot{m}_{t,i}, \forall \dot{m}_{v,i}$ and $\forall \dot{m}_{d,i}$
Mathematical formulation	$\dot{m}_{d,o} \cdot h^h = \dot{m}_{t,i} \cdot h_{t,i} + \dot{m}_{v,i} \cdot h_{v,i} + \dot{m}_{d,i} \cdot h_{d,i}$
Comments	The mixing enthalpy is used to compute the properties of the hot fluid inside the condenser

**Equation 4**

Title	Energy released during the condensation of the steam at the inlets
Validity domain	$\forall \dot{m}_{t,i}, \forall \dot{m}_{v,i}$ , and $\forall \dot{m}_{d,i}$
Mathematical formulation	$W = \dot{m}_{t,i} \cdot (h_{t,i} - h_l^{\text{sat}}) + \dot{m}_{v,i} \cdot (h_{v,i} - h_l^{\text{sat}}) + \dot{m}_{d,i} \cdot (h_{d,i} - h_l^{\text{sat}})$
Comments	<p>There are three sources of steam:</p> <ol style="list-style-type: none"> <li>1. Steam coming from the turbine,</li> <li>2. Steam coming from the boiler outlet or from the turbine inlet valve,</li> <li>3. Water or steam coming from the drain, e.g., outlets of water heaters.</li> </ol> <p>It is assumed that the steam is completely condensed or in other words that the efficiency of the condenser is equal to one</p>

**Equation 5**

Title	Power exchanged between the hot and the cold fluids
Validity domain	$W > 0$
Mathematical formulation	$T^{\text{sat}} - T_{c,o} = (T^{\text{sat}} - T_{c,i}) \cdot e^{-\frac{h_{\text{cond}} \cdot A \cdot (T_{c,i} - T_{c,o})}{W}}$
Comments	<p>This equation is obtained from the standard LMTD expression, cf. (9.39):</p> $W = h_{\text{cond}} \cdot A \cdot \frac{\Delta T_2 - \Delta T_1}{\ln\left(\frac{\Delta T_2}{\Delta T_1}\right)}$ <p>with <math>\Delta T_1 = T^{\text{sat}} - T_{c,i}</math> and <math>\Delta T_2 = T^{\text{sat}} - T_{c,o}</math>. It is therefore assumed that the hot fluid stays in the condensation zone at the saturation temperature between the inlet and the outlet of the condenser (no desuperheating zone and no subcooled zone). This is a valid assumption when the condenser is under normal operating conditions: The steam coming from the turbine is at the saturation temperature, and the outgoing condensate is also at the same saturation temperature. For other specific transients, such as turbine bypass following a turbine trip, where superheated steam is directly sent to the condenser, one can use the dynamic condenser model component instead; cf. Sect. 9.5.4.</p> <p>The heat exchange coefficient <math>h_{\text{cond}}</math> is computed with a correlation given by the Heat Exchange Institute (HEI) standard:</p> $h_{\text{cond}} = K_{\text{cond}} \cdot \frac{C}{C_{\text{ref}}} \cdot \frac{K(T_{c,i})}{K(T_{c,\text{ref}})} \cdot \sqrt{\frac{\dot{m}_c}{\dot{m}_{c,\text{ref}}}}$ <p>For the 9th HEI standard (1996), <math>K(T)</math> is given by:</p> $K(T) = -0.05 \cdot (T - 273.16)^2 + 3.3 \cdot (T - 273.16)^2 + 52.0$

(continued)

(continued)

**Equation 5**

	$K_{\text{cond}}$ and $A$ can be given as inputs by the user or computed from measurements using inverse computation. $K_{\text{cond}}$ can also be computed using correlations for condensation; cf. Sect. 9.2.4.2. Then, the above HEI correlation is a correction for $K_{\text{cond}}$ . This correlation varies according the HEI standard under consideration
--	---

**Equation 6**

Title	Momentum balance equation (cold fluid)
Validity domain	$\forall \dot{m}_c$
Mathematical formulation	$\Delta P_c = \Lambda_c \cdot \frac{\dot{m}_c \cdot  \dot{m}_c }{\rho_c}$
Comments	Only friction pressure losses are taken into account

In order to have a full system of equations that can be solved, this set of equations must be completed by the state equations for the following water and steam properties:  $h_l^{\text{sat}}$ ,  $T^{\text{sat}}$ ,  $T_{c,i}$ ,  $T_{c,o}$ ,  $\rho_c$ , and  $\rho_l$ .

### 9.7.1.4 Modelica Component Model: *StaticCondenser*

The governing equations are implemented in the *StaticCondenser* located in the *WaterSteam.HeatExchangers* sub-library.

Figure 9.34a represents the graphical icon of the component with its six connectors.

### 9.7.1.5 Component Model Validation

The model *TestStaticCondenser* used to validate the *StaticCondenser* component model is represented in Fig. 9.34b. This model uses the following component models:

- One *StaticCondenser* component model;
- Three *SourceP* component models;
- Six *SingularPressureLoss* component models;
- Four *SourceQ* component models;
- One *SinkP* component model;
- One *Sink* component model.

In the test-case scenario, the *StaticCondenser* component receives: (1) the steam mass flow rate and specific enthalpy at the steam inlet, (2) the cold fluid mass flow rate and specific enthalpy at the cold fluid inlet, (3) the cold fluid pressure at the cold fluid outlet, and (4) the condenser pressure. The component computes: (1) the

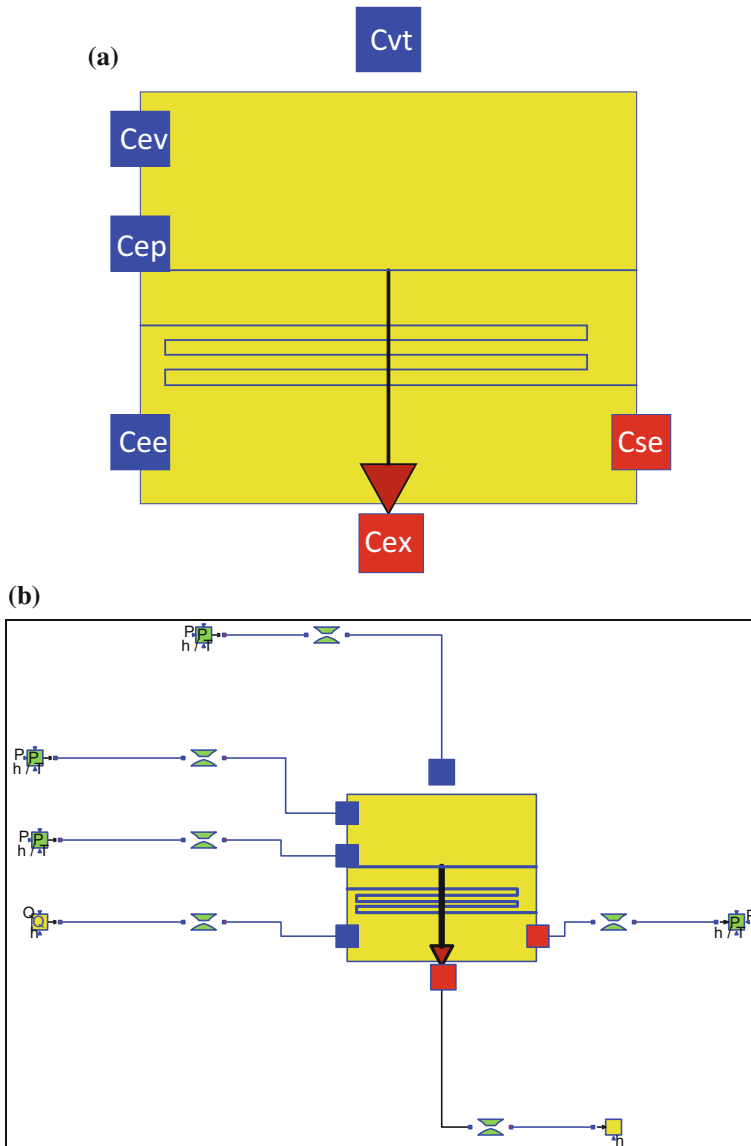


**Fig. 9.34** **a** Icon of the *StaticCondenser* component model and **b** test-case for the *StaticCondenser* component model

cold fluid specific enthalpy at the cold fluid outlet, (2) the cold fluid pressure at the cold fluid inlet, (3) the hot fluid specific enthalpy at the hot fluid outlet, (4) the condenser heat exchange surface, and (5) the thermal power exchanged.

## Test-Case Parameterization and Boundary Conditions

The model data are:

- Heat exchange surface = 47,786 m<sup>2</sup>
- Pressure loss coefficient for the water side = 0
- Water level in the condenser = 0
- Reference heat exchange coefficient = 3400.57 W/m<sup>2</sup>/K
- Reference mass flow rate = 37,700 kg/s
- Reference temperature = 293 K
- Reference fouling coefficient = 1
- Actual fouling coefficient = 1
- Steam specific enthalpy at the inlet =  $2275.1 \times 10^3$  J/kg
- Steam mass flow rate at the inlet = 832.66 kg/s
- Cooling water pressure at the outlet = 328,800 Pa
- Cooling water specific enthalpy at the inlet =  $60 \times 10^3$  J/kg
- Cooling water mass flow rate at the inlet = 42,261 kg/s
- Pressure loss coefficient of each *SingularPressureLoss* component model = 0.001.

## Model Calibration

The calibration procedure consists in setting the pressure in the cavity (hot fluid) to a known measurement value and computing by model inversion the value of the heat exchange surface of the condenser (alternatively: of the heat exchange coefficient, or of the fouling coefficient, or of the mass flow rate of the cold fluid at the inlet).

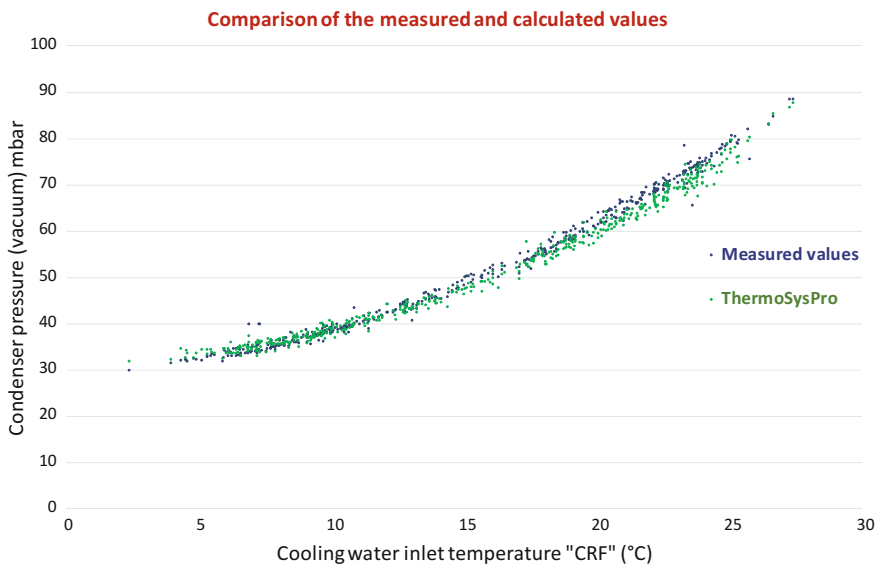


**Fig. 9.35** Simulation results for *StaticCondenser*: comparison between the measured values on site and the calculated values

## Simulation Results

The results of the simulation runs are given in Fig. 9.35.

Figure 9.35 shows that the calculated values are very close to the measured values on site.

## References

- CEA-GRETh (1997) Manuel technique du GRETh
- Chato JC (1962) Laminar condensation inside horizontal and inclined tubes. *Ashrae J* 4(2):52–60
- Chen JC (1966) Correlation for boiling heat transfer to saturated fluids in convective flow. *Ind Eng Chem Proc Des Dev* 5(3):322–329
- Fraas AP, Ozisik MN (1965) Heat exchanger design. Wiley
- Gungor KE, Winterton RHS (1986) A general correlation for flow boiling in tubes and annuli. *Int J Heat Mass Transf* 29(3):351–358
- Hilpert R (1933) Wärmeabgabe von geheizten Drähten und Rohren im Luftstrom. *Forschung auf dem Gebiet des Ingenieurwesens A* 4(5):215–224
- Incropera F, DeWitt P, Bergman T, Lavine A (2006) Fundamentals of heat transfer. Wiley
- Jens WH, Lottes PA (1951) Analysis of heat transfer, burnout, pressure drop and density date for high pressure water. USAEC report ANL-4627, Argonne National Lab
- Kakaç S, Liu H, Pramuanjaroenkij A (2012) Heat exchangers: selection, rating and thermal design. CRC Press
- Kays WM, London AL (1964) Compact heat exchangers, 2nd edn. McGraw-Hill, New York

- Kern DQ (1950) Process heat transfer. McGraw-Hill, New York
- Nusselt WA (1916) The surface condensation of water vapor. Z Ver Deut Ing 60:541–546
- Sacadura JF (1978) Initiation aux transferts thermiques. Technique et documentation, Paris
- Shah M (1979) A general correlation for heat transfer during film condensation inside pipes. Int J Heat Mass Transf 22:547–556
- Thom JRS, Walker WM, Fallon TA, Reisting GFS (1965–1966) Boiling in sub-cooled water during flow up heated tubes or annuli. Proc Inst Mech Eng (London) 180:226–246
- Wylie EB, Streeter VL (1993) Fluid transients in systems. Prentice Hall

# Chapter 10

## Steam Turbine Modeling



**Abstract** Steam turbines are one of the most important equipment for generating electricity. A steam turbine is a rotating device that converts a large part of steam kinetic and thermal energy into mechanical energy for driving a generator. High-temperature steam from the boiler is fed to the steam turbine, where it imparts its energy to the rotor blades. In each blade row, the steam releases a part of its energy, thus becoming cooler and progressively losing pressure, this energy being imparted to the turbine shaft in the form of mechanical energy. This chapter describes the steam turbine model and gives a detailed description of the physical equations: modeling assumptions and fundamental equations. A test-case is given that includes the structure of the model, parameterization data, and results of simulation. The full description of the physical equations is independent of programming languages and tools.

### 10.1 Basic Description

The problem to be solved is how to compute the mechanical work  $\dot{W}$  produced by an adiabatic expansion of steam flow within one turbine multistage group.

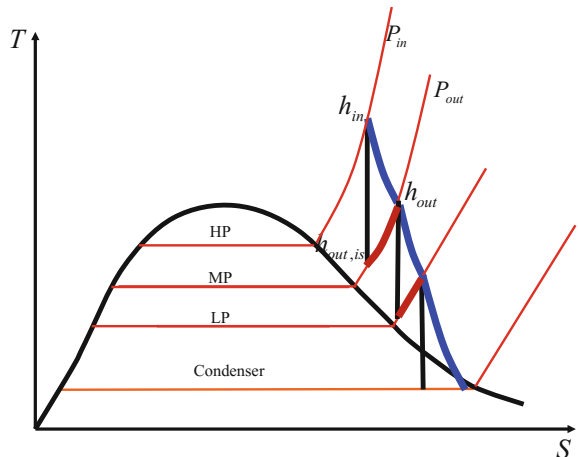
Only stationary or quasi-stationary compressible flow is considered through the turbine, so the turbine multistage group is assumed to be a static component.

Let us suppose first that the steam is dry throughout the expansion, as shown for the expansion going from the high-pressure (HP) group to the medium-pressure (MP) group in Fig. 10.1.

As the expansion within the turbine group is not reversible,  $\dot{W}$  is not a state function, so it cannot be directly related to the thermodynamic state of the system by property functions.

However, as work  $\dot{W}_{\text{rev}}$  produced by an ideal reversible transformation is a state function,  $\dot{W}$  may be related to  $\dot{W}_{\text{rev}}$ , and hence to the state of the system, using the isentropic efficiency:

**Fig. 10.1** Expansions in the three multistage groups of a turbine



$$\eta_{is} = \frac{\dot{W}}{\dot{W}_{rev}} \quad (10.1)$$

As the expansion is assumed to be adiabatic, the static energy balance equation yields:

$$\dot{W} = \dot{m} \cdot \Delta h \quad (10.2)$$

where  $\dot{m}$  is the mass flow rate going through the turbine group and  $\Delta h$  is the variation of specific enthalpy between the inlet (the upstream side of the group) and the outlet (the downstream side of the group).

$$\Delta h = h_{in} - h_{out} \quad (10.3)$$

In the same way:

$$\dot{W}_{rev} = \dot{m} \cdot \Delta h_{is} \quad (10.4)$$

where  $\Delta h_{is}$  is the variation of specific enthalpy between the inlet and the outlet for a reversible transformation:

$$\Delta h_{is} = h_{in} - h_{out,is} \quad (10.5)$$

Therefore:

$$\eta_{is} = \frac{\Delta h}{\Delta h_{is}} \quad (10.6)$$

The isentropic efficiency is a function that reaches its maximum value under nominal operating conditions:

$$\eta_{\text{is}} = f_{\eta} \left( \frac{P_{\text{out}}}{P_{\text{in}}}, \frac{\omega}{\sqrt{T_{\text{in}}}} \right) \quad (10.7)$$

where  $P_{\text{in}}$  and  $T_{\text{in}}$  are respectively the fluid pressure and temperature at the inlet,  $P_{\text{out}}$  is the fluid pressure at the outlet, and  $\omega$  is the rotational speed. The efficiency curves  $f_{\eta}$  can be given by tables, or approximated by polynomials.

The final mechanical work produced takes into account the energy losses due to kinetic losses and hydrodynamic friction:

$$\dot{W}_{\text{t}} = \dot{m} \cdot \Delta h \cdot r_s - \dot{W}_{\text{f}} \quad (10.8)$$

where  $r_s$  is a coefficient that accounts for kinetic losses and  $\dot{W}_{\text{f}}$  denotes the energy losses due to friction.

It is assumed hereafter that the fluid is an ideal gas undergoing isentropic (adiabatic frictionless) expansion.

If the gas is at choked flow (sonic) conditions at the inlet of the turbine group, using the nozzle analogy for the entire group (Bidard and Bonnin 1979):

$$\dot{m} = \Phi_c \cdot A_{\text{in}} \cdot \sqrt{P_{\text{in}} \cdot \rho_{\text{in}}} \quad (10.9)$$

where  $\Phi_c$  is a dimensionless constant,  $A_{\text{in}}$  is the flow cross-sectional area at the inlet, and  $\rho_{\text{in}}$  is the fluid density at the inlet.

$$\Phi_c \propto \sqrt{\gamma \cdot \left( \frac{2}{\gamma + 1} \right)^{\frac{\gamma+1}{\gamma-1}}} \quad (10.10)$$

with  $\gamma = \frac{c_p}{c_v}$  being the specific heat ratio, and the sign  $\propto$  meaning “proportional to.”

Let us introduce the dimensionless variables for pressure and flow:

$$X = \frac{P_{\text{out}}}{P_{\text{in}}} \quad (10.11)$$

$$\Phi = \frac{\dot{m}}{A_{\text{in}} \cdot \sqrt{P_{\text{in}} \cdot \rho_{\text{in}}}} \quad (10.12)$$

$X$  is the expansion rate, and  $\Phi$  is the dimensionless mass flow rate. For a single stage, choked flow occurs when:

$$X < X_c = \left( \frac{2}{\gamma + 1} \right)^{\frac{\gamma}{\gamma-1}} \quad (10.13)$$

For choked flow ( $X < X_c$ ):

$$\Phi = \Phi_c \quad (10.14)$$

For non-choked flow ( $X \geq X_c$ ), Stodola's ellipse is used:

$$\Phi = \Phi_c \cdot \sqrt{1 - \left(\frac{X - X_c}{1 - X_c}\right)^2} \quad (10.15)$$

A rationale for (10.15) is the following. Considering that the turbine is made of infinitely close stages and that the fluid is non-choked, the pressure loss in each stage is given by (cf. (13.5)):

$$dP = \frac{1}{2} \cdot \frac{\dot{m}^2}{\rho \cdot A^2} \cdot d\xi \quad (10.16)$$

Considering a polytropic expansion  $P \cdot \rho^{-k} = C$ , cf. (2.78), (10.16) writes

$$P^{\frac{1}{k}} \cdot dP = \frac{1}{2} \cdot \frac{\dot{m}^2}{A^2} \cdot d\lambda \quad (10.17)$$

with

$$d\lambda = C^{\frac{1}{k}} \cdot d\xi \quad (10.18)$$

As the mass flow rate  $\dot{m}$  is constant for a stage group (i.e., no bleeds), integrating (10.17) between the first stage with non-choked flow and the last stage yields

$$P_{in}^{\frac{k+1}{k}} - P_{out}^{\frac{k+1}{k}} = P_{in}^{\frac{k+1}{k}} \cdot (1 - X^{\frac{k+1}{k}}) = \frac{k+1}{2 \cdot k} \cdot \frac{\dot{m}^2}{A^2} \cdot \lambda \quad (10.19)$$

At the junction of choked and non-choked flows  $X = X_c$ , the mass flow rates obtained from Eqs. (10.9) and (10.19) are equal. Assuming in addition that the junction is very close to the inlet (i.e.,  $X_c \approx 0$ ), then:

$$\dot{m}^2 = \Phi_c^2 \cdot A^2 \cdot \rho \cdot P_{in} = \frac{2 \cdot k}{k+1} \cdot \frac{A^2 \cdot P_{in}^{\frac{k+1}{k}}}{\lambda} \cdot (1 - X_c^{\frac{k+1}{k}}) \quad (10.20)$$

Hence, from (10.20), at the junction

$$\lambda = \frac{2 \cdot k}{k+1} \cdot \frac{P_{in}^{\frac{1}{k}}}{\rho \cdot \Phi_c^2} \cdot (1 - X_c^{\frac{k+1}{k}}) \quad (10.21)$$

From (10.18),  $\lambda$  is constant throughout the whole stage group as it is proportional to the turbine mass flow coefficient  $\xi$  which is constant; cf. Eq (5) in (Cooke 1985).

Then, from (10.12), (10.19), and (10.21):

$$\Phi^2 = \frac{\dot{m}^2}{A^2 \cdot \rho \cdot P_{\text{in}}} = \frac{2 \cdot k}{k + 1} \cdot \frac{P_{\text{in}}^{\frac{1}{k}}}{\lambda \cdot \rho} \cdot (1 - X^{\frac{k+1}{k}}) = \Phi_c^2 \cdot \frac{1 - X^{\frac{k+1}{k}}}{1 - X_c^{\frac{k+1}{k}}} \quad (10.22)$$

As  $X_c \approx 0$

$$\Phi = \Phi_c \cdot \sqrt{1 - X^{\frac{k+1}{k}}} \quad (10.23)$$

Equation (10.23) yields Stodola's ellipse law for  $k = 1$ , i.e., if the expansion is isothermal under the ideal gas law.

If  $X_c$  is not close to zero, by inserting into (10.23) the change of variable that consists in replacing  $X$  by  $(X - X_c)/(1 - X_c)$  in order to ensure  $\Phi(X_c) = 1$  and  $\Phi(1) = 0$ :

$$\Phi = \Phi_c \cdot \sqrt{1 - \left(\frac{X - X_c}{1 - X_c}\right)^{\frac{k+1}{k}}} \quad (10.24)$$

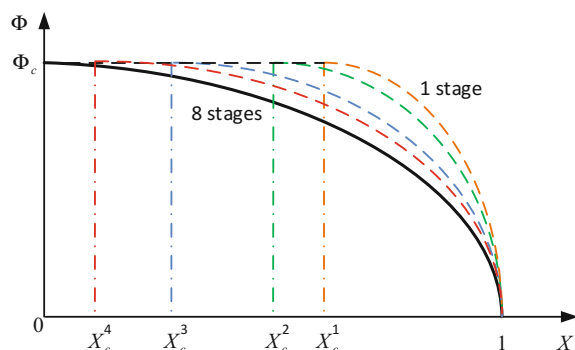
Equation (10.15) is obtained by setting  $k = 1$  into (10.24).

Therefore, for non-chocked flow,  $\Phi$  is not a constant anymore, but varies as a function of  $X$  such that  $\Phi(X = X_c) = \Phi_c$  and  $\Phi(X = 1) = 0$ .  $X_c$  decreases and tends to zero when the number of stages increases (see dashed curves in Fig. 10.2). Therefore, choking never occurs when the number of stages is sufficiently high (see solid line in Fig. 10.2).

For choked flow conditions, the dashed straight line  $\Phi = \Phi_c$  corresponding to  $0 < X < X_c$  should be used. However,  $\Phi = \Phi_c$  has an infinite number of solutions in the segment  $[0, X_c]$  if the dashed curve is used. For this reason, the ellipse law is used for all flow regimes, i.e., for any  $X \in [0, 1]$ ; cf. solid curve in Fig. 10.2

**Fig. 10.2** Stodola's ellipse

$$\frac{\Phi^2}{\Phi_c^2} + X^2 = 1 \text{ (solid line)}$$



obtained by setting  $X_c$  to zero in (10.15). This approximation is acceptable when the number of stages is sufficiently high so that  $X_c$  is sufficiently close to zero. Stodola found empirically that this is valid down to as few as eight 50% reaction stages (Stodola 1922; Cooke 1985).

Hence, stating that  $X_c = 0$  in (10.15), and using (10.11) and (10.12):

$$\begin{aligned}\dot{m} &= \Phi_c \cdot A_{in} \cdot \sqrt{\rho_{in} \cdot P_{in}} \cdot \sqrt{1 - \left(\frac{P_{out}}{P_{in}}\right)^2} \\ &= \Phi_c \cdot A_{in} \cdot \sqrt{\rho_{in} \cdot \frac{P_{in}^2 - P_{out}^2}{P_{in}}}\end{aligned}\quad (10.25)$$

This relation is commonly used even if the expansion is not isothermal, i.e., for  $1 < k < \gamma$  where  $\gamma$  is the ratio of specific heats.

Using (10.11), (10.12), and (10.23):

$$\dot{m} = \Phi_c \cdot A_{in} \cdot \sqrt{\rho_{in} \cdot P_{in}} \cdot \sqrt{1 - \left(\frac{P_{out}}{P_{in}}\right)^{\frac{k+1}{k}}}\quad (10.26)$$

Therefore, if the polytropic exponent  $k$  is known, then (10.26) that does not assume isothermal expansion can be used instead of (10.25).

$k$  can be computed from the following relation, if the initial and final states of the expansion are known from measurements:

$$\frac{T_{out}}{T_{in}} = \left(\frac{P_{out}}{P_{in}}\right)^{\frac{k-1}{k}}\quad (10.27)$$

that yields:

$$k = \frac{\log\left(\frac{P_{out}}{P_{in}}\right)}{\log\left(\frac{T_{out}}{T_{in}}\right) - \log\left(\frac{P_{out}}{P_{in}}\right)}\quad (10.28)$$

One can use the temperature  $T_{in}$  at the inlet instead of the density  $\rho_{in}$  considering the ideal gas law:

$$\frac{P_{in}}{\rho_{in}} = R_g \cdot T_{in}\quad (10.29)$$

where  $R_g$  is the specific gas constant for the dry steam.

$$R_g = \frac{\mathfrak{R}}{M_g}\quad (10.30)$$

where  $\mathfrak{R}$  is the universal gas constant and  $M_g$  is the molar mass of the steam.

Then, using (10.12):

$$\Phi = \frac{\dot{m} \cdot \sqrt{R_g \cdot T_{in}}}{A_{in} \cdot P_{in}} \quad (10.31)$$

Using (10.25):

$$\dot{m} = C_s \cdot P_{in} \cdot \sqrt{\frac{1 - \left(\frac{P_{out}}{P_{in}}\right)^2}{T_{in}}} = C_s \cdot \sqrt{\frac{P_{in}^2 - P_{out}^2}{T_{in}}} \quad (10.32)$$

with:

$$C_s = \frac{\Phi_c \cdot A_{in}}{\sqrt{R_g}} \quad (10.33)$$

Using the polytropic exponent, cf. (10.26):

$$\dot{m} = C_s \cdot P_{in} \cdot \sqrt{\frac{1 - \left(\frac{P_{out}}{P_{in}}\right)^{\frac{k+1}{k}}}{T_{in}}} \quad (10.34)$$

If the steam is not dry at the inlet, let us suppose that the vapor mass fraction at the inlet  $x_{in}$  is close enough to 1 for the mixture to be still considered as an ideal gas. This is consistent with the fact that the steam should not be too humid in order to avoid damage on the turbine.

Then,  $R_g$  must be replaced in (10.33) by the specific gas constant of the mixture:

$$R = \frac{\mathfrak{R}}{M} \quad (10.35)$$

which depends upon  $x_{in}$  as:

$$\frac{1}{M} = \frac{1 - x_{in}}{M_l} + \frac{x_{in}}{M_g} \approx \frac{x_{in}}{M_g} \quad (10.36)$$

as  $1 - x_{in}$  is close to 0 and  $M_l > M_g$ , where  $M$ ,  $M_l$ , and  $M_g$  are respectively the molar mass of the mixture, liquid, and gas.

This yields:

$$R \approx x_{in} \cdot R_g \quad (10.37)$$

From (10.32), the variation of the mass flow rate with the expansion is then given by:

$$\dot{m} \approx C_s \cdot P_{in} \cdot \sqrt{\frac{1 - \left(\frac{P_{out}}{P_{in}}\right)^2}{x_{in} \cdot T_{in}}} = C_s \cdot \sqrt{\frac{P_{in}^2 - P_{out}^2}{x_{in} \cdot T_{in}}} \quad (10.38)$$

or using the polytropic exponent:

$$\dot{m} \approx C_s \cdot P_{in} \cdot \sqrt{\frac{1 - \left(\frac{P_{out}}{P_{in}}\right)^{\frac{k+1}{k}}}{x_{in} \cdot T_{in}}} \quad (10.39)$$

If the steam is not dry at the inlet, or if it is dry at the inlet but crosses the saturation line during the expansion, the isentropic efficiency is modified according to the Baumann rule (Leyzerovich 2005):

$$\eta_{is}^{wet} = \frac{\Delta h}{\Delta h_{is}} = \eta_{is} \cdot (1 - (1 - x_m) \cdot C_{Bau}) \quad (10.40)$$

$C_{Bau}$  is the Baumann coefficient,  $\eta_{is}^{wet}$  is the isentropic efficiency for the wet steam,  $\eta_{is}$  is the isentropic efficiency for the dry steam, and  $x_m$  is the average vapor mass fraction in the humid part of the expansion:

$$x_m = \frac{x_{in} + x_{out}}{2} \quad (10.41)$$

where  $x_{out}$  is the vapor mass fraction at the outlet of the turbine group.

## 10.2 Stodola Turbine Modeling

The steam turbine transforms the steam thermal energy into mechanical energy following the Rankine cycle. A body of the turbine is composed of a group of stages that uses wet or dry steam.

The model of the steam turbine is composed of the steam turbine itself and a nozzle (diffuser); cf. Fig 10.3.

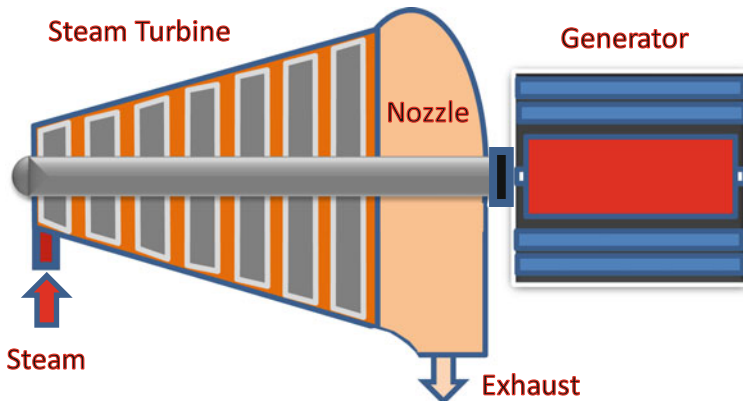


**Fig. 10.3** Schematic diagram of a steam turbine

### 10.2.1 Nomenclature

Symbols	Definition	Unit	Mathematical definition
$A_{nz}$	Nozzle area	$\text{m}^2$	
$C_s$	Stodola's ellipse coefficient	—	
$h_i$	Fluid specific enthalpy at the inlet	$\text{J/kg}$	
$h_{is}$	Fluid specific enthalpy after isentropic expansion	$\text{J/kg}$	
$h_o$	Fluid specific enthalpy at the outlet	$\text{J/kg}$	
$\dot{m}$	Fluid mass flow rate	$\text{kg/s}$	
$P_i$	Fluid pressure at the inlet	$\text{Pa}$	
$P_o$	Fluid pressure at the outlet	$\text{Pa}$	
$T_i$	Fluid temperature at the inlet	$\text{K}$	
$v_o$	Fluid velocity at the outlet	$\text{m/s}$	$\frac{\dot{m}}{\rho_o \cdot A_{nz}}$
$W$	Mechanical power produced by the turbine	$\text{W}$	
$W_{\text{fric}}$	Power losses due to hydrodynamic friction	%	
$x_i$	Vapor mass fraction at the inlet	—	
$x_o$	Vapor mass fraction at the outlet	—	
$\eta_{is}$	Isentropic efficiency for the dry steam	—	
$\eta_{is}^{\text{wet}}$	Isentropic efficiency for wet steam	—	
$\eta_{nz}$	Nozzle efficiency	—	
$\eta_{\text{sta}}$	Efficiency to account for kinetic losses	—	

### 10.2.2 Assumptions

The steam turbine is modeled according to the following assumptions:

- Subsonic fluid.
- Model is quasi-static because the dynamic response of the turbine is faster than the network queries (inertia is neglected).
- Supercritical or subcritical flow at the inlet and the outlet.

### 10.2.3 Governing Equations

The *StodolaTurbine* component model is based on the ellipse law (Stodola's theory developed by Aurel Stodola in 1922).

Equation 1a

Title	Stodola's ellipse law: mass flow rate for subcritical flow
Validity domain	$\forall \dot{m}$ and $x_i > 0$
Mathematical formulation	$\dot{m} = C_s \cdot \sqrt{\frac{P_i^2 - P_o^2}{x_i \cdot T_i}}$
Comments	Corresponds to (10.38)

Equation 1b

Title	Stodola's ellipse law: mass flow rate for supercritical flow
Validity domain	$\forall \dot{m}$
Mathematical formulation	$\dot{m} = C_s \cdot \sqrt{\frac{P_i^2 - P_o^2}{T_i}}$
Comments	Corresponds to (10.38) with $x_i = 1$

Equation 2

Title	Fluid specific enthalpy at the outlet
Mathematical formulation	$h_o = h_i + \eta_{is} \cdot x_m \cdot (h_{is} - h_i) + \frac{(1 - \eta_{nz}) \cdot v_o^2}{2}$
Comments	<p>Corresponds to (10.40) with <math>C_{Bau} = 1</math>.</p> <p>The last term of the equation corresponds to the kinetic energy of the steam at the outlet.</p> <p>The nozzle efficiency <math>\eta_{nz}</math> is less than unity for a turbine with nozzle and equal to unity for a turbine without nozzle.</p> <p>The isentropic efficiency can be given by a characteristic equation which is a function of the mass flow rate:</p> $\eta_{is} = f_\eta(\dot{m})$

Equation 3

Title	Energy balance equation (mechanical power produced by the turbine)
Validity domain	$\forall \dot{m}$
Mathematical formulation	$W = \eta_{\text{sta}} \cdot \dot{m} \cdot (h_i - h_o) \cdot \left(1 - \frac{W_{\text{fric}}}{100}\right)$

### 10.2.4 Modelica Component Model: StodolaTurbine

The governing equations are implemented in the *StodolaTurbine* component model located in the *WaterSteam.Machines* sub-library. Figure 10.4a represents the graphical icon of the component with its four connectors.

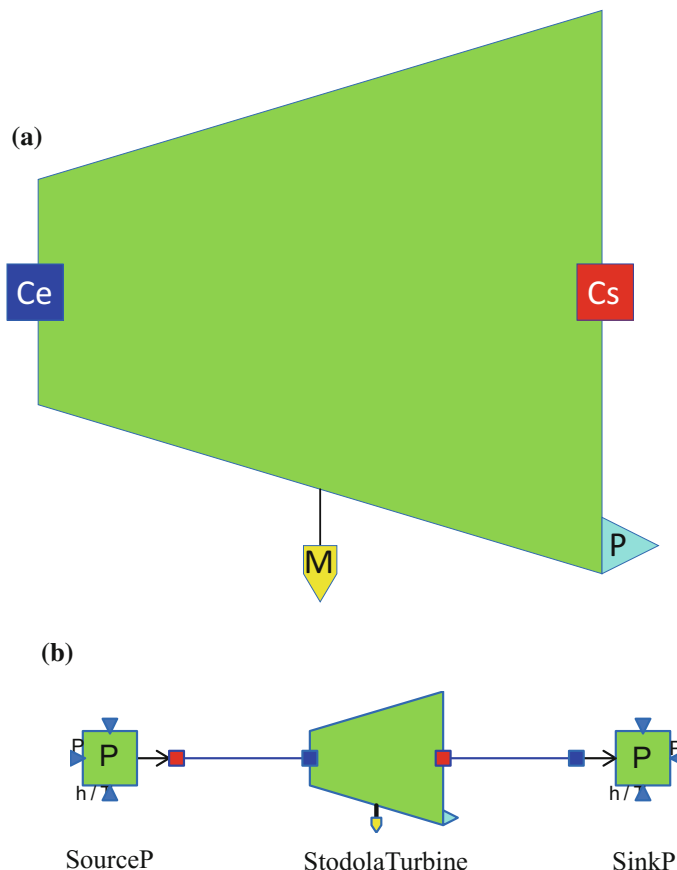


Fig. 10.4 a Icon representation of the *StodolaTurbine* component model and b test-case for the *StodolaTurbine* component model

### 10.2.5 Test-Case

The model *TestStodolaTurbine* used to validate the *StodolaTurbine* component model is represented in Fig. 10.4b. This model uses the following component models:

- One *StodolaTurbine* component model;
- One *SourceP* component model;
- One *SinkP* component model.

In this test-case scenario, the *StodolaTurbine* component receives: (1) the steam specific enthalpy and pressure at the inlet, and (2) the steam pressure at the outlet. The component computes: (1) the steam mass flow rate, (2) the steam specific enthalpy at the outlet, and (3) the mechanical power produced by the turbine.

#### 10.2.5.1 Test-Case Parameterization and Boundary Conditions

The model data are:

- Stodola's ellipse coefficient =  $2 \times 10^6$
- Nominal isentropic efficiency = 0.94
- Fluid specific enthalpy at the inlet =  $3475 \times 10^3$  J/kg
- Fluid pressure at the inlet =  $270 \times 10^5$  Pa
- Fluid pressure at the outlet =  $100 \times 10^5$  Pa.

#### 10.2.5.2 Model Calibration

The calibration step consists in setting the steam mass flow rate in the *StodolaTurbine* component model to a known measurement value to compute by model inversion the value of the Stodola's ellipse coefficient.

Other possible calibration: setting the steam specific enthalpy at the outlet to a known measurement value to compute by model inversion the value of the nominal isentropic efficiency.

#### 10.2.5.3 Simulation Results

The simulation of the test scenario gives the numerical results below:

- Mass flow rate = 600.17 kg/s
- Fluid temperature at the outlet = 701.9 K
- Fluid specific enthalpy at the outlet =  $3182.7 \times 10^3$  J/kg
- Mechanical power =  $175.406 \times 10^6$  W.

## References

- Bidard R, Bonnin J (1979) Energétique et turbomachines. Eyrolles, Paris
- Cooke DH (1985) On prediction of off-design multistage turbine pressures by Stodola's ellipse. Trans ASME 107:596–606
- Leyzerovich A (2005) Wet-steam turbines for nuclear power plants. PenWell Books
- Stodola A (1922) Dampf und gasturbinen V2: mit einem anhang über die aussichten der warmekraftmaschinen. Kessinger Pub Co

# Chapter 11

## Gas Turbine Modeling



**Abstract** A gas turbine is a type of internal combustion engine used for the generation of electricity. It is a rotating device that converts the hot flue gases resulting from air compression and combustion with gas into mechanical energy. A significant fraction of the mechanical power produced is used by the compressor, while the rest is converted into electricity in the generator. The exhausted gases are released to the atmosphere. Therefore, this cycle is classified as an open Brayton cycle. This chapter describes the two components of a gas turbine model, the compressor and the combustion turbine, and gives a detailed description of the physical equations: modeling assumptions and fundamental equations. A test-case is given that includes the structure of the model, parameterization data, and results of the simulation. The full description of the physical equations is independent of programming languages and tools.

### 11.1 Basic Principles

A gas turbine is a type of internal combustion engine following a Brayton cycle (cf. Fig. 11.1). The cycle is open as the flue gases are released to the atmosphere. It is composed of an upstream compressor coupled to a downstream turbine with a combustion chamber in between (cf. Fig. 11.2). Most commonly, combustion turbines are of axial flow type where the gas flow is parallel to the turbine axis.

The gas turbine converts thermal energy in the combustion products into mechanical energy on the shaft. The hot flue gases flow through the turbine, where they expand to the exhaust pressure, producing work on the shaft. A significant fraction of the mechanical power is used by the compressor, while the rest is converted into electricity in the generator.

The cooling of the gas turbine blades is essential for long life as it is continuously subject to high-temperature gases. The air cooling is the most commonly used method for cooling the turbine blades.

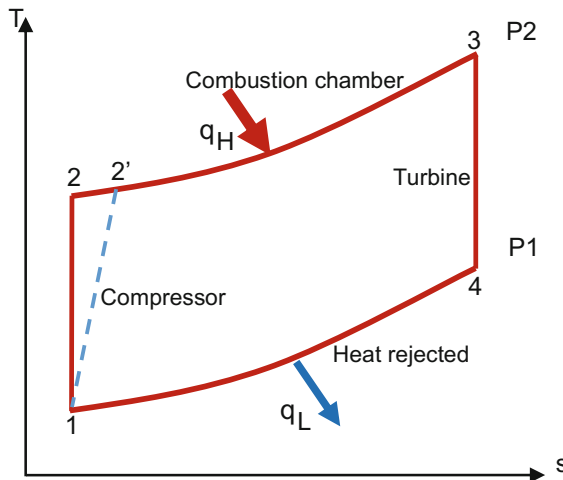


**Fig. 11.1** Ideal Brayton cycle in a temperature–entropy diagram

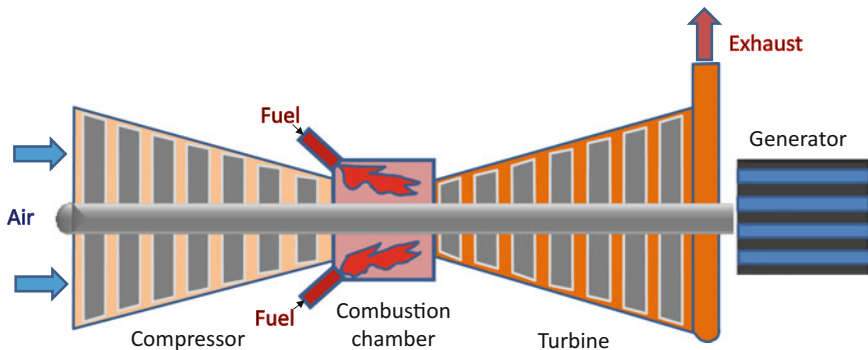


**Fig. 11.2** Schematic diagram of a gas turbine

For a gas turbine, the gas speed at the combustion turbine inlet reaches sonic speed with a Mach number equal to 1. The flow in the turbine is then at choked flow conditions.

The objective of the rest of this paragraph is to compute the power required by the compressor.

Assuming that the air is an ideal gas, that the compression is adiabatic, and that the turbine inlet and outlet are at the same altitude, from (5.5) the static energy balance equation writes:

$$-w_{12} = h_2 - h_1 \quad (11.1)$$

where  $w_{12}$  is the specific work in J/kg provided to the gas by the compressor,  $h_1$  is the fluid specific enthalpy at the compressor inlet, and  $h_2$  is the fluid specific enthalpy at the compressor outlet.

Assuming that the specific heat capacity  $c_p$  is constant throughout process 1–2 (the variation of specific heat with the temperature is small for the air), then from (2.18) the work produced by the compressor is:

$$-w_{12} = c_p \cdot (T_2 - T_1) = c_p \cdot T_1 \cdot \left( \frac{T_2}{T_1} - 1 \right) \quad (11.2)$$

where  $T_1$  and  $T_2$  are, respectively, the fluid temperature at the compressor inlet and outlet.

From the isentropic temperature and pressure relation for ideal gases (Laplace or Poisson's equation):

$$P_1 \cdot v_1^\gamma = P_2 \cdot v_2^\gamma \quad (11.3)$$

where  $P_1$  and  $v_1$  are, respectively, the fluid pressure and specific volume at the compressor inlet, and  $P_2$  and  $v_2$  are, respectively, the fluid pressure and specific volume at the compressor outlet.

$\gamma$  is the ratio of specific heats:

$$\gamma = c_p/c_v \quad (11.4)$$

Using the ideal gas law (2.77):

$$\frac{P_1 \cdot v_1}{P_2 \cdot v_2} = \frac{T_1}{T_2} \quad (11.5)$$

Using (11.3) and (11.5) yields:

$$\frac{T_2}{T_1} = \left( \frac{v_1}{v_2} \right)^{\gamma-1} = \left( \frac{P_2}{P_1} \right)^{\frac{\gamma-1}{\gamma}} \quad (11.6)$$

Using (11.2) and (11.6):

$$-w_{12} = c_p \cdot T_1 \cdot \left[ \left( \frac{P_2}{P_1} \right)^{\frac{\gamma-1}{\gamma}} - 1 \right] \quad (11.7)$$

In order to calculate the actual specific work, the concept of isentropic efficiency is used. The compressor isentropic efficiency  $\eta_{is}$  is defined as the ratio of the isentropic compression work to the actual compression work, when considering the process as isentropic:

$$\eta_{\text{is}} = \frac{h_2 - h_1}{h_{2'} - h_1} \quad (11.8)$$

where  $h_{2'}$  is the actual specific enthalpy at the compressor outlet; cf. Fig. 11.1.

Another ideal reference commonly used is the polytropic process. The polytropic evolution is used to describe any reversible process on open or closed systems. The polytropic process is described with the equation:

$$\frac{T_2}{T_1} = \left( \frac{P_2}{P_1} \right)^{\frac{n-1}{n}} \quad (11.9)$$

where  $n$  is the polytropic index with  $1 < n < \gamma$  as the fluid receives work and releases heat in the compression phase.

For an isentropic compression, one can write the Mayer relation:

$$R = c_p - c_v \quad (11.10)$$

Combining (11.4) and (11.10) yields:

$$c_p = \frac{\gamma}{\gamma - 1} \cdot R \quad (11.11)$$

Using the ideal gas law (2.77) with Eqs. (11.2), (11.9), and (11.11), and replacing  $\gamma$  by  $n$ , the specific polytropic work provided by the compressor to the gas is defined as:

$$-w_{\text{poly}} = \frac{n}{n-1} \cdot P_1 \cdot v_1 \cdot \left[ \left( \frac{P_2}{P_1} \right)^{\frac{n-1}{n}} - 1 \right] \quad (11.12)$$

The polytropic process equation can describe multiple compression and expansion processes.

## 11.2 Reference Quantities

A number of quantities have been defined to facilitate the analysis of flow characteristics and to allow comparison of the aerodynamic performance of different gas turbines. These quantities include the pressure ratio and the corrected mass flow rate (mass flow parameter).

For the compressor, the pressure ratio is defined as:

$$\pi_c = \frac{P_2}{P_1} \quad (11.13)$$

For the compressor, the corrected mass flow rate is defined as:

$$\dot{m}_{\text{cor\_c}} = \frac{\dot{m}_c \cdot \sqrt{T_1}}{P_1} \quad (11.14)$$

where  $\dot{m}_c$  is the gas mass flow rate at the compressor inlet.

For the turbine, the pressure ratio is defined as:

$$\pi_t = \frac{P_4}{P_3} \quad (11.15)$$

where  $P_3$  and  $P_4$  are, respectively, the pressure at the turbine inlet and outlet.

For the turbine, the corrected mass flow rate is defined as:

$$\dot{m}_{\text{cor\_t}} = \frac{\dot{m}_t \cdot \sqrt{T_3}}{P_3} \quad (11.16)$$

where  $T_3$  and  $\dot{m}_t$  are, respectively, the gas temperature and mass flow rate at the turbine inlet.

### 11.3 Static Modeling of Compressor

Nearly, all modern combustion turbines use multistage axial compressors. The compressor is used to increase the pressure of the atmospheric air that flows through it, in some cases up to 30 times higher than the atmospheric pressure.

The air density depends on the temperature, so when the ambient temperature decreases, the inlet air mass flow rate of the compressor increases.

In this paragraph, only a static model of the compressor is presented.

#### 11.3.1 Nomenclature

Symbols	Definition	Unit	Mathematical definition
$h_i$	Fluid specific enthalpy at the inlet	J/kg	
$h_{is}$	Fluid specific enthalpy after the isentropic compression	J/kg	

(continued)

(continued)

Symbols	Definition	Unit	Mathematical definition
$h_o$	Fluid specific enthalpy at the outlet	J/kg	
$\dot{m}$	Fluid mass flow rate	kg/s	$q \cdot \rho_i$
$P_i$	Fluid pressure at the inlet	Pa	
$P_o$	Fluid pressure at the outlet	Pa	
$q$	Fluid volumetric flow rate	m <sup>3</sup> /s	
$W_c$	Compressor power ( <i>negative value</i> )	W	
$X$	Ratio between the actual and nominal compression rate	–	$\pi / \pi_n$
$\eta$	Isentropic efficiency	–	
$\eta_n$	Nominal isentropic efficiency	–	
$\pi$	Compression rate	–	$P_o / P_i$
$\pi_n$	Nominal compression rate	–	
$\rho_i$	Fluid density at the inlet	kg/m <sup>3</sup>	

### 11.3.2 Governing Equations

The steady-state model is based on a polynomial equation of the isentropic efficiency obtained and validated against experimental data from several combined cycle power plants.

Equation 1

Title	Fluid specific enthalpy at the outlet of the compressor
Validity domain	$\forall h_i$
Mathematical formulation	$h_o = h_i + \frac{(h_{is} - h_i)}{\eta_{is}}$
Comments	Corresponds to (11.8)

Equation 2

Title	Compressor power
Validity domain	$\dot{m} \geq 0$
Mathematical formulation	$W_c = \dot{m} \cdot (h_i - h_0)$
Comments	Corresponds to (11.1)

Equation 3	
Title	Isentropic efficiency
Validity domain	$X > 0$
Mathematical formulation	$\eta = f_\eta(X) \cdot \eta_n$
Comments	<p><math>f_\eta(X)</math> is the compressor map expressed as a polynomial function of <math>X</math>. The following map function is independent of the compressor size and gives satisfactory results for the combined cycle power plant of Sect. 6.5:</p> $f_\eta(X) = -0.634857 \cdot X^2 + 1.46222 \cdot X + 0.1725914$

### 11.3.3 Modelica Component Model: Compressor

The governing equations are implemented in the *Compressor* component model located in the *FlueGases.Machines* sub-library. Figure 11.3a represents the graphical icon of the component with its three connectors.

### 11.3.4 Test-Case

The model *TestCompressor* used to validate the *Compressor* component model is represented in Fig. 11.3b. This model uses the following component models:

- One *Compressor* component model;
- One *SourcePQ* component model (from the *FlueGases* package);
- One *SinkP* component model (from the *FlueGases* package).

This component receives as inputs the characteristics of the air at the inlet (mass flow rate, temperature, pressure, and composition) and the air pressure at the outlet. It calculates the air temperature at the outlet, the volume flow rate, and the compressor power.

#### 11.3.4.1 Test-Case Parameterization and Boundary Conditions

The model data are:

- Nominal compression rate = 16
- Fluid temperature at the inlet = 288 K
- Fluid temperature at the outlet = 680 K
- Fluid mass flow rate at the inlet = 420 kg/s
- Fluid pressure at the inlet =  $10^5$  Pa
- Fluid pressure at the outlet =  $18.5 \times 10^5$  Pa
- H<sub>2</sub>O mass fraction in the fluid = 0.003
- O<sub>2</sub> mass fraction in the fluid = 0.23

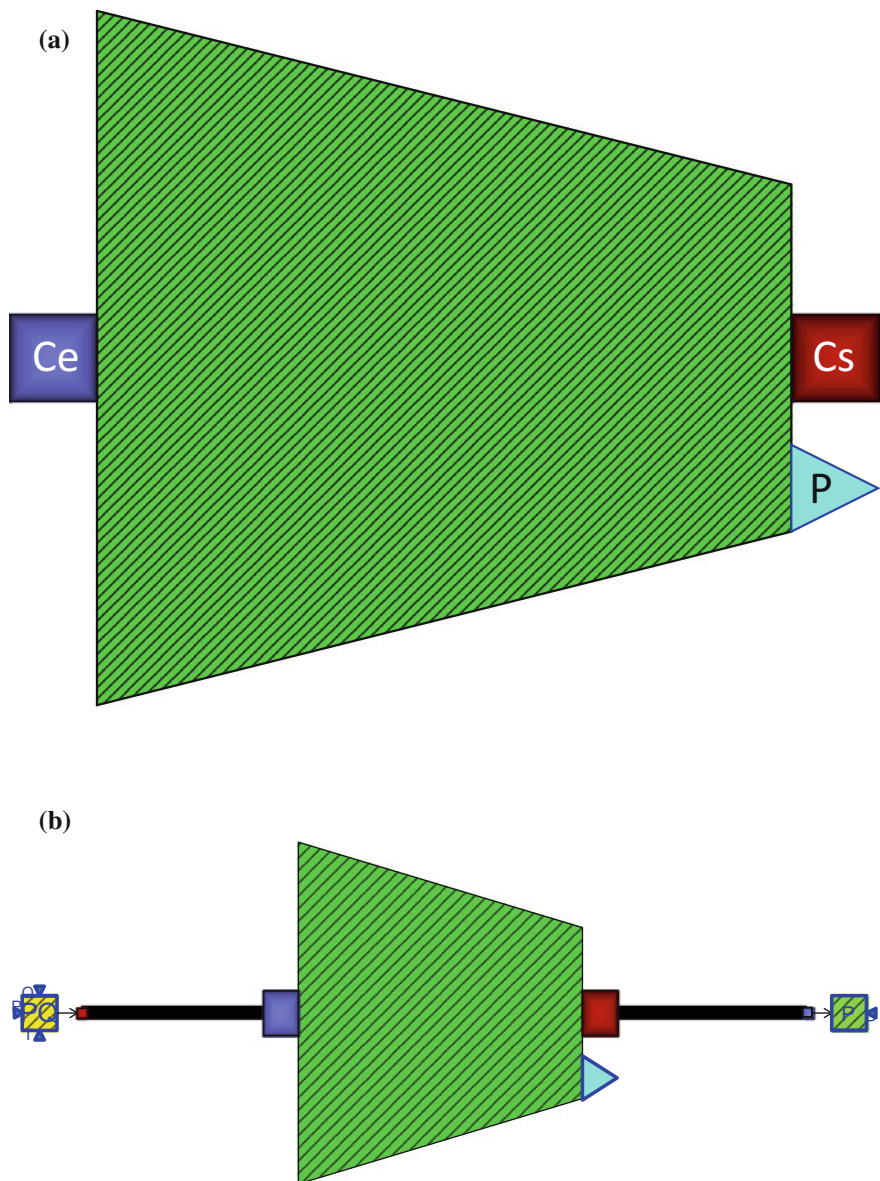


**Fig. 11.3** **a** Icon representation of the *Compressor* component model and **b** test-case for the *Compressor* component model

### 11.3.4.2 Model Calibration

The calibration step consists in setting the value of the air temperature at the outlet to a known measurement value and computing by model inversion the value of the nominal isentropic efficiency.

### 11.3.4.3 Simulation Results

The simulation of the test scenario was successful and led to the numerical results below:

- Nominal isentropic efficiency = 0.8523
- Isentropic efficiency = 0.8524
- Fluid volumetric flow rate =  $349.33 \text{ m}^3/\text{s}$
- Compressor power =  $-1.71218 \times 10^8 \text{ W}$

## 11.4 Static Modeling of the Combustion Turbine

### 11.4.1 Nomenclature

Symbols	Definition	Unit	Mathematical definition
$h_i$	Fluid specific enthalpy at the inlet	J/kg	
$h_{is}$	Fluid specific enthalpy after the isentropic expansion	J/kg	
$h_o$	Fluid specific enthalpy at the outlet	J/kg	
$\dot{m}$	Fluid mass flow rate	kg/s	
$\dot{m}_{cor}$	Corrected mass flow rate (mass flow rate parameter)	—	
$P_i$	Fluid pressure at the inlet	Pa	
$P_o$	Fluid pressure at the outlet	Pa	
$W_c$	Compressor power ( <i>negative value</i> )	W	
$W_m$	Mechanical power	W	
$W_t$	Turbine power (total power)	W	
$X$	Ratio between the actual and nominal expansion rate	—	$\pi / \pi_n$
$\eta_{is}$	Isentropic efficiency	—	
$\eta_n$	Nominal isentropic efficiency	—	
$\pi$	Expansion rate	—	$P_o/P_i$
$\pi_n$	Nominal expansion rate	—	

### 11.4.2 Assumptions

The following assumptions are made:

- Steady-state flow;
- Supersonic flow ( $\dot{m}_{\text{cor}} = \text{constant}$ ).

### 11.4.3 Governing Equations

The steady-state model is based on a polynomial equation of the isentropic efficiency obtained and validated against experimental data from several combined cycle power plants.

Equation 1	
Title	Fluid specific enthalpy at the outlet
Validity domain	$\forall h_i$
Mathematical formulation	$h_o = h_i + \eta_{\text{is}} \cdot (h_{\text{is}} - h_i)$
Comments	This equation is obtained from (10.6) with $\Delta h = h_o - h_i$ and $\Delta h_{\text{is}} = h_{\text{is}} - h_i$

Equation 2	
Title	Isentropic efficiency
Validity domain	$X > 0$
Mathematical formulation	$\eta_{\text{is}} = f_{\eta_{\text{is}}}(X) \cdot \eta_n$
Comments	$f_{\eta_{\text{is}}}(X)$ is the turbine map expressed as a polynomial function of $X$ . The following map function is independent of the turbine size and gives satisfactory results for the combined cycle power plant of Sect. 6.5: $f_{\eta_{\text{is}}}(X) = -0.04778 \cdot X^2 + 0.09555 \cdot X + 0.95223$

Equation 3	
Title	Total turbine power
Validity domain	$\forall \dot{m}$
Mathematical formulation	$W_t = \dot{m} \cdot (h_i - h_o)$
Comments	Corresponds to (10.2)

Equation 4	
Title	Mechanical power
Validity domain	$\forall \dot{m}$
Mathematical formulation	$W_m = W_t + W_c$
Comments	The mechanical power produced on the shaft of the electricity generator is the total turbine power minus the power used by the compressor (which is counted negatively)

Equation 5	
Title	Mass flow rate
Validity domain	$\forall P_i$ and $\forall T_i$
Mathematical formulation	$\dot{m}_{cor} = \frac{\dot{m} \cdot \sqrt{T_i}}{P_i}$
Comments	This equation calculates the mass flow rate from the corrected mass flow rate which is a parameter provided by the user

#### 11.4.4 Modelica Component Model: CombustionTurbine

The governing equations are implemented in the *CombustionTurbine* component model located in the *FlueGases.Machines* sub-library. Figure 11.4a represents the graphical icon of the component with its four connectors.

#### 11.4.5 Test-Case

The model *TestCombustionTurbine* used to validate the *CombustionTurbine* component model is represented in Fig. 11.4b. This model uses the following component models:

- One *CombustionTurbine* component model;
- One *SourceQ* component model (from the *FlueGases* package);
- One *SinkP* component model (from the *FlueGases* package);
- One *Constant* block.

This component receives as inputs the characteristics of the flue gases (mass flow rate, temperature, and composition) at the inlet, the flue gases pressure at the outlet, and the compressor power. It calculates the flue gases outlet temperature, the flue gases inlet pressure, the mechanical power, and the total power.

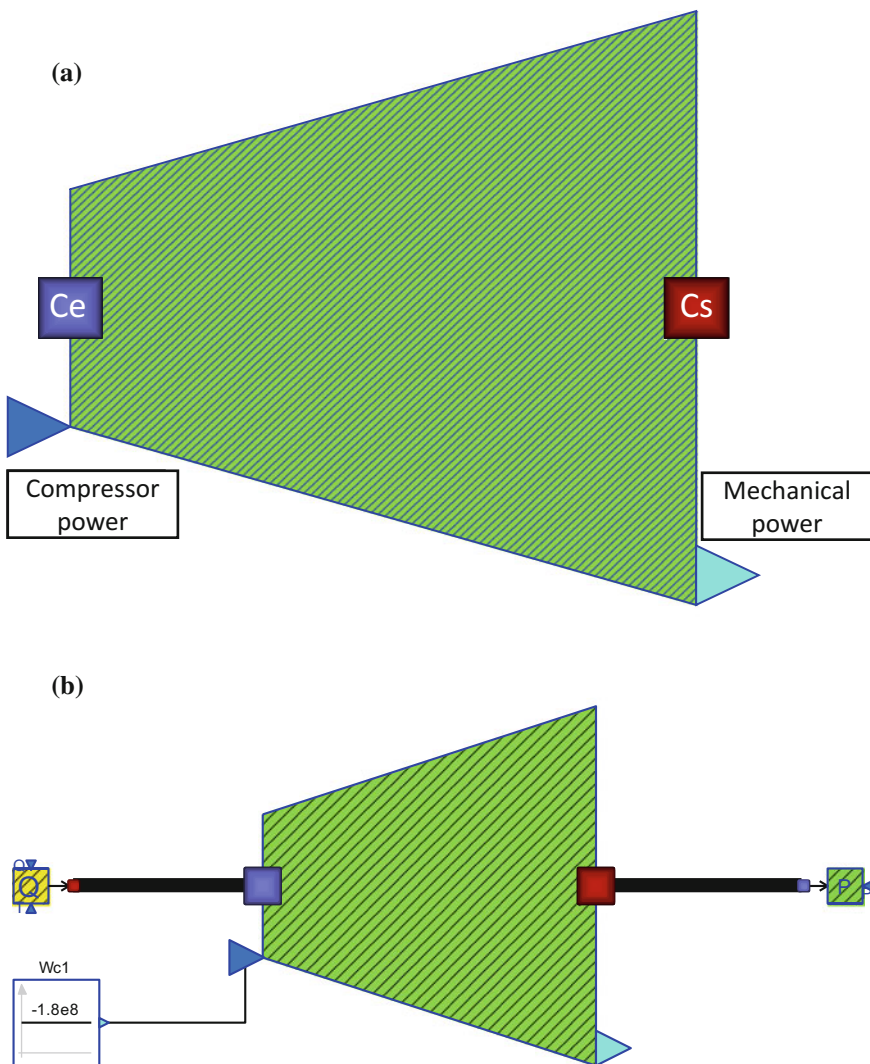


**Fig. 11.4** **a** Icon representation of the *CombustionTurbine* component model and **b** test-case for the *CombustionTurbine* component model

#### 11.4.5.1 Test-Case Parameterization and Boundary Conditions

The model data are:

- Nominal expansion rate = 0.06667
- Fluid temperature at the inlet = 1500 K
- Fluid temperature at the outlet = 680 K
- Fluid mass flow rate at the inlet = 430 kg/s
- Fluid pressure at the inlet =  $15 \times 10^5$  Pa
- Fluid pressure at the outlet =  $10^5$  Pa
- CO<sub>2</sub> mass fraction in the fluid = 0.06
- H<sub>2</sub>O mass fraction in the fluid = 0.06
- O<sub>2</sub> mass fraction in the fluid = 0.14

#### 11.4.5.2 Model Calibration

The calibration step consists in setting the value of the flue gases pressure at the inlet and the fluid temperature at the outlet to known measurement values and computing by model inversion the values of the corrected mass flow rate and of the nominal expansion.

#### 11.4.5.3 Simulation Results

The simulation of the test scenario gives the numerical results below:

- Nominal isentropic efficiency = 0.94753
- Isentropic efficiency = 0.9475
- Corrected mass flow (reduced mass flow rate) = 0.0111
- Mechanical power =  $1.82759 \times 10^8$  W

# Chapter 12

## Centrifugal Pump Modeling



**Abstract** Centrifugal pumps are one of the most important components in power plants. They are also widely used in industry. This chapter presents the different types of pump components (dynamic and static centrifugal pumps) and gives a detailed description of the physical equations for each of them: modeling assumptions and fundamental equations. A test-case is given for each model that includes the structure of the model, parameterization data and results of simulation. The full description of the physical equations is independent of the programming languages and tools.

### 12.1 Basic Description

Centrifugal pumps are one of the most important components in power plants. They are also widely used in industry. They can be single-stage or multi-stage. Their rotating part can be propelled by an electric motor or by a steam turbine.

Centrifugal pumps are used to generate flow or to increase the pressure of a liquid. To those ends, they convert mechanical energy into kinetic energy. The pressure at the outlet of the pump corresponds to the transformation of kinetic energy into static pressure (cf. Fig. 12.1), as depicted by the Bernoulli equation (4.17). However, the Bernoulli equation cannot be used here because energy losses cannot be neglected. So the momentum balance equation is replaced by a more general homologous relation called pump characteristic, as shown in the sequel.

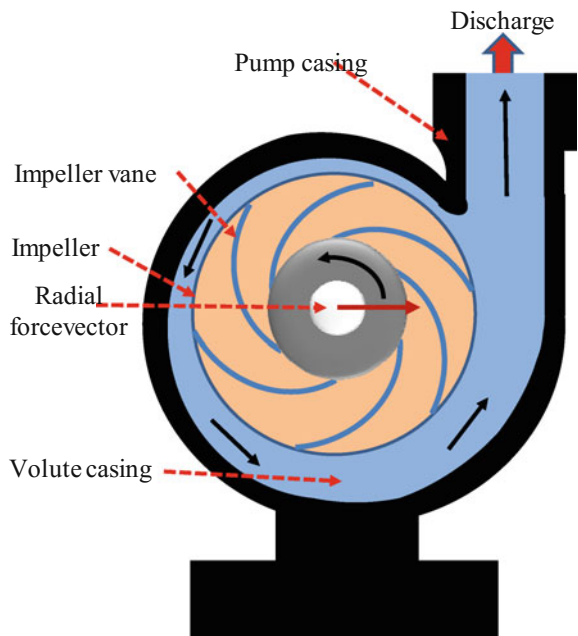
The problem is to compute the variation of fluid pressure  $\Delta P$  through the pump from the mechanical work received from the rotating shaft.

$$\Delta P = P_{\text{out}} - P_{\text{in}} \quad (12.1)$$

where  $P_{\text{in}}$  is the pressure at the inlet and  $P_{\text{out}}$  is the pressure at the outlet.

Assuming incompressible flow, and neglecting thermal inertia, the pump is considered as a static component w.r.t. the fluid balance equations. However, mechanical inertia is taken into account with the rotating mass dynamic equation.

**Fig. 12.1** Schematic diagram of a centrifugal pump



The static energy balance equation (5.5) applied to the fluid yields:

$$\dot{m} \cdot \Delta h = \dot{W}_h + \dot{W}_f \quad (12.2)$$

where  $\dot{m}$  is the mass flow rate through the pump,  $\Delta h$  is the variation of the fluid specific enthalpy between the inlet and the outlet,  $\dot{W}_h$  is the mechanical work produced by the shaft on the fluid, and  $\dot{W}_f$  is the heat released to the fluid by friction of the shaft.

Equation (12.2) is not valid for zero flows, as  $\Delta h$  is undefined when  $\dot{m} = 0$  (see also Sect. 5.2.1).

$$\Delta h = h_{\text{out}} - h_{\text{in}} \quad (12.3)$$

$$\dot{W}_h = T_h \cdot \omega \quad (12.4)$$

$$\dot{W}_f = T_f \cdot \omega \quad (12.5)$$

where  $\omega$  is the shaft angular speed,  $T_h$  is the hydraulic torque on the shaft and  $T_f$  is the friction torque on the shaft.

The friction torque may be given by:

$$T_f = \begin{cases} \text{sign}(\bar{\omega}) \cdot T_{f_0} \cdot (1 - |\bar{\omega}|) & \text{if } |\bar{\omega}| < 1 \\ 0 & \text{if } |\bar{\omega}| \geq 1 \end{cases} \quad (12.6)$$

with

$$\bar{\omega} = \frac{\omega}{\omega_{\text{nom}}} \quad (12.7)$$

$\omega_{\text{nom}}$  is the nominal angular speed of the pump, and  $T_{f_0}$  is the value of the friction torque for  $\omega = 0$ . The friction torque prevents oscillations of the rotational speed when the pump is stopped.

The hydraulic torque is computed by considering the hydraulic efficiency of the pump:

$$\eta_h = \frac{\dot{W}_u}{\dot{W}_h} \quad (12.8)$$

$\dot{W}_u$  is the useful mechanical work produced by the pump:

$$\dot{W}_u = q \cdot \Delta P \quad (12.9)$$

$q$  is the average volumetric flow rate:

$$q = \frac{\dot{m}}{\rho} \quad (12.10)$$

where  $\rho$  is the average fluid density between the inlet and the outlet.

From (12.4), (12.8), and (12.9), the value of the hydraulic torque is given by:

$$T_h = \frac{q \cdot \Delta P}{\eta_h \cdot \omega} \quad (12.11)$$

$\eta_h$  is given by the following dimensionless homologous relation:

$$\eta_h = f_\eta \left( \frac{q}{\omega} \right) \quad (12.12)$$

The momentum balance equation is replaced by the dimensionless homologous relation for the pump head:

$$\frac{\Delta P}{\rho \cdot \omega^2} = f_h \left( \frac{q}{\omega} \right) \quad (12.13)$$

The functions  $f_h$  and  $f_\eta$  are the dimensionless characteristics of the pump that are usually provided by the manufacturer. They can be given by tables or approximated by polynomials.

The pump head is defined as

$$h_n = \frac{\Delta P}{\rho \cdot g} \quad (12.14)$$

Using the dimensionless quantities

$$\bar{h}_n = \frac{h_n}{h_{nom}} \quad (12.15)$$

$$\bar{T}_h = \frac{T_h}{T_{nom}} \quad (12.16)$$

$$\bar{q} = \frac{q}{q_{nom}} \quad (12.17)$$

with  $h_{nom}$ ,  $T_{nom}$ , and  $q_{nom}$  being, respectively, the nominal pump head, nominal hydraulic torque, and nominal volumetric flow, (12.13) can be rewritten as

$$\frac{\bar{h}_n}{\bar{\omega}^2} = \bar{f}_h \left( \frac{\bar{q}}{\bar{\omega}} \right) \quad (12.18)$$

and (12.11) can be replaced by the dimensionless homologous relation

$$\frac{\bar{T}_h}{\bar{\omega}^2} = \bar{g}_h \left( \frac{\bar{q}}{\bar{\omega}} \right) \quad (12.19)$$

As (12.18) and (12.19) are singular when  $\omega = 0$ , they can be, respectively, replaced by (Wylie and Streeter 1993)

$$\frac{\bar{h}_n}{\bar{q}^2 + \bar{\omega}^2} = F(\theta) \quad (12.20)$$

$$\frac{\bar{T}_h}{\bar{q}^2 + \bar{\omega}^2} = G(\theta) \quad (12.21)$$

with

$$\theta = \arctan \left( \frac{\bar{q}}{\bar{\omega}} \right), \quad \theta \in [0, 2\pi] \quad (12.22)$$

which is a variant of the Suter representation (Kolev 2005).

Equation (12.20) complies with the dimensionless homologous relation (12.18) because

$$\frac{\bar{h}_n}{\bar{q}^2 + \bar{\omega}^2} = \frac{\bar{h}_n}{\bar{\omega}^2 \cdot \left(1 + \left(\frac{\bar{q}}{\bar{\omega}}\right)^2\right)}$$

and therefore

$$\frac{\bar{h}_n}{\bar{\omega}^2} = \left(1 + \left(\frac{\bar{q}}{\bar{\omega}}\right)^2\right) \cdot F\left(\arctan\left(\frac{\bar{q}}{\bar{\omega}}\right)\right) = \bar{f}_h\left(\frac{\bar{q}}{\bar{\omega}}\right)$$

The same holds for (12.21).

Finally, the rotating mass dynamic equation for the shaft is:

$$J \cdot \frac{d\omega}{dt} = T_m - T_h - T_f \quad (12.23)$$

where  $T_m$  is the torque delivered by the motor and  $J$  is the shaft inertia.

The nominal operating point corresponds to  $\bar{\omega} = \bar{q} = \bar{T}_h = \bar{h}_n = 1$  and consequently to  $\theta = \frac{\pi}{4}$ .

Figure 12.2 presents the different operating domains of a centrifugal pump as a function of  $\theta$  (Knapp 1937; Wylie and Streeter 1993; Coppolani et al. 2004; Kolev 2005).

Figure 12.3 gives an example of  $F(\theta)$  and  $G(\theta)$  for the specific speed  $N_s = 25$  (SI units) based on data obtained from Hollander's experiments (Wylie and Streeter 1993). The specific speed is defined as

$$N_s = N_{\text{nom}} \cdot \frac{\sqrt{q_{\text{nom}}}}{(h_n)_{\text{nom}}^{3/4}} \quad (12.24)$$

with  $N_{\text{nom}}$  being the nominal pump speed expressed in revolutions per minute:

$$N_{\text{nom}} = \frac{30}{\pi} \cdot \omega_{\text{nom}} \quad (12.25)$$

To compare the hydraulic torque given by the analytical expression (12.11) with the hydraulic torque given by the homologous relation (12.21), the analytical expression (12.11) is rewritten as a function of  $\theta$  taking a second-order polynomial for  $\eta_h$ :

$$\frac{\bar{T}_h}{\bar{q}^2 + \bar{\omega}^2} = G'(\theta) \quad (12.26)$$

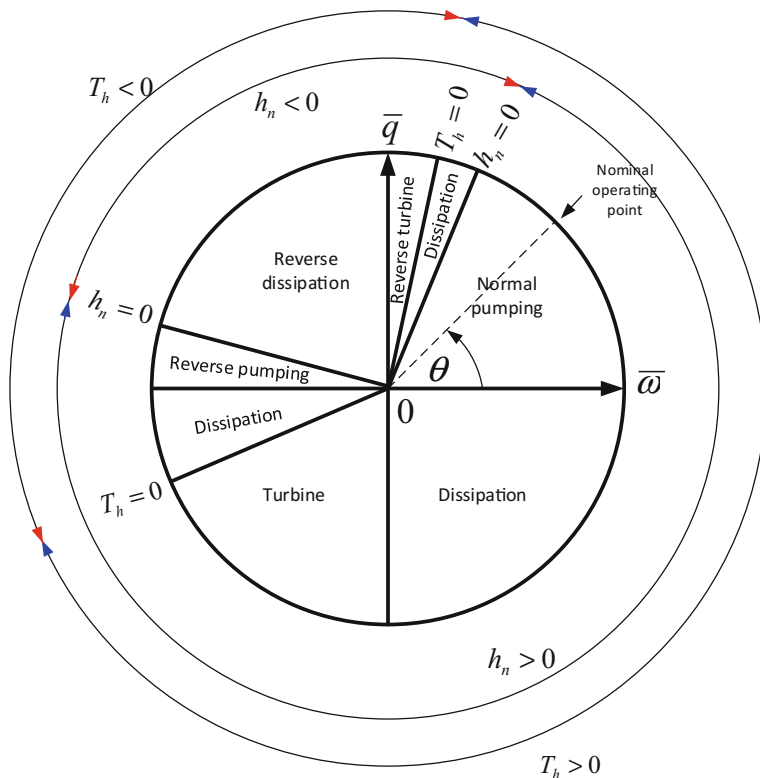


**Fig. 12.2** Centrifugal pump operating domains

with

$$G'(\theta) = \frac{F(\theta)}{2 - \tan(\theta)} \quad (12.27)$$

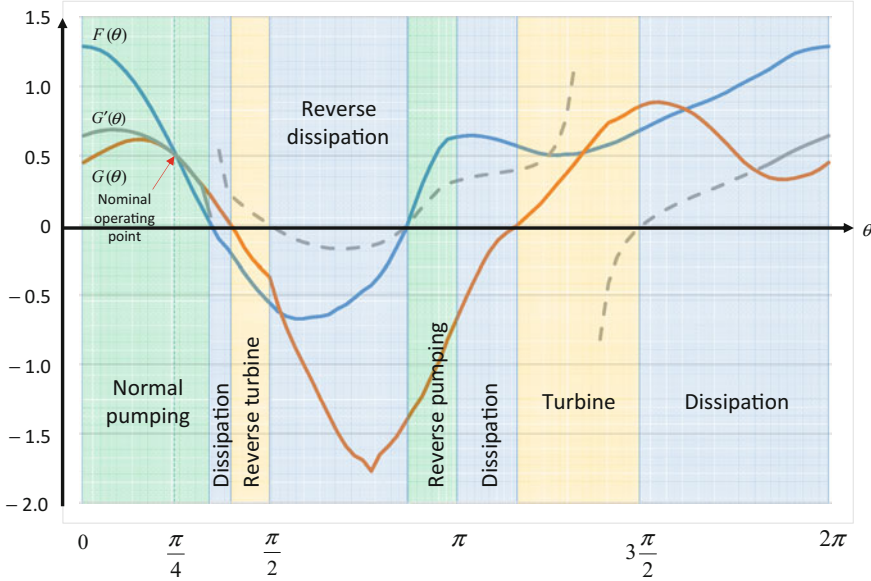
$G'(\theta)$  is not defined for  $\theta = \arctan(2) \approx 0.35 \cdot \pi \pm n \cdot \pi$ .

Figure 12.3 shows that  $G'(\theta)$  is tangent to  $G(\theta)$  around the nominal operating point  $\theta = \frac{\pi}{4}$ , deviates from  $G(\theta)$  when not in the vicinity of the nominal point, and is often unphysical (i.e., has the wrong sign) when not in the normal pumping region. Therefore, (12.11) is valid only in the normal pump operation region and accurate around the nominal operating point.

The derivation of (12.27) follows.

From (12.11) and (12.15–12.17):

$$\bar{T}_h = \frac{\bar{q} \cdot \bar{h}_n}{\bar{\eta}_h \cdot \bar{\omega}} \quad (12.28)$$



**Fig. 12.3**  $F(\theta)$  (blue curve),  $G(\theta)$  (orange curve), and  $G'(\theta)$  (gray solid and dashed curve)

with

$$\bar{\eta}_h = \frac{\eta_h}{\eta_{h,nom}} \quad (12.29)$$

$\eta_{h,nom}$  being the nominal hydraulic efficiency.

From (12.20), (12.22), and (12.28):

$$\frac{\bar{T}_h}{\bar{q}^2 + \bar{\omega}^2} = \frac{1}{\bar{\eta}_h} \cdot \frac{\bar{q}}{\bar{\omega}} \cdot F(\theta) = \frac{1}{\bar{\eta}_h} \cdot \tan(\theta) \cdot F(\theta) \quad (12.30)$$

Expressing  $\bar{\eta}_h$  as a second-order polynomial:

$$\bar{\eta}_h = -(b-1) \cdot \left( \frac{\bar{q}}{\bar{\omega}} \right)^2 + b \cdot \frac{\bar{q}}{\bar{\omega}} \quad (12.31)$$

where  $b$  is a constant. One can verify that  $\bar{\eta}_h = 1$  for the nominal point  $\bar{q} = \bar{\omega} = 1$  and that  $\bar{\eta}_h = 0$  when  $\bar{q} = 0$  [see (12.8), (12.9), (12.17), and (12.29)]. Assuming that the hydraulic efficiency  $\bar{\eta}_h$  is maximum for the nominal operating point  $\bar{q} = \bar{\omega} = 1$  yields  $b = 2$ .

Then

$$\bar{\eta}_h = -\tan^2(\theta) + 2 \cdot \tan(\theta) \quad (12.32)$$

Inserting (12.32) into (12.30) with  $b = 2$  yields (12.27).

## 12.2 Static Centrifugal Pump

### 12.2.1 Nomenclature

Symbols	Definition	Unit	Mathematical definition
$a_2$	$x^2$ coefficient of the pump parabolic characteristic $h_n = f_h(q/\omega)$	$\text{s}^2/\text{m}^5$	
$a_1$	$x$ coefficient of the pump parabolic characteristic $h_n = f_h(q/\omega)$	$\text{s}/\text{m}^2$	
$a_0$	Constant coefficient of the pump parabolic characteristic $h_n = f_h(q/\omega)$	m	
$b_2$	$x^2$ coefficient of the pump parabolic characteristic $\eta_h = f_\eta(q/\omega)$	$\text{s}^2/\text{m}^6$	
$b_1$	$x$ coefficient of the pump parabolic characteristic $\eta_h = f_\eta(q/\omega)$	$\text{s}/\text{m}^3$	
$b_0$	Constant coefficient of the pump parabolic characteristic $\eta_h = f_\eta(q/\omega)$	—	
$F(\theta)$	Pump head full characteristic	—	
$g$	Gravity constant	$\text{m}/\text{s}^2$	
$h_i$	Fluid specific enthalpy at the inlet	$\text{J}/\text{kg}$	
$h_o$	Fluid specific enthalpy at the outlet	$\text{J}/\text{kg}$	
$h_n$	Pump head	m	$h_n = \frac{P_o - P_i}{\rho \cdot g}$
$\dot{m}$	Fluid mass flow rate through the pump	$\text{kg}/\text{s}$	
$N$	Rotational speed of the pump	rev/min	$\frac{30}{\pi} \cdot \omega$
$N_{\text{nom}}$	Nominal rotational speed of the pump	rev/min	$\frac{30}{\pi} \cdot \omega_{\text{nom}}$
$P_i$	Fluid pressure at the inlet	Pa	
$P_o$	Fluid pressure at the outlet	Pa	
$q$	Volumetric flow rate through the pump	$\text{m}^3/\text{s}$	$\frac{\dot{m}}{\rho}$
$q_{\text{nom}}$	Nominal volumetric flow rate through the pump	$\text{m}^3/\text{s}$	
$\bar{q}$	Reduced volumetric flow rate through the pump	—	$\frac{q}{q_{\text{nom}}}$
$W_h$	Hydraulic power	W	
$W_m$	Mechanical power	W	
$\eta_h$	Hydraulic efficiency	—	

(continued)

(continued)

Symbols	Definition	Unit	Mathematical definition
$\eta_m$	Product of the pump mechanical and electrical efficiencies	–	
$\theta$	Angle between coordinates $(\omega, q)$ in the pump operating domain	rad	$\arctan\left(\frac{\bar{q}}{\bar{\omega}}\right)$
$\rho$	Average fluid density between the inlet and the outlet	kg/m <sup>3</sup>	
$\omega$	Pump rotational velocity	rad/s	
$\omega_{\text{nom}}$	Pump nominal rotational velocity	rad/s	
$\bar{\omega}$	Reduced rotational speed	–	$\frac{\omega}{\omega_{\text{nom}}} = \frac{N}{N_{\text{nom}}}$

### 12.2.2 Governing Equations

For the static model, the rotational speed of the pump  $N$  is a fixed input. Alternatively, the mechanical power can be provided as a fixed input and the rotational speed is calculated.

The model depends on the available characteristics from the manufacturer. Usually, characteristics are only provided for the operating domain limited to  $\bar{\omega} > 0$ ,  $q > 0$  and  $h_n > 0$  (cf. Fig. 12.2). Such characteristics are sufficient if simulation near the nominal operating is sufficient. However, for large transients involving other operating regimes, the full characteristic spanning the entire operating domain is needed. Therefore, two sets of equations are given, the first numbered with extension-a involving a partial parabolic characteristic, as usually provided by the manufacturers, and the second numbered with extension-b involving full characteristics.

---

#### Equation 1

---

Title	Energy balance equation
Validity domain	$\forall \bar{\omega}$ and $\forall q \neq 0$ such that $0 < \eta_h \leq 1$
Mathematical formulation	$g \cdot h_n = \eta_h \cdot (h_o - h_i)$
Comments	<p>Derivation of Eq. 1. Neglecting friction, the static balance equation (12.2) writes:</p> $\dot{W}_h = \dot{m} \cdot \Delta h$ <p>From (12.8) and (12.9)</p> $\dot{W}_h = \frac{q \cdot \Delta P}{\eta_h}$ <p>From (12.10) and (12.14), it follows that</p> $q \cdot \rho \cdot g \cdot h_n = \eta_h \cdot \rho \cdot q \cdot \Delta h$ <p>Hence,</p> $g \cdot h_n = \eta_h \cdot \Delta h = \eta_h \cdot (h_o - h_i)$

**Equation 2**

Title	Energy balance equation: mechanical power
Validity domain	$\forall \bar{\omega}$ and $\forall q$ such that $0 < \eta_m \leq 1$
Mathematical formulation	$W_m = \frac{\rho \cdot q \cdot (h_o - h_i)}{\eta_m}$
Comments	Using (12.2), (12.3), and (12.10), the mechanical balance equation (12.23) applied to powers (instead of torques) yields, considering that the pump angular velocity is constant: $\eta_m \cdot W_m = W_h = \dot{m} \cdot \Delta h = \rho \cdot q \cdot (h_o - h_i)$ where $\eta_m$ is the fraction of useful mechanical power

**Equation 3**

Title	Energy balance equation: hydraulic power
Validity domain	$\forall \bar{\omega}$ and $\forall q$ such that $0 < \eta_h \leq 1$
Mathematical formulation	$W_h = \frac{q \cdot (P_o - P_i)}{\eta_h}$
Comments	Equation 3 follows from (12.8) and (12.9)

**Equation 4-a**

Title	Pump partial parabolic characteristic
Validity domain	$\bar{\omega} > 0$ and $q > 0$
Mathematical formulation	$h_n = a_2 \cdot q \cdot  q  + a_1 \cdot q \cdot \bar{\omega} + a_0 \cdot \bar{\omega}^2$
Comments	Taking a parabola for function $\bar{f}_h$ in (12.18) yields: $\frac{\bar{h}_n}{\bar{\omega}^2} = \alpha_2 \cdot \left(\frac{\bar{q}}{\bar{\omega}}\right)^2 + \alpha_1 \cdot \left(\frac{\bar{q}}{\bar{\omega}}\right) + \alpha_0$ Therefore $\bar{h}_n = \alpha_2 \cdot \bar{q}^2 + \alpha_1 \cdot \bar{q} \cdot \bar{\omega} + \alpha_0 \cdot \bar{\omega}^2$ or $h_n = a_2 \cdot q^2 + a_1 \cdot q \cdot \bar{\omega} + a_0 \cdot \bar{\omega}^2$ with $a_2 = \frac{\alpha_2 \cdot h_{nom}}{q_{nom}^2}$ $a_1 = \frac{\alpha_1 \cdot h_{nom}}{q_{nom}}$ $a_0 = \alpha_0$ In order to provide a single solution for $q$ when $q$ is calculated from the knowledge of $h_n$ (this being a consequence of the causality analysis, cf. Sect. 1.5), $q^2$ is replaced by $q \cdot  q $ . This also means that the characteristic defined by Eq. 4-a is only physically valid for $q > 0$ (although it is mathematically valid $\forall q$ )

The physical meaning of a parabolic characteristic is the following. Let us consider the kinetic energy provided by the pump to the fluid:

$$\Delta E_c = \frac{1}{2} \cdot \dot{m} \cdot (r^2 \cdot \omega^2 - v^2)$$

where  $\dot{m}$  is the mass flow rate through the pump,  $r$  is the radius of the impeller,  $\omega$  is the pump rotational speed and  $v$  is the fluid velocity at the inlet of the pump (therefore  $r \cdot \omega$  is the velocity at the outlet of the

(continued)

(continued)

**Equation 4-a**

Title	Pump partial parabolic characteristic
	<p>pump). If the kinetic energy provided to the fluid is entirely converted into pressure, then from Bernoulli's theorem (cf. Sect. 13.1):</p> $\frac{\Delta P}{\rho} = \frac{1}{2} \cdot (r^2 \cdot \omega^2 - v^2)$ <p>where <math>\Delta P = P_o - P_i</math> is the variation of the fluid pressure between the inlet and the outlet of the pump. Then</p> $h_n = \frac{1}{2 \cdot g} \cdot (r^2 \cdot \omega^2 - v^2)$ <p>or</p> $h_n = \frac{1}{2 \cdot g} \cdot \left[ r^2 - \frac{1}{A^2} \cdot \left( \frac{q}{\omega} \right)^2 \right]$ <p>where <math>A</math> is the fluid cross-sectional area at the inlet.</p> <p>This corresponds to a parabolic characteristic</p>

**Equation 4-b**

Title	Pump full characteristic
Validity domain	$\forall \bar{\omega}$ and $\forall q$ such that $\bar{\omega} \cdot q \neq 0$
Mathematical formulation	$\frac{\bar{h}_n}{\bar{q}^2 + \bar{\omega}^2} = F(\theta)$
Comments	<p>This equation corresponds to (12.20). The characteristic <math>F(\theta)</math> depends on the specific speed <math>N_s</math>; cf. (12.24)</p> <p>To extend the validity domain to all values of <math>\bar{\omega}</math> and <math>q</math>, one can write Eq. 4-b as</p> $\bar{h}_n = (\bar{q}^2 + \bar{\omega}^2) \cdot F(\theta)$ <p>and choose an arbitrary value for <math>\theta</math> when <math>\omega = 0</math> and <math>q = 0</math> among the values <math>\theta \in \left\{ 0, \frac{\pi}{2}, \pi, \frac{3\pi}{2}, 2\pi \right\}</math></p>

**Equation 5**

Title	Hydraulic parabolic efficiency
Validity domain	$\bar{\omega} > 0$ and $q > 0$ such that $0 < \eta_h \leq 1$
Mathematical formulation	$\eta_h = b_2 \cdot \frac{q \cdot  q }{\bar{\omega}^2} + b_1 \cdot \frac{q}{\bar{\omega}} + b_0$
Comments	The derivation of Eq. 5 is similar to Eq. 4 starting from the homologous relation (12.12)

**Equation 6**

Title	Fluid average density
Validity domain	$\forall P$ and $\forall h$ inside the validity domain of $f_p$
Mathematical formulation	$\rho = f_p \left( \frac{P_i + P_o}{2}, \frac{h_i + h_o}{2} \right)$
Comments	<p><math>f_p</math> is the state equation for the density.</p> <p>Notice that the pump does not follow the upwind scheme; cf. (4.113).</p> <p>The average density is calculated at the midpoint of the compression.</p>

### 12.2.3 Modelica Component Model: StaticCentrifugalPump

The governing equations are implemented in the *StaticCentrifugalPump* component model located in the *WaterSteam.Machines* sub-library. Figure 12.4a represents the graphical icon of the component with its three connectors.

### 12.2.4 Test-Case

The model *TestStaticCentrifugalPump* used to validate the *StaticCentrifugalPump* component model is represented in Fig. 12.4b. This model uses the following component models:

- One *StaticCentrifugalPump* component model;
- One *Tank* model component model;
- One *ControlValve* component model;
- One *Pulse* block.

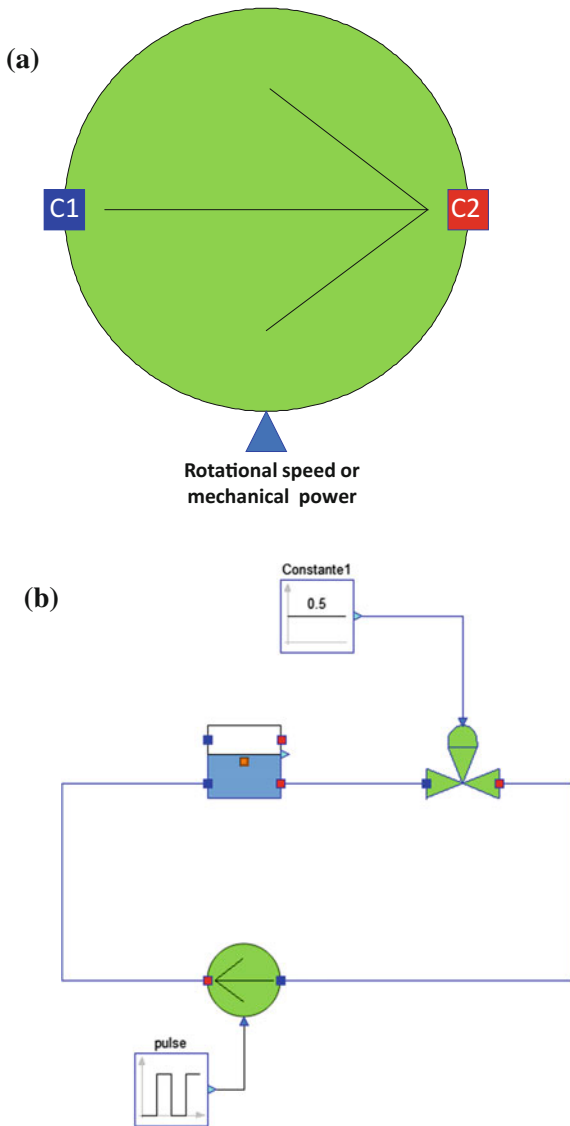
In this test-case scenario, the *StaticCentrifugalPump* component receives: (1) the fluid specific enthalpy and pressure at the inlet, and (2) the fluid pressure at the outlet. The component computes: (1) the fluid mass flow rate, (2) the fluid specific enthalpy at the outlet, and (3) the mechanical power.

#### 12.2.4.1 Test-Case Parameterization and Boundary Conditions

The model data are:

- $a_2$  (pump) =  $-88.67 \text{ s}^2/\text{m}^5$
- $a_1$  (pump) = 0
- $a_0$  (pump) = 43.15 m
- $b_2$  (pump) =  $-3.7751 \text{ s}^2/\text{m}^6$
- $b_1$  (pump) = 3.61  $\text{s}/\text{m}^3$
- $b_0$  (pump) = -0.0075464
- Nominal rotational speed = 1400 rev/min
- Fluid specific enthalpy in the tank =  $10^5 \text{ J/kg}$
- Pressure above the water level in the tank =  $10^5 \text{ Pa}$
- Altitude of inlet 2 (tank) = 10 m
- Altitude of outlet 2 (tank) = 10 m
- Maximum mass flow rate coefficient of the valve = 8005.42 U.S.

**Fig. 12.4 a** Icon of the *StaticCentrifugalPump* component model.  
**b** Test-case for the *StaticCentrifugalPump* component model



#### 12.2.4.2 Model Calibration

The calibration step consists in setting the fluid mass flow rate in the *StaticCentrifugalPump* to a known measurement value to compute by model inversion the value of the coefficient  $a_2$  (the  $x^2$  coefficient of the pump characteristic).

### 12.2.4.3 Simulation Results

Figure 12.5 shows the results of the simulation for a scenario of pump rotational speed variation from 1400 rev/min to 0 and from 0 to 1400 rev/min.

## 12.3 Centrifugal Pump

The centrifugal pump model is an extension of the static centrifugal pump model (cf. Sect. 12.2) to all operating domains of the pump (cf. Figure 12.2). It also features a dynamic rotating mass equation for the shaft.

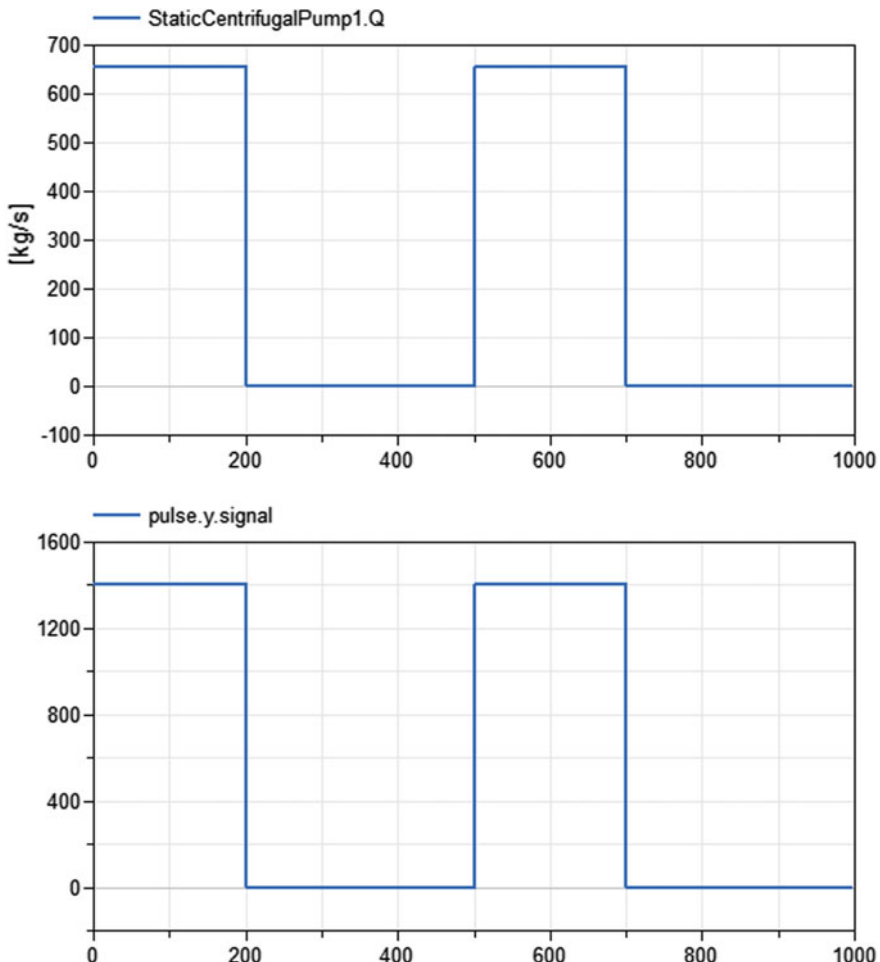


**Fig. 12.5** Simulation results for *StaticCentrifugalPump*: mass flow rate and pump rotational speed

### 12.3.1 Nomenclature

The following nomenclature is given in addition to the nomenclature used for the static centrifugal pump (cf. Sect. 12.2.1).

Symbols	Definition	Unit	Mathematical definition
$G(\theta)$	Hydraulic torque full characteristic	–	
$J$	Shaft inertia	$\text{kg m}^2$	
$T_h$	Hydraulic torque	$\text{N m}$	
$T_m$	Motor torque	$\text{N m}$	

### 12.3.2 Governing Equations

The equations for this component model are given in addition to the equations for the static centrifugal pump (cf. Sect. 12.2.2). Therefore, they are numbered in continuity with the static centrifugal pump model equations.

<b>Equation 7</b>	
Title	Rotational mass equation
Validity domain	$\forall \bar{\omega}$ and $\forall q$
Mathematical formulation	$J \cdot \frac{d\omega}{dt} = T_m - T_h$
Comments	This equation replaces the fixed input for the rotational speed (or the mechanical power) of the static pump model. It is derived from (12.23) by neglecting the friction torque

<b>Equation 8-a</b>	
Title	Hydraulic torque with an analytic formula
Validity domain	$\bar{\omega} > 0$ , $q > 0$ and $h_n > 0$
Mathematical formulation	$T_h = \frac{q \cdot (P_o - P_i)}{\eta_h \cdot \omega}$
Comments	This equation replaces the fixed input for the rotational speed (or the mechanical power) of the static pump model. It corresponds to (12.11). This equation is accurate only around the nominal point ( $\bar{\omega} = \bar{q} = 1$ ); cf. Sect. 12.1

<b>Equation 8-b</b>	
Title	Hydraulic torque with a full characteristic
Validity domain	$\forall \bar{\omega}$ and $\forall q$ such that $\bar{\omega} \cdot q \neq 0$
Mathematical formulation	$\frac{\bar{T}_h}{\bar{q}^2 + \bar{\omega}^2} = G(\theta)$

(continued)

(continued)

**Equation 8-b**

Title	Hydraulic torque with a full characteristic
Comments	<p>This equation corresponds to (12.21). The characteristic <math>G(\theta)</math> depends on the specific speed <math>N_s</math>; cf. (12.24)</p> <p>To extend the validity domain to all values of <math>\bar{\omega}</math> and <math>q</math>, one can write Eq. 8-b as</p> $\bar{T}_h = (\bar{q}^2 + \bar{\omega}^2) \cdot G(\theta)$ <p>and choose an arbitrary value for <math>\theta</math> when <math>\omega = 0</math> and <math>q = 0</math> among the values <math>\theta \in \{0, \frac{\pi}{2}, \pi, 3\frac{\pi}{2}, 2\pi\}</math></p>

### 12.3.3 Modelica Component Model: CentrifugalPump

The governing equations are implemented in the *CentrifugalPump* component model located in the *WaterSteam.Machines* sub-library. Figure 12.6a represents the graphical icon of the component with its three connectors.

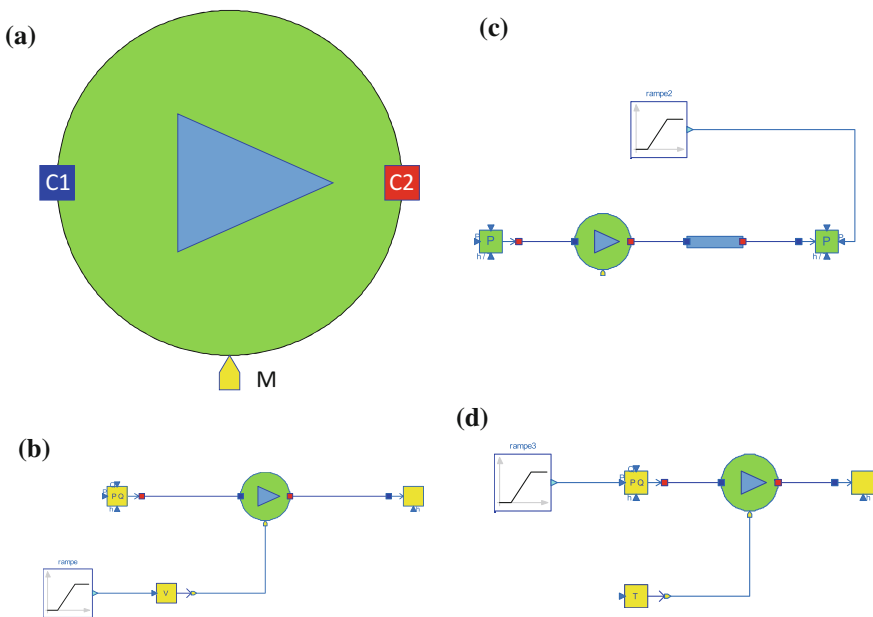


**Fig. 12.6** **a** Icon of the *CentrifugalPump* component model. **b** Test-case for the *CentrifugalPump* component model for scenarios 1 and 2. **c** Test-case for the *CentrifugalPump* component model for scenario 3. **d** Test-case for the *CentrifugalPump* component model for scenario 4

### 12.3.4 Test-Case

The objective is to ensure that the component model is robust to all operating regimes of the pump as shown in Fig. 12.2.

To that end, several scenarios are defined in order to challenge a wide range of values for angle  $\theta$ :

- Scenario no 1: stopping the pump while keeping the mass flow rate equal to zero. The mass flow rate through the pump is constantly set to zero and the pump angular velocity varies linearly from the nominal speed to zero. For this scenario,  $\theta$  takes two values: 0 and  $-180^\circ$ .
- Scenario no 2: stopping the pump while keeping the mass flow rate at a constant value different from zero. The mass flow rate through the pump is constantly set to 100 kg/s and the pump angular velocity varies linearly from nominal speed to zero. For this scenario,  $\theta$  varies continuously from  $8^\circ$  to  $90^\circ$ .
- Scenario no 3: flow reversal at constant rotational speed. The rotational speed of the pump is set to its nominal value. The pressure at the inlet is set to 3 bars. The pressure at the outlet is initially set to 4 bars, then rises linearly until 48 bars. For this scenario,  $\theta$  varies continuously from  $44^\circ$  to  $-83^\circ$ .
- Scenario no 4: going from one-phase to two-phase flow. The pump is stopped (i.e., the motor torque is set to zero). The mass flow rate is set to 10 kg/s. The fluid specific enthalpy is set to 650 kJ. The pressure at the inlet decreases continuously from 7.2 to 2 bars. For this scenario,  $\theta$  varies continuously from  $71^\circ$  to  $74^\circ$ .

The models used to validate the *CentrifugalPump* component model are represented in Fig. 12.6b–d. They all use the *CentrifugalPump* component model and boundary conditions for the fluid and the motor torque. In addition, a lumped straight pipe model is used for scenario 3.

The results of the simulation for the four scenarios are shown in Fig. 12.7.

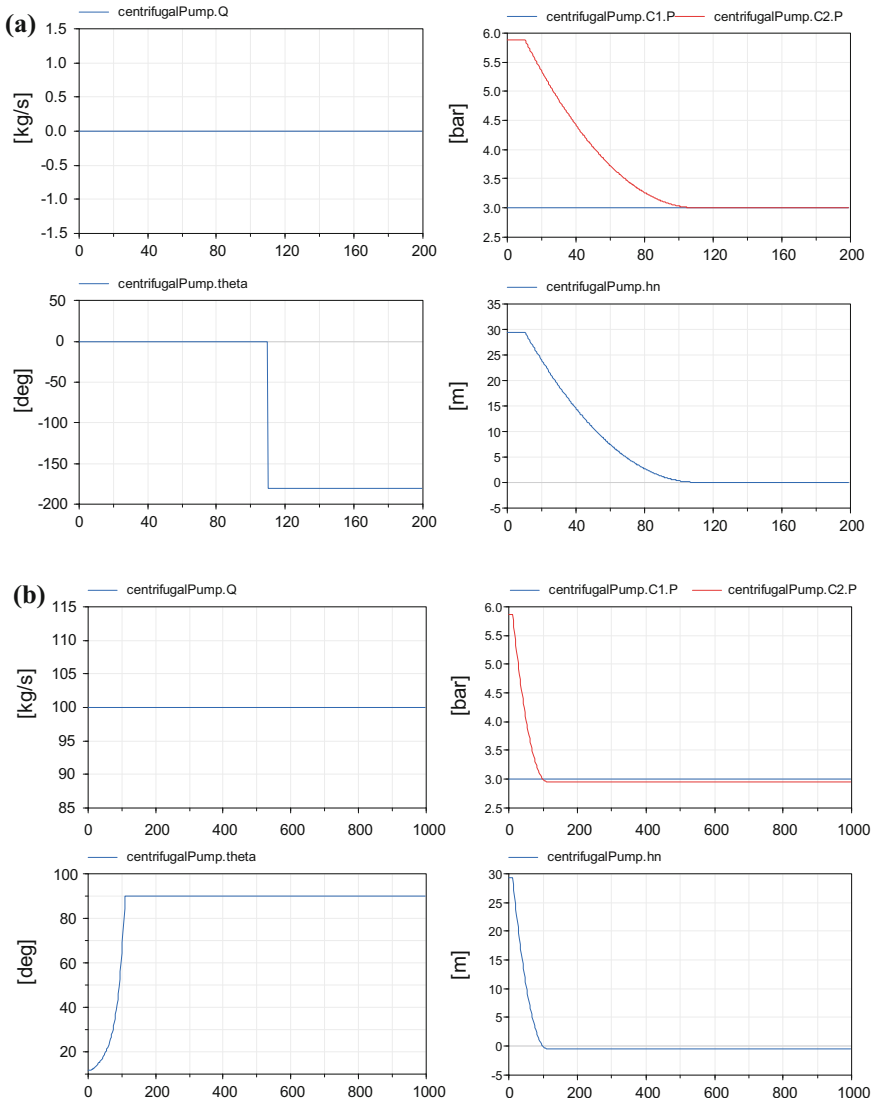


**Fig. 12.7** **a** Simulation results for *CentrifugalPump* “scenario 1”: fluid mass flow rate (top left), angle  $\theta$  (bottom left), fluid pressure at the inlet and at the outlet (top right), and pump head (bottom right). **b** Simulation results for *CentrifugalPump* “scenario 2”: fluid mass flow rate (top left), angle  $\theta$  (bottom left), fluid pressure at the inlet and at the outlet (top right), and pump head (bottom right). **c** Simulation results for *CentrifugalPump* “scenario 3”: fluid mass flow rate (top left), angle  $\theta$  (bottom left), fluid pressure at the inlet and at the outlet (top right), and pump head (bottom right). **d** Simulation results for *CentrifugalPump* “scenario 4”: fluid mass flow rate (top left), angle  $\theta$  (bottom left), fluid pressure at the inlet and at the outlet (top right), and pump head (bottom right)

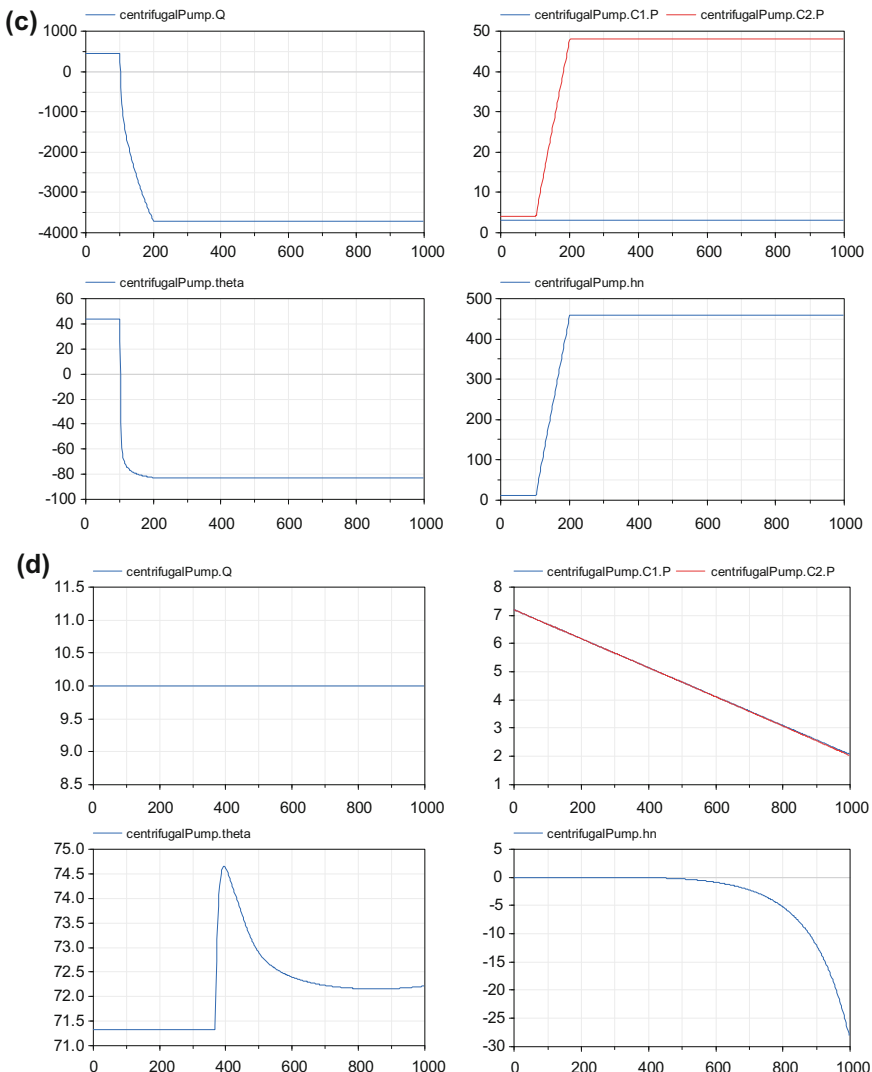


**Fig. 12.7** (continued)

## References

- Coppolani P, Hassenboehler N, Joseph J, Petetrot JF, Py JP, Zampa JS (2004) La chaudière des réacteurs à eau sous pression. INSTN, EDP Sciences
- Knapp RT (1937) Complete characteristics of centrifugal pumps and their use in the prediction of transient behavior. Trans ASME 59:683–689
- Kolev NI (2005) Multiphase flow dynamics. Springer
- Wylie EB, Streeter VL (1993) Fluid transients in systems. Prentice Hall

# Chapter 13

## Pressure Loss Modeling



**Abstract** This chapter gives an introduction to the Bernoulli equation and the different correlations to calculate the friction pressure loss coefficient for single- and two-phase flow (evaporation and condensation). Detailed descriptions of the physical equations for pressure loss components are provided (lumped straight pipe, pipe pressure loss, singular pressure loss, bend, control valve, check valve, dynamic check valve, etc): modeling assumptions, fundamental equations, and correlations with their validity domains. A test-case for each component model is given that includes the structure of the model, parameterization data, model calibration, and results of simulation. The full description of the physical equations is independent of the programming languages and tools.

### 13.1 Bernoulli's Equation

The Bernoulli equation states that the pressure of a fluid decreases as its velocity increases and vice versa as the consequence of the conservation of energy. A fluid that is flowing steadily possesses three types of energy: potential energy due to pressure, gravitational potential energy due to elevation, and kinetic energy due to velocity. If no energy is added or removed from the system, the sum of these three energy components remains constant. The energy form of the Bernoulli equation is defined as:

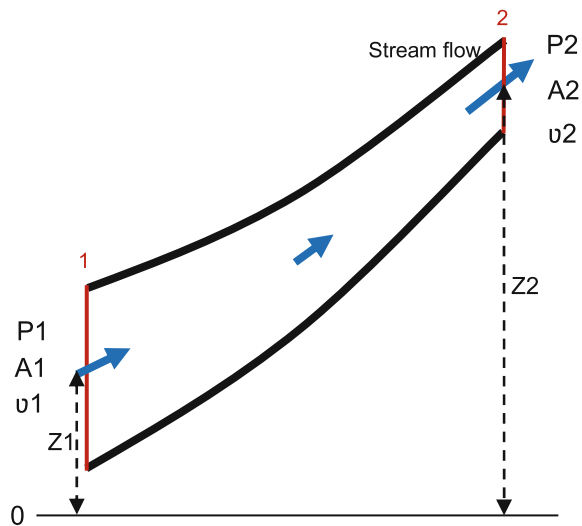
$$\frac{P_1}{\rho} + g \cdot z_1 + \frac{v_1^2}{2} = \frac{P_2}{\rho} + g \cdot z_2 + \frac{v_2^2}{2} \quad (13.1)$$

where  $P_i$  is the static pressure,  $v_i$  is the fluid velocity,  $z_i$  is the elevation of the pipe, and  $\rho$  is the fluid density assumed to be the same at all points in the fluid. Index  $i$  represents the inlet ( $i = 1$ ) and the outlet ( $i = 2$ ) of the pipe, and more generally any section of the pipe.

The Bernoulli equation is derived from first principles in Sect. 4.1.3.1.

The Bernoulli equation applies only along a streamline if and only if the following conditions are met:

**Fig. 13.1** Schematic diagram of a pipe (streaming fluid)



- The flow is steady.
- The flow is incompressible (e.g., most liquid flows and gases moving at low Mach number).
- There is no heat or work interactions between sections 1 and 2 (see Fig. 13.1).
- Friction by viscous forces is neglected.

The head form of the Bernoulli equation is defined as:

$$\frac{P_1}{\rho \cdot g} + z_1 + \frac{v_1^2}{2 \cdot g} = \frac{P_2}{\rho \cdot g} + z_2 + \frac{v_2^2}{2 \cdot g} \quad (13.2)$$

which corresponds to (13.1) divided by the gravity constant  $g$ .

The mass flow rate at any section of a pipe is:

$$\dot{m} = \rho \cdot v_1 \cdot A_1 = \rho \cdot v_2 \cdot A_2 \quad (13.3)$$

where  $A_i$  is the internal cross section of the pipe.

## 13.2 Closure Laws: Coefficient of Friction

We are here interested in pressure losses due to friction between the fluid and the wall, or to singularities arising from sudden changes in the geometry of the fluid equipment.

### 13.2.1 Single-Phase Flow

Many thermal power plant components are based on simple pipe models. One of them is the heat exchanger. In a pipe, the pressure drop of a fluid flowing through the pipe depends on the flow velocity, the roughness of the inner surface of the pipe, the cross section of the pipe, and the fluid properties. Pressure losses are captured by the friction term in the momentum balance equation (c.f. 4.11):

$$A_x \cdot dP_{f,x} = \text{sgn}(v_x) \cdot \pi_{w,x} \cdot \tau_{w,x} \cdot dx \quad (13.4)$$

Equation (13.4) shows that pressure losses are positive when the mass flow rate is positive. Therefore, the sign convention for the differential  $dP_{f,x}$  is opposite to the usual differential sign convention so that  $\int_{x=\text{in}}^{x=\text{out}} dP_{f,x} = P_{f,\text{in}} - P_{f,\text{out}}$ .

Assuming turbulent flow and using the Idel'cik notation:

$$dP_{f,x} = \frac{1}{2} \cdot \text{sgn}(v_x) \cdot \rho_x \cdot v_x^2 \cdot d\xi_x = \frac{1}{2} \cdot \frac{\dot{m}(x) \cdot |\dot{m}(x)|}{\rho_x \cdot A_x^2} \cdot d\xi_x \quad (13.5)$$

where  $\xi_x$  is the pressure loss coefficient and  $v_x$  is the average velocity of the fluid at section  $A_x$ .

For single-phase flow,  $\xi$  is in general a function of the Reynolds number and geometrical coefficients:

$$\xi_x = \xi(Re_x, \text{geom\_coef}) \quad (13.6)$$

with

$$Re_x = \frac{\rho_x \cdot v_x \cdot D_{H,x}}{\mu_x} = \frac{4 \cdot \dot{m}(x)}{\mu_x \cdot \pi_{w,x}} \quad (13.7)$$

where  $D_{H,x}$  is the hydraulic diameter of the pipe,  $\mu_x$  is the fluid viscosity, and  $\pi_{w,x}$  is the wetted perimeter.

Not all flow conduits are circular pipes. In such case, the hydraulic diameter (i.e., equivalent diameter) of the pipe is defined as:

$$D_{H,x} = \frac{4 \cdot A_x}{\pi_{w,x}} \quad (13.8)$$

Example for straight pipes:

$$d\xi_x = \frac{\lambda_x}{D_{H,x}} \cdot dx \quad (13.9)$$

where  $\lambda_x$  is the friction coefficient given by different expressions depending on the flow regime.

For a laminar flow:

$$\lambda_x = \frac{64}{Re_x} \quad (13.10)$$

For turbulent flows ( $Re_x > 2300$ ), the implicit Colebrook correlation can be used (Colebrook and White 1937):

$$\lambda_x = 0.25 \cdot \left[ \log_{10} \left( \frac{2.51}{Re_x \cdot \sqrt{\lambda_x}} + \frac{\varepsilon_x}{3.7 \cdot D_{H,x}} \right) \right]^{-2} \quad (13.11)$$

where  $\varepsilon_x$  is the roughness of the pipe. Notice that (13.11) is implicit as  $\lambda_x$  appears on both sides of the equation.

Approximated explicit versions of (13.11) have been proposed:

- The Eck correlation (Eck 1973; Asker et al. 2014):

$$\lambda_x = 0.25 \cdot \left[ \log_{10} \left( \frac{15}{Re_x} + \frac{\varepsilon_x}{3.7 \cdot D_{H,x}} \right) \right]^{-2} \quad (13.12)$$

- The Zigrang correlation (Zigrang and Sylvester 1982):

$$\lambda_x = 0.25 \cdot \left[ \log_{10} \left( \frac{13}{Re_x} + \frac{\varepsilon_x}{3.7 \cdot D_{H,x}} \right) \right]^{-2} \quad (13.13)$$

For straight pipes,  $D_{H,x}$  and  $A_x$  are constant and may be replaced by their constant values  $D_H$  and  $A$ . Using (13.9) and integrating (13.5) over the pipe length (cf. Fig. 3.2) yields:

$$\Delta P_f(a \rightarrow b) = \int_0^L dP_{f,x} = \frac{1}{2} \cdot \frac{1}{D_H \cdot A^2} \cdot \int_0^L \frac{\lambda_x}{\rho_x} \cdot \dot{m}(x) \cdot |\dot{m}(x)| \cdot dx \quad (13.14)$$

with  $\lambda_x$  and  $\rho_x$  being functions of the fluid state:

$$\lambda_x = \lambda(T_x, \rho_x) \quad (13.15)$$

$$\rho_x = \rho(P_x, T_x) \quad (13.16)$$

If the flow is adiabatic (i.e., no energy exchange through the pipe wall), if the upwind scheme (4.113) is used, and if the fluid is considered as incompressible, then the thermodynamic state  $(T_x, \rho_x)$  remains quasi-constant throughout the pipe. Consequently,  $\lambda_x$  and  $\dot{m}(x)$  are also quasi-constant, and  $\rho_x$ ,  $\lambda_x$  and  $\dot{m}(x)$  may be replaced by their constant values  $\rho_{a:b}$ ,  $\lambda_{a:b}$  and  $\dot{m}(a \rightarrow b)$ .

Then, the total pressure loss between volumes  $a$  and  $b$  for incompressible single-phase flow is given by the Darcy–Weisbach equation:

$$\Delta P_f(a \rightarrow b) = \frac{1}{2} \cdot \frac{\lambda_{a:b} \cdot L}{D_H} \cdot \frac{\dot{m}(a \rightarrow b) \cdot |\dot{m}(a \rightarrow b)|}{\rho_{a:b} \cdot A_{a:b}^2} \quad (13.17)$$

For singularities,  $L$  and  $D_H$  are very small, so:

$$\Delta P_f(a \rightarrow b) = \frac{1}{2} \cdot \xi_{a:b} \cdot \frac{\dot{m}(a \rightarrow b) \cdot |\dot{m}(a \rightarrow b)|}{\rho_{a:b} \cdot A_{a:b}^2} \quad (13.18)$$

where  $\xi_{a:b}$  is the pressure loss coefficient corresponding to the singularity. Formally speaking,

$$\xi_{a:b} = \lim_{\substack{L \rightarrow 0 \\ D_H \rightarrow 0}} \frac{\lambda_{a:b} \cdot L}{D_H}$$

For valves, the flow coefficient  $C_V$  is defined such that:

$$\frac{\Delta P_f(a \rightarrow b)}{\Delta P_{f,\text{ref}}} \cdot \frac{C_V^2}{C_{V,\text{ref}}^2} = \frac{\frac{\dot{m}(a \rightarrow b) \cdot |\dot{m}(a \rightarrow b)|}{\rho_{a:b}}}{\frac{\dot{m}_{\text{ref}}^2}{\rho_{\text{ref}}}} \quad (13.19)$$

where the index ref denotes a reference state.

Therefore,

$$\Delta P_f(a \rightarrow b) \cdot C_V^2 = K \cdot \frac{\dot{m}(a \rightarrow b) \cdot |\dot{m}(a \rightarrow b)|}{\rho_{a:b} \cdot \rho_{\text{ref}}} \quad (13.20)$$

with

$$K = \frac{\Delta P_{f,\text{ref}} \cdot C_{V,\text{ref}}^2}{q_{\text{ref}}^2} \quad (13.21)$$

$q_{\text{ref}}$  is the volumetric flow rate of reference:  $q_{\text{ref}} = \dot{m}_{\text{ref}} / \rho_{\text{ref}}$ .

The reference state corresponds to the volume (in US gallons) of water at 60 °F (15.5556 °C) that flows each minute through the valve with a pressure drop of 1 psi across the valve.

Therefore,  $K$  is a constant that depends only on the units system utilized for (13.21). In US units,  $K = 1$ . Inserting this value of  $K$  in (13.20) gives the usual definition of the flow coefficient:

$$C_V = q \cdot \sqrt{\frac{\rho}{\rho_{\text{water}, 60^\circ\text{F}}} \cdot \frac{1}{\Delta P}}$$

where  $q = \dot{m}^2 / \rho$  is the volumetric mass flow rate through the valve expressed in US gallons per minute,  $\Delta P$  is the pressure drop across the valve expressed in psi, and  $\rho$  is the fluid density (the unit for the density is not important as only the dimensionless specific gravity  $\rho / \rho_{\text{water}, 60^\circ\text{F}}$  features in the definition of the flow coefficient).

In SI units, the value of  $K$  is obtained by expressing the values of all variables in (13.21) in SI units, except  $C_{V,\text{ref}}$  that remains in US units, thus by setting  $\Delta P_{f,\text{ref}} = 1 \text{ psi} = 6.89476 \times 10^3 \text{ Pa}$ ,  $q_{\text{ref}} = 1 \text{ gpm} = 6.30901966 \text{ } 10^{-5} \text{ m}^3/\text{s}$  and  $C_{V,\text{ref}} = 1$ :

$$K = 1.732189 \times 10^{12} \quad (13.22)$$

From (13.18) and (13.20), the relation between the flow coefficient  $C_V$  and the pressure loss coefficient  $\zeta_{a:b}$  is:

$$C_V = A_{a:b} \cdot \sqrt{\frac{2 \cdot K}{\zeta_{a:b} \cdot \rho_{\text{water}, 60^\circ\text{F}}}} \quad (13.23)$$

### 13.2.2 Homogeneous Two-Phase Flow Model

For two-phase flow in straight pipes, according to the Lockhart–Martinelli model, the pressure loss is higher as compared to single-phase flow. This increase in pressure loss is captured by a two-phase friction multiplier  $\Phi_{lo}^2$ :

$$dP_{f,x} = \Phi_{lo,x}^2 \cdot dP_{f,lo,x} \quad (13.24)$$

where the pressure loss  $dP_{f,lo,x}$  is computed as in the case of single-phase flow.

Using the Thom correlation:

$$\Phi_{lo,x}^2 = 1 + \frac{4200 \cdot x_{v,x}}{(19 + P_x) \cdot e^{\frac{P_x}{84}}} \quad (13.25)$$

where  $x_{v,x}$  is the vapor mass fraction at location  $x$  along the pipe.

### 13.3 General Assumptions for Pressure Loss Modeling

Pressure losses are modeled as flow component of the staggered grid scheme (cf. Chap. 17) that features only the momentum balance equations (the mass and energy balance equations are to be found in volumes).

The consequences are the following:

- The flow inside pressure losses is adiabatic. Non-adiabatic pipes must be modeled by connecting pressure losses to volumes as done for heat exchangers (cf. Chap. 9).
- The upwind scheme is used, so the specific enthalpy inside the components is equal to the specific enthalpy at the inlet.
- The properties of the fluid are computed for the average pressure  $(P_i + P_o)/2$  as justified in Sect. 4.3.4, where  $P_i$  is the pressure at the inlet and  $P_o$  is the pressure at the outlet.

### 13.4 Pipe and Singular Pressure Loss Modeling

This component represents in a generic way the pressure losses inside a pipe or a singularity using a single-friction pressure loss coefficient. It can also represent the pressure losses inside a circuit of connected pipes and singularities with a pressure loss coefficient equivalent to the whole circuit, as shown in Fig. 13.2. It does not take into account the inertia due to momentum inside pipes. The lumped straight pipe should be used instead to take that effect into account.

For water/steam, the flow regime can be single-phase or homogeneous two-phase flow.

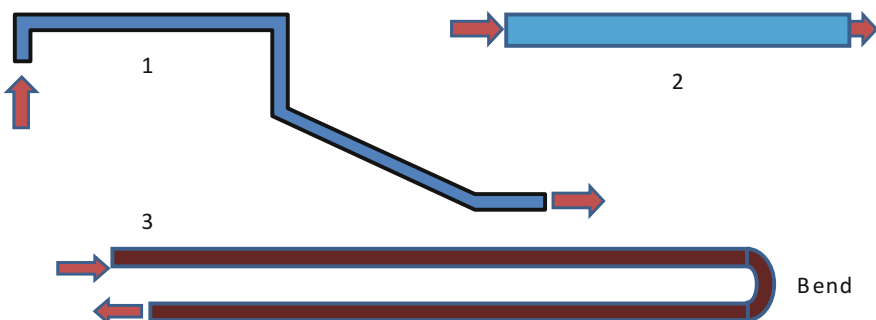


**Fig. 13.2** Schematic diagram of various singular pressure losses consisting in pipes with or without singularities

### 13.4.1 Nomenclature

Symbols	Definition	Unit	Mathematical definition
$g$	Gravity constant	$\text{m/s}^2$	
$h$	Fluid specific enthalpy at the inlet	$\text{J/kg}$	
$\dot{m}$	Fluid mass flow rate	$\text{kg/s}$	
$P_i$	Fluid pressure at the inlet	$\text{Pa}$	
$P_o$	Fluid pressure at the outlet	$\text{Pa}$	
$z_i$	Inlet altitude	$\text{m}$	
$z_o$	Outlet altitude	$\text{m}$	
$\Delta P$	Pressure loss of the fluid between the inlet and the outlet	$\text{Pa}$	$P_i - P_o$
$\Delta P_f$	Friction pressure loss between the inlet and the outlet	$\text{Pa}$	
$\Delta P_g$	Gravity pressure loss between the inlet and the outlet	$\text{Pa}$	$\rho \cdot g \cdot (z_o - z_i)$
$\Lambda$	Friction pressure loss coefficient	$\text{m}^{-4}$	
$\rho$	Fluid density	$\text{kg/m}^3$	

### 13.4.2 Governing Equations

The model is based on the momentum balance equation. The model is formulated in order to correctly handle possible flow reversal conditions. It represents the simplest possible model for a flow component of the staggered grid scheme (cf. Chap. 17).

Equation 1	
Title	Static momentum balance equation
Validity domain	$\forall \dot{m}$
Mathematical formulation	$\Delta P = \Delta P_f + \Delta P_g$
Comments	In case of a singularity, $z_o = z_i$ and consequently $\Delta P_g = 0$

Equation 2	
Title	Friction pressure losses
Validity domain	$\forall \dot{m}$
Mathematical formulation	$\Delta P_f = \Lambda \cdot \frac{\dot{m} \cdot  \dot{m} }{\rho}$
Comments	This equation corresponds to both (13.17) and (13.18) The pressure loss coefficient $\Lambda$ is a parameter to be provided by the user or that can be obtained by inverse calculation from the mass flow rate or the pressure loss

(continued)

(continued)

**Equation 2**

Title	Friction pressure losses
	<p>For pipes, cf. (13.17):</p> $\Lambda = \frac{1}{2} \cdot \frac{\lambda_{a:b} \cdot L}{D_H \cdot A_{a:b}^2}$ <p>For singularities, cf. (13.18):</p> $\Lambda = \frac{1}{2} \cdot \frac{\zeta_{a:b}}{A_{a:b}^2}$ <p>This shows that <math>\Lambda</math> captures the geometry of the component</p>

### 13.4.3 Modelica Component Models: PipePressureLoss and SingularPressureLoss

The equations are separated in two different models, one for the pipe pressure loss and the other for the singular pressure loss. The only differences in the two models are the presence of parameters for the inlet and outlet altitudes in the pipe model (which are absent in the singular pressure loss model), and the icons.

For the pipe pressure loss, the governing equations are implemented in the *PipePressureLoss* component model located in the *WaterSteam.PressureLosses* sub-library. Figure 13.3a represents the graphical icon of the component with its two connectors.

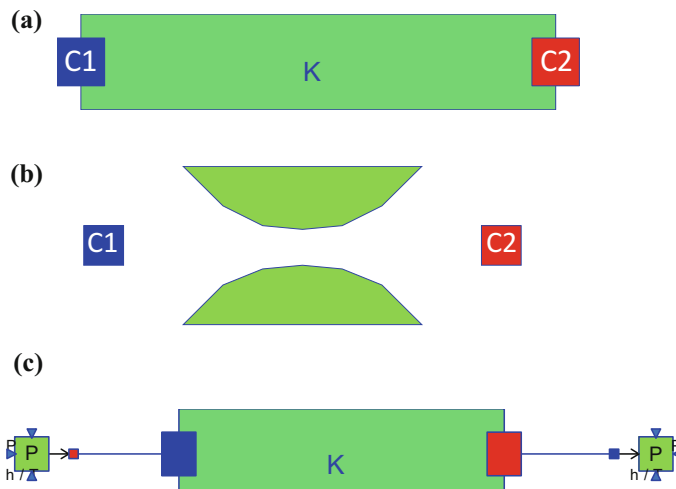


**Fig. 13.3** **a** Icon representation of the *PipePressureLoss* component model. **b** Icon representation of the *SingularPressureLoss* component model. **c** Test-case for the *PipePressureLoss* component model

For the singular pressure loss, the governing equations are implemented in the *SingularPressureLoss* component model located in the *WaterSteam.PressureLosses* sub-library. Figure 13.3b represents the graphical icon of the component with its two connectors.

### 13.4.4 Test-Case

The model *TestPipePressureLoss* used to validate the *PipePressureLoss* component model is represented in Fig. 13.3c. This model uses the following component models:

- One *PipePressureLoss* or *SingularPressureLoss* component model;
- One *SourceP* component model;
- One *SinkP* component model.

In this test-case scenario, the *PipePressureLoss* component receives: (1) the fluid pressure and specific enthalpy at the inlet and (2) the fluid pressure at the outlet. The component computes the fluid mass flow rate going through the pipe.

#### 13.4.4.1 Test-Case Parameterization and Boundary Conditions

The model data are:

- Friction pressure loss coefficient =  $10 \text{ m}^{-4}$
- Inlet altitude of the pipe = 0
- Outlet altitude of the pipe = 0
- Fluid temperature at the inlet = 290 K
- Fluid pressure at the inlet =  $3 \times 10^5 \text{ Pa}$
- Fluid pressure at the outlet =  $10^5 \text{ Pa}$ .

#### 13.4.4.2 Model Calibration

The calibration step consists in setting the fluid mass flow rate in the pipe to a known measurement value to compute by model inversion the value of the friction pressure loss coefficient.

Other possible calibration: setting the fluid mass flow rate in the pipe to a known measurement value to compute by model inversion the value of the fluid pressure at the inlet or at the outlet.

### 13.4.4.3 Simulation Results

The fluid mass flow rate going through the pipe is equal to 4469.54 kg/s.

## 13.5 Lumped Straight Pipe Modeling

The lumped straight pipe is a component for modeling the pressure loss of a fluid circulating inside a pipe, between the inlet and the outlet of the pipe; cf. Fig. 13.4.

Therefore, the model only involves the momentum balance equation. It does not feature the mass and energy balance equations. According to the staggered grid scheme (cf. Chap. 17), the mass and energy balance equations are to be found in volumes. Therefore, the lumped straight pipe cannot be used alone: It must be connected to volumes in order to have a complete model featuring mass, energy, and momentum balance equations.

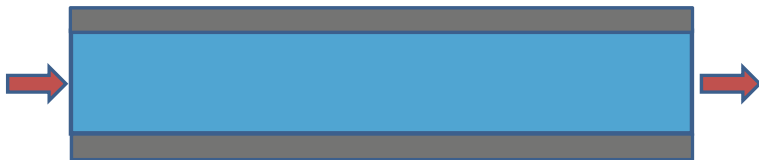


**Fig. 13.4** Schematic diagram of a lumped straight pipe

### 13.5.1 Nomenclature

Symbols	Definition	Unit	Mathematical definition
$A$	Internal cross section of the pipe	$\text{m}^2$	$\pi \cdot D^2 / 4$
$D$	Internal diameter of the pipe	m	
$g$	Gravity constant	$\text{m/s}^2$	
$h$	Fluid specific enthalpy at the inlet	J/kg	
$L$	Length of the pipe	m	
$\dot{m}$	Fluid mass flow rate	kg/s	
$P_i$	Fluid pressure at the pipe inlet	Pa	
$P_o$	Fluid pressure at the pipe outlet	Pa	
$Re$	Fluid Reynolds number	–	$\frac{4 \cdot  \dot{m} }{\pi \cdot D \cdot \mu}$
$z_i$	Inlet altitude of the pipe	m	
$z_o$	Outlet altitude of the pipe	m	
$\Delta P$	Pressure loss of the fluid between the pipe inlet and outlet	Pa	$P_i - P_o$

(continued)

(continued)

Symbols	Definition	Unit	Mathematical definition
$\Delta P_f$	Friction pressure loss between the pipe inlet and outlet	Pa	
$\Delta P_g$	Gravity pressure loss	Pa	$\rho \cdot g \cdot (z_o - z_i)$
$\varepsilon$	Pipe roughness	m	
$\Lambda_f$	Friction pressure loss coefficient	—	
$\mu$	Fluid dynamic viscosity	Pa.s	
$\rho$	Fluid density	kg/m <sup>3</sup>	

### 13.5.2 Governing Equations

The model is based on the momentum balance equation and is formulated in order to correctly handle possible flow reversal conditions.

#### Equation 1-a

Title	Dynamic momentum balance equation
Validity domain	$\forall \dot{m}$ (cf. comments)
Mathematical formulation	$\Delta P = \Delta P_f + \Delta P_g + \frac{L}{A} \cdot \frac{d\dot{m}}{dt}$
Comments	This equation corresponds to (4.99), assuming that the fluid density $\rho$ is constant along the pipe. It takes into account the fluid inertia inside the pipe. However, it is valid only if the mass flow rate wavelength is large as compared to the pipe length $L$ , therefore if there is no water hammer effect inside the pipe. It can for instance be used to model water level oscillations in tanks communicating through a pipe

#### Equation 1-b

Title	Static momentum balance equation
Validity domain	$\forall \dot{m}$
Mathematical formulation	$\Delta P = \Delta P_f + \Delta P_g$
Comments	This equation corresponds to (4.99), assuming that the fluid density $\rho$ is constant along the pipe, and neglecting the inertia captured in the differential term

Equation 2	
Title	Friction pressure losses
Validity domain	$\forall \dot{m}$
Mathematical formulation	$\Delta P_f = \frac{\Lambda_f \cdot L}{D} \cdot \frac{\dot{m} \cdot  \dot{m} }{2 \cdot A^2 \cdot \rho}$
Comments	<p>This equation corresponds to (13.17)</p> <p>The friction pressure loss coefficient <math>\Lambda_f</math> can be given by a fixed parameter or computed by various correlations such as (13.11), (13.12), or (13.13)</p> <p>Using (Idel'Cik 1986), for <math>\varepsilon &gt; 5 \times 10^{-5}</math></p> $\Lambda_f = [2 \cdot \log_{10}(\frac{3.7}{\varepsilon})]^{-2}$ <p>and for <math>\varepsilon \leq 5 \times 10^{-5}</math></p> $\Lambda_f = [1.8 \cdot \log_{10}(Re) - 1.64]^{-2}$

### 13.5.3 Modelica Component Model: LumpedStraightPipe

The governing equations are implemented in the *LumpedStraightPipe* component model located in the *WaterSteam.PressureLosses* sub-library. Figure 13.5a represents the graphical icon of the component with its two connectors.

#### 13.5.4 Test-Case

The model *TestLumpedStraightPipe* used to validate the *LumpedStraightPipe* component model is represented in Fig. 13.5b. This model uses the following component models:

- One *LumpedStraightPipe* component model;
- Two *Tank* component models.

In this test-case scenario, the *LumpedStraightPipe* component receives: (1) the fluid pressure and specific enthalpy at the inlet and (2) the fluid pressure at the outlet. The component computes the fluid mass flow rate going through the pipe.

##### 13.5.4.1 Test-Case Parameterization and Boundary Conditions

The model data are:

- Internal diameter of the pipe = 0.2 m
- Length of the pipe = 10 m
- Inlet altitude of the pipe = 0
- Outlet altitude of the pipe = 0

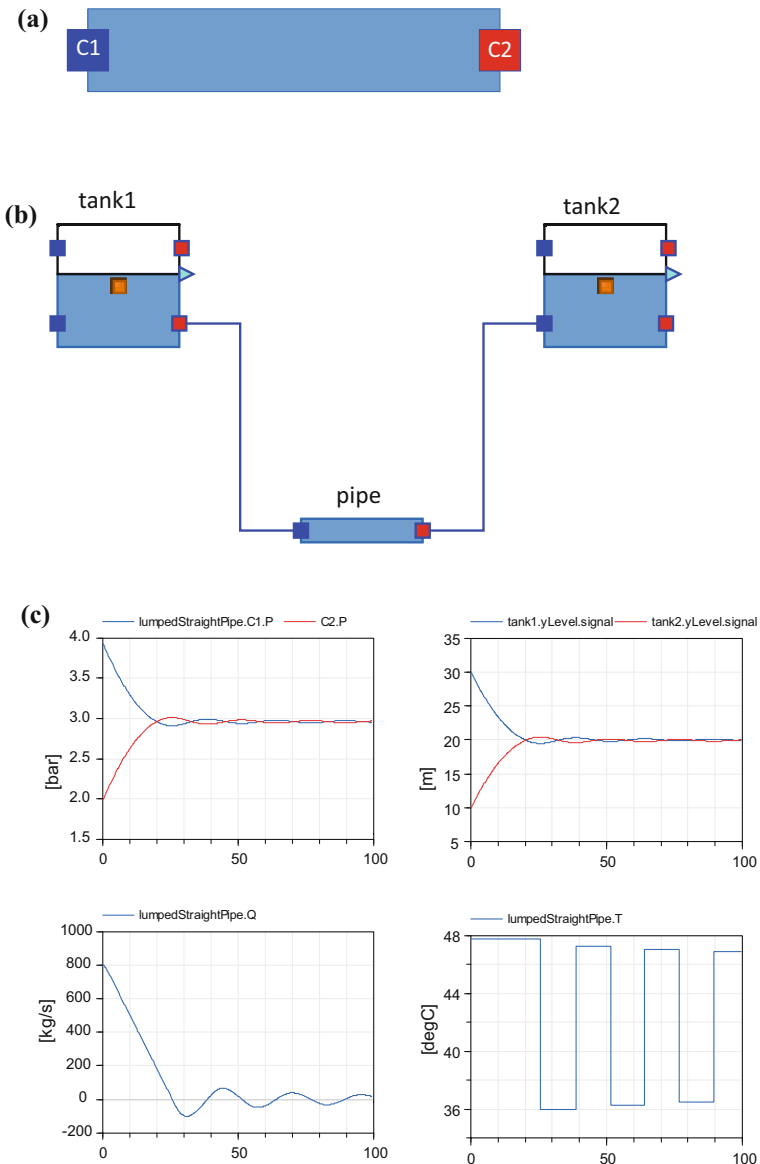


**Fig. 13.5** **a** Icon representation of the *LumpedStraightPipe* component model. **b** Test-case for the *LumpedStraightPipe* component model. **c** Simulation results for *LumpedStraightPipe*: fluid pressure at the inlet and at the outlet of the pipe (top left), fluid mass flow rate in the pipe (bottom left), fluid level in tank1 and tank2 (top right) and fluid temperature in the pipe (bottom right)

- Friction pressure loss coefficient = 0.012
- Tank cross sectional area =  $1 \text{ m}^2$
- Fluid specific enthalpy in tank1 =  $2 \times 10^5 \text{ J/kg}$
- Fluid specific enthalpy in tank2 =  $10^5 \text{ J/kg}$
- Pressure above the level in tank1 and tank2 =  $10^5 \text{ Pa}$
- Altitude of inlet 1 (tank1 and tank2) = 40 m
- Altitude of inlet 2 (tank1 and tank2) = 0.1 m
- Altitude of outlet 1 (tank1 and tank2) = 40 m
- Altitude of outlet 2 (tank1 and tank2) = 0.1 m
- Initial liquid level in tank1 = 30 m
- Initial liquid level in tank2 = 10 m.

#### 13.5.4.2 Model Calibration

The calibration step consists in setting the fluid mass flow rate to a known measurement value to compute by model inversion the value of the fluid pressure loss coefficient in the pipe.

#### 13.5.4.3 Simulation Results

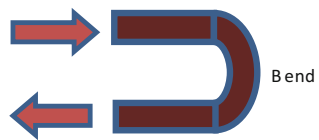
Figure 13.5c shows the simulation results for a scenario that consists in starting the simulation with different water levels and temperatures in each tank. The water levels become equal, but because of the mechanical inertia due to the fluid momentum in the pipe, level equilibrium is attained after flow oscillations between positive (direct flow) and negative (backflow) values. The last curve shows how flow oscillations affect the fluid temperature in the pipe according to the upwind scheme; cf. (4.113): The temperature is always equal to the temperature of the upstream volume. The sharp fluid temperature transitions in the pipe between the temperature of tank1 (hot) and tank2 (cold) is due to the fact that diffusion is negligible as soon as there is significant mass flow rate in the pipe.

### 13.6 Bend Modeling

The bend is a type of singular pressure loss that models the pressure loss of a fluid circulating inside a bend; cf. Fig. 13.6. For water/steam, the flow regime can be single-phase or homogeneous two-phase flow.

The difference between this component and the singular pressure loss component is that the friction pressure loss coefficient is calculated using a correlation that is a function of the geometry of the bend instead of being given by single parameter.

**Fig. 13.6** Schematic diagram of a bend



### 13.6.1 Nomenclature

Symbols	Definition	Unit	Mathematical definition
$A_1$	Factor for the singular pressure loss coefficient	–	
$B_1$	Factor for the singular pressure loss coefficient	–	
$C_1$	Factor for the singular pressure loss coefficient	–	
$D$	Internal diameter of the bend	m	
$h$	Fluid specific enthalpy at the inlet	J/kg	
$K_e$	Roughness factor	–	
$\dot{m}$	Fluid mass flow rate	kg/s	
$P_i$	Fluid pressure at the inlet	Pa	
$P_o$	Fluid pressure at the outlet	Pa	
$R$	Bend radius	m	
$Re$	Reynolds number	–	$\frac{4 \cdot  \dot{m} }{\pi \cdot D \cdot \mu}$
$Re_{lim}$	Limiting Reynolds number	–	
$\delta$	Bend angle	°	
$\Delta P$	Pressure loss between the inlet and the outlet	Pa	$P_i - P_o$
$\varepsilon$	Pipe roughness	m	
$\zeta$	Hydraulic pressure loss coefficient	–	
$\zeta_m$	Singular pressure loss coefficient	–	
$\zeta_f$	Friction pressure loss coefficient	–	
$\lambda$	Friction pressure loss coefficient	–	
$\mu$	Fluid dynamic viscosity	Pa s	
$\rho$	Fluid density	kg/m <sup>3</sup>	

### 13.6.2 Assumptions

The gravity pressure loss between the outlet and the inlet of the bend is neglected.

### 13.6.3 Governing Equations

The model is based on the momentum balance equation. The model is formulated in order to correctly handle possible flow reversal conditions. The correlations used in this model are provided by Idel'Cik (1986).

Equation 1	
Title	Static momentum balance equation
Validity domain	$\forall \dot{m}$
Mathematical formulation	$\Delta P = 8 \cdot \zeta \cdot \frac{\dot{m} \cdot  \dot{m} }{\pi^2 \cdot D^4 \cdot \rho}$
Comments	This equation corresponds to (13.18) with $A_{a:b} = \frac{\pi \cdot D^2}{4}$ and $\zeta = \zeta_{a:b}$ .

Equation 2	
Title	Hydraulic pressure loss coefficient
Validity domain	$\forall \dot{m}$ with $Re > Re_{\text{lim}}$
Mathematical formulation	$\zeta = K_e \cdot \zeta_m + \zeta_f$ $K_e = \begin{cases} 2 & \text{if } \varepsilon \geq 10^{-3} \\ 1 + 10^3 \cdot \varepsilon & \text{if } \varepsilon < 10^{-3} \text{ and } R/D < 1.5 \\ 1 + 10^6 \cdot \varepsilon^2 & \text{if } \varepsilon < 10^{-3} \text{ and } R/D \geq 1.5 \end{cases}$ $\zeta_m = A_1 \cdot B_1 \cdot C_1$ $\zeta_f = 0.0175 \cdot \lambda \cdot R/D \cdot \delta$
Comments	<p>The limiting Reynolds number is given by</p> $Re_{\text{lim}} = \begin{cases} 2 \times 10^5 & \text{if } \varepsilon < 5 \times 10^{-5} \\ \max(560/\varepsilon, 2 \times 10^5) & \text{if } \varepsilon \geq 5 \times 10^{-5} \end{cases}$ <p>For <math>0.5 &lt; R/D &lt; 1.5</math> and <math>0 &lt; \delta &lt; 180^\circ</math>, <math>A_1</math>, <math>B_1</math> and <math>C_1</math> are given by the following expressions:</p> $A_1 = \begin{cases} 0.9 \cdot \sin(\delta) & \text{if } \delta < 70^\circ \\ 1 & \text{if } \delta \geq 70^\circ \text{ and } \delta \leq 100^\circ \\ 0.7 + \frac{0.35 \cdot \delta}{90} & \text{if } \delta > 100^\circ \end{cases}$ $B_1 = \begin{cases} 0.21/(R/D)^{2.5} & \text{if } R/D < 1 \\ 0.21/(R/D)^{0.5} & \text{if } R/D \geq 1 \end{cases}$ $C_1 = 1$ <p><math>\lambda</math> is given by the following correlation:</p> $\lambda = \begin{cases} \left[ 2 \cdot \log_{10} \left( \frac{3,7}{\varepsilon} \right) \right]^{-2} & \text{if } \varepsilon > 5 \times 10^{-5} \\ [1.8 \cdot \log_{10}(Re) - 1.64]^{-2} & \text{if } \varepsilon \leq 5 \times 10^{-5} \end{cases}$ <p>Idel'Cik provides other correlations for other types of bends</p>

### 13.6.4 Modelica Component Model: Bend

The governing equations are implemented in the *Bend* component model located in the *WaterSteam.PressureLosses* sub-library. Figure 13.7a represents the graphical icon of the component with its two connectors.

### 13.6.5 Test-Case

The model *TestBend* used to validate the *Bend* component model is represented in Fig. 13.7b. This model uses the following component models:

- One *Bend* component model;
- One *SourceP* component model;
- One *SinkP* component model.

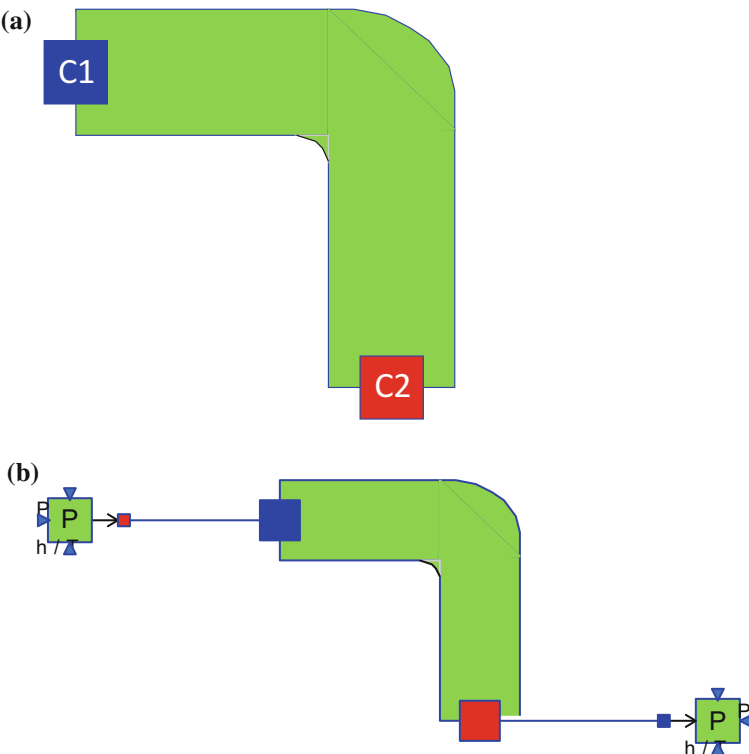


**Fig. 13.7** **a** Representation of the *Bend* component model. **b** Test-case for the *Bend* component model

In this test-case scenario, the *Bend* component receives: (1) the fluid pressure and specific enthalpy at the inlet and (2) the fluid pressure at the outlet. The component computes the fluid mass flow rate going through the bend.

### 13.6.5.1 Test-Case Parameterization and Boundary Conditions

The model data are:

- Internal diameter of the pipe bend = 0.2 m
- Bend radius = 0.2 m
- Bend angle =  $90^\circ$
- Fluid temperature at the inlet = 290 K
- Fluid pressure at the inlet =  $3 \times 10^5$  Pa
- Fluid pressure at the outlet =  $10^5$  Pa.

### 13.6.5.2 Model Calibration

The calibration step consists in setting the fluid mass flow rate in the bend to a known measurement value to compute by model inversion the value of the bend diameter.

### 13.6.5.3 Simulation Results

The fluid mass flow rate going through the pipe is equal to 1328 kg/s.

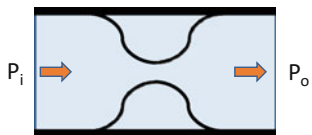
## 13.7 Diaphragm Modeling

A diaphragm is a device for measuring pressure losses in order to compute mass flow rates; cf. Fig. 13.8.

For water/steam, the flow regime can be single-phase or homogeneous two-phase flow.

This component model simulates the friction pressure losses only. The difference between this component and the singular pressure loss component is that the friction pressure loss coefficient is calculated using a correlation that is a function of the geometry of the diaphragm instead of being given by a single parameter.

**Fig. 13.8** Schematic diagram of a diaphragm



### 13.7.1 Nomenclature

Symbols	Definition	Unit	Mathematical definition
$D$	Diaphragm diameter	m	
$h$	Fluid specific enthalpy at the inlet	J/kg	
$\dot{m}$	Fluid mass flow rate	kg/s	
$P_i$	Fluid pressure at the inlet	Pa	
$P_o$	Fluid pressure at the outlet	Pa	
$Re$	Reynolds number	–	$\frac{4 \cdot  \dot{m} }{\pi \cdot D \cdot \mu \cdot \Omega}$
$Re_{lim}$	Limiting Reynolds number	–	$10^5$
$\Delta P$	Fluid pressure loss	Pa	$P_i - P_o$
$\zeta_f$	Friction pressure loss coefficient	–	
$\mu$	Fluid dynamic viscosity	Pa s	
$\rho$	Fluid density	kg/m <sup>3</sup>	
$\Omega$	Diaphragm aperture (between 0 and 1)	–	

### 13.7.2 Assumptions

Diaphragm aperture with sharp ridges.

### 13.7.3 Governing Equations

The model is based on the momentum balance equation. The model is formulated in order to correctly handle possible flow reversal conditions. The correlations used in this model are provided by Idel'Cik (1986).

#### Equation 1

Title	Static momentum balance equation
Validity domain	$\forall \dot{m}$
Mathematical formulation	$\Delta P = 8 \cdot \zeta_f \cdot \frac{\dot{m} \cdot  \dot{m} }{\pi^2 \cdot D^4 \cdot \rho}$
Comments	This equation corresponds to (13.18) with $A_{a:b} = \frac{\pi \cdot D^2}{4}$ and $\zeta_f = \xi_{a:b}$

Equation 2

Title	Friction pressure loss coefficient
Validity domain	$\forall in \text{ with } Re > Re_{\lim}$ $\Omega > 0$
Mathematical formulation	$\zeta_f = \left(\frac{1.707 - \Omega}{\Omega}\right)^2$
Comments	For Reynolds numbers less than $Re_{\lim}$ , cf. Idel'Cik

### 13.7.4 Modelica Component Model: Diaphragm

The governing equations are implemented in the *Diaphragm* component model located in the *WaterSteam.PressureLosses* sub-library. Figure 13.9a represents the graphical icon of the component with its two connectors.

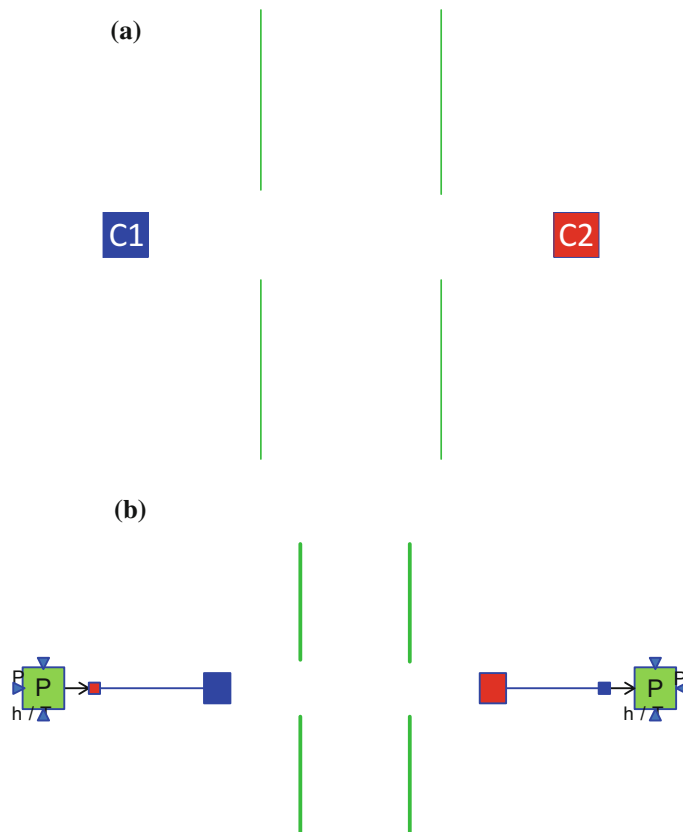


**Fig. 13.9** a Icon representation of the *Diaphragm* component model. b Test-case for the *Diaphragm* component model

### 13.7.5 Test-Case

The model *TestDiaphragm* used to validate the *Diaphragm* component model is represented in Fig. 13.9b. This model uses the following component models:

- One *Diaphragm* component model,
- One *SourceP* component model,
- One *SinkP* component model.

In this test-case scenario, the *Diaphragm* component model receives: (1) the fluid pressure and specific enthalpy at the inlet and (2) the fluid pressure at the outlet. The component computes the fluid mass flow rate going through the diaphragm.

#### 13.7.5.1 Test-Case Parameterization and Boundary Conditions

The model data are:

- Diaphragm diameter = 0.2 m
- Diaphragm aperture = 0.5
- Fluid temperature at the inlet = 290 K
- Fluid pressure at the inlet =  $3 \times 10^5$  Pa
- Fluid pressure at the outlet =  $10^5$  Pa.

#### 13.7.5.2 Model Calibration

The calibration step consists in setting the fluid mass flow rate in the diaphragm to a known measurement value to compute by model inversion the value of the fluid pressure at the inlet or at the outlet.

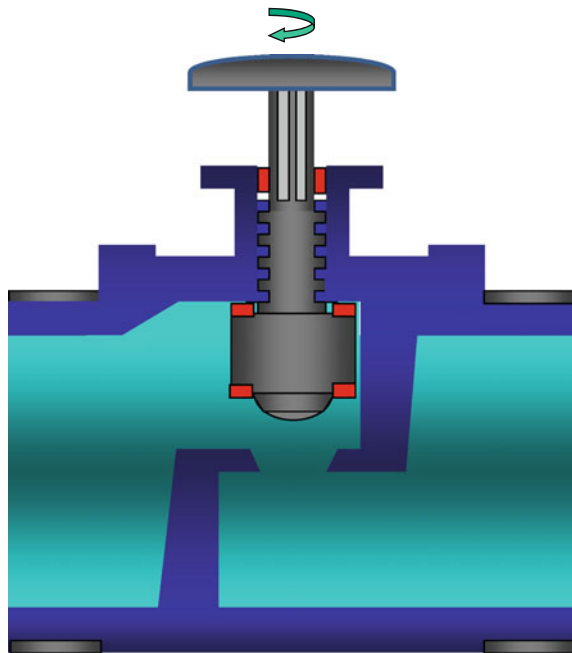
#### 13.7.5.3 Simulation Results

The fluid mass flow rate going through the diaphragm is equal to 260.13 kg/s.

## 13.8 Control Valve Modeling

Control valves are used to control the fluid conditions such as flow, pressure, temperature, or liquid level. To that end, the fluid flow rate through the valve is set at varying values between minimal flow and full capacity by adjusting the position of the valve; cf. Fig. 13.10. The valve is usually automatically driven by an

**Fig. 13.10** Schematic diagram of a control valve



electrical, hydraulic, or pneumatic actuator controlled by a regulator. A control valve is the critical part of any control loop.

For water/steam, the flow regime is single-phase or homogeneous two-phase flow.

### 13.8.1 Nomenclature

Symbols	Definition	Unit	Mathematical definition
$C_v$	Flow coefficient of the valve	U.S.	
$h$	Fluid specific enthalpy at the valve inlet	J/kg	
$\dot{m}$	Fluid mass flow rate	kg/s	
$P_i$	Fluid pressure at the valve inlet	Pa	
$P_o$	Fluid pressure at the valve outlet	Pa	
$\Delta P$	Fluid pressure loss between the inlet and the outlet	Pa	$P_i - P_o$
$\rho$	Fluid density	kg/m <sup>3</sup>	
$\rho_{\text{water},60^{\circ}\text{F}}$	Density of water at 60 °F (15.5556 °C).	kg/m <sup>3</sup>	
$\Omega$	Valve position (between 0 and 1)	—	

### 13.8.2 Assumptions

The modeling assumptions are the following:

- Subsonic fluid;
- Incompressible fluid;
- Inertia is neglected: The volume inside the valve is assumed to be negligible.

### 13.8.3 Governing Equations

The component model uses the notion of flow coefficient  $C_v$  of the valve which is almost universal. The flow coefficient was introduced in 1944 by Masoneilan (Masoneilan 1997). It is used for the sizing of the valve and for computing the mass flow rate through the valve.

The model is formulated in order to correctly handle possible flow reversal conditions.

Equation 1	
Title	Static momentum balance equation
Validity domain	$\forall \dot{m}$ and $C_v \geq 0$ For $C_v = 0$ , $\Delta P$ must be defined (cf. Sect. 5.2.3).
Mathematical formulation	$\Delta P \cdot C_v \cdot  C_v  = 1.732189 \times 10^{12} \cdot \frac{\dot{m} \cdot  \dot{m} }{\rho \cdot \rho_{\text{water}, 60^\circ F}}$
Comments	This equation is obtained by combining (13.20) with (13.22) $C_v^2$ in (13.20) is replaced by $C_v \cdot  C_v $ in order to avoid negative values for $C_v$ when performing inverse calculations on $C_v$
	However, for other fluids than water, e.g., steam or flue gases, it is necessary to calculate the $C_v$ (when the valve is fully open) by model inversion using experimental data $C_v$ is a function of the position $\Omega$ of the valve: $C_v = f_v(\Omega)$ $f_v$ is called the valve characteristic. $0 \leq \Omega \leq 1$ : the valve is fully closed for $\Omega = 0$ and fully open for $\Omega = 1$ $C_v = 0$ when the valve is fully closed: $0 = f_v(0)$ $C_{v,\max}$ is the maximum possible value for $C_v$ . It is obtained when the valve is fully open: $C_{v,\max} = f_v(1)$ If the characteristic is linear, then $C_v = \Omega \cdot C_{v,\max}$ In general, the characteristic is nonlinear and given by an experimental curve Control valves are often assumed to be leaking; hence, $C_v$ never completely reaches zero when the valve is closed. This solves the indetermination problem of $\Delta P$ when $C_v = 0$

### 13.8.4 Modelica Component Model: ControlValve

The governing equations are implemented in the *ControlValve* component model located in the *WaterSteam.PressureLosses* sub-library. Figure 13.11a represents the graphical icon of the component with its three connectors.

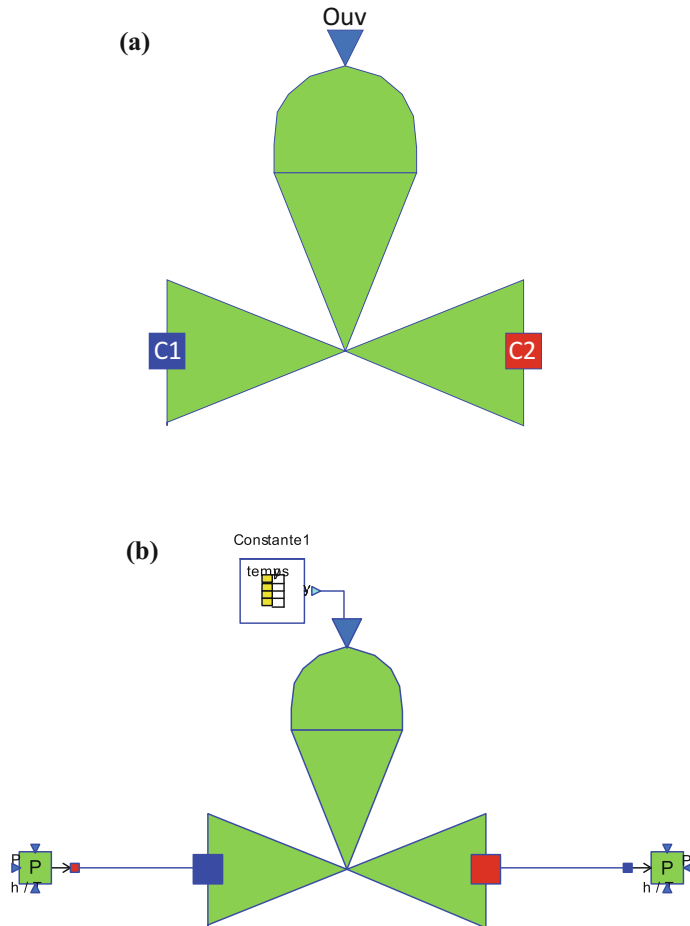


**Fig. 13.11** a Icon representation of the *ControlValve* component model. b Test-case for the *ControlValve* component model

### 13.8.5 Test-Case

The model *TestControlValve* used to validate the *ControlValve* component model is represented in Fig. 13.11b. This model uses the following component models:

- One *ControlValve* component model;
- One *SourceP* component model;
- One *SinkP* component model;
- One *TimeTable* block.

In this test-case scenario, the *ControlValve* component receives: (1) the fluid pressure and specific enthalpy at the inlet, (2) the fluid pressure at the outlet, and (3) the valve position. The component computes the fluid mass flow rate going through the valve.

#### 13.8.5.1 Test-Case Parameterization and Boundary Conditions

The model data are:

- Maximum flow coefficient of the valve = 8005.42 U.S.
- Fluid temperature at the inlet = 290 K
- Fluid pressure at the inlet =  $3 \times 10^5$  Pa
- Fluid pressure at the outlet =  $10^5$  Pa.

#### 13.8.5.2 Model Calibration

The calibration step consists in setting the fluid mass flow rate in the valve to a known measurement value to compute by model inversion the value of the maximum flow coefficient of the valve.

Other possible calibration: setting the fluid mass flow rate in the valve to a known measurement value to compute by model inversion the value of the fluid pressure at the inlet or at the outlet.

#### 13.8.5.3 Simulation Results

Figure 13.12 shows the simulation results for a scenario that consists in closing the valve from position 0.9 to 0.2.

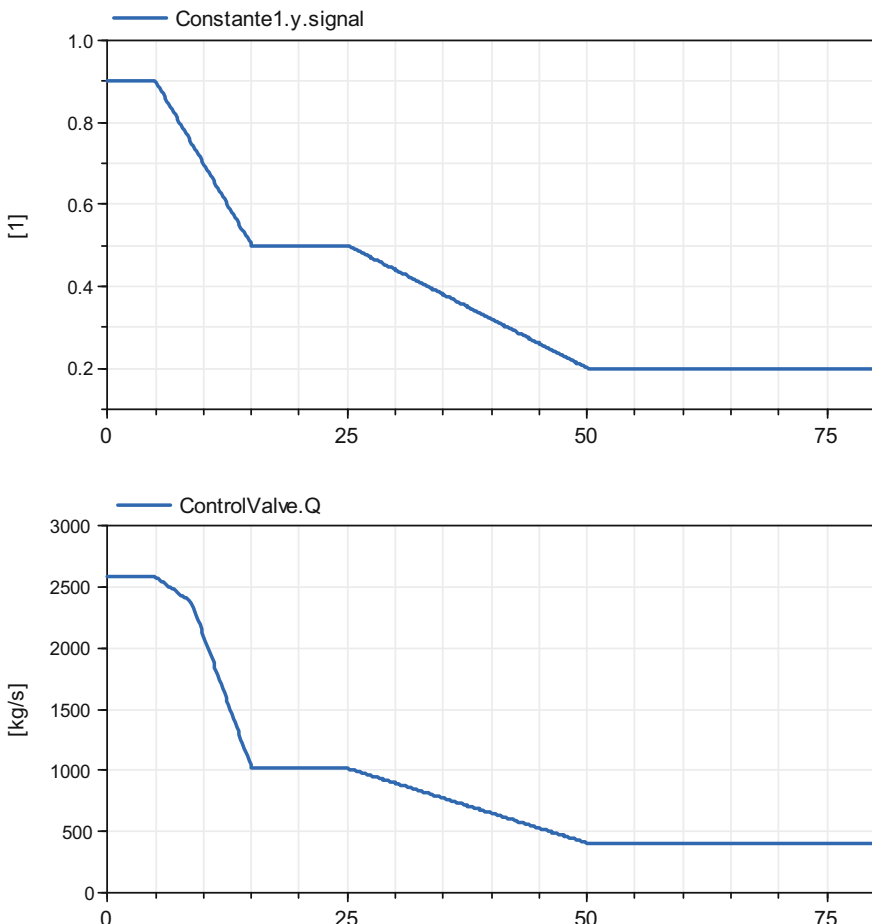


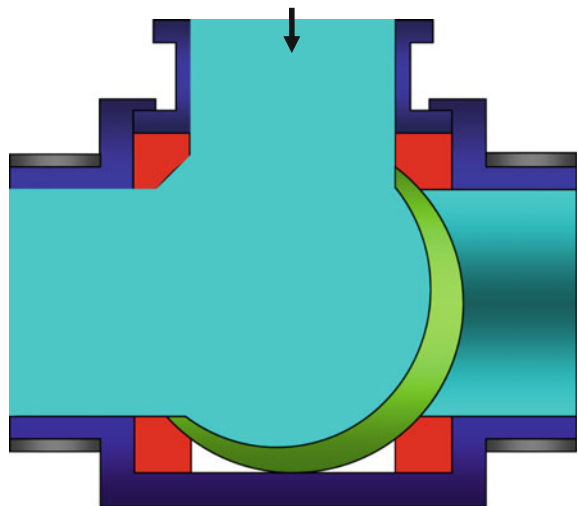
**Fig. 13.12** Simulation results for *ControlValve*: evolution of the valve position (*Constante1.y.signal*) and the fluid mass flow rate (*ControlValve.Q*)

## 13.9 Three-Way Valve Modeling

The function of a three-way valve is to direct the fluid in two directions; cf. Fig. 13.13. When the valve is fully open, the fluid moves in one direction, and when it is fully closed, it moves in the other direction. When it is partially open, a fraction of the fluid moves in one direction, and the rest moves in the other direction.

For water/steam, the flow regime is single-phase or homogeneous two-phase flow.

**Fig. 13.13** Schematic diagram of a three-way valve



### 13.9.1 Modelica Component Model: ThreeWayValve

The three-way valve is modeled as two control valves with respective positions  $\Omega_1$  and  $\Omega_2$  such that  $\Omega_1 + \Omega_2 = 1$ . The position of the three-way valve is  $\Omega$  and  $\Omega_1 = \Omega$  (the other alternative being  $\Omega_2 = \Omega$ ). Therefore, when the three-way valve is fully open, control valve 1 is fully open and control valve 2 is fully closed: The fluid flows to direction 1. When the three-way valve is fully closed, control valve 1 is fully closed and control valve 2 is fully open: The fluid flows to direction 2. When the two control valves are partially open, the fluid flows in both directions.

The three-way valve model is composed of the following component models; cf. Fig. 13.14b:

- Two *ControlValve* component models;
- One *VolumeA* component model;
- One *PipePressureLoss* component model;
- One *Constant* block;
- One *Add* block.

The *ThreeWayValve* component model is located in the *WaterSteam.PressureLosses* sub-library. Figure 13.14a represents the graphical icon of the component with its four connectors.

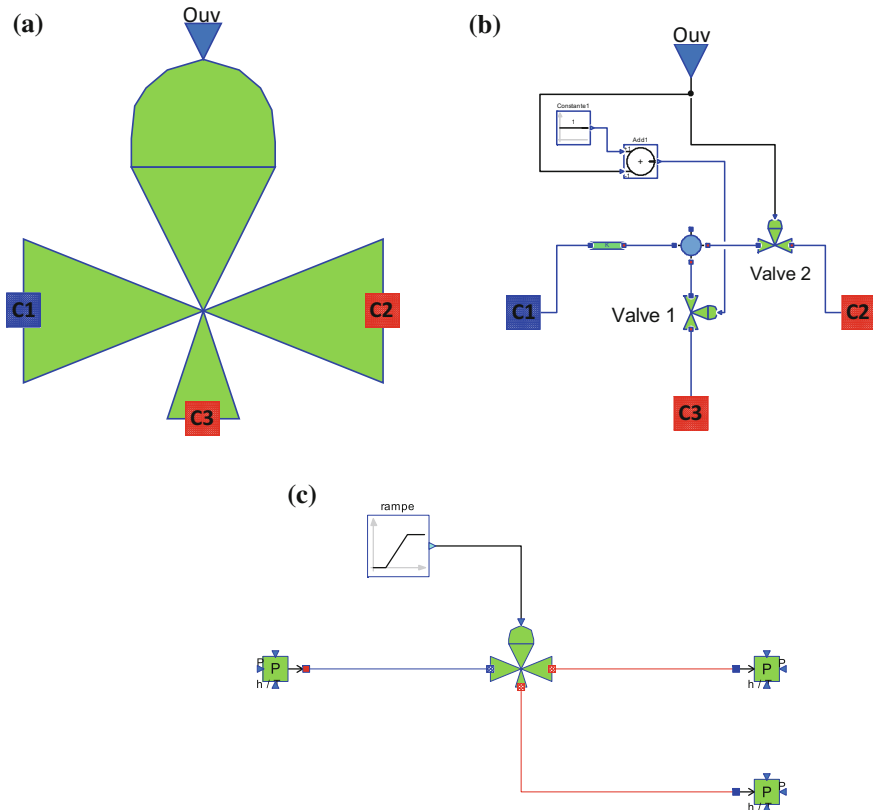


**Fig. 13.14** a Icon representation of the *ThreeWayValve* component model. b Model of the *ThreeWayValve* component model. c Test-case for the *ThreeWayValve* component model

### 13.9.2 Test-Case

The model *TestThreeWayValve* used to validate the *ThreeWayValve* component model is represented in Fig. 13.14c. This model uses the following component models:

- One *ThreeWayValve* component model;
- One *SourceP* component model;
- Two *SinkP* component models;
- One *Ramp* block.

In this test-case scenario, the *ThreeWayValve* component receives: (1) the fluid pressure and specific enthalpy at the inlet, (2) the fluid pressure at the two outlets, and (3) the valve position. The component computes the fluid mass flow rate at the two outlets.

### 13.9.2.1 Test-Case Parameterization and Boundary Conditions

The model data are:

- Maximum flow coefficient of the valves = 8005.42 U.S.
- Fluid temperature at the inlet = 290 K
- Fluid pressure at the inlet =  $3 \times 10^5$  Pa
- Fluid pressure at the outlet =  $10^5$  Pa.

### 13.9.2.2 Model Calibration

The calibration step consists in setting the mass flow rate of the fluid in each direction to known measurement values to compute by model inversion the values of the maximum flow coefficient for each valve (with, e.g., the valve position  $\Omega = 0.5$ ).

### 13.9.2.3 Simulation Results

Figure 13.15 shows the simulation results for a scenario that consists in opening the valve from position 0 (valve fully closed) to 1 (valve fully open).

## 13.10 Switch Valve Modeling

A switch valve is a type of valve that has only two stable positions: (a) open: the fully open position and (b) closed: the fully closed position; cf. Fig. 13.16. When the valve is open, the fluid flows through the valve with a pressure loss. When the valve is closed, the mass flow rate is zero (unless the valve is leaking). For ideal valves, the pressure loss is zero when the valve is open. Ideal valves are similar to ideal switches in electric circuits.

Switch valves are usually controlled by a binary control signal elaborated by the control system of the plant. However, the position of the valve is controlled by the valve actuator in a way that is similar to a control valve: The controller takes the binary signal from the control system as input and produces the continuous valve position in the range 0 (fully closed) to 1 (fully open) as output. However, contrary to control valves, only 0 and 1 are stable positions of the switch valve.

For this component model, it is assumed that the valve operates instantaneously between its two stable positions. If this assumption is not valid, then the control valve (cf. Sect. 13.8) should be used instead, with an actuator that models the continuous valve position signal between the open and close positions.

For water/steam, the flow regime is single-phase or homogeneous two-phase flow.

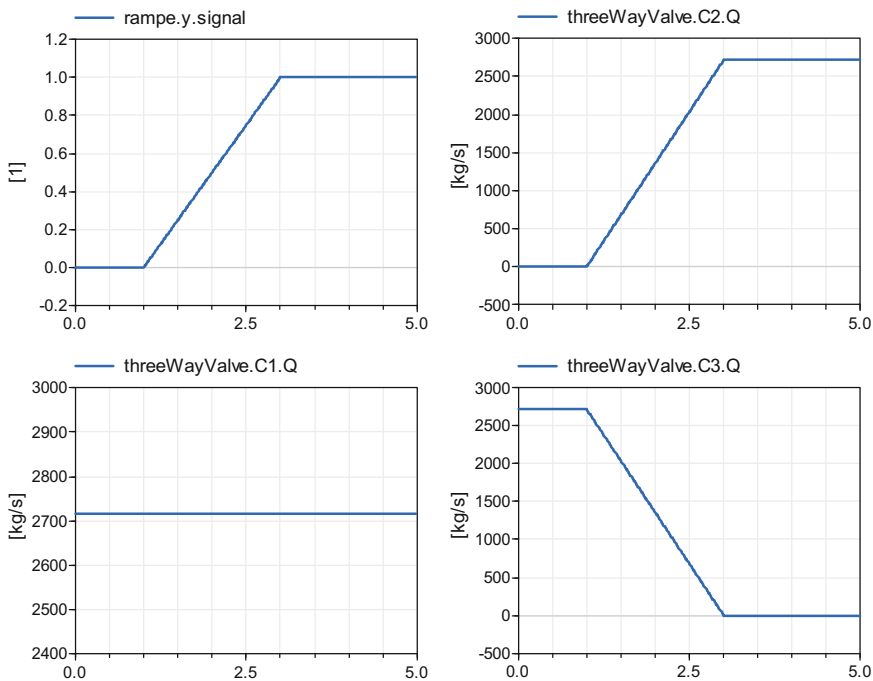
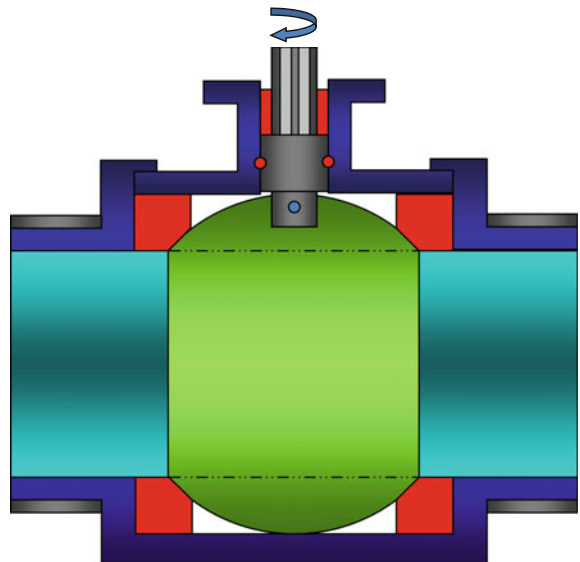


**Fig. 13.15** Simulation results for *ThreeWayValve*: ramp signal (*rampe.y.signal*), mass flow rate at the inlet (*threeWayValve.C1.Q*), mass flow rate at outlet 1 (*threeWayValve.C2.Q*) and at outlet 2 (*threeWayValve.C3.Q*)

**Fig. 13.16** Schematic diagram of a switch valve



### 13.10.1 Nomenclature

Symbols	Definition	Unit	Mathematical definition
$h$	Fluid specific enthalpy at the valve inlet	J/kg	
$P_i$	Fluid pressure at the valve inlet	Pa	
$P_o$	Fluid pressure at the valve outlet	Pa	
$\dot{m}$	Fluid mass flow rate	kg/s	
$\Delta P$	Pressure loss of the fluid between the inlet and the outlet	Pa	$P_i - P_o$
$\Lambda$	Friction pressure loss coefficient	$m^{-4}$	
$\rho$	Fluid density	$kg/m^3$	
$\Omega$	Valve position (0 or 1)	-	

### 13.10.2 Assumptions

The modeling assumptions are:

- Subsonic fluid;
- Incompressible fluid;
- Inertia is neglected: The volume inside the valve is assumed to be negligible;
- Only the two stable positions of the valve are represented. Therefore, the valve is assumed to switch positions instantly.

### 13.10.3 Governing Equations

The model is based on a simple pressure loss equation when the valve is open that switches dynamically to zero flow equation when the valve closes.

Equation 1	
Title	Static momentum balance equation
Validity domain	$\forall \dot{m}$ For $\dot{m} = 0$ , $\Delta P$ must be defined (cf. Sect. 5.2.3).
Mathematical formulation	$\begin{cases} \dot{m} = 0 & \text{if } \Omega = 0 \\ \Delta P = \Lambda \cdot \frac{\dot{m} \cdot  \dot{m} }{\rho} & \text{if } \Omega = 1 \end{cases}$
Comments	This formulation switches dynamically between two equations with different computational causalities (cf. Sect. 1.5) when $\Omega$ switches between 0 and 1. When $\Omega = 0$ , the valve is fully closed, so there is no

(continued)

(continued)

Equation 1	
Title	Static momentum balance equation
	<p>pressure loss across the valve. In such case, <math>\Delta P</math> is not computed by the switch valve model, so one should ensure that <math>P_i</math> and <math>P_o</math> are properly defined in the component models adjacent to the valve (cf. Sect. 5.2.3).</p> <p>This equation corresponds to (13.18) with <math>\Lambda = \frac{\xi_{a:b}}{2 \cdot A_{a:b}^2}</math> for <math>\Omega = 1</math> and <math>\Lambda = +\infty</math> for <math>\Omega = 0</math></p>

### 13.10.4 Modelica Component Model: SwitchValve

The governing equations are implemented in the *SwitchValve* component model located in the *WaterSteam.PressureLosses* sub-library. Figure 13.17a represents the graphical icon of the component with its three connectors.

### 13.10.5 Test-Case

The model *TestSwitchValve* used to validate the *SwitchValve* component model is represented in Fig. 13.17b. This model uses the following component models:

- One *SwitchValve* component model;
- Two *LumpedStraightPipe* component models;
- One *Pulse* block;
- One *SourceP* component model;
- One *SinkP* component model.

In this test-case scenario, the *SwitchValve* component receives: (1) the fluid pressure and specific enthalpy at the inlet, (2) the fluid pressure at the outlet, and (3) the valve position. The component computes the fluid mass flow rate going through the valve.

#### 13.10.5.1 Test-Case Parameterization and Boundary Conditions

The model data are:

- Friction pressure loss coefficient =  $1000 \text{ m}^{-4}$
- Fluid temperature at the inlet = 290 K
- Fluid pressure at the inlet =  $3 \times 10^5 \text{ Pa}$
- Fluid pressure at the outlet =  $10^5 \text{ Pa}$ .

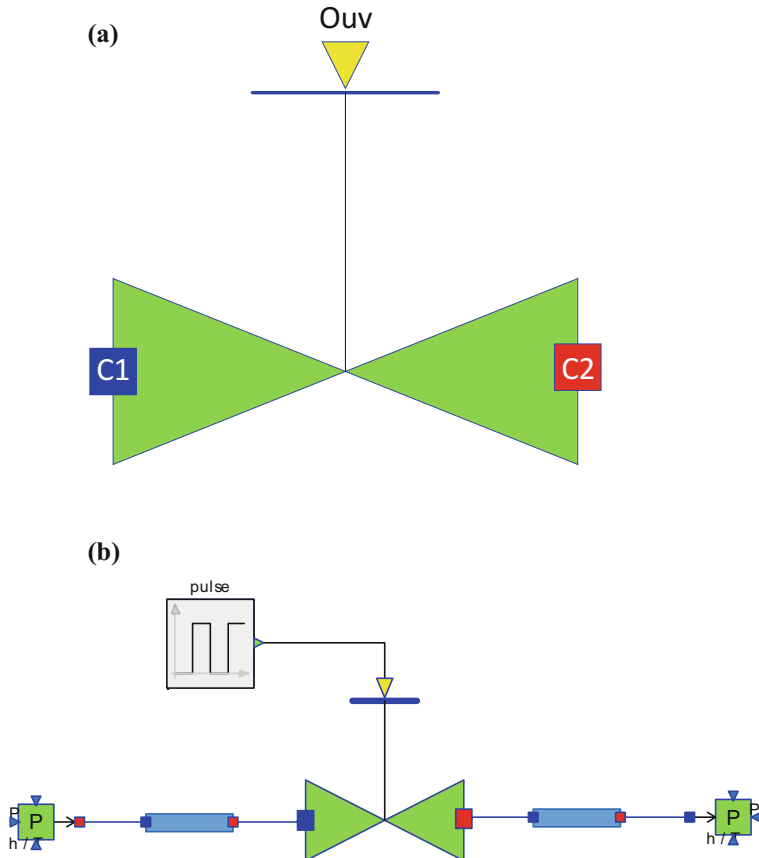


**Fig. 13.17** **a** Icon representation of the *SwitchValve* component model. **b** Test-case for the *SwitchValve* component model

### 13.10.5.2 Model Calibration

The calibration step consists in setting the fluid mass flow rate in the valve to a known measurement value to compute by model inversion the value of the friction pressure loss coefficient.

Other possible calibration: setting the fluid mass flow rate in the valve to a known measurement value to compute by model inversion the value of the fluid pressure at the inlet or at the outlet.

### 13.10.5.3 Simulation Results

Figure 13.18 shows the simulation results for a scenario that consists in closing and opening the valve.

## 13.11 Check Valve Modeling

Check valves are a type of valve which only allows flow in one direction; cf. Fig. 13.19. They are typically installed in pipes or channels in order to prevent backflow for safety reasons. They operate automatically and most do not have any external control (they are not actuator operated).

Check valves feature a clapper that opens on direct flow and closes on backflow. In this model, the movement of the clapper between the open and close positions is assumed to be instantaneous. Therefore, the inertia of the clapper is not taken into account.

The model presented here accounts for all types of check valves as it only depends on two parameters:  $\Delta P_{\text{close}}$ , the pressure loss under which the valve closes, and  $\Delta P_{\text{open}}$ , the pressure loss above which the valve opens.

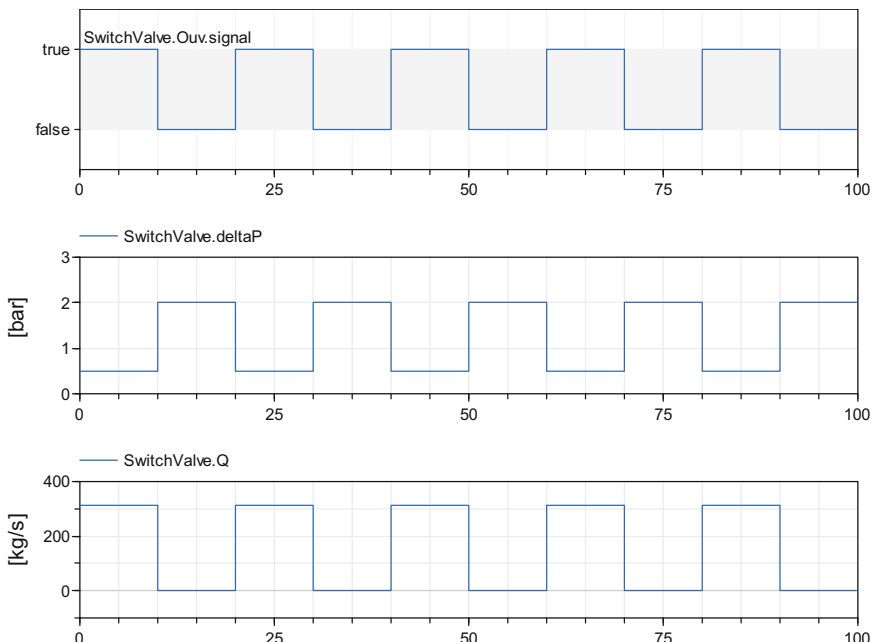
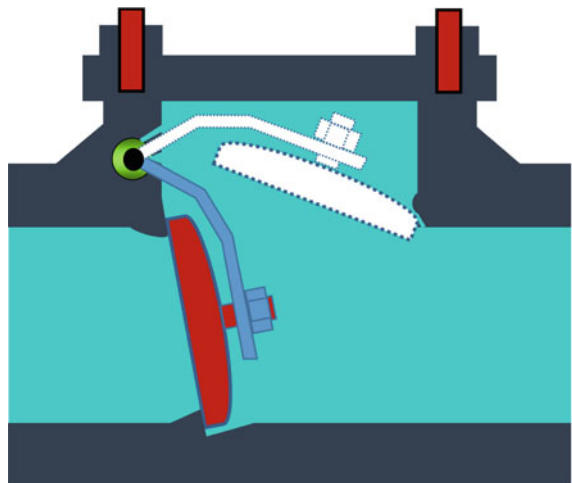


**Fig. 13.18** Simulation results for *SwitchValve*: valve position (*SwitchValve.Ouv.signal*), fluid pressure loss (*SwitchValve.deltaP*), and mass flow rate (*SwitchValve.Q*)

**Fig. 13.19** Schematic diagram of a check valve



### 13.11.1 Nomenclature

Symbols	Definition	Unit	Mathematical definition
$h$	Fluid specific enthalpy at the inlet	J/kg	
$\dot{m}$	Fluid mass flow rate	kg/s	
$P_i$	Fluid pressure at the inlet	Pa	
$P_o$	Fluid pressure at the outlet	Pa	
$\Delta P$	Pressure loss of the fluid between the inlet and the outlet	Pa	$P_i - P_o$
$\Delta P_{close}$	Pressure loss under which the valve closes	Pa	
$\Delta P_{open}$	Pressure loss above which the valve opens	Pa	
$\Lambda$	Friction pressure loss coefficient	$m^{-4}$	
$\rho$	Fluid density	$kg/m^3$	

### 13.11.2 Governing Equations

The model is based on a simple pressure loss equation when the valve is open that switches dynamically to zero flow equation when the valve closes.

Equation	
Title	Static momentum balance equation
Validity domain	$\forall \dot{m}$

(continued)

(continued)

Equation	
Title	Static momentum balance equation
Mathematical formulation	For $\dot{m}$ , $\Delta P$ must be defined (cf. Sect. 5.2.3). $\begin{cases} \dot{m} = 0 & \text{if } \Delta P < \Delta P_{\text{close}} \\ \Delta P = \Lambda \cdot \frac{\dot{m} \cdot  \dot{m} }{2 \cdot \rho} & \text{if } \Delta P > \Delta P_{\text{open}} \end{cases}$
Comments	This equation corresponds to (13.18) with $\Lambda = \frac{\xi_{a:b}}{A_{a:b}^2}$ when the valve is open, and with $\Lambda = +\infty$ when the valve is closed. The model is similar to the switch valve. However, to the contrary of the switch valve, the check valve is operated by the pressure difference $\Delta P$ between the inlet and the outlet instead of the valve position $\Omega$ set by the actuator. The valve closes when $\Delta P$ drops below $\Delta P_{\text{close}}$ and opens when $\Delta P$ rises above $\Delta P_{\text{open}}$ . To avoid chattering, $\Delta P_{\text{open}}$ and $\Delta P_{\text{close}}$ should be set such that $\Delta P_{\text{close}} < \Delta P_{\text{open}}$

### 13.11.3 Modelica Component Model: CheckValve

The governing equations are implemented in the *CheckValve* component model located in the *WaterSteam.PressureLosses* sub-library. Figure 13.20a represents the graphical icon of the component with its two connectors.

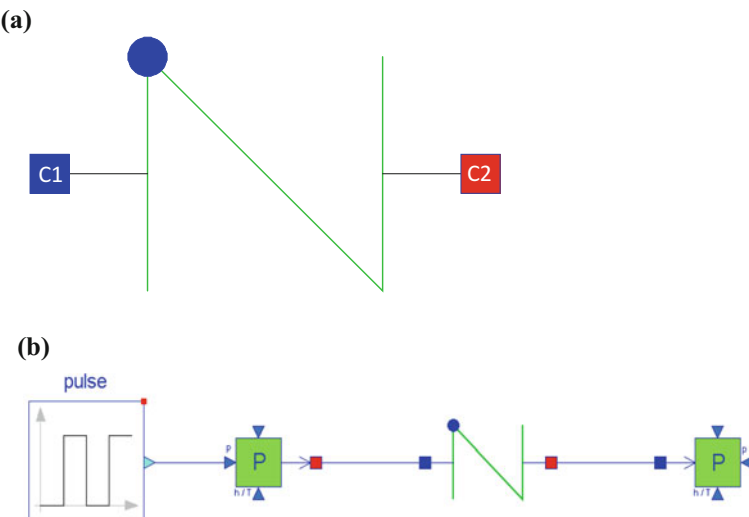


**Fig. 13.20** a Icon representation of the *CheckValve* component model. b Test-case for the *Checkvalve* component model

### 13.11.4 Test-Case

The model *TestCheckValve* used to validate the *CheckValve* component model is represented in Fig. 13.20b. This model uses the following component models:

- One *CheckValve* component model;
- One *SourceP* component model;
- One *SinkP* component model;
- One *Pulse* block.

In this test-case scenario, the *Checkvalve* component receives: (1) the fluid pressure and specific enthalpy at the inlet and (2) the fluid pressure at the outlet. The component computes the fluid mass flow rate going through the check valve.

#### 13.11.4.1 Test-Case Parameterization and Boundary Conditions

The model data are:

- Friction pressure loss coefficient of the pipes =  $1000 \text{ m}^{-4}$
- Pressure loss when the valve opens = 10 Pa
- Pressure loss when the valve closes = 0
- Fluid temperature at the inlet = 290 K
- Fluid pressure at the inlet =  $3 \times 10^5 \text{ Pa}$
- Fluid pressure at the outlet =  $6 \times 10^5 \text{ Pa}$ .

#### 13.11.4.2 Model Calibration

The calibration step consists in setting the fluid mass flow rate in the check valve to a known measurement value to compute by model inversion the value of the pressure loss coefficient.

#### 13.11.4.3 Simulation Results

Figure 13.21 shows the simulation results for a scenario where the pressure at the inlet of the check valve varies between  $9 \times 10^5 \text{ Pa}$  and  $3 \times 10^5 \text{ Pa}$ .

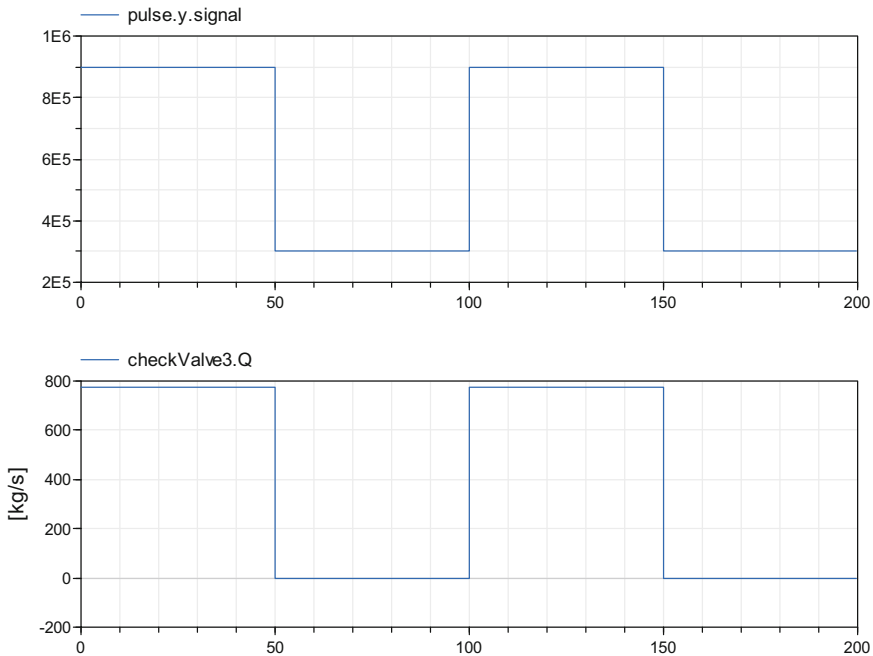


**Fig. 13.21** Simulation results for *Checkvalve*: input pressure (*pulse.y.signal*) and mass flow rate (*CheckValve3.Q*)

## 13.12 Dynamic Check Valve Modeling

The difference between this component model and the check valve component model (cf. Sect. 13.11) is that the inertia of the movement of the clapper is taken into account.

The model presented here only accounts for clapper check valves only.

### 13.12.1 Nomenclature

Symbols	Definition	Unit	Mathematical definition
$A$	Clapper hydraulic area	$\text{m}^2$	
$C_f$	Friction torque acting on the clapper	N m	
$C_h$	Hydraulic torque acting on the clapper	N m	
$C_s$	Spring torque acting on the clapper	N m	
$C_t$	Total torque acting on the clapper	N m	

(continued)

(continued)

Symbols	Definition	Unit	Mathematical definition
$C_v$	Flow coefficient of the valve	U.S.	
$C_w$	Weight torque acting on the clapper	N m	
$g$	Gravity constant	$\text{m/s}^2$	
$h$	Fluid specific enthalpy at the inlet	$\text{J/kg}$	
$J$	Clapper moment of inertia	$\text{kg m}^2$	
$K_1$	Clapper friction law coefficient #1	—	
$K_2$	Clapper friction law coefficient #2	—	
$\dot{m}$	Fluid mass flow rate through the valve	$\text{kg/s}$	
$M$	Clapper mass	kg	
$n$	Clapper friction law exponent	—	
$P_i$	Fluid pressure at the valve inlet	Pa	
$P_o$	Fluid pressure at the valve outlet	Pa	
$r$	Clapper radius	m	$\sqrt{A/\pi}$
$\Delta P$	Fluid pressure loss between the inlet and the outlet	Pa	$P_i - P_o$
$\theta$	Clapper aperture angle	rad	
$\theta_{\min}$	Minimum clapper aperture angle (valve fully closed)	rad	
$\theta_{\max}$	Maximum clapper aperture angle (valve fully open)	rad	
$\rho$	Fluid density	$\text{kg/m}^3$	
$\rho_{\text{water}, 60^\circ F}$	Density of water at $60^\circ \text{F}$ ( $15.5556^\circ \text{C}$ ).	$\text{kg/m}^3$	
$\omega$	Clapper angular velocity	$\text{rad/s}$	
$\Omega$	Valve position	—	$1 - \cos(\theta)$

### 13.12.2 Governing Equations

The dynamic check valve is modeled as a control valve whose position  $\Omega$  is controlled by the flow through the clapper aperture angle  $\theta$ ; cf. Fig. 13.22.

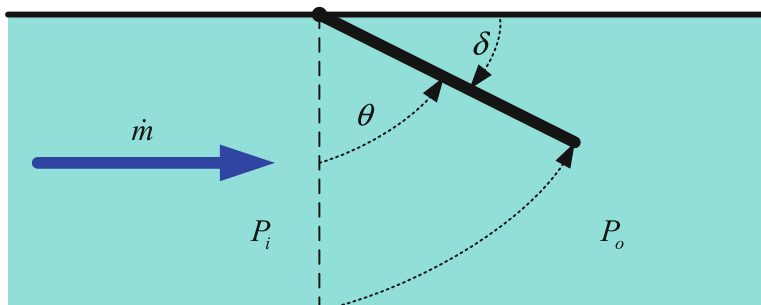


Fig. 13.22 Diagram of the dynamic check valve model

Equation 1	
Title	Static momentum balance equation
Validity domain	$\forall \dot{m}$ and $C_v \geq 0$ For $C_v = 0$ , $\Delta P$ must be defined (cf. Sect. 5.2.3).
Mathematical formulation	$\Delta P \cdot C_v \cdot  C_v  = 1.732189 \times 10^{12} \cdot \frac{\dot{m} \cdot  \dot{m} }{\rho \cdot \rho_{\text{water}, 60^\circ F}}$
Comments	<p>This equation is the same as the control valve's <math>C_v = f_v(\Omega)</math> where <math>f_v</math> is the valve characteristic (Idel'cik 1986) provides correlations for <math>\xi_{a:b}</math>; cf. (13.18)</p> <p>For a swing check valve:</p> $\xi_{a:b} \cong 0.35 \times 10^{0.0323 \cdot \delta}$ <p>where <math>\delta = \frac{180}{\pi} \cdot \left( \frac{\pi}{2} - \theta \right)</math> is the angle shown in Fig. 13.22 expressed in degrees (<math>^\circ</math>)</p> <p>Equation (13.23) can then be used to compute <math>C_v</math> from <math>\xi_{a:b}</math>:</p> $C_v = \sqrt{\frac{2 \cdot 1.732189 \times 10^{12}}{\rho_{\text{water}, 60^\circ F} \cdot 0.35 \times 10^{0.0323 \cdot \delta}}}$
Equation 2	
Title	Clapper equation
Validity domain	$\theta_{\min} < \theta < \theta_{\max}$
Mathematical formulation	<p>Clapper fully closed <math>\theta = \theta_{\min}</math></p> <p>Clapper moving <math>J \cdot \frac{d\omega}{dt} = C_t</math></p> <p>Clapper fully open <math>\theta = \theta_{\max}</math></p> <p><math>\theta = \theta_{\min}</math></p> <p><math>\theta = \theta_{\max}</math></p> <p><math>C_t</math> becomes <math>&gt; 0</math></p> <p><math>C_t</math> becomes <math>&lt; 0</math></p>
Comments	<p>The rotating mass equation is formulated as a multi-mode model (cf. Sect. 1.4) with three states:</p> <ul style="list-style-type: none"> <li>• Clapper fully closed</li> <li>• Clapper moving</li> <li>• Clapper fully open</li> </ul>

(continued)

(continued)

## Equation 2

Title	Clapper equation
	<p>with the transitions conditions between modes.</p> <p>In order to be numerically solved, this multi-mode model is transformed into the following DAE (this is possible because contrary to multi-mode models, the clapper model does not exhibit singularities):</p> $J \cdot \frac{d\omega}{dt} = \begin{cases} C_t & \text{if } \theta_{\min} < \theta < \theta_{\max} \\ C_t & \text{if } \theta \leq \theta_{\min} \text{ and } C_t > 0 \\ C_t & \text{if } \theta \geq \theta_{\max} \text{ and } C_t < 0 \\ 0 & \text{else} \end{cases}$ <p>The angular acceleration is zero when the clapper hits the mechanical stop (<math>C_t = 0</math>)</p> $\omega = \begin{cases} \frac{d\theta}{dt} & \text{when } \theta_{\min} < \theta < \theta_{\max} \\ 0 & \text{when } \theta \leq \theta_{\min} \text{ or } \theta \geq \theta_{\max} \end{cases}$ <p>The angular velocity is reset to zero when the clapper hits the mechanical stops.</p> <p>The equal sign is replaced by <math>\leq</math> or <math>\geq</math> in the transition conditions <math>\theta = \theta_{\min}</math> and <math>\theta = \theta_{\max}</math> because equal signs are not recognized by solvers to compare real values</p>

### 13.12.3 Modelica Component Model: DynamicCheckValve

The governing equations are implemented in the *DynamicCheckValve* component model located in the *WaterSteam.PressureLosses* sub-library. Figure 13.23a represents the graphical icon of the component with its two connectors.

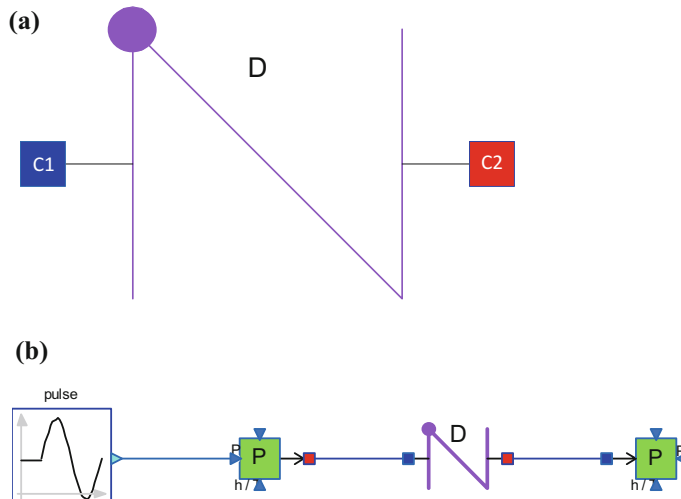


**Fig. 13.23** a Icon representation of the *DynamicCheckValve* component model. b Test-case for the *DynamicCheckValve* component model

### 13.12.4 Test-Case

The model *TestDynamicCheckValve* used to validate the *DynamicCheckValve* component model is represented in Fig. 13.23b. This model uses the following component models:

- One *DynamicCheckValve* component model;
- One *SourceP* component model;
- One *SinkP* component model;
- One *Pulse* block.

In this test-case scenario, the *DynamicCheckValve* component receives: (1) the fluid pressure and specific enthalpy at the inlet and (2) the fluid pressure at the outlet. The component computes the fluid mass flow rate going through the check valve.

#### 13.12.4.1 Test-Case Parameterization and Boundary Conditions

The model data are:

- Maximum flow coefficient of the valves = 1000 U.S.
- Fluid temperature at the inlet = 290 K
- Fluid pressure at the inlet =  $3 \times 10^5$  Pa
- Fluid pressure at the outlet =  $6 \times 10^5$  Pa
- Clapper moment of inertia = 10 kg m<sup>2</sup>
- Clapper spring stiffness = 0.2 N m
- Clapper friction law coefficient #2 = 100
- Clapper friction law exponent = 5
- Clapper mass = 1 kg
- Clapper hydraulic area = 1 m<sup>2</sup>.

#### 13.12.4.2 Model Calibration

The calibration step consists in setting the fluid mass flow rate in the check valve fully open to a known measurement value to compute by model inversion the value of the maximum flow coefficient of the check valve.

#### 13.12.4.3 Simulation Results

Figure 13.24 shows the simulation results for where the pressure at the inlet of the check valve varies between  $9 \times 10^5$  Pa and  $3 \times 10^5$  Pa. Notice that as the clapper does not close instantaneously, there is a brief backflow when the valve starts to close.

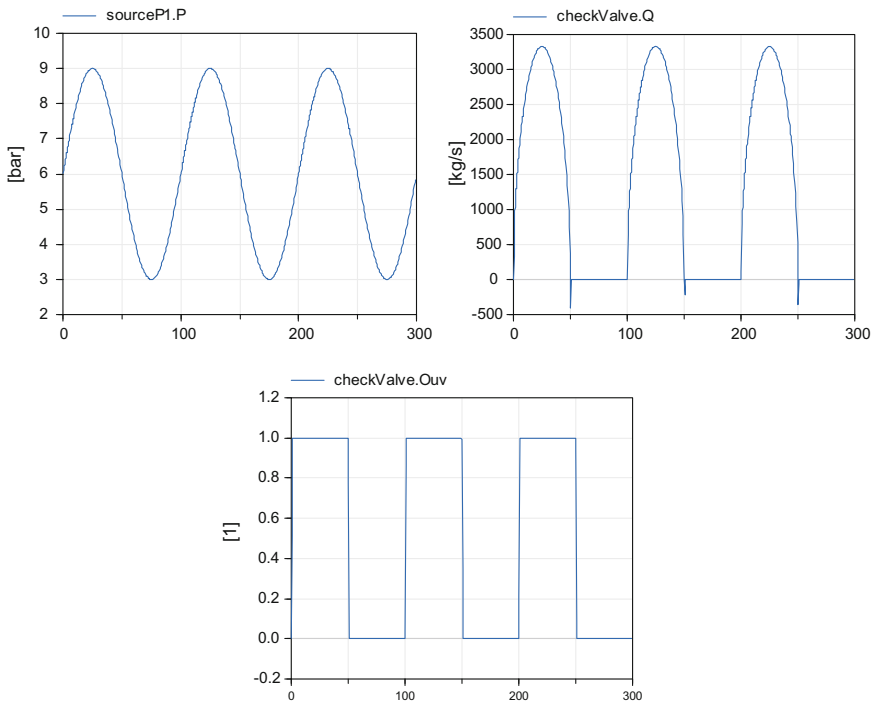


**Fig. 13.24** Simulation results for *DynamicCheckValve*: input pressure (*sourceP1.P*), mass flow rate (*CheckValve.Q*), and valve position (*CheckValve.Ouv*)

### 13.13 Dynamic Relief Valve Modeling

Relief valves are a type of valve used to limit the pressure in a system; cf. Fig. 13.25a. It is designed to open at a predetermined pressure in order to protect equipment subject to pressures that exceed their design limits. When the set pressure of the valve is exceeded, the pressure is relieved by allowing the pressurized fluid to flow through the relief valve. Once the system pressure reaches the valve reseating pressure, the relief valve closes.

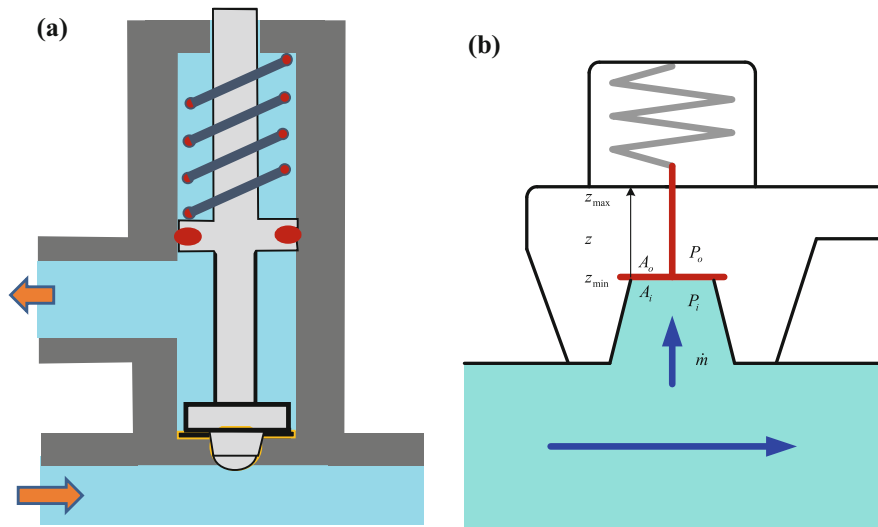


**Fig. 13.25** **a** Schematic diagram of a relief valve. **b** Diagram of the dynamic relief valve model

### 13.13.1 Nomenclature

Symbols	Definition	Unit	Mathematical definition
$A_i$	Clapper section at the inlet	$\text{m}^2$	
$A_o$	Clapper section at the outlet	$\text{m}^2$	
$C_v$	Flow coefficient of the valve	U.S.	
$D$	Valve damping	—	
$f_d$	Force acting on the clapper due to damping	N	
$f_h$	Hydraulic force acting on the clapper	N	
$f_s$	Force acting on the clapper due to the spring	N	
$f_t$	Total force acting on the clapper	N	
$f_w$	Force acting on the clapper due to the weight of the clapper	N	
$h$	Fluid specific enthalpy at the valve inlet	J/kg	
$h_c$	Valve height	m	$h_c = z_{\max} - z_{\min}$
$K_e$	Valve spring stiffness	N/m	
$\dot{m}$	Fluid mass flow rate	kg/s	
$M$	Valve mass	kg	
$P_i$	Fluid pressure at the inlet	Pa	
$P_o$	Fluid pressure at the outlet	Pa	
$v$	Clapper velocity	m/s	$\frac{dz}{dt}$

(continued)

(continued)

Symbols	Definition	Unit	Mathematical definition
$z$	Clapper position	m	
$z_{\min}$	Clapper minimum position (valve fully closed)	m	
$z_{\max}$	Clapper maximum position (valve fully open)	m	
$\delta$	Difference between the free spring length and the spring length when the valve is closed	m	
$\Delta P$	Pressure loss of the fluid between the valve inlet and outlet	Pa	$P_i - P_o$
$\rho$	Fluid density	kg/m <sup>3</sup>	
$\rho_{\text{water},60^\circ F}$	Density of water at 60 °F (15.5556 °C).	kg/m <sup>3</sup>	
$\Omega$	Valve position	—	

### 13.13.2 Assumptions

The modeling assumptions are:

- Subsonic fluid;
- Incompressible fluid;
- Inertia is neglected: The volume inside the valve is assumed to be negligible.

### 13.13.3 Governing Equations

The dynamic check valve is modeled as a control valve whose position  $\Omega$  is controlled by the pressure inside the valve; cf. Fig. 13.25b.

Equation 1	
Title	Static momentum balance equation
Validity domain	$\forall \dot{m}$ and $C_v \geq 0$ For $C_v = 0$ , $\Delta P$ must be defined (cf. Sect. 5.2.3)
Mathematical formulation	$\Delta P \cdot C_v \cdot  C_v  = 1.732189 \times 10^{12} \cdot \frac{\dot{m} \cdot  \dot{m} }{\rho \cdot \rho_{\text{water},60^\circ F}}$
Comments	This equation is the same as the control valve $C_v = f_v(\Omega)$ where $f_v$ is the valve characteristic It is assumed that $\Omega = \frac{z - z_{\min}}{z_{\max} - z_{\min}}$ Idel'Cik 1986 provides correlations for $\xi_{ab}$ ; cf. (13.18): $\xi_{ab} = f\left(\frac{z - z_{\min}}{D_i}\right)$ where $D_i$ is the clapper diameter at the inlet, e.g.,

(continued)

(continued)

## Equation 1

Title	Static momentum balance equation
	$\xi_{a:b} = 0.6 + \frac{0.15}{\left(\frac{z - z_{\min}}{D_i}\right)^2}$ <p>for a conic clapper</p> <p>Equation (13.23) can then be used to compute <math>C_v</math> from <math>\xi_{a:b}</math>:</p> $C_v = \sqrt{\frac{2 \cdot 1.732189 \times 10^{12}}{\rho_{\text{water}, 60^\circ F}} \cdot \frac{A_i}{\sqrt{f \left(\frac{z - z_{\min}}{D_i}\right)}}}$ <p>Hence, for a conic clapper:</p> $C_v = \sqrt{\frac{\pi \cdot A_i \cdot 1.732189 \times 10^{12}}{0.3 \cdot \rho_{\text{water}, 60^\circ F}} \cdot \frac{h_c \cdot \Omega}{\sqrt{1 + \frac{\pi}{A_i} \cdot h_c^2 \cdot \Omega^2}}}$

## Equation 2

Title	Clapper equation
Validity domain	$z_{\min} \leq z \leq z_{\max}$
Mathematical formulation	<p>Clapper fully closed <math>z = z_{\min}</math></p> <p>Clapper moving <math>M \cdot \frac{d^2z}{dt^2} = f_t</math></p> <p>Clapper fully open <math>z = z_{\max}</math></p> <p><math>f_t</math> becomes <math>&gt; 0</math></p> <p><math>f_t</math> becomes <math>&lt; 0</math></p> <p><math>z = z_{\min}</math></p> <p><math>z = z_{\max}</math></p>
Comments	<p>The rotating mass equation is formulated as a multi-mode model (cf. Sect. 1.4) with three states:</p> <ul style="list-style-type: none"> <li>• Clapper fully closed</li> <li>• Clapper moving</li> <li>• Clapper fully open</li> </ul> <p>with the transitions conditions between modes</p> <p>In order to be numerically solved, this multi-mode model is transformed into the following DAE (this is possible because contrary to multi-mode models, the clapper model does not exhibit singularities):</p> $f_t = f_w + f_d + f_s + f_h$ $f_w = -M \cdot g$ $f_d = -D \cdot \frac{dz}{dt}$ $f_s = -K_e \cdot (z - z_{\min} + \delta)$ $f_h = P_i \cdot A_i - P_o \cdot A_o$

(continued)

(continued)

Equation 2

Title	Clapper equation
	$M \cdot \frac{dv}{dt} = \begin{cases} f_t & \text{if } z_{\min} < z < z_{\max} \\ f_t & \text{if } z \leq z_{\min} \text{ and } f_t > 0 \\ f_t & \text{if } z \geq z_{\max} \text{ and } f_t < 0 \\ 0 & \text{else} \end{cases}$ <p>The acceleration is zero when the clapper hits the mechanical stops (<math>f_t = 0</math>).</p> $v = \begin{cases} \frac{dz}{dt} & \text{when } z_{\min} < z < z_{\max} \\ 0 & \text{when } z \leq z_{\min} \text{ or } z \geq z_{\max} \end{cases}$ <p>The velocity is reset to zero when the clapper hits the mechanical stops The equal sign is replaced by <math>\leq</math> or <math>\geq</math> in the transition conditions <math>z = z_{\min}</math> and <math>z = z_{\max}</math> because equal signs are not recognized by solvers to compare real values</p> <p>The minimum pressure <math>P_{\min_1}</math> that opens the valve is given by:  <math>M \cdot g + K_e \cdot \delta = P_{\min_1} \cdot A_i - P_o \cdot A_o</math></p> <p>The minimum pressure <math>P_{\min_2}</math> that keeps the valve fully open is given by:  <math>M \cdot g + K_e \cdot (z_{\max} - z_{\min} + \delta) = P_{\min_2} \cdot A_i - P_o \cdot A_o</math></p>

### 13.13.4 Modelica Component Model: DynamicReliefValve

The governing equations are implemented in the *DynamicReliefValve* model component located in the *WaterSteam.PressureLosses* sub-library. Figure 13.26a represents the graphical icon of the component with its two connectors.

### 13.13.5 Test-Case

The model *TestDynamicReliefValve* used to validate the *DynamicReliefValve* component model is represented in Fig. 13.26b. This model uses the following component models:

- One *DynamicReliefValve* component model;
- Two *LumpedStraightPipe* component models;
- One *VolumeD* component model;
- Two *SinkP* component models;
- One *Ramp* block.

In this test-case scenario, the pressure inside the pressure source increases from 15 bars to 30 bars in 200 s. The relief valve is set to open when the pressure at the inlet reaches 20 bars, and to be fully open when the pressure at the inlet reaches 25 bars. The formula given in Eq. 1 of Sect. 13.13.3 for a conic clapper is used to compute the valve flow coefficient versus the valve position.

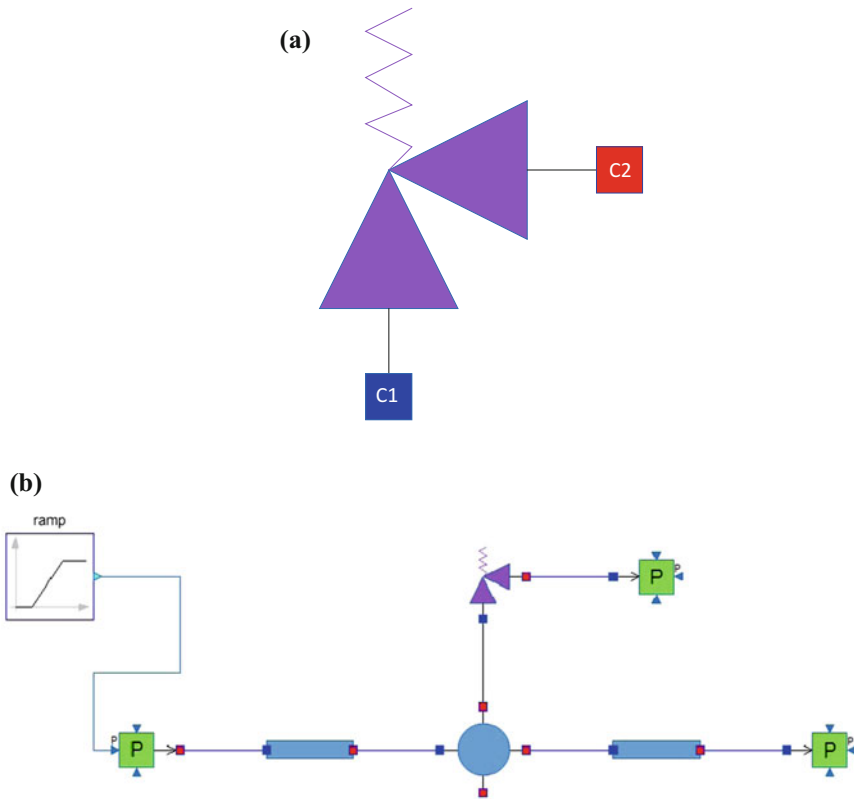


**Fig. 13.26** **a** Icon representation of the *DynamicReliefValve* component model. **b** Test-case for the *DynamicReliefValve* component model

### 13.13.5.1 Test-Case Parameterization and Boundary Conditions

The model data are:

- Flow coefficient of the valve cf. Table 13.1
- Pressure at the inlet when the valve opens =  $20 \times 10^5$  Pa
- Pressure at the inlet when the valve is fully open =  $25 \times 10^5$  Pa
- Fluid temperature at the inlet = 290 K
- Fluid pressure at the outlet =  $10^5$  Pa
- Valve spring damping = 1

**Table 13.1** Valve flow coefficient

$\Omega$	0	0.1	0.2	0.3	0.4	0.5	0.6	0.7	0.8	0.9	1
$C_V$	0	2745	4915	6391	7339	7949	8351	8625	8818	8958	9063

- Valve mass = 100 kg
- Maximum clapper position = 0.6 m
- Clapper section at the inlet =  $0.125 \text{ m}^2$
- Clapper section at the outlet =  $0.125 \text{ m}^2$
- Internal diameter of the upstream pipe = 0.4 m
- Internal diameter of the downstream pipe = 0.2 m
- Length of the pipes = 10 m
- Inlet altitude of the pipes = 0
- Outlet altitude of the pipes = 0
- Friction pressure loss coefficient of the pipes = 0.03.

### 13.13.5.2 Simulation Results

Figure 13.27 shows the simulation results for a scenario where the increase of pressure at the inlet of the relief valve is sufficient to open the valve.

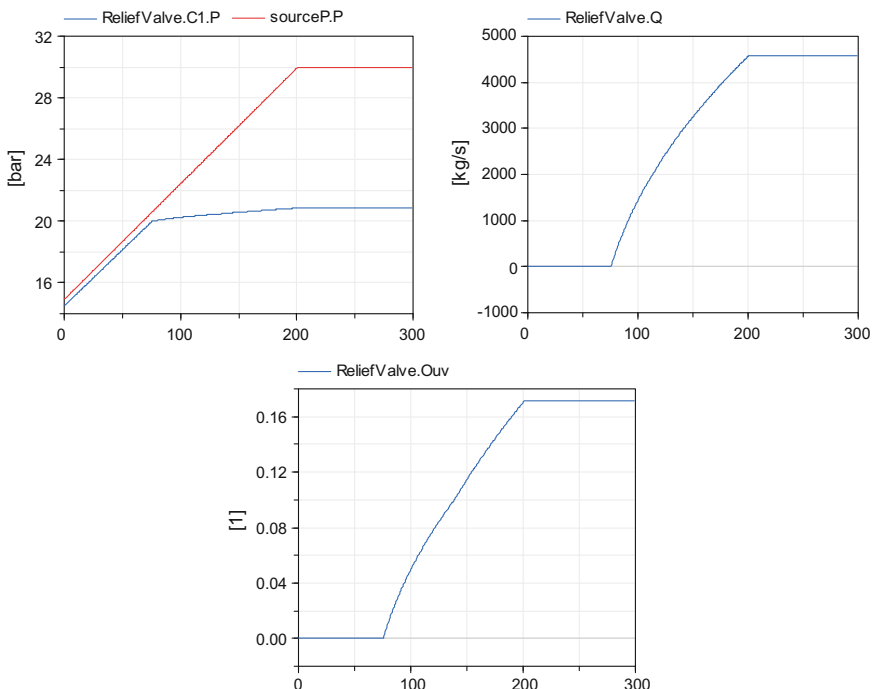


**Fig. 13.27** Simulation results for *DynamicReliefValve*: pressure at the source (`sourceP.P`), pressure at the inlet of the valve (`ReliefValve.C1.P`), fluid mass flow rate in the valve (`ReliefValve.Q`), and valve position (signal `ReliefValve.Ouv`)

## References

- Asker M, Turgut OE, Coban MT (2014) A review of non-iterative friction factor correlations for the calculation of pressure drop in pipes. Bitlis Eren Univ J Sci Technol 4(1):1–8
- Colebrook CF, White CM (1937) Experiments with fluid friction in roughened pipes. Proc R Soc A 161(906)
- Eck B (1973) Technische Strömungslehre. Springer, New York
- İdelecik IE (1986) Memento des pertes de charge, 3rd edn. Eyrolles
- Masoneilan (1997) Comment choisir les vannes de réglage. DRESSER Valve Division, Bulletin OZ1000 F 08/97
- Zigrang DJ, Sylvester ND (1982) Explicit approximations to the solution of Colebrook's friction factor equation. AIChE J 28(3)

# Chapter 14

## Volume Modeling



**Abstract** A volume, as its name suggests, is a fluid mixing or splitting component. For water/steam, the flow regime can be single-phase or two-phase flow. Regarding two-phase flow, two kinds of models are presented: one for the homogeneous flow model and the other for the two-fluid formulation with two zones (a liquid and a steam zone). The phenomena taken into account are the condensation flow of the steam phase into the liquid phase, the vaporization flow of the liquid phase into the steam phase and the thermal exchanges between the two phases, between the two phases in the volume and the cooling fluid flowing outside the volume through the tube bundle, and between the two phases in the volume and the ambient. In this chapter, the different types of volume components are presented: simple dynamic volume, dynamic drum, pressurizer, two-phase cavity, tank, static drum, mixer, splitter, and steam dryer. Detailed descriptions of the physical equations for the component models are provided: modeling assumptions, fundamental equations, and correlations with their validity domains. A test-case for each component model is given that includes the structure of the model, parameterization data, model calibration, and results of simulation. The full description of the physical equations is independent of programming languages and tools.

### 14.1 Simple Dynamic Volume Modeling

This component represents fluid mixing in a volume; cf. Fig. 14.1. It is modeled as a non-adiabatic one-phase volume or two-phase (homogeneous fluid) volume where the fluid flow representation is based on the dynamic mass and energy balance equations, and the thermal exchange between the fluid and other sources of heat is taken into consideration.

The purpose of this model is to serve as a basic volume for the staggered grid scheme (cf. Chap. 17).

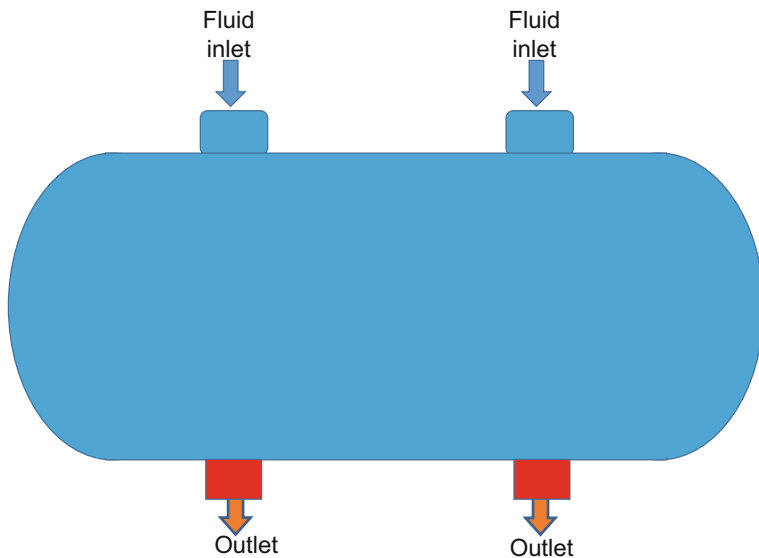


**Fig. 14.1** Schematic diagram of a volume

### 14.1.1 Nomenclature

Symbols	Definition	Unit	Mathematical definition
$h$	Fluid specific enthalpy in the volume	J/kg	
$h_i$	Specific enthalpy of the fluid at the inlets of the volume	J/kg	
$h_o$	Specific enthalpy of the fluid at the outlets of the volume	J/kg	
$\dot{m}_i$	Mass flow rate at the inlets of the volume	kg/s	
$\dot{m}_o$	Mass flow rate at the outlets of the volume	kg/s	
$P$	Fluid pressure in the volume	Pa	
$u$	Fluid specific internal energy	J/kg	$h - \frac{P}{\rho}$
$V$	Volume of the fluid	$m^3$	
$W$	Thermal power received by the fluid from other sources of heat	W	
$\rho$	Fluid density	$kg/m^3$	

### 14.1.2 Assumptions

The fluid is considered to be single-phase or homogeneous two-phase flow; cf. Sect. 4.2.1.

### 14.1.3 Governing Equations

The model of the fluid flow in the volume is based on the dynamic mass and energy balance equations. The model is formulated in order to correctly handle possible flow reversal conditions.

The state variables of the system of equations are:

- The fluid average pressure;
- The fluid average specific enthalpy.

Equation 1

Title	Dynamic mass balance equation
Validity domain	$\forall \dot{m}_i$ and $\forall \dot{m}_o$
Mathematical formulation	$V \cdot \frac{d\rho}{dt} = \sum_i \dot{m}_i - \sum_o \dot{m}_o$
Comments	<p>The mass balance equation derives from (4.7). The fluid volume is constant</p> <p>The derivative term can be developed using <math>P</math> and <math>h</math> as state variables; cf. Sect. 9.5.3.3 Eq. 1.</p> <p>This yields:</p> $V \cdot \left[ \left( \frac{\partial \rho}{\partial P} \right)_h \cdot \frac{dP}{dt} + \left( \frac{\partial \rho}{\partial h} \right)_P \cdot \frac{dh}{dt} \right] = \sum_i \dot{m}_i - \sum_o \dot{m}_o$

Equation 2a

Title	Dynamic energy balance equation
Validity domain	$\forall \dot{m}_i$ and $\forall \dot{m}_o$
Mathematical formulation	$V \cdot \frac{d(\rho \cdot u)}{dt} = \sum_i \dot{m}_i \cdot h_i - \sum_o \dot{m}_o \cdot h_o + W$
Comments	<p>The energy balance equation derives from (4.28), neglecting diffusion. The fluid volume is constant</p> <p>The derivative term can be developed using <math>P</math> and <math>h</math> as state variables; cf. Sect. 9.5.3.3 Eq. 3. This yields:</p> $\begin{aligned} V \cdot & \left[ \left( \frac{P}{\rho} \cdot \left( \frac{\partial \rho}{\partial P} \right)_h - 1 \right) \cdot \frac{dP}{dt} + \left( \frac{P}{\rho} \cdot \left( \frac{\partial \rho}{\partial h} \right)_P + \rho \right) \cdot \frac{dh}{dt} \right] \\ & = \sum_i \dot{m}_i \cdot \left[ h_i - \left( h - \frac{P}{\rho} \right) \right] - \sum_o \dot{m}_o \cdot \left[ h_o - \left( h - \frac{P}{\rho} \right) \right] + W \end{aligned}$

Equation 2b	
Title	Simple dynamic energy balance equation
Validity domain	$\forall \dot{m}_i$ and $\forall \dot{m}_o$
Mathematical formulation	$\rho \cdot V \cdot \frac{dh}{dt} = \sum_i \dot{m}_i \cdot h_i - \sum_o \dot{m}_o \cdot h_o + W$
Comments	This equation is obtained from Eq. 2a considering the fluid as incompressible (the partial derivatives of the density are zero) and neglecting the derivative of the pressure w. r. t. time, or considering that $u \approx h$ (i.e., $P/\rho \ll u$ )

#### 14.1.4 Modelica Component Model: VolumeATh

The governing equations are implemented in several components whose names are prefixed with *Volume*: *VolumeA*, *VolumeATh*, *VolumeB*, *VolumeBTh*, etc. They are located in the *WaterSteam.Volumes* sub-library. The difference between the different *Volume* components lies in the number of inputs and outputs and whether they exchange energy with the environment. Here, the *VolumeATh* component model is presented. Figure 14.2a represents the graphical icon of the component with its five connectors.

#### 14.1.5 Test-Case

The model *TestVolumeATh* used to validate the *VolumeATh* component model is represented in Fig. 14.2b. It uses the following component models:

- One *VolumeATh* component model;
- Two *ControlValve* component models;
- One *LumpedStraightPipe* component model;
- One *SourceQ* component model;
- One *SourceP* component model;
- One *SinkP* component model;
- One *Ramp* block;
- One *Constant* block;
- One *TimeTable* block.

In this test-case scenario, the *VolumeATh* component receives: (1) the fluid mass flow rate and specific enthalpy at inlet Ce1, (2) the fluid pressure and specific enthalpy at outlet Ce2, and (3) the thermal power CTh.W exchanged with the environment. The component computes: (1) the specific enthalpy of the fluid in the volume and (2) the mass flow rate of the fluid at outlet Cs1.

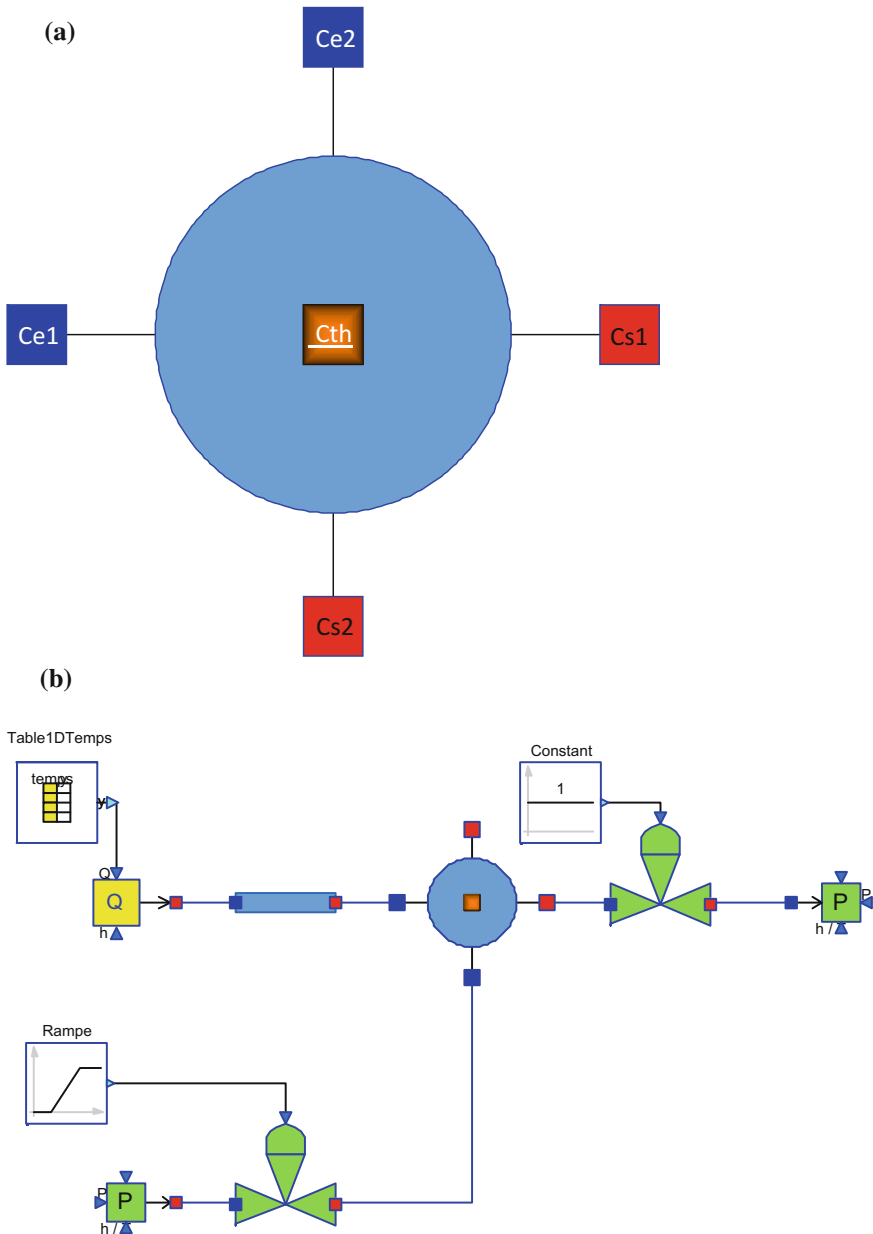


**Fig. 14.2** **a** Icon of the *VolumeATh* component model. **b** Test-case for the *VolumeATh* component model

### 14.1.5.1 Test-Case Parameterization and Boundary Conditions

The model data are:

- Volume of the component volume =  $1 \text{ m}^3$
- Length of the pipe =  $0.1 \text{ m}$
- Pipe diameter =  $1 \text{ m}$
- Outlet valve maximum flow coefficient =  $8005.42 \text{ U.S.}$
- Inlet valve maximum flow coefficient =  $80 \text{ U.S.}$
- Inlet valve specific enthalpy =  $10^5 \text{ J/kg}$
- Valve pressure at the inlet =  $3 \times 10^5 \text{ Pa}$
- Fluid mass flow rate at the inlet of the pipe =  $(10 \text{ at } 0 \text{ s}, -10 \text{ at } 5 \text{ s}, 0 \text{ at } 8 \text{ s}) \text{ kg/s}$
- Fluid specific enthalpy at the inlet of the pipe =  $10^5 \text{ J/kg}$
- Fluid pressure in the pressure sink =  $10^5 \text{ Pa}$
- Fluid specific enthalpy in the pressure sink =  $2 \cdot 10^5 \text{ J/kg}$ .

### 14.1.5.2 Model Calibration

The calibration procedure consists in setting the fluid mass flow rate going through the valve at inlet Ce2 to a known measurement value to compute by model inversion the value of the maximum flow coefficient of the valve.

### 14.1.5.3 Simulation Results

Figure 14.3 shows the simulation results for a scenario that consists in varying the mass flow rate at the two inlets of the volume (curves 1 and 2). Curves 3 and 5 show, respectively, the mass flow rate at outlet 1 and the specific enthalpy of the mixture in the volume.

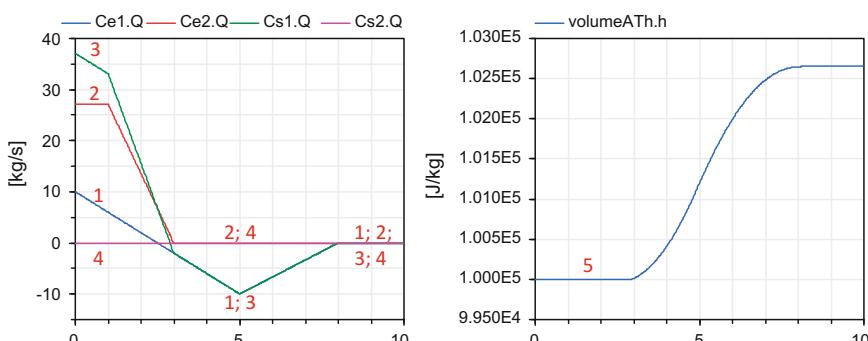


**Fig. 14.3** Simulation results for *VolumeATh*: (1) fluid mass flow rate at inlet 1 (*Ce1.Q*), (2) fluid mass flow rate at inlet 2 (*Ce2.Q*), (3) fluid mass flow rate at outlet 1 (*Cs1.Q*), (4) fluid mass flow rate at outlet 2 (*Cs2.Q*), and (5) fluid specific enthalpy in the volume

## 14.2 Dynamic Drum Modeling

A drum is a reservoir of steam and water at the top end of the boiler. It is used to separate water from steam in the water/steam mixture generated in the boiler and to store both separated fluids; cf. Figure 14.4.

The drum is represented as a dynamic non-adiabatic two-phase volume, with vertical or horizontal cylindrical geometry. The physical model is based on a

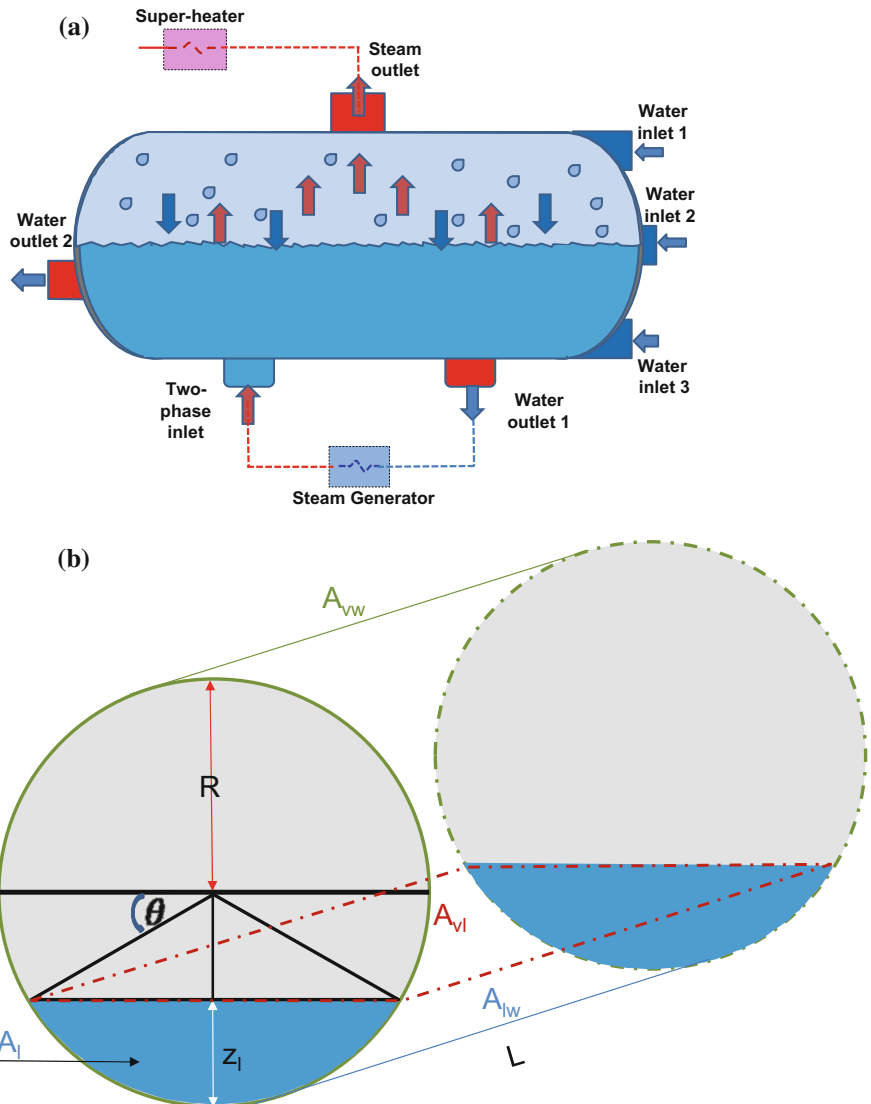


**Fig. 14.4** a Schematic diagram of a drum. b Heat exchange surfaces inside a horizontal drum

non-equilibrium two-phase formulation of the fluid balance equations. The two phases are assumed to be undergoing isobaric transformations and will be in the sequel referred to as liquid phase and vapor phase, respectively, although each phase contains (in general) small amounts of the other phase, i.e., bubbles in the liquid phase and droplets in the vapor phase; cf. Sect. 4.2.

The model takes into account the condensation flow of the vapor phase into the liquid phase (i.e., the flow of droplets), and reciprocally the vaporization flow of the liquid phase into the steam phase (i.e., the flow of bubbles).

There is another component similar to the *DynamicDrum* component called *TwoPhaseVolume*. The main difference between the two components lies in the number of connectors to accommodate their respective roles in the plant: The dynamic drum is a steam separator for the evaporator, whereas the two-phase volume is a condenser.

### 14.2.1 Nomenclature

Symbols	Definition	Unit	Mathematical definition
$A_l$	Cross-sectional area of the liquid phase in the cavity (see Fig. 14.4b)	$\text{m}^2$	For a vertical cavity: $\pi \cdot R^2$ For a horizontal cavity: $(\frac{\pi}{2} - \theta) \cdot R^2$ $- R \cdot \cos(\theta) \cdot (R - z_l)$
$A_{aw}$	Contact surface between the ambient and the cavity wall	$\text{m}^2$	$A_{lw} + A_{vw}$
$A_{lw}$	Contact surface between the liquid phase and the cavity wall (see Fig. 14.4b)	$\text{m}^2$	For a vertical cavity: $2 \cdot \pi \cdot R \cdot z_l + A_l$ For a horizontal cavity: $(\pi - 2 \cdot \theta) \cdot R \cdot L + 2 \cdot A_l$
$A_{vl}$	Contact surface between the vapor phase and the liquid phase (see Fig. 14.4b)	$\text{m}^2$	For a vertical cavity: $A_l$ For a horizontal cavity: $2 \cdot R \cdot L \cdot \cos(\theta)$
$A_{vw}$	Contact surface between the vapor phase and the cavity wall (see Fig. 14.4b)	$\text{m}^2$	For a vertical cavity: $2 \cdot \pi \cdot R \cdot (L - z_l) + A_l$ For a horizontal cavity: $(\pi + 2 \cdot \theta) \cdot R \cdot L + 2(\pi \cdot R^2 - A_l)$
$c_{p,w}$	Specific heat capacity of the drum wall	$\text{J/kg/K}$	
$C_{cond}$	Condensation rate	$\text{s}^{-1}$	
$C_{evap}$	Evaporation rate	$\text{s}^{-1}$	
$g$	Acceleration due to gravity	$\text{m/s}^2$	

(continued)

(continued)

Symbols	Definition	Unit	Mathematical definition
$h_{ev}$	Specific enthalpy of the water/steam mixture coming from the evaporator	J/kg	
$h_{i_1}$	Specific enthalpy of the liquid phase at inlet 1, coming from the economizer (see Fig. 14.4a)	J/kg	
$h_{i_2}$	Specific enthalpy of the liquid phase at inlet 2 (see Fig. 14.4a)	J/kg	
$h_{i_3}$	Specific enthalpy of the liquid phase at inlet 3 (see Fig. 14.4a)	J/kg	
$h_l$	Specific enthalpy of the liquid phase in the cavity	J/kg	
$h_{l,ev}$	Specific enthalpy of the liquid coming from the evaporator	J/kg	
$h_{l,o_1}$	Specific enthalpy of the liquid phase at outlet 1, going to the evaporator (see Fig. 14.4a)	J/kg	
$h_{l,o_2}$	Specific enthalpy of the liquid phase at outlet 2 (see Fig. 14.4a)	J/kg	
$h_l^{\text{sat}}$	Saturation enthalpy of the liquid in the cavity	J/kg	
$h_v$	Specific enthalpy of the vapor phase in the cavity	J/kg	
$h_{v,ev}$	Specific enthalpy of the vapor coming from the evaporator	J/kg	
$h_{v,o}$	Specific enthalpy of the vapor phase at the outlet of the drum, going to the super-heater	J/kg	
$h_v^{\text{sat}}$	Saturation enthalpy of the vapor in the cavity	J/kg	
$K_{lw}$	Convective heat exchange coefficient between the liquid and the wall	W/m <sup>2</sup> /K	
$K_{vl}$	Convective heat exchange coefficient between the liquid and the vapor in the cavity	W/m <sup>2</sup> /K	
$K_{vw}$	Convective heat exchange coefficient between the vapor and the wall	W/m <sup>2</sup> /K	

(continued)

(continued)

Symbols	Definition	Unit	Mathematical definition
$K_{wa}$	Convective heat exchange coefficient between the wall and the ambient	W/m <sup>2</sup> /K	
$L$	Cavity length	m	
$\dot{m}_{cond}$	Condensation mass flow rate inside the cavity	kg/s	
$\dot{m}_{ev}$	Fluid mass flow rate entering the cavity coming from the evaporator	kg/s	
$\dot{m}_{evap}$	Evaporation mass flow rate inside the cavity	kg/s	
$\dot{m}_{l,o_1}$	Mass flow rate of outgoing condensate 1 (going to the evaporator)	kg/s	
$\dot{m}_{l,o_2}$	Mass flow rate of outgoing condensate 2	kg/s	
$\dot{m}_{i_1}$	Mass flow rate of the liquid at inlet 1 (coming from the economizer)	kg/s	
$\dot{m}_{i_2}$	Mass flow rate of the liquid at inlet 2	kg/s	
$\dot{m}_{i_3}$	Mass flow rate of the liquid at inlet 3	kg/s	
$\dot{m}_v$	Mass flow rate of the vapor going to the super-heater	kg/s	
$M_w$	Mass of the wall cavity	kg	
$P$	Pressure of the liquid and vapor phases inside the cavity	Pa	
$P_b$	Pressure of the liquid phase at the bottom of the cavity	Pa	$P + \rho_l \cdot g \cdot z_l$
$R$	Cavity radius	m	
$T_a$	Ambient temperature	K	
$T_l$	Liquid temperature	K	
$T_{sat}$	Saturation temperature	K	
$T_v$	Vapor temperature	K	
$T_w$	Cavity wall temperature	K	
$u$	Fluid specific internal energy	J/kg	
$V$	Volume of the cavity	m <sup>3</sup>	$V_l + V_v$
$V_l$	Volume of the liquid in the cavity	m <sup>3</sup>	$A_l \cdot z_l$
$V_v$	Volume of the vapor in the cavity	m <sup>3</sup>	

(continued)

(continued)

Symbols	Definition	Unit	Mathematical definition
$W$	Power directly provided to the liquid phase	W	
$W_{aw}$	Power exchanged from the ambient to the drum wall	W	
$W_{lw}$	Power exchanged from the liquid to the drum wall	W	
$W_{vl}$	Power exchanged from the vapor to the liquid	W	
$W_{vw}$	Power exchanged from the vapor to the drum wall	W	
$x_{ev}$	Vapor mass fraction of the fluid coming from the evaporator	–	
$x_l$	Vapor mass fraction in the liquid phase	–	
$X_{lo}$	Vapor mass fraction in the liquid phase from which the liquid starts to evaporate	–	
$x_v$	Vapor mass fraction in the vapor phase	–	
$X_{vo}$	Vapor mass fraction in the vapor phase from which the liquid starts to condensate	–	
$z_l$	Liquid level in the cavity	m	$V_l/A_l$
$\theta$	Cf. Fig. 14.4b	rad	$\arcsin\left(\frac{R - z_l}{R}\right)$
$\lambda_l$	Liquid thermal conductivity in the cavity	W/m/K	
$\rho_l$	Liquid density in the cavity	kg/m <sup>3</sup>	
$\rho_v$	Vapor density in the cavity	kg/m <sup>3</sup>	

### 14.2.2 Assumptions

The drum is modeled according to the following assumptions:

- The two phases are always present (there is no phase appearance or disappearance).
- Pressure losses are not taken into account in the drum.
- The liquid and vapor phases are not necessarily in thermal equilibrium.
- The liquid and vapor phases are assumed to be always in pressure equilibrium.

For some operating conditions, the liquid and the vapor phases in the cavity are not necessarily in thermal equilibrium, for the following reasons:

- The steam may enter the cavity superheated (the steam temperature is then higher than the saturation temperature).
- The liquid can be subcooled by the incoming drain and the wetted tube bundle (the liquid temperature is then lower than the saturation temperature).

### 14.2.3 Governing Equations

The *DynamicDrum* component represents the dynamics of the thermal-hydraulic phenomena of the fluids inside the drum. In particular, the model takes into account the thermal exchanges between the fluid in the cavity and the cooling fluid flowing through the tube bundle. Also, the heat transfer between (1) the liquid phase and vapor phase, (2) the fluid and the wall, and (3) the drum and the external medium (ambient environment) is considered in the model. The drum cavity is considered as a vertical or horizontal cylinder.

The state variables of the system are:

- The pressure in the cavity;
- The specific enthalpy of the liquid phase;
- The specific enthalpy of the vapor phase;
- The temperature of the wall;
- The volume of the liquid phase;
- The volume of the vapor phase.

Equation 1

Title	Dynamic mass balance equation for the liquid phase
Validity domain	$\forall \dot{m}$ and $0 < V_l < V$
Mathematical formulation	$\rho_l \frac{dV_l}{dt} + V_l \left[ \left( \frac{\partial \rho_l}{\partial P} \right)_h \cdot \frac{dP}{dt} + \left( \frac{\partial \rho_l}{\partial h_l} \right)_P \cdot \frac{dh_l}{dt} \right]$ $= \dot{m}_{l_1} + \dot{m}_{l_2} + \dot{m}_{l_3} - \dot{m}_{l,o_1} - \dot{m}_{l,o_2}$ $+ (1 - x_{ev}) \cdot \dot{m}_{ev} + \dot{m}_{cond} - \dot{m}_{evap}$
Comments	<p>The derivation of this equation is similar to Eq. 1 of the dynamic modeling of a simple condenser (cf. Sect. 9.5.3.3)</p> <p>It is assumed that the liquid fraction of the fluid mixture coming from the evaporator goes directly to the liquid phase</p>

Equation 2

Title	Dynamic mass balance equation for the vapor phase
Validity domain	$\forall \dot{m}$ and $0 < V_v < V$
Mathematical formulation	$\rho_v \cdot \frac{dV_v}{dt} + V_v \cdot \left[ \left( \frac{\partial \rho_v}{\partial P} \right)_h \cdot \frac{dP}{dt} + \left( \frac{\partial \rho_v}{\partial h_v} \right)_P \cdot \frac{dh_v}{dt} \right]$ $= -\dot{m}_v + x_{ev} \cdot \dot{m}_{ev} + \dot{m}_{evap} - \dot{m}_{cond}$
Comments	The derivation of this equation is similar to Eq. 1 of the dynamic modeling of a simple condenser (cf. Sect. 9.5.3.3)

Equation 3

Title	Dynamic energy balance equation for the liquid phase
Validity domain	$\forall \dot{m}$ and $0 < V_l < V$
Mathematical formulation	$V_l \cdot \left[ \left( \frac{P}{\rho_l} \cdot \left( \frac{\partial \rho_l}{\partial P} \right)_h - 1 \right) \cdot \frac{dP}{dt} + \left( \frac{P}{\rho_l} \cdot \left( \frac{\partial \rho_l}{\partial h_l} \right)_P + \rho_l \right) \cdot \frac{dh_l}{dt} \right]$ $= \dot{m}_{i_1} \cdot \left( h_{i_1} - \left( h_l - \frac{P}{\rho_l} \right) \right) + \dot{m}_{i_2} \cdot \left( h_{i_2} - \left( h_l - \frac{P}{\rho_l} \right) \right)$ $+ \dot{m}_{i_3} \cdot \left( h_{i_3} - \left( h_l - \frac{P}{\rho_l} \right) \right) - \dot{m}_{l,o_1} \cdot \left( h_{l,o_1} - \left( h_l - \frac{P}{\rho_l} \right) \right)$ $- \dot{m}_{l,o_2} \cdot \left( h_{l,o_2} - \left( h_l - \frac{P}{\rho_l} \right) \right) + \dot{m}_{\text{cond}} \cdot \left( h_l^{\text{sat}} - \left( h_l - \frac{P}{\rho_l} \right) \right)$ $- \dot{m}_{\text{evap}} \cdot \left( h_v^{\text{sat}} - \left( h_l - \frac{P}{\rho_l} \right) \right)$ $+ (1 - x_{\text{ev}}) \cdot \dot{m}_{\text{ev}} \cdot \left( h_{l,\text{ev}} - \left( h_l - \frac{P}{\rho_l} \right) \right)$ $+ W_{vl} - W_{lw} + W$
Comments	<p>The derivation of this equation is similar to Eq. 3 of the dynamic modeling of a simple condenser (cf. Sect. 9.5.3.3)</p> <p>The value of <math>h_{l,\text{ev}}</math> is given by:</p> $h_{l,\text{ev}} = \begin{cases} h_{\text{ev}} & \text{for } x_{\text{ev}} = 0 \\ h_l^{\text{sat}} & \text{for } x_{\text{ev}} > 0 \end{cases}$

Equation 4

Title	Dynamic energy balance equation for the vapor phase
Validity domain	$\forall \dot{m}$ and $0 < V_v < V$
Mathematical formulation	$V_v \cdot \left[ \left( \frac{P}{\rho_v} \cdot \left( \frac{\partial \rho_v}{\partial P} \right)_h - 1 \right) \cdot \frac{dP}{dt} + \left( \frac{P}{\rho_v} \cdot \left( \frac{\partial \rho_v}{\partial h_v} \right)_P + \rho_v \right) \cdot \frac{dh_v}{dt} \right]$ $= -\dot{m}_v \cdot \left( h_{v,o} - \left( h_v - \frac{P}{\rho_v} \right) \right) - \dot{m}_{\text{cond}} \cdot \left( h_v^{\text{sat}} - \left( h_v - \frac{P}{\rho_v} \right) \right)$ $+ \dot{m}_{\text{evap}} \cdot \left( h_v^{\text{sat}} - \left( h_v - \frac{P}{\rho_v} \right) \right)$ $+ x_{\text{ev}} \cdot \dot{m}_{\text{ev}} \cdot \left( h_{v,\text{ev}} - \left( h_v - \frac{P}{\rho_v} \right) \right) - W_{vl} - W_{vw}$
Comments	<p>The derivation of this equation is similar to Eq. 3 of the dynamic modeling of a simple condenser (cf. Sect. 9.5.3.3).</p> <p>The value of <math>h_{v,\text{ev}}</math> is given by:</p> $h_{v,\text{ev}} = \begin{cases} h_{\text{ev}} & \text{for } x_{\text{ev}} = 1 \\ h_v^{\text{sat}} & \text{for } x_{\text{ev}} < 1 \end{cases}$

**Equation 5**

Title	Energy accumulation in the wall
Validity domain	$\forall T_w$
Mathematical formulation	$M_w \cdot c_{p,w} \cdot \frac{dT_w}{dt} = W_{lw} + W_{vw} + W_{aw}$

**Equation 6**

Title	Power exchanged between the vapor and liquid phases
Validity domain	$\forall T_v$ and $\forall T_l$
Mathematical formulation	$W_{vl} = K_{vl} \cdot A_{vl} \cdot (T_v - T_l)$

**Equation 7**

Title	Power exchanged between the liquid and the drum wall
Validity domain	$\forall T_l$ and $\forall T_w$
Mathematical formulation	$W_{lw} = K_{lw} \cdot A_{lw} \cdot (T_l - T_w)$

**Equation 8**

Title	Power exchanged between the vapor and the drum wall
Validity domain	$\forall T_v$ and $\forall T_w$
Mathematical formulation	$W_{vw} = K_{vw} \cdot A_{vw} \cdot (T_v - T_w)$

**Equation 9**

Title	Power exchanged between the ambient and the drum wall
Validity domain	$\forall T_a$ and $\forall T_w$
Mathematical formulation	$W_{aw} = K_{aw} \cdot A_{aw} \cdot (T_a - T_w)$

**Equation 10**

Title	Condensation mass flow rate
Validity domain	$\forall x_v$ close to $X_{vo}$
Mathematical formulation	$\dot{m}_{cond} = \max(C_{cond} \cdot \rho_v \cdot V_v \cdot (X_{vo} - x_v), 0)$
Comments	Cf. (4.96a).

**Equation 11**

Title	Evaporation mass flow rate
Validity domain	$\forall x_l$ close to $X_{lo}$
Mathematical formulation	$\dot{m}_{evap} = \max(C_{evap} \cdot \rho_l \cdot V_l \cdot (x_l - X_{lo}), 0)$
Comments	Cf. (4.96b).

This set of equations must be completed by the water and steam state equations for  $h_l^{\text{sat}}$ ,  $h_v^{\text{sat}}$  and  $x_{ev}$  in order to have a complete system of equations that can be solved.

### 14.2.4 Modelica Component Model: DynamicDrum

The governing equations are implemented in the *DynamicDrum* component model located in the *WaterSteam.Volumes* sub-library.

Figure 14.5a represents the graphical icon of the component with its ten connectors.

### 14.2.5 Test-Case

The model *TestDynamicDrum* used to validate the *DynamicDrum* component model is represented in Fig. 14.5b. It uses the following component models:

- One *DynamicDrum* component model;
- Two *ControlValve* component models;
- One *LumpedStraightPipe* component model;
- One *HeatExchangerWall* component model;
- One *DynamicTwoPhaseFlowPipe* component model;
- One *SourceP* component model;
- One *SinkQ* component model;
- One *HeatSource* component model;
- Two *Constant* blocks;
- One *TimeTable* block;
- One *Drum\_LevelControl* block.

In this test-case scenario, the *DynamicDrum* component receives: (1) the water mass flow rate and specific enthalpy at the inlet, (2) the steam mass flow rate at the outlet, and (3) the fluid mass flow rate and specific enthalpy at the outlet of the evaporator. The component computes: (1) the drum pressure, (2) the specific enthalpy of the liquid in the drum, (3) the specific enthalpy of the steam in the drum, (4) the wall temperature, and (5) the liquid level in the drum.

#### 14.2.5.1 Test-Case Parameterization and Boundary Conditions

The model data are:

- Cavity length = 16.27 m
- Cavity radius = 1.05 m
- Liquid level in the cavity = 1.05 m
- Fluid specific enthalpy at the inlet of the feed water valve =  $14 \times 10^5$  J/kg
- Fluid pressure at the inlet of the feed water valve =  $133 \times 10^5$  Pa
- Fluid pressure at the outlet of the steam valve =  $127 \times 10^5$  Pa

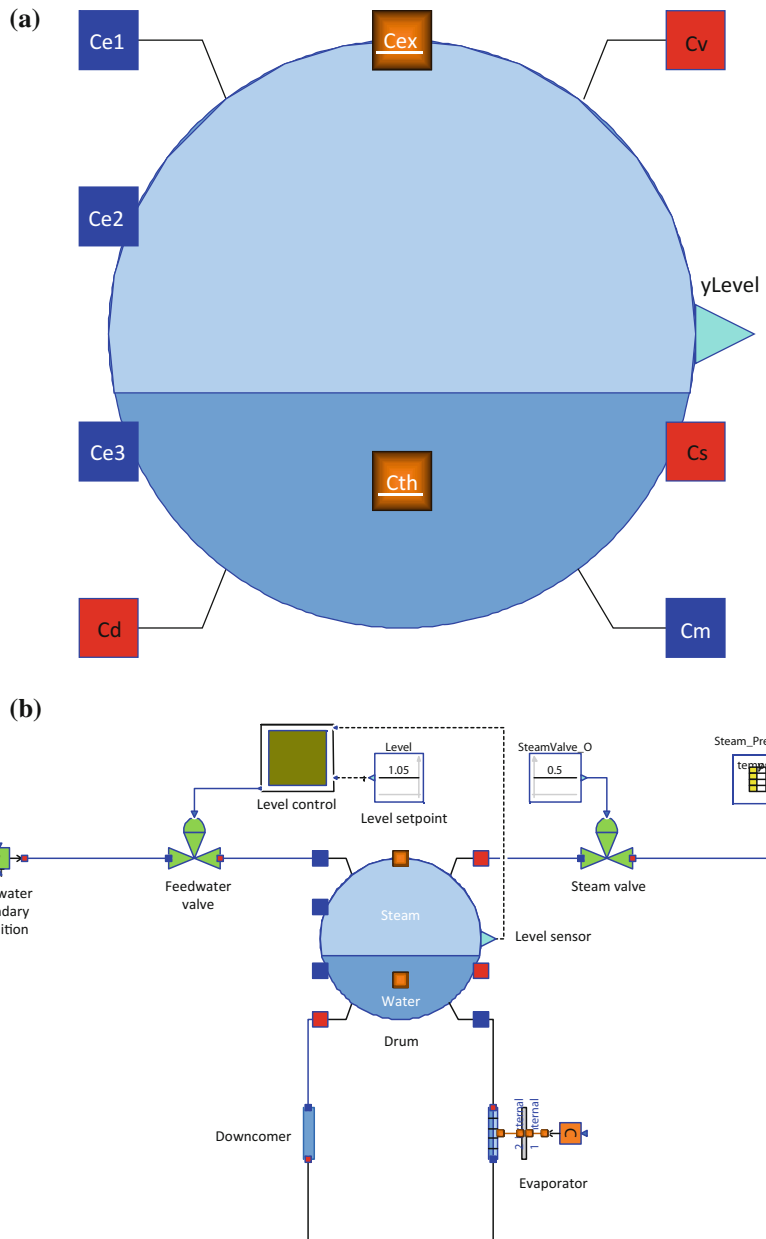


**Fig. 14.5** **a** Icon of the *DynamicDrum* component model. **b** Test-case for the *DynamicDrum* component model

- Fluid mass flow rate in the down-comer = 130 kg/s
- Evaporator pipe diameter = 0.03 m
- Evaporator pipe length = 20 m
- Number of pipes (evaporator) = 1400
- Evaporator wall thickness = 0.002 m
- Input power (evaporator) =  $10^8$  W.

#### 14.2.5.2 Model Calibration

The calibration procedure consists in setting the fluid mass flow rate of the fluid coming from the evaporator (in the *LumpedStraightPipe* model), the drum pressure, the liquid level in the drum to known measurement values to compute by model inversion the values of the mass flow rate of the steam at the outlet, the friction pressure loss coefficient of the *LumpedStraightPipe* model (*lambda*), and the flow coefficient of the water control valve (*Cvmax*).

#### 14.2.5.3 Simulation Results

The simulation of the test scenario gives the numerical results below:

- Cavity pressure = 128,732 Pa
- Steam mass flow rate (*Cv.Q*) = 79.298 kg/s
- Water mass flow rate (*Ce1.Q*) = 79.298 kg/s
- Friction pressure loss coefficient of the down-comer = 0.0859
- Maximum flow coefficient of the feed water valve = 458.04 U.S.

Figure 14.6 shows the results of the simulation for a scenario of pressure variation at the outlet of the steam valve that simulates the scenario of a decrease followed by an increase in steam load (curve 1). Curve 3 shows the corresponding swell and shrink effect: The water level inside the drum increases then decreases. When the pressure inside the drum decreases (curve 2), the saturation pressure inside the evaporator decreases, resulting in an increase in the steam mass flow rate produced by the evaporator (curve 4). The increase in steam volume in the evaporator located below the drum pushes the water level upward, the main reason for the increase in water level being, however, the increase in the feed water mass flow rate due to the decrease in drum pressure.

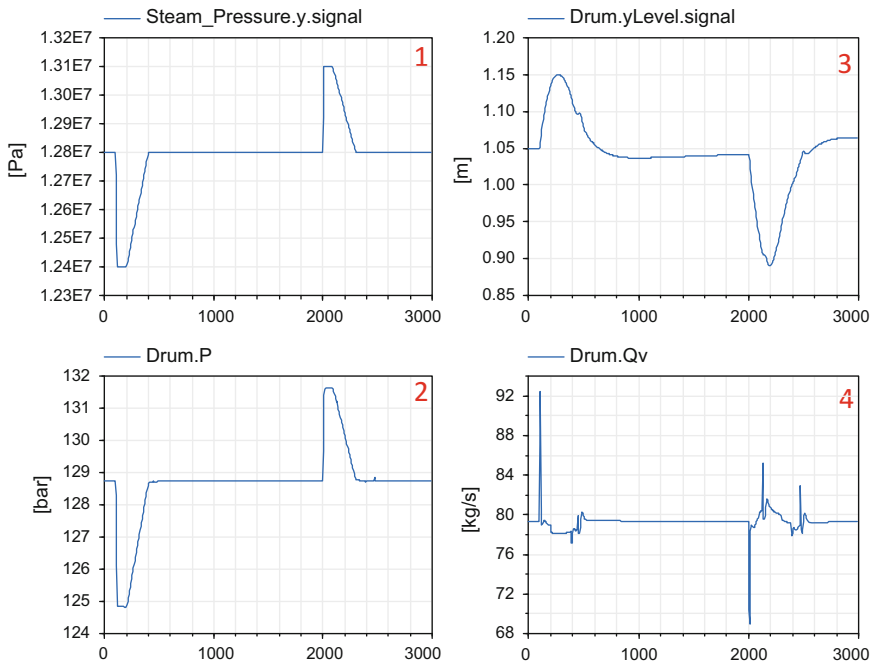


**Fig. 14.6** Simulation results for *DynamicDrum*: (1) pressure variation at the outlet of the steam valve, (2) drum pressure, (3) drum level, and (4) steam mass flow rate from the evaporator

### 14.3 Pressurizer Modeling

The pressurizer is a component used in pressurized water reactors to control the pressure inside the primary system to ensure that the reactor coolant remains always liquid (i.e., that boiling does not occur in any part of the primary system by ensuring that the fluid pressure is always above the saturation line). It is a cylindrical tank terminated by two hemispherical heads, coated internally with stainless steel and disposed vertically. The pressure inside the pressurizer is controlled by constantly keeping the pressurizer in two-phase condition by acting on the fluid temperature, as the pressure is a function of the temperature in two-phase fluids. To that end, the pressurizer is equipped with electric heating rods at the bottom to increase the temperature, and spray tubes at the top to lower the temperature, with a level control. The pressurizer is also equipped with several safety valves (discharge valves) and several valves on the depressurization line, dedicated to the mitigation of serious accidents (cf. Figure 14.7).

A steady small spray mass flow rate is maintained which condenses small amounts of steam that fall into the liquid phase. Correlatively, the heating rods generate bubbles in the liquid phase that go into the vapor phase. This ensures a constant stirring of the liquid phase that prevents thermal stratification.

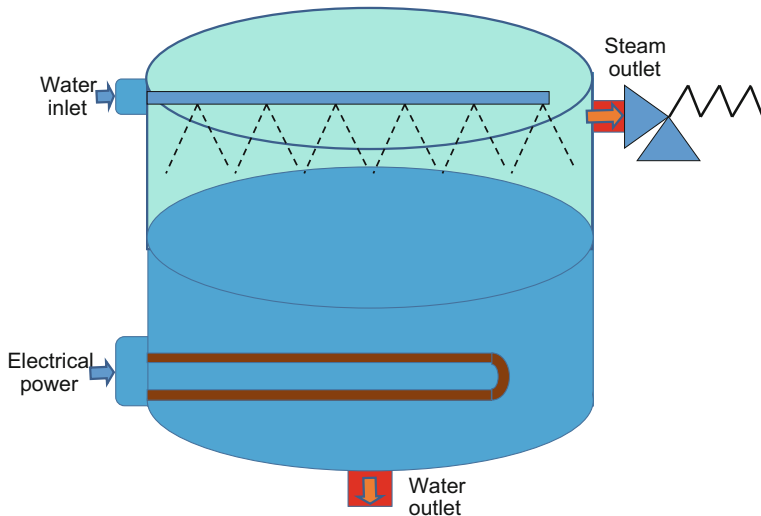


**Fig. 14.7** Schematic diagram of a pressurizer

The pressurizer is modeled as a dynamic non-adiabatic two-phase volume, with vertical cylindrical geometry. The physical model is based on a non-equilibrium two-phase formulation of the fluid balance equations. The two phases are assumed to be isobaric and will be respectively referred to as the liquid phase and the steam phase in the sequel.

The model takes into account the condensation flow of the steam phase into the liquid phase and, reciprocally, the vaporization flow of the liquid phase into the steam phase.

### 14.3.1 Nomenclature

Symbols	Definition	Unit	Mathematical definition
$A_e$	External pressurizer surface	$\text{m}^2$	
$A_{lw}$	Heat exchange surface between the liquid phase and the wall	$\text{m}^2$	$2 \cdot \pi \cdot R \cdot z_l$
$A_p$	Pressurizer cross-sectional area	$\text{m}^2$	$\pi \cdot R^2$
$A_{vw}$	Heat exchange surface between the steam phase and the wall	$\text{m}^2$	$2 \cdot \pi \cdot R \cdot \left( \frac{V}{A_p} - z_l \right)$
$c_{p,w}$	Specific heat capacity of the wall	$\text{J/kg/K}$	
$C_{cond}$	Condensation rate	$\text{s}^{-1}$	
$C_{evap}$	Evaporation rate	$\text{s}^{-1}$	
$g$	Acceleration due to gravity	$\text{m/s}^2$	

(continued)

(continued)

Symbols	Definition	Unit	Mathematical definition
$h_l$	Specific enthalpy of the liquid phase in the pressurizer	J/kg	
$h_{l,i}$	Specific enthalpy of the liquid at the inlet of the pressurizer	J/kg	
$h_{l,o}$	Specific enthalpy of the liquid at the outlet of the pressurizer	J/kg	
$h_l^{\text{sat}}$	Saturation enthalpy of the liquid in the pressurizer	J/kg	
$h_v$	Specific enthalpy of the steam phase in the pressurizer	J/kg	
$h_{v,o}$	Specific enthalpy of the steam at the outlet of the pressurizer	J/kg	
$h_v^{\text{sat}}$	Saturation enthalpy of the steam in the pressurizer	J/kg	
$K_{lw}$	Convective heat exchange coefficient between the liquid and the wall of the pressurizer	W/m <sup>2</sup> /K	
$K_{vl}$	Convective heat exchange coefficient between the liquid and the steam in the pressurizer	W/m <sup>2</sup> /K	
$K_{vw}$	Convective heat exchange coefficient between the steam and the wall of the pressurizer	W/m <sup>2</sup> /K	
$K_{wa}$	Convective heat exchange coefficient between the wall of the pressurizer and the ambient	W/m <sup>2</sup> /K	
$\dot{m}_{\text{cond}}$	Condensation mass flow rate inside the pressurizer	kg/s	
$\dot{m}_{\text{evap}}$	Evaporation mass flow rate inside the pressurizer	kg/s	
$\dot{m}_{l,i}$	Mass flow rate of the liquid at the inlet of the pressurizer	kg/s	
$\dot{m}_{l,o}$	Mass flow rate of the liquid at the outlet of the pressurizer	kg/s	
$\dot{m}_v$	Mass flow rate of the steam at the outlet of the pressurizer	kg/s	
$M_w$	Mass of the wall of the pressurizer	kg	
$P$	Pressure inside the pressurizer	Pa	
$P_b$	Fluid pressure at the bottom of the pressurizer	Pa	$P + \frac{g}{A_p} \cdot (\rho_l \cdot V_l + \rho_v \cdot V_v)$
$R$	Pressurizer cross-sectional radius	m	
$T_a$	Ambient temperature	K	

(continued)

(continued)

Symbols	Definition	Unit	Mathematical definition
$T_l$	Liquid temperature in the pressurizer	K	
$T_v$	Steam temperature in the pressurizer	K	
$T_w$	Wall temperature of the pressurizer	K	
$V$	Pressurizer volume	$\text{m}^3$	
$V_l$	Volume of the liquid in the pressurizer	$\text{m}^3$	$A_p \cdot z_l$
$V_v$	Volume of the steam in the pressurizer	$\text{m}^3$	$V - V_l$
$W_{eh}$	Power released by the electrical heaters	W	
$W_{lw}$	Power exchanged from the liquid to the pressurizer wall	W	
$W_{vl}$	Power exchanged from the steam to the liquid	W	
$W_{vw}$	Power exchanged from the steam to the pressurizer wall	W	
$W_{wa}$	Power exchanged from the pressurizer wall to the ambient	W	
$y$	Liquid level expressed as a percent of the scale of level measure	%	$0 \leq y \leq 1$
$z_l$	Liquid level inside the pressurizer for the controller: water level + margin	m	$z_m \cdot y + \frac{\frac{V}{A_p} - z_m}{2}$
$z_m$	Scale of level measure	m	
$\rho_l$	Density of the liquid inside the pressurizer	$\text{kg}/\text{m}^3$	
$\rho_v$	Density of the steam inside the pressurizer	$\text{kg}/\text{m}^3$	

### 14.3.2 Assumptions

The pressurizer is modeled according to the following assumptions:

- There is always a water level inside the pressurizer: The pressurizer is always operating in two-phase conditions (there is no phase appearance or disappearance).
- Pressure losses are not taken into account in the pressurizer.
- The liquid and steam phases are not necessarily in thermal equilibrium.
- The liquid and steam phases are assumed to be always in pressure equilibrium.

### 14.3.3 Governing Equations

The *Pressurizer* component model represents the dynamic of the thermal hydraulic phenomena of the fluids inside the pressurizer. The physical model is based on a non-equilibrium two-phase formulation of the fluid balance equation. Also, the heat transfer between (1) the liquid phase and the steam phase, (2) the fluid and the wall, and (3) the pressurizer and the external medium (ambient environment) are considered in the model. The pressurizer cavity is considered as a vertical cylinder.

The state variables of the system are:

- The pressure inside the pressurizer;
- The specific enthalpy of the liquid phase;
- The specific enthalpy of the steam phase;
- The temperature of the wall;
- The volume of the liquid phase;
- The volume of the steam phase.

Equation 1

Title	Dynamic mass balance equation for the liquid phase
Validity domain	$\forall \dot{m}$ and $0 < V_l < V$
Mathematical formulation	$\rho_l \cdot \frac{dV_l}{dt} + V_l \left[ \left( \frac{\partial \rho_l}{\partial P} \right)_h \cdot \frac{dP}{dt} + \left( \frac{\partial \rho_l}{\partial h} \right)_p \cdot \frac{dh_l}{dt} \right]$ $= \dot{m}_{l,i} - \dot{m}_{l,o} + \dot{m}_{cond} - \dot{m}_{evap}$
Comments	<p>The derivation of this equation is similar to Eq. 1 of the dynamic modeling of a simple condenser (cf. Sect. 9.5.3.3)</p> <p>As</p> $V_l = A_p \cdot z_m \cdot y$ <p>the equation can be written as</p> $A_p \cdot z_m \cdot \left[ \rho_l \cdot \frac{dy}{dt} + y \cdot \left[ \left( \frac{\partial \rho_l}{\partial P} \right)_h \cdot \frac{dP}{dt} + \left( \frac{\partial \rho_l}{\partial h} \right)_p \cdot \frac{dh_l}{dt} \right] \right]$ $= \dot{m}_{l,i} - \dot{m}_{l,o} + \dot{m}_{cond} - \dot{m}_{evap}$

Equation 2

Title	Dynamic mass balance equation for the steam phase
Validity domain	$\forall \dot{m}$ and $0 < V_v < V$
Mathematical formulation	$\rho_v \cdot \frac{dV_v}{dt} + V_v \cdot \left[ \left( \frac{\partial \rho_v}{\partial P} \right)_h \cdot \frac{dP}{dt} + \left( \frac{\partial \rho_v}{\partial h} \right)_p \cdot \frac{dh_v}{dt} \right]$ $= \dot{m}_{evap} - \dot{m}_v - \dot{m}_{cond}$
Comments	The derivation of this equation is similar to Eq. 1 of the dynamic modeling of a simple condenser (cf. Sect. 9.5.3.3).

---

Equation 3

---

Title	Dynamic energy balance equation for the liquid phase
Validity domain	$\forall \dot{m}$ and $0 < V_l < V$
Mathematical formulation	$V_l \cdot \left( \rho_l \cdot \frac{dh_l}{dt} - \frac{dP}{dt} \right) = (\dot{m}_{l,i} + \dot{m}_{\text{cond}}) \cdot (h_l^{\text{sat}} - h_l)$ $- \dot{m}_{\text{evap}} \cdot (h_v^{\text{sat}} - h_l) - \dot{m}_{l,o} \cdot (h_{l,o} - h_l)$ $+ W_{vl} - W_{lw} + W_{eh}$
Comments	The derivation of this equation is similar to Eq. 3 of the dynamic modeling of a simple condenser (cf. Sect. 9.5.3.3), considering that the liquid is incompressible (the partial derivatives of the density are zero). Regarding the right-hand side of the equation, the term $\dot{m}_{l,i} \cdot (h_l^{\text{sat}} - h_l)$ accounts for the fact that the spray is first heated to saturated liquid by the contact with the steam inside the pressurizer (this phenomenon is accounted for in the energy balance equation for the steam phase; cf. Eq. 4), and then the saturated liquid is mixed with the liquid inside the pressurizer

---



---

Equation 4

---

Title	Dynamic energy balance equation for the steam phase
Validity domain	$\forall \dot{m}$ and $0 < V_v < V$
Mathematical formulation	$V_v \cdot \left( \rho_v \cdot \frac{dh_v}{dt} - \frac{dP}{dt} \right) = \dot{m}_{\text{evap}} \cdot (h_v^{\text{sat}} - h_v)$ $- \dot{m}_{\text{cond}} \cdot (h_l^{\text{sat}} - h_v) - \dot{m}_{l,i} \cdot (h_l^{\text{sat}} - h_{l,i})$ $- \dot{m}_v \cdot (h_{v,o} - h_v) - W_{vl} - W_{vw}$
Comments	The derivation of this equation is similar to Eq. 3 of the dynamic modeling of a simple condenser (cf. Sect. 9.5.3.3), considering that the liquid is incompressible (the partial derivatives of the density are zero). Regarding the right-hand side of the equation, the term $\dot{m}_{l,i} \cdot (h_l^{\text{sat}} - h_{l,i})$ accounts for the fact that the spray extracts heat from the steam inside the pressurizer to be heated to saturated liquid

---



---

Equation 5

---

Title	Energy accumulation in the wall
Validity domain	$\forall T_w$
Mathematical formulation	$M_w \cdot c_{p,w} \cdot \frac{dT_w}{dt} = W_{lw} + W_{vw} + W_{aw}$

---



---

Equation 6

---

Title	Power exchange between the steam phase and the liquid phase
Comments	$\forall T_v$ and $\forall T_l$
Mathematical formulation	$W_{vl} = K_{vl} \cdot A_p \cdot (T_v - T_l)$

---

Equation 7

---

Title	Power exchange between the liquid and the pressurizer wall
Comments	$\forall T_l$ and $\forall T_w$
Mathematical formulation	$W_{lw} = K_{lw} \cdot A_l \cdot (T_l - T_w)$

---

Equation 8

---

Title	Power exchange between the steam and the pressurizer wall
Comments	$\forall T_v$ and $\forall T_w$
Mathematical formulation	$W_{vw} = K_{vw} \cdot A_v \cdot (T_v - T_w)$

---

Equation 9

---

Title	Power exchange between the pressurizer wall and the ambient
Comments	$\forall T_w$ and $\forall T_a$
Mathematical formulation	$W_{wa} = K_{wa} \cdot A_e \cdot (T_w - T_a)$

---

Equation 10

---

Title	Condensation mass flow rate
Mathematical formulation	$\dot{m}_{cond} = C_{cond} \cdot \rho_v \cdot V_v \cdot \frac{h_v^{\text{sat}} - h_v}{h_v^{\text{sat}} - h_l^{\text{sat}}}$
Comments	Cf. (4.96a) where it is assumed that $x_{g,0} = 1$ and where $x_v = \frac{h_v - h_l^{\text{sat}}}{h_v^{\text{sat}} - h_l^{\text{sat}}} \quad (\text{cf. 4.48})$

---

Equation 11

---

Title	Evaporation mass flow rate
Mathematical formulation	$\dot{m}_{evap} = C_{evap} \cdot \rho_l \cdot V_l \cdot \frac{h_l - h_v^{\text{sat}}}{h_v^{\text{sat}} - h_l^{\text{sat}}}$
Comments	Cf. (4.96b) where it is assumed that $x_{l,0} = 0$ and where $x_l = \frac{h_l - h_v^{\text{sat}}}{h_v^{\text{sat}} - h_l^{\text{sat}}} \quad (\text{cf. 4.48}).$

---

This set of equations must be completed by the state equations for water/steam in order to have a complete system of equations that can be solved. The state equations are to be given for  $h_l^{\text{sat}}$ ,  $h_v^{\text{sat}}$ ,  $\rho_l$ , and  $\rho_v$ .

#### 14.3.4 Modelica Component Model: Pressurizer

The governing equations are implemented in the *Pressurizer* component model located in the *WaterSteam.Volumes* sub-library. Figure 14.8a represents the graphical icon of the component with its six connectors.

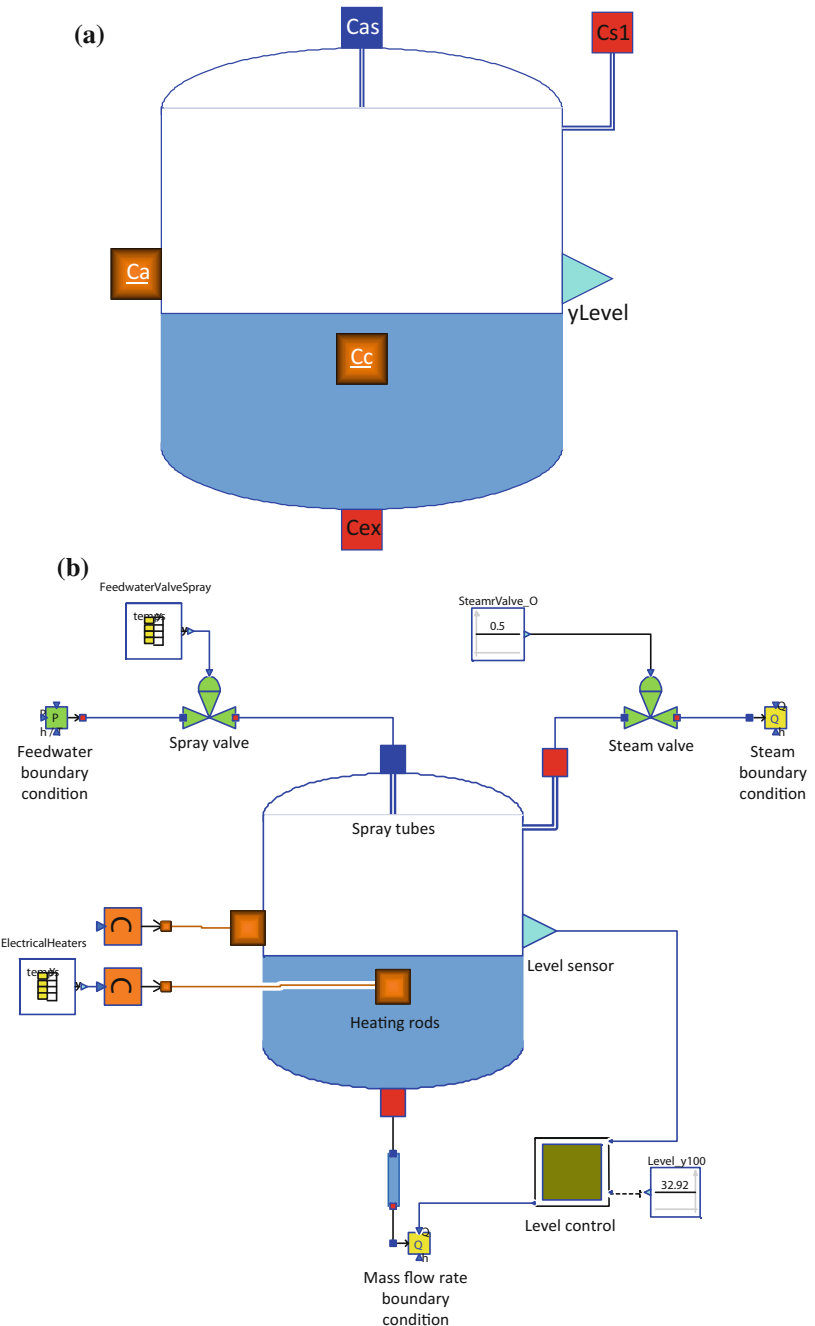


**Fig. 14.8** **a** Icon of the *Pressurizer* component model. **b** Test-case for the *Pressurizer* component model

### 14.3.5 Test-Case

The model *TestPressurizer* used to validate the *Pressurizer* component model is represented in Fig. 14.8b. It uses the following component models:

- One *Pressurizer* component model;
- Two *ControlValve* component models;
- Two *HeatSource* component models;
- One *LumpedStraightPipe* component model;
- One *SourceP* component model;
- Two *SinkQ* component models;
- Two *Constant* blocks;
- One *TimeTable* blocks;
- One *Drum\_LevelControl* block.

In this test-case scenario, the pressurizer component receives: (1) the water mass flow rate and specific enthalpy at the outlet, (2) the steam mass flow rate at the outlet, (3) the water pressure and specific enthalpy at the inlet, (4) the ambient temperature at the inlet, and (5) the power released by the electrical heaters. The component computes: (1) the pressurizer pressure, (2) the specific enthalpies of the fluids in the pressurizer (liquid and steam), (3) the wall temperature, and (4) the liquid level in the pressurizer.

#### 14.3.5.1 Test-Case Parameterization and Boundary Conditions

The model data are:

- Pressurizer volume =  $61.12 \text{ m}^3$
- Pressurizer cross-sectional radius = 1.27 m
- Height of the level measuring range = 10.15 m
- Initial water level as a percent of the measure scale = 60%
- Liquid water as a percent of the measure scale = 32.92%
- Pressurizer pressure =  $155 \times 10^5 \text{ Pa}$
- Length of the pipes (*lumpedStraightPipe*) = 1 m
- Pipe diameter (*lumpedStraightPipe*) = 1 m
- Inlet altitude of the pipes (*lumpedStraightPipe*) = 1 m
- Ambient temperature (*HeatSource*) = 310 K
- Fluid specific enthalpy at the feed water valve inlet =  $1270 \times 10^3 \text{ J/kg}$
- Fluid pressure at the inlet of the feed water valve =  $160 \times 10^5 \text{ Pa}$
- Steam mass flow rate at the outlet = 0
- Water mass flow rate at the outlet = 0
- Maximum flow coefficient of the steam valve = 5000 U.S.
- Maximum flow coefficient of the feed water valve = 5000 U.S.

### 14.3.5.2 Model Calibration

The calibration procedure consists in setting the pressurizer pressure and the liquid level in the pressurizer to known measurement values to compute by model inversion the inlet power released by the electrical heaters and the flow coefficient of the water control valve.

### 14.3.5.3 Simulation Results

The simulation of the test scenario led to the numerical results below:

- Water mass flow rate at the inlet of the feed water valve = 0.001 kg/s
- Feed water valve position (between 0 and 1) =  $2 \times 10^{-5}$
- Power released by the electrical heaters = 166,663 W.

Figure 14.9 shows the results of the simulation for a scenario that consists in the spurious opening of the spray valve (curve 1). This results in activating the electrical heating rods (curve 2), a decrease in the pressure inside the pressurizer (curve 4), and a swell and shrink of the water level (curve 5).

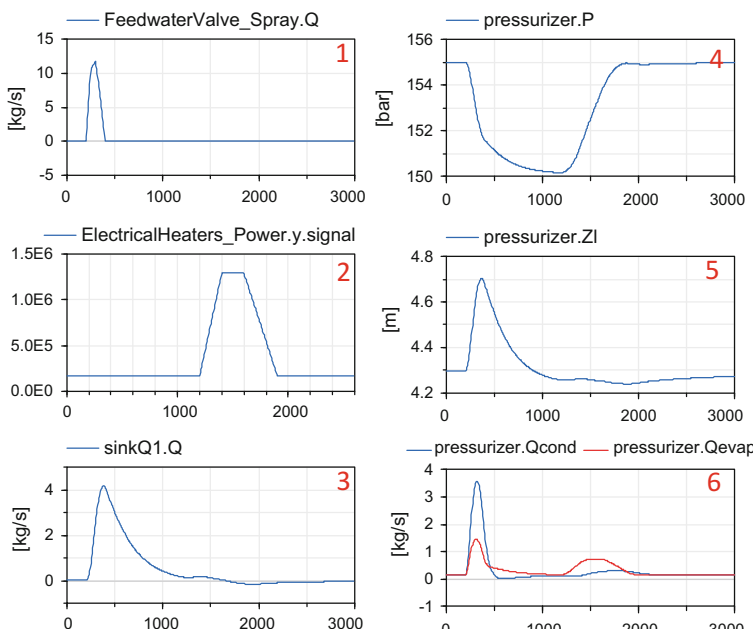


**Fig. 14.9** Simulation results for *Pressurizer*: (1) mass flow rate of the sprayed water, (2) power released by the electrical heating rods, (3) water mass flow rate at the outlet of the pressurizer, (4) pressure in the pressurizer, (5) water level in the pressurizer, and (6) condensation and evaporation mass flow rates inside the pressurizer

## 14.4 Two-Phase Cavity Modeling

The two-phase cavity is a reservoir used to separate the water from the steam in the water/steam mixture and store the separated phases; cf. Fig. 14.10.

The two-phase cavity component is modeled as a dynamic non-adiabatic two-phase volume, with vertical or horizontal cylindrical geometry. The physical model is based on a non-equilibrium two-phase formulation of the fluid balance equations. The two phases are assumed to be isobaric and are referred to as the liquid zone and the steam zone, respectively, in the sequel.

The model takes into account the condensation flow of the steam phase into the liquid phase and, reciprocally, the vaporization flow of the liquid phase into the steam phase.

The *TwoPhaseCavity* component is subdivided into two distinct zones: (1) the *desuperheating* and *condensation* zone located in the upper part of the component and (2) the *subcooled* zone located in the lower part of the component. It is used as a cavity for the *DynamicWaterHeating* model (two-phase shell-and-tube heat exchanger) for which four configurations of the model are possible.

The pipes inside the cavity are divided into three categories:

- The pipes drowned in the liquid, equal to half of the total length of the U-tubes partially immersed in water and partially immersed in steam, labeled Pipes 1 in Fig. 14.10a.
- The pipes immersed in steam, equal to half of the total length of the U-tubes partially immersed in water and partially immersed in steam, labeled Pipes 2 in Fig. 14.10a.
- The U-tubes completely immersed in steam, labeled Pipes 3 in Fig. 14.10a.

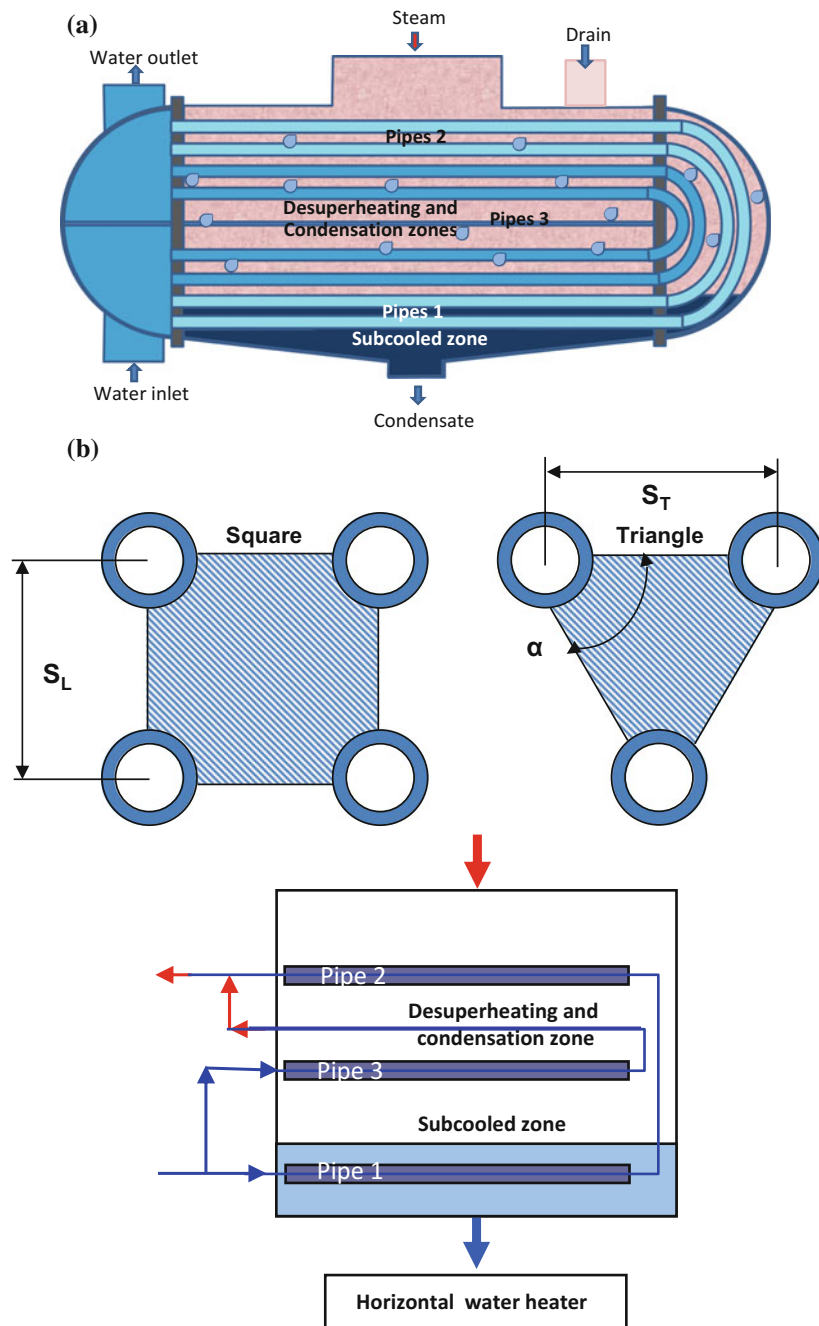


**Fig. 14.10** **a** Schematic diagram of a two-phase cavity. **b** Geometry of the tube bundle (square and triangular step) and heat exchanger zones inside a two-phase cavity

### 14.4.1 Nomenclature

Symbols	Definition	Unit	Mathematical definition
$A_l$	Cross-sectional area of the liquid phase in the cavity (cf. Fig. 14.4b)	$\text{m}^2$	For a vertical cavity: $\pi \cdot R^2$ For a horizontal cavity: $\left(\frac{\pi}{2} - \theta\right) \cdot R^2$ $- R \cdot \cos(\theta) \cdot (R - z_l)$
$A_{lw}$	Contact surface between the liquid phase and the cavity wall (cf. Fig. 14.4b)	$\text{m}^2$	For a vertical cavity: $2 \cdot \pi \cdot R \cdot z_l + A_l$ For a horizontal cavity: $(\pi - 2 \cdot \theta) \cdot R \cdot L + 2 \cdot A_l$
$A_{vl}$	Heat exchange surface between the vapor phase and the liquid phase (cf. Fig. 14.4b)	$\text{m}^2$	For a vertical cavity: $A_l$ For a horizontal cavity: $2 \cdot R \cdot L \cdot \cos(\theta)$
$A_{vw}$	Contact surface between the vapor phase and the cavity wall (cf. Fig. 14.4b)	$\text{m}^2$	For a vertical cavity: $2 \cdot \pi \cdot R \cdot (L - z_l) + A_l$ For a horizontal cavity: $(\pi + 2 \cdot \theta) \cdot R \cdot L$ $+ 2(\pi \cdot R^2 - A_l)$
$A_{wa}$	Internal cavity surface	$\text{m}^2$	$A_{vw} + A_{lw}$
$c_{p,l}$	Specific heat capacity of the liquid phase in the cavity	$\text{J/kg/K}$	
$c_{p,v}$	Specific heat capacity of the vapor phase in the cavity	$\text{J/kg/K}$	
$c_{p,w}$	Specific heat capacity of the cavity wall	$\text{J/kg/K}$	
$C_{cond}$	Condensation coefficient with inverse time	$\text{s}^{-1}$	
$C_{evap}$	Evaporation coefficient with inverse time	$\text{s}^{-1}$	
$\text{COP}_l$	Corrective term for the heat exchange coefficient for Pipes 1 (desuperheating zone)	-	
$\text{COP}_v$	Corrective term for the heat exchange coefficient for Pipes 2 and Pipes 3 (condensation and subcooled zones)	-	
$D_e$	Pipe external diameter, for one pipe	$\text{m}$	

(continued)

(continued)

Symbols	Definition	Unit	Mathematical definition
$D_h$	Cross-sectional equivalent diameter (Sacadura 1978), cf. Fig. 14.10b	m	For a square step: $\frac{4 \cdot S_L^2}{\pi \cdot D_e} - D_e$ For a triangular step: $\frac{2 \cdot S_L \cdot S_T}{\pi \cdot D_e \cdot \frac{z}{120}} - D_e$ or $\frac{3.464 \cdot S_L^2}{\pi \cdot D_e} - D_e$
$D_s$	Shell internal diameter	m	
$g$	Acceleration due to gravity	m/s <sup>2</sup>	
$h$	Specific enthalpy of the fluid in the cavity (liquid or vapor)	J/kg	
$h_{\text{cond}2,i}$	Convective coefficient of heat transfer by condensation between the vapor and the tube bundle for Pipes 2	W/m <sup>2</sup> /K	
$h_{\text{cond}3,i}$	Convective coefficient of heat transfer by condensation between the vapor and the tube bundle for Pipes 3	W/m <sup>2</sup> /K	
$h_{\text{conv}1,i}$	Convective coefficient of heat transfer between the condensate and the tube bundle for Pipes 1	W/m <sup>2</sup> /K	
$h_{\text{drain},i}$	Specific enthalpy at the drain inlet	J/kg	
$h_{fg}$	Latent energy at the cavity pressure	J/kg	
$h_l$	Specific enthalpy of the liquid phase in the cavity	J/kg	
$h_{l,\text{drain},i}$	Specific enthalpy of the liquid at the drain inlet	J/kg	
$h_{l,o}$	Specific enthalpy of the liquid at the outlet (outgoing condensate)	J/kg	
$h_l^{\text{sat}}$	Saturation enthalpy of the liquid in the cavity	J/kg	
$h_v$	Specific enthalpy of the vapor phase in the cavity	J/kg	
$h_{v,\text{drain},i}$	Specific enthalpy of the vapor at the drain inlet	J/kg	
$h_{v,i}$	Specific enthalpy of the steam at the inlet, coming from the steam turbine	J/kg	
$h_v^{\text{sat}}$	Saturation enthalpy of the vapor in the cavity	J/kg	
$K_{\text{corr}}$	Corrective term for the heat exchange coefficient between the liquid and the steam	-	

(continued)

(continued)

Symbols	Definition	Unit	Mathematical definition
$K_{lw}$	Convective heat exchange coefficient between the liquid and the wall	W/m <sup>2</sup> /K	
$K_{vl}$	Convective heat exchange coefficient between the liquid and the vapor in the cavity	W/m <sup>2</sup> /K	
$K_{vw}$	Convective heat exchange coefficient between the vapor and the wall	W/m <sup>2</sup> /K	
$K_{wa}$	Convective heat exchange coefficient between the wall and the ambient	W/m <sup>2</sup> /K	
$L$	Cavity length	m	
$L_t$	Total pipes length	m	
$L_1$	Total length of Pipes 1	m	
$L_2$	Total length of Pipes 2	m	$L_2 = L_1$
$L_3$	Total length of Pipes 3	m	
$L_c$	Distance between two plates in the shell (support plate spacing in the cooling zone)	m	
$N_t$	Number of pipes in a vertical row (tube bank)	-	
$N_1$	Number of Pipes 1	-	
$N_2$	Number of Pipes 2	-	
$N_3$	Number of Pipes 3	-	
$N_s$	Number of segments for Pipes 1 and Pipes 2	-	
$N_{s3}$	Number of segments for Pipes 3	-	$2 \cdot N_s$
$M_w$	Mass of the wall cavity	kg	
$\dot{m}_{l,o}$	Mass flow rate of the outgoing condensate	kg/s	
$\dot{m}_v$	Mass flow rate of the incoming vapor	kg/s	
$\dot{m}_{\text{drain},i}$	Mass flow rate at the drain inlet	kg/s	
$\dot{m}_{\text{cond}}$	Condensation mass flow rate inside the cavity	kg/s	
$\dot{m}_{\text{evap}}$	Evaporation mass flow rate inside the cavity	kg/s	
$P$	Cavity pressure	Pa	
$P_b$	Fluid pressure at the bottom of the cavity	Pa	$P + \rho_l \cdot g \cdot z_l$
$Pr_l$	Prandtl number of the liquid phase	-	$\frac{\mu_l \cdot c_{pl}}{\lambda_l}$
$Pr_v$	Prandtl number of the vapor phase	-	$\frac{\mu_v \cdot c_{pv}}{\lambda_v}$
$Q_s$	Surface mass flow rate in the shell	kg/s/m <sup>2</sup>	$\frac{\dot{m}_{l,o}}{D_s \cdot L_c \cdot \left( \frac{S_L - D_c}{S_L} \right)}$

(continued)

(continued)

Symbols	Definition	Unit	Mathematical definition
$R$	Radius of the cavity cross-sectional area	m	
$Re_l$	Reynolds number of the condensate flowing between the drowned tubes	-	$\frac{Q_s \cdot D_h}{\mu_l}$
$Re_{l,w}$	Reynolds number of the condensate flowing against cavity wall	-	
$Re_{v,l}$	Reynolds number of the vapor flowing against the free surface of the condensate	-	
$Re_{v,w}$	Reynolds number of the vapor flowing against the cavity wall	-	
$S_L$	Longitudinal step, cf. Fig. 14.10b	m	
$S_T$	Transverse step, cf. Fig. 14.10b	m	
$T_a$	Ambient temperature	K	
$T_l$	Liquid temperature in the cavity	K	
$T_w$	Wall temperature of the cavity	K	
$T_{w1,i}$	Wall temperature for Pipes 1	K	
$T_{w2,i}$	Wall temperature for Pipes 2	K	
$T_{w3,i}$	Wall temperature for Pipes 3	K	
$T_{sat}$	Saturation temperature in the cavity	K	
$T_v$	Vapor temperature in the cavity	K	
$u$	Fluid specific internal energy	J/kg	$h - \frac{P}{\rho}$
$V$	Volume of the cavity	$m^3$	$V_l + V_v$
$V_l$	Volume of the liquid phase in the cavity	$m^3$	$V_l = A_l \cdot z_l$
$V_v$	Volume of the vapor phase in the cavity	$m^3$	
$W_{1t}$	Total power exchanged from the liquid to Pipes 1	W	
$W_{2t}$	Total power exchanged from the vapor to Pipes 2	W	
$W_{3t}$	Total power exchanged from the vapor to Pipes 3	W	
$W_{4t}$	Total power exchanged for desuperheating of the steam	W	
$W_{vl}$	Power exchanged from the vapor to the liquid	W	
$W_{lw}$	Power exchanged from the liquid to the cavity wall	W	

(continued)

(continued)

Symbols	Definition	Unit	Mathematical definition
$W_{vv}$	Power exchanged from the vapor to the cavity wall	W	
$W_{aw}$	Power exchanged from the ambient environment to the cavity wall	W	
$x_v$	Vapor mass fraction in the vapor phase	-	
$X_{vo}$	Vapor mass fraction in the vapor phase from which the liquid starts to condensate	-	
$x_l$	Vapor mass fraction in the liquid phase	-	
$X_{lo}$	Vapor mass fraction in the liquid phase from which the liquid starts to evaporate	-	
$x_{mv}$	Vapor mass fraction at the inlet of the drain	-	
$z_l$	Liquid level in the cavity	m	$V_l/A_l$
$\alpha$	Average bend angle (pipes triangular step), cf. Fig. 14.10b	°	
$\lambda_l$	Thermal conductivity of the liquid	W/m/K	
$\lambda_v$	Thermal conductivity of the vapor	W/m/K	
$\Delta S_{ext1}$	Heat exchange surface for each segment of Pipes 1	$m^2$	$\pi.D_e.L_1.N_1/N_s$
$\Delta S_{ext2}$	Heat exchange surface for each segment of Pipes 2	$m^2$	$\pi.D_e.L_2.N_2/N_s$
$\Delta S_{ext3}$	Heat exchange surface for each segment of Pipes 3	$m^2$	$\pi.D_e.L_3.N_3/N_{s3}$
$\rho_l$	Density of the liquid in the cavity	kg/m <sup>3</sup>	
$\rho_v$	Density of the vapor in the cavity	kg/m <sup>3</sup>	
$\mu_l$	Dynamic viscosity of the liquid in the cavity	kg/(m s)	
$\mu_{lT}$	Dynamic viscosity of the liquid at the wall temperature	kg/(m s)	
$\mu_v$	Dynamic viscosity of the vapor in the cavity	kg/(m s)	
$\theta$	Chord angle of the liquid in the horizontal cavity, cf. Fig. 14.4b	rad	$\arcsin\left(\frac{R - z_l}{R}\right)$

#### 14.4.2 Assumptions

The two-phase cavity is modeled according to the following assumptions:

- Pressure losses are not taken into account in the cavity.
- The liquid and vapor phases are not necessarily in thermal equilibrium.

- The liquid and vapor phases are assumed to be always in pressure equilibrium.

In some operating conditions, the liquid and the vapor phases in the cavity are not necessarily in thermal equilibrium for the following reasons:

- The vapor may enter the cavity superheated (the vapor temperature is then higher than the saturation temperature).
- The liquid can be subcooled by the incoming drain and the wetted tube bundle (the liquid temperature is then lower than the saturation temperature).

### 14.4.3 Governing Equations

The *TwoPhaseCavity* component represents the dynamics of the thermal hydraulic phenomena of the fluids inside the cavity. In particular, the model takes into account the thermal exchanges between the fluid in the cavity and the cooling fluid flowing through the tube bundle. Also, the heat transfer between (1) the liquid phase and vapor phase, (2) the fluid and the wall, and (3) the cavity and the external medium (ambient environment) is considered in the model. The cavity is considered as a vertical or horizontal cylinder.

The state variables of the system are:

- The average pressure in the cavity;
- The specific enthalpy of the liquid phase;
- The specific enthalpy of the vapor phase;
- The temperature of the wall;
- The volume of the liquid phase;
- The volume of the vapor phase.

Equation 1

Title	Dynamic mass balance equation for the liquid phase
Validity domain	$\forall \dot{m}$ and $0 < V_l < V$
Mathematical formulation	$\rho_l \frac{dV_l}{dt} + V_l \cdot \left[ \left( \frac{\partial \rho_l}{\partial P} \right)_h \cdot \frac{dP}{dt} + \left( \frac{\partial \rho_l}{\partial h} \right)_p \cdot \frac{dh_l}{dt} \right]$ $= -\dot{m}_{l,o} + (1 - x_{mv}) \cdot \dot{m}_{drain,i} + \dot{m}_{cond} - \dot{m}_{evap}$
Comments	The derivation of this equation is similar to Eq. 1 of the dynamic modeling of a simple condenser (cf. Sect. 9.5.3.3)

Equation 2

Title	Dynamic mass balance equation for the steam phase
Validity domain	$\forall \dot{m}$ and $0 < V_v < V$
Mathematical formulation	$\rho_v \cdot \frac{dV_v}{dt} + V_v \cdot \left[ \left( \frac{\partial \rho_v}{\partial P} \right)_h \cdot \frac{dP}{dt} + \left( \frac{\partial \rho_v}{\partial h} \right)_p \cdot \frac{dh_v}{dt} \right]$ $= \dot{m}_v + x_{mv} \cdot \dot{m}_{drain,i} + \dot{m}_{evap} - \dot{m}_{cond}$
Comments	The derivation of this equation is similar to Eq. 1 of the dynamic modeling of a simple condenser (cf. Sect. 9.5.3.3)

**Equation 3**

Title	Dynamic energy balance equation for the liquid phase
Validity domain	$\forall \dot{m}$ and $0 < V_l < V$
Mathematical formulation	$V_l \cdot \left[ \left( \frac{P}{\rho_l} \cdot \left( \frac{\partial \rho_l}{\partial P} \right)_h - 1 \right) \cdot \frac{dP}{dt} + \left( \frac{P}{\rho_l} \cdot \left( \frac{\partial \rho_l}{\partial h_l} \right)_P + \rho_l \right) \cdot \frac{dh_l}{dt} \right]$ $= -\dot{m}_{l,o} \cdot \left( h_{l,o} - \left( h_l - \frac{P}{\rho_l} \right) \right) + \dot{m}_{cond} \cdot \left( h_l^{sat} - \left( h_l - \frac{P}{\rho_l} \right) \right)$ $- \dot{m}_{evap} \cdot \left( h_v^{sat} - \left( h_l - \frac{P}{\rho_l} \right) \right)$ $+ (1 - x_{mv}) \cdot \dot{m}_{drain,i} \cdot \left( h_{l,drain,i} - \left( h_l - \frac{P}{\rho_l} \right) \right) + W_{vl} - W_{lw} - W_{lt}$
Comments	<p>The derivation of this equation is similar to Eq. 3 of the dynamic modeling of a simple condenser (cf. Sect. 9.5.3.3)</p> <p>The value of <math>h_{l,drain,i}</math> is given by:</p> $h_{l,drain,i} = \begin{cases} h_{drain,i} & \text{for } x_{mv} = 0 \\ h_l^{sat} & \text{for } x_{mv} > 0 \end{cases}$

**Equation 4**

Title	Dynamic energy balance equation for the vapor phase
Validity domain	$\forall \dot{m}$ and $0 < V_v < V$
Mathematical formulation	$V_v \cdot \left[ \left( \frac{P}{\rho_v} \cdot \left( \frac{\partial \rho_v}{\partial P} \right)_h - 1 \right) \cdot \frac{dP}{dt} + \left( \frac{P}{\rho_v} \cdot \left( \frac{\partial \rho_v}{\partial h_v} \right)_P + \rho_v \right) \cdot \frac{dh_v}{dt} \right]$ $= \dot{m}_v \cdot \left( h_{v,i} - \left( h_v - \frac{P}{\rho_v} \right) \right) - \dot{m}_{cond} \cdot \left( h_l^{sat} - \left( h_v - \frac{P}{\rho_v} \right) \right)$ $+ \dot{m}_{evap} \cdot \left( h_v^{sat} - \left( h_v - \frac{P}{\rho_v} \right) \right)$ $+ x_{mv} \cdot \dot{m}_{drain,i} \cdot \left( h_{v,drain,i} - \left( h_v - \frac{P}{\rho_v} \right) \right)$ $- W_{vl} - W_{vw} - W_{2t} - W_{3t} - W_{4t}$
Comments	<p>The derivation of this equation is similar to Eq. 3 of the dynamic modeling of a simple condenser (cf. Sect. 9.5.3.3)</p> <p>The value of <math>h_{v,drain,i}</math> is given by:</p> $h_{v,drain,i} = \begin{cases} h_{drain,i} & \text{for } x_{mv} = 1 \\ h_v^{sat} & \text{for } x_{mv} < 1 \end{cases}$

**Equation 5**

Title	Energy accumulation in the wall
Validity domain	$T_w <$ melting temperature of the tubes metal
Mathematical formulation	$M_w \cdot c_{p,w} \cdot \frac{dT_w}{dt} = W_{lw} + W_{vw} + W_{aw}$

**Equation 6**

Title	Power exchanged from the liquid to Pipes 1 (subcooled)
Validity domain	$\forall T_l$ and $\forall T_{w1,i}$
Mathematical formulation	$W_{lt} = \Delta S_{ext1} \cdot \sum_{i=1}^{N_s} h_{conv1,i} \cdot (T_l - T_{w1,i})$
Comments	The power is exchanged by convection from the liquid to the pipes

**Equation 7**

Title	Power exchanged from the vapor to Pipes 2
Validity domain	$\forall T_v$ and $\forall T_{w2,i}$
Mathematical formulation	$W_{2t} = \Delta S_{ext2} \cdot \sum_{i=1}^{N_s} h_{cond2,i} \cdot (T_v - T_{w2,i})$
Comments	The power is exchanged by convection from the vapor to the pipes

**Equation 8**

Title	Power exchanged from the vapor to Pipes 3
Validity domain	$\forall T_v$ and $\forall T_{w3,i}$
Mathematical formulation	$W_{3t} = \Delta S_{ext3} \cdot \sum_{i=1}^{N_s} h_{cond3,i} \cdot (T_v - T_{w3,i})$
Comments	The power is exchanged by convection from the vapor to the pipes

**Equation 9**

Title	Power exchanged for desuperheating of the vapor
Validity domain	$\forall \dot{m}_v$
Mathematical formulation	$W_{4t} = \begin{cases} \dot{m}_v \cdot (h_{v,i} - h_v^{\text{sat}}) & \text{for } h_{v,i} > h_v^{\text{sat}} \\ 0 & \text{for } h_{v,i} < h_v^{\text{sat}} \end{cases}$
Comments	The power is exchanged from the vapor to the pipes

**Equation 10**

Title	Power exchanged from the vapor to the liquid
Validity domain	$\forall T_v$ and $\forall T_l$
Mathematical formulation	$W_{vl} = K_{vl} \cdot A_p \cdot (T_v - T_l)$
Comments	<p>The power is exchanged by convection from the vapor to the liquid at the interface between the two phases</p> <p>The coefficient <math>K_{vl}</math> can be computed with the following correlation (Attalla 2013):</p> $K_{vl} = K_{corr} \cdot 0.105 \cdot \lambda_v \cdot Re_{v,l}^{0.68} \cdot Pr_v^{0.333} \cdot \frac{1}{2,R} \cdot \left(\frac{L}{2,R}\right)^{-0.103}$ <p><math>Re_{v,l}</math> is the Reynolds number of the remaining steam after condensation flowing against the condensate free surface. <math>Re_{v,l}</math> is difficult to assess, but assuming that the hydraulic diameter is equal to the cavity diameter <math>2 \cdot R</math>, one can take the following value:</p> $Re_{v,l} = \frac{2 \cdot \dot{m}_v}{\pi \cdot R \cdot \mu_v}$

**Equation 11**

Title	Power exchanged from the liquid to the cavity wall
Validity domain	$\forall T_l$ and $\forall T_w$
Mathematical formulation	$W_{lw} = K_{lw} \cdot A_l \cdot (T_l - T_w)$
Comments	<p>The power is exchanged by convection from the liquid to the cavity wall</p> <p>The coefficient <math>K_{lw}</math> can be computed by the Von Karman correlation (Sacadura 1978):</p> $K_{lw} = 0.0366 \cdot \frac{\lambda_l}{z_l} \cdot Re_{l,w}^{0.8} \cdot Pr_l^{0.333}$ <p><math>Re_{l,w}</math> is the Reynolds number of the condensate flowing against the cavity wall:</p> $Re_{l,w} = \frac{\dot{m}_{l,o} \cdot z_l}{\pi \cdot R^2 \cdot \mu_l}$

**Equation 12**

Title	Power exchanged from the vapor to the cavity wall
Validity domain	$\forall T_v$ and $\forall T_w$
Mathematical formulation	$W_{vw} = K_{vw} \cdot A_v \cdot (T_v - T_w)$
Comments	<p>The power is exchanged by convection from the vapor to the cavity wall</p> <p>The coefficient <math>K_{vw}</math> can be computed by the Von Karman correlation (Sacadura 1978):</p> $K_{vw} = 0.0366 \cdot \frac{\lambda_v}{L - z_l} \cdot Re_{v,w}^{0.8} \cdot Pr_v^{0.333}$ <p><math>Re_{v,w}</math> is the Reynolds number of the steam flowing against the cavity wall:</p> $Re_{v,w} = \frac{\dot{m}_v \cdot (L - z_l)}{\pi \cdot R^2 \cdot \mu_v}$

**Equation 13**

Title	Power exchanged from the ambient to the cavity wall
Validity domain	$\forall T_a$ and $\forall T_w$
Mathematical formulation	$W_{aw} = K_{aw} \cdot A_e \cdot (T_a - T_w)$
Comments	The power is exchanged by convection from the ambient to the cavity wall

**Equation 14**

Title	Condensation mass flow rate
Validity domain	$\forall x_v$ close to $X_{vo}$
Mathematical formulation	$\dot{m}_{cond} = \max(C_{cond} \cdot \rho_v \cdot V_v \cdot (X_{vo} - x_v), 0)$
Comments	Cf. (4.96a)

Equation 15

Title	Evaporation mass flow rate
Validity domain	$\forall x_l$ close to $X_{lo}$
Mathematical formulation	$\dot{m}_{evap} = \max(C_{evap} \cdot \rho_l \cdot V_l \cdot (x_l - X_{lo}), 0)$
Comments	Cf. (4.96b)

Equation 16

Title	Convective heat transfer coefficient in zone 1 corresponding to the drowned tubes
Validity domain	$100 < Re_l < 10^6$
Mathematical formulation	$h_{conv1} = \frac{\lambda_l}{D_e} \cdot 0.36 \cdot COP_l \cdot Re_l^{0.55} \cdot Pr_l^{0.33} \cdot \left(\frac{\mu_l}{\mu_{IT}}\right)^{0.14}$
Comments	This equation uses the correlation from Sacadura (1978)

Equation 17

Title	Convective heat transfer coefficient in zones 2 and 3 corresponding to the condensation zone
Mathematical formulation	$h_{cond2} = \begin{cases} 1, 13.COPv \cdot \left[ \frac{g \cdot \rho_l (\rho_l - \rho_v) \lambda_l^3 \cdot h_{fg}}{L_2 \cdot \mu_l (T_{sat} - T_{w2})} \right]^{0.25} & \text{vertical cavity} \\ 0, 728.COPv \cdot \left[ \frac{g \cdot \rho_l (\rho_l - \rho_v) \lambda_l^3 \cdot h_{fg}}{Nt_n \cdot \mu_l (T_{sat} - T_{w2}) D_e} \right]^{0.25} & \text{horizontal cavity} \end{cases}$ $h_{cond3} = \begin{cases} 1, 13.COPv \cdot \left[ \frac{g \cdot \rho_l (\rho_l - \rho_v) \lambda_l^3 \cdot h_{fg}}{L_3 \cdot \mu_l (T_{sat} - T_{w3})} \right]^{0.25} & \text{vertical cavity} \\ 0, 728.COPv \cdot \left[ \frac{g \cdot \rho_l (\rho_l - \rho_v) \lambda_l^3 \cdot h_{fg}}{Nt_n \cdot \mu_l (T_{sat} - T_{w3}) D_e} \right]^{0.25} & \text{horizontal cavity} \end{cases}$
Comments	This equation uses the correlation from (Incropera et al. 2006)

This set of equations must be completed by the state equations for water and steam in order to have a complete system of equations that can be solved. The state equations are to be given for  $h_l^{sat}$ ,  $h_v^{sat}$ ,  $\rho_l$ ,  $\rho_v$ , and  $x_{mv}$ .

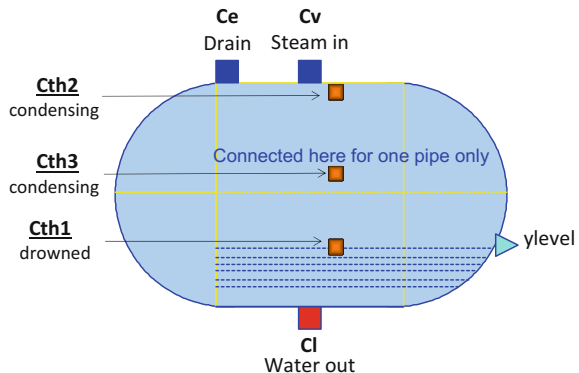
#### 14.4.4 Modelica Component Model: TwoPhaseCavity

The governing equations are implemented in the *TwoPhaseCavity* component model located in the *WaterSteam.Volumes* sub-library. Figure 14.11 represents the graphical icon of the component with its seven connectors.

#### 14.4.5 Test-Case

See §9.5.2.2 where the *TwoPhaseCavity* component model is utilized in the *DynamicWaterHeater* component model.

**Fig. 14.11** Icon of the *TwoPhaseCavity* component model



## 14.5 Tank Modeling

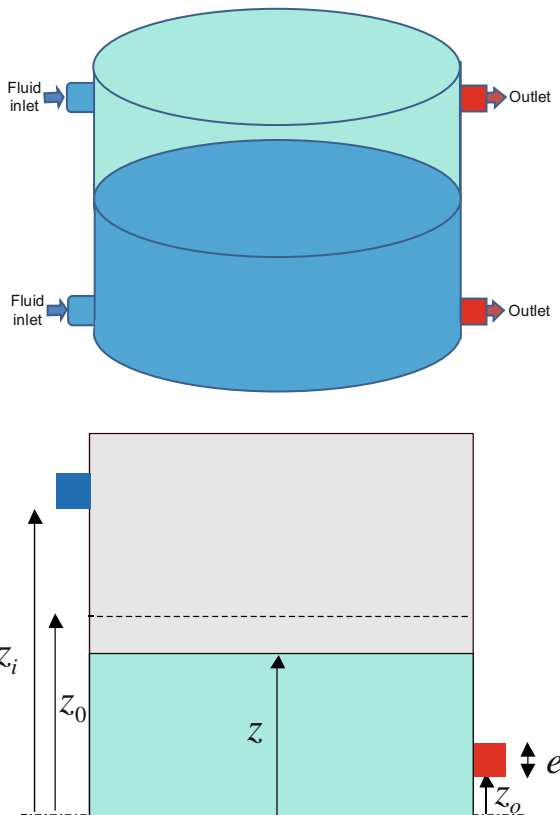
The tank is a reservoir that contains water. It is modeled as an open volume with a constant sky pressure; cf. Fig. 14.12. The reservoir is assumed to be a vertical cylinder (with a constant horizontal section). The tank models the mass and energy mixing of the input flows and a possible thermal exchange with the environment. Overflow through the orifices is taken into account.

### 14.5.1 Nomenclature

Symbols	Definition	Unit	Mathematical definition
$a_i$	Cross-sectional area of inlet i	m	
$a_o$	Cross-sectional area of outlet o	m	
$A$	Cross-sectional area of the liquid in the tank	$\text{m}^2$	
$h$	Specific enthalpy of the liquid in the tank	J/kg	
$h_i$	Specific enthalpy of the liquid at inlet i	J/kg	
$h_o$	Specific enthalpy of the liquid at outlet o	J/kg	
$\dot{m}_i$	Mass flow rate of the liquid at inlet i	kg/s	
$\dot{m}_o$	Mass flow rate of the liquid at outlet o	kg/s	

(continued)

**Fig. 14.12** Schematic diagram of a tank



(continued)

Symbols	Definition	Unit	Mathematical definition
$P$	Liquid average pressure in the tank	Pa	$P_{atm} + \rho.g.z/2$
$P_{atm}$	Pressure above the fluid level (sky pressure)	Pa	
$P_i$	Pressure of the liquid at inlet i	Pa	
$P_o$	Pressure of the liquid at outlet o	Pa	
$W$	Thermal power exchanged between the fluid and the heat source	W	
$z$	Liquid level in the tank	m	
$z_i$	Altitude of inlet i	m	
$z_o$	Altitude of outlet o	m	
$\xi_i$	Pressure loss coefficient for inlet i	-	
$\xi_o$	Pressure loss coefficient for outlet o	-	
$\rho$	Liquid density in the tank	kg/m <sup>3</sup>	

### 14.5.2 Governing Equations

The model of the fluid flow in the *Tank* component is based on the dynamic mass and energy balance equations. The model is formulated in order to correctly handle possible flow reversal conditions through the orifices.

The side effects corresponding to overflow through the orifices are supported: Outgoing flow can pass through an orifice only if its altitude is above the orifice. To that end, the orifice is represented as a variable pressure loss similar to a valve.

The state variables of the system are:

- The liquid level in the tank;
- The specific enthalpy of the fluid.

Equation 1

Title	Dynamic mass balance equation
Validity domain	$\forall \dot{m}$ and $z > 0$
Mathematical formulation	$\rho \cdot A \cdot \frac{dz}{dt} = \sum_i \dot{m}_i - \sum_o \dot{m}_o$
Comments	This equation derives from (4.7) assuming that the fluid is incompressible (i.e., the partial derivatives of the density are zero), the mass of fluid inside the tank being $M = \rho \cdot A \cdot z$

Equation 2

Title	Dynamic energy balance equation
Validity domain	$\forall \dot{m}$ and $z > 0$
Mathematical formulation	$\rho \cdot A \cdot z \cdot \frac{dh}{dt} = \sum_i \dot{m}_i \cdot (h_i - h) + \sum_o \dot{m}_o \cdot (h_o - h) + W$
Comments	<p>From (4.28) assuming that the fluid is incompressible (i.e., the partial derivatives of the density are zero) and neglecting diffusion, the energy balance equation writes:</p> $\rho \cdot \frac{d(A \cdot z \cdot u)}{dt} = \sum_i \dot{m}_i \cdot h_i + \sum_o \dot{m}_o \cdot h_o + W \quad (1)$ <p>The differential term can be developed using the mass balance equation (cf. Eq. 1):</p> $\begin{aligned} \rho \cdot \frac{d(A \cdot z \cdot u)}{dt} &= \rho \cdot A \cdot z \cdot \frac{du}{dt} + \rho \cdot A \cdot \frac{dz}{dt} \cdot u \\ &= \rho \cdot A \cdot z \cdot \frac{du}{dt} + \left( \sum_i \dot{m}_i - \sum_o \dot{m}_o \right) \cdot u \quad (2) \\ &\approx \rho \cdot A \cdot z \cdot \frac{dh}{dt} + \left( \sum_i \dot{m}_i - \sum_o \dot{m}_o \right) \cdot h \end{aligned}$ <p>because <math>\frac{\rho}{\rho} \ll u</math> for liquid water at ambient pressure.</p> <p>Combining (1) with (2) yields Eq. 2.</p>

Equation 3

Title	Pressure losses at the inlets
Validity domain	$\forall \dot{m}_i$
Mathematical formulation	$\Delta P_i \cdot \Omega_i^2 = \frac{1}{2} \cdot \xi_i \cdot \frac{\dot{m}_i \cdot  \dot{m}_i }{\rho \cdot a_i^2}$ with $\Delta P_i = P_i - (P_{atm} + \rho \cdot g \cdot \max(z - z_i, 0))$
Comments	<p>The orifice (i.e., the junction between the tube and the tank) is modeled as a singular pressure loss; cf. (13.18) that varies with the level of water:</p> $\Delta P_i = \frac{1}{2} \cdot \xi_i \cdot \frac{\dot{m}_i \cdot  \dot{m}_i }{\rho \cdot (\Omega_i \cdot a_i)^2}$ <p>where <math>\Omega_i</math> is the ratio between the cross-sectional area of the flow through the orifice and the cross-sectional of the tube to or from the orifice. <math>\Omega_i = 0</math> when the orifice is empty and <math>\Omega_i = 1</math> when the orifice is full.</p> <p>When <math>\dot{m}_i \geq 0</math> (direct flow), then <math>\Omega_i = 1</math>. This means that the tube is always full when the fluid is entering the tank. Assuming uniform distribution of the flow velocity at the inlet, the pressure loss coefficient can be taken equal to unity (cf. Idel'Cik 1986): <math>\xi_i = 1</math>.</p> <p>When <math>\dot{m}_i &lt; 0</math> (backflow), i.e., when the overflowing fluid is leaving the tank, <math>\Omega_i</math> depends on the level of water w. r. t. the orifice.</p> <p>For a circular orifice of diameter <math>d_i</math>:</p> $\Omega_i = \begin{cases} 0 & \text{for } z \leq z_i - \frac{d_i}{2} \\ 1 & \text{for } z \geq z_i + \frac{d_i}{2} \\ \frac{\pi + 2 \cdot \theta_i + \sin(2 \cdot \theta_i)}{2 \cdot \pi} & \text{for } z_i - \frac{d_i}{2} \leq z \leq z_i + \frac{d_i}{2} \end{cases}$ <p>with <math>\theta_i = \arcsin((z - z_i)/d_i/2)</math>.</p> <p>For a square orifice of side <math>d_i</math>:</p> $\Omega_i = \begin{cases} 0 & \text{for } z \leq z_i - \frac{d_i}{2} \\ 1 & \text{for } z \geq z_i + \frac{d_i}{2} \\ \frac{z - z_i + d_i/2}{d_i} & \text{for } z_i - \frac{d_i}{2} \leq z \leq z_i + \frac{d_i}{2} \end{cases}$ <p>The value of <math>\xi_i</math> depends on the geometry of the junction. If the junction is not protruding inside the tank, then one can take <math>\xi_i = 0.5</math>; cf. (Idel'Cik 1986).</p>

Equation 4

Title	Pressure losses at the outlets
Validity domain	$\forall \dot{m}_o$
Mathematical formulation	$\Delta P_o \cdot \Omega_o^2 = \frac{1}{2} \cdot \xi_o \cdot \frac{\dot{m}_o \cdot  \dot{m}_o }{\rho \cdot a_o^2}$ with $\Delta P_o = P_{atm} + \rho \cdot g \cdot \max(z - z_o, 0) - P_o$
Comments	Comments are similar to Eq. 3 except that the flow is leaving the tank when $\dot{m}_o > 0$ .

### 14.5.3 Modelica Component Model: Tank

The governing equations are implemented in the *Tank* component model located in the *WaterSteam.Volumes* sub-library. Figure 14.13a represents the graphical icon of the component with its six connectors.

### 14.5.4 Test-Case

The model *TestTank* used to validate the *Tank* component model is represented in Fig. 14.13b. It uses the following component models:

- One *Tank* component model;
- One *ControlValve* component model;
- Two *LumpedStraightPipe* component models;
- One *Ramp* block;
- One *SourceP* component model;
- Two *SinkP* component models.

In this test-case scenario, the *Tank* component receives: (1) the liquid pressure and temperature at the inlet and (2) the fluid pressure at the outlet. The component computes: (1) the liquid specific enthalpy in the tank, (2) the liquid pressure in the tank, (3) the upstream liquid pressure at the inlet, (4) the downstream liquid pressure at the outlet, and (5) the liquid level in the tank.

#### 14.5.4.1 Test-Case Parameterization and Boundary Conditions

The model data are:

- Tank cross-sectional area = 1 m<sup>2</sup>
- Fluid specific enthalpy in the tank = 10<sup>5</sup> J/kg
- Pressure above the level in the tank = 10<sup>5</sup> Pa
- Altitude of inlet 1 (tank) = 40 m
- Altitude of outlet 1 (tank) = 40 m
- Initial liquid level in the tank = 30 m
- Fluid specific enthalpy at the inlet of the control valve = 10<sup>5</sup> J/kg
- Fluid pressure at the inlet of the control valve = 3 10<sup>5</sup> Pa
- Pipe diameter = 0.2 m
- Pipe length = 10 m
- Inlet and outlet altitude of the pipe = 0
- Friction pressure loss coefficient of the pipe = 0.03
- Maximum flow coefficient of the control valve = 8005.42 U.S.

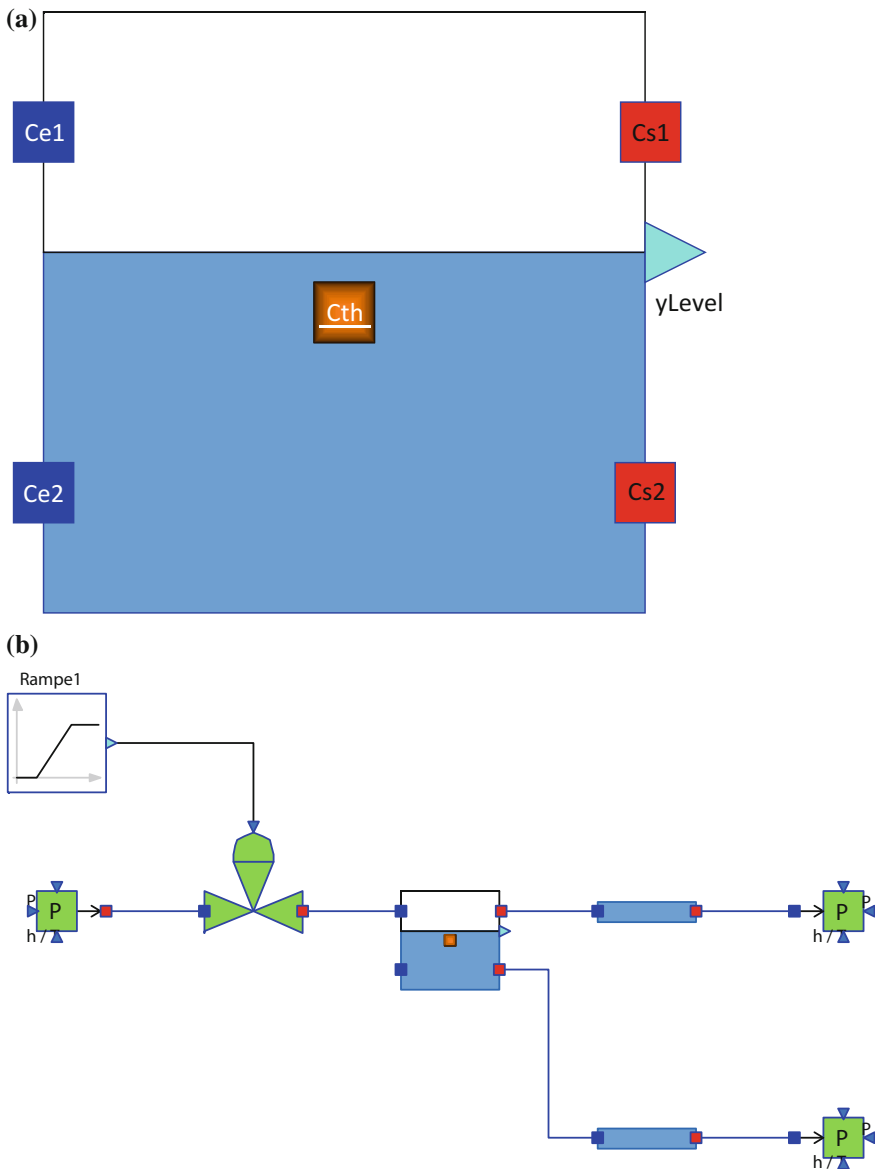


Fig. 14.13 a Icon of the *Tank* component model. b Test-case for the *Tank* component model

#### 14.5.4.2 Model Calibration

The calibration procedure consists in setting the fluid mass flow rate going through the valve and the fluid mass flow rate going through the pipe to known measurement values to compute by model inversion the values of the maximum flow coefficient of the valve and the friction pressure loss coefficient of the pipe.

#### 14.5.4.3 Simulation Results

Figure 14.14 shows the simulation results for a scenario that consists in opening the valve (curve 1). Curves 2, 3, and 4 show, respectively, the mass flow rates at inlet 1 and at outlets 1 and 2. It will be noted that the mass flow rate at outlet 1 of the tank (curve 3) is zero for about 8 s because the level in the tank (curve 8) has not reached the altitude of outlet 1.

### 14.6 Static Drum Modeling

The static drum is a reservoir of steam and water at the top end of the boiler. It is used to separate the water from the steam in the water/steam mixture generated in the boiler and to store both separated fluids; see Fig. 14.15.

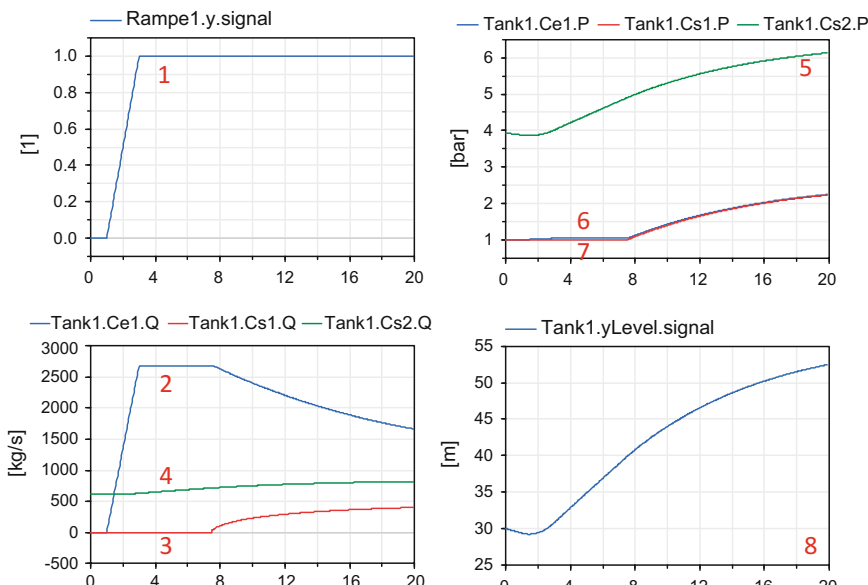


**Fig. 14.14** Simulation results for *Tank*: (1) position of the valve (between 0 and 1), (2) mass flow rate at the inlet, (3) mass flow rate at outlet 1, (4) mass flow rate at outlet 2, (5) pressure at outlet 2, (6) pressure at the inlet, (7) pressure at outlet 1, and (8) liquid level in the tank

The *StaticDrum* component is modeled as a volume. The physical model is based on the mass and energy balance equations.

This component can also be used as a simple steam generator.

### 14.6.1 Nomenclature

Symbols	Definition	Unit	Mathematical definition
$h_{\text{eco},i}$	Specific enthalpy of the liquid at the inlet of the drum, coming from the economizer	J/kg	
$h_{\text{eva},i}$	Specific enthalpy of the fluid at the inlet of the drum, coming from the evaporator	J/kg	
$h_{\text{steam},i}$	Specific enthalpy of the steam at the inlet	J/kg	
$h_{\text{sup},i}$	Specific enthalpy of the fluid at the inlet	J/kg	

(continued)

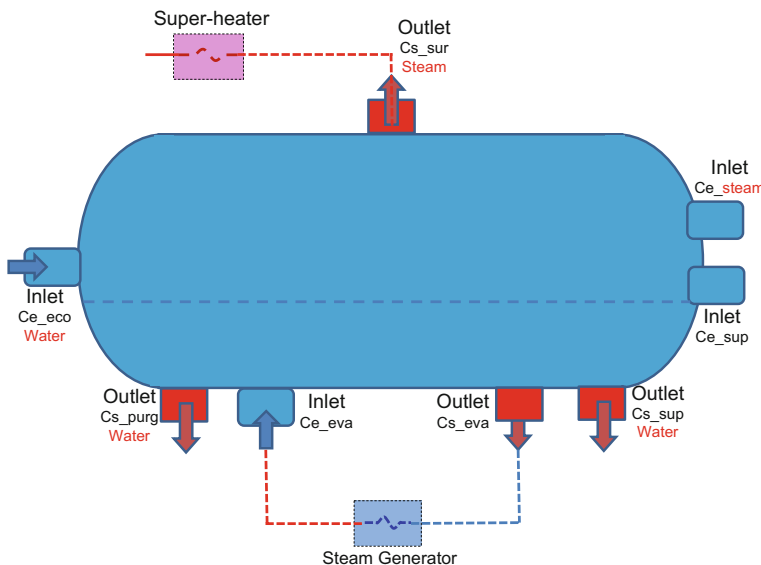


Fig. 14.15 Schematic diagram of a drum

(continued)

Symbols	Definition	Unit	Mathematical definition
$h_{\text{drain},o}$	Specific enthalpy of the liquid at the outlet, going to the drain	J/kg	
$h_{\text{eva},o}$	Specific enthalpy of the fluid at the outlet, going to the evaporator	J/kg	
$h_{\text{sup},o}$	Specific enthalpy of the liquid at the outlet	J/kg	
$h_{\text{sur},o}$	Specific enthalpy of the steam at the outlet, going to the super-heater	J/kg	
$\dot{m}_{\text{drain},o}$	Mass flow rate of the liquid at the outlet, going to the drain	kg/s	
$\dot{m}_{\text{eco},i}$	Mass flow rate of the fluid at the inlet, coming from the economizer	kg/s	
$\dot{m}_{\text{eva},i}$	Mass flow rate of the fluid at the inlet, coming from the evaporator	kg/s	
$\dot{m}_{\text{eva},o}$	Mass flow rate of the liquid at the outlet, going to the evaporator	kg/s	
$\dot{m}_{\text{steam},i}$	Mass flow rate of the steam at the inlet	kg/s	
$\dot{m}_{\text{sup},i}$	Mass flow rate of the fluid at the inlet	kg/s	
$\dot{m}_{\text{sup},o}$	Mass flow rate of the liquid at the outlet	kg/s	
$\dot{m}_{\text{sur},o}$	Mass flow rate of the steam at the outlet, going to the super-heater	kg/s	
$W$	Thermal power exchanged from the heat source to the fluid	W	
$x$	Steam mass fraction at the outlet going to the super-heater (steam separation efficiency)	–	

### 14.6.2 Assumptions

The static drum is modeled according to the following assumptions:

- Heat exchange between the liquid and steam phases is neglected.
- Heat exchange between the drum and the external medium is neglected.
- Pressure losses are not taken into account.

### 14.6.3 Governing Equations

The *StaticDrum* model is based on the static mass and energy balance equations.

Equation 1	
Title	Static mass balance equation
Validity domain	$\forall \dot{m}$
Mathematical formulation	$0 = \dot{m}_{\text{eco},i} + \dot{m}_{\text{eva},i} + \dot{m}_{\text{sup},i} + \dot{m}_{\text{steam},i}$ $- \dot{m}_{\text{drain},o} - \dot{m}_{\text{eva},o} - \dot{m}_{\text{sup},o} - \dot{m}_{\text{sur},o}$
Comments	Cf. (5.2)

Equation 2	
Title	Static energy balance equation
Validity domain	$\exists \dot{m}$ such that $\dot{m} \neq 0$
Mathematical formulation	$0 = \dot{m}_{\text{eco},i} \cdot h_{\text{eco},i} + \dot{m}_{\text{eva},i} \cdot h_{\text{eva},i} + \dot{m}_{\text{sup},i} \cdot h_{\text{sup},i}$ $+ \dot{m}_{\text{steam},i} \cdot h_{\text{steam},i} - \dot{m}_{\text{drain},o} \cdot h_{\text{drain},o} - \dot{m}_{\text{eva},o} \cdot h_{\text{eva},o}$ $- \dot{m}_{\text{sup},o} \cdot h_{\text{sup},o} - \dot{m}_{\text{sur},o} \cdot h_{\text{sur},o} + W$
Comments	This equation is valid if not all mass flow rates are equal to zero (cf. Sect. 5.2.1). Otherwise, the mixing specific enthalpy inside the drum is undefined

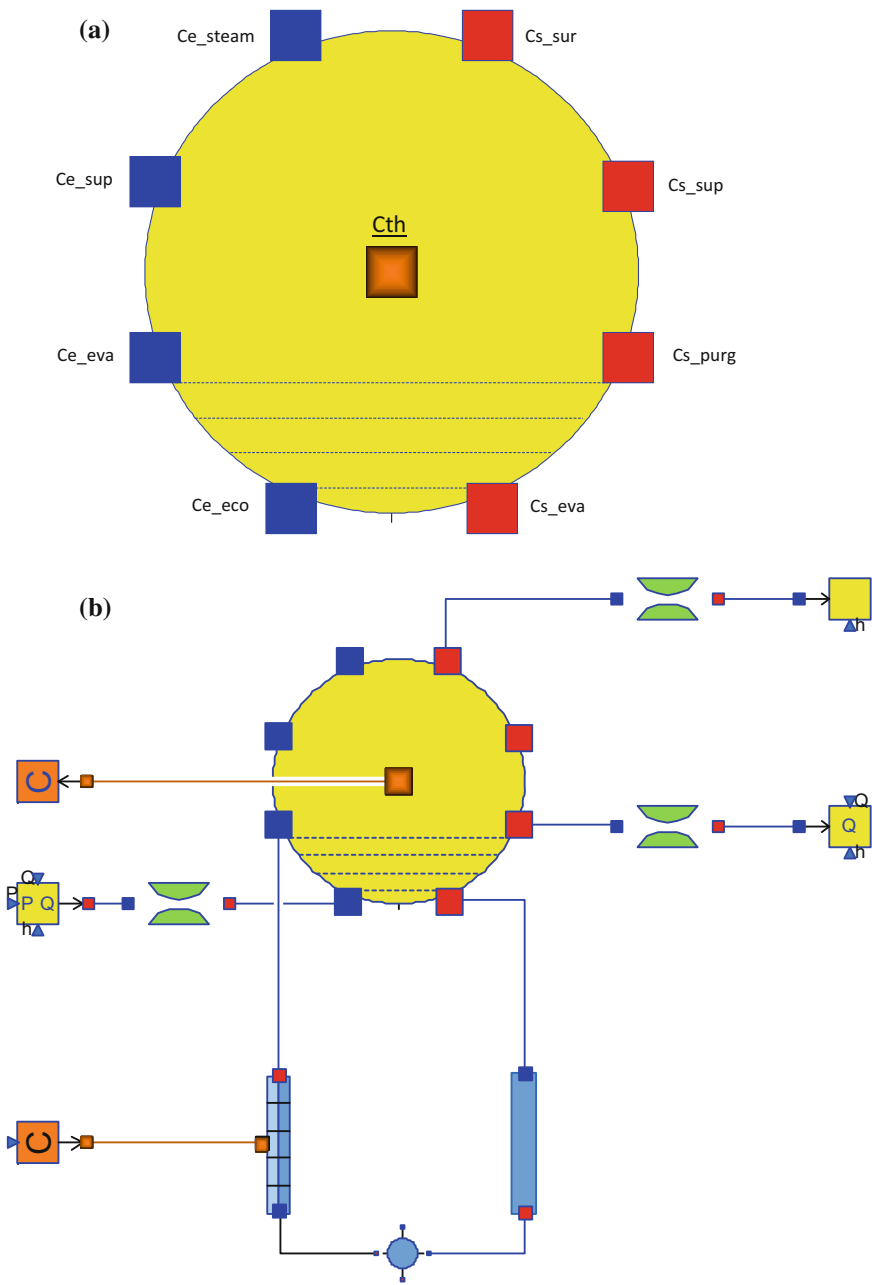
Equation 3	
Title	Specific enthalpy at the drum liquid outlets
Validity domain	$\exists \dot{m}$ such that $\dot{m} \neq 0$
Mathematical formulation	$h_{\text{eva},o} = h_{\text{sup},o} = h_{\text{drain},o} = h_l^{\text{sat}}$
Comments	The liquid inside the drum is assumed to be always at saturation

Equation 4	
Title	Specific enthalpy at the drum vapor outlet
Validity domain	$\exists \dot{m}$ such that $\dot{m} \neq 0$ and $x$ is close to 1
Mathematical formulation	$h_{\text{sur},o} = (1 - x) \cdot h_l^{\text{sat}} + x \cdot h_v^{\text{sat}}$
Comments	The vapor inside the drum is assumed to be always at saturation with possibly small amounts of water

### 14.6.4 Modelica Component Model: *StaticDrum*

The governing equations are implemented in the *StaticDrum* component model located in the *WaterSteam.Junctions* sub-library. Figure 14.16a represents the graphical icon of the component with its nine connectors.



**Fig. 14.16** **a** Icon of the *StaticDrum* component model. **b** Test-case for the *StaticDrum* component model

### 14.6.5 Test-Case

The model *TestStaticDrum* used to validate the *StaticDrum* component model is represented in Fig. 14.16b. It uses the following component models:

- One *StaticDrum* component model;
- One *VolumeA* component model;
- One *DynamicTwoPhaseFlowPipe* component model;
- One *LumpedStraightPipe* component model;
- One *HeatSource* component model;
- One *HeatSink* component model;
- One *SourcePQ* component model;
- One *SinkQ* component model;
- One *Sink* component model;
- Three *SingularPressureLoss* component models.

In this test-case scenario, the *StaticDrum* component receives: (1) the water mass flow rate and specific enthalpy at the inlet coming from the economizer, (2) the water/steam mass flow rate and specific enthalpy at the inlet coming from the evaporator, and (3) the water mass flow rate at the outlet going to the drain. The component computes: (1) the mass flow rate and the specific enthalpy at the outlet going to the super-heater, (2) the specific enthalpy at the outlet going to the drain, and (3) the thermal power received by the fluid (*HeatSink*).

#### 14.6.5.1 Test-Case Parameterization and Boundary Conditions

The model data are:

- Steam mass fraction at the outlet going to the super-heater (separation efficiency) = 1
- Fluid mass flow rate at the outlet of the economizer = 100 kg/s
- Fluid specific enthalpy at the outlet of the economizer =  $1.4 \times 10^6$  J/kg
- Fluid pressure at the outlet of the economizer =  $10^7$  Pa
- Fluid mass flow rate at the outlet going to the drain = 10 kg/s
- Fluid mass flow rate in the down-comer = 30 kg/s
- Inlet altitude of the pipes (down-comer) = 10 m
- Number of pipes (down-comer) = 10
- Evaporator pipe diameter = 0.05 m
- Evaporator pipe length = 10 m
- Number of pipes in the evaporator = 10
- Outlet altitude of the evaporator = 10 m
- Input thermal power provided to the evaporator =  $2 \times 10^7$  W
- Pressure loss coefficient (*singularPressureLoss*) =  $10^{-4}$ .

### 14.6.5.2 Model Calibration

The calibration procedure consists in setting the fluid mass flow rate of the fluid coming from the evaporator (in the *LumpedStraightPipe* model) to a known measurement value to compute by model inversion the value of the friction pressure loss coefficient (lambda) of the *LumpedStraightPipe* model.

### 14.6.5.3 Simulation Results

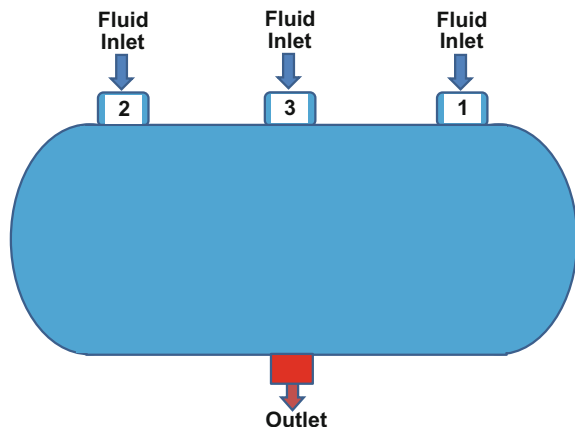
The simulation of the test scenario led to the numerical results below:

- Steam mass flow rate = 90 kg/s
- Specific enthalpy of the steam at the outlet = 2,725,470 J/kg
- Specific enthalpy of the liquid at the outlet going to the drain = 1,407,870 J/kg
- Specific enthalpy of the fluid coming from the evaporator = 2,074,530 J/kg
- Input thermal power to the evaporator =  $99.371 \times 10^6$  W
- Friction pressure loss coefficient of the down-comer = 0.0403.

## 14.7 Static Mixer Modeling

This static model describes the mixing of a fluid as an adiabatic single-phase or two-phase homogeneous flow mixer; cf. Fig. 14.17. The model of the fluid flow in the mixer is based on the static mass and energy balance equations.

**Fig. 14.17** Schematic diagram of a mixer



### 14.7.1 Nomenclature

Symbols	Definition	Unit	Mathematical definition
$h_{i_1}$	Specific enthalpy of the fluid at inlet 1	J/kg	
$h_{i_2}$	Specific enthalpy of the fluid at inlet 2	J/kg	
$h_{i_3}$	Specific enthalpy of the fluid at inlet 3	J/kg	
$h_o$	Specific enthalpy of the fluid at the outlet of the mixer	J/kg	
$\dot{m}_{i_1}$	Mass flow rate of the fluid at inlet 1	kg/s	
$\dot{m}_{i_2}$	Mass flow rate of the fluid at inlet 2	kg/s	
$\dot{m}_{i_3}$	Mass flow rate of the fluid at inlet 3	kg/s	
$\dot{m}_o$	Mass flow rate of the fluid at the outlet	kg/s	
$\alpha_1$	Extraction coefficient for inlet 1 (output of the model)	—	$\frac{\dot{m}_{i_1}}{\dot{m}_o}$
$\alpha_2$	Extraction coefficient for inlet 2 (output of the model)	—	$\frac{\dot{m}_{i_2}}{\dot{m}_o}$
$\alpha_{i_1}$	Mass fraction coefficient for inlet 1	—	
$\alpha_{i_2}$	Mass fraction coefficient for inlet 2	—	

### 14.7.2 Assumptions

The two-phase flow is considered as a mixture of both phases (homogeneous flow, cf. Sect. 4.2.1).

### 14.7.3 Governing Equations

The model of the fluid flow in the mixer is based on the static mass and energy balance equations.

Equation 1	
Title	Static mass balance equation
Validity domain	$\forall \dot{m}$
Mathematical formulation	$0 = \dot{m}_{i_1} + \dot{m}_{i_2} + \dot{m}_{i_3} - \dot{m}_o$
Comments	<p>Cf. (5.2)</p> <p>It is possible to define the values of <math>\dot{m}_{i_1}</math> and <math>\dot{m}_{i_2}</math> as a fraction of the output mass flow rate:</p> $\dot{m}_{i_1} = \alpha_{i_1} \cdot \dot{m}_o$ $\dot{m}_{i_2} = \alpha_{i_2} \cdot \dot{m}_o$ <p>This option is useful when the mass flow rate at the outlet is known and one wants to compute the mass flow rates at the inlets</p>

Equation 2	
Title	Static energy balance equation
Validity domain	$\exists \dot{m}$ such that $\dot{m} \neq 0$
Mathematical formulation	$0 = \dot{m}_{i_1} \cdot h_{i_1} + \dot{m}_{i_2} \cdot h_{i_2} + \dot{m}_{i_3} \cdot h_{i_3} - \dot{m}_o \cdot h_o$
Comments	This equation is valid if not all mass flow rates are equal to zero (cf. Sect. 5.2.1) Otherwise, the mixing specific enthalpy inside the mixer is undefined

#### 14.7.4 Modelica Component Model: Mixer3

The governing equations are implemented in the *Mixer3* component model located in the *WaterSteam.Junctions* sub-library. Figure 14.18a represents the graphical icon of the component with its eight connectors.

#### 14.7.5 Test-Case

The model *TestMixer3* used to validate the *Mixer3* component model is represented in Fig. 14.18b. It uses the following component models:

- One *Mixer3* component model;
- Four *SingularPressureLoss* component models;
- One *SourceQ* component model;
- One *SourceP* component model;
- One *Source* component model;
- One *SinkQ* component model;
- One *Constant* block.

In this test-case scenario, the *Mixer3* component receives: (1) the specific enthalpies of the fluids at the three inlets (Ce1, Ce2, and Ce3), (2) the mass fraction coefficient for inlet 1 (*Talpha1*), (3) the fluid pressure at inlet 2, (4) the mass flow rate of the fluid at inlet 3, and (5) the mass flow rate of the fluid at the outlet (*Cs*). The component computes: (1) the specific enthalpy of the fluid in the mixer, (2) the mass flow rate of the fluid at inlet 1, and (3) the mass flow rate of the fluid at inlet 2.

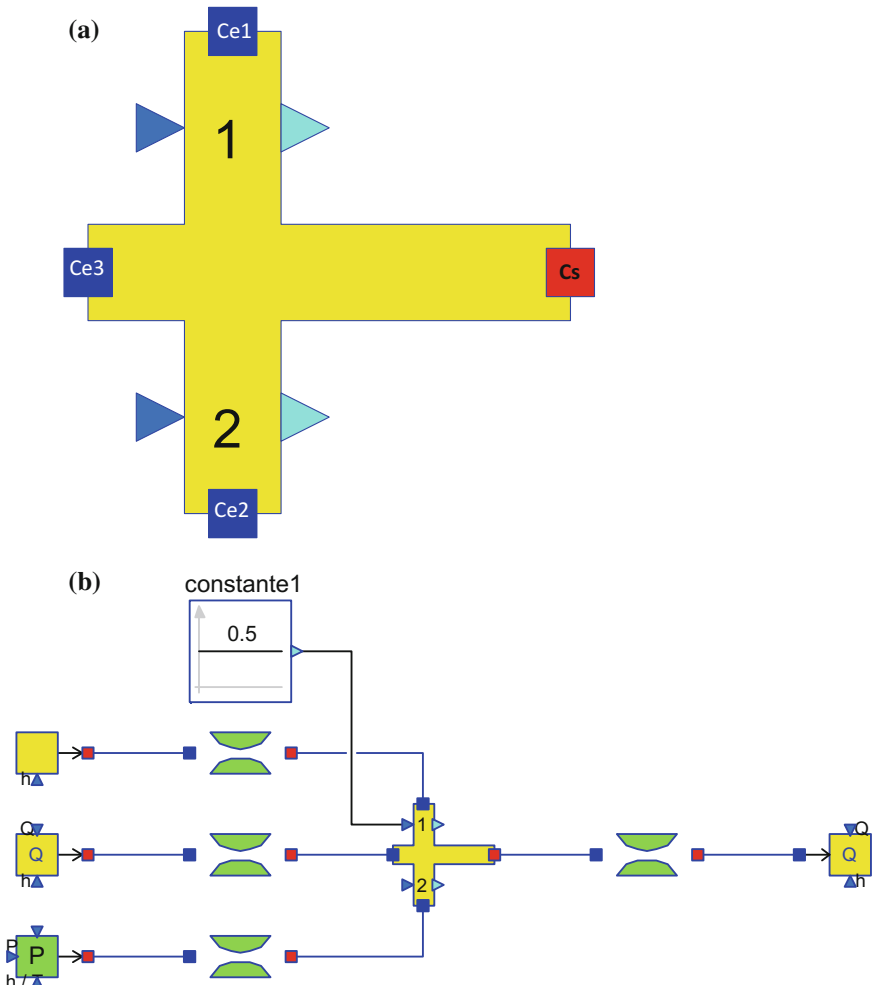


**Fig. 14.18** **a** Icon of the *Mixer3* component model. **b** Test-case for the *Mixer3* component model

#### 14.7.5.1 Test-Case Parameterization and Boundary Conditions

The model data are:

- Fluid specific enthalpy at inlet 1 =  $10^5$  J/kg
- Fluid temperature at inlet 2 = 290 K
- Fluid pressure at inlet 2 =  $3 \times 10^5$  Pa
- Fluid mass flow rate at inlet 3 = 100 kg/s
- Fluid specific enthalpy at inlet 3 =  $10^5$  J/kg
- Fluid mass flow rate at the outlet = 100 kg/s
- Pressure loss coefficient (*singularPressureLoss*) =  $10^{-4}$ .

#### 14.7.5.2 Simulation Results

The simulation of the test scenario led to the numerical results below:

- Fluid mass flow rate at inlet 1 ( $Ce1$ ) = 50 kg/s
- Fluid mass flow rate at inlet 2 ( $Ce2$ ) = -50 kg/s
- Extraction coefficient for inlet 1 ( $\alpha_1$ ) = 0.5
- Extraction coefficient for inlet 2 ( $\alpha_2$ ) = -0.5.

## 14.8 Static Splitter Modeling

This static model describes the splitting of a fluid as an adiabatic single-phase or homogeneous two-phase flow splitter; cf. Figure 14.19. The model of the fluid flow in the splitter is based on the static mass and energy balance equations.

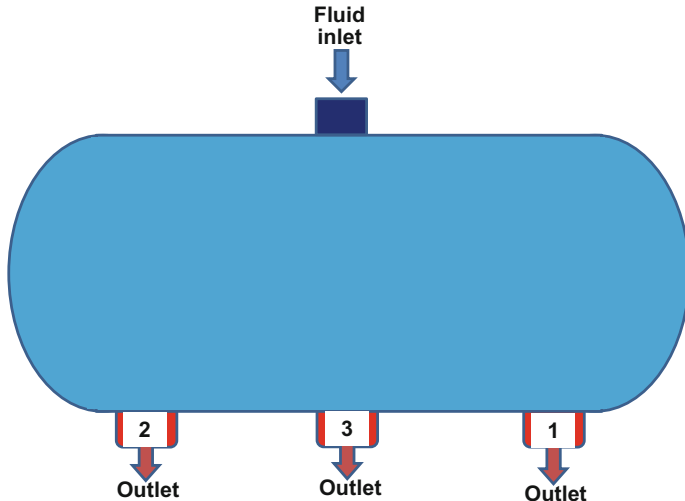


**Fig. 14.19** Schematic diagram of a splitter

### 14.8.1 Nomenclature

Symbols	Definition	Unit	Mathematical definition
$h_i$	Specific enthalpy of the fluid at the inlet of the splitter	J/kg	
$h_{o_1}$	Specific enthalpy of the fluid at outlet 1	J/kg	
$h_{o_2}$	Specific enthalpy of the fluid at outlet 2	J/kg	
$h_{o_3}$	Specific enthalpy of the fluid at outlet 3	J/kg	
$\dot{m}_i$	Fluid mass flow rate at the inlet	kg/s	
$\dot{m}_{o_1}$	Fluid mass flow rate at outlet 1	kg/s	
$\dot{m}_{o_2}$	Fluid mass flow rate at outlet 2	kg/s	
$\dot{m}_{o_3}$	Fluid mass flow rate at outlet 3	kg/s	
$\alpha_1$	Extraction coefficient for outlet 1 (output of the model)	—	$\frac{\dot{m}_{o_1}}{\dot{m}_i}$
$\alpha_2$	Extraction coefficient for outlet 2 (output of the model)	—	$\frac{\dot{m}_{o_2}}{\dot{m}_i}$
$\alpha_{o_1}$	Mass fraction coefficient for outlet 1	—	
$\alpha_{o_2}$	Mass fraction coefficient for outlet 2	—	

### 14.8.2 Assumptions

The two-phase flow is considered as a mixture of both phases (homogeneous flow, cf. Sect. 4.2.1).

### 14.8.3 Governing Equations

The model of the fluid flow in the splitter is based on the static mass and energy balance equations. The model is formulated in order to correctly handle possible flow reversal conditions.

Equation 1	
Title	Static mass balance equation
Validity domain	$\forall \dot{m}$
Mathematical formulation	$0 = \dot{m}_i - \dot{m}_{o_1} - \dot{m}_{o_2} - \dot{m}_{o_3}$
Comments	Cf. (5.2) It is possible to define the value of $\dot{m}_{o_1}$ and $\dot{m}_{o_2}$ as a fraction of the input mass flow rate:

(continued)

(continued)

**Equation 1**

$$\dot{m}_{o_1} = \alpha_{o_1} \cdot \dot{m}_i$$

$$\dot{m}_{o_2} = \alpha_{o_2} \cdot \dot{m}_i$$

This option is useful when the mass flow rate at the inlet is known and one wants to compute the mass flow rates at the outlets

**Equation 2**

Title	Static energy balance equation
Validity domain	$\exists \dot{m}$ such that $\dot{m} \neq 0$
Mathematical formulation	$0 = \dot{m}_i \cdot h_i - \dot{m}_{o_1} \cdot h_{o_1} - \dot{m}_{o_2} \cdot h_{o_2} - \dot{m}_{o_3} \cdot h_{o_3}$
Comments	This equation is valid if not all mass flow rates are equal to zero (cf. Sect. 5.2.1). Otherwise, the mixing specific enthalpy inside the splitter is undefined

### 14.8.4 Modelica Component Model: Splitter3

The governing equations are implemented in the *Splitter3* component model located in the *WaterSteam.Junctions* sub-library. Figure 14.20a represents the graphical icon of the component with its eight connectors.

### 14.8.5 Test-Case

The model *TestSplitter3* used to validate the *Splitter3* component model is represented in Fig. 14.20b. It uses the following component models:

- One *Splitter3* component model;
- Three *SingularPressureLoss* component models;
- One *SourceQ* component model;
- One *SinkP* component model;
- Two *Sink* component models;
- Two *Constant* blocks.

In this test-case scenario, the *Splitter3* component model receives: (1) the specific enthalpy and the mass flow rate of the fluid at the inlet (*Ce*), (2) the mass fraction coefficient for outlet 1 (*Ialpha1*), (3) the mass fraction coefficient for outlet 2 (*Ialpha2*), and (4) the fluid pressure at outlet 3 (*Cs3*). The component computes: (1) the specific enthalpy of the fluid in the splitter and (2) the mass flow rate of the fluid at the three outlets (*Cs1*, *Cs2*, and *Cs3*).

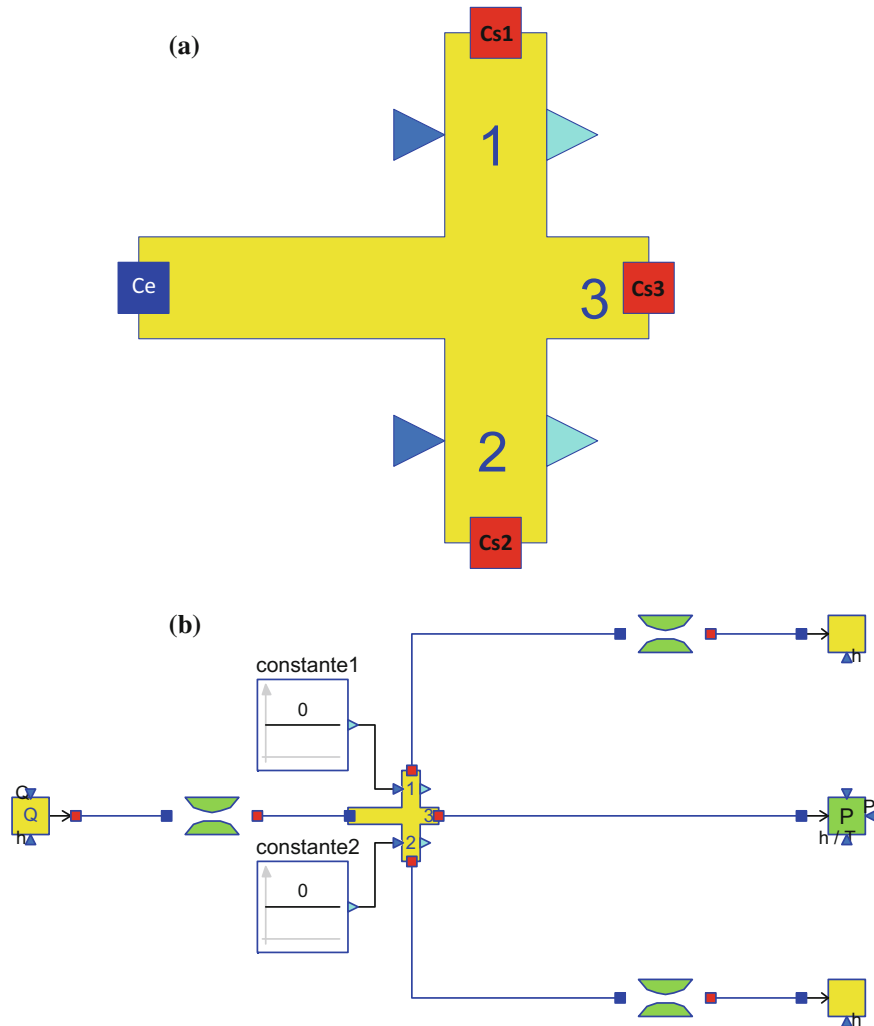


**Fig. 14.20** **a** Icon of the *Splitter3* component model. **b** Test-case for the *Splitter3* component model

#### 14.8.5.1 Test-Case Parameterization and Boundary Conditions

The model data are:

- Mass fraction coefficient for outlet 1 = 0
- Mass fraction coefficient for outlet 2 = 0
- Fluid specific enthalpy at the inlet =  $10^5$  J/kg
- Fluid mass flow rate at the inlet = 100 kg/s
- Fluid temperature at outlet 3 = 290 K

- Fluid pressure at outlet 3 =  $10^5$  Pa
- Pressure loss coefficient (*singularPressureLoss*) =  $10^{-4}$ .

#### 14.8.5.2 Simulation Results

The simulation of the test scenario led to the numerical results below:

- Fluid mass flow rate at outlet 1 ( $Cs1$ ) = 0
- Fluid mass flow rate at outlet 2 ( $Cs2$ ) = 0
- Fluid mass flow rate at outlet 3 ( $Cs3$ ) = 100 kg/s
- Extraction coefficient for outlet 1 ( $\alpha_1$ ) = 0
- Extraction coefficient for outlet 2 ( $\alpha_2$ ) = 0.

## 14.9 Steam Dryer Modeling

Wet steam is steam containing some quantity of water. Wet steam can reduce the plant efficiency and cause damage to most items and equipment of the plant.

The steam dryer is a reservoir of steam and water used to separate water from the steam generated in the boiler; cf. Fig. 14.21.

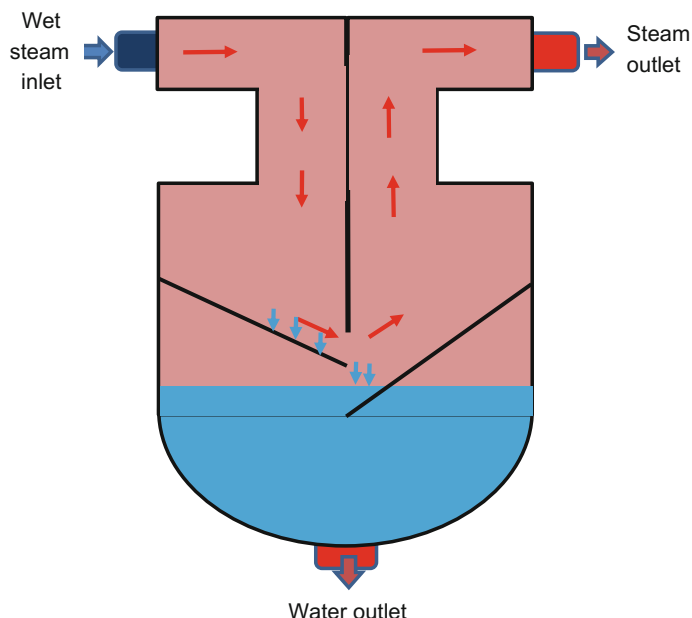


**Fig. 14.21** Schematic diagram of a steam dryer

### 14.9.1 Nomenclature

Symbols	Definition	Unit	Mathematical definition
$h_i$	Specific enthalpy of the fluid at the inlet of the dryer	J/kg	
$h_{l,o}$	Specific enthalpy of the liquid at the outlet	J/kg	
$h_l^{\text{sat}}$	Saturation enthalpy of the liquid	J/kg	
$h_{v,o}$	Specific enthalpy of the steam at the outlet	J/kg	
$\dot{m}_i$	Fluid mass flow rate at the inlet	kg/s	
$\dot{m}_{l,o}$	Liquid mass flow rate at the outlet	kg/s	
$\dot{m}_{v,o}$	Steam mass flow rate at the outlet	kg/s	
$P$	Fluid pressure in the dryer	Pa	
$x_i$	Steam mass fraction at the inlet	—	
$\eta$	Steam dryer efficiency	—	$0 \leq \eta \leq 1$

### 14.9.2 Assumptions

The steam dryer is modeled according to the following assumptions:

- Heat exchange between the liquid and steam phases is neglected.
- Heat exchange between the steam dryer and the external medium is neglected.
- Pressure losses are not taken into account.

### 14.9.3 Governing Equations

The *SteamDryer* model is based on the static mass and energy balance equations.

Equation 1	
Title	Static mass balance equation
Validity domain	$\forall \dot{m}$
Mathematical formulation	$0 = \dot{m}_i - \dot{m}_{l,o} - \dot{m}_{v,o}$
Comments	<p>The value of the steam mass flow rate at the outlet (<math>\dot{m}_{v,o}</math>) is given by:</p> $\dot{m}_{v,o} = \begin{cases} 0 & \text{for } x_i = 0 \\ \dot{m}_i \cdot (1 - \eta \cdot (1 - x_i)) & \text{for } x_i > 0 \end{cases}$ <p>The efficiency gives the discrepancy between an ideal steam separator where no water remains in the steam after separation and a real steam separator where small quantities of water remain in the steam</p>

Equation 2	
Title	Static energy balance equation
Validity domain	$\exists \dot{m}$ such that $\dot{m} \neq 0$
Mathematical formulation	$0 = \dot{m}_i \cdot h_i - \dot{m}_{l,o} \cdot h_{l,o} - \dot{m}_{v,o} \cdot h_{v,o}$
Comments	<p>This equation is valid if not all mass flow rates are equal to zero (cf. Sect. 5.2.1) Otherwise, the mixing specific enthalpy inside the steam dryer is undefined</p> <p>The value of the specific enthalpy of the liquid at the outlet <math>h_{l,o}</math> is given by:</p> $h_{l,o} = \begin{cases} h_i^{\text{sat}} & \text{for } x_i > 0 \\ h_i & \text{for } x_i = 0 \end{cases}$

#### 14.9.4 Modelica Component Model: SteamDryer

The governing equations are implemented in the *SteamDryer* component model located in the *WaterSteam.Junctions* sub-library. Figure 14.22a represents the graphical icon of the component with its three connectors.

#### 14.9.5 Test-Case

The model *TestSteamDryer* used to validate the *SteamDryer* component model is represented in Fig. 14.22b. It uses the following component models:

- One *SteamDryer* component model;
- Three *SingularPressureLoss* component models;
- One *SourcePQ* component model;
- Two *Sink* component models.

In this test-case scenario, the *SteamDryer* component receives: the specific enthalpy, the pressure and the mass flow rate of the fluid at the inlet (Cev). The component computes: the specific enthalpy and the mass flow rate of the fluid at the two outlets (Csv and Csl).

##### 14.9.5.1 Test-Case Parameterization and Boundary Conditions

The model data are:

- Vapor mass fraction at outlet 1 = 0.9
- Fluid mass flow rate at the inlet = 100 kg/s
- Fluid specific enthalpy at the inlet =  $2.4 \times 10^6$  J/kg

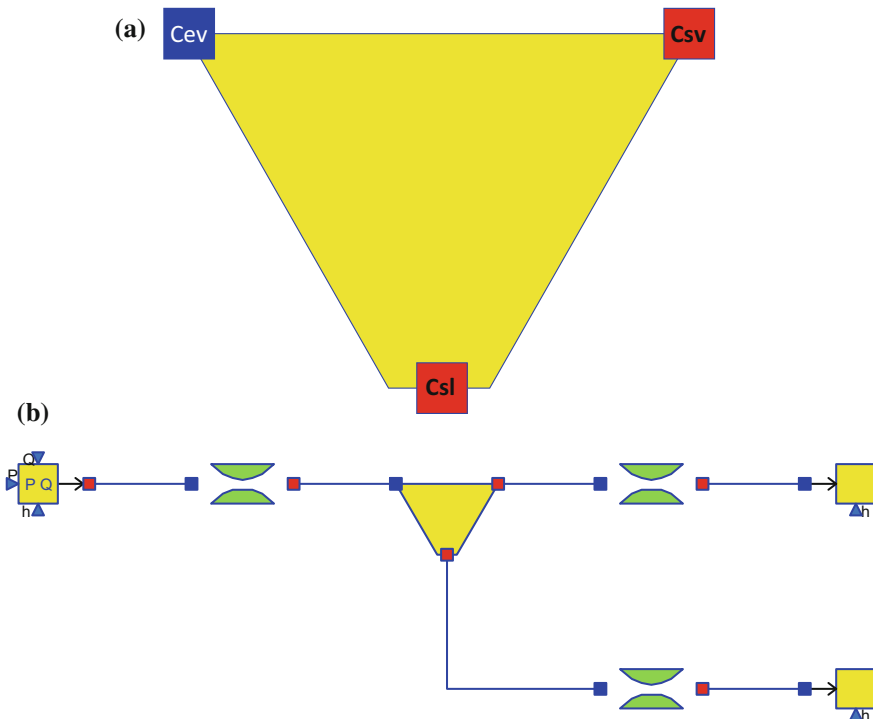


**Fig. 14.22** **a** Icon of the *SteamDryer* component model. **b** Test-case for the *SteamDryer* component model

- Fluid pressure at the inlet =  $10^7$  Pa
- Pressure loss coefficient (*singularPressureLoss*) =  $10^{-4}$ .

#### 14.9.5.2 Simulation Results

The simulation of the test scenario led to the numerical results below:

- Steam mass flow rate at outlet 1 (Csv) = 77.77 kg/s
- Steam specific enthalpy at outlet 1 (Csv) = 2,683,620 J/kg
- Liquid mass flow rate at outlet 2 (CsI) = 22.23 kg/s
- Liquid specific enthalpy at outlet 2 (CsI) = 1,407,870 J/kg
- Steam mass fraction at the inlet = 0.753.

## References

- Attalla M (2013) Stagnation region heat transfer due to a turbulent circular impinging air jets. J Eng Sci 41(4). Assiut University, Faculty of Engineering
- Idel'cik IE (1986) Memento des pertes de charge, 3rd edn. Eyrolles
- Incropera F, DeWitt P, Bergman T, Lavine A (2006) Fundamentals of heat transfer. Wiley
- Sacadura JF (1978) Initiation aux transferts thermiques. Technique et documentation, Paris

# Chapter 15

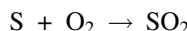
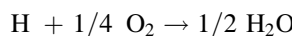
## Internal Combustion Engine Modeling



**Abstract** This chapter presents the motor component. The detailed description of the physical equations for internal combustion engines is provided. A test-case is given that includes parameterization data, model calibration and results of simulation. The full description of the physical equations is independent of the programming languages and tools.

The internal combustion engine is a heat engine that converts thermal and kinetic energy in the combustion products into mechanical energy. Similarly to a gas turbine, the combustion and conversion processes take place at the same time in the combustion chamber; cf. Fig. 15.1a. In the combustion chamber, energy is added by spraying fuel into the air. The fuel ignition generates high-temperature high-pressure flue gases. The force from the expanding gas is transferred to the piston in order to rotate the crankshaft. The engine is cooled with water. The heat engine presented here works according to the four-stroke-cycle principle based on the Beau de Rochas cycle or the Otto cycle. Figure 15.1b shows the diagram for the Otto cycle on a pressure–volume (P–V) diagram. It is considered as a polytropic process with both heat and work transfer to the surroundings (cf. Sect. 2.11).

The species in the flue gases at the exhaust are governed by the following chemical reactions:



The flue gases also contain excess air (i.e., air that was not used during combustion) in the form of oxygen ( $\text{O}_2$ ) and nitrogen ( $\text{N}_2$ ). It assumed that there is no unburnt fuel, so that the combustion is complete.

The Otto ideal cycle is made of six processes:

- Process 0–1: admission (intake) of gasoline/air mixture into the cylinder;
- Process 1–2: isentropic compression;

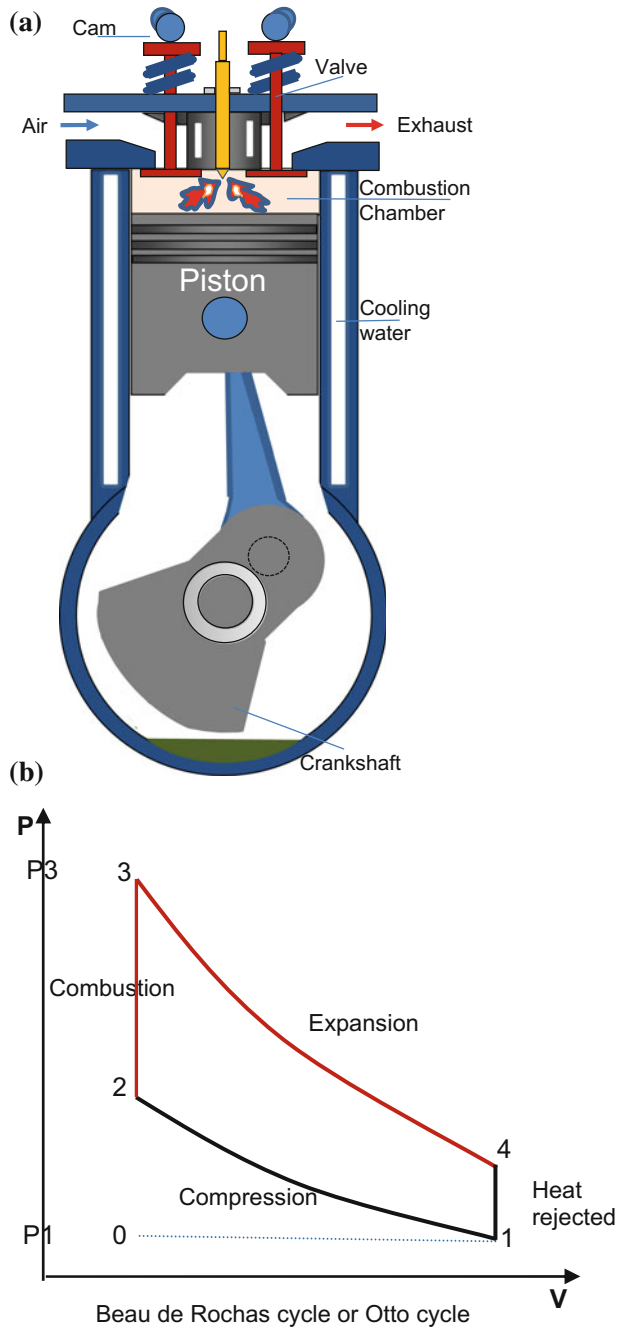


**Fig. 15.1** **a** Schematic diagram of an internal combustion engine. **b** Beau de Rochas cycle or Otto cycle in a pressure–volume diagram

- Process 2–3: constant volume heat addition (instant combustion);
- Process 3–4: isentropic expansion of the products of combustion;
- Process 4–1: constant volume cooling (heat rejection);
- Process 1–0: exhaust of the flue gases.

## 15.1 Nomenclature

Symbols	Definition	Unit	Mathematical definition
$c_{p,a}$	Air specific heat capacity	J/kg/K	
$c_{p,f}$	Fuel specific heat capacity	J/kg/K	
$c_{p,g}$	Flue gases specific heat capacity at the end of the combustion phase	J/kg/K	
$c_{p,g}^{23}$	Flue gases specific heat capacity between point 2 and point 3; cf. Fig. 15.1b	J/kg/K	
$E_X$	Dry air stoichiometry necessary for the combustion of one kilogram of fuel (theoretical dry air requirement)	–	
$E_{X,a}$	Combustion air ratio (excess air factor)	–	$\frac{\dot{m}_a \cdot (1 - X_{h2o,a})}{\dot{m}_f \cdot E_X}$
$h_{a,i}$	Air specific enthalpy at the intake	J/kg	
$\tilde{h}_{a,r}$	Air reference specific enthalpy	J/kg	$2501569 \cdot X_{h2o,a}$
$h_f$	Fuel specific enthalpy at the intake	J/kg	$c_{p,f} \cdot (T_f - 273.16)$
$\tilde{h}_{f,r}$	Fuel reference specific enthalpy	J/kg	0
$h_{g,o}$	Flue gases specific enthalpy at the exhaust	J/kg	
$\tilde{h}_{g,r}$	Flue gases reference specific enthalpy	J/kg	$2501569 \cdot X_{h2o,g}$
$h_{w,i}$	Water specific enthalpy at the inlet	J/kg	
$h_{w,o}$	Water specific enthalpy at the outlet	J/kg	
LHV	Fuel lower heating value	J/kg	
$\dot{m}_a$	Air mass flow rate	kg/s	
$\dot{m}_g$	Flue gases mass flow rate	kg/s	
$\dot{m}_f$	Fuel mass flow rate (crude fuel)	kg/s	
$\dot{m}_w$	Cooling water mass flow rate	kg/s	
$M_a$	Air molar mass	kg/kmol	28.9
$M_{af}$	Air–fuel mixture molar mass	kg/kmol	

(continued)

(continued)

Symbols	Definition	Unit	Mathematical definition
$M_{\text{CO}_2}$	$\text{CO}_2$ molar mass	kg/kmol	$M_C + 2 \cdot M_O$
$M_{\text{H}_2\text{O}}$	$\text{H}_2\text{O}$ molar mass	kg/kmol	$M_O + 2 \cdot M_H$
$M_{\text{SO}_2}$	$\text{SO}_2$ molar mass	kg/kmol	$M_S + 2 \cdot M_O$
$M_C$	Carbon atomic mass	kg/kmol	12.01115
$M_{\text{fuel}}$	Fuel molar mass	kg/kmol	
$M_g$	Flue gases molar mass	kg/kmol	
$M_H$	Hydrogen atomic mass	kg/kmol	1.00797
$M_O$	Oxygen atomic mass	kg/kmol	15.9994
$M_N$	Nitrogen atomic mass	kg/kmol	14
$M_S$	Sulfur atomic mass	kg/kmol	32.064
$n_c$	Compression polytropic index	—	
$n_e$	Expansion polytropic index	—	
$P_{a,i}$	Air pressure at the intake	Pa	
$P_{a,2}$	Air-fuel mixture pressure at the end of the compression phase	Pa	
$P_{g,o}$	Flue gases pressure at the exhaust	Pa	$P_{a,i} - \Delta P_f$
$P_{g,3}$	Flue gases pressure at the end of the combustion phase	Pa	
$P_{g,4}$	Flue gases pressure at the end of the expansion phase	Pa	
$P_{w,i}$	Water pressure at the inlet	Pa	
$P_{w,o}$	Water pressure at the outlet	Pa	
$R_v$	Engine volume ratio: volume of the piston at the end of the expansion phase divided by the volume of the piston after the compression phase	—	
$T_{a,i}$	Air temperature at the intake	K	
$T_f$	Fuel temperature at the intake	K	
$T_{g,o}$	Flue gases temperature at the exhaust	K	
$T_{g,3}$	Flue gases temperature at the end of the combustion phase	K	
$T_{g,4}$	Flue gases temperature at the end of the expansion phase	K	
$T_{m,1}$	Air-fuel mixture temperature	K	
$T_{m,2}$	Air-fuel mixture temperature at the end of the compression phase	K	

(continued)

(continued)

Symbols	Definition	Unit	Mathematical definition
$W_m$	Engine mechanical power	W	
$X_{\text{CO}_2,\text{a}}$	$\text{CO}_2$ mass fraction in the air at the intake	–	
$X_{\text{CO}_2,\text{g}}$	$\text{CO}_2$ mass fraction in the flue gases	–	
$X_{\text{H}_2\text{O},\text{a}}$	$\text{H}_2\text{O}$ mass fraction in the air at the intake	–	
$X_{\text{H}_2\text{O},\text{g}}$	$\text{H}_2\text{O}$ mass fraction in the flue gases	–	
$X_{\text{O}_2,\text{a}}$	$\text{O}_2$ mass fraction in the air at the intake	–	
$X_{\text{O}_2,\text{g}}$	$\text{O}_2$ mass fraction in the flue gases	–	
$X_{\text{SO}_2,\text{a}}$	$\text{SO}_2$ mass fraction in the air at the intake	–	
$X_{\text{SO}_2,\text{g}}$	$\text{SO}_2$ mass fraction in the flue gases	–	
$X_{\text{C,f}}$	C mass fraction in the fuel	–	
$X_{\text{CD,f}}$	Ashes mass fraction in the fuel	–	
$X_{\text{H,f}}$	H mass fraction in the fuel	–	
$X_{\text{O,f}}$	O mass fraction in the fuel	–	
$X_{\text{S,f}}$	S mass fraction in the fuel	–	
$X_{\text{lth}}$	Thermal loss fraction to the ambient	–	
$X_{\text{lw}}$	Thermal loss fraction to the cooling water	–	
$\delta P_w$	Water pressure loss as percent of the pressure at the inlet	–	$100 \cdot \frac{\Delta P_w}{P_{w,i}}$
$\Delta P_f$	Pressure difference between the air pressure at the intake and the flue gases pressure at the exhaust	Pa	
$\Delta P_w$	Water pressure loss	Pa	$P_{w,i} - P_{w,o}$
$\gamma$	Flue gases heat capacity ratio	–	$\frac{c_p}{c_v}$
$\eta_m$	Engine mechanical efficiency	–	
$\Lambda$	Pressure loss coefficient in the combustion chamber	$\text{m}^{-4}$	

## 15.2 Governing Equations

Equation 1	
Title	Mass balance equation for the flue gases
Validity domain	$\dot{m}_a \geq 0$ and $\dot{m}_f \geq 0$
Mathematical formulation	$\dot{m}_g = \dot{m}_a + \dot{m}_f$
Comments	Flue gases result from the combustion of fuel with air. It is assumed that there is no unburnt fuel

Equation 2	
Title	Engine mechanical power
Validity domain	$\dot{m}_f \geq 0$
Mathematical formulation	$W_m = \eta_m \cdot \dot{m}_f \cdot LHV$
Comments	<p>The fuel lower heating value LHV is the total heat produced by the combustion, minus the amount of heat necessary to vaporize the water contained in the fuel and the water produced during the hydrogen combustion process. Only the lower heating value is converted into mechanical energy and the efficiency of the energy conversion is given by <math>\eta_m</math>.</p> <p>The efficiency <math>\eta_m</math> can be provided in various ways such as a fixed parameter or a characteristic curve</p> $\eta_m = f_\eta(\dot{m}_f \cdot LHV)$ <p>The efficiency can also be computed by inverting Eq. (2) and providing a known value for <math>W_m</math></p>

Equation 3	
Title	Energy balance equation for the cooling water
Validity domain	$\dot{m}_w \neq 0$
Mathematical formulation	$X_{lw} \cdot \dot{m}_f \cdot LHV = \dot{m}_w \cdot (h_{w,i} - h_{w,o})$
Comments	This equation calculates the specific enthalpy $h_{w,o}$ of the cooling water at the outlet from the fraction of combustion heat $X_{lw}$ released to the water

Equation 4	
Title	Flue gases specific enthalpy at the exhaust (point 0 in Fig. 15.1b)
Validity domain	$\dot{m}_f \geq 0$
Mathematical formulation	$\dot{m}_f \cdot (h_f + LHV) + \dot{m}_a \cdot h_{a,i} = W_m + \dot{m}_g \cdot h_{g,o} + (X_{lth} + X_{lw}) \cdot \dot{m}_f \cdot LHV$
Comments	<p>This equation calculates the specific enthalpy <math>h_{g,o}</math> of the flue gases at the exhaust using the conservation of energy over the whole cycle</p> <p>As the start and end of the cycle are at the same pressure and volume, from (2.20) and (2.35), the variation of enthalpy over a cycle (i.e., from intake to exhaust) is:</p> $\Delta H_{cycle} = H_0 - H_i = -Q - W_m$ <p>where <math>H_0</math> is the enthalpy at the exhaust, <math>H_i</math> is the enthalpy at the intake, <math>Q</math> is the heat released to the outside and <math>W_m</math> is the mechanical work produced. <math>\Delta H_{cycle} \neq 0</math> because the cycle 0–5 is not closed.</p> <p><math>H_i</math> is the thermal and chemical energy (LHV) of the fuel and air:</p> $H_i = \dot{m}_f \cdot h_f + \dot{m}_a \cdot h_{a,i} + \dot{m}_l \cdot LHV$ <p><math>H_0</math> is the thermal energy of the flue gases:</p> $H_0 = \dot{m}_g \cdot h_{g,o}$ <p><math>Q</math> is the thermal losses released to the cooling water, expressed as a fraction of the combustion energy:</p> $Q = (X_{lth} + X_{lw}) \cdot \dot{m}_f \cdot LHV$ <p>The specific enthalpies <math>h_f</math> and <math>h_a</math> are computed using properties tables from the known temperatures <math>T_f</math> and <math>T_a</math> of the fuel and the air at the intake. As the properties tables use different references, <math>h_f</math> and <math>h_{a,i}</math> must be replaced by <math>\tilde{h}_f</math> and <math>\tilde{h}_{a,i}</math> using (2.19):</p> $h_f \rightarrow \tilde{h}_f = h_f - \tilde{h}_{f,r}$ $h_{a,i} \rightarrow \tilde{h}_{a,i} = h_{a,i} - \tilde{h}_{a,r}$ <p>where the sign → means “is replaced by.”</p> <p>The same applies to <math>h_{g,o}</math> in order to compute the temperature <math>T_{g,o}</math> of the flue gases:</p> $h_{g,o} \rightarrow \tilde{h}_{g,o} = h_{g,o} - \tilde{h}_{g,r}$

Equation 5	
Title	Air-fuel mixture temperature at the intake (point 1 in Fig. 15.1b)
Validity domain	$\dot{m}_a \neq 0$ or $\dot{m}_f \neq 0$
Mathematical formulation	$T_{m,1} \cdot (\dot{m}_f \cdot c_{p,f} + \dot{m}_a \cdot c_{p,a}) = \dot{m}_f \cdot c_{p,f} \cdot T_f + \dot{m}_a \cdot c_{p,a} \cdot T_a$
Comments	<p>This equation calculates the mixing temperature <math>T_{m,1}</math> of the fuel and the air at the beginning of the cycle.</p> <p>Mixing occurs at constant pressure without any heat exchange to the outside. Therefore, the variation of total enthalpy is zero during the mixing; cf. (2.39). Before the mixing, the fuel and the air are at different temperatures, respectively, denoted by <math>T_f</math> and <math>T_a</math>, and after the mixing, they are at the same temperature <math>T_{m,1}</math>.</p> $\Delta H_{mixing} = (h_{f,m1} + h_{a,m1}) - (h_f + h_a) = 0$ <p>where <math>h_f</math> and <math>h_a</math> are, respectively, the specific enthalpies of the fuel and the air before the mixing, and <math>h_{f,m1}</math> and <math>h_{a,m1}</math> are, respectively, the specific enthalpies of the fuel and the air after the mixing.</p>

(continued)

(continued)

**Equation 5**

Title	Air-fuel mixture temperature at the intake (point 1 in Fig. 15.1b)
	<p>Therefore</p> $\Delta H_{\text{mixing}} = (h_{f,m1} - h_f) + (h_a - h_{a,m1}) = 0$ <p>From (2.19):</p> $\Delta H_{\text{mixing}} = \dot{m}_f \cdot c_{p,f} \cdot (T_{m1} - T_f) + \dot{m}_a \cdot c_{p,a} \cdot (T_{m1} - T_a) = 0$ <p>which yields Eq. (5)</p>

**Equation 6**

Title	Air-fuel mixture pressure at the end of the compression phase (point 2 in Fig. 15.1b)
Validity domain	$\forall P_{a,1}$ and $\forall P_{a,2}$
Mathematical formulation	$\frac{P_{a,2}}{P_{a,1}} = R_v^{n_c}$
Comments	This equation calculates the pressure $P_{a,2}$ at the end of the compression, assuming that the air follows a polytropic compression; cf. (2.78)

**Equation 7**

Title	Air-fuel mixture temperature at the end of the compression phase (point 2 in Fig. 15.1b)
Validity domain	$\forall T_{m,1}$ and $\forall T_{m,2}$
Mathematical formulation	$\frac{T_{m,2}}{T_{m,1}} = R_v^{n_c-1}$
Comments	<p>This equation calculates the temperature <math>T_{m,2}</math> at the end of the compression phase.</p> <p>This equation is derived by using the equation for polytropic processes (2.78) combined with the equation for ideal gases (2.75), which yields</p> $\frac{T_2}{T_1} = \left(\frac{V_1}{V_2}\right)^{n_c-1} = R_v^{n_c-1}$ <p>since <math>R_v = \frac{V_1}{V_2}</math>, where <math>V_1</math> and <math>V_2</math> are, respectively, the volume before and after the compression phase.</p> <p>It is therefore assumed that the flue gases follow the ideal gas law for the calculation of temperatures</p>

**Equation 8**

Title	Flue gases pressure at the end of the combustion phase (point 3 in Fig. 15.1b)
Validity domain	$\forall P_{a,2}$ , $\forall T_{m,2}$ , $\forall P_{g,3}$ and $\forall T_{g,3}$
Mathematical formulation	$\frac{P_{g,3}}{P_{a,2}} = \frac{T_{g,3}}{T_{m,2}} \cdot \frac{M_{af}}{M_g}$
Comments	<p>This equation calculates the pressure at the end of the combustion phase <math>P_{g,3}</math>, using the ideal gas law (2.75) with (2.76).</p> <p>The air-fuel mixture molar mass is given by:</p> $M_{af} = \frac{\dot{m}_a \cdot M_a + \dot{m}_f \cdot M_f}{\dot{m}_a + \dot{m}_f}$ <p>The flue gases molar mass is given by:</p>

(continued)

(continued)

**Equation 8**

Title	Flue gases pressure at the end of the combustion phase (point 3 in Fig. 15.1b)
	$M_g = (1 - X_{\text{CO}_2,g} - X_{\text{H}_2\text{O},g} - X_{\text{O}_2,g} - X_{\text{SO}_2,g}) \cdot 2 \cdot M_N$ $+ X_{\text{CO}_2,g} \cdot M_{\text{CO}_2} + X_{\text{H}_2\text{O},g} \cdot M_{\text{H}_2\text{O}}$ $+ X_{\text{O}_2,g} \cdot 2 \cdot M_{\text{O}_2} + X_{\text{SO}_2,g} \cdot M_{\text{SO}_2}$ <p>It is assumed that air contains nitrogen (<math>\text{N}_2</math>) and oxygen (<math>\text{O}_2</math>) only</p>

**Equation 9**

Title	Flue gases temperature at the end of the combustion phase (point 3 in Fig. 15.1b)
Validity domain	$\dot{m}_f \geq 0$ and $\dot{m}_g > 0$
Mathematical formulation	$\dot{m}_g \cdot c_{p,g}^{23} \cdot (T_{g,3} - T_{m,2}) = \dot{m}_f \cdot \text{LHV}$
Comments	This equation calculates the temperature $T_{g,3}$ . All the energy produced by the combustion is transferred to the flue gases

**Equation 10**

Title	Flue gases pressure at the end of the expansion phase (point 4 in Fig. 15.1b)
Validity domain	$\forall P_{f,3}$ and $\forall P_{f,4}$
Mathematical formulation	$\frac{P_{f,4}}{P_{f,3}} = \frac{1}{R_v^{\eta_d}}$
Comments	This equation calculates the pressure at the end of the expansion phase $P_{g,4}$ , assuming that the flue gases follow a polytropic compression; cf. (2.78)

**Equation 11**

Title	Flue gases temperature at the end of the expansion phase (point 4 in Fig. 15.1b)
Validity domain	$\forall T_{g,3}$ and $\forall T_{g,4}$
Mathematical formulation	$\frac{T_{g,4}}{T_{g,3}} = \frac{1}{R_v^{\eta_d-1}}$
Comments	This equation calculates the temperature $T_{g,4}$ ; cf. comments of Eq. (7)

**Equation 12**

Title	Flue gases temperature at the end of the exhaust phase (point 1 in Fig. 15.1b)
Validity domain	$\forall T_{g,4}$ , $\forall P_{g,4}$ , $\forall T_{g,o}$ and $\forall P_{g,o}$
Mathematical formulation	$\frac{T_{g,o}}{T_{g,4}} = \left( \frac{P_{g,o}}{P_{g,4}} \right)^{\frac{\gamma-1}{\gamma}}$
Comments	This equation calculates the temperature $T_{g,o}$ for an adiabatic process; cf. (11.6)

**Equation 13**

Title	Dry air stoichiometry for the combustion of one kilogram of fuel
Validity domain	$X_{\text{h2o,f}} < 1$ and $X_{\text{o2,a}} > 0$
Mathematical formulation	$E_X = M_O \cdot \frac{\frac{2 \cdot X_{\text{C,f}}}{M_C} + \frac{X_{\text{H,f}}}{2 \cdot M_H} + \frac{2 \cdot X_{\text{S,f}}}{M_S} - \frac{X_{\text{O,f}}}{M_O}}{\frac{X_{\text{o2,a}}}{1 - X_{\text{h2o,a}}}}$
Comments	The derivation of this equation is identical to Eq. (7) in Chap. 7

**Equation 14**

Title	$\text{CO}_2$ mass fraction in the flue gases
Validity domain	$\dot{m}_g \neq 0$
Mathematical formulation	$X_{\text{co2,g}} = \frac{\dot{m}_a}{\dot{m}_g} \cdot X_{\text{co2,a}} + \frac{\dot{m}_f}{\dot{m}_g} \cdot X_{\text{f,C}} \cdot \frac{M_{\text{co2}}}{M_C}$
Comments	The derivation of this equation is identical to Eq. (8) in Chap. 7

**Equation 15**

Title	$\text{H}_2\text{O}$ mass fraction in the flue gases
Validity domain	$\dot{m}_g \neq 0$
Mathematical formulation	$X_{\text{h2o,g}} = \frac{\dot{m}_a}{\dot{m}_g} \cdot X_{\text{h2o,a}} + \frac{\dot{m}_f}{\dot{m}_g} \cdot X_{\text{H,f}} \cdot \frac{M_{\text{h2o}}}{2 \cdot M_H}$
Comments	The derivation of this equation is identical to Eq. (9) in Chap. 7

**Equation 16**

Title	$\text{O}_2$ mass fraction in the flue gases
Validity domain	$\dot{m}_g \neq 0$
Mathematical formulation	$X_{\text{o2,g}} = \frac{\dot{m}_a}{\dot{m}_g} \cdot X_{\text{o2,a}} - M_O \cdot \frac{\dot{m}_f}{\dot{m}_g} \cdot \left( \frac{2 \cdot X_{\text{C,f}}}{M_C} + \frac{X_{\text{H,f}}}{2 \cdot M_H} + \frac{2 \cdot X_{\text{S,f}}}{M_S} \right) + \frac{\dot{m}_f}{\dot{m}_g} \cdot X_{\text{O,f}}$
Comments	The derivation of this equation is identical to Eq. (10) in Chap. 7

**Equation 17**

Title	$\text{SO}_2$ mass fraction in the flue gases
Validity domain	$\dot{m}_g \neq 0$
Mathematical formulation	$X_{\text{so2,g}} = \frac{\dot{m}_a}{\dot{m}_g} \cdot X_{\text{so2,a}} + \frac{\dot{m}_f}{\dot{m}_g} \cdot X_{\text{S,f}} \cdot \frac{M_{\text{so2}}}{M_S}$
Comments	The derivation of this equation is identical to Eq. (11) in Chap. 7

This set of equations must be completed by state equations for all substances in order to have a complete system of equations that can be solved. The state equations are to be given for  $c_{\text{p,a}}$ ,  $c_{\text{p,g}}^{23}$ ,  $h_{\text{a,i}}$  and  $T_{\text{g,o}}$ .

### 15.3 Modelica Component Model: *InternalCombustionEngine*

The governing equations are implemented in the *InternalCombustionEngine* located in the *MultiFluids.Machines* sub-library. Figure 15.2a represents the graphical icon of the component with its five connectors.

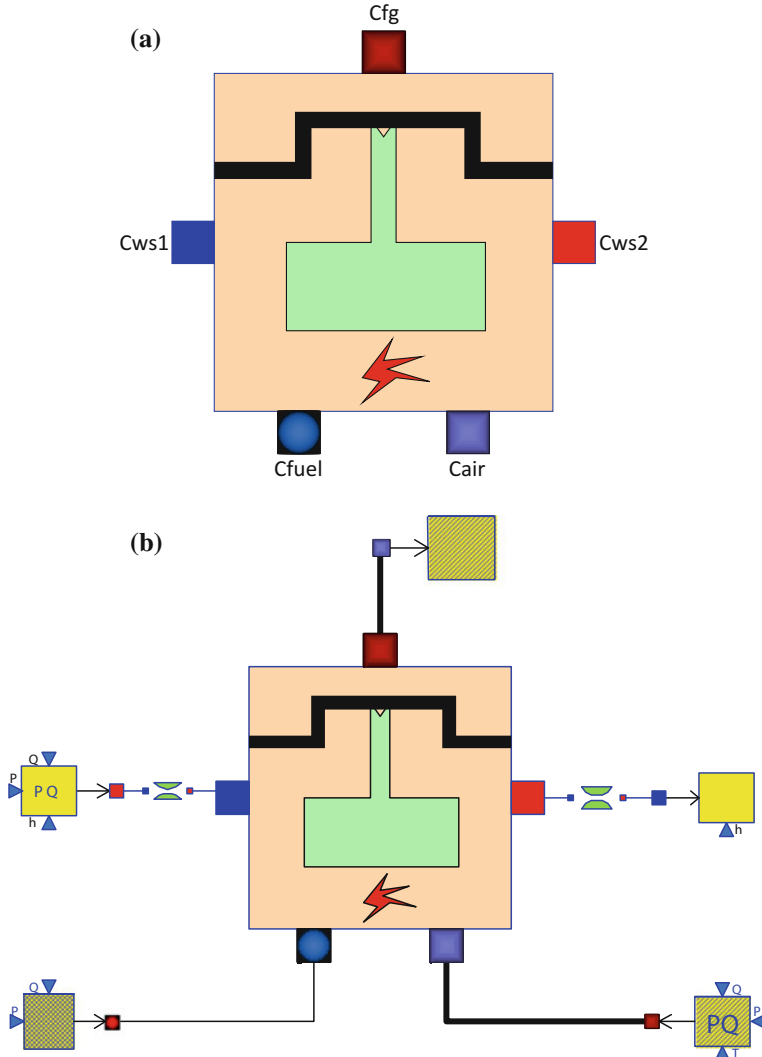


**Fig. 15.2** a Icon of the *InternalCombustionEngine* component model. b Test-case for the *InternalCombustionEngine* component model

## 15.4 Test-Case

The model *TestInternalCombustionEngine* used to validate the *InternalCombustionEngine* component model is represented in Fig. 15.2b. This model uses the following component models:

- One *InternalCombustionEngine* component model;
- One *SourcePQ* component model (for the flue gases);
- One *Sink* component model (for the flue gases);
- One *SourcePQ* component model (for water/steam);
- One *Sink* component model (for water/steam);
- One *FuelSourcePQ* component model (for the fuel).

In this test-case scenario, the *InternalCombustionEngine* component receives: (1) the air pressure, mass flow rate, temperature, and composition at the inlet; (2) the fuel pressure, mass flow rate, temperature, lower heat value, and composition at the inlet; and (3) the water pressure, mass flow rate, and specific enthalpy at the inlet. The component computes (1) the flue gases temperature, pressure, and composition at the outlet; (2) the water pressure and specific enthalpy at the outlet; and (3) the mechanical and electrical power produced by the engine.

### 15.4.1 Test-Case Parameterization and Boundary Conditions

The model data are:

- Mechanical efficiency type = 2
- $a$  ( $x^2$  coefficient of the linear mechanical efficiency) =  $-5.4727 \times 10^{-9}$
- $b$  ( $x$  coefficient of the linear mechanical efficiency) =  $4.9359 \times 10^{-5}$
- $c$  (constant coefficient of the linear mechanical efficiency) = 0.30814
- Engine electrical efficiency = 0.97
- Thermal loss fraction to the cooling water = 0.05
- Thermal loss fraction to the ambient = 0.2
- Gas average molar mass = 20 g/mol
- Water pressure loss as percent of the pressure at the inlet = 1%
- Pressure difference between the inlet and the outlet (air–flue gases) = 0
- Engine volume ratio = 6.45
- Compression polytropic coefficient = 1.28
- Expansion polytropic coefficient = 1.33
- Air temperature at the inlet = 303.16 K
- Air pressure at the inlet =  $1.91 \times 10^5$  Pa
- Air mass flow rate at the inlet = 1.9627 kg/s
- $\text{CO}_2$  mass fraction in the air at the inlet = 0

- H<sub>2</sub>O mass fraction in the air at the inlet = 0.005
- O<sub>2</sub> mass fraction in the air at the inlet = 0.25
- SO<sub>2</sub> mass fraction in the air at the inlet = 0
- Water specific enthalpy at the inlet = 334410 J/kg
- Water pressure at the inlet =  $4.1 \times 10^5$  Pa
- Water mass flow rate at the inlet = 15.3 kg/s
- Fuel temperature at the inlet = 299 K
- Fuel pressure at the inlet =  $2.103 \times 10^5$  Pa
- Fuel mass flow rate at the inlet = 0.0676 kg/s
- Lower heating value of the fuel =  $50 \times 10^6$  J/kg
- Fuel humidity = 0
- C mass fraction in the fuel = 0.75
- H mass fraction in the fuel = 0.25
- Ashes mass fraction in the fuel = 0
- Fuel density = 0.744 kg/m<sup>3</sup>.

#### ***15.4.2 Model Calibration***

The calibration step consists in setting the water specific enthalpy at the outlet to a known measurement value to compute by model inversion the value of the water mass flow rate at the inlet.

Other possible calibration procedures:

- Setting the mechanical power to a known measurement value to compute by model inversion the value of the mass flow rate of the fuel;
- Setting the combustion air ratio to a known measurement value to compute by model inversion the value of the air mass flow rate.

#### ***15.4.3 Simulation Results***

The simulation of the test scenario gives the numerical results below:

- Flue gases temperature at the exhaust = 797.66 K
- Water specific enthalpy at the outlet = 378,593 J/kg
- Mechanical power = 1,394,080 W
- Combustion air ratio = 1.677.

# Chapter 16

## Solar Collector Modeling



**Abstract** Solar thermal power plants are a key technology for electricity generation from renewable energy resources. Concentrated solar power (CSP) systems collect and concentrate sunlight (solar radiation) to produce thermal energy which can be stored and used to produce electricity in a thermodynamic cycle (Rankine cycle or Brayton cycle). There are several types of concentrating solar power systems.

**Central Receiver Systems (CRSs):** CRSs use a field of distributed mirrors—heliostats—that individually track the sun and focus the sunlight on the receiver by concentrating the sunlight 600–1000 times. The wall temperature of the receiver can reach up to 650 °C. Thus, the solar energy is transferred to the working fluid and then used to generate steam to power a conventional turbine.

**Linear Parabolic Trough Collectors (PTSCs):** PTSCs concentrate the solar radiation through long rectangular curved mirrors. The mirrors are tilted toward the sun, focusing sunlight on the absorber pipe that runs down the focus line of parabolic trough collectors. The absorber pipes heat up the oil to nearly 400 °C, and a heat exchanger transfers the heat of the oil to a water/steam cycle (Rankine cycle).

**Linear Fresnel Reflectors (LFRs):** LFRs concentrate the solar radiation through long parallel rows of flat mirrors. These modular mirrors focus the sunlight onto the receiver, which consists of a system of tubes through which working fluid is pumped.

In this chapter, we present two types of solar collector components, the PTSC and the LFR, and give a detailed description of the physical equations for each of them. We give a test-case for each model that includes the structure of the model, parameterization data, and results of simulation. The full description of the physical equations is independent of the programming languages and tools.

## 16.1 Linear Parabolic Trough Collector (PTSC)

A PTSC receiver (Fig. 16.1) contains a parabolic reflective surface and a receiver tube. The receiver tube is located at the focus line of the parabolic reflective surface which transfers the absorbed solar energy to a synthetic heat transfer fluid pumped through the absorber tube. The absorber tube is located inside the receiver tube and coated with blackened nickel to ensure high absorption. The absorber tube is contained in a glass envelope that is transparent to solar radiation. The annulus gap between the absorber tube and the glass envelope is vacuumed in order to reduce heat losses to the ambient.

The absorber tubes heat up the synthetic oil to nearly 400 °C, and a heat exchanger transfers the heat of the thermal oil to a water/steam cycle in order to produce electricity.

### 16.1.1 Nomenclature

Symbols	Definition	Unit	Mathematical definition
$A_{g,i}$	External glass surface for cell $i$	$\text{m}^2$	$\pi \cdot (D_g + 2 \cdot e) \cdot \frac{L}{N}$
$A_r$	Reflector surface (Barakos 2006)	$\text{m}^2$	$4f \cdot \tan\left(\frac{\varphi_R}{2}\right) \cdot L$
$A_{t,i}$	External pipe surface (absorber) for cell $i$	$\text{m}^2$	$\frac{\pi \cdot D \cdot L}{N}$
$c_{p,g}$	Specific heat capacity of the glass	J/kg/K	
$D$	External pipe diameter (absorber)	m	
$D_g$	Internal glass diameter	m	
DNI	Incident energy (direct normal irradiance)	W/m <sup>2</sup>	
$e$	Glass thickness or wall thickness	m	
$f$	Focal length	m	
$F_{12}$	View factor to surroundings (radiation heat loss)	—	
$h_c$	Convective heat transfer coefficient between the ambient air and the glass envelop	W/m <sup>2</sup> /K	
$K$	Incidence angle modifier	—	$\cos(\theta)$
$L$	Absorber pipe length	m	

(continued)

(continued)

Symbols	Definition	Unit	Mathematical definition
$m_g$	Glass mass for cell $i$	kg	$\rho_g \cdot \frac{L}{N} \cdot \frac{\pi}{4} \cdot ((D_g + 2e)^2 - D_g^2)$
$N$	Number of cells (segments)	—	
$R$	Mirror reflectivity	—	
$T_{\text{atm}}$	Atmospheric temperature	K	
$T_{g,i}$	Glass temperature for cell $i$	K	
$T_{\text{sky}}$	Sky temperature	K	$0.0552 \cdot T_{\text{atm}}^{1.5}$
$T_{w,i}$	Temperature of the outer absorber surface for cell $i$	K	
$W_{\text{abs,g},i}$	Power absorption by the glass envelop for cell $i$	W	
$W_{\text{abs,t}}$	Solar radiation absorbed by the receiver	W	
$W_{\text{cond,t:g},i}$	Conduction power between the outer absorber surface and the inner glass surface for cell $i$	W	
$W_{\text{conv,g:air},i}$	Convection power loss from the outer glass envelop surface to the ambient air for cell $i$	W	
$W_{\text{rad,t},i}$	Radiation power from the outer absorber surface and the inner glass surface for cell $i$	W	
$W_{\text{rad,g:sky},i}$	Radiation power loss from the outer glass envelop surface to the sky for cell $i$	W	
$W_{t,i}$	Total power transferred to the pipe (absorber) for cell $i$	W	
$\tau$	Glass transmissivity	—	
$\alpha_g$	Glass absorptivity	—	
$\alpha_t$	Tube absorptivity	—	
$\gamma$	Interception factor	—	
$\varepsilon_g$	Glass emissivity	—	
$\varepsilon_t$	Tube emissivity	—	
$\eta_{\text{opt}}$	Optical efficiency	—	
$\theta$	Zenith angle	°	
$\lambda$	Gas thermal conductivity between the tube and the glass	W/(m K)	
$\rho_g$	Glass density	kg/m <sup>3</sup>	
$\sigma$	Stefan–Boltzmann constant	W/(m <sup>2</sup> K <sup>4</sup> )	$5.67 \times 10^{-8}$
$(\tau\alpha)_n$	Transmissivity-absorptivity factor	—	
$\varphi_R$	Rim angle	°	
$\phi_{\text{sun}}$	Solar radiation (direct normal irradiance—DNI)	W/m <sup>2</sup>	

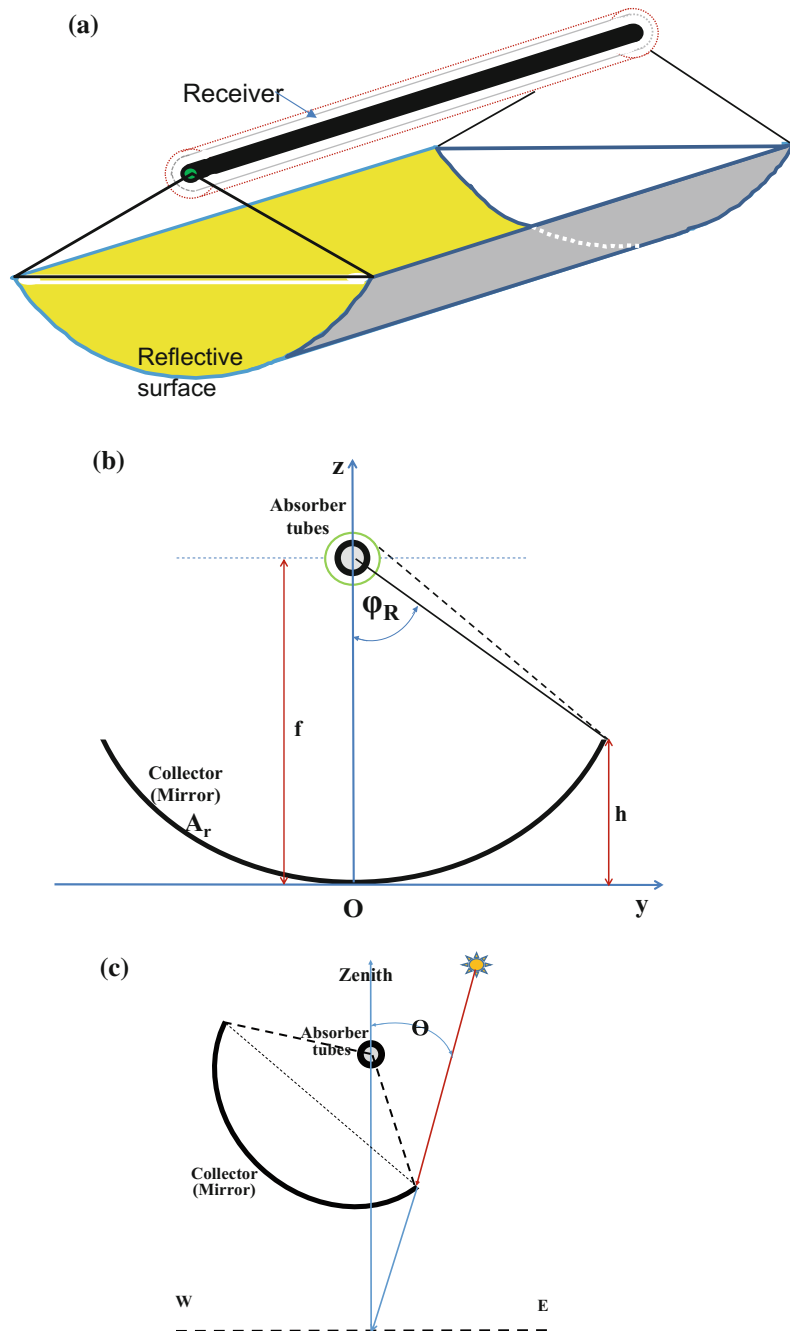


**Fig. 16.1** **a** Schematic diagram of a PTSC receiver, **b** characteristics of the PTSC receiver parabola, **c** PTSC receiver zenith angle

### 16.1.2 Assumptions

The PTSC receiver is modeled according to the following assumptions:

- 1D modeling.
- Mass accumulation is considered in each mesh cell (glass).
- The phenomenon of longitudinal heat conduction in the glass wall is neglected.

### 16.1.3 Governing Equations

The *SolarCollector* model is a steady-state model (accumulation is considered in the glass), based on first principle energy balance equations and on heat transfer phenomena occurring in PTSC receiver tube (Qu et al. 2006). The model takes into account heat losses from the receiver to the outside by radiation, conduction, and convection; cf. Fig. 16.2.

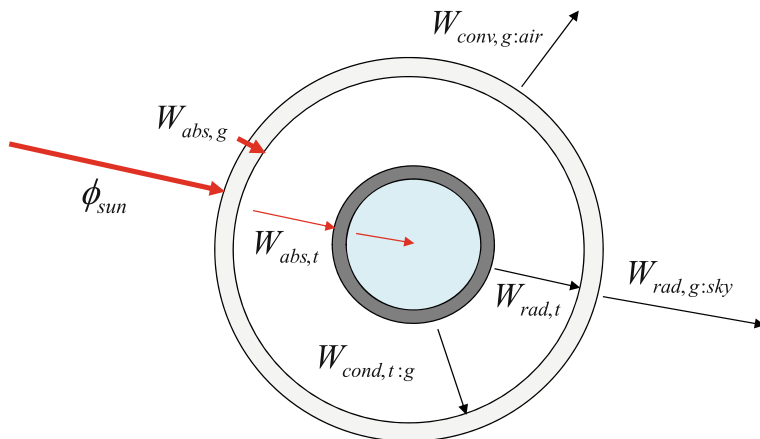


**Fig. 16.2** Thermal loss in a PTSC receiver tube

---

Equation 1

---

Title	Solar radiation absorbed by the receiver (reflector total power)
Mathematical formulation	$W_{\text{abs,t}} = \eta_{\text{opt}} \cdot \phi_{\text{sun}} \cdot A_r$
Comments	<p>The optical efficiency is given by Qu et al. (2006):  <math>\eta_{\text{opt}} = R \cdot (\tau\alpha)_n \cdot \gamma \cdot K</math></p> <p>The transmissivity-absorptivity factor is given by Kaushika and Arulanantham (1996):  <math>(\tau\alpha)_n = \tau \cdot \alpha \cdot \frac{1}{1 - (1 - \alpha) \cdot (1 - \tau)}</math></p> <p>where <math>\tau</math> is the transmissivity and <math>\alpha</math> is the absorptivity</p>

---



---

Equation 2

---

Title	Energy balance equation for the glass
Mathematical formulation	$m_g \cdot c_{p,g} \cdot \frac{dT_{g,i}}{dt} = W_{\text{abs,g},i} + W_{\text{rad,t},i} + W_{\text{cond,t:g},i} - W_{\text{rad,g:sky},i} - W_{\text{conv,g:air},i}$
Comments	<p>This equation calculates the glass temperature <math>T_{g,i}</math>.</p> <p>Similar to Eq. 1, the power absorption by one segment of the glass envelop is given by:</p> $W_{\text{abs,g},i} = \eta_{\text{opt}} \cdot \phi_{\text{sun}} \cdot \frac{A_r}{N} = R \cdot \alpha_g \cdot \gamma \cdot K \cdot \phi_{\text{sun}} \cdot \frac{A_r}{N}$ <p>The radiation power from the outer absorber surface to the inner glass surface is given by (cf. (2.83)):</p> $W_{\text{rad,t},i} = \sigma \cdot A_{t,i} \cdot \epsilon_t \cdot (T_{w,i}^4 - T_{g,i}^4)$ <p>The conduction power from the outer absorber surface to the inner glass surface is given by (cf. (2.80)):</p> $W_{\text{cond,t:g},i} = \frac{A_{t,i} \cdot \lambda \cdot (T_{w,i} - T_{g,i})}{\frac{\rho}{2} \ln \left( \frac{T_g}{D} \right)}$ <p>See Incropera et al. (2006) for a demonstration of this equation.</p> <p>The radiation power loss from the outer glass envelop surface to the sky is given by (cf. (2.83)):</p> $W_{\text{rad,g:sky},i} = F_{12} \cdot \sigma \cdot A_{g,i} \cdot \epsilon_g \cdot (T_{g,i}^4 - T_{\text{sky}}^4)$ <p>The convection power loss from the outer glass envelop surface to the ambient air is given by (cf. (2.84)):</p> $W_{\text{conv,g:air},i} = A_{g,i} \cdot h_c \cdot (T_{g,i} - T_{\text{atm}})$ <p><math>h_c</math> is given as input by the user</p>

---



---

Equation 3

---

Title	Energy balance equation for the pipe (power transferred to the absorber)
Mathematical formulation	$W_{t,i} = \frac{W_{\text{abs,t}}}{N} - W_{\text{rad,g:sky},i} - W_{\text{conv,g:air},i}$
Comments	The net power received by each tube segment is equal to the total power absorbed by the receiver for that segment minus the losses by radiation to the sky and convection to the ambient for that segment

---

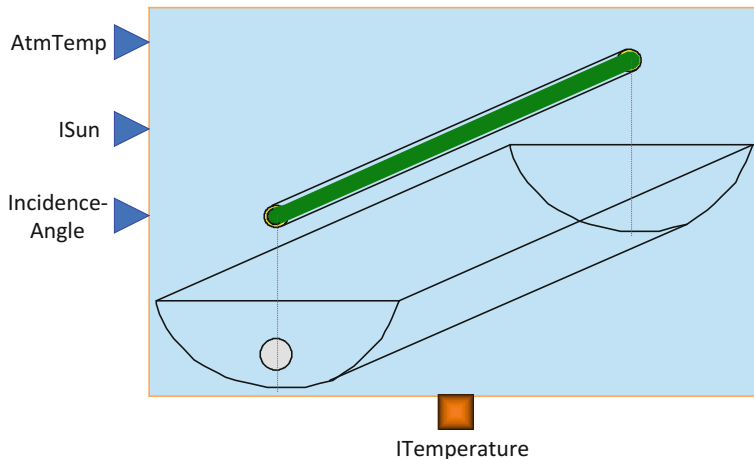


**Fig. 16.3** Icon of the *SolarCollector* component model

#### 16.1.4 Modelica Component Model: SolarCollector

The governing equations are implemented in the *SolarCollector* component model located in the *Solar.Collectors* sub-library. Figure 16.3 represents the graphical icon of the component with its four connectors.

#### 16.1.5 Test-Case

See Sect. 6.7 where the component is utilized in a complete concentrated solar power plant model.

## 16.2 Linear Fresnel Reflector (LFR)

The linear Fresnel reflector (LFR) is similar to the parabolic trough collector (PTSC). The LFR concentrates the solar radiation through long parallel rows of flat mirrors. These modular mirrors focus the sunlight onto the receiver, which consists of a system of tubes through which the working fluid is pumped; cf. Fig. 16.4. In addition, another mirror is placed above the absorber tube (in the cavity) to reduce optical losses.

Flat mirrors allow more reflective surface in the same amount of space than a parabolic reflector, and they are much cheaper than parabolic reflectors. Also,

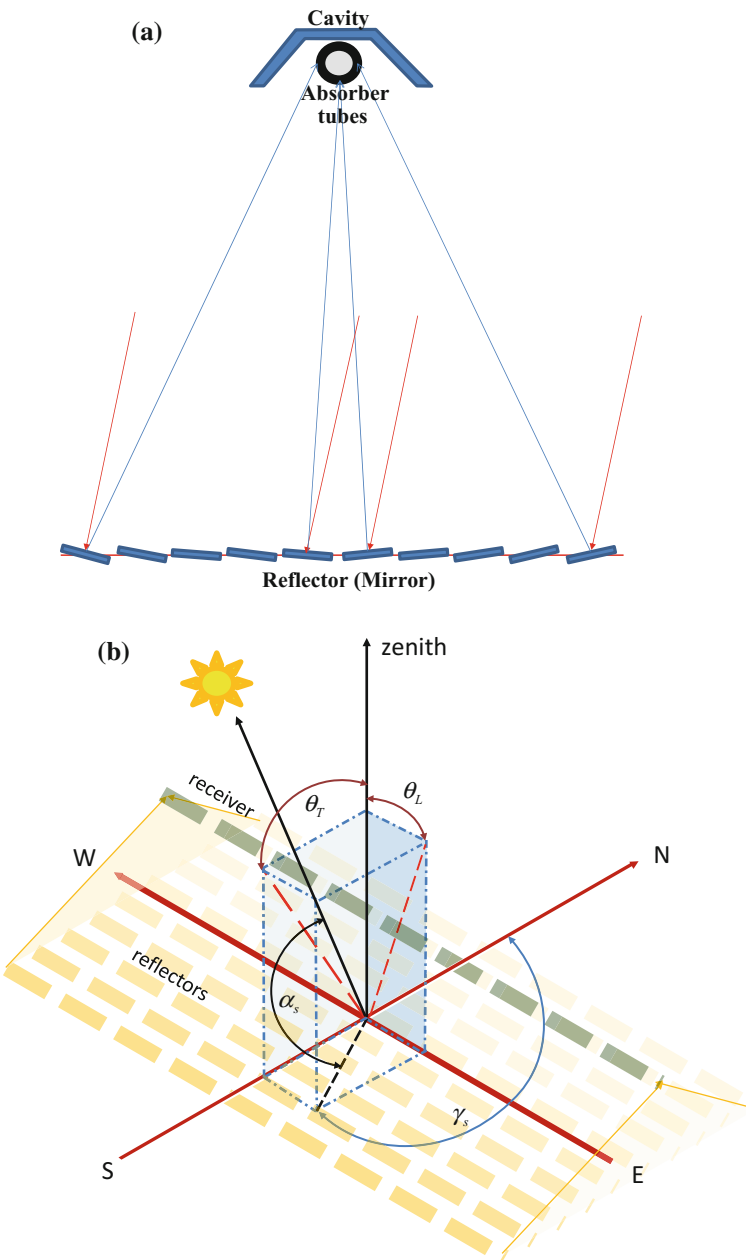


**Fig. 16.4** **a** Schematic diagram of a linear Fresnel reflector and **b** solar optics of a LFR: main angles

unlike the linear parabolic trough collector, the receiver is not moving and thus made up of fewer moving parts. This eliminates the need for strengthening materials.

### 16.2.1 Nomenclature

Symbols	Definition	Unit	Mathematical definition
$a$	Absorptivity of the collector	–	0.955
$A$	Area of all collectors	$\text{m}^2$	
$A_{t,i}$	External pipe surface (absorber) for cell $i$	$\text{m}^2$	$\frac{\pi \cdot D \cdot L}{N}$
$D$	External pipe diameter (absorber)	m	
$F_{12}$	View factor to surroundings (radiation heat loss)	–	
$h_c$	Convective heat transfer coefficient between the ambient air and the pipe	$\text{W}/\text{m}^2/\text{K}$	
$K_L$	Longitudinal incidence angle modifier	–	
$K_T$	Transversal incidence angle modifier	–	
$L$	Length of the collector	m	$\frac{A}{w}$
$N$	Number of cells (sections) in the solar field	–	
$T_{\text{atm}}$	Atmospheric temperature	K	
$T_{\text{sky}}$	Sky temperature	K	$0.0552 \cdot T_{\text{atm}}^{1.5}$
$T_{w,i}$	Temperature of the outer receiver surface for cell $i$	K	
$w$	Aperture width of the collector	m	
$W_{\text{abs}}$	Solar radiation absorbed by the receiver	W	
$W_{\text{conv},i}$	Convection power loss from the outer pipe surface to the ambient air for cell $i$	W	
$W_{\text{rad},i}$	Radiation power losses from the outer pipe surface to the ambient for cell $i$	W	
$W_{t,i}$	Thermal power transferred to the fluid for each cell (section) for cell $i$	W	
$z$	Height of the collector	m	
$\alpha_s$	Sun elevation angle (angle between the straight line to the sun and the horizontal plane)	°	
$\gamma_s$	Sun azimuth angle (angle between the North and the solar position projected on the horizontal plane)	°	
$\varepsilon_t$	Tube emissivity	–	
$\eta_{\text{av}}$	Mean availability of the solar field	–	$\leq 1$
$\eta_{\text{cl}}$	Mean cleanliness factor	–	$\leq 1$

(continued)

(continued)

Symbols	Definition	Unit	Mathematical definition
$\eta_{\text{opt}}$	Optical efficiency at normal irradiation	—	
$a$	Mean sun tracking system factor	—	$\leq 1$
$\theta_L$	Longitudinal incidence angle (angle between the zenith and the projection of the straight line to the sun onto the longitudinal plane “North–South”)	°	
$\theta_T$	Transverse incidence angle (angle between the zenith and the projection of the straight line to the sun onto the transverse plane “North–South”)	°	
$\rho$	Reflexivity of the primary reflector	—	$\approx 0.935$
$\sigma$	Stefan–Boltzmann constant	$\text{W}/(\text{m}^2 \text{ K}^4)$	$5.67 \times 10^{-8}$
$\tau$	Transmissivity of the pipe wall	—	$\approx 0.965$
$\phi_{\text{sun}}$	Solar radiation (direct normal irradiance—DNI)	$\text{W}/\text{m}^2$	
$\chi$	Geometric default factor		0.725

### 16.2.2 Governing Equations

Equation 1

Title	Thermal power received by the receiver
Mathematical formulation	$W_{\text{rec}} = A \cdot \phi_{\text{sun}} \cdot \eta_{\text{opt}} \cdot K_T \cdot K_L \cdot \eta_{\text{av}} \cdot \eta_{\text{tr}} \cdot \eta_{\text{cl}}$
Comments	<p>The optical efficiency at normal irradiation is given by Morin et al. (2012):</p> $\eta_{\text{opt}} = \rho \cdot a \cdot \tau \cdot \chi$ <p>It is also possible for the user to directly provide a value for <math>\eta_{\text{opt}}</math>. The polynomial function <math>K_T</math> is obtained by polynomial interpolation based on the values obtained from Novatec Solar (2012). So, the transverse incidence angle modifier is given by:</p> $K_T = 3 \times 10^{-10} \cdot  \theta_T ^5 - 5 \times 10^{-8} \cdot  \theta_T ^4 + 1 \times 10^{-6} \cdot  \theta_T ^3 - 3 \times 10^{-5} \cdot  \theta_T ^2 - 4 \times 10^{-4} \cdot  \theta_T  + 0.995$ <p>The longitudinal incidence angle modifier is given by:</p> $K_L = \cos(\theta_L) \cdot (1 - \frac{\varepsilon}{L} \cdot \tan(\theta_L))$ <p>The longitudinal incidence angle is given by Feldhoff (2012):</p> $\theta_L = a \cdot \cos\left(\sqrt{(1 - \cos^2(\alpha_s) \cdot \cos^2(\gamma_s))}\right)$ <p>The transverse incidence angle is given by Feldhoff (2012):</p> $\theta_T = \begin{cases} 90 & \text{for }  \sin(\alpha_s)  \leq 10^{-6} \\ \arctan\left(\frac{\sin(\gamma_s)}{\tan(\alpha_s)}\right) & \text{for }  \sin(\alpha_s)  > 10^{-6} \end{cases}$

---

Equation 2

---

Title	Energy balance equation for each cell (power transferred to the fluid)
Mathematical formulation	$W_{t,i} = \frac{W_{\text{abs}}}{N} - W_{\text{rad},i} - W_{\text{conv},i}$
Comments	The net power received by each tube segment is equal to the total power absorbed by the receiver for that segment minus the losses by radiation to the sky and convection to the ambient for that segment

---

Equation 3

---

Title	Radiation power losses
Mathematical formulation	$W_{\text{rad},i} = 0.5 \cdot F_{12} \cdot \sigma \cdot A_{t,i} \cdot \varepsilon_t \cdot (T_{w,i}^4 - T_{\text{sky}}^4)$
Comments	Cf. (2.83)

---

Equation 4

---

Title	Convection power losses to the ambient
Mathematical formulation	$W_{\text{conv},i} = A_{t,i} \cdot h_c \cdot (T_{w,i} - T_{\text{atm}})$
Comments	Cf. (2.84) $h_c$ is given as input by the user

---

### 16.2.3 Modelica Component Model: FresnelField

The governing equations are implemented in the *FresnelField* component model located in the *Solar.Collectors* sub-library. Figure 16.5a represents the graphical icon of the component with its five connectors.

### 16.2.4 Test-Case

The model *TestFresnelField* used to validate the *FresnelField* component model is represented in Fig. 16.5b. This model uses the following component models:

- One *FresnelField* component model;
- One *HeatExchangerWall* component model;
- One *DynamicTwoPhaseFlowPipe* component model;
- One *SourceQ* component model;
- One *SinkP* component model;
- Three *Ramp* blocks.

In the test-case scenario, the model receives: (1) the fluid mass flow rate and specific enthalpy at the inlet, (2) the fluid pressure at the outlet, and (3) the DNI. The component computes: (1) the thermal power transferred to the fluid, (2) the fluid specific enthalpy at the outlet, and (3) the fluid pressure at the inlet.

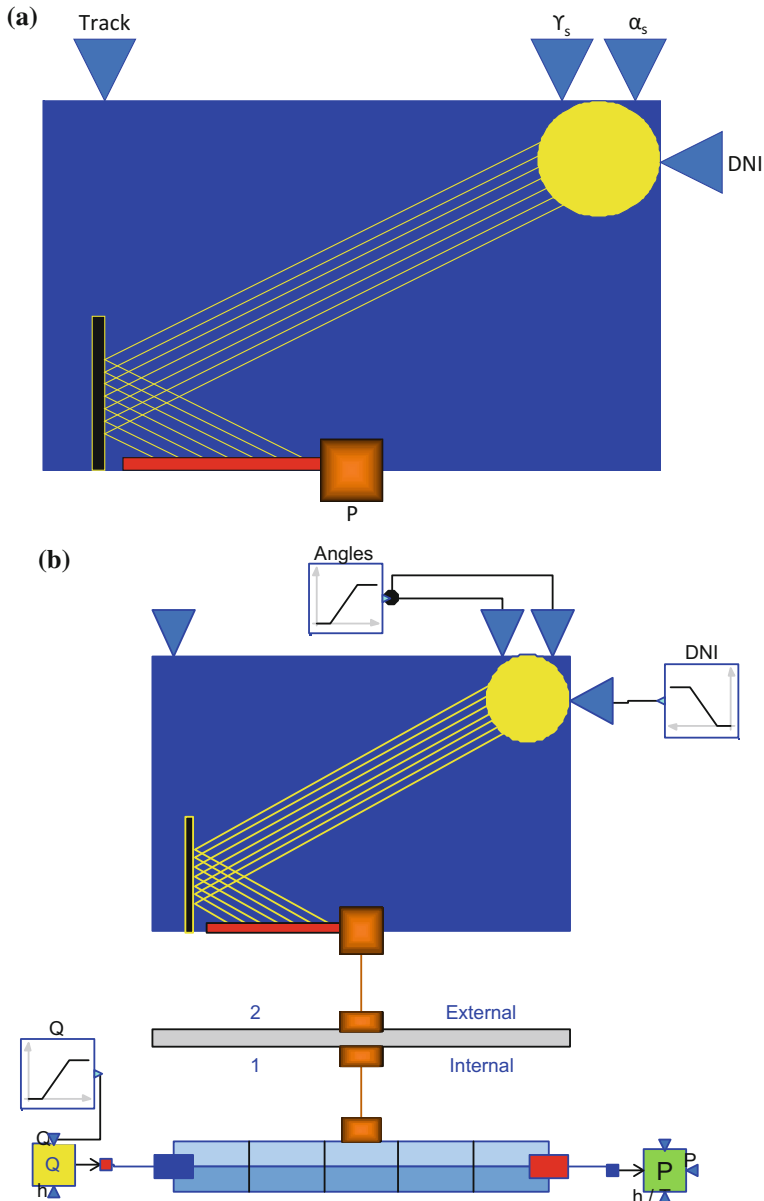


**Fig. 16.5** **a** Icon of the *FresnelField* component model and **b** test-case for the *FresnelField* component model

#### 16.2.4.1 Test-Case Parameterization and Boundary Conditions

The model data are:

- Aperture area of the collectors =  $5.5 \times 10^4 \text{ m}^2$
- mode\_efficiency = 1
- Global optical efficiency at normal irradiation = 0.625
- Reflexivity of the primary reflector = 0.935
- Absorptivity of the collector = 0.955
- Transmissivity of the glass envelope = 0.965
- Geometric default factor = 0.725
- Mean availability of the solar field = 1
- Mean cleanliness factor = 1
- Height of a collector = 7.4 m
- Length of a collector = 54 m
- Aperture width of a collector = 11.46 m
- Internal tube diameter = 0.07 m
- Heat transfer coefficient between the ambient and the pipe = 4 W/m<sup>2</sup>/K
- View factor to surroundings (radiation heat loss) = 0.6366
- Tube emissivity = 0.8
- Atmospheric temperature = 300 K
- Number of sections in the field = 30
- Internal diameter of the pipe = 0.07 m
- Length of the pipe = 50 m
- Inlet altitude of the pipe = 0
- Outlet altitude of the pipe = 0
- Pipe wall thickness = 0.004 m
- Wall thermal conductivity = 20 W/m/K
- Water specific enthalpy at the inlet = 1500 kJ/kg
- Water pressure at the outlet =  $125 \times 10^5 \text{ Pa}$ .

#### 16.2.4.2 Model Calibration

The calibration procedure consists in setting the fluid pressure at the inlet to a known measurement value and computing by model inversion the value of the pressure loss coefficient in the pipe.

Another possible calibration consists in setting the fluid specific enthalpy at the outlet to a known measurement value and computing by model inversion the value of the collector area.

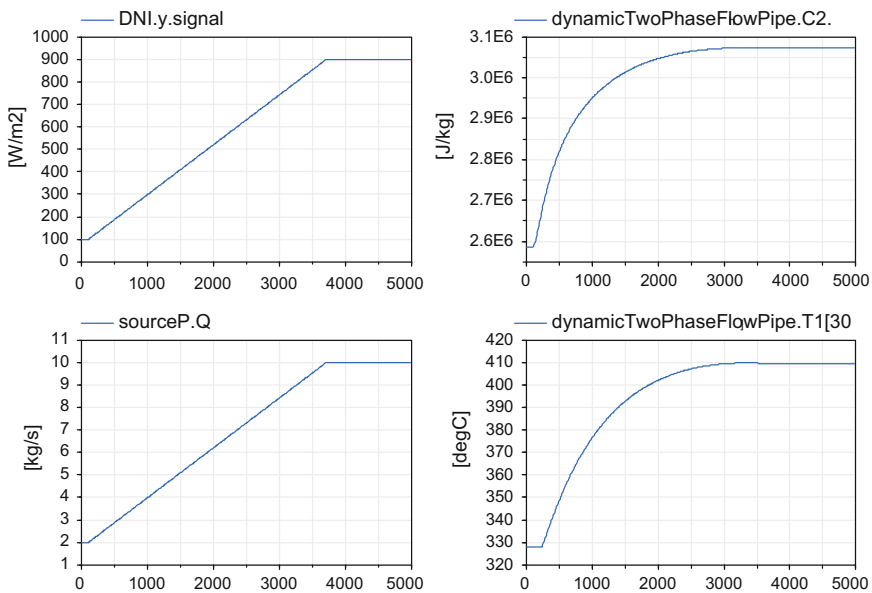


**Fig. 16.6** Simulation results: DNI, water/steam mass flow rate for one pipe, steam specific enthalpy at the outlet, and steam temperature at the outlet of the absorber pipe

#### 16.2.4.3 Simulation Results

Figure 16.6 shows the results of the simulation. When the DNI goes from 100 to 900 W/m<sup>2</sup>, the temperature of the steam at the outlet of the absorber pipe increases from 328 to 410 °C.

## References

- Barakos G (2006) Design, simulation and performance of reflecting parabolic solar collector. Socrates Program, European Summer School, Technological Educational Institute of Patra
- Feldhoff JF (2012) Linear fresnel collectors, a technology overview. SFERA Summer School, 28 Jun 2012, Almería, Spain (DLR)
- Incropera F, DeWitt P, Bergman T, Lavine A (2006) Fundamentals of heat transfer. Wiley, New Jersey
- Kaushika ND, Arulanantham M (1996) Transmittance-absorptance product of solar glazing with transparent insulation materials. Sol Energy Mater Sol Cells 44:383–395

- Morin G, Dersch J, Platzer W, Eck M, Häberle A (2012) Comparison of linear fresnel and parabolic trough collector power plants. Sol Energy 86(1):1–12
- Novatec Solar (2012) Turnkey solar boiler, mass produced in industrial precision—with performance guarantee. Novatec Brochure, available from [http://novatecsolar.com/files/120510\\_novatec\\_solar\\_product\\_brochure\\_english\\_web.pdf](http://novatecsolar.com/files/120510_novatec_solar_product_brochure_english_web.pdf)
- Qu M, Archer D, Masson S (2006) A linear parabolic trough solar collector performance model. Renew Energy Resour Greener Future VIII-3-3

# Chapter 17

## Implementation of the Fluid Equations into Component Models



**Abstract** This chapter introduces the notion of staggered grid scheme and explains how it can be used to implement the thermal hydraulics equations into component models. The staggered grid is made of two superimposed grids, the first implementing the mass and energy balance equations, and the second implementing the momentum balance equations. Components from each grid are then connected together via so-called connectors. Connections are made according to well defined rules in order to exchange the variables common to different balance equations so that the full state of the system can be computed. Several alternatives are possible for the structure of the connectors. The fundamental choices made for the structure of ThermoSysPro are given.

### 17.1 The Staggered Grid Scheme

#### 17.1.1 Nomenclature

Symbol	Definition	Unit
$h$	Fluid specific enthalpy	$\text{J kg}^{-1}$
$h_a$	Average specific enthalpy inside volume $a$	$\text{J kg}^{-1}$
$M(a)$	Component model associated with volume $a$	
$M(b:a)$	Component model associated with boundary $b:a$	
$\dot{m}(b \rightarrow a)$	Mass flow rate through boundary $b:a$ , positively from $b$ to $a$	$\text{kg s}^{-1}$
$P$	Fluid pressure	Pa
$P_a$	Average pressure in volume $a$	Pa
$s(x)$	Step function	—
$T$	Fluid temperature	K
$T_a$	Average temperature in volume $a$	K
$u$	Fluid specific internal energy	$\text{J kg}^{-1}$
$\Delta_{b \rightarrow a} h$	Variation of the specific enthalpy of the mass flow rate $\dot{m}(b \rightarrow a)$	$\text{J kg}^{-1}$
$\rho$	Fluid density	$\text{kg m}^{-3}$

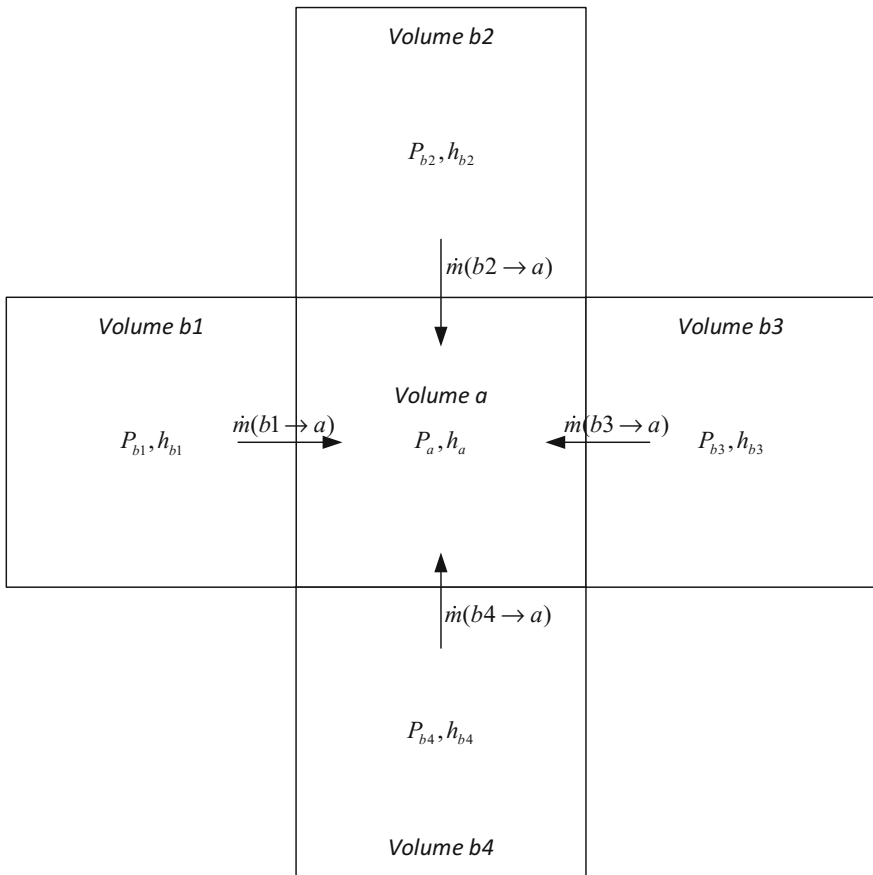


**Fig. 17.1** Thermodynamic states and mass flow rates (Bouskela and El Hefni 2014)

### 17.1.2 Principle of the Staggered Grid Scheme

The model equations are divided into two main groups (cf. Fig. 17.1):

1. Those that compute the thermodynamic states  $(P_a, h_a)$  or  $(P_a, T_a)$ . In the following, only the  $(P_a, h_a)$  representation is considered as the discussion for the  $(P_a, T_a)$  representation is similar.
2. Those that compute the mass flow rates  $\dot{m}(b \rightarrow a)$ .

The thermodynamic state is a scalar field computed by the mass and energy balance equations.

The mass flow rates constitute a vector field computed by the momentum balance equations.

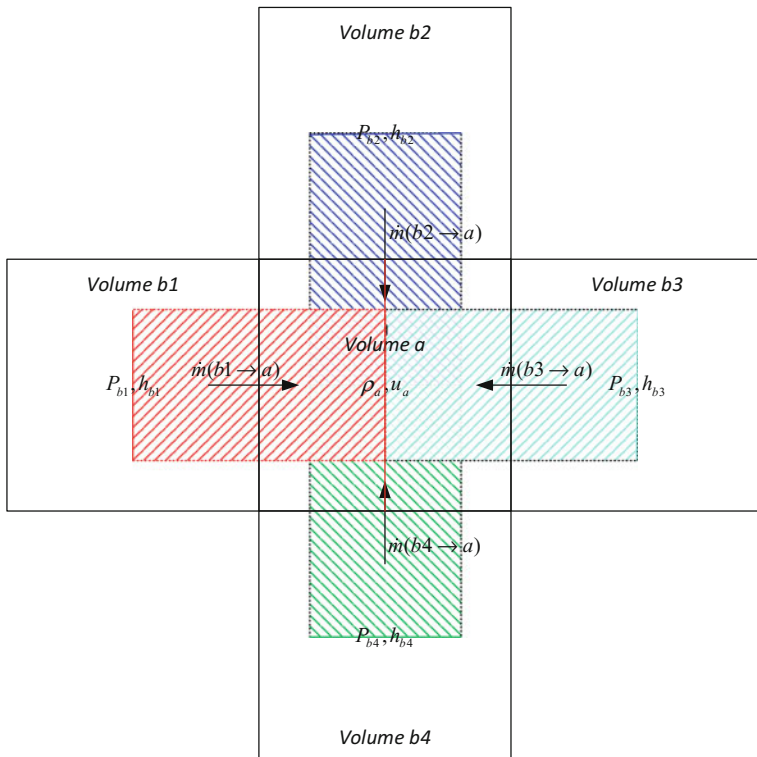


**Fig. 17.2** Staggered grid scheme

The mass and energy balance equations that compute the thermodynamic state  $(P_a, h_a)$  are implemented within the component model that represents volume  $a$ .

The momentum balance equation that computes the mass flow rate  $\dot{m}(b \rightarrow a)$  is implemented within the component model that represents the boundary  $b:a$  between volume  $a$  and volume  $b$ . However, this component model extends from the center of volume  $a$  to the center of volume  $b$  in order to take into account the pressure losses along the fluid path (cf. Fig. 17.2).

$\dot{m}(b \rightarrow a)$  is oriented positively from  $b$  to  $a$ . Consequently:

$$\dot{m}(a \rightarrow b) = -\dot{m}(b \rightarrow a)$$

There are thus two grid schemes: a first one that represents the scalar field  $(P_a, h_a)$  and a second one that represents the vector field  $\dot{m}(b \rightarrow a)$ . When superimposed, these two grid schemes give the so-called staggered grid scheme (cf. Fig. 17.2).

### 17.1.3 Volume Components and Flow Components

#### 17.1.3.1 Volume Components

By definition, the volume components are the component models associated with the mass and energy balance equations. They are also called thermal cells.

Volume components compute the thermodynamic states  $(P_a, h_a)$ .

The volume component that computes the thermodynamic state  $(P_a, h_a)$  is denoted as  $M(a)$ .

A volume component can have any number of fluid inlets or outlets as it can have any number of neighboring volume components.

A volume component  $M(a)$  represents an isobaric process because the fluid is at the same pressure at all inlets and outlets of the component, which is the average pressure  $P_a$  inside the volume.

#### 17.1.3.2 Flow Components

By definition, the flow components are the component models associated with the momentum balance equations. They are also called hydraulic cells.

Flow components compute the mass flow rates  $\dot{m}(b \rightarrow a)$ .

The flow component that computes the mass flow rate  $\dot{m}(b \rightarrow a)$  is denoted as  $M(b:a)$ . Notice that the mass flow rate  $\dot{m}(b \rightarrow a)$  is always constant within  $M(b:a)$ , but this property is not related to the conservation of mass: It is due to the fact that  $\dot{m}(b \rightarrow a)$  is the mass flow rate through the boundary  $b:a$  between volumes  $b$  and  $a$  and that  $M(b:a)$  represents this boundary.

A flow component has always one inlet and one outlet because it represents a boundary between two volumes.

For the following discussion, recall that according to (4.28),  $h_{b:a}$  is associated with the energy balance equation in volume  $a$ .

A flow component  $M(b:a)$  can be of two kinds: a tube component and a machine component.

#### Tube Components

A tube component  $M(b:a)$  is associated with an adiabatic pressure loss between volumes  $b$  and  $a$ . It represents an isenthalpic process because according to the upwind scheme (4.113), the fluid specific enthalpy  $h_{b:a}$  is constant between the inlet and the outlet of the component (cf. also (4.130)).

Then, for the adiabatic process:

$$h_{b:a} = s(\dot{m}(b \rightarrow a)) \cdot h_b + s(\dot{m}(a \rightarrow b)) \cdot h_a \quad (17.1)$$

which is equivalent to

$$h_{b:a} = \begin{cases} h_b & \text{if } \dot{m}(b \rightarrow a) > 0 \\ h_a & \text{if } \dot{m}(a \rightarrow b) > 0 \end{cases} \quad (17.2)$$

### **Machine Components**

A machine component  $M(b:a)$  is associated with a thermodynamic machine such as a pump or a turbine. It represents a thermodynamic process subject to the second law of thermodynamics that produces or absorbs mechanical work (cf. Sect. 2.8.2). Therefore, the fluid receives or releases heat during the process. The corresponding variation of specific enthalpy between the inlet  $b$  and the outlet  $a$  of the component is denoted as  $\Delta_{b \rightarrow a} h$ . It is computed using formulas such as (10.6) or (12.2) combined with (12.8) (cf. also comments of Eq. (1) in Sect. 12.2.2).

To account for the fact that the process is not adiabatic, the upwind scheme is modified as follows:

$$h_{b:a} = s(\dot{m}(b \rightarrow a)) \cdot (h_b + \Delta_{b \rightarrow a} h) + s(\dot{m}(a \rightarrow b)) \cdot h_a \quad (17.3)$$

which is equivalent to

$$h_{b:a} = \begin{cases} h_b + \Delta_{b \rightarrow a} h & \text{if } \dot{m}(b \rightarrow a) > 0 \\ h_a & \text{if } \dot{m}(a \rightarrow b) > 0 \end{cases} \quad (17.4)$$

$\Delta_{b \rightarrow a} h$  is positive if heat is provided to the fluid during the thermodynamic process; otherwise, it is negative.

It is assumed for (17.3) or (17.4) that the machine operates only for direct flows, i.e., when  $\dot{m}(b \rightarrow a) > 0$ . Otherwise, the machine is stopped and behaves like an adiabatic pressure loss, so that the regular upwind scheme (17.1) or (17.2) is applicable.

Equations (17.3) and (17.4) are a generalization of the upwind scheme to non-adiabatic processes, as when  $\Delta_{b \rightarrow a} h = 0$ , they are equivalent to (17.1) or (17.2).

#### **17.1.4 Connecting Volume Components to Flow Components**

In order to compute the mass, energy, and momentum balance equations throughout the network of component models, information must be shared between the different components.

Expanding the staggered grid scheme of Fig. 17.2 shows how volume components are related to flow components; cf. Fig. 17.3.

Volume components  $M(a)$  and  $M(b)$  provide, respectively, the thermodynamic states  $(P_a, h_a)$  and  $(P_b, h_b)$  to flow component  $M(b:a)$ .

Flow component  $M(b:a)$  provides the mass flow rate  $\dot{m}(b \rightarrow a)$  to volume components  $M(a)$  and  $M(b)$ .

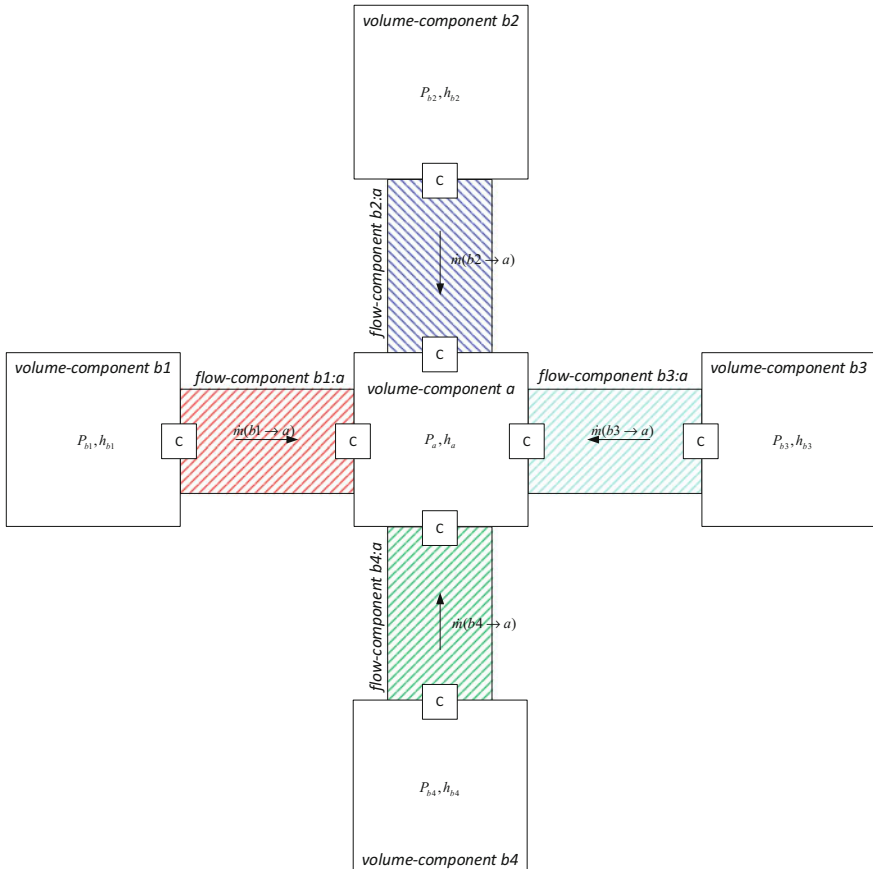


**Fig. 17.3** Expanded staggered grid scheme

The variables to be shared between components are grouped into so-called *fluid connectors*. Figure 17.3 shows how connectors represented as small boxes with capital letter  $C$  can be used to share variables between two neighboring components. However, this style is graphically not flexible, so the idea is to split a connector into two identical connectors, each attached to one of the neighboring components, and declare that they share the same variables by connecting them, as explained in the sequel.

A fluid connector attached to volume component  $M(a)$  and containing variables  $x$ ,  $y$ , and  $z$  is denoted as  $C_{\text{fluid},a}(x, y, z)$ .  $C_{\text{fluid},a,x}$ ,  $C_{\text{fluid},a,y}$ , and  $C_{\text{fluid},a,z}$  denote, respectively, variables  $x$ ,  $y$ , and  $z$  within  $C_{\text{fluid},a}$ . In a similar way,  $C_{\text{fluid},b:a}$  denotes a fluid connector attached to flow component  $M(b:a)$ .

Sharing connectors  $C_1(x, y, z)$  and  $C_2(x, y, z)$  is denoted (in this book)  $C_1 \equiv C_2$  and means that  $C_1.x \equiv C_2.x$ ,  $C_1.y \equiv C_2.y$  and  $C_1.z \equiv C_2.z$ , the sign “ $\equiv$ ” stating that the two variables on each side represent the same quantity (they are identical).

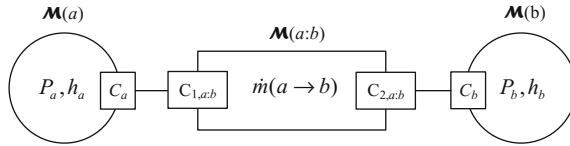


**Fig. 17.4** Connecting two volume components to a flow component

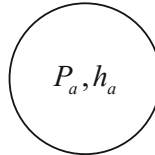


**Fig. 17.5** Closed volume

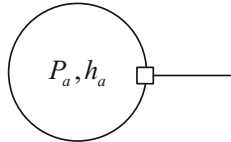


**Fig. 17.6** Source or sink

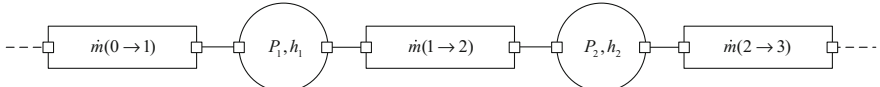


**Fig. 17.7** Discretized non-adiabatic pipe

When  $C_{\text{fluid},a}$  is connected to  $C_{\text{fluid},b:a}$ , then  $C_{\text{fluid},a} \equiv C_{\text{fluid},b:a}$  (the two connectors are identical).

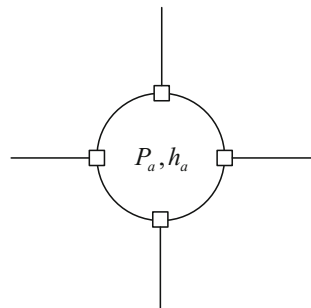
Sharing two connectors is graphically represented as shown in Fig. 17.4, where connector  $C_a$  is shared with connector  $C_{1,a:b}$  by connecting them with a line. This is how Modelica connectors are graphically connected. In the same way,  $C_b$  is connected to  $C_{2,a:b}$ .

Figure 17.3 shows that a connector is always shared between one volume component and one flow component only. Therefore, only one-to-one (1:1) connections need to be considered, and they always connect a volume component to a flow component.

The number of connectors that a component may have is equal to the number of its neighbors. Therefore, flow components have always two connectors, whereas volume components can have 0 to  $n$  connectors (i.e., as many as needed).

Volume components without any connectors ( $n = 0$ ) are closed volumes; cf. Fig. 17.5.

**Fig. 17.8** Mixing volume with four connectors



Volume components with one connector ( $n = 1$ ) are used to represent pressure sources or sinks (infinite reservoirs at constant pressure and temperature which act as boundary conditions); cf. Fig. 17.6.

Volume components with two connectors ( $n = 2$ ) are used to discretize non-adiabatic or compressible pipes in conjunction with flow components; cf. Fig. 17.7.

Volume components with three connectors or more ( $n \geq 3$ ) are used to represent frictionless mixing volumes; cf. Fig. 17.8.

### 17.1.5 Structure of the Connectors

In the following discussion, it is assumed that diffusion is neglected.

Section 17.1.4 shows how the physical state  $(P_a, h_a, \dot{m}(b \rightarrow a))$  is shared between volume component  $M(a)$  and flow components  $M(b:a)$  for all  $b \in V(a)$ ,  $V(a)$  being the set of volumes  $b$  neighboring  $a$ .

Let us check whether sharing those states between neighboring components is sufficient to compute the complete state of the system, i.e., the complete distribution of  $(P_a, h_a, \dot{m}(b \rightarrow a))$  for all volumes  $a$  in the complete connected model.

To compute the complete distribution of  $(P_a, h_a, \dot{m}(b \rightarrow a))$ , it is necessary and sufficient to compute all mass, energy, and momentum balance equations.

Inspecting the balance equations given by (4.7), (4.28), and (4.99), together with (17.1)–(17.4) and (2.28)–(2.31) that transform the  $(\rho, u)$  state representation into the  $(P, h)$  state representation, shows that for a given volume  $a$ :

1. To compute the right-hand side of the mass and energy balance equations, all flow components  $M(b:a)$  must provide  $\dot{m}(b \rightarrow a)$  to volume component  $M(a)$ .
2. To compute the terms  $h_{b:a}$  in the energy balance equation, all volume components  $M(b)$  must provide  $h'_b = h_b + \Delta_{b \rightarrow a}h$  to volume component  $M(a)$  through flow component  $M(b:a)$ .
3. To compute the momentum balance equations, volume component  $M(a)$  must provide  $(P_a, h_a)$  to flow component  $M(b:a)$ .

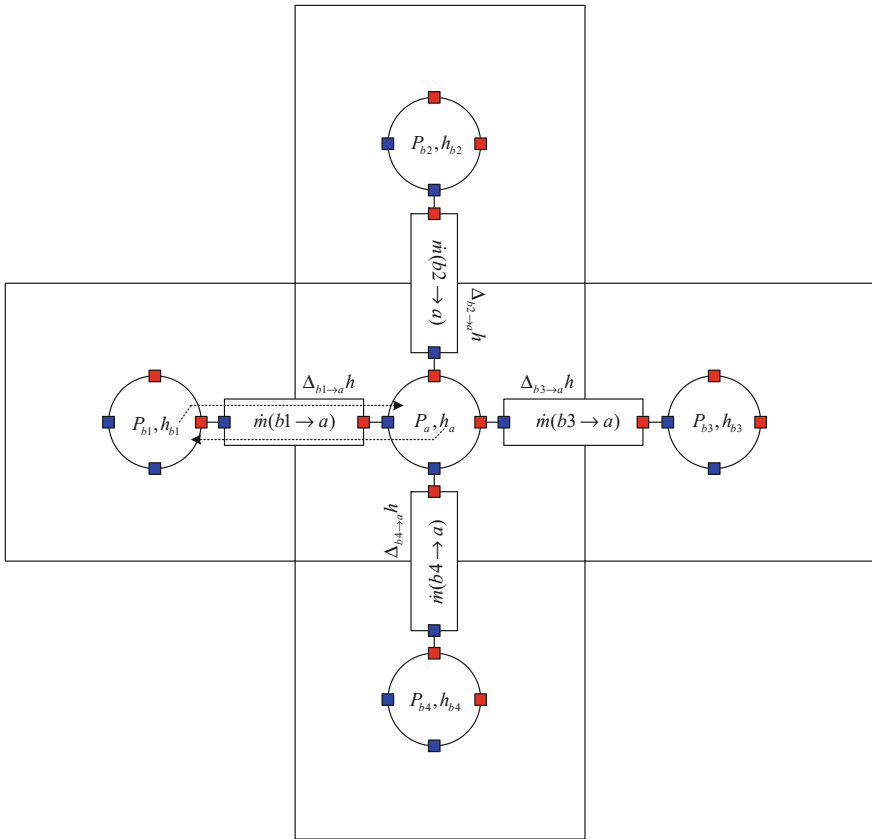


**Fig. 17.9** Information shared through the connectors

Therefore, the structure of the connector for volume  $a$  is:

$$C_{\text{fluid},a} = (P_a, h_a, h'_b, \dot{m}(b \rightarrow a)) \quad (17.5)$$

with

$$h'_b = h_b + \Delta_{b \rightarrow a}h \quad (17.6)$$

This representation is valid for all state representations, in particular for the  $(P, h)$  and  $(P, T)$  state representations. In case of flue gases, the chemical composition of the fluid should also be included in the connector.

Fig. 17.9 shows the information shared through the connectors between neighboring control volumes.

Thus, fluid connector (17.5) ensures that the full model can be computed.

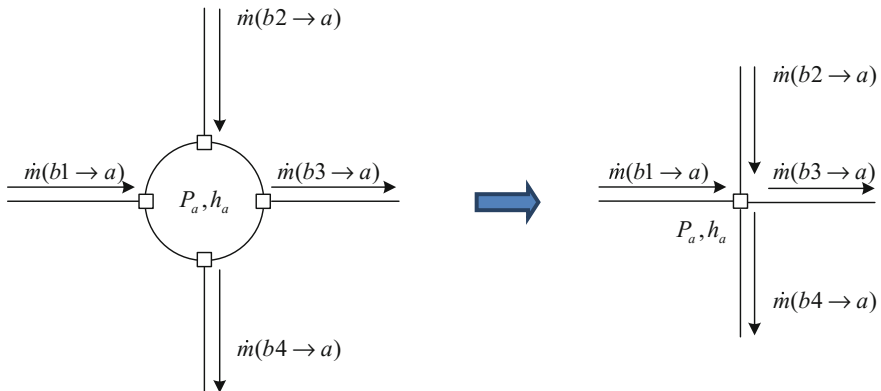
### 17.1.6 Case of Static Volume Components

#### 17.1.6.1 Static Volume Components with More Than Two Connectors

Static volume components can be considered to have zero (or quasi-zero) volumes, such as singular pressure losses. A better graphical representation would then be to represent these components as points, with the consequence that all their connectors would be superimposed (cf. Fig. 17.10).

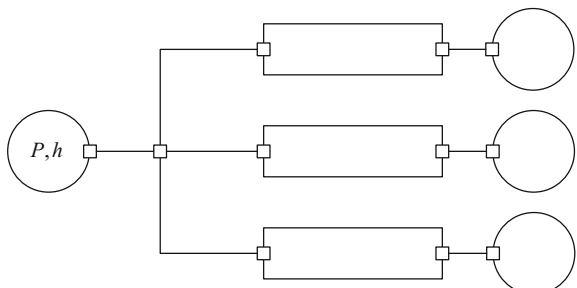
In Fig. 17.10, all connectors of the mixing volume collapse into a single connector that is shared by all flow components. This representation leads to some interpretation difficulties, as the superimposed connectors could be interpreted as sharing the same information, which is in fact not the case:  $P_a$  and  $h_a$  represent indeed the same information for all connections, but  $\dot{m}(b \rightarrow a)$  and  $h_b$  represent a different information for different connections. This is why the representation on the right-hand side of Fig. 17.10 is avoided.

As an example of such interpretation difficulty, see Fig. 17.11. It is tempting to interpret this model as setting the same boundary condition ( $P, h$ ) to the three pipes and forget that water flows from one pipe to another (see Fig. 17.12).



**Fig. 17.10** Static volume component represented as a point (right)

**Fig. 17.11** Connecting a single source to three flow components



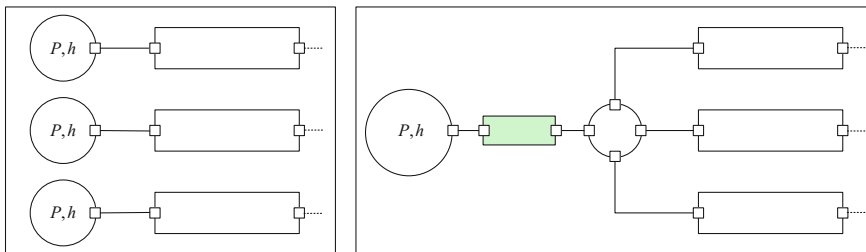


**Fig. 17.12** Two interpretations of model in Fig. 17.11: wrong (left) and correct (right)

In Fig. 17.12, a pipe without pressure loss has been added on the right-hand side model to comply with the staggered grid scheme.

### 17.1.6.2 Static Volume Components with Two Connectors

In this case, there is no difficulty in representing the volume component as a point, as the two superimposed connectors carry exactly the same information. It is also possible to omit the representation of the volume component altogether, resulting in directly connecting the two adjacent flow components (cf. Fig. 17.13).

Connecting flow components directly is convenient to represent lines of flow components, such as in Fig. 17.14, which shows a source connected to a valve which is connected to a pipe which is connected to a pump which is connected to a sink.

When directly connecting flow components together, it seems that  $P_a$  and  $h_a$  in the bottom component line of Fig. 17.13 are not computed anymore, as the volume component that computes them disappears completely from the model. Let us see whether these two quantities can still be computed.

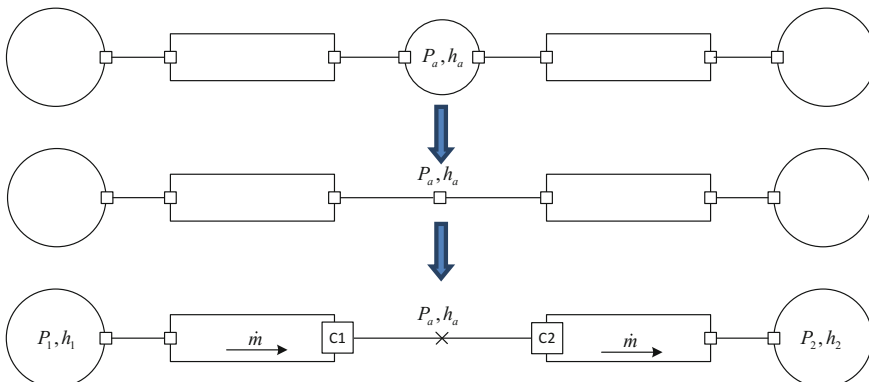


**Fig. 17.13** Connecting two flow components together

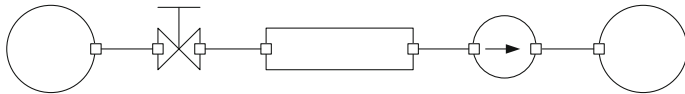


**Fig. 17.14** Line of flow components

Using (5.25):

$$P_1 - P_a = f_1(\dot{m}) \quad (17.7)$$

$$P_a - P_2 = f_2(\dot{m}) \quad (17.8)$$

Equations (17.7) and (17.8) enable to compute  $P_a$  and  $\dot{m}$  as  $P_1$  and  $P_2$  are known boundary conditions.

Using (17.1):

$$h_{1:a} = s(\dot{m}) \cdot h_1 + s(-\dot{m}) \cdot h_a \quad (17.9)$$

$$h_{a:2} = s(\dot{m}) \cdot h_a + s(-\dot{m}) \cdot h_2 \quad (17.10)$$

$h_1$  and  $h_2$  are known boundary conditions.  $\dot{m}$  is computed with (17.7)–(17.8). There are three unknowns left:  $h_a$ ,  $h_{1:a}$ , and  $h_{a:2}$  for two equations: (17.9) and (17.10). Therefore, one equation is missing, which is the energy balance equation that corresponds to the missing component  $M(a)$ . Therefore,  $h_a$  cannot be computed, as it should be computed by  $M(a)$ , unless the energy balance equation in  $M(a)$  is restored. Let us see how this can be done.

Neglecting diffusion and applying the static energy balance equation (5.5) to volume  $a$  yields:

$$h_{1:a} = h_{a:2} \quad (17.11)$$

One can then prove that  $h_a$  can be computed and its value is given by

$$h_a = h_{1:a} = h_{a:2} = s(\dot{m}) \cdot h_1 + s(-\dot{m}) \cdot h_2 \quad (17.12)$$

which is consistent with the upwind scheme, and shows that all models in Fig. 17.15 are equivalent.

*Proof* From (17.9) to (17.11):

$$s(\dot{m}) \cdot h_1 + s(-\dot{m}) \cdot h_a = s(\dot{m}) \cdot h_a + s(-\dot{m}) \cdot h_2$$

$$(s(\dot{m}) - s(-\dot{m})) \cdot h_a = s(\dot{m}) \cdot h_1 - s(-\dot{m}) \cdot h_2$$

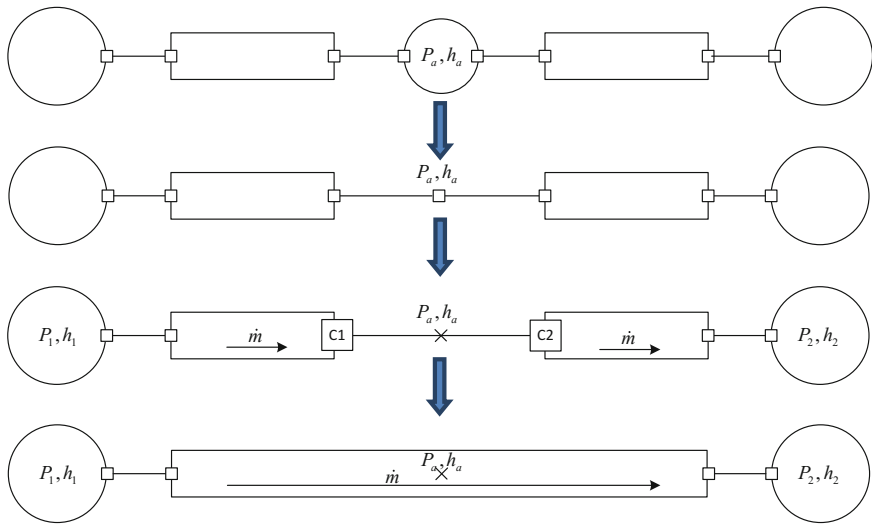


**Fig. 17.15** Connecting two flow components together

From (5.10):

$$\operatorname{sgn}(s(\dot{m})) \cdot h_a = s(\dot{m}) \cdot h_1 - s(-\dot{m}) \cdot h_2$$

Noticing that  $\operatorname{sgn}(x) \cdot \operatorname{sgn}(x) = 1$  and using (5.10), (5.12), and (5.13):

$$\begin{aligned} h_a &= \operatorname{sgn}(s(\dot{m})) \cdot (s(\dot{m}) \cdot h_1 - s(-\dot{m}) \cdot h_2) \\ &= (s(\dot{m}) - s(-\dot{m})) \cdot (s(\dot{m}) \cdot h_1 - s(-\dot{m}) \cdot h_2) \\ &= (s^2(\dot{m}) - s(\dot{m}) \cdot s(-\dot{m})) \cdot h_1 - (s(\dot{m}) \cdot s(-\dot{m}) - s^2(-\dot{m})) \cdot h_2 \\ &= s(\dot{m}) \cdot h_1 + s(-\dot{m}) \cdot h_2 \end{aligned}$$

Then, from (17.9):

$$\begin{aligned} h_{1:a} &= s(\dot{m}) \cdot h_1 + s(-\dot{m}) \cdot h_a \\ &= s(\dot{m}) \cdot h_1 + s(-\dot{m}) \cdot (s(\dot{m}) \cdot h_1 + s(-\dot{m}) \cdot h_2) \\ &= s(\dot{m}) \cdot h_1 + s(\dot{m}) \cdot s(-\dot{m}) \cdot h_1 + s^2(-\dot{m}) \cdot h_2 \\ &= s(\dot{m}) \cdot h_1 + s(-\dot{m}) \cdot h_2 \end{aligned}$$

In a similar way,

$$h_{a:2} = s(\dot{m}) \cdot h_1 + s(-\dot{m}) \cdot h_2$$

This proof is also valid for non-adiabatic processes: It suffices to replace  $h_b$  by  $h'_b$  for all relevant volumes  $b$ ; cf. (17.6).

If more than two flow components are connected together, it suffices to repeat the proof for the additional flow components. Therefore, (17.12) is applicable to a line of flow components.

However,  $h_{1:a}$  and  $h_{a:2}$  cannot be found in the fluid connector as defined by (17.5) so (17.11) cannot be generated automatically by connecting  $C1$  to  $C2$ . Therefore, a better structure for the fluid connector is to add  $h_{b:a}$  to connector (17.5), yielding

$$C_{\text{fluid},a} = (P_a, h_a, h'_b, h_{b:a}, \dot{m}(b \rightarrow a)) \quad (17.13)$$

Then, (17.11) can be generated automatically when connecting  $C1$  to  $C2$ . Hence, connector (17.13) restores automatically the staggered grid scheme when flow components are connected together. This method uses the approximation of neglecting diffusion.

The upwind scheme (17.4) computes  $h_{b:a}$  directly from the specific enthalpies of the two adjacent volumes  $b$  and  $a$ .  $h'_b$  is only used to compute  $h_{b:a}$ . So, if the upwind scheme is implemented in flow components, then it is not necessary to pass  $h'_b$  along from volume  $b$  to volume  $a$  through the line of flow components that connects them. Then, the fluid connector can be reduced to

$$C_{\text{fluid},a} = (P_a, h_a, h_{b:a}, \dot{m}(b \rightarrow a)) \quad (17.14)$$

Indeed, using fluid connector (17.14) for both connectors of flow component  $M(a:b)$  yields

$$\begin{cases} C_{\text{fluid},a} = (P_a, h_a, h_{b:a}, \dot{m}(b \rightarrow a)) \\ C_{\text{fluid},b} = (P_b, h_b, h_{a:b}, \dot{m}(a \rightarrow b)) \end{cases}$$

Then, the upwind scheme (17.4) can be implemented in  $M(a:b)$ :

$$C_{\text{fluid},b} \cdot h_{b:a} = C_{\text{fluid},a} \cdot h_{a:b} = h_{b:a} = \begin{cases} C_{\text{fluid},b} \cdot h_b + \Delta_{b \rightarrow a} h & \text{if } C_{\text{fluid},b} \cdot \dot{m}(b \rightarrow a) > 0 \\ C_{\text{fluid},a} \cdot h_a & \text{if } C_{\text{fluid},a} \cdot \dot{m}(a \rightarrow b) > 0 \end{cases}$$

with

$$C_{\text{fluid},b} \cdot \dot{m}(b \rightarrow a) = -C_{\text{fluid},a} \cdot \dot{m}(a \rightarrow b)$$

$\Delta_{b \rightarrow a} h$  is computed within  $M(a:b)$ .  $C_{\text{fluid},b}.h_b$  and  $C_{\text{fluid},a}.h_a$  are, respectively, computed by the energy balance equations in volume components  $M(a)$  and  $M(b)$ .

Therefore, if diffusion is neglected and the upwind scheme (17.4) is implemented in flow components, then fluid connector (17.14) can be used to connect flow components together in the staggered grid scheme.

### 17.1.7 Flow Network Global Orientation

The orientation of the flow component  $M(b:a)$  is given by the vector  $\vec{A}(b \rightarrow a)$  which represents the surface unit vector for boundary  $b:a$  oriented positively from  $b$  to  $a$ . The sign of the mass flow rate  $\dot{m}(b \rightarrow a)$  crossing boundary  $b:a$  is equal to the sign of  $\vec{v} \cdot \vec{A}(b \rightarrow a)$ , where  $\vec{v}$  is the fluid velocity through the boundary.

For a given network, it is possible to assign different orientations to flow components, such as the ones given at random in Fig. 17.16.

However, it is better to choose the network orientation according to the flow direction under nominal operating conditions. This means that flows will be negative only during transitory flow reversals, which is what one would expect when inspecting simulation results.

To that end, each flow component is oriented by giving a particular role to each of its two connectors: One connector is the flow origin, while the other is the flow destination under nominal operating conditions. The flow is then positive when going from the origin to the destination, and negative otherwise, cf. Fig. 17.17, where the origin connector is blue and the destination connector is red. The network can then be globally oriented by connecting connectors of different colors while complying with the rules of the staggered grid scheme; cf. Fig. 17.18: Two flow

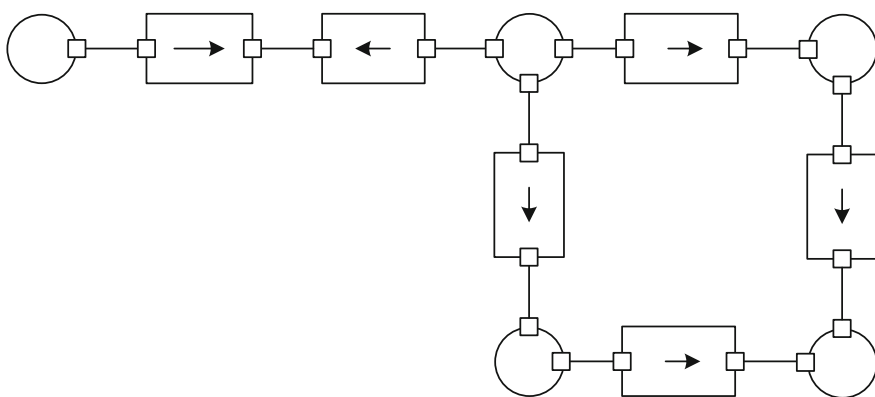
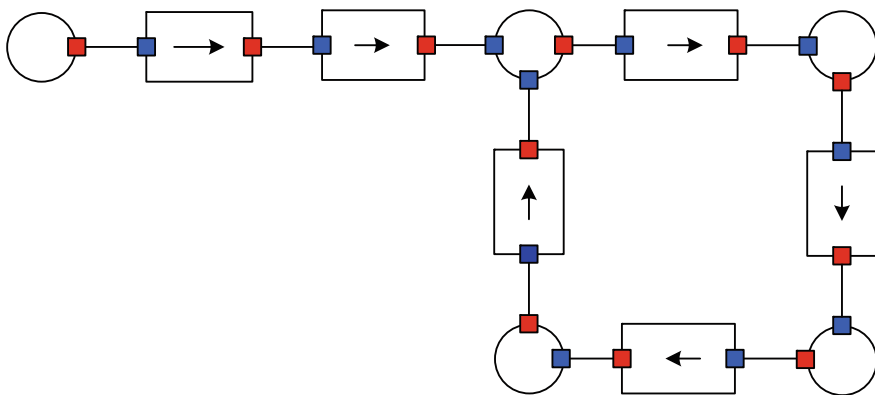


Fig. 17.16 Random network orientation



**Fig. 17.17** Origin connector (blue) and destination connector (red)



**Fig. 17.18** Globally oriented network

components can be connected together, but volume components must always be connected via flow components (even if they have exactly two connectors).

Flows are positive when leaving a component through a red connector and entering a component through a blue connector.

## 17.2 Fundamental Choices for ThermoSysPro

### 17.2.1 Current Situation with ThermoSysPro V3.x

The following choices are made:

1. The model equations are formulated in lumped form such as (4.5) using the  $(P, h)$  state representation for water/steam and the  $(P, T)$  state representation for flue gases (cf. Sect. 2.5).
2. Equations are expressed in the form of DAEs such as (1.7).

3. The staggered grid scheme is used (cf. Sect. 17.1).
4. Diffusion is neglected (cf. Sects. 4.3.2 and 5.2).
5. The upwind scheme is used; cf. (17.4).
6. The average pressure is used at boundary  $b:a$ , even for compressible fluids (cf. Sect. 4.3.4).
7. It is possible to connect flow components together (cf. Sect. 17.1.6.2).
8. Flow reversal is not handled for flue gases. This means that for flue gases, mass flow rates are assumed to be always positive so that the upwind scheme (17.4) reduces to

$$h_{b:a} = h_b + \Delta_{b \rightarrow a} h \quad (17.15)$$

9. Consequently, the fluid connector is:

- For water/steam components:

$$C_{\text{fluid},a} = (P_a, h_a, h_{b:a}, \dot{m}(b \rightarrow a)) \quad (17.16)$$

corresponding to (17.14).

- For flue gases components:

$$C_{\text{flue gases},a} = (P_a, T_a, \dot{m}(b \rightarrow a), X_{a,i}) \quad (17.17)$$

where  $X_{a,i}$  denotes the mass fraction of chemical substance  $i$  in volume  $a$ , with  $\sum_i X_{a,i} = 1$ .

Figure 17.19 shows the ThermoSysPro logo.

**Fig. 17.19** ThermoSysPro logo



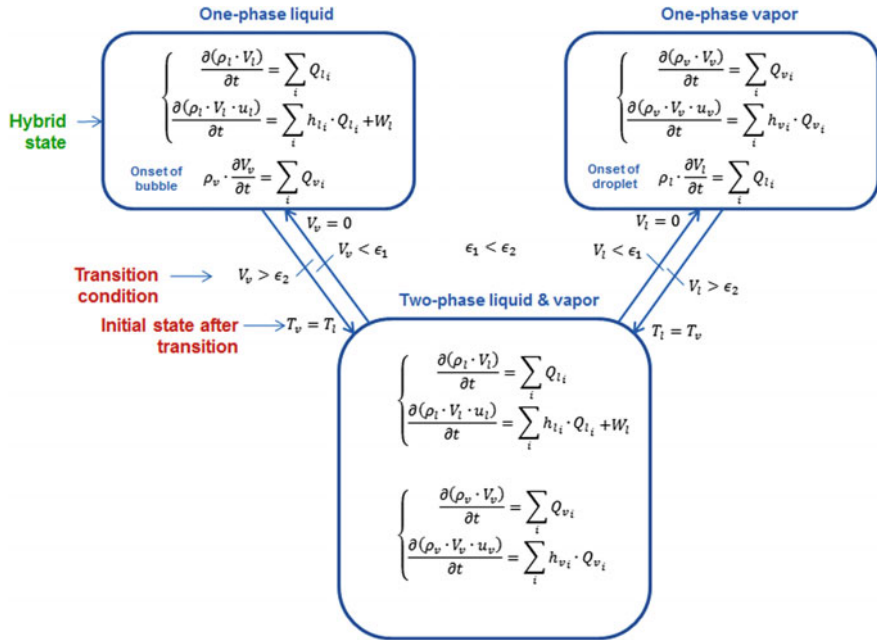


**Fig. 17.20** Transitions between single- and two-phase flows represented in multi-mode form (Bouskela 2016)

### 17.2.2 Future Directions for ThermoSysPro V4.x

Future directions for ThermoSysPro 4.x are as follows:

1. Diffusion will be taken into account.
2. The  $(P, h)$  state representation will be used for all fluid connectors. Therefore, flow reversals will be handled for all fluids, including flue gases.
3. Equations will be expressed in multi-mode form when necessary (e.g., to represent transitions between single- and two-phase flows; cf. Fig. 17.20 and Sect. 1.4).

## References

- Bouskela D (2016) Multi-mode physical modelling of a drum boiler, complex adaptive systems. Proc Comput Sci 95:516–523
- Bouskela D, El Hefni B (2014) A physical solution for solving the zero-flow singularity in static thermal-hydraulics mixing models. In: Proceedings of the 10th international modelica conference, Lund, Sweden